UNCLASSIFIED

AD NUMBER

AD820760

NEW LIMITATION CHANGE

TO

Approved for public release, distribution unlimited

FROM

Distribution authorized to U.S. Gov't. agencies and their contractors; Critical Technology; MAY 1967. Other requests shall be referred to Naval Air Systems Command, Washington, DC 20360.

AUTHORITY

USNASC notice, 23 Dec 1970

THIS PAGE IS UNCLASSIFIED

HSER 4348
VOLUME ~~2 of 4~~ 2 of 4

ENGINEERING REPORT

SHROUDED PROPELLER TEST PROGRAM DATA

AD820760

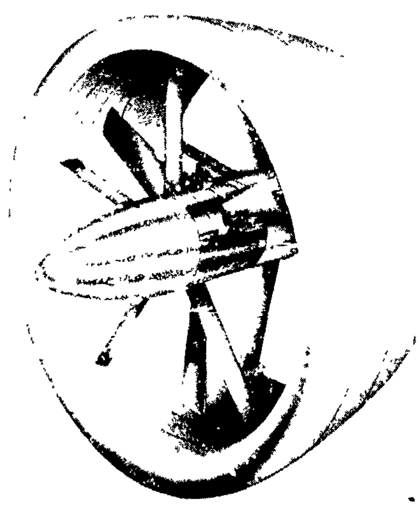

PHASE 1

CONTRACT NOw 64-0707-d

MAY, 1967

Hamilton Standard
DIVISION OF UNITED AIRCRAFT CORPORATION

HSER 4348
VOLUME ~~2 of 4~~ 2 of 4

ENGINEERING REPORT

SHROUDED PROPELLER TEST PROGRAM DATA

PREPARED BY: UNITED AIRCRAFT RESEARCH LABORATORIES

APPROVED BY: Carl Rohrbach
C. ROHRBACH - HEAD OF AERODYNAMICS & HYDRODYNAMICS

W. Fortmann
W. FORTMANN - CHIEF OF TECHNICAL STAFF

A. D. Croxall
A. D. CROXALL - CHIEF PROJECT ENGINEER

THE WORK COVERED BY THIS REPORT WAS CARRIED OUT FOR HAMILTON STANDARD BY THE UNITED AIRCRAFT CORPORATION RESEARCH LABORATORIES

PHASE 1

CONTRACT NO. 64-0707-d
MAY ,1967

Hamilton Standard
DIVISION OF UNITED AIRCRAFT CORPORATION

United Aircraft Research Laboratories

UNITED AIRCRAFT CORPORATION

EAST HARTFORD, CONNECTICUT

Report E330590-1

Wind Tunnel Tests

of Shrouded Propellers

VOLUME II OF IV

REPORTED BY A. W. Simmonds

A. W. Simmonds

APPROVED BY A. Fasano

A. Fasano
Supervisor, Low Speed
Wind Tunnels

DATE 3/20/67

NO. OF PAGES 334 - Volume II

COPY NO. 19

Report E330590-1

Wind Tunnel Tests of

Shrouded Propellers

TABLE OF CONTENTS

TABLE OF CONTENTS
(Contd.)

INDEX TO CONTENTS OF VOLUMES

INDEX TO CONTENTS OF VOLUMES
(Contd.)

Report E330590-1

Wind Tunnel Tests of

Shrouded Propellers

SUMMARY

Wind tunnel tests of a shrouded propeller model were conducted for the Hamilton Standard Division of the United Aircraft Corporation in the 18- and 8-ft test sections of the UARL Large Subsonic Wind Tunnel during December 1965 and May 1966. The test model comprised a shroud-propeller assembly which was attached to a propeller dynamometer through strain-gage balances. The balances provided shroud chord force, shroud normal force, propeller thrust and propeller torque data. Various pressure measurements were also obtained including shroud inlet pitot-static pressures, shroud exit total pressures, shroud surface pressure distributions, non-steady shroud surface pressures and velocity-angularity radial traverse probe data. These data were obtained for propellers with varying blade planform, number of blades and blade-shroud tip clearance. Attendant shroud variables included lip contour, length, axial position, exit area and inlet-exit guide vanes. Test data for these model configurations were obtained through ranges of blade rotational speed at various blade pitch angles and at tunnel Mach numbers from 0.02 to 0.60.

A complete transcript of test data and descriptive information pertinent to the test models, equipment and techniques were transmitted to Hamilton personnel shortly after the test was completed. This report presents an explanatory text, detailed tabulations of the performance and pressure data, and a comprehensive graphical presentation of the performance data.

This project was undertaken for Hamilton Standard under Purchase Order No. E277698 dated March 31, 1965 and Supplement No. 2 dated February 1, 1966.

INTRODUCTION

The subject shrouded propeller tests comprise the experimental phase of an experimental-analytical program contracted by Hamilton Standard with the Navy Bureau of Weapons. The data obtained are intended to provide detailed and systematically varied performance curves which are sufficient to permit empirical performance estimates for most shrouded propeller configurations. The data also serve as a reference for the analytic predictions which will evolve from the analytical phase of the Navy contract. The data obtained are presented herein in detailed tabular and graphical formats; the test apparatus and techniques are also described.

TEST FACILITY, PROPELLER DYNAMOMETER AND TEST MODELS

Wind Tunnel Facility

The UARL Large Subsonic Wind Tunnel shown in Fig. 1 is a single-return, closed-throat facility with interchangeable 18- and 8-ft octagonal test sections. Maximum tunnel velocity is approximately 200 mph in the 18-ft section and near sonic Mach numbers can be obtained in the 8-ft section. Tunnel stagnation pressure equals atmospheric pressure, and the stagnation temperature of the airstream is held constant in the 40 to 130 F range by means of air exchanger valves. Electric power may be supplied to test models by two motor generator sets each of which develop a maximum of 375 hp at frequencies of 0 to 400 cps. Auxiliary vacuum systems and a 400 psig air supply are also available. A small digital computer and a high-speed data acquisition system capable of sampling 20 channels of dynamic data, 200 steady pressures or 150 steady temperatures are available in the tunnel control room. A detailed description of the wind tunnel and its auxiliary equipment is given in Ref. 1.

Propeller Dynamometer and Shroud Balance

The model propellers were driven by the UARL propeller dynamometer which consists of two variable-speed motors, mounted in tandem, and housed within a

streamlined cast-steel pod with an integral support strut (Fig. 2). The motors are mounted in hydrostatic bearings to restrain all motion except axial motion along, or rotational motion about, the longitudinal axis of the dynamometer. These motions were restrained by load cells which measure thrust and torque of the model propeller. Each motor is capable of delivering 375 hp at 12,000 rpm; together they provide a maximum torque of 330 lb-ft at any operational speed. Model speed was controlled by variable frequency power supplied by two motor-generator sets and measured with a Berkley EPUT meter and 60 tooth gear signal generator. The dynamometer was faired such that there is negligible axial static pressure gradient in the plane of the propeller (Ref. 2). The dynamometer is also designed so that the model propeller and hub are the only portion of the metric system exposed to the airstream. Pressure instrumentation was provided within the dynamometer in order to correct the measured thrust for any difference in pressure between the front face of the hub and an equal area in the rear fairing (Fig. 2). Further details of the propeller dynamometer are presented in Ref. 2.

The shroud strain-gage balance system shown in Fig. 3 was used to support the shroud on the propeller dynamometer and to measure shroud normal and chord forces. The balance ground structure was provided by a new fairing of heavy gage rolled boiler plate machined to provide essentially the same shape as the metal fairing normally used. The shroud was supported on the ground structure by a three-point linkage schematically illustrated in Fig. 4. Support points P_1 and P_2 shown in Figs. 3 and 4 were fixed in the y-z plane (Fig. 4) by two "A" frames which were free to pivot at both ends. Points P_1 and P_2 were restrained in the axial direction by flexured load cells (C_4, C_5) which attached to the non-metric structure. Points P_1 and P_2 permitted lateral as well as vertical rotation and thus only axial chord forces (C_4, C_5) were transmitted through these points. Forces N_1 and N_2 were obtained directly from load cells which measured a bending moment in the lateral plane between points P_1 and P_2 and the shroud. Support point P_3 was fixed in space by a rigid normal force support arm projecting forward from the fairing of the extension shaft housing. A flexured load cell (N_3) was located between the side arm and shroud. The interference effect of the support arm of point P_3 and the tare and interference effect of the "A" frames were obtained by use of dummy images of these supports.

Propeller Dynamometer and Shroud Installation

The shroud-dynamometer was initially installed in each test section at a yaw angle of 0 deg and with the thrust axis coincident with the tunnel centerline

elevation. Figures 5 to 8 illustrate the installation although the dynamometer is shown at non-zero yaw angles (28 deg in 18-ft test section, 8 deg in 8-ft test section) as used during stress tests not described herein. Dynamometer monitoring instrumentation consisted of an EPUT meter for rotational speed, a vibration meter with provision for selecting vertical or horizontal motion and a Speed-O-Max display for numerous thermocouple temperatures. Pressure leads from the dynamometer and electrical leads from the dynamometer and shroud balance were connected at the dynamometer strut bulkhead (Fig. 2) then led across the tunnel balance chamber to the appropriate facility in the control room. Electrical leads from the shroud transient pressure transducers were led across the shroud balance linkage, along and down the leading edge of the dynamometer, and into the balance chamber where they were directed into the control room and connected to a Visicorder. Pressure tubing leads from the shroud and exit rake were led downstream across the shroud balance linkage, along and down the leading edge of the dynamometer, and into the balance chamber where they were connected to a patch panel. Pressure tubing leads from the inlet rake and spinner (P_1 in Fig. 2) were led upstream through the spinner and a sting, through the sting support struts, and into the balance chamber where they were connected to the patch panel. At the patch panel the leads were directed to the high-speed data acquisition system and manometer boards in the tunnel control room. The electrical and pressure leads from the traversing probe were led into the balance chamber and then directed to the appropriate facility in the control room. During pre-performance stress tests, the electrical leads from the blade strain gages were directed along the trailing edge of the blade and through the hub to a slip ring assembly mounted on the upstream surface of the hub. The electrical leads from the slip ring assembly were led upstream through the spinner and sting and down the sting support strut into the balance chamber where they were directed to the appropriate HSD equipment in the control room.

Test Models

The test models consisted of a 20-inch chord shroud with provisions for varying shroud geometry, a 15-inch chord shroud (short chord) of fixed geometry and four sets of propeller blades. The 20-inch chord shroud geometric variations included shroud axial position (two locations), shroud lip shape (two nose sections), shroud diffuser shape and exit area (four aft sections), shroud adjustable pitch inlet guide vanes (set of five), and shroud adjustable pitch exit guide vanes (set of five). Specifications for the shroud components and guide vanes are presented in Appendix I, Figs. I-1 through I-4. Changes in shroud geometry were provided through use of a central support ring which supported the shroud components and transferred aerodynamic loads from the model to the shroud balance.

The support ring as shown in Fig. 9 was fabricated from aluminum to form a channel section with component variation attachment points and was machined to provide a close tolerance inner surface ring concentric with the propeller tip path. The support ring could be located downstream of the position shown in Fig. 9 by the removal of spacers at the upper and lower support points. The forward position places the propeller at the 40 percent chord station of the 20-inch shroud and the aft position locates the propeller at the 25 percent station of that shroud. Figures 10 and 11 show the support ring with exit vanes and with typical shroud diffuser and inlet sections attached, respectively. The diffusers were fabricated from laminated mahogany and machined to provide the exterior contour. Also shown in Fig. 11 is the location of shroud surface static pressure orifices (90 and 315 deg azimuth) and the normal force load cell fairing. A surface pressure transducer on the inner surface and outer surface of the shroud upstream of the propeller plane was also installed for portions of the program. Figures 12 and 13 show the complete shroud model including lip section, center ring fairing blocks, diffuser, aluminum inlet vanes, aluminum exit vanes and exit total pressure rake. Figures 12 and 13 also show the propeller hub spinner which is specified in Appendix I, Fig. I-5.

The test models included four sets of propeller blades comprising rectangular, wide tip and narrow tip planform three-way configurations and comprising a narrow tip four-way configuration. A blade of each of the four propeller sets is shown in Fig. 14 and the geometry of each blade is described in Appendix I, Figs. I-6 through I-9. The blades were aluminum and the three-way rectangular set incorporated fiberglass tips which provided for tip clearance variations between the blade tip and shroud. The blades installed in the 7.5-inch diameter steel hub provided a disc diameter of approximately 30 inches. All three-way propellers had an activity factor of 168 per blade and a design camber of 0.4. The four-way propeller had an activity factor of 126 per blade and a design camber of 0.4. Changes in blade angle were accomplished by manually turning worm gears in the hub that mesh with integral gear sectors on the blade root. Figure 15 shows the rectangular blades installed in the three-way hub (HSD Dwg. SK 27388), and Fig. 16 shows the narrow tip blades, with strain gage instrumentation attached, installed in the four-way hub (HSD Dwg. SK 27388).

Provisions for mounting of inlet pitot-static rakes and an exit total pressure rake were provided in addition to the static pressure orifices and surface pressure transducers incorporated in the model shroud components. The 15-orifice pitot-static inlet rake and the 25-orifice total pressure exit rake were both non-metrically supported from the spinner and dynamometer cowl fairing, respectively. A probe which traversed the exit of each shroud and just behind the propellers was mounted from the tunnel wall. A complete description of this instrumentation is provided in Appendix II.

The configuration designation system used herein is based on 16 symbols, each consisting of a letter with subscripts denoting variables and superscripts, where applicable, denoting angle deflections. A typical example would be $L_1C_1E_1B_3P_RT_1$, which defines the complete shroud-propeller model with inlet lip one (L_1), propeller located at 40 percent shroud chord (C_1), diffuser exit area ratio of 1.1 (E_1), three-way hub (B_3), rectangular planform blade (P_R) and basic blade tip-shroud clearance (T_1). The symbols are concisely defined in Table I and illustrated in Figs. 9 to 16. Special forms of these symbols used in computer tabulations are included in parenthesis after the symbol definition in Table I.

TEST PROCEDURES

Initial Testing

The initial testing consisted of traversing probe calibration, tunnel blockage calibration, hub tare, tare and interference, and pre-performance stress runs. The traversing probe calibration, as described in Appendix II, defined the parameters required for interpretation of velocity-angularity data. The blockage calibrations, as described in Appendix III, provided a technique for setting tunnel speed. The hub tare runs, as described in Appendix IV, defined the hub skin friction drag which was to be subtracted from the thrust measurements.

The tare and interference runs, as described in Appendix V, defined the effects of the side arm and "A" frame which were to be deleted from the shroud normal and chord-force data. The pre-performance stress runs were conducted with strain-gaged blades to define safe operating limits. The blade stress signals were transmitted through a slip ring assembly within the hub spinner and monitored on a Visicorder by Hamilton personnel. Based on observed stress levels of specific blades selected by HSD personnel, a safe operating range (windmill rpm to 8000 rpm) was established for all the blades tested. Propeller dynamic balance calibrations were interspersed in the test program and were conducted following assembly and static balancing of each hub propeller configuration. These calibrations consisted of monitoring horizontal and vertical vibration as sensed by the vibration gages immediately downstream of the hub as shown in Fig. 2. A safe operating limit of ±0.005 inch has been established for the subject test rig.

Performance Testing

The performance test program consisted of recording and processing propeller thrust and torque, shroud chord and normal force, and shroud inlet and exit pressures for various model blade angles through a range of rotational speed at constant Mach number, shroud configuration and yaw angle (zero). Each rotational speed setting constituted a test point and each range of rotational speed defined a data run. This testing was conducted without strain gage instrumentation on the blades.

The performance data instrumentation consisted of one EPUT meter for propeller rotational speed and ten strain gage unit (sgu) potentiometers for torque, thrust, delta thrust, normal force (three load cells), chord force (two load cells), and local Mach number at the hub (two transducers). This instrumentation incorporated a locking circuit which provided a simultaneous visual sample of each signal which was manually recorded and at the same time punched into a digital computer in the tunnel control room for processing. The almost simultaneous reduction of the basic data permitted a manual on-line graphic presentation of the data in coefficient form. The inlet and exit pressure data were displayed on manometer boards in the control room and recorded photographically, or on magnetic tape with the high-speed data acquisition system. When these data were recorded on magnetic tape, a back-up record was usually obtained through a photographic record of the pressures as displayed on the manometer boards. These data were reduced concurrent with the test program at the UARL Computation Laboratory.

Performance data in the Mach number ranges from 0.02 to 0.20 and 0.3 to 0.6 were obtained in the 18-ft and 8-ft test sections, respectively. A functional sequence of shroud configurations with attendant run numbers and figure numbers is presented in Table II, and a detailed listing of each run obtained during the entire program is given in Table III.

Pressure Testing

The pressure program consisted of recording and processing pressures sensed by a probe traversed radially across the shroud exit area (T_P) and behind the propeller disc (T_{P_2}) for various model blade angles at constant rotational speed, Mach number and shroud configuration. Each radial station setting constituted a test point and each complete traverse across the shroud exit area or behind the

propeller disc defined a pressure run. In the 8-ft test section pressures were also recorded at a specified rotational speed below and above the design rotational speed for one radial position of the traversing probe.

The installation of the probe in the clear 8-ft section preceding the 8-ft section test phase constitutes a third probe position identified in Table I. In addition to the traverse probe data, pressures sensed with the inlet pitot-static rake, the exit total pressure rake and the static orifices on the shroud were recorded on magnetic tape and processed at the computation laboratory. For some shroud-propeller configurations, transient pressures sensed by pressure transducers mounted flush with the inner and outer surface of the shroud lip were recorded on a Visicorder.

STATEMENT OF ACCURACY

At the conclusion of the test program a statistical analysis based on methods outlined in Ref. 3 was made of approximately 300 static zero shifts noted for each of the four balance components. Estimates of static data accuracy (two standard deviations) based on these results are tabulated below.

Component	System Capacity	Measured Force or Moment	Coefficient (5000 RPM)
Thrust, lb	700	±0.93	±0.002
Torque, ft-lb	500	±0.54	±0.002
Chord Force, lb	±1000	±1.26	±0.004
Normal Force, lb	±2000	±1.82	±0.003

Accuracy in setting propeller rotational speed and propeller blade angle is estimated as ±1 rpm and ±0.1 deg, respectively. Accuracy in setting tunnel Mach number is estimated as 0.005. Overall data repeatability as influenced by all of these parameters and also by model configuration duplication is illustrated in Figs. 17 to 26 of the Data Repeatability tab section. Figures 17 to 20 present data repeatability through the speed regime of the 18-ft tunnel; Figs. 21 and 22 present data repeatability between the 18-ft and 8-ft test sections for a common Mach number of 0.2 and Figs. 23 to 26 present data repeatability in the 8-ft test section. The plots presented are a sampling of the repeat runs conducted throughout the test program and are felt to be representative of the overall data repeatability.

An arithmetic mean estimate of the pressure data repeatability based on a small number of samples indicated values of ±0.06 in surface pressure coefficient, ±0.5 deg in traverse probe yaw angle (ZETA), ±1.0 deg in traverse probe pitch angle (THETA), and ±5 fps in traverse probe velocity (V'). The accuracy in setting the traversing probe radial position was estimated as 0.012 inches.

DATA REDUCTION AND PRESENTATION

The reduction and presentation of the performance and pressure data which were obtained during the runs listed in Table II are discussed herein. Additional calibration and tare data are described in Appendices II through V. The data reduction equations for the performance data are presented in Appendix VI in the initial five sections. The first section (Eqs. 1 to 5) is preliminary in nature and includes standard calculations for determining tunnel air density, velocity and dynamic pressure, and an equation for solid and wake blockage corrections to tunnel velocity. The symbols used in these equations and all subsequently discussed equations are defined in the List of Symbols. The second group of equations (Eqs. 6 to 9) converts the force and moment gage readings to thrust, torque, chord force and normal force. The third and fourth groups of equations (Eqs. 10 to 16) indicate expressions for tare corrections and balance interactions to the basic force and moment equations. The fifth group of equations (Eqs. 17 to 28) converts thrust, torque, chord force and normal force to aerodynamic coefficient form and also includes standard calculations for advance ratio, shaft horsepower and propeller tip speed. These equations also indicate the "A"-frame tare and interference correction on chord force.

The parameters defined by Eqs. 17 to 28 represent the required performance data in their final algebraic form. The data reduction equations for the pressure data are presented in the remaining two sections. Section VI presents an equation for dynamic pressure (Eq. 29) corrected for solid blockage at Mach numbers greater than 0.2 and an equation for pressure coefficient (Eq. 30). The seventh and final group of equations (Eqs. 31 to 38) includes expressions for converting traversing probe pressures to inclined velocity and to projected velocity parallel to the thrust axis.

The presentation of the performance data is in the form of aerodynamic coefficient plots and tabulations. The plots are divided into seven tab-sectioned groups as indicated in Table IV "List of Figures." The groups are descriptively annotated as: Data Repeatability, Basic Shroud Characteristics, Shroud Contour

Effects, Propeller Location and Chord Effects, Vane Effects, Blade Geometry Effects and Blade Tip Clearance Effects.

The first tab section presents a comparison of the data repeatability and is discussed in the preceding section of this report (Statement of Accuracy). The remaining tab-sectioned groups are presented so that the effects of a specific change in model geometry is presented in an individual tab section and is easily compared with the basic model characteristics presented in the second tab section. Within each tab-sectioned group the salient aerodynamic parameters for low (M = 0.02 to 0.15) and high (M = 0.20 to 0.60) speed performance are presented in sets of two and three figures, respectively. The low-speed performance plots present power coefficient and thrust coefficient, versus advance ratio on the first figure of the set and net thrust coefficient and chord force versus advance ratio on the second figure of the set.

The first data presented in the Basic Shroud Characteristics tab section are a single figure set since the shroud was not installed and net thrust coefficient and chord force data were not pertinent. The high-speed performance plots present efficiency, net efficiency and power coefficient versus advance ratio. The contents of the Vane Effects tab section differ slightly from the described format in that, in addition to the typical performance plots, the effect of vane angle at two propeller blade angles for Mach numbers of 0.05 and 0.20 is presented. In addition to the graphic presentation of the performance data, a complete tabulation of these data is presented in Table V.

Concurrent with the acquisition of performance data and in addition to the pressure data obtained during the "Pressure Data" phases of the test program, a very large quantity of shroud inlet velocity and shroud exit pressure data was obtained. Complete tabulations of these data have been transmitted to HSD personnel and only selections of these results are presented herein. The presentation of these data is in the form of data tabulations in Tables VI and VII. A complete tabulation of the shroud inlet velocities obtained during the performance data runs in the 18-ft test section is presented in Table VI. Table VII presents shroud inlet velocities and exit pressures at, or above, the design rpm (5500) for the performance data runs in the 8-ft test section. A complete tabulation of the traversing probe data obtained during the "Pressure Data" phase of the program and the accompanying inlet, exit and model surface pressure data are presented in Tables VIII and IX, respectively.

REFERENCES

1. UAC Research Laboratories Report and Organization. UAC Research Laboratories Report R-10100, April 1950.

2. Lanz, Henry: Description of UAC 12,000 RPM Propeller Test Rig. UAC Research Laboratories Report R-14493-1, November 1953.

3. Ireson, W. and E. Grant: Handbook of Industrial Engineering and Management. Prentice-Hall, Inc. Englewood Cliffs, New Jersey, 1955.

4. Pope, Allen: Wind Tunnel Testing. John Wiley & Sons, New York, 1954.

5. Wells, W. J.: Blockage Corrections for the UAC 8-Foot High Speed Wind Tunnel. UAC Research Dept. Report M-4500-50, January 14, 1954.

6. Grose, Ronald M.: Wind Tunnel Tests of Shrouded Propellers at Mach Numbers from 0 to 0.60. United Aircraft Research Laboratories, December 1958 (WADC Technical Report 58-604).

7. Black, D.: Tare and Interference (T&I) for the Shroud "A"-Frame Support System for the 8-Foot Tunnel Testing. Memorandum to A. Simmonds, June 24, 1966.

LIST OF SYMBOLS

A	Ordinate intercept of hub skin friction tare equation, lb, Ref. App. IV
A_e	Area of the shroud exit, station 100% chord, sq ft
A_P	Disc area of 2.494 ft diameter propeller (T_1), sq ft
A_T	Cross sectional area of test section; 49 sq ft for 8-ft test section
B	Slope of hub skin friction tare versus local Mach number, lb/M_ℓ, Ref. App. IV
b	Blade local chord, ft
C	Shroud chord force, lb
c	Shroud chord length, in.
C_c	Shroud chord force coefficient, positive upstream, (CC)
C_{c_t}	"A"-frame chord force tare coefficient, Ref. App. V, VI
$C_{c_{t\&i}}$	"A"-frame chord force tare and interference coefficient, Ref. App. V, VI
C_L	Integrated design lift coefficient
C_{LD}	Blade design lift coefficient
C_N	Shroud normal force coefficient, positive to right looking upstream, (CN)
c_n	Interaction slope of chord force on normal force, lb N/lb C, Ref. App. VII
C_P	Power or pressure coefficient, (CP)
C_T	Thrust coefficient, (CT)
$C_{T_{NET}}$	Net thrust coefficient, (CT NET)
C_u	Shroud chord force uncorrected for balance interaction, lb

LIST OF SYMBOLS
(Contd.)

d_p	Actual model propeller diameter, ft, Ref. Table I
d_s	Shroud minimum internal diameter, 30.0 in.
e	Ordinate intercept of "A"-frame tare and interference equation, Ref. App. V, VI
f_{h_t}	Hub skin friction tare on thrust, lb, Ref. App. IV
f	Slope in "A"-frame tare and interference equation, Ref. App. V, VI
g	Acceleration due to gravity, 32.16 ft/sec/sec
h	Blade local thickness, ft
H_o	Barometric pressure, psf, (HO)
HP	Horsepower, (HP)
J	Advance ratio
K	Shroud shape factor, 1.03, (Ref. 4)
K_1	Slope of torque strain gage unit (sgu) read-out instrument, ft-lb/sgu Ref. App. VII
K_2	Slope of thrust sgu read-out instrument, lb/sgu, Ref. App. VII
K_3	Slope of ΔT sgu read-out instrument, lb/sgu, Ref. App. VII
K_4	Slope of normal force N_1 (upper bending moment load cell), read-out instrument, lb/sgu, Ref. App. VII
K_5	Slope of normal force N_2 (lower bending moment load cell), read-out instrument, lb/sgu, Ref. App. VII
K_6	Slope of normal force N_3 (side arm load cell), read-out instrument, lb/sgu, Ref. App. VII
K_7	Slope of chord force C_4 (upper "A"-frame load cell), read-out instrument, lb/sgu, Ref. App. VII

LIST OF SYMBOLS
(Contd.)

K_8	Slope of chord force C_5 (lower "A"-frame load cell), read-out instrument, lb/sgu, Ref. App. VII
K_9	Slope of local (hub), total pressure read-out instrument, psf/sgu, Ref. App. VII
K_{10}	Slope of local (hub), static pressure read-out instrument, psf/sgu, Ref. App. VII
$\bar{K}$	Constant for determining static pressure at traversing probe; obtained from probe calibration data, Ref. App. II
LER	Leading edge radius, % chord
M	Mach number, uncorrected for solid and wake blockage (performance data) tabulations and plots; or, corrected for solid blockage only (pressure data), (M)
M_ℓ	Mach number at 20 deg azimuth approximately 1.5 inches above hub surface, Ref. App. IV
M_r	Mach number pressure ratio at traversing probe, Ref. App. II
M_{TP}	Mach number at traversing probe, Ref. App. VI
N	Shroud normal force, lb
n	Rotational speed, rps
$\bar{N}$	Rotational speed, (RPM)
n_c	Interaction slope of normal force on chord force, lb C/lb N_u, Ref. App. VII
N_u	Shroud normal force uncorrected for balance interaction, lb
P	Pressure, psi
PTR	Propeller test rig

LIST OF SYMBOLS
(Contd.)

Δp_t	Hub pressure differential tare (buoyancy) on thrust, lb
Q	Torque, ft-lb
q	Dynamic pressure corrected for solid and wake blockage (performance data); or, corrected for solid blockage only (pressure data), psf (Q)
Q_P	Torque uncorrected for thrust interaction on torque, ft-lb
q_t	Interaction slope of torque on thrust, lb T/ft-lb Q_F, Ref. App. VII
q_u	Dynamic pressure uncorrected for solid and wake blockage, psf
R	Gas constant, 1716 ft^2/sec^2 ^oR; nominal blade radius, 30 in.
r	Local propeller radius, in.
T	Thrust, lb
TER	Trailing edge radius, % chord
ΔT	Increment of thrust due to axial pressure differential across hub, lb
t	Shroud thickness, in.
T_{NET}	Net thrust (T+C), lb
T_P	Thrust uncorrected for hub pressure differential tare, hub skin friction tare, and balance interactions, lb
t_q	Interaction slope of thrust on torque, ft-lb Q/lb T, Ref. App. VII
T_{SC}	Settling chamber temperature, ^oR, (TSC)
V	Velocity component at traversing probe; or, free airstream velocity (18-ft section pressure data uncorrected and 8-ft section data corrected for solid blockage), fps, (V)
V'	Velocity component parallel to thrust axis at traversing probe, fps (V PRIME)

LIST OF SYMBOLS
(Contd.)

V_O	Velocity of airstream corrected for blockage, fps (VO)
V_S	Volume of shroud, 13 cu ft
V_T	Propeller tip speed, fps (VT)
V_u	Velocity of airstream uncorrected for solid and wake blockage, fps
β	Blade twist, deg, Ref. App. I
γ	Ratio of specific heat of air, 1.4
Z	Angle of yaw at traversing probe, deg, (ZETA)
η	Propeller efficiency, (ETA)
η_{NET}	Net propeller efficiency, (ETA NET)
θ	Blade angle at 3/4 blade radius, (THETA 3/4); or pitch angle at traversing probe, (THETA), deg, Ref. App. II
θ_r	Ratio of pressure differential across axial static orifices to traverse orifices on traversing probe, Ref. App. II
π	Constant, 3.1416
ρ	Mass density of free airstream, slugs/cu ft, (RHO)
τ_1	Model span to width factor, 0.83 (Ref. 4)
ψ	Angle of yaw, deg, (PSI)

Subscripts

ℓ	Local condition
m	Model surface
o	Initial or zero gage reading or ambient condition

LIST OF SYMBOLS
(Contd.)

Subscripts (Contd.)

P	Parameters uncorrected for interactions, buoyancy, and tares
R	Strain gage reading, sgu
s	Static pressure
t	Total pressure
∞	Free stream static pressure, (INF)
1-5	Orifices on traversing probe (see Fig. II-4)

APPENDIX I

HSD SHROUDED PROPELLER TEST

Model Dimensional Data

The presentation in this appendix comprises tabulation of the shroud, inlet and exit guide vane, and spinner dimensions. Plots of propeller blade width ratio, thickness ratio, twist angle and design lift coefficient are also presented.

HSD SHROUDED PROPELLER TEST

MODEL DIMENSIONAL DATA

LIP ORDINATES

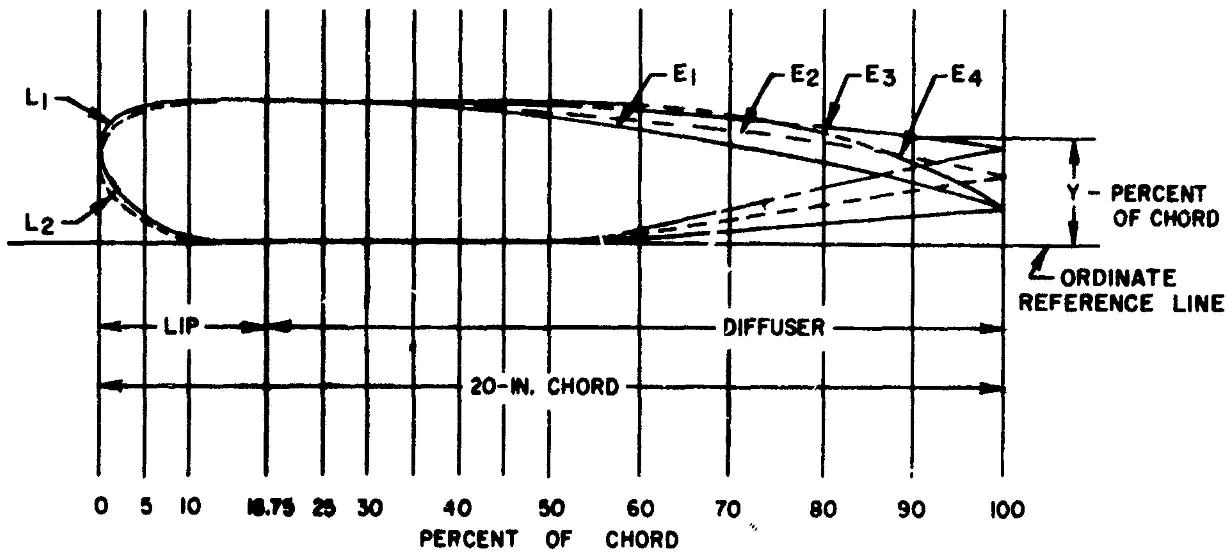

Station Percent of Chord	Lip, L_1 Ordinate,Y		Lip, L_2 Ordinate,Y	
	Upper	Lower	Upper	Lower
0.0	10.050	10.050	8.753	8.753
0.25	11.325	8.400	10.175	7.200
0.5	11.885	7.715	10.740	6.560
0.75	12.260	7.160	11.160	6.055
1.00	12.535	6.695	11.475	5.630
1.50	12.970	5.930	12.000	4.950
2.00	13.305	5.255	12.395	4.385
2.50	13.555	4.705	12.725	3.950
3.00	13.760	4.205	13.015	3.460
4.00	14.090	3.335	13.500	2.735
5.00	14.335	2.640	13.835	2.190
6.00	14.500	2.085	14.110	1.735
8.00	14.730	1.215	14.485	1.000
10.00	14.870	0.645	14.740	0.525
13.00	14.960	0.170	14.900	0.160
16.00	14.990	0.020	14.965	0.035
18.75	15.000	0.00	15.000	0.0
$t/c = 15\%$ $t/ds = 10\%$				

HSD SHROUDED PROPELLER TEST

MODEL DIMENSIONAL DATA

DIFFUSER ORDINATES

Station Percent of Chord	Diffuser, E_1 Ordinate, Y		Diffuser, E_2 Ordinate, Y		Diffuser, E_3 Ordinate, Y		Diffuser, E_4 Ordinate, Y	
	Upper	Lower	Upper	Lower	Upper	Lower	Upper	Lower
20.0	15.000	0.0	15.000	0.0	15.000	0.0	15.000	0.0
25.0	15.000		15.000		15.000			
30.0	14.910		14.940		14.965			
35.0	14.640		14.800		14.925			
40.0	14.235		14.525		14.835			
45.0	13.775		14.190		14.730			
50.0	13.225		13.800		14.575			
52.5	12.935	0.040	-	0.150	-	0.110	14.960	0.040
55.0	12.610	0.205	13.365	0.400	14.350	0.540	14.875	0.205
60.0	11.910	0.580	12.895	1.105	14.060	1.600	14.690	0.580
65.0	11.175	0.965	12.375	1.825	13.700	2.665	14.320	0.965
70.0	10.335	1.355	11.835	2.560	13.290	3.720	13.680	1.355
75.0	9.475	1.745	11.230	3.295	12.825	4.785	12.800	1.745
80.0	8.520	2.130	10.550	4.015	12.330	5.860	11.800	2.130
85.0	7.490	2.510	9.800	4.750	11.810	6.920	10.500	2.510
90.0	6.360	2.900	8.960	5.480	11.285	7.990	8.795	2.900
95.0	5.100	3.290	8.025	6.210	10.760	9.055	6.550	3.290
97.5	4.435	3.480	7.565	6.600	10.510	9.595	-	-
100.0	3.760	3.760	7.035	7.035	10.180	10.180	3.860	3.860
	A_e/A_p = 1.1		A_e/A_p = 1.2		A_e/A_p = 1.3		A_e/A_p = 1.1	
	*TER = 0.085%		*TER = 0.085%		*TER = 0.085%		*TER = 0.200%	

*TER = Trailing Edge Radius, % Chord

HSD SHROUDED PROPELLER TEST
MODEL DIMENSIONAL DATA
SHORT CHORD ORDINATES

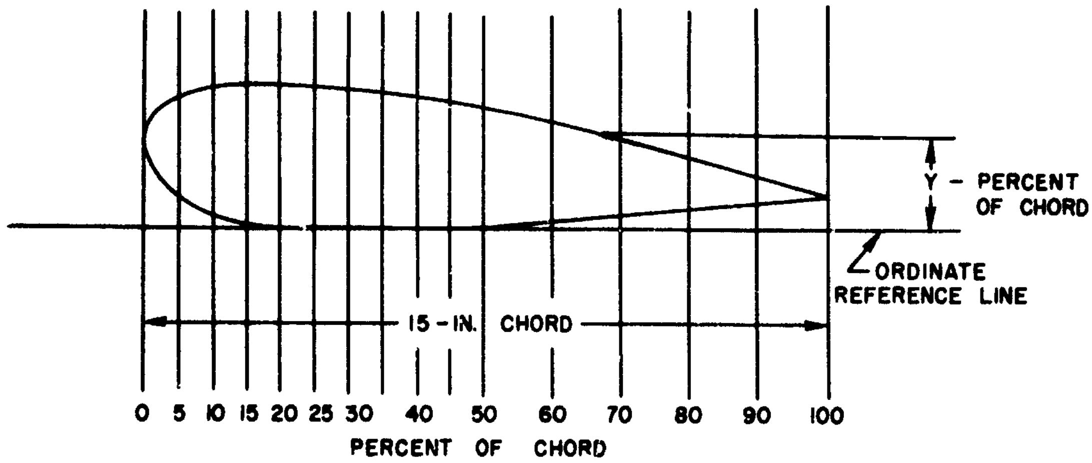

Station Percent of Chord	Short Chord, L_{1SC}, C_{1SC}, E_{1SC} Ordinate, Y	
	Upper	Lower
0.0	13.399	13.399
0.33	15.098	11.199
0.67	15.845	10.286
1.00	16.345	9.546
1.33	16.712	8.926
2.00	17.292	7.906
2.67	17.738	7.006
3.33	18.072	6.273
4.00	18.345	5.606
5.33	18.785	4.446
6.67	19.111	3.520
8.00	19.331	2.780
10.67	19.638	1.620
13.33	19.825	0.860
17.33	19.945	0.227
21.33	19.985	0.027
25.00	19.998	0.0

Station Percent of Chord	Short Chord, L_{1SC}, C_{1SC}, E_{1SC} Ordinate, Y	
	Upper	Lower
26.66	20.000	0.0
33.33	19.318	
40.00	18.531	
49.66	17.498	
50.66	16.732	
53.33	16.178	0.053
59.99	14.731	0.713
66.66	13.265	1.413
73.33	11.745	2.120
79.99	10.199	2.813
86.66	8.566	3.506
93.32	6.813	4.200
96.66	5.913	4.553
100.00	5.013	5.013
	A_e/A_p = 1.1	
	*TER = 0.113%	

*TER = Trailing Edge Radius

HSD SHROUDED PROPELLER TEST

MODEL DIMENSIONAL DATA

INLET AND EXIT GUIDE VANE ORDINATES

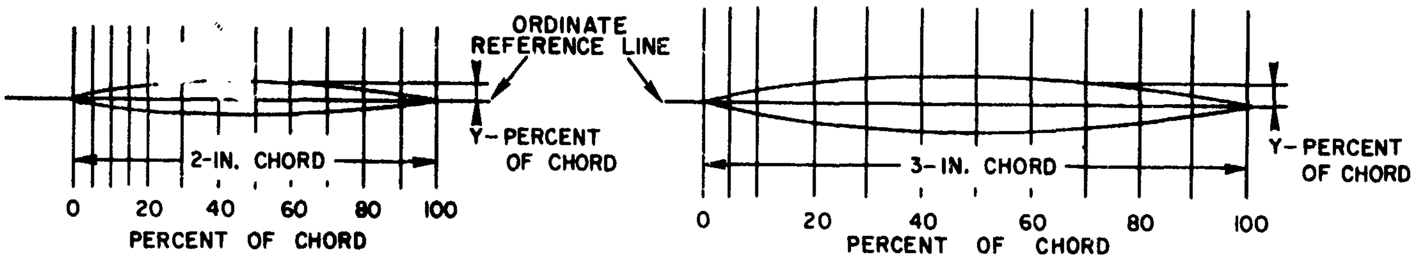

Station Percent of Chord	Inlet Vane, I Ordinate, Y Upper & Lower
0	0.0
1.25	1.050
2.5	1.500
5.0	2.100
7.5	2.500
10	2.900
15	3.450
20	3.900
30	4.500
40	4.850
50	5.000
60	4.850
70	4.400
80	3.500
90	2.100
95	1.150
100	0.100
	*LER = 0.55%

Thickness ratio = 10% chord
*LER = leading edge radius, % chord

Station Percent of Chord	Exit Vane, V Ordinate, Y Upper & Lower
0.0	0.0
1.25	1.067
2.5	1.500
5.0	2.100
7.5	2.533
10	2.867
15	3.433
20	3.867
30	4.500
40	4.867
50	5.000
60	4.867
70	4.400
80	3.500
90	2.100
95	1.167
100	1.000
	*LER = 0.533%

Thickness ratio = 10% chord
*LER = leading edge radius, % chord

HSD SHROUDED PROPELLER TEST

MODEL DIMENSIONAL DATA

SPINNER ORDINATES

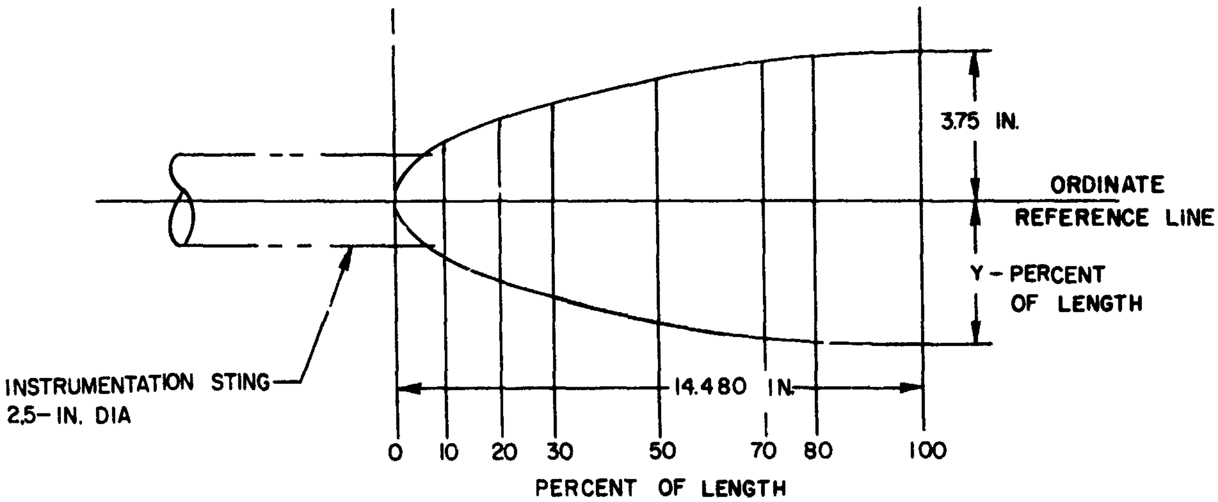

Station Percent of Length	Spinner Ordinate, Y Upper and Lower
0	0.0
1	2.69
2	3.81
3	4.74
4	5.56
5	6.31
10	9.36
15	11.73
20	13.65
25	15.32
30	16.81
35	18.15
40	19.36
45	20.45
50	21.42
60	23.08
70	24.33
80	25.21
90	25.74
100	25.90

HSD SHROUDED PROPELLER TEST

MODEL DIMENSIONAL DATA

4-WAY NARROW TIP BLADE GEOMETRY
SK 57142
DESIGN $C_L = 0.4$

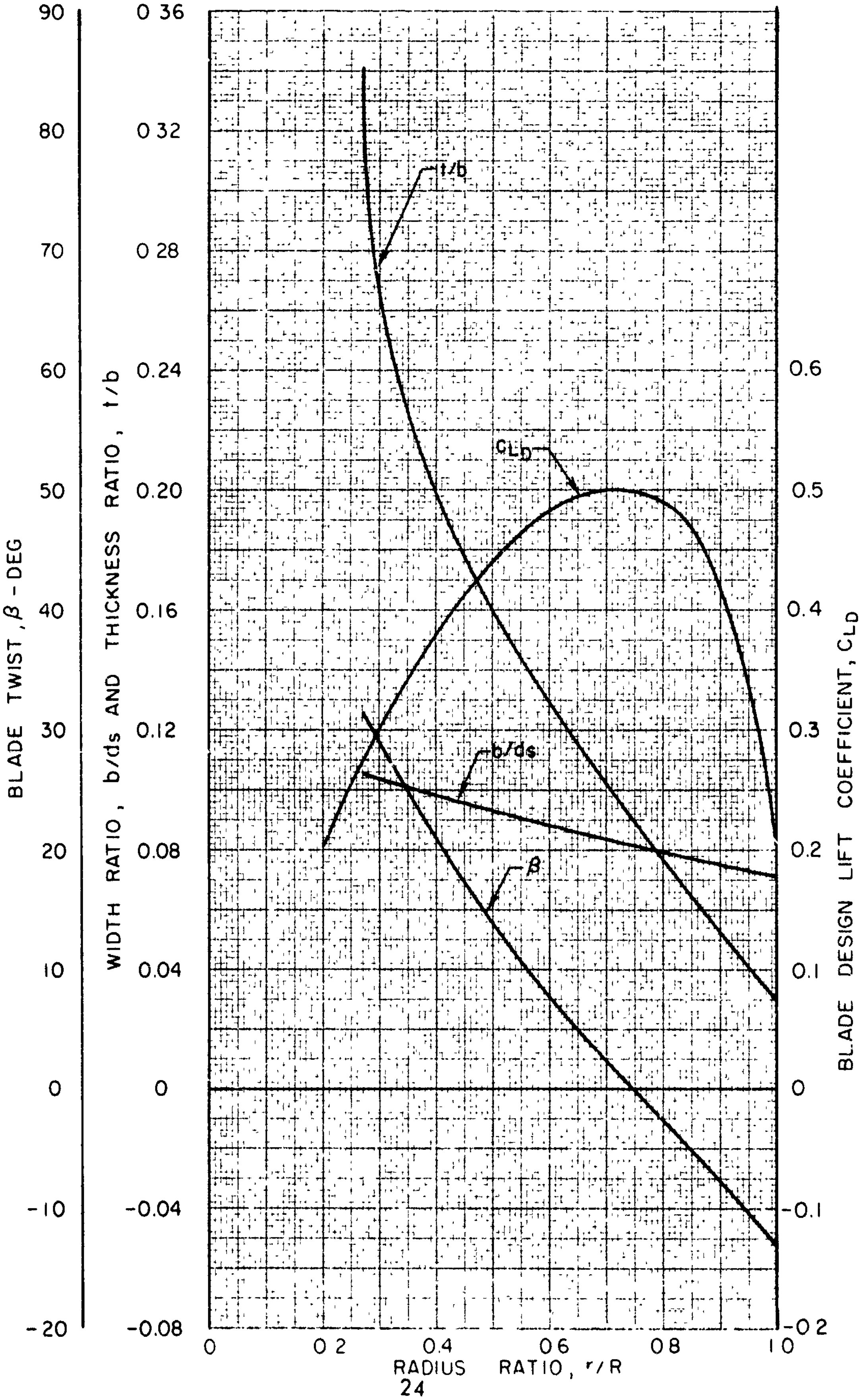

HSD SHROUDED PROPELLER TEST

MODEL DIMENSIONAL DATA

3-WAY RECTANGULAR BLADE GEOMETRY
SK 57143
DESIGN $C_L = 0.4$

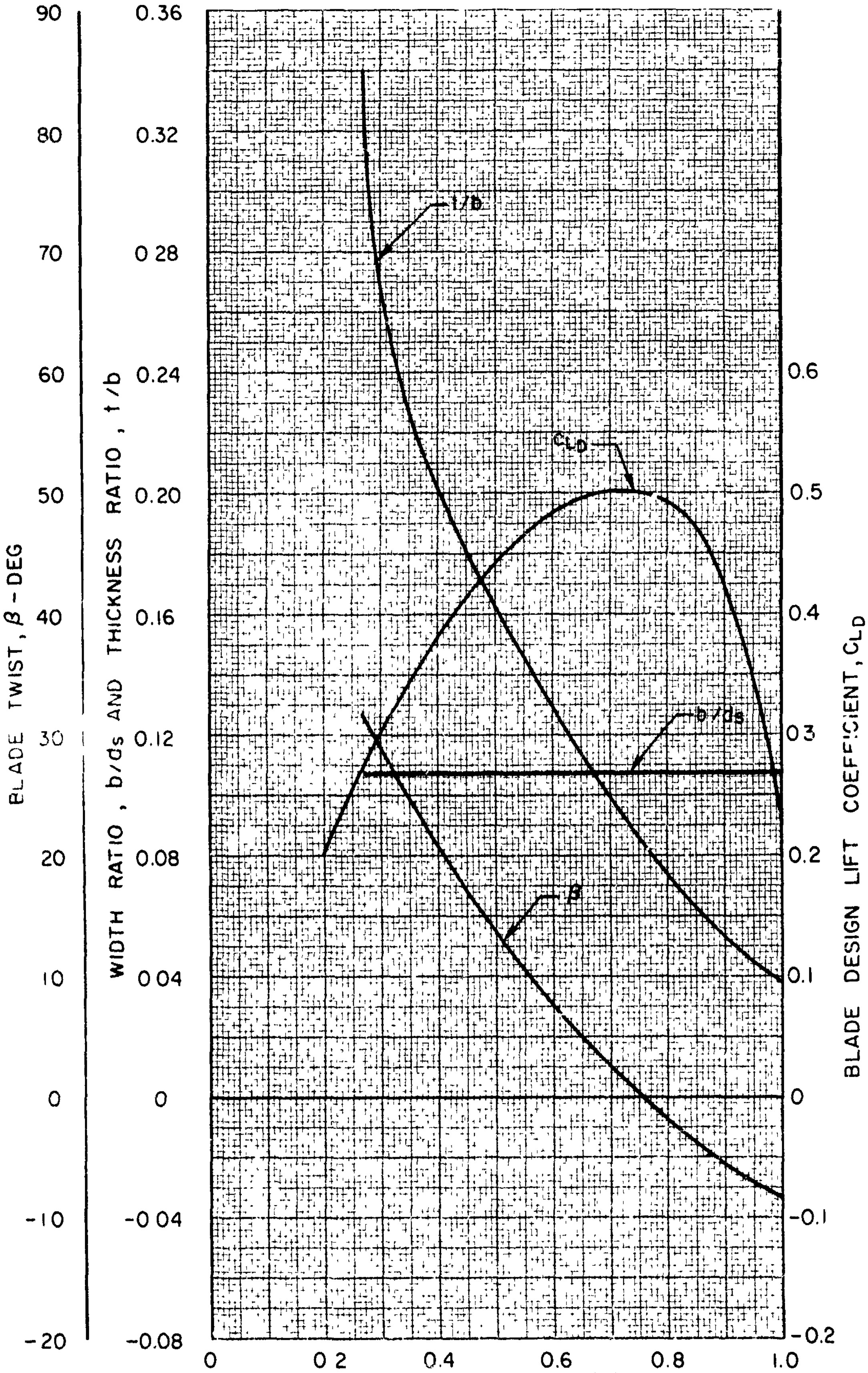

HSD SHROUDED PROPELLER TEST

MODEL DIMENSIONAL DATA

3-WAY WIDE TIP BLADE GEOMETRY
SK 57144
DESIGN $C_L = 0.4$

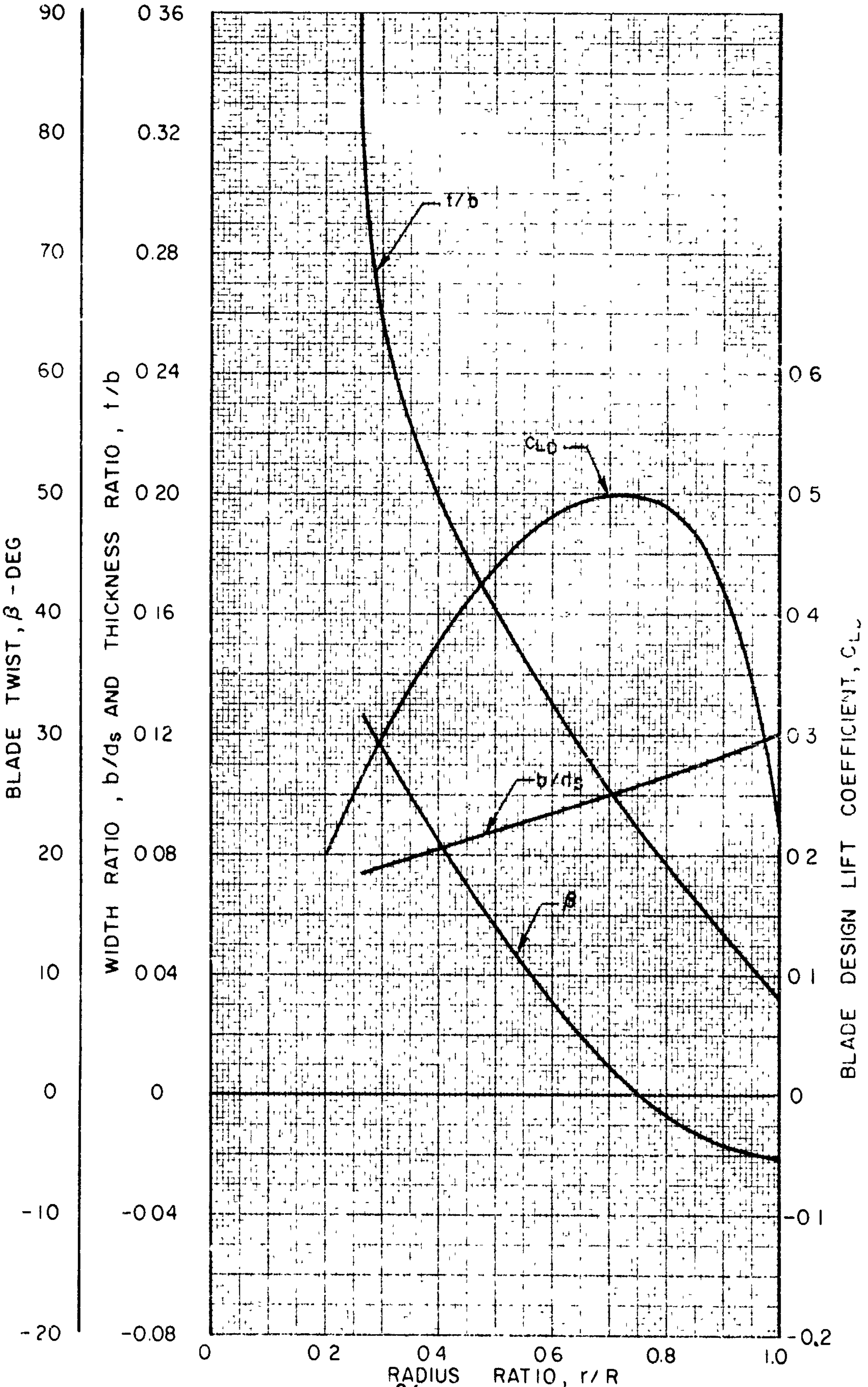

HSD SHROUDED PROPELLER TEST

MODEL DIMENSIONAL DATA

3-WAY NARROW TIP BLADE GEOMETRY
SK 57145
DESIGN C_L = 0 4

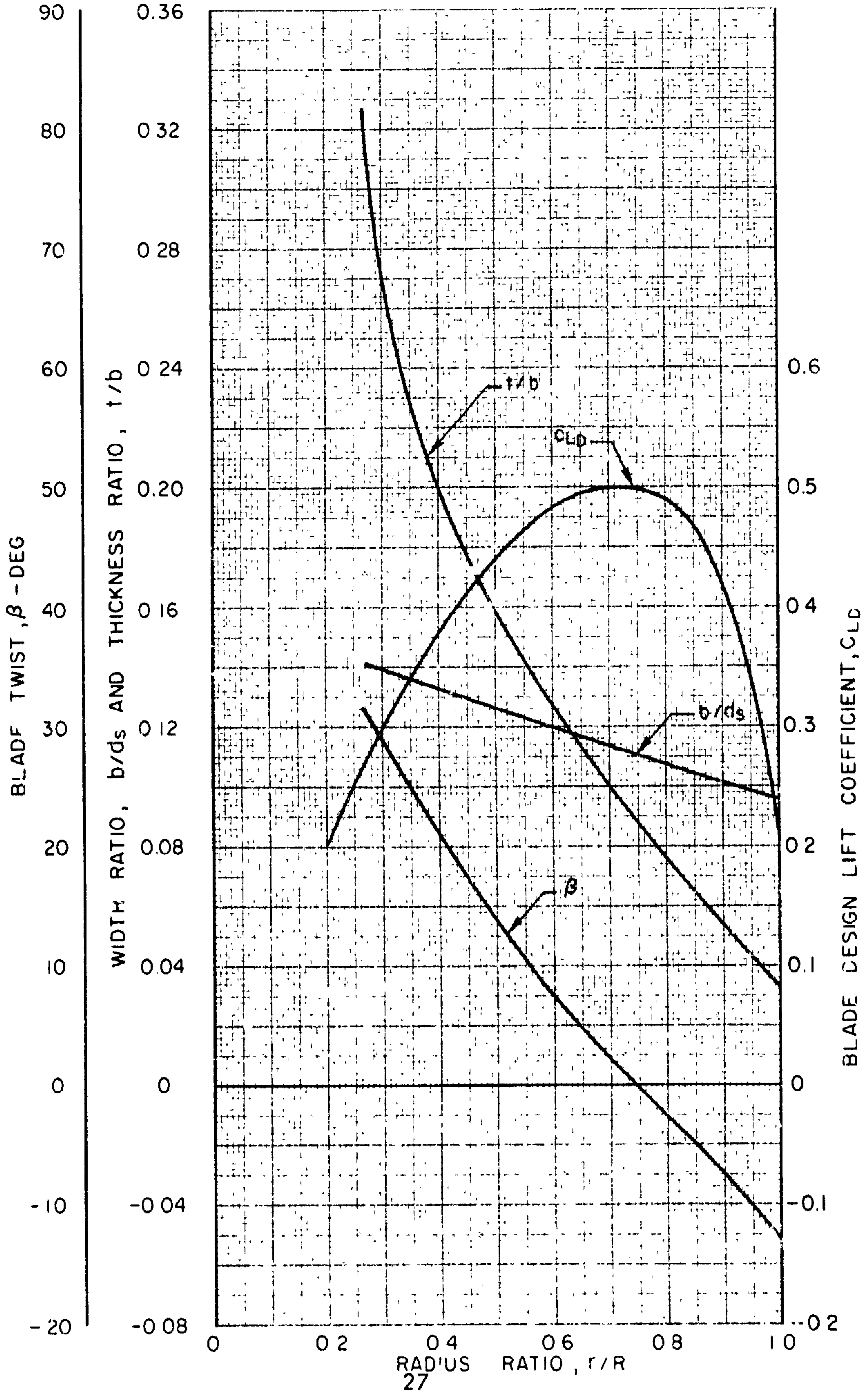

APPENDIX II

HSD SHROUDED PROPELLER TEST

Pressure Sensing Instrumentation and Traversing Probe Calibration

This appendix describes the pressure sensing instrumentation used and presents a relationship for the complete solid blockage correction to pressure coefficient values in Table IX. As shown in Fig. II-1, the instrumentation consisted of either one or two inlet pitot-static rakes, an exit total pressure rake, shroud surface static pressure orifices at two azimuth angles, a traversing probe applicable to two axial stations and two transient pressure transducers. Except for the transient data, pressures sensed by these devices were converted to electrical signals with transducers and recorded on magnetic tape with a high-speed data acquisition system in the tunnel control room. Pressures sensed by the transient pressure transducer were recorded on Visicorder paper and transmitted to HSD during the test period; these results were retained by Hamilton and have not been incorporated in this report. In addition to the magnetic tape record, a photographic record of the pressures as displayed on manometer boards was obtained. Sketches of an inlet pitot-static rake, the exit total pressure rake and the traversing probe are presented in Figs. II-2, II-3, and II-4, respectively. Figures II-5 and II-6 present the results of the traversing probe calibration conducted immediately prior to the 8-ft section test and used in the final reduction of traversing probe data obtained in the 8- and 18-ft test sections.

The traversing probe calibration was performed to extend the scope of the original calibration provided by the probe manufacturer to higher speeds and pitch angles. The results of the UARL calibration did not agree with the original calibration provided with the probe and therefore the probe was returned to the manufacturer for further calibration. A lack of repeatability between the original and second calibration performed by the manufacturer, with respect to the parameter $\bar{K}$, weakened both UARL's and HSD's confidence in these calibration data. It was mutually agreed between UARL and HSD to utilize the UARL calibration data for reduction of the traversing probe data obtained during the test period in the 8-ft test section; and in addition, to extrapolate these data for reduction of the previously obtained traversing probe data obtained during the test period in the 18-ft test section. These calibration data were used in conjunction with Eqs. 31 through 38 of Appendix VI to define the velocity and angularity of the airflow at the probe station.

The test technique employed with the traversing probe consisted of recording pressures P_1 through P_5 at discrete radial stations at shroud azimuth 166.5 deg

APPENDIX II
(Contd.)

for particular shroud chord locations (T_P and T_{P2}). Radial positioning of the probe was remotely controlled at a console in the tunnel control room which also provided for rotating the probe to balance the pressures P_2 and P_3 shown in Fig. II-4. Nulling of these pressures provided a yaw angle (ZETA) in numerical display through an electro-mechanical system integral in the control console. With a discrete radial position and yaw angle the parameters M_r and θ_r were determined by Eqs. 31 and 32 of Appendix VI, respectively. With values of M_r and θ_r, pitch angle (THETA) and subsequently parameter $\bar{K}$ were determined from the calibration data presented in Figs. II-5 and II-6, respectively. Linear interpolation was used to determine pitch angle and $\bar{K}$ for values of M_r and θ_r parameter intermediate to the presented curves. The parameter $\bar{K}$ was used to determine a corrected static pressure (Eq. 35) which in turn leads to the determination of Mach number, velocity component and axial velocity by Eqs. 36 through 38, respectively.

Pressure coefficient values presented in Table IX were obtained in accordance with the data reduction equations presented in Appendix VI and as such, are not based on a test section static pressure corrected for solid blockage. The effect of this correction can be expressed as an additive pressure coefficient of 0.06. Pressure coefficient with dynamic pressure corrected for solid blockage and with static pressure uncorrected and corrected for solid blockage may be expressed as:

$$C_P = \frac{\frac{P_\ell}{H_o} - \frac{P_\infty}{H_o}}{q/H_o}$$ (dynamic pressure corrected for solid blockage)

$$C_{P_C} = \frac{\frac{P_\ell}{H_o} - \frac{P_{\infty C}}{H_o}}{q/H_o}$$ (dynamic and test section static pressure corrected for solid blockage)

The increment in pressure coefficient may be presented as:

$$\Delta C_P = C_{P_C} - C_P = \frac{\frac{P_\infty}{H_o} - \frac{P_{\infty C}}{H_o}}{q/H_o}$$

APPENDIX II
(Contd.)

Expressing the ratios of static-to-stagnation pressure as functions of Mach number we have:

$$\Delta C_P = \frac{P_\infty}{q}\left[1 - \left(\frac{1 + .2M^2}{1 + .2M_C^2}\right)^{3.5}\right]$$

and

$$C_{P_C} = C_P + \Delta C_P = C_P + \frac{P_\infty}{q}\left[1 - \left(\frac{1 + .2M^2}{1 + .2M_C^2}\right)^{3.5}\right]$$

Pressure coefficient increments (ΔC_P) for the Mach number range traversed in the 8-ft test section phase are:

Mach number, M	0.3	0.4	0.5	0.6
C_P	0.0626	0.0601	0.0584	0.0567

Note that the corrected pressure coefficient described above is based on solid but not wake blockage in the static pressure and dynamic pressure terms. Wake blockage was not applied since dependent thrust data were not obtained during the pressure testing. This effect would however reduce the above factors within the ±0.06 value indicated for repeatability in the text.

A static pressure identification system for the tabulated pressure coefficients presented in Table IX is presented in Table II-7.

HSD SHROUDED PROPELLER TEST
PRESSURE SENSING INSTRUMENTATION ARRANGEMENT

VIEW LOOKING DOWNSTREAM

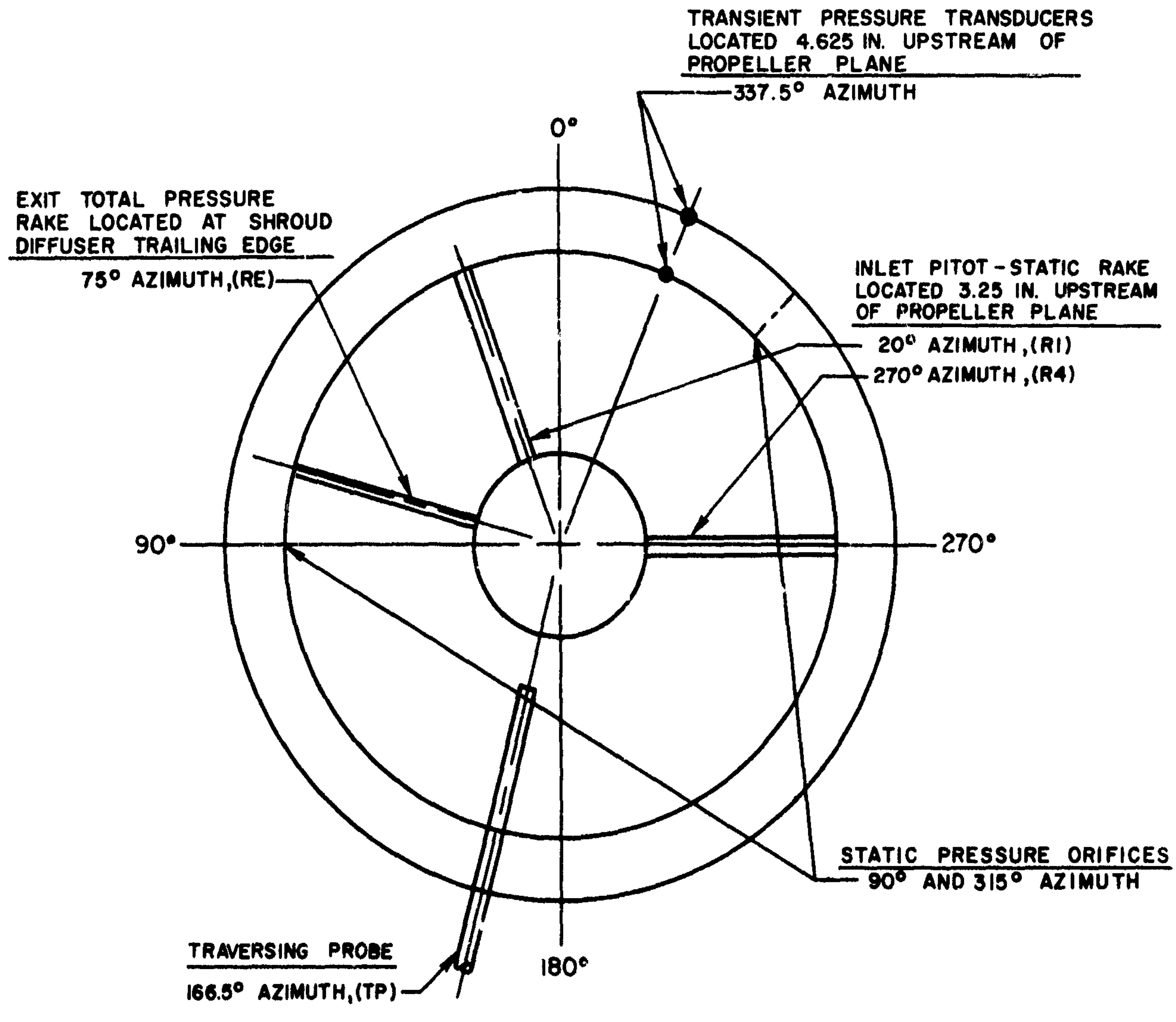

HSD SHROUDED PROPELLER TEST

INLET RAKE ORIFICE LOCATIONS AND DESIGNATIONS

NOTE: DIMENSIONS SHOWN IN INCHES

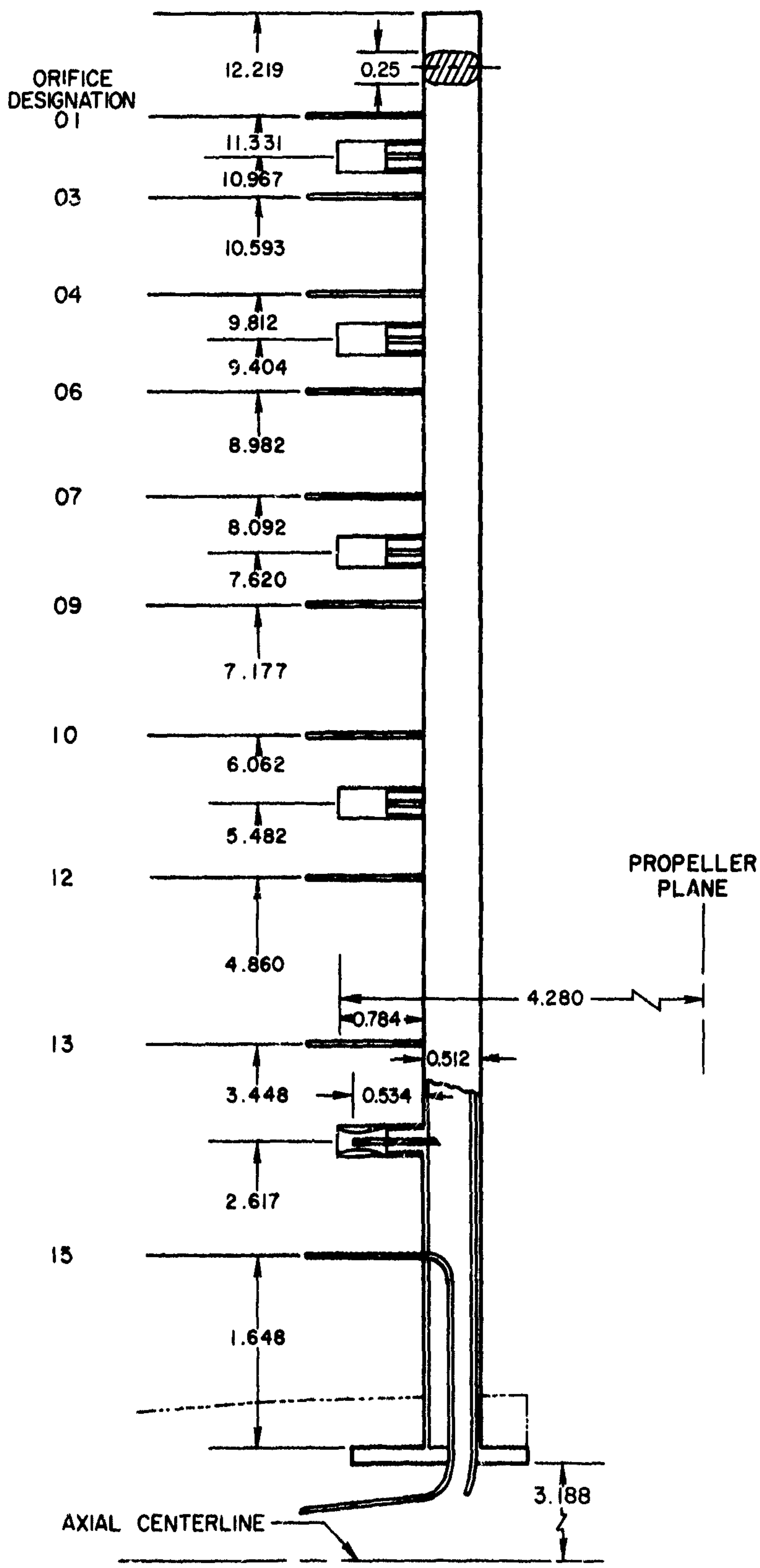

HSD SHROUDED PROPELLER TEST

EXIT RAKE ORIFICE LOCATIONS AND DESIGNATIONS

NOTE: DIMENSIONS SHOWN IN INCHES

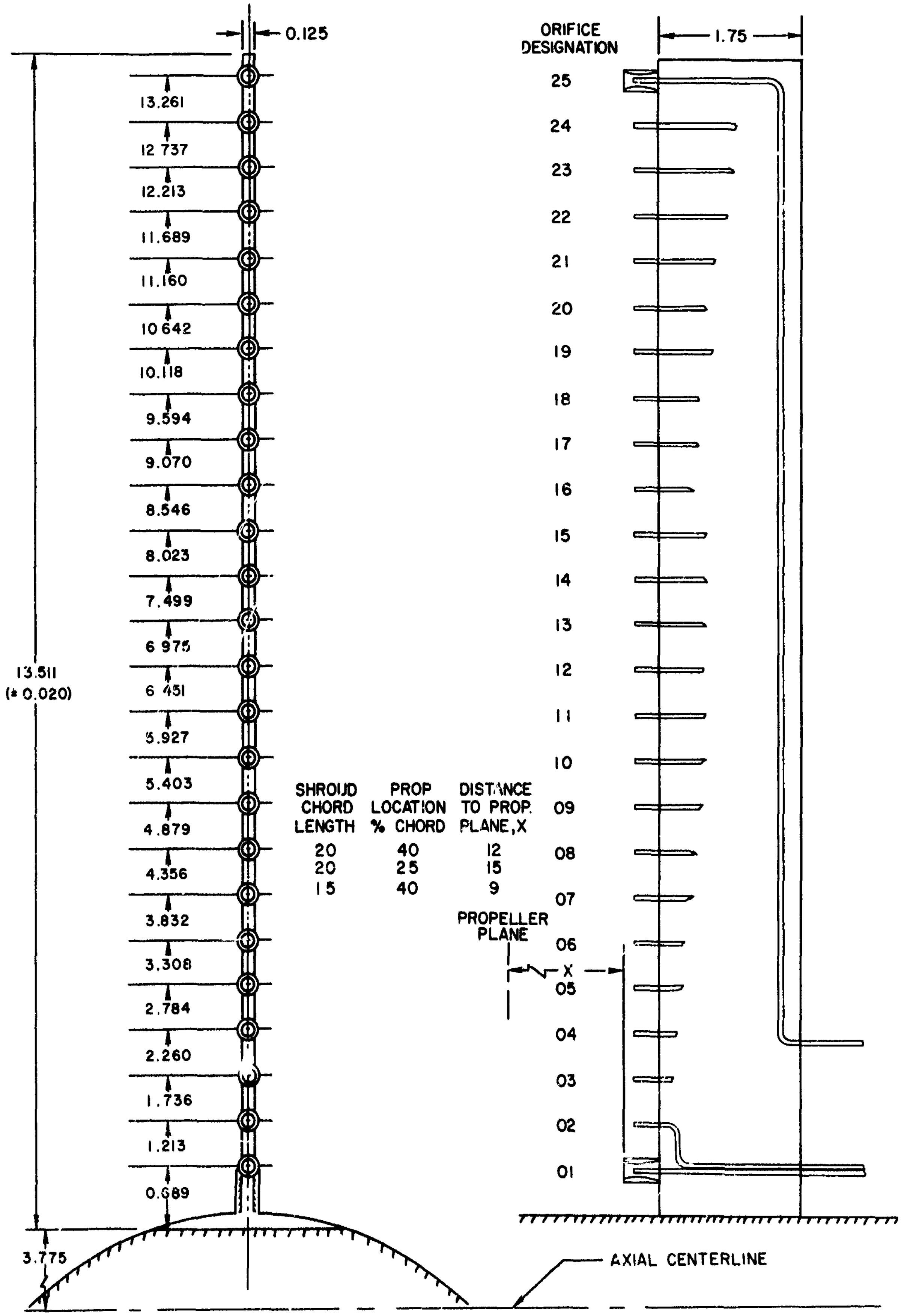

HSD SHROUDED PROPELLER TEST

TRAVERSING PROBE INSTALLATION

NOTE: DIMENSIONS SHOWN IN INCHES
POSITIVE ANGLES SHOWN

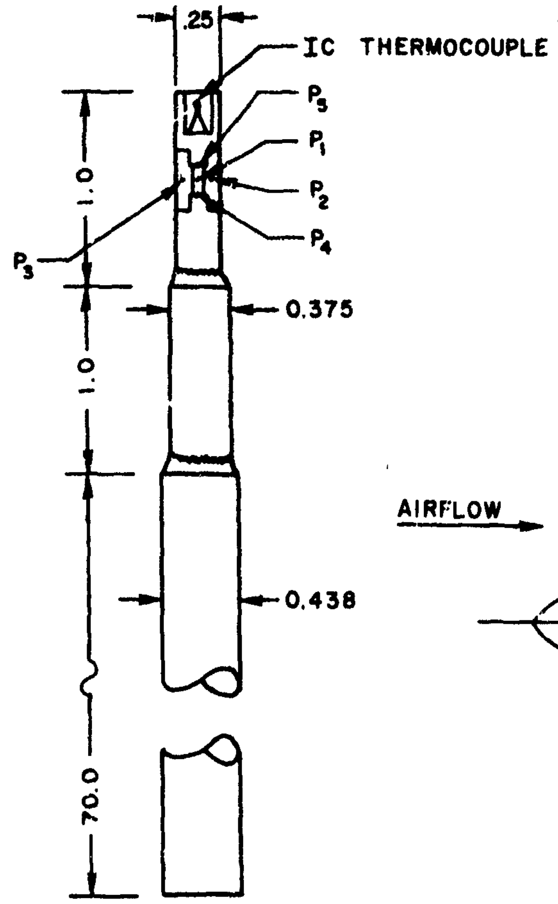

SHROUD CHORD LENGTH	PROP LOCATION % CHORD	DISTANCE TO PROP PLANE, X
20	40	12
20	25	15
15	40	9

TOP VIEW

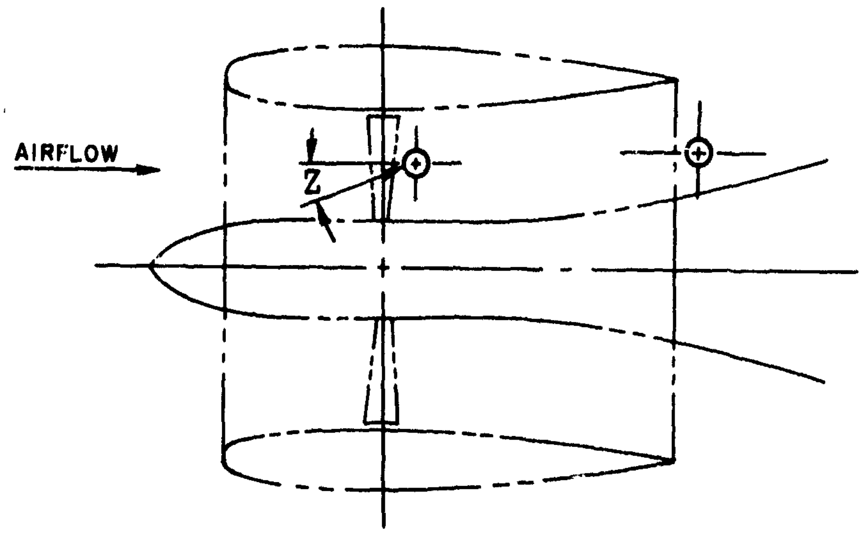

VIEW FROM UPSTREAM

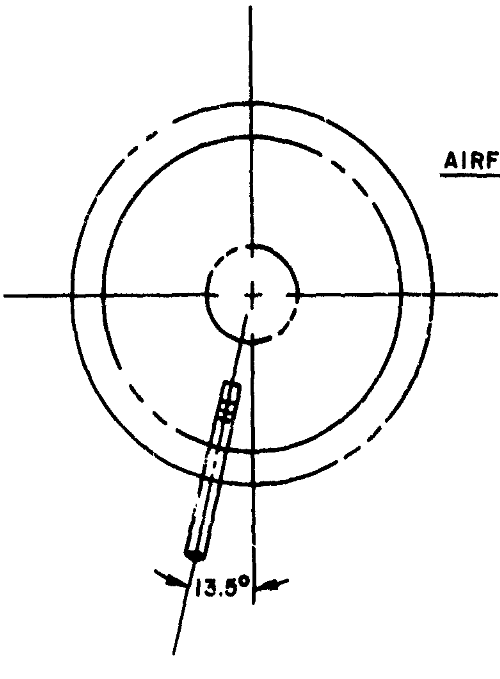

SIDE VIEW

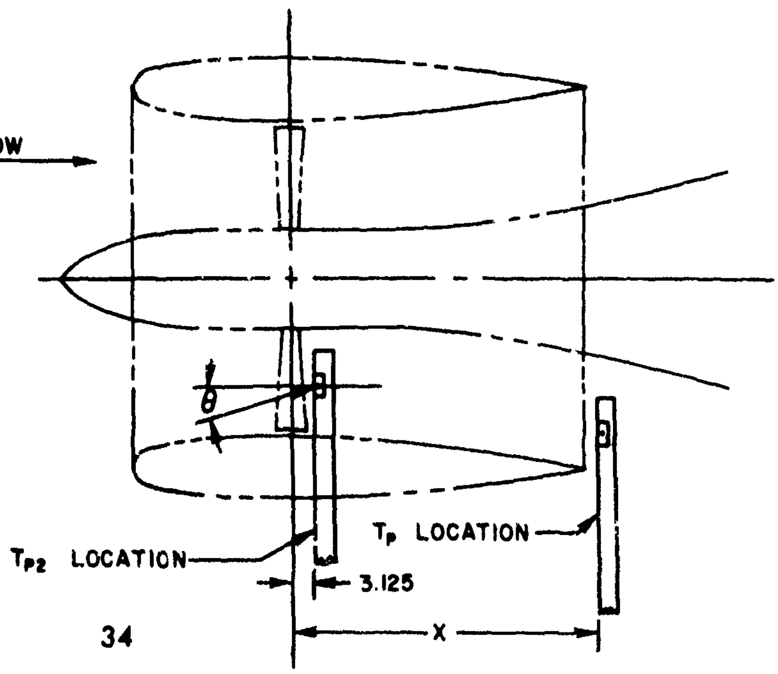

HSD SHROUDED PROPELLER TEST

TRAVERSING PROBE CALIBRATION

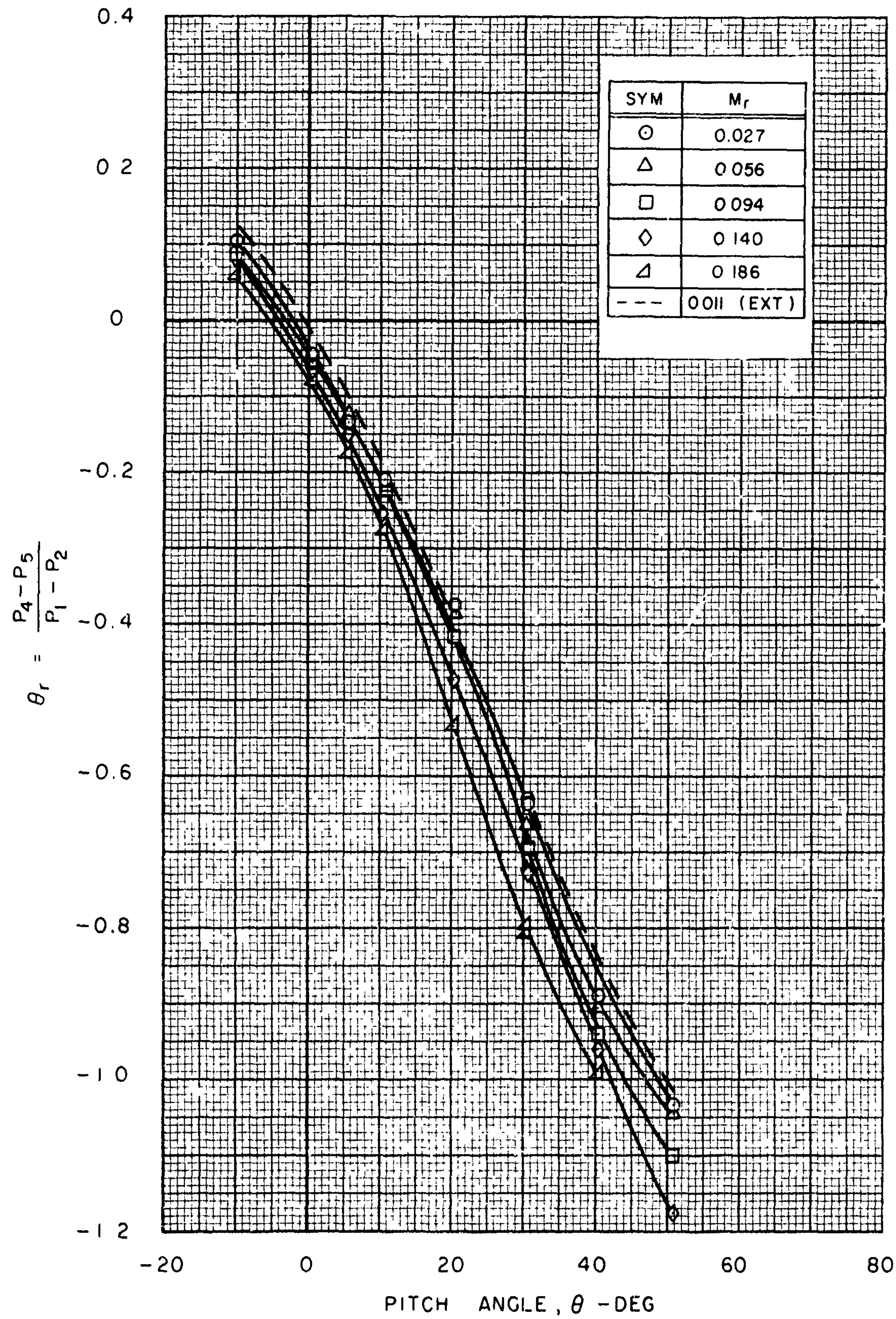

HSD SHROUDED PROPELLER TEST

TRAVERSING PROBE CALIBRATION

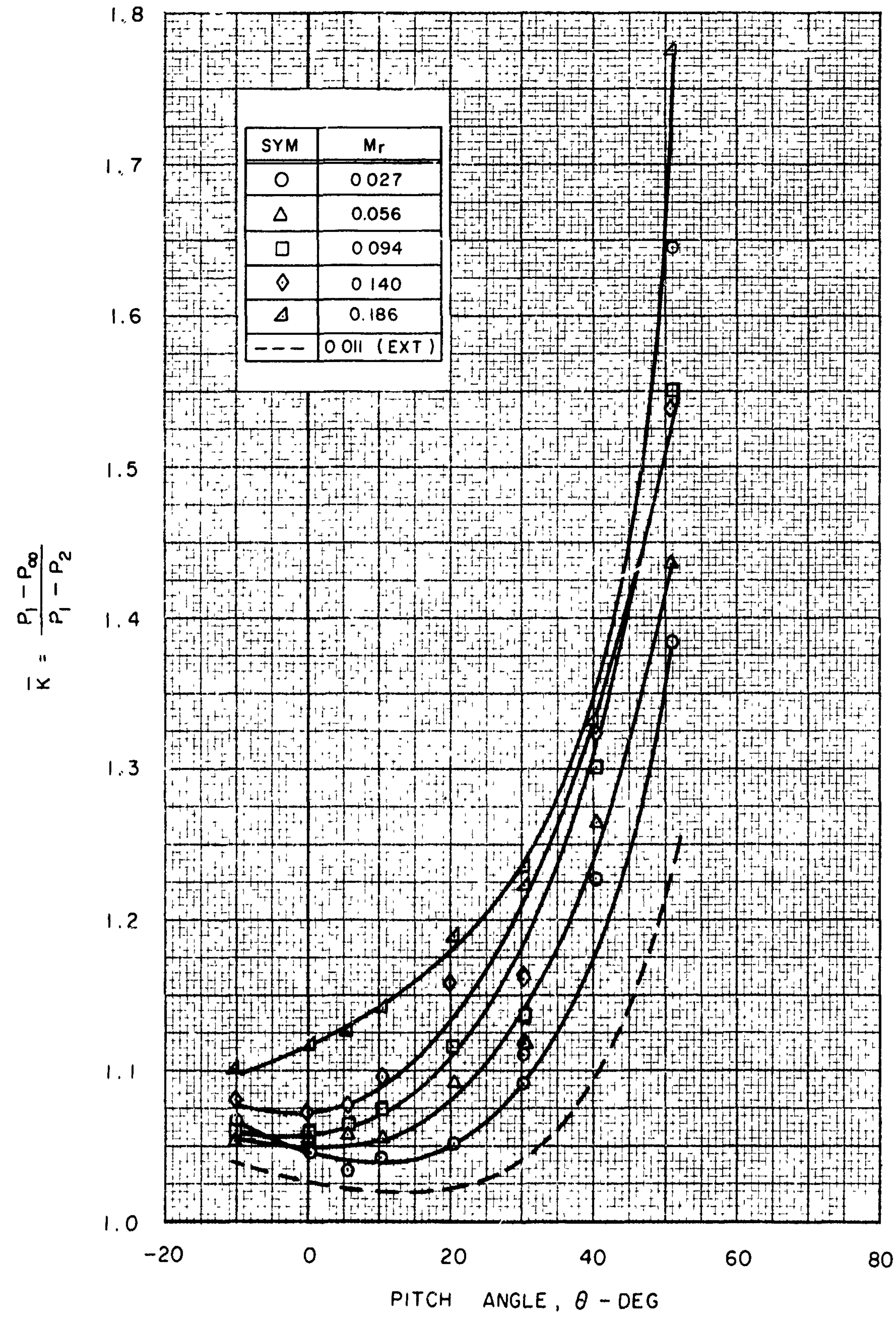

HSD SHROUDED PROPELLER TEST

Surface Pressure Orifice Identification System for Table IX

I - Symbols

S - Shroud

B - Inside Surface

LEO - Leading Edge

T - Outside

1 - 90 deg azimuth

2 - 315 deg azimuth

II - Orifice Legend

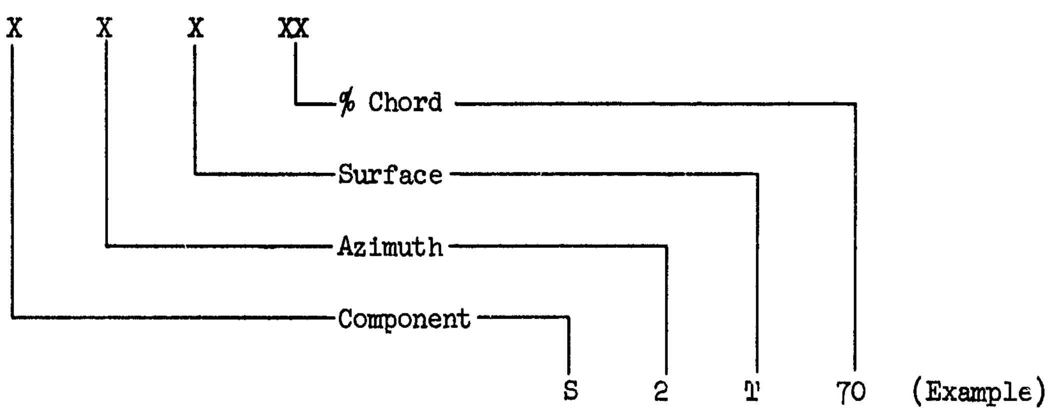

APPENDIX III

HSD SHROUDED PROPELLER TEST

Tunnel Blockage Calibrations

Various tunnel calibrations were performed in order to establish a solid and wake blockage correction for the dynamometer-shroud model in both 18- and 8-ft test sections. The initial efforts associated with the 18-ft test section operation indicated that the dynamometer and shroud blockage was negligible. Tunnel speed was then set from a propeller-plane wall pressure which accounts for the remaining wake blockage thrust effect. Subsequent efforts for the 8-ft test section indicated significant blockage due to the shroud (but not the dynamometer). A simple solid blockage correction was found to agree with measured speed increments due to the shroud and thus this correction and a comparable correction for the propeller thrust effect were used in the 8-ft test section. These calibrations are described below.

In the 18-ft test section the average static pressure in the propeller plane at the two vertical walls of the test section was compared with an average of four static pressures on the 45 degree sides of the octagonal test section (speed ring) located 167.56 inches upstream of the propeller plane. This comparison was made with the propeller test rig installed in the test section with and without the shroud present. As shown in Fig. III-1 the static pressure at the tunnel walls in the propeller plane does not differ from the upstream value due to the addition of the dynamometer with or without the shroud. Blockage effects of the dynamometer and shroud in the 18-ft test section were thus considered negligible and tunnel speeds were set in the propeller plane at the tunnel walls to account for the remaining thrust effect on wake blockage.

In the 8-ft test section the propeller is close to the beginning of the test section and thus it was not possible to establish an upstream pressure reference which was equal to the test section static pressure without being influenced by the model. A reference pressure in the test section bellmouth was therefore selected (speed bump, 81.4 inches upstream of the propeller; average of three pressures). The speed bump (Fig. 7) data is plotted in Fig. III-2 against data from orifices in the propeller plane at the top wall of the test section for the clear test section and for the dynamometer with and without the shroud. As indicated in Fig. III-2 an increase in speed of

APPENDIX III
(Contd.)

approximately 4 percent is caused by the presence of the dynamometer and shroud (primarily from shroud). Since the dynamometer itself does not significantly increase the propeller plane wall pressure it appears that its blockage interference is negligible. The shroud, however, increases the wall speed about 4% and approximately half of this increment (Ref. 5) may be applicable at the center of the tunnel as a blockage interference correction. Since it is difficult to accurately determine the tunnel centerline correction from the measured wall data for a realistic model, a simpler and more conventional solid blockage correction was calculated at a reasonable 3.2% as shown in Appendix VI. Tunnel speed in the 8-ft test section was therefore set from the upstream speed bump value calibrated to give clear tunnel speed. The clear tunnel speed was then increased by 3.2% to account for shroud solid blockage and by a varying amount dependent on propeller thrust to account for the thrust effect (App. VI and Ref. 4).

HSD SHROUDED PROPELLER TEST

BLOCKAGE EFFECT OF PROPELLER TEST RIG WITH AND WITHOUT SHROUD 18-FT TEST SECTION

SYM	RUN NO	MACH NO	CONFIGURATION	$\theta_{3/4}$
○	1	VARY	PTR W/O SHROUD AND BLADES	—
△	2,3	↓	$L_1C_1F_3B_4R_1$	↓

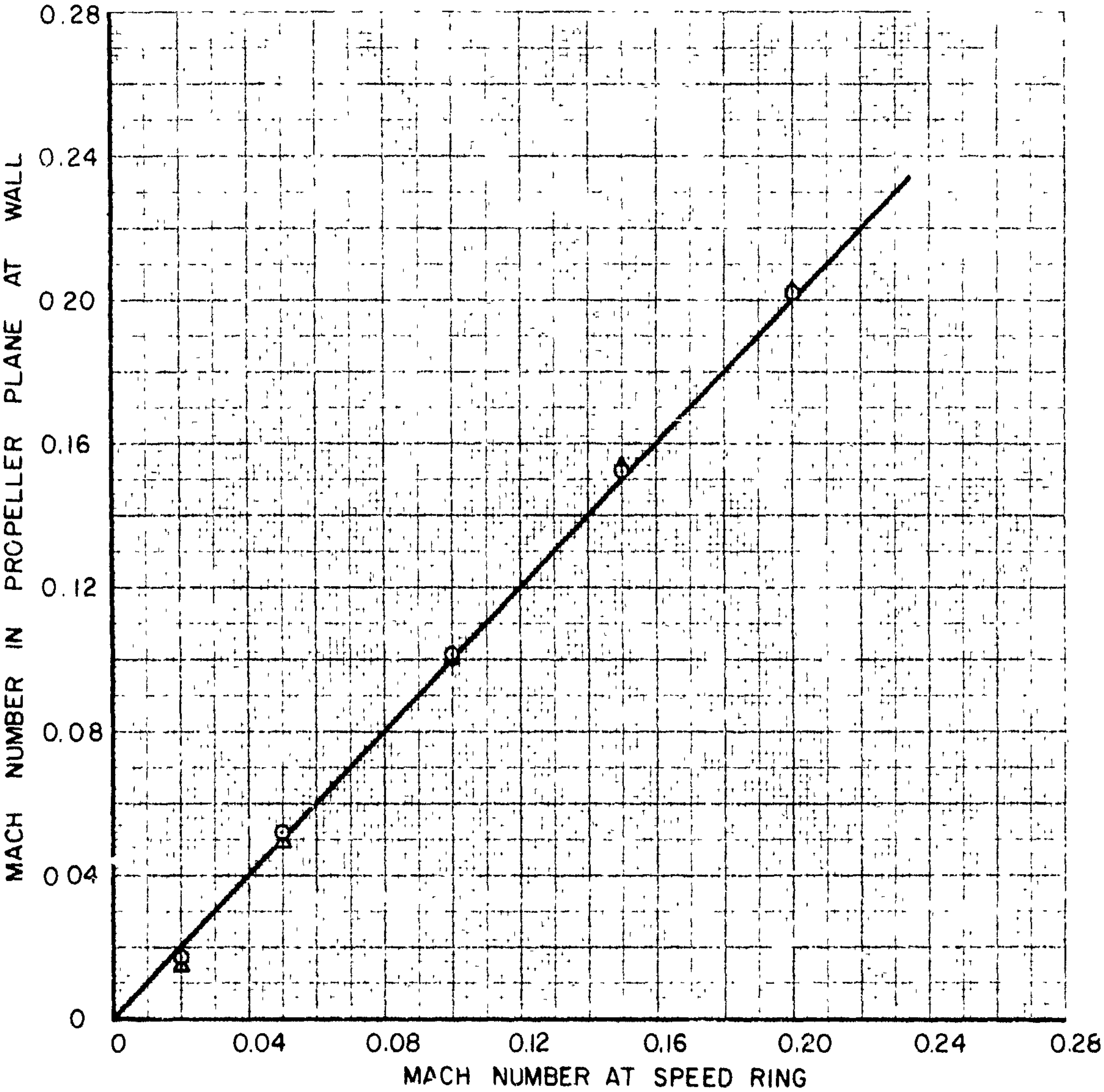

HSD SHROUDED PROPELLER TEST

BLOCKAGE EFFECT OF PROPELLER TEST RIG WITH AND WITHOUT SHROUD

8 - FT TEST SECTION

SYM	RUN NO.	MACH NO.	CONFIGURATION	$\theta_{3/4}$
⊙	413	VARY	T_{P3} (CLEAR TEST SECTION)	—
△	423	↓	$L_1 C_1 E_3 B_3 R_1$	↓
□	422	↓	PTR W/O SHROUD & BLADES	↓

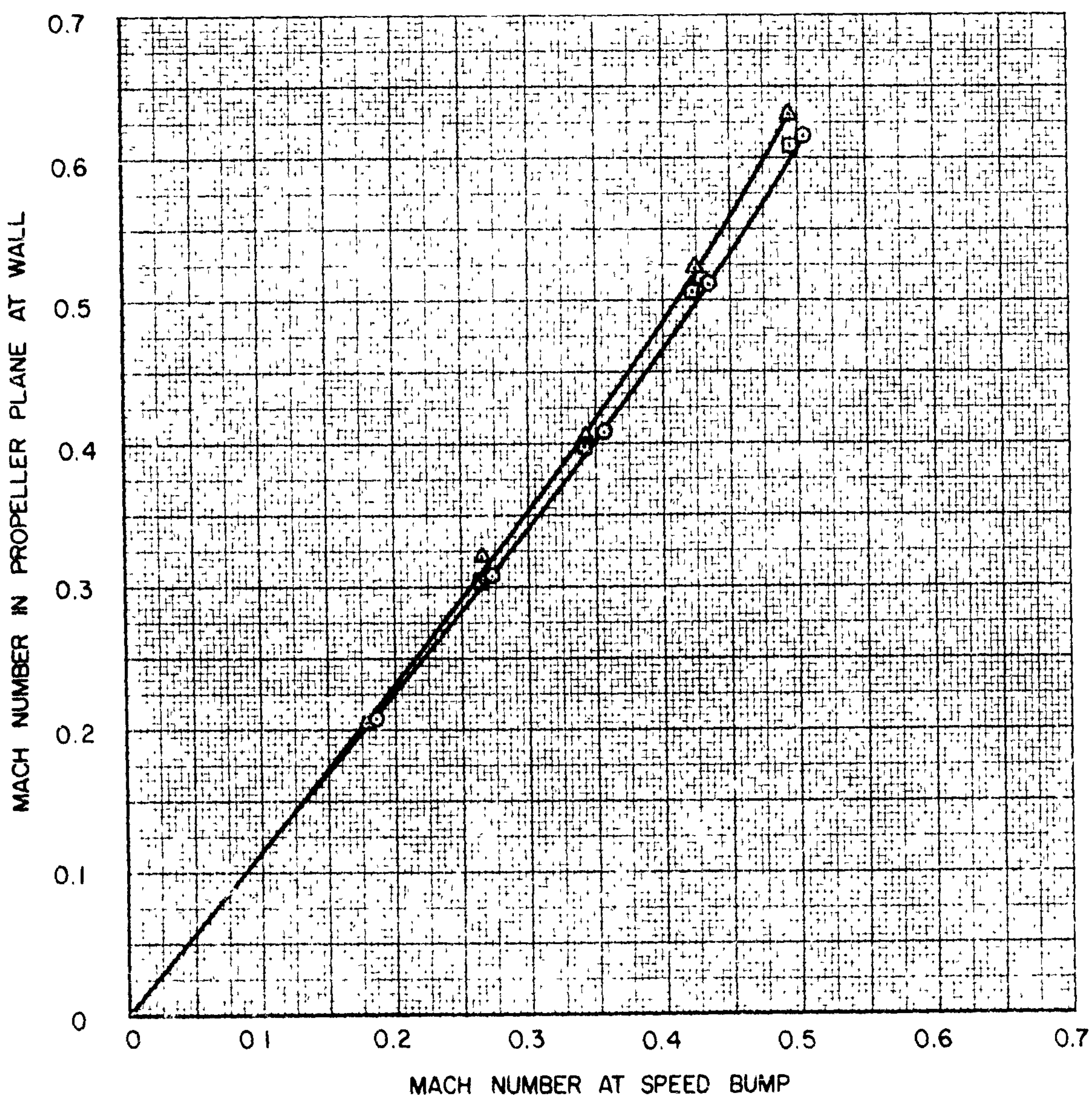

APPENDIX IV

HSD SHROUDED PROPELLER TEST

Propeller Hub Skin Friction Tare

The forces measured by the dynamometer's thrust balance represent a summation of the propeller thrust, a hub-skin friction drag and a thrust force derived from the pressure differential across the hub. The pressure differential thrust is determined from direct measurement of the pressures across the hub at each data point. The hub skin friction drag tare was determined from a calibration made without blades through a Mach number range at zero hub rotational speed. The gross thrust measured during this calibration is equal to the independently measured pressure thrust plus the skin friction drag since the propeller thrust is equal to zero. Hub skin friction tare values measured in this manner are shown in Fig. IV-1. A linear function of local Mach number was fitted to the data as shown in this plot to simplify computer application of the data. Local Mach number was selected, rather than tunnel speed, to account for the effect due to the shroud presence. It should be noted that these results are applicable only with the finite spinner.

HSD SHROUDED PROPELLER TEST

PROPELLER HUB SKIN FRICTION TARE

SYM	RUN NO.	MACH NO.	CONFIGURATION	θ 3/4
⊙	2	VARY	$L_1\ C_1\ E_3\ B_4\ R_1$	—
△	3	↓	↓ ↓ ↓ ↓ ↓	↓
⊡	427	↓	↓ ↓ ↓ B_3 ↓	↓

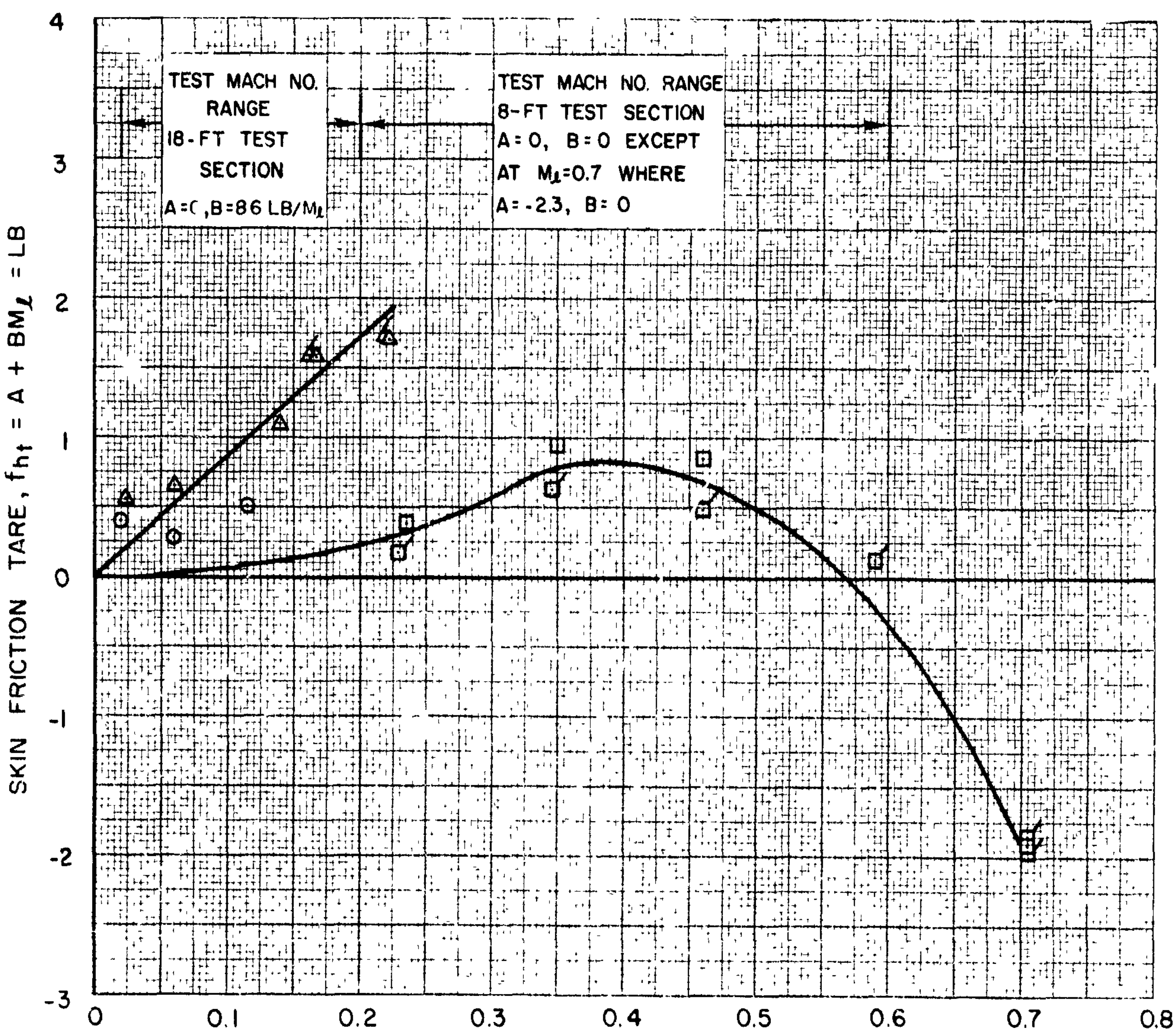

APPENDIX V

HSD SHROUDED PROPELLER TEST

"A"-Frame Tare and Interference and Side Arm Interference Effects

The tare and interference effect of the "A"-frame (Fig. V-1) on chord force and the interference effect of the side arm (Fig. V-2) on normal force are presented in this appendix. The tare and interference effects of the "A"-frame on normal force and the interference on the side arm on chord force were assumed negligible (Ref. 6) and corrections for these effects were not applied to the performance data presented in this report. In the case of the side arm interference on normal force, the effect was small in both test sections (less than 1% of the normal force system capacity of 2,000 lbs) and was not applied to the subject data. Results of the normal force measurements without and with the dummy side arm installed are presented in Fig. V-3.

Unlike the side arm interference, the "A"-frame tare and interference effect on chord force was significant in both test sections. For data obtained in the 18-ft test section the difference in shroud chord force coefficient without and with the single dummy "A"-frame installed (this configuration produces half the effect of the two "A"-frames) was determined. These differences were then doubled (to account for the two "A"-frames) and represented by linear functions of power coefficient (App. VI, Eq. 11). The corrections which were employed in reducing the data were based on four runs made with the basic shroud configuration ($L_1C_1E_1$) and three runs made with the 1.3 exit area ratio ($L_1C_1E_3$) as noted below.

Run Number W/O Image	Run Number W/Image	Mach No.	Shroud Configuration	Correction Applicable to:
18	22	0.02	$L_1C_1E_1$	$L_1C_1E_1$, $L_1C_2E_1$, $L_{1SC}C_{1SC}E_{1SC}$
19	23	0.10		
20	24	0.20		
28	27			
94	99	0.02	$L_1C_1E_3$	$L_1C_1E_3$
95	98	0.10		
96	97	0.20		

For intermediate Mach numbers and for the 1.2 exit area ratio shroud (E_2) the corrections were interpolated from the preceding results. Ten other tare and interference runs were also made with the short chord shroud configuration; but, due to inconsistent results did not contribute to the evaluation of the corrections employed. The following table presents the slope (f) constants for the "A"-frame tare and interference chord force correction in the 18-ft test section (Eq. 11 of Appendix VI). The intercept (e) value was zero through the Mach number range for all configurations tested.

Shroud Configuration	Constant	Mach Number 0.02	0.05	0.10	0.15	0.20
All, unless noted below	f	0.0433	0.0319	0.0237	0.0190	0.0156
$L_1C_1E_2$	↓	0.0529	0.0409	0.0318	0.0265	0.0221
$L_1C_1E_3$	↓	0.0625	0.0496	0.0400	0.0337	0.0285

For the 8-ft test section data, an "A"-frame correction to chord force was obtained based on chord force measurements of the two isolated (no shroud) "A"-frames rather than from the dummy "A"-frame image. This change in technique was made because the previous data obtained with the dummy "A"-frames were somewhat inconsistent; a direct measurement of isolated "A"-frame chord force was thus made to improve the correction. With the measurements of "A"-frame chord force presented in Fig. V-4 and the approach described in Ref. 7, a chord force correction as a function of propeller advance ratio and thrust coefficient was derived as given in Eq. 12 of Appendix VI. The revised correction does not include the "interference" of tare and interference, nor does it account for changes in tare and interference that could be associated with variations in "A"-frame shroud attachment proximities. However, these effects should be small and thus it is possible to reduce the required tare and interference runs to a single data run. In order to check the correction, data without the dummy "A"-frame were corrected for the effect of one "A"-frame by applying one half of the correction noted above. The corrected data were then compared to measured results with the dummy "A"-frame present. This comparison as shown in Fig. V-5 was satisfactory. The following table presents the constant terms in the chord force correction (App. VI, Eq. 12) for the data obtained on the 8-ft test section. For the intermediate Mach numbers the correction constants were obtained from interpolation of the curve presented in Fig. V-5.

Constant	Mach Number 0.3	0.4	0.5	0.6
e	0.00405	0.00390	0.00435	0.00510
f = 2.71e	0.01100	0.01059	0.01182	0.01385

HSD SHROUDED PROPELLER TEST

"A"-FRAME IMAGE SYSTEM

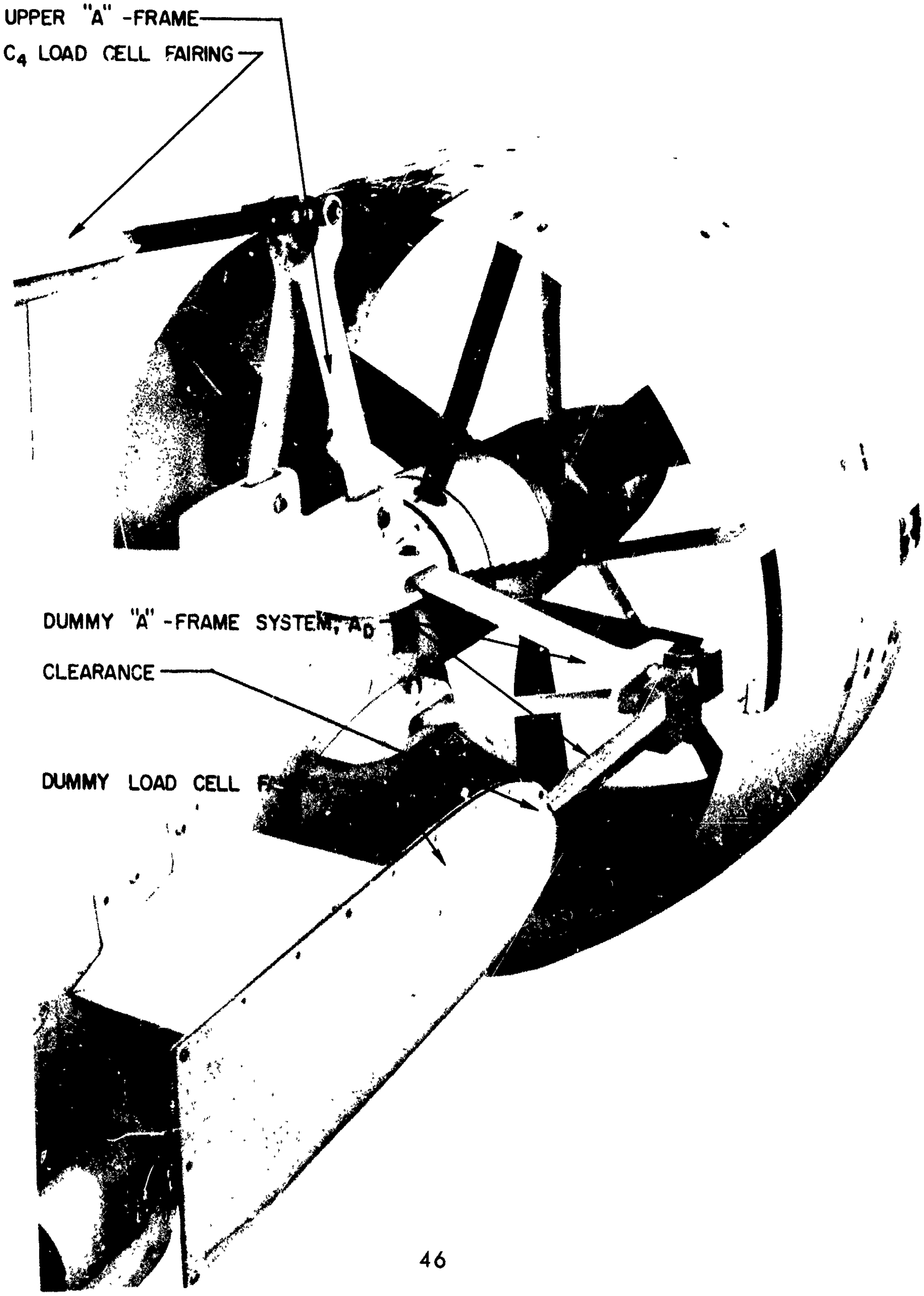

HSD SHROUDED PROPELLER TEST

SIDE ARM IMAGE SYSTEM

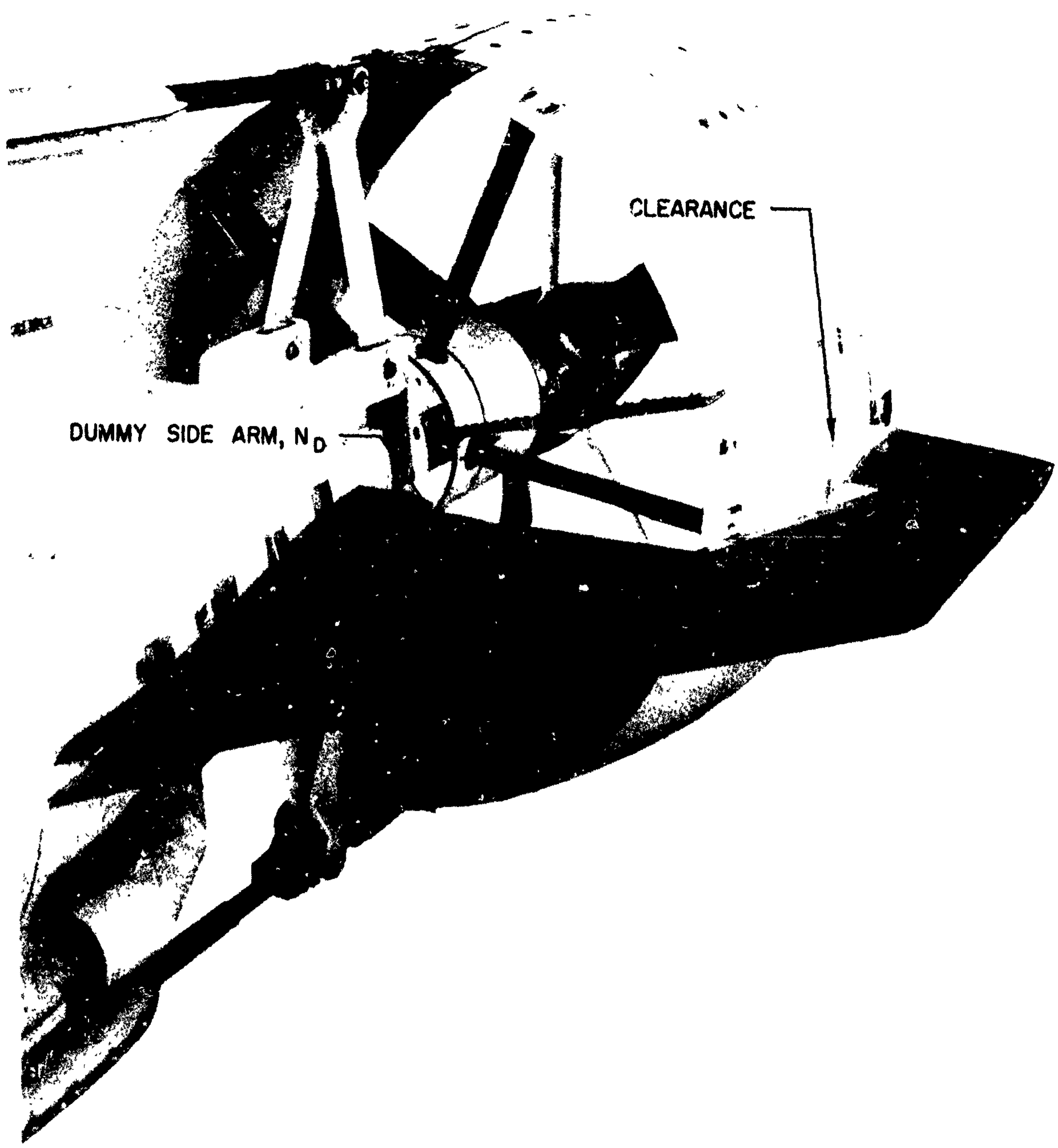

HSD SHROUDED PROPELLER TEST

EFFECT OF SIDE ARM ON NORMAL FORCE COEFFICIENT

SYM	RUN NO	MACH NO.	CONFIGURATION	$\theta_{3/4}$
⊙	18	0.02	$L_1\ C_1\ E_1\ B_3\ P_{WT}\ T_1\ R_1$	30
●	29		N_D	
△	19	0.10		
▲	30		N_D	
⊡	20	0.20		
■	31		N_D	
◇	465	0.30	R_E	
◆	497		N_D	
◿	468			38
◢	498		N_D	
▽	469	0.40		
▼	499		N_D	
D	475			46
◗	495		N_D	
◺	476	0.50		
◣	496		N_D	
◖	481			54
◖	500		N_D	

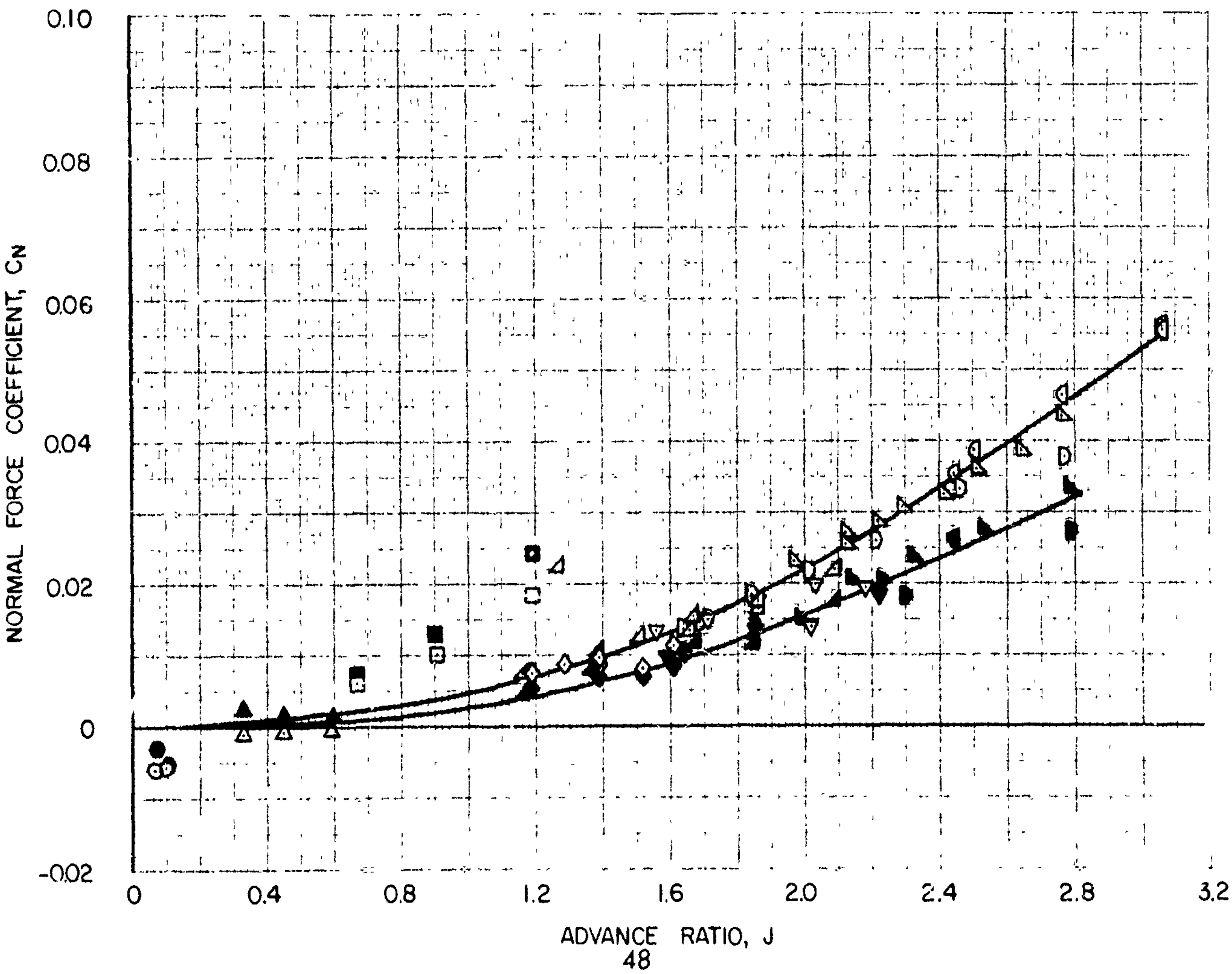

HSD SHROUDED PROPELLER TEST

"A"-FRAME DRAG TARE

SYM	RUN NO.	MACH NO.	CONFIGURATION	$\theta_{3/4}$
⊙	422	VARY	PTR W/O SHROUD & BLADES	—

$$C_{C_t} = \left[e + f\left(\frac{C_T}{J^2}\right)\right] J^2 \qquad \text{(APP VI, EQ 12)}$$

WHERE: $f = 2.71e$

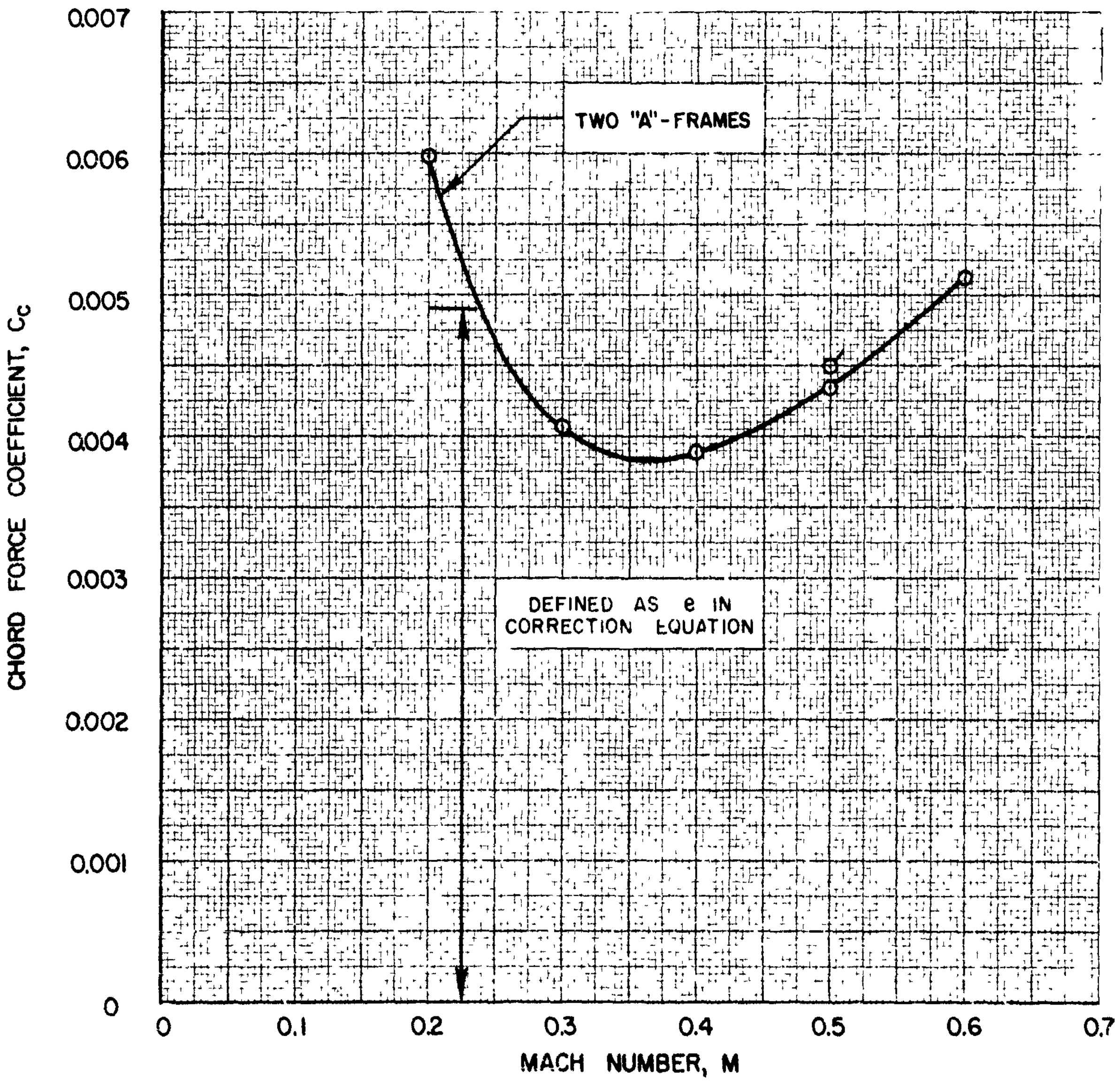

HSD SHROUDED PROPELLER TEST

COMPARISON OF "A"-FRAME TARE CORRECTION WITH TEST DATA

SYM	RUN NO.	MACH NO	CONFIGURATION	$\theta_{3/4}$
●	465	0.3	$L_1 C_1 E_1 B_3 P_{WT} T_1 R_1 R_E$	30.0
○	488	↓	↓ A_D	↓
▲	468	↓	↓	38.0
△	489	↓	↓ A_D	↓
■	475	0 4	↓	46 0
□	491	↓	↓ A_D	↓

NOTE. DATA WITHOUT "A"-FRAME (SHADED SYMBOLS) CORRECTED FOR ONE "A"-FRAME EFFECT (X) AND COMPARED WITH DATA OBTAINED WITH DUMMY "A"-FRAME ADDED (UNSHADED SYMBOLS)

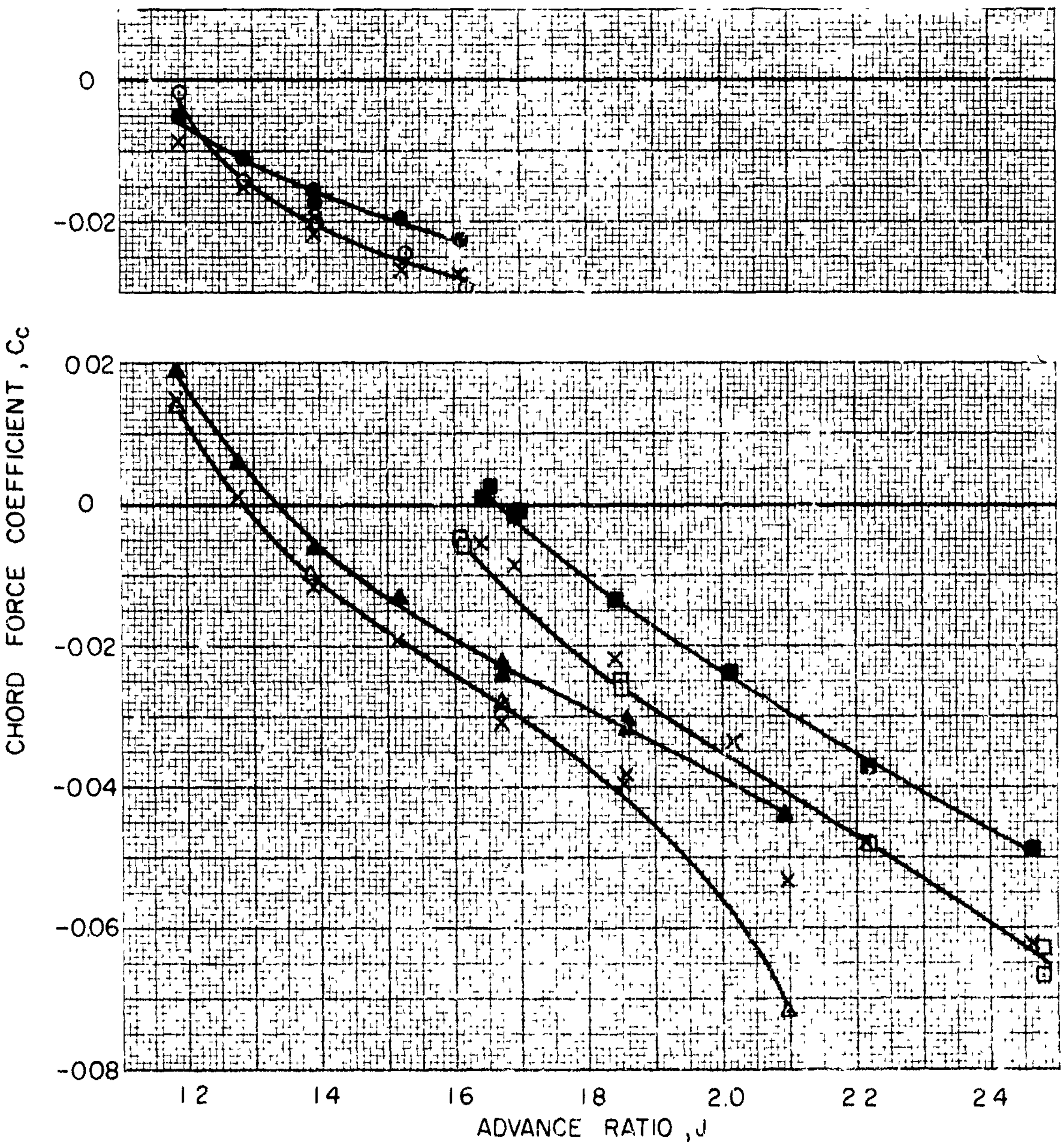

APPENDIX VI

HSD SHROUDED PROPELLER TEST DATA REDUCTION EQUATIONS

I - Preliminary Equations

$$\rho_C = \frac{H_O}{R\,T_{SC}} \tag{1}$$

$$\rho = \rho_0\left(1 + \frac{\gamma - 1}{2}M^2\right)^{-\frac{1}{\gamma - 1}} \tag{2}$$

$$V_u = M\left(\frac{\gamma\, g\, R\; T_{SC}}{1 + \frac{\gamma - 1}{2}M^2}\right)^{1/2} \tag{3}$$

$$q_u = \frac{\rho\, V_u^{\,2}}{2} \tag{4}$$

$$q = \frac{\rho\, V_0^{\,2}}{2} \quad \text{where} \quad V_0 = V_u \;\; @ \;\; M \le 0.2 \tag{5}$$

and

$$V_0 = V_u\left[1 + \frac{K\,\tau_1\, V_S}{A_T^{\,3/2}} - \frac{T_{NET}}{4A_T\, q_u\left(1 + \frac{T_{NET}}{q_u A_P}\right)^{1/2}}\right] \quad @ \quad M > 0.2$$

II - Conversion of Strain Gage Readings

$$T_P = K_2\left(T_R - T_0\right) \tag{6}$$

$$Q_P = K_1\left(Q_R - Q_0\right) \tag{7}$$

APPENDIX VI
(Contd.)

II - Conversion of Strain Gage Readings (Contd.)

$$C_u = K_7\left(C_{4_R} - C_{4_C}\right) + K_8\left(C_{5_R} - C_{5_0}\right) \tag{8}$$

$$N_u = K_6\left(N_{3_R} - N_{3_0}\right) - K_4\left(N_{1_R} - N_{1_C}\right) - K_5\left(N_{2_R} - N_{2_0}\right) \tag{9}$$

III - Hub Skin Friction Tare and "A" Frame Tare and Interference

$$f_{h_t} = A + BM_\ell \quad \text{where} \quad \frac{P_{s\ell}}{P_{t\ell}} = \frac{H_0 - K_{10}\left(P_{s\ell_R} - P_{s\ell_0}\right)}{H_0 - K_9\left(P_{s\ell_R} - P_{s\ell_0}\right)} \tag{10}$$

and

$$M_\ell = \left[\frac{\left(\frac{P_{s\ell}}{P_{t\ell}}\right)^{-.286} - 1}{\frac{\gamma - 1}{2}}\right]^{1/2}$$

$$C_{C_{tai}} = e + f\,C_P \quad @ \quad M \leq 0.2 \tag{11}$$

$$C_{C_t} = \left[e + f\left(\frac{C_T}{J^2}\right)\right] J^2 \quad @ \quad M \geq 0.3 \tag{12}$$

IV - Balance Interactions, Hub Buoyancy and Hub Skin Friction Tare Correction

$$T = T_P + f_{h_t} - K_3\left(\Delta T_R - \Delta T_0\right) - Q_P q_t \tag{13}$$

$$Q = Q_P - T_P\, t_q \tag{14}$$

APPENDIX VI
(Contd.)

IV - Balance Interactions, Hub Buoyancy and Hub Skin Friction Tare Correction (Contd.)

$$C = C_u - N_u n_c \tag{15}$$

$$N = N_u - C_u C_n \tag{16}$$

V - Conversion of Force Components to Performance Parameters

$$n = \bar{N}/60 \tag{17}$$

$$J = \frac{V_0}{n\,d_p} \tag{18}$$

$$C_P = \frac{2\pi Q}{\rho n^2 d_p^5} \tag{19}$$

$$C_C = \frac{C}{\rho n^2 d_p^4} + C_{C_{tai}} \quad @ \quad M \le 0.2 \tag{20}$$

$$C_C = \frac{C}{\rho n^2 d_p^4} + C_{C_t} \quad @ \quad M \ge 0.3 \tag{21}$$

$$C_T = \frac{T}{\rho n^2 d_p^4} \tag{22}$$

$$C_{T_{NET}} = C_T + C_C \tag{23}$$

$$\eta = \left(\frac{C_T}{C_P}\right) J \tag{24}$$

$$\eta_{NET} = \left(\frac{C_{T_{NET}}}{C_P}\right) J \tag{25}$$

APPENDIX VI
(Contd.)

V - Conversion of Force Components to Performance Parameters (Contd.)

$$C_N = \frac{N}{\rho n^2 d_p{}^4} \qquad (26)$$

$$V_T = \pi n d_p \qquad (27)$$

$$HP = \frac{\bar{N} Q}{5252} \qquad (28)$$

VI - Calculation of Pressure Coefficient

$$q = \frac{\rho V_0{}^2}{2} \quad \text{where} \quad V_0 = V_u \;@\; M \leq 0.2 \qquad (29)$$

$$\text{and} \quad V_0 = V_u \left(\frac{1 + K\tau_i V_s}{A_T{}^{3/2}} \right) \;@\; M > 0.2$$

$$C_P = \frac{P_{s_m} - P_{s\infty}}{q} \qquad (30)$$

VII - Reduction of Traversing Probe Data

$$M_r = \frac{P_1 - P_2}{P_1} \qquad (31)$$

$$\theta_r = \frac{P_4 - P_5}{P_1 - P_2} \qquad (32)$$

$$\theta = f\left(\theta_r, M_r\right) \quad \text{From Fig. II-5} \qquad (33)$$

APPENDIX VI
(Contd.)

VII - Reduction of Traversing Probe Data (Contd.)

$$\overline{K} = (M_r, \theta) \qquad \text{From Fig. II-6} \tag{34}$$

$$P_S = P_1 - \overline{K}\,(P_1 - P_2) \tag{35}$$

$$M_{TP} = \left[\frac{\left(\frac{P_S}{P_1}\right)^{-\frac{\gamma}{\gamma-1}} - 1}{\frac{\gamma-1}{2}} \right]^{1/2} \tag{36}$$

$$V = M_{TP} \left[\frac{\gamma\, g\, R\, T_{SC}}{1 + \frac{\gamma-1}{2} M^2} \right]^{1/2} \tag{37}$$

$$V' = V \cos\theta \ \cos Z \tag{38}$$

APPENDIX VII

HSD SHROUDED PROPELLER TEST

Balance Load Cell Slopes

Constant	Description	Numerical Value 18-Ft Section	8-Ft Section
C_n	Interaction slope of chord force on normal force, lb N/lb/C	0.021714	0.010630 0.040650*
K_1	Slope of torque strain gage unit read-out instrument, ft-lb/sgu	0.049140	0.049852
K_2	Slope of thrust sgu read-out instrument, lb/sgu	0.072161	0.073019
K_3	Slope of ΔT sgu read-out instrument, lb/sgu	0.004421	0.008842
K_4	Slope of normal force N_1 (upper bending moment load cell), read-out instrument, lb/sgu	0.018153	0.017400 0.04442*
K_5	Slope of normal force N_2 (lower bending moment load cell) read-out instrument, lb/sgu	0.019328	0.019460 0.053980*
K_6	Slope of normal force N_3 (side arm load cell), read-out instrument, lb/sgu	0.190553	0.185400 0.217760*
K_7	Slope of chord force C_4 (upper "A"-frame load cell), read-out instrument, lb/sgu	0.044366	0.042520 0.042580*
K_8	Slope of chord force C_5 (lower "A"-frame load cell), read-out instrument, lb/sgu	0.044805	0.043820 0.044630*

APPENDIX VII
(Contd.)

Constant	Description	Numerical Value 18-Ft Section	Numerical Value 8-Ft Section
K_9	Slope of local (hub), total pressure read-out instrument, psf/sgu	0.0	0.0202
K_{10}	Slope of local (hub) static pressure read-out instrument, psf/sgu	0.0288	0.0719
n_c	Interaction slope of normal force on chord, force, lb C/lb N	-0.031438	-0.045426 0.029290*
q_t	Interaction slope of torque on thrust, lb T/ft-lb Q_p	0.0	0.0
t_q	Interaction slope of thrust on torque, ft-lb Q/lb T	0.0	0.0

*Used for configuration with propeller plane located at 25% shroud chord (C_2).

TABLE I

HSD Shrouded Propeller Test

Component Designation Symbols

		Figure
A_D	Chord force "A" frame dummy, (AD)	V-1
B_x	Propeller hub configuration	
	where subscript x = 3 3-way nub (B3)	15
	= 4 4-way hub (B4)	16
C_x	Shroud - propeller plane relationship	
	where subscript x = 1 propeller plane located at 40% shroud chord, (C1)	9
	= 1SC short chord shroud with propeller plane located at 40% shroud chord, (C1SC)	-
	= 2 propeller plane located at 25% shroud chord, (C2)	9
E_x	Diffuser section	
	where subscript x = 1 shroud exit area divided by shroud internal area at propeller equal 1.1, (E1)	10
	= 1SC short chord shroud diffuser with shroud exit area divided by shroud internal area at propeller equal 1.1, (E1SC)	-
	= 2 shroud exit area divided by shroud internal area at propeller equal 1.2, (E2)	-

TABLE I
(Contd.)

			Figure
E_x	Diffuser section (Contd.)		
	where subscript x = 3	shroud exit area divided by shroud internal area at propeller equal 1.3, (E3)	-
	= 4	NACA series 16 section with shroud exit area divided by shroud internal area at propeller equal 1.1, (E4)	-
I^x	Five inlet guide vanes with numerical superscript indicating deflection angle in degrees. Clockwise rotation when viewed from tip positive		12
L_x	Inlet lip		
	where subscript x = 1	inlet lip 1, (L1)	11
	= 1SC	short chord shroud inlet lip, (L1SC)	-
	= 2	inlet lip 2, (L2)	-
N_D	Side arm dummy, (ND)		V-2
P_{xx}	Planform of propeller blades		14-16
	where subscript x = R	rectangular planform, (PR)	
	= WT	wide tip planform (PWT)	
	= NT	narrow tip planform, (PNT)	
PTR	Propeller dynamometer, PTR		2
R_x	Inlet rake		II-2
	where subscript x = 1	20 deg azimuth, (R1)	
	= 4	270 deg azimuth, (R4)	

TABLE I
(Contd.)

		Figure
R_E	Exit rake at 75 deg azimuth	II-3
TP	Traversing probe at 166.5 deg shroud azimuth, at trailing edge of basic (E_1) shroud diffuser (tunnel station -71.75 in.), (TP)	II-4
T_{P2}	Traversing probe at 166.5 deg shroud azimuth, immediately downstream of blade plane (tunnel station -82.00 in.), (TP2)	II-4
T_{P3}	Traversing probe protruding from tunnel floor at tunnel station -9 in., (TP3)	-
T_x	Blade tip-shroud clearance	
	where subscript x = 1 29.925 in. diameter propeller, (T1)	
	= 2 29.850 in. diameter propeller, (T2)	
	= 3 29.700 in. diameter propeller, (T3)	

Note: Minimum internal shroud diameter = 30.0 in. for all shrouds

V^x	Five exit vanes with numerical superscript indicating deflection angle in degrees. Counterclockwise rotation when viewed from tip positive.	13

TABLE II

HSD Shrouded Propeller Test
Test Schedule

I - 18-Ft Test Section Performance Data (Table V)

Configuration									Run Number	Figure Number
L_1	C_1	E_1	B_3	P_{WT}	T_1	R_1			18-21,28,32-36,38-49	18-20,28-34
							R_E		260-272	28-34
				P_{NT}					51-58,213-220	172-176
L_2				P_{WT}					61-74	19,20,47-51
L_1		E_2							77-80,82-92	61-65
		E_3							93-96,101-104,106-116	17,18,75-79
		E_4							117-129	17,89-93
									130-134	27
L_1	C_1	E_1		P_R	T_1				175-179,181-186	158-162
			B_4	P_{NT}					188-199	21,22,186-190
			B_3	P_R	T_2				201-211	200-204
L_{1SC}	C_{1SC}	E_{1SC}	B_3	P_{NT}	T_1				230-233,235-242	117-121
L_1	C_1	E_1	B_3	P_R	T_3	R_1	R_E		247-258	214-218
	C_2			P_{WT}	T_1				278-285,287-290	103-107
	C_1							V	291-303	143-145,152-157
								I	304-315	131-133,137-142
L_{1SC}	C_{1SC}	E_{1SC}	B_3	P_R	T_3	R_1	R_E		348-351,358-363	-

E330590-1

TABLE II

HSD Shrouded Propeller Test
Test Schedule

II - 18-Ft Test Section Pressure Data

Configuration									Run Numbers	Tabulations Presented	
										*Pressure (Table IX)	Trav. Probe (Table VIII)
L_1	C_1	E_1	B_3	P_{WT}	T_1	R_4	R_E	T_P	137-139	-	X
									141-143	X	
									144	-	
									149,150	X	
			B_4	P_{NT}		R_1			158,159,162,163	-	
			B_3	P_{NT}					165,166,168,169	X	
				P_R					171-174		
				P_{WT}					316-321		
				P_R	T_3				323-326		
		E_3		P_{WT}	T_1				328,329,331,332		
L_{1SC}	C_{1SE}	E_{1SC}	B_3	P_{WT}	T_1				334,335,340-341		

*Surface pressures, inlet rake, exit rake

TABLE II

HSD Shrouded Propeller Test
Test Schedule

III - 8-Ft Test Section Performance Data.

Configuration	Run Numbers	Figure Number
L_1 C_1 E_1 B_4 P_{NT} T_1 R_1 R_E	434-446	21,22,191-199
B_3 P_R	449-458,460,461	163-171
P_{WT}	463-479,481,482, 485-487,702-704	25,26,35-46
I	501-504,722-729	131-136
V	505-508	146-151
E_2	509-521	66-74
E_3	522-527,529-533	80-88
E_4	539-551	94-102
L_2 E_1	552-565	52-60
L_1 C_2	566-577	108-116
L_{1SC} C_{1SC} E_{1SC} B_3 P_{NT}	585-590,592-598,600-603	122-130
L_1 C_1 E_1 P_R T_2	612-614,616-625,708-713, 717-720	205-213
P_{NT} T_1	627-639	177-185
P_R T_3	641-653	23,24,219-227
P_{WT} T_1 I V	730-734	-

TABLE II

HSD Shrouded Propeller Test
Test Schedule

I - 8-Ft Test Section Pressure Data

Configuration	Run Numbers	Tabulations Presented	
		*Pressure (Table IX)	Trav.Probe (Table VIII)
L_1 C_1 E_1 B_3 P_R T_3 R_1 R_E T_P	654	X	X
	655,656		
P_{NT} T_1	658-660		
B_4	662-664		
B_3 P_{WT}	666-676		
I	677-679		
B_3 P_R	681-684		
E_3 P_{WT}	686-688		
L_{1SC} C_{1SC} E_{1SC} P_{NT}	691-693		
L_1 C_1 E_1 P_{WT} T_{P2}	695-698,700,701		

*Surface pressures, inlet rake, exit rake

TABLE III

HSD SHROUDED PROPELLER TEST

WIND TUNNEL RUN LOG

RUN NO.	CONFIGURATION	$\theta_{3/4}$	TEST CONDITIONS MACH NO.	TEST CONDITIONS RPM	TEST OBJECTIVE	REMARKS
1	PTR w/o shroud and blades	-	Varied	0	Calib.	PTR installed 12-2-65
2	$L_1C_1E_3B_4R_1$					Run aborted
3						Rerun of run 2
4	$E_1B_3P_RT_1R_1I^{10}$+Gages	10	0.0	Varied	Static balance	Fouling indicatin
5	+					Rerun of run 4
6	+	35	0.02		Blade stress	
7	+	20				
8	+	40	0.10			
9	+		0.20			
10		30	0.02		Performance	Blades damaged
11	P_{WT} +Gages	10	0.0		Static balance	
12	+	20	0.02		Blade stress	
13	+		0.15			
14	+	35	0.02			
15	+		0.15			
16	+	40	0.10			
17	+		0.20			
18		30	0.02		Performance	
19			0.10			
20			0.20			

TABLE III

HSD SHROUDED PROPELLER TEST

WIND TUNNEL RUN LOG

RUN NO.	CONFIGURATION	$\theta_{3/4}$	TEST CONDITIONS MACH NO.	TEST CONDITIONS RPM	TEST OBJECTIVE	REMARKS
21	$L_1C_1E_1B_3P_{WT}T_1R_1$	30	0.10	Varied	Performance	Repeat of run 19
22	A_D		0.02			
23			0.10			
24			0.20			
25		10	0		Static balance	
26		30	0.20		Performance	Repeat of run 24
27		40	0.20			
28						
29	N_D	30	0.02			
30			0.10			
31			0.20			
32			0.05			
33			0.10			Repeat of run 19
34			0.20			Repeat of run 20
35			0.05			Repeat of run 32
36		20				
37			0.10			Instrumentation inoperative
38		30				Repeat of run 33
39		40	0.20			Repeat of run 28
40	R_E	20	0.10			Rerun of run 37

E330590-1

TABLE III

HSD SHROUDED PROPELLER TEST

WIND TUNNEL RUN LOG

RUN NO.	CONFIGURATION	$\theta_{3/4}$	TEST CONDITIONS MACH NO.	RPM	TEST OBJECTIVE	REMARKS
41	$L_1C_1E_1B_3P_{WT}T_1R_1R_E$	25	0.05	Varied	Performance	
42			0.10			
43			0.20			
44		35				
45			0.10			
46			0.05			
47		30	0.10			Repeat of run 38
48						
49						
50	P_{NT} R_1	10	0		Static balance	
51		20	0.05		Performance	
52			0.10			
53			0.20			
54		25	0.05			
55			0.10			
56			0.20			
57		30				
58			0.10			
59			0.05			Blades damaged
60	L_2 P_{WT}	10	0		Static balance	

TABLE III

HSD SHROUDED PROPELLER TEST

WIND TUNNEL RUN LOG

RUN NO.	CONFIGURATION	$\theta_{3/4}$	TEST CONDITIONS MACH NO.	TEST CONDITIONS RPM	TEST OBJECTIVE	REMARKS
61	$L_2C_1E_1B_3P_{WT}T_1R_1R_E$	20	0.10	Varied	Performance	
62			0.05			
63		25				
64			0.10			
65			0.20			
66		30				
67			0.10			
68			0.05			
69		35				
70			0.10			
71			0.20			
72		40				
73		25				Repeat of run 65
74						Repeat of run 73
75	L_1 P_R	10	0		Static balance	Aborted blade failure
76	E_2 P_{WT}					
77		20	0.05		Performance	
78			0.10			
79		25	0.05			
80			0.10			

TABLE III

HSD SHROUDED PROPELLER TEST

WIND TUNNEL RUN LOG

RUN NO.	CONFIGURATION	$\theta_{3/4}$	TEST CONDITIONS MACH NO.	TEST CONDITIONS RPM	TEST OBJECTIVE	REMARKS
81	$L_1C_1E_2B_3P_{WT}T_1R_1R_E$	25	0.20	Varied	Performance	Aborted high vibration
82						Rerun of run 81
83		30	0.05			
84			0.02			
85			0.10			
86			0.20			
87		35	0.20			
88			0.10			
89			0.02			
90	+Tufts	25	0.02			
91	+	20	0.02			
92	+	40	0.20			
93	E_3	20	0.02			
94		30				
95			0.10			
96			0.20			
97	A_D					
98			0.10			
99			0.02			
100						Repeat of run 99

E330590-1

TABLE III

HSD SHROUDED PROPELLER TEST

WIND TUNNEL RUN LOG

RUN NO.	CONFIGURATION	$\theta_{3/4}$	TEST CONDITIONS MACH NO.	TEST CONDITIONS RPM	TEST OBJECTIVE	REMARKS
101	$L_1C_1E_3B_3P_{WT}T_1R_1R_E$	30	0.02	Varied	Performance	Repeat of run 94
102						Repeat of run 101
103			0.10			Repeat of run 95
104			0.05			
105	A_D		0.05			
106		20				
107			0.10			
108		25	0.02			
109			0.05			
110			0.10			
111			0.20			
112		35				
113			0.10			
114			0.05			
115			0.02			
116		40	0.20			
117	E_4					
118		20	0.10			
119			0.02			
120		25				

TABLE III

HSD SHROUDED PROPELLER TEST

WIND TUNNEL RUN LOG

RUN NO.	CONFIGURATION	$\theta_{3/4}$	TEST CONDITIONS		TEST OBJECTIVE	REMARKS
			MACH NO.	RPM		
121	$L_1C_1E_4B_3P_{WT}T_1R_1R_E$	25	0.10	Varied	Performance	
122			0.20			
123		30				
124			0.10			
125			0.02			
126		35				
127			0.10			
128			0.20			
129			0.02			Repeat of run 126
130		30	0.20			w/o shroud
131			0.10			
132			0.05			
133		25	0.10			
134			0.05			
135			-	-	-	Tunnel fan maintenance
136	$L_1C_1E_1$ T_1 T_P	30	0.05	5500	Pressure	Aborted Epsco inoperative
137						Rerun of run 136
138				6500		
139				7500		
140	R_4		0.10	5500		Aborted Epsco inoperative

TABLE III

HSD SHROUDED PROPELLER TEST

WIND TUNNEL RUN LOG

RUN NO.	CONFIGURATION	$\theta_{3/4}$	TEST CONDITIONS MACH NO.	TEST CONDITIONS RPM	TEST OBJECTIVE	REMARKS
141	$L_1C_1E_1B_3P_{WT}T_1R_4R_ET_P$	30	0.10	5500	Pressure	
142				6500		
143				7500		
144		25	0.05	5500		
145			-	-		Epsco inoperative
146						
147						
148						
149			0.05	6500		
150				7500		
151	B_4P_{NT} R_1 +Gage	10	0	Varied	Static balance	
152	+	20	0.02		Blade stress	
153	+		0.15			
154	+	35	0.02			
155	+		0.15			
156	+	40	0.10			
157	+		0.20			
158		30	0.05	5500	Pressure	
159				7500		
160			0.20	5500		Aborted, trav. probe inoperative

TABLE III

HSD SHROUDED PROPELLER TEST

WIND TUNNEL RUN LOG

RUN NO.	CONFIGURATION	$\theta_{3/4}$	TEST CONDITIONS MACH NO.	TEST CONDITIONS RPM	TEST OBJECTIVE	REMARKS
161	$L_1C_1E_1B_4P_{NT}T_1R_1R_ET_P$	30	0.20	5500	Pressure	Trav. probe inoperative
162						Rerun of run 160
163				7500		
164	B_3	10	0	Varied	Static balance	
165		30	0.05	5500	Pressure	
166				7500		
167			0.20	5500		
168						
169				7500		
170	P_R	10	0	Varied	Static balance	
171		30	0.05	5500	Pressure	
172				7500		
173			0.20	5500		
174				7500		
175		20	0.02	Varied	Performance	
176			0.10			
177		25	0.02			
178			0.10			
179			0.20			
180		10	0		Static balance	

TABLE III

HSD SHROUDED PROPELLER TEST

WIND TUNNEL RUN LOG

RUN NO.	CONFIGURATION	$\theta_{3/4}$	TEST CONDITIONS		TEST OBJECTIVE	REMARKS
			MACH NO.	RPM		
181	$L_1C_1E_1B_3P_R\ T_1R_1R_E$	30	0.20	Varied	Performance	
182			0.10			
183			0.02			
184		35				
185			0.10			
186			0.20			
187	B_4P_{NT}	10	0		Static balance	
188		20	0.02		Performance	
189			0.10			
190			0.20			
191		25	0.02			
192			0.10			
193			0.20			
194		30				
195			0.10			
196			0.02			
197		35				
198			0.10			
199			0.20			
200	$B_3P_RT_2$	10	0		Static balance	

E330590-I

TABLE III

HSD SHROUDED PROPELLER TEST

WIND TUNNEL RUN LOG

RUN NO.	CONFIGURATION	$\theta_{3/4}$	TEST CONDITIONS MACH NO.	TEST CONDITIONS RPM	TEST OBJECTIVE	REMARKS
201	$L_1C_1E_1B_3P_R\ T_2R_1R_E$	20	0.02	Varied	Performance	
202			0.10			
203		25	0.02			
204			0.10			
205			0.20			
206		30	0.20			
207			0.10			
208			0.02			
209		35	0.02			
210			0.10			
211			0.20			
212	$P_{NT}T_1$	10	0		Static balance	
213		20	0.02		Performance	
214		25				
215		30				
216			0.05			Rerun of run 59
217		35	0.02			
218			0.05			
219			0.10			
220			0.20			

TABLE III

HSD SHROUDED PROPELLER TEST

WIND TUNNEL RUN LOG

RUN NO.	CONFIGURATION	$\theta_{3/4}$	TEST CONDITIONS MACH NO.	TEST CONDITIONS RPM	TEST OBJECTIVE	REMARKS
221	$L_{1SC}C_{1SC}E_{1SC}B_3P_{WT}T_1R_1R_EA_D$	10	-	Varied	Static balance	
222		30	0.02		Performance	Run aborted
223						Rerun of run 222
224			0.10			Blades damaged
225	P_{NT}	10	0		Static balance	
226		30	0.02		Performance	
227			0.10			
228			0.20			
229		35	0.20			
230						
231			0.10			
232			0.02			
233		30	0.02			
234			0.10			Shroud balance instr.inoperative
235						
236			0.20			
237		20	0.02			
238			0.10			
239			0.20			
240		25	0.02			

TABLE III

HSD SHROUDED PROPELLER TEST

WIND TUNNEL RUN LOG

RUN NO.	CONFIGURATION	$\theta_{3/4}$	TEST CONDITIONS MACH NO.	RPM	TEST OBJECTIVE	REMARKS
241	$L_{1SC}C_{1SC}E_{1SC}B_3P_{NT}T_1R_1R_E$	25	0.10	Varied	Performance	
242			0.20			
243	A_D		0.02			
244			0.10			
245			0.20			
246	$L_1C_1E_1$ P_R T_3	10	0		Static balance	
247		20	0.20		Performance	
248			0.10			
249			0.02			
250		25				
251			0.10			
252			0.20			
253		30				
254			0.10			
255			0.02			
256		35				
257			0.10			
258			0.20			
259	$P_{WT}T_1$	10	0		Static balance	
260		15	0.02		Performance	

TABLE III

HSD SHROUDED PROPELLER TEST

WIND TUNNEL RUN LOG

RUN NO.	CONFIGURATION	$\theta_{3/4}$	TEST CONDITIONS		TEST OBJECTIVE	REMARKS
			MACH NO.	RPM		
261	$L_1C_1E_1B_3P_{WT}T_1R_1R_E$	15	0.05	Varied	Performance	
262			0.10			
263		20	0.02			
264			0.15			
265			0.20			
266		25	0.15			
267			0.02			
268		30	0.15			
269		35				
270			0.02			
271		40	0.10			
272			0.15			
273	C_2	20	0.02			
274			0.10			
275			0.02			Rerun of run 273
276			0.20			
277		30	0.02			
278						Rerun of run 277
279			0.10			
280			0.20			

E330590-1

TABLE III

HSD SHROUDED PROPELLER TEST

WIND TUNNEL RUN LOG

RUN NO.	CONFIGURATION	$\theta_{3/4}$	TEST CONDITIONS MACH NO.	TEST CONDITIONS RPM	TEST OBJECTIVE	REMARKS
281	$L_1C_2E_1B_3P_{WT}T_1R_1R_E$	20	0.20	Varied	Performance	Rerun of run 276
282			0.10			Rerun of run 274
283			0.02			Rerun of run 275
284		25				
285			0.10			
286			0.20			Aborted high vibration
287						Rerun of run 286
288		35				
289			0.10			
290			0.02			
291	C_1 V^0		0.05			
292			0.20			
293		25				
294			0.05			
295	V^{10}					
296			0.20			
297		35	0.20			
298			0.05			
299	V^{-10}	25				
300	V^{-5}					

TABLE III

HSD SHROUDED PROPELLER TEST

WIND TUNNEL RUN LOG

RUN NO.	CONFIGURATION	$\theta_{3/4}$	TEST CONDITIONS MACH NO.	TEST CONDITIONS RPM	TEST OBJECTIVE	REMARKS
301	$L_1C_1E_1B_3P_{WT}T_1R_1R_EV^{-5}$	25	0.20	Varied	Performance	
302		35	0.20			
303			0.05			
304	I^0					
305			0.20			
306		25				
307			0.05			
308	I^{10}					
309			0.20			
310		35				
311			0.05			
312	I^{-10}					
313			0.20			
314		25	0.05			
315			0.20			
316	$I^{10}T_P$	35	0.05	5500	Pressure	
317				7500		
318			0.20	5500		
319				7500		
320	I^{-10}			5500		

TABLE III

HSD SHROUDED PROPELLER TEST

WIND TUNNEL RUN LOG

RUN NO	CONFIGURATION	$\theta_{3/4}$	TEST CONDITIONS MACH NO.	TEST CONDITIONS RPM	TEST OBJECTIVE	REMARKS
321	L_1 C_1 E_1 $B_3P_{WT}T_1R_1R_EI^{-10}T_P$	35	0.20	7500	Pressure	
322	P_R T_3	10	0	Varied	Static balance	
323		35	0.05	5500	Pressure	
324				7500		
325			0.20	5500		
326				7500		
327	E_3 $P_{WT}T_1$	10	0	Varied	Static balance	
328		30	0.05	5500	Pressure	
329				7500		
330			0.20	5500		Aborted, trav. probe inoper.
331						Rerun of run 330
332				7500		
333	$L_{1SC}C_{1SC}E_{1SC}$		0.05	5500		Epsco inoper.
334						Rerun of run 33
335			0.20			
336			0.05	7500		N_3 flexure broken
337						Epsco inoper.
338						Run aborted resonant noise
339						Run aborted resonant noise
340						Rerun of run 336

E330590-1

TABLE III

HSD SHROUDED PROPELLER TEST

WIND TUNNEL RUN LOG

RUN NO.	CONFIGURATION	$\theta_{3/4}$	TEST CONDITIONS MACH NO.	TEST CONDITIONS RPM	TEST OBJECTIVE	REMARKS
341	$L_{1SC}C_{1SC}E_{1SC}B_3P_{WT}T_1R_1R_ET_P$	30	0.20	7000	Pressure	
342		35		Varied	Performance	
343						
344			0.10			
345						
346						Blades damaged
347	P_RT_3	10	0		Static balance	
348		35	0.20		Performance	
349			0.05			
350			0.10			
351			0.05			
352	A_D					
353			0.10			
354			0.20			
355		30				
356			0.10			
357			0.05			
358						
359						
360			0.10			

E330590-1

TABLE III

HSD SHROUDED PROPELLER TEST

WIND TUNNEL RUN LOG

RUN NO.	CONFIGURATION	$\theta_{3/4}$	TEST CONDITIONS		TEST OBJECTIVE	REMARKS
			MACH NO.	RPM		
361	$L_{1SC}C_{1SC}E_{1SC}B_3P_RT_3R_1R_E$	30	0.20	Varied	Performance	
362		10	0.05			
363		0				Final data run in 18-ft section
	Phase I program in 18-ft test section concluded Jan. 7, 1966					
	1-P stress program conducted for HSD under Project No. 330798					
	and 330821 initiated Jan. 7, 1966. Data runs 364 to 411 completed					
	satisfactorily and PTR removed Jan. 12, 1966.					
	Phase I program in 8-ft test section initiated April 28, 1966.					
412	T_{P3}	-	0.20	-	Trav.Probe Calib.	Probe installed 8-ft sec.4-28-66
413			Varied			α = 0 deg
414						α = 40 deg
415						α = 20 deg
416						α = 5 deg
417						α = 10 deg
418						α = 30 deg
419						α = 50 deg
420						α = 0 deg Repeat of Run 413
421						α = -10 deg probe removed 4-29-66

E330590-1

TABLE III

HSD SHROUDED PROPELLER TEST

WIND TUNNEL RUN LOG

RUN NO.	CONFIGURATION	$\theta_{3/4}$	TEST CONDITIONS MACH NO.	RPM	TEST OBJECTIVE	REMARKS
	Propeller test rig installed in 8-ft test section April 29, 1966.					
422	PTR w/o shroud and blades + R_1	-	Varied	0	Calib.	
423	$L_1C_1E_3B_3$ R_1					
424						Rerun of run 423
425						
426						
427						
428	$E_1B_4P_{NT}T_1$ + gages	10	0.0	Varied	Static Balance	
429		45	0.30		Blade Stress	
430		55	0.45			
431		50	0.45			
432		60	0.60			
433		45	0.30			Repeat of run 429
434	R_E	20	0.20		Performance	Repeat of 18-ft tunnel run 190
435		34	0.30			
436		38				
437		42				
438		42	0.40			
439		46	0.30			
440			0.40			

E330590-1

TABLE III

HSD SHROUDED PROPELLER TEST

WIND TUNNEL RUN LOG

RUN NO.	CONFIGURATION	$\theta_{3/4}$	TEST CONDITIONS MACH NO.	TEST CONDITIONS RPM	TEST OBJECTIVE	REMARKS
441	$L_1C_1E_1B_4P_{NT}T_1R_1R_E$	46	0.50	Varied	Performance	
442		50	0.40			
443			0.50			
444		54	0.40			
445			0.50			
446		58				
447	B_3P_R	10	0.0		Static Balance	
448						
449		34	0.30		Performance	
450		38				
451		42				
452			0.40			
453		46	0.30			
454			0.40			
455			0.50			
456		50	0.40			
457			0.50			
458		54	0.40			
459			0.50			N. inoperative, run aborted
460						Rerun of run 459

E330590-1

TABLE III

HSD SHROUDED PROPELLER TEST

WIND TUNNEL RUN LOG

RUN NO.	CONFIGURATION	$\theta_{3/4}$	TEST CONDITIONS MACH NO.	RPM	TEST OBJECTIVE	REMARKS
461	$L_1C_1E_1B_3P_RT_1R_1R_E$	42	0.5	Varied	Performance	
462	P_{WT}	10	0.0		Static Balance	
463		25	0.20		Performance	
464		30				
465			0.30			
466		34				
467		35	0.20			
468		38	0.30			
469			0.40			
470						Repeat of run 469
471		40	0.20			
472		42	0.30			
473			0.40			
474			0.50			
475		46	0.40			
476			0.50			
477			0.60			
478		50	0.40			
479			0.50			
480		54				Fouling indication

TABLE III

HSD SHROUDED PROPELLER TEST

WIND TUNNEL RUN LOG

RUN NO	CONFIGURATION	$\theta_{3/4}$	TEST CONDITIONS		TEST OBJECTIVE	REMARKS
			MACH NO.	RPM		
481	$L_1C_1E_1B_3P_{WT}T_1R_1R_E$	54	0.50	Varied	Performance	Fouling indication, rerun of run 480
482		50				Rerun of run 479
483			0.60			Blade-shroud interference
484						
485						Rerun of run 483
486		54				
487		58				
488	A_D	30	0.30			
489		38				
490			0.40			
491		46				
492			0.50			
493		54				
494		46	0.40			Repeat of run 491
495	N_D					
496			0.50			
497		30	0.30			
498		38				
499			0.40			
500		54	0.50			

E330590-1

TABLE III

HSD SHROUDED PROPELLER TEST

WIND TUNNEL RUN LOG

RUN NO.	CONFIGURATION	$\theta_{3/4}$	TEST CONDITIONS MACH NO.	TEST CONDITIONS RPM	TEST OBJECTIVE	REMARKS
501	$L_1C_1E_1B_3P_{WT}T_1R_1R_EI^o$	42	0.40	Varied	Performance	
502		46				
503			0.50			
504		50				
505	V^o					
506		42	0.40			
507		46				
508			0.50			
509	E_2	30	0.30			
510		34				
511		38				
512			0.40			
513		42	0.30			
514			0.40			
515			0.50			
516		46	0.40			
517			0.50			
518		50	0.40			
519			0.50			
520		54				

E330590-1

TABLE III

HSD SHROUDED PROPELLER TEST

WIND TUNNEL RUN LOG

RUN NO.	CONFIGURATION	$\theta_{3/4}$	TEST CONDITIONS MACH NO.	RPM	TEST OBJECTIVE	REMARKS
521	$L_1C_1E_2B_3P_{WT}T_1R_1$	54	0.50	Varied	Performance	Repeat of run 520
522	E_3	34	0.30			
523		38				
524		42				
525			0.40			
526		46	0.30			
527			0.40			
528			0.50			Windmill speed too high. No data
529		50	0.40			
530			0.50			
531						Repeat of run 530
532		58				
533		54	0.40			
534	A_D	38	0.30			
535		42	0.40			
536		46	0.30			
537		50	0.50			
538			0.40			
539	E_4	30	0.30			
540		34				

TABLE III

HSD SHROUDED PROPELLER TEST

WIND TUNNEL RUN LOG

RUN NO.	CONFIGURATION	$\theta_{3/4}$	TEST CONDITIONS		TEST OBJECTIVE	REMARKS
			MACH NO.	RPM		
541	$L_1 C_1 E_4 B_3 P_{WT} T_1 R_1 R_E$	38	0.30	Varied	Performance	
542			0.40			
543		42	0.30			
544			0.40			
545			0.50			
546		46	0.40			
547			0.50			
548		50	0.40			
549			0.50			
550		54				
551		42	0.30			Repeat of run 543
552	L_2 E_1	30	0.31			
553		34				
554		38				
555			0.41			
556		42	0.31			
557			0.41			
558			0.52			
559		46	0.41			
560			0.52			

TABLE III

HSD SHROUDED PROPELLER TEST

WIND TUNNEL RUN LOG

RUN NO.	CONFIGURATION	$\theta_{3/4}$	TEST CONDITIONS MACH NO.	TEST CONDITIONS RPM	TEST OBJECTIVE	REMARKS
561	$L_2C_1E_1B_3P_{WT}T_1R_1R_E$	50	0.41	Varied	Performance	
562			0.52			
563		54				
564		34	0.31			Repeat of run 553
565						Repeat of run 564
566	L_1C_2	30				
567		34				
568		38				
569			0.41			
570		42	0.31			
571			0.41			
572			0.52			
573		46	0.41			
574			0.52			
575		50	0.41			
576			0.52			
577		54				
578	A_D	30	0.31			
579		38				
580			0.41			

TABLE III

HSD SHROUDED PROPELLER TEST

WIND TUNNEL RUN LOG

RUN NO.	CONFIGURATION	$\theta_{3/4}$	TEST CONDITIONS MACH NO.	TEST CONDITIONS RPM	TEST OBJECTIVE	REMARKS
581	L_1 C_2 E_1 $B_3P_{WT}T_1R_1R_EA_D$	46	0.41	Varied	Performance	
582			0.52			
583		54				
584	$L_{1SC}C_{1SC}E_{1SC}$ P_{NT}	10	0.0		Static Balance	
585		30	0.31		Performance	
586		34				
587		38				
588			0.41			
589		42	0.31			
590			0.41			
591			0.52			Windmill speed too high. No data
592			0.41			Repeat of run 590
593		46	0.31			
594			0.41			
595			0.52			
596		50	0.41			
597			0.52			
598		54				
599		46				Repeat of run 595 run aborted
600						Rerun of run 599

E330590-1

TABLE III

HSD SHROUDED PROPELLER TEST

WIND TUNNEL RUN LOG

RUN NO.	CONFIGURATION	$\theta_{3/4}$	TEST CONDITIONS MACH NO.	TEST CONDITIONS RPM	TEST OBJECTIVE	REMARKS
601	$L_{1SC}C_{1SC}E_{1SC}B_3P_{NT}T_1R_1R_E$	46	0.31	Varied	Performance	Repeat of run 593
602			0.41			Repeat of run 594
603						Repeat of run 602
604	A_D					
605						Repeat of run 604
606			0.52			
607		30	0.31			
608		38				
609			0.41			
610		54	0.52			
611	L_1 C_1 E_1 P_R T_2	10	0.0		Static Balance	
612		30	0.31		Performance	
613		34				
614		38				
615			0.41			Large static zero shift on N_1
616						Rerun of run 615
617		42	0.31			
618			0.41			
619			0.52			
620		46	0.41			

E330590-1

TABLE III

HSD SHROUDED PROPELLER TEST

WIND TUNNEL RUN LOG

RUN NO.	CONFIGURATION	$\theta_{3/4}$	TEST CONDITIONS MACH NO.	TEST CONDITIONS RPM	TEST OBJECTIVE	REMARKS
621	$L_1C_1E_1B_3P_R\ T_2R_1R_E$	46	0.52	Varied	Performance	
622		50	0.41			
623			0.52			
624		54				
625		34	0.31			Repeat of run 613
626	$P_NT T_1$	10	0.0		Static Balance	
627		30	0.31		Performance	
628		34				
629		38				
630			0.41			
631		42	0.31			
632			0.41			
633			0.52			
634		58				
635		46	0.41			
636			0.52			
637		50	0.41			
638			0.52			
639		54				
640	$P_R\ T_3$	10	0.0		Static Balance	

E330590-1

TABLE III

HSD SHROUDED PROPELLER TEST

WIND TUNNEL RUN LOG

RUN NO.	CONFIGURATION	$\theta_{3/4}$	TEST CONDITIONS		TEST OBJECTIVE	REMARKS
			MACH NO.	RPM		
641	$L_1C_1E_1B_3P_R\ T_3R_1R_E$	30	0.30	Varied	Performance	
642		34				
643		38				
644			0.40			
645		42	0.30			
646			0.40			
647			0.50			
648		34	0.30			Repeat of run 642
649		46	0.40			
650			0.50			
651		50	0.40			
652			0.50			
653		54				
654	T_P	38	0.30		Pressure	
655		46	0.40			
656		50	0.50			
657	P_NT_{T1}	10	0.0		Static Balance	
658		38	0.30		Pressure	
659		46	0.40			
660		50	0.50			

TABLE III

HSD SHROUDED PROPELLER TEST

WIND TUNNEL RUN LOG

RUN NO.	CONFIGURATION	$\theta_{3/4}$	TEST CONDITIONS		TEST OBJECTIVE	REMARKS
			MACH NO.	RPM		
661	$L_1C_1E_1B_4P_{NT}T_1R_1R_ET_P$	10	0.0	Varied	Static Balance	
662		38	0.30		Pressure	
663		46	0.40			
664		50	0.50			
665	B_3P_{WT}	10	0.0		Static Balance	
666		30	0.20		Pressure	
667		34	0.30			
668		35	0.20			
669		38	0.30			
670		42	0.40			
671		46				
672			0.50			
673		50				
674			0.60			Blade-shroud interference
675		54	0.40			
676		46				Repeat of run 671
677	I^o	42				
678		46				
679			0.50			
680	P_R	10	0		Static Balance	

TABLE III

HSD SHROUDED PROPELLER TEST

WIND TUNNEL RUN LOG

RUN NO.	CONFIGURATION	$\theta_{3/4}$	TEST CONDITIONS MACH NO.	RPM	TEST OBJECTIVE	REMARKS
681	L_1 C_1 E_1 B_3P_R $T_1R_1R_ET_P$	38	0.30	Varied	Pressure	
682		50	0.40			
683			0.50			
684		46	0.40			
685	E_3 P_{WT}	10	0.0		Static Balance	
686		42	0.30		Pressure	
687		50	0.40			
688		58	0.50			
689	$L_{1SC}C_{1SC}E_{1SC}$ P_{WT}	10	0.0		Static Balance	
690		42	0.30		Pressure	Tp not in position, run aborted
691						Rerun of run 690
692		46	0.40			
693		50	0.50			
694	L_1 C_1 E_1 B_3P_{WT} T_{P2}	10	0.0		Static Balance	
695		34	0.30	5500	Pressure	
696		38				
697		42	0.40			
698		46				
699			0.50			High vibration, run aborted
700						Rerun of run 699

TABLE III

HSD SHROUDED PROPELLER TEST

WIND TUNNEL RUN LOG

RUN NO.	CONFIGURATION	$\theta_{3/4}$	TEST CONDITIONS MACH NO.	TEST CONDITIONS RPM	TEST OBJECTIVE	REMARKS
701	$L_1C_1E_1B_3P_{WT}T_1R_1R_ET_{P2}$	50	0.50	5500	Pressure	
702	↓	15	0.10	Varied	Performance	Reverse thrust
703	↓	10	↓	↓	↓	↓
704	↓	5	↓	↓	↓	↓
705	P_R T_2	10	0.0	↓	Static Balance	
706	↓	30	0.30	↓	Performance	Blade angle setting off
707	↓	34	↓	↓	↓	↓
708	↓	↓	↓	↓	↓	Rerun of run 707
709	↓	38	↓	↓	↓	
710	↓	↓	0.40	↓	↓	
711	↓	30	0.30	↓	↓	Rerun of run 706
712	↓	42	↓	↓	↓	
713	↓	↓	0.40	↓	↓	
714	↓	↓	0.50	↓	↓	High vibration, run aborted
715	↓	46	0.40	↓	↓	
716	↓	10	0.0	↓	Static Balance	
717	↓	46	0.52	↓	Performance	
718	↓	50	0.42	↓	↓	
719	↓	↓	0.52	↓	↓	
720	↓	54	↓	↓	↓	

E330690-1

TABLE III

HSD SHROUDED PROPELLER TEST

WIND TUNNEL RUN LOG

RUN NO.	CONFIGURATION	$\theta_{3/4}$	TEST CONDITIONS MACH NO.	RPM	TEST OBJECTIVE	REMARKS
721	$L_1C_1E_1B_3P_{WT}T_1R_1R_EI^o$	10	0.0	Varied	Static Balance	
722		34	0.32		Performance	
723		38				
724		42	0.42			Repeat of run 501
725						Repeat of run 724
726			0.40			Repeat of run 725
727		50				
728		54	0.50			
729		42	0.30			
730	V^o		0.40			
731						
732		38	0.30			
733		46	0.50			
734	I^5	42	0.40			
	Phase I program in 8-ft test section concluded May 16, 1966.					
	1-P stress program conducted for HSD under Project No. 330821 and 330899					
	initiated May 16, 1966. Data runs 735 to 754 completed satisfactorily and					
	PTR removed May 19, 1966.					

TABLE IV

HSD Shrouded Propeller Test

List of Figures

TABLE IV
(Contd.)

Figure	Tab Section: Photographs and Sketches
16	Narrow Tip Blades with Strain Gage Instrumentation Installed in 4-Way Hub
	Tab Section: Data Repeatability
17-20	Comparison of Data Repeatability in 18-Ft Test Section
21, 22	Comparison of Data in 18- and 8-Ft Test Section
23-26	Comparison of Data Repeatability in 8-Ft Test Section
	Tab Section: Basic Shroud Characteristics
27	Effect of Blade Angle on Propeller Performance
28-46	Effect of Blade Angle on Shrouded Propeller Performance
	Tab Section: Shroud Contour Effects
47-59	Effect of Inlet Lip (L_2) on Shrouded Propeller Performance
61-74	Effect of Diffuser (E_2) on Shrouded Propeller Performance
75-88	Effect of Diffuser (E_3) on Shrouded Propeller Performance
89-102	Effect of Diffuser (E_4) on Shrouded Propeller Performance
	Tab Section: Propeller Location and Chord Effects
103-116	Effect of Propeller Location on Shrouded Propeller Performance
117-130	Effect of Chord Length on Shrouded Propeller Performance
	Tab Section: Inlet and Exit Vane Effects
131-136	Effect of Inlet Vanes on Shrouded Propeller Performance
137-142	Effect of Inlet Vane Angle on Shrouded Propeller Performance

TABLE IV
(Contd.)

Figure	Tab Section: Inlet and Exit Vane Effects (Contd.)
143-151	Effect of Exit Vanes on Shrouded Propeller Performance
152-157	Effect of Exit Vane Angle on Shrouded Propeller Performance
	Tab Section: Blade Geometry Effects
158-185	Effect of Blade Planform on Shrouded Propeller Performance
186-199	Effect of 4-Way Blades on Shrouded Propeller Performance
	Tab Section: Blade Tip Clearance Effects
200-227	Effect of Blade Tip Clearance on Shrouded Propeller Performance

HSD SHROUDED PROPELLER TEST

UARL LARGE SUBSONIC WIND TUNNEL

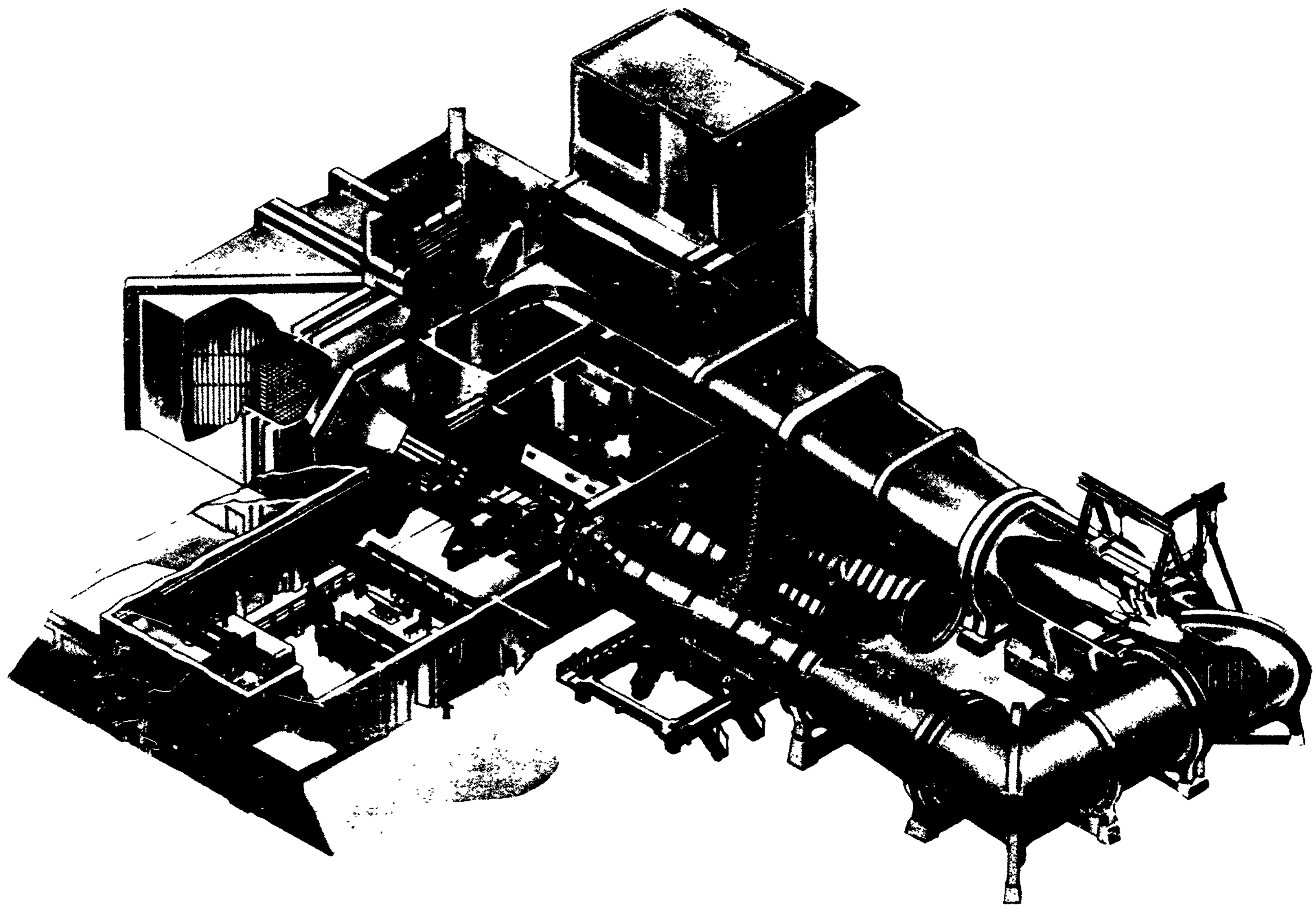

FIG. 1

HSD SHROUDED PROPELLER TEST
SCHEMATIC DRAWING OF PROPELLER DYNAMOMETER

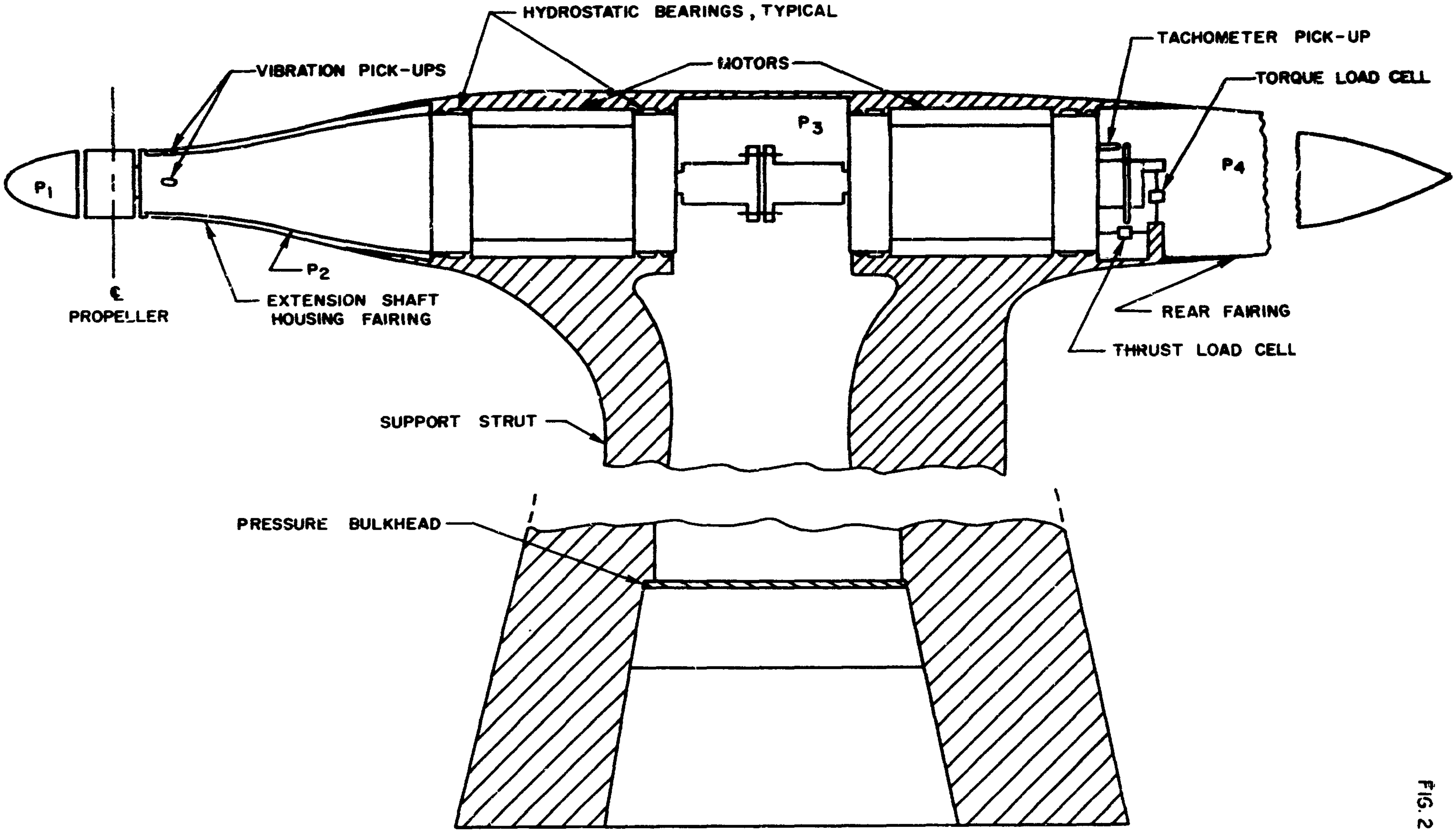

FIG. 2

HSD SHROUDED PROPELLER TEST

BALANCE SYSTEM

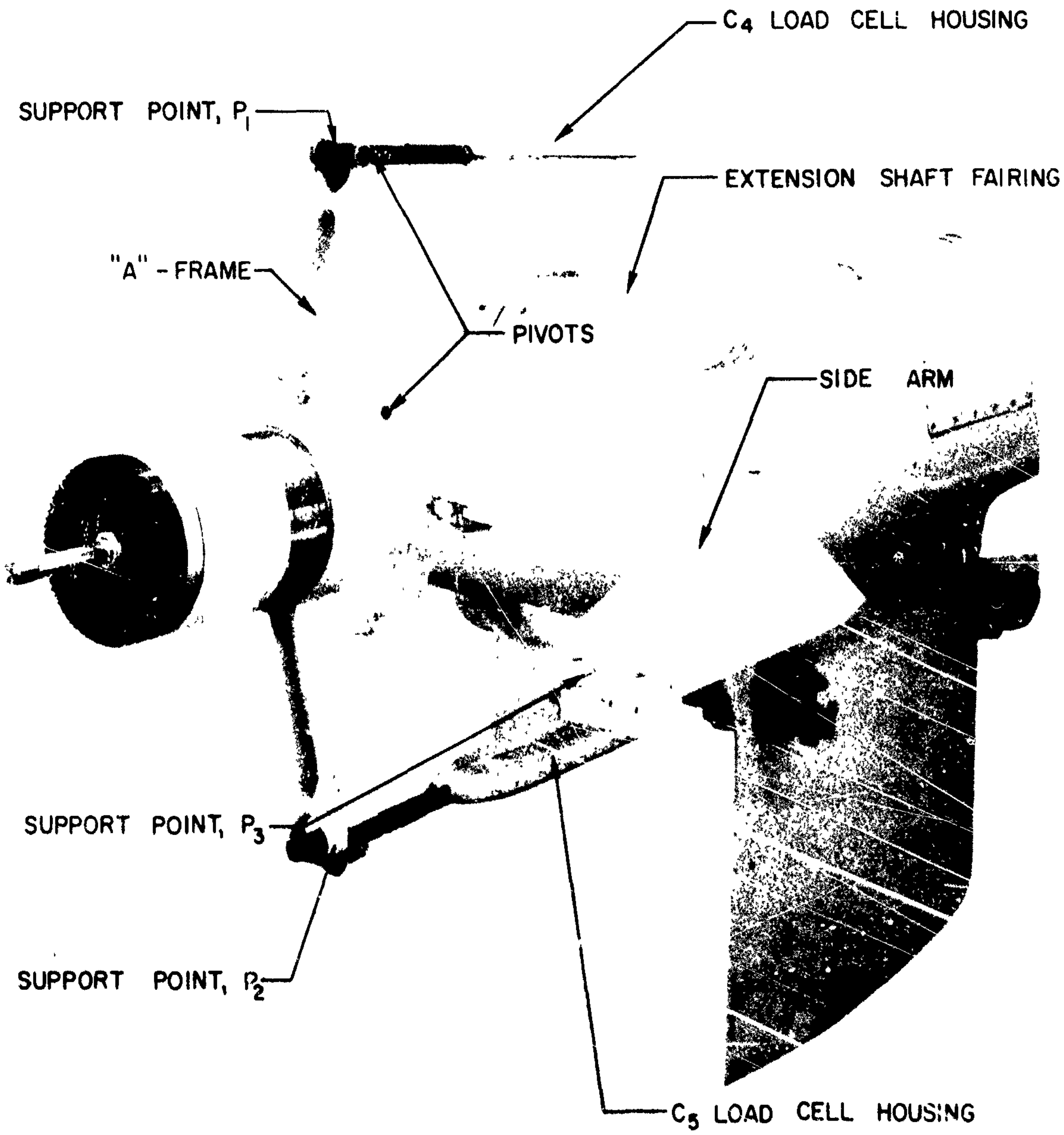

HSD SHROUDED PROPELLER TEST

SCHEMATIC DIAGRAM OF SHROUD BALANCE

$$N = N_3 - N_1 - N_2$$
$$C = C_4 + C_5$$

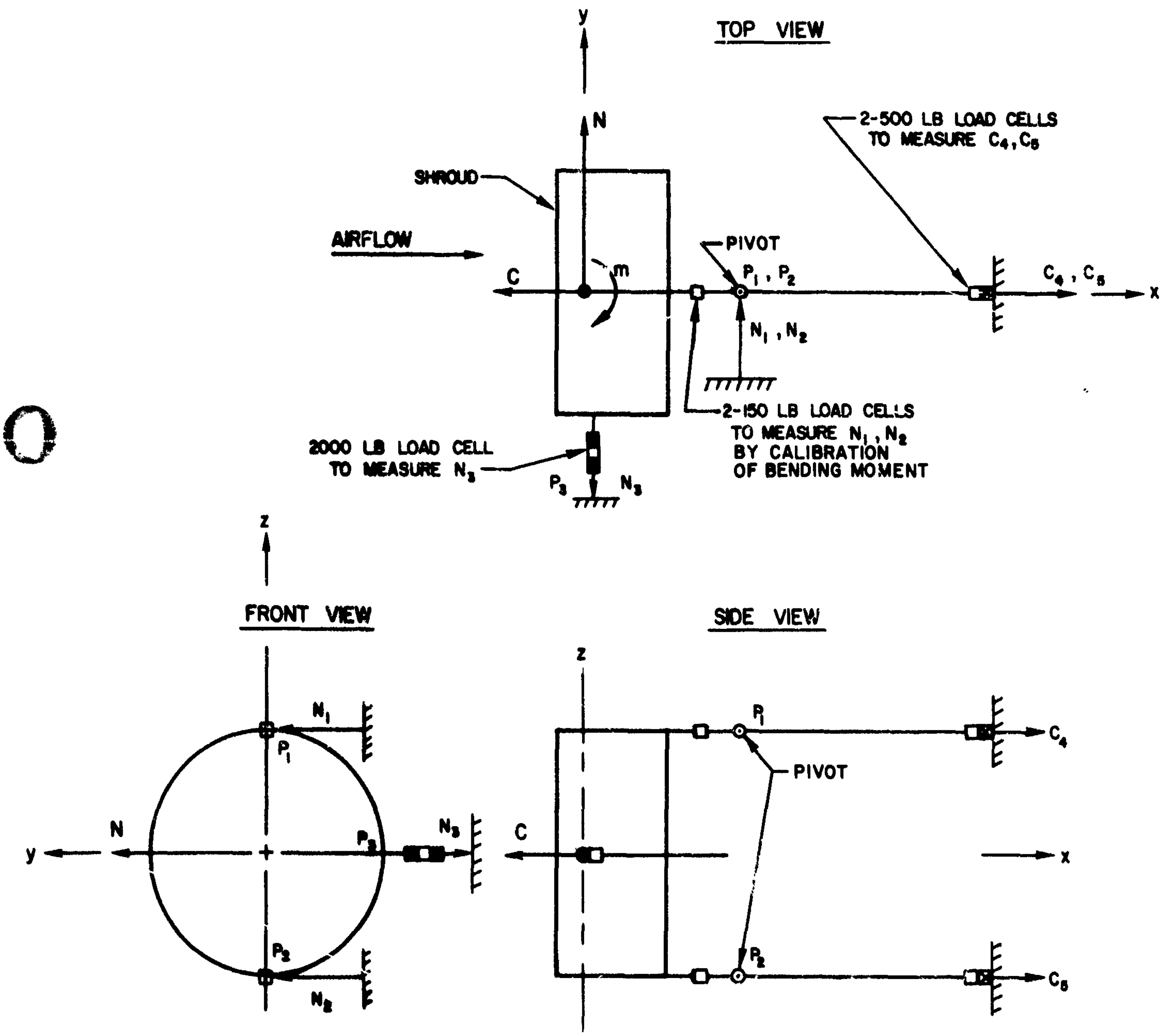

HSD SHROUDED PROPELLER TEST

MODEL PROPELLER TEST DYNAMOMETER INSTALLED IN 18-FT TEST SECTION

VIEW LOOKING DOWNSTREAM

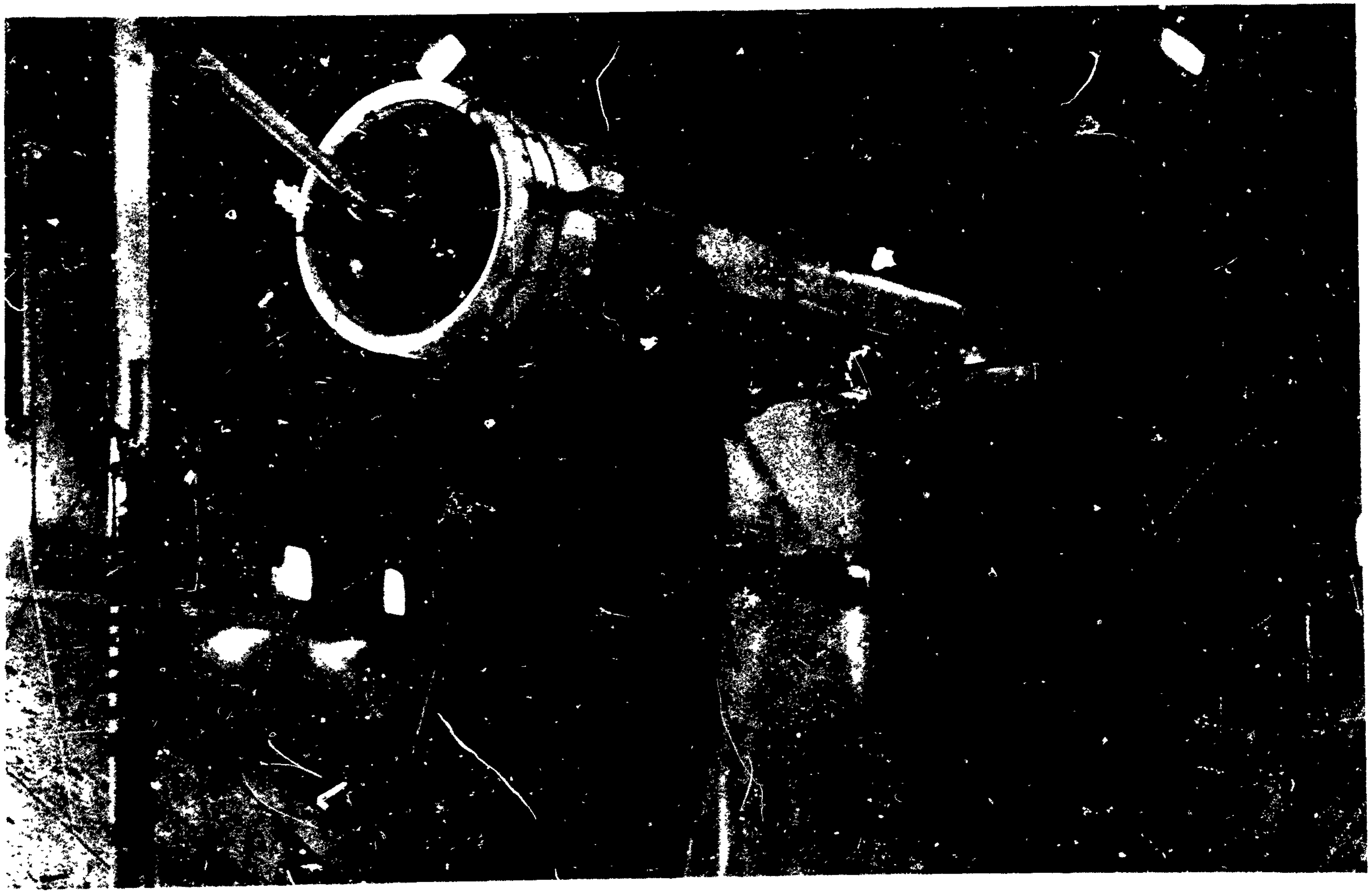

FIG. 5

HSD SHROUDED PROPELLER TEST

MODEL PROPELLER TEST DYNAMOMETER INSTALLED IN 18-FT TEST SECTION

VIEW LOOKING UPSTREAM

HSD SHROUDED PROPELLER TEST

MODEL PROPELLER TEST DYNAMOMETER INSTALLED IN 8-FT TEST SECTION

VIEW LOOKING DOWNSTREAM

HSD SHROUDED PROPELLER TEST

MODEL PROPELLER TEST DYNAMOMETER INSTALLED IN 8-FT TEST SECTION

VIEW LOOKING UPSTREAM

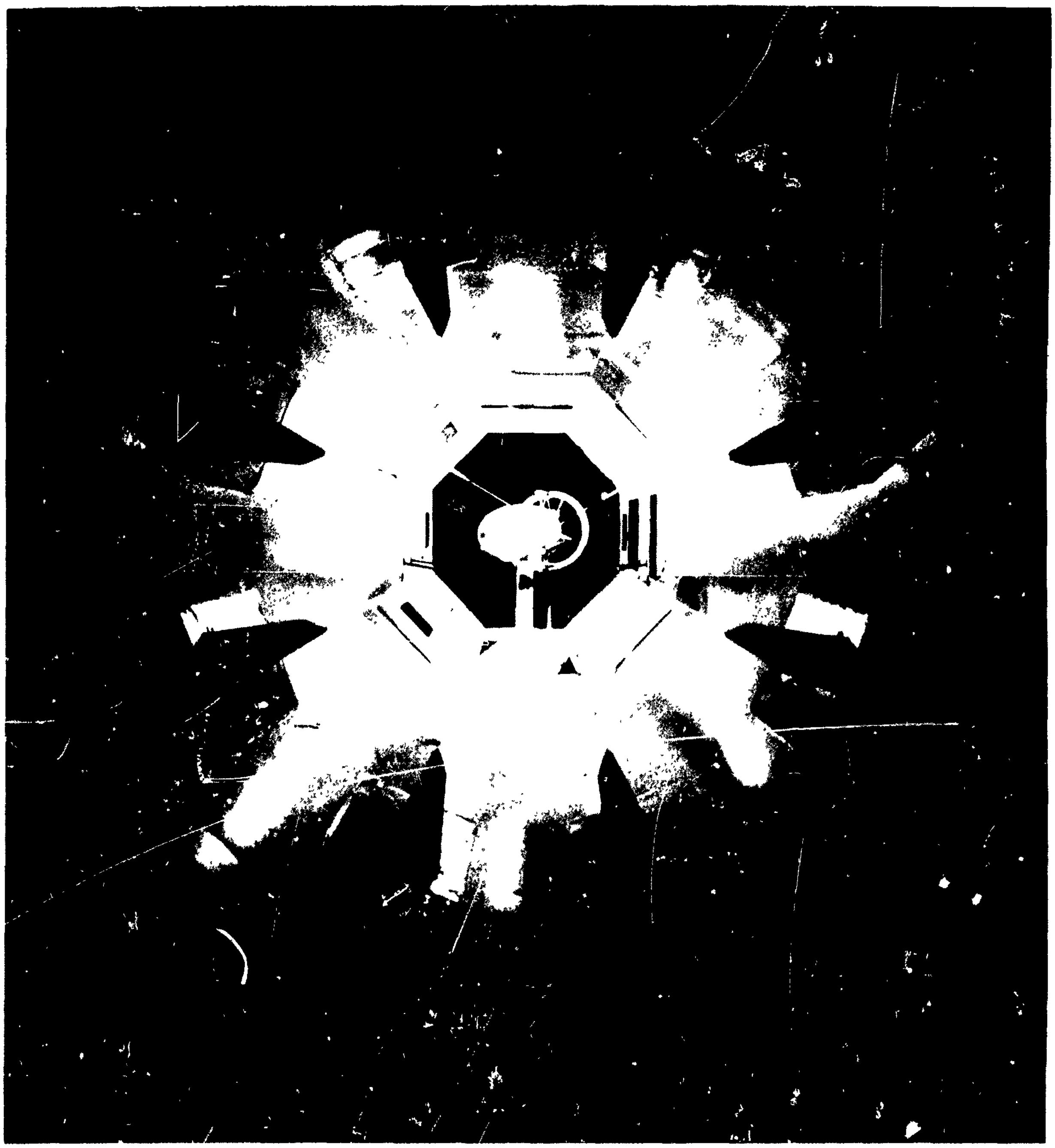

HSD SHROUDED PROPELLER TEST

SHROUD SUPPORT RING INSTALLATION

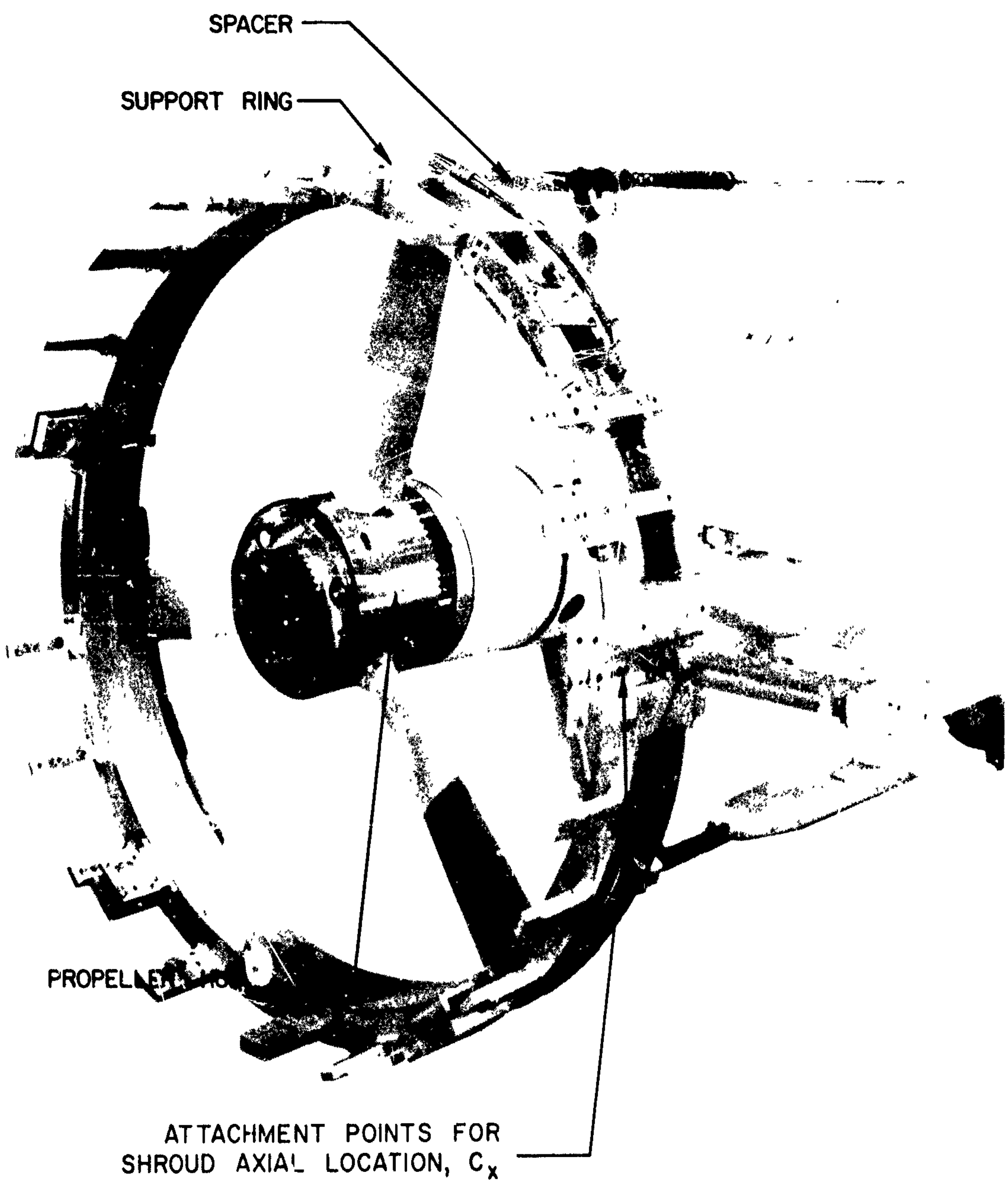

E330590-1

FIG. 10

HSD SHROUDED PROPELLER TEST

SHROUD DIFFUSER AND EXIT VANE INSTALLATION

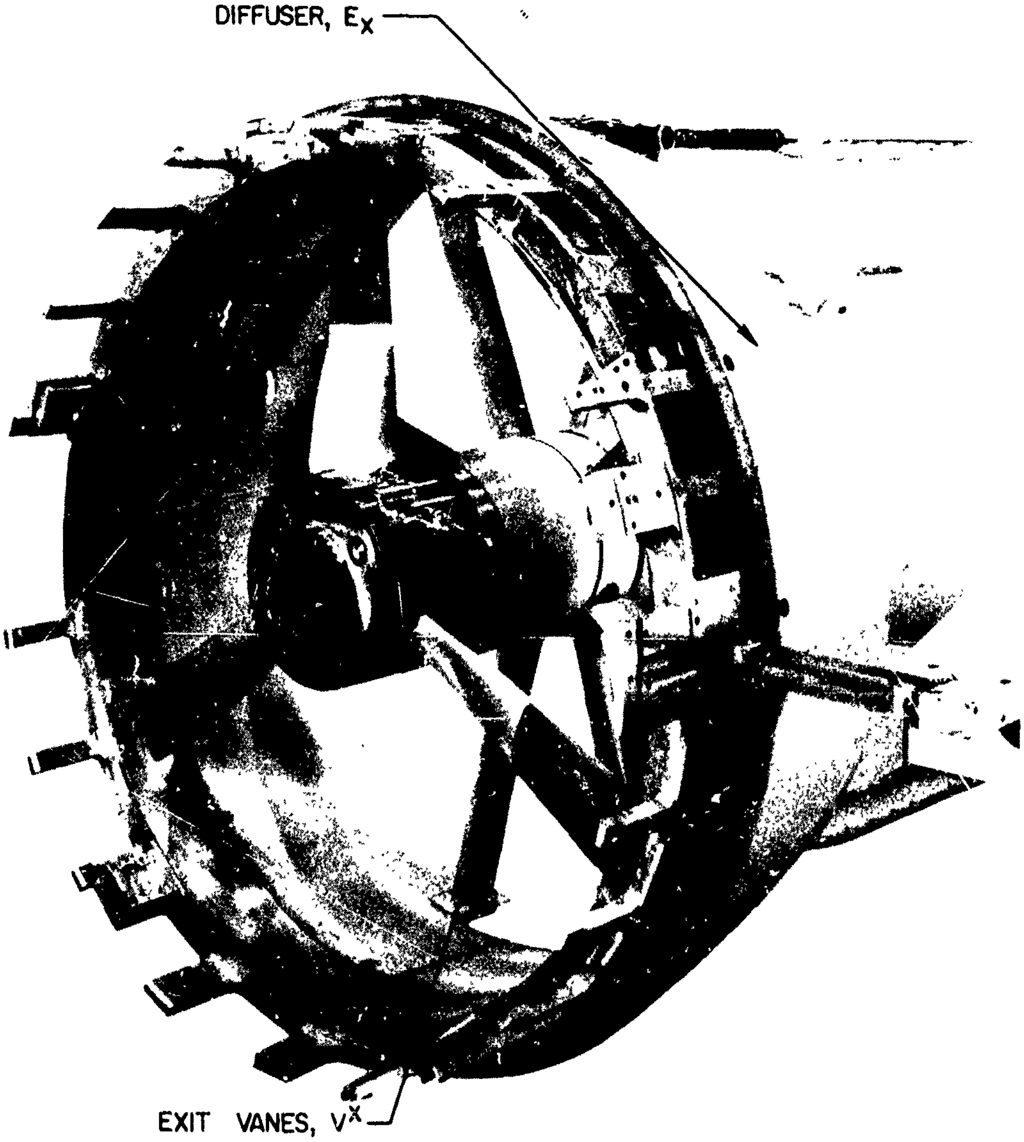

E330590-1

FIG. 11

HSD SHROUDED PROPELLER TEST

SHROUD CENTER SECTION AND LIP INSTALLATION

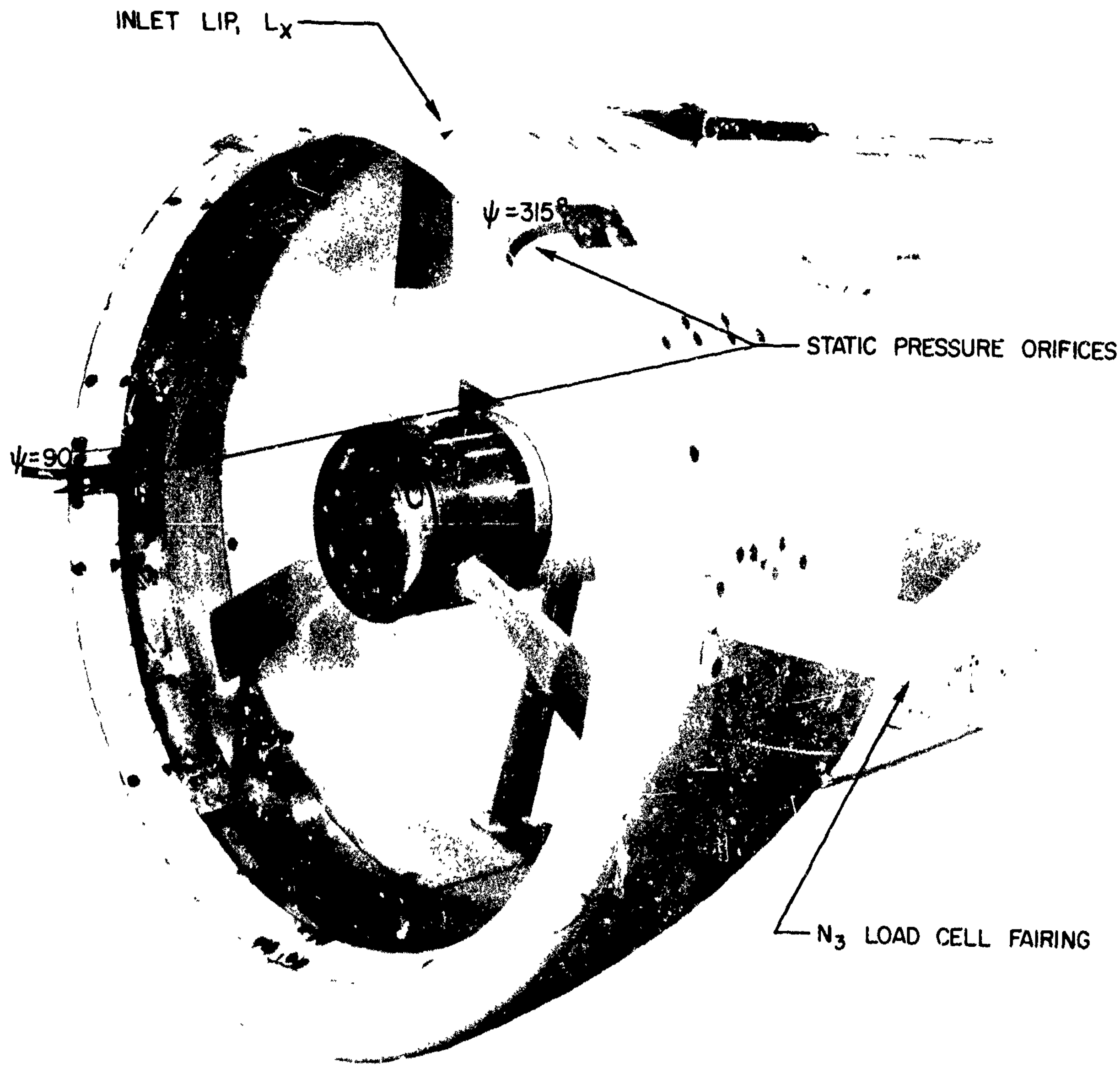

HSD SHROUDED PROPELLER TEST

COMPLETE MODEL SHOWING SPINNER AND INLET VANES INSTALLED

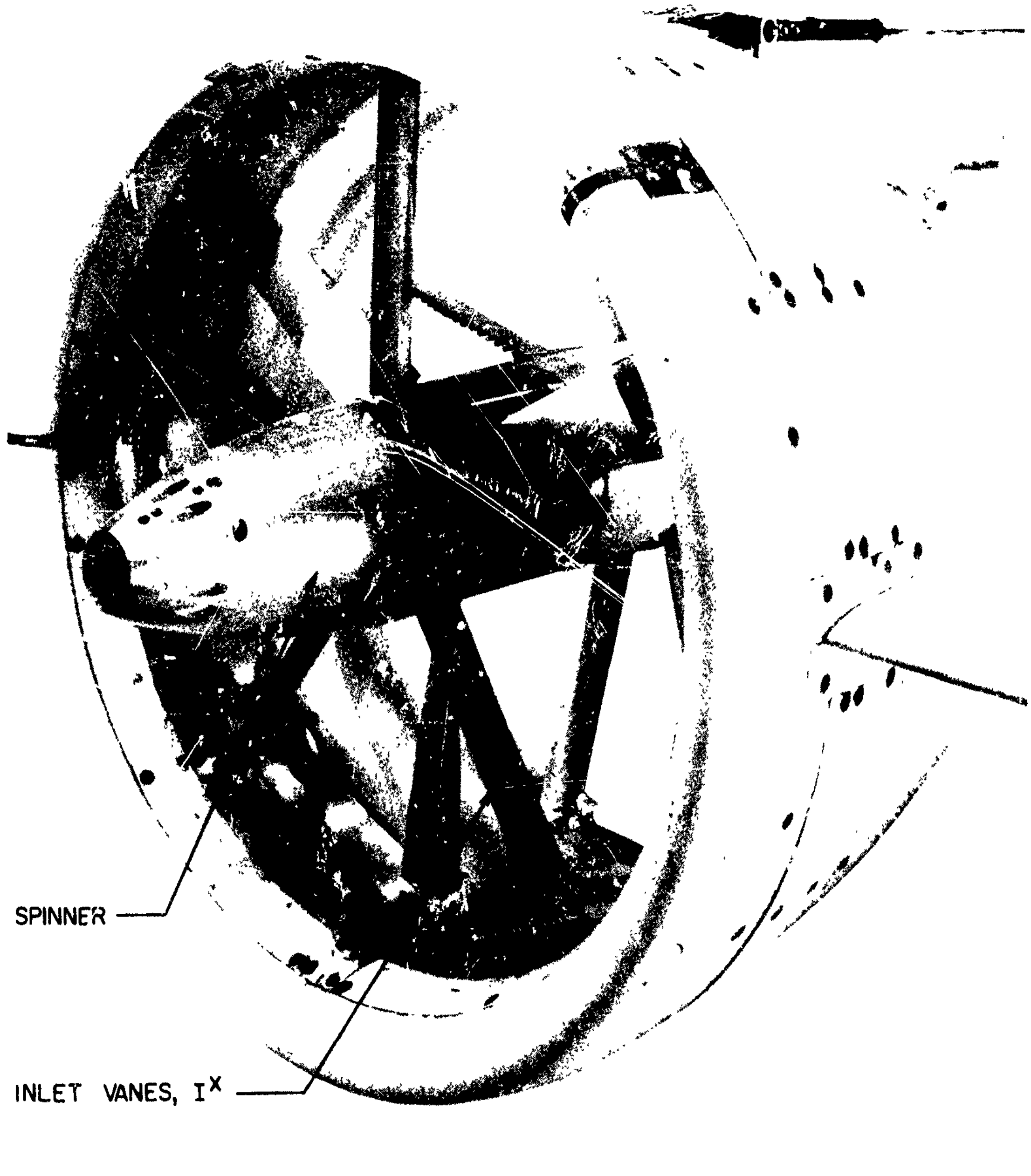

HSD SHROUDED PROPELLER TEST

COMPLETE MODEL SHOWING EXIT VANES AND EXIT RAKE INSTALLED

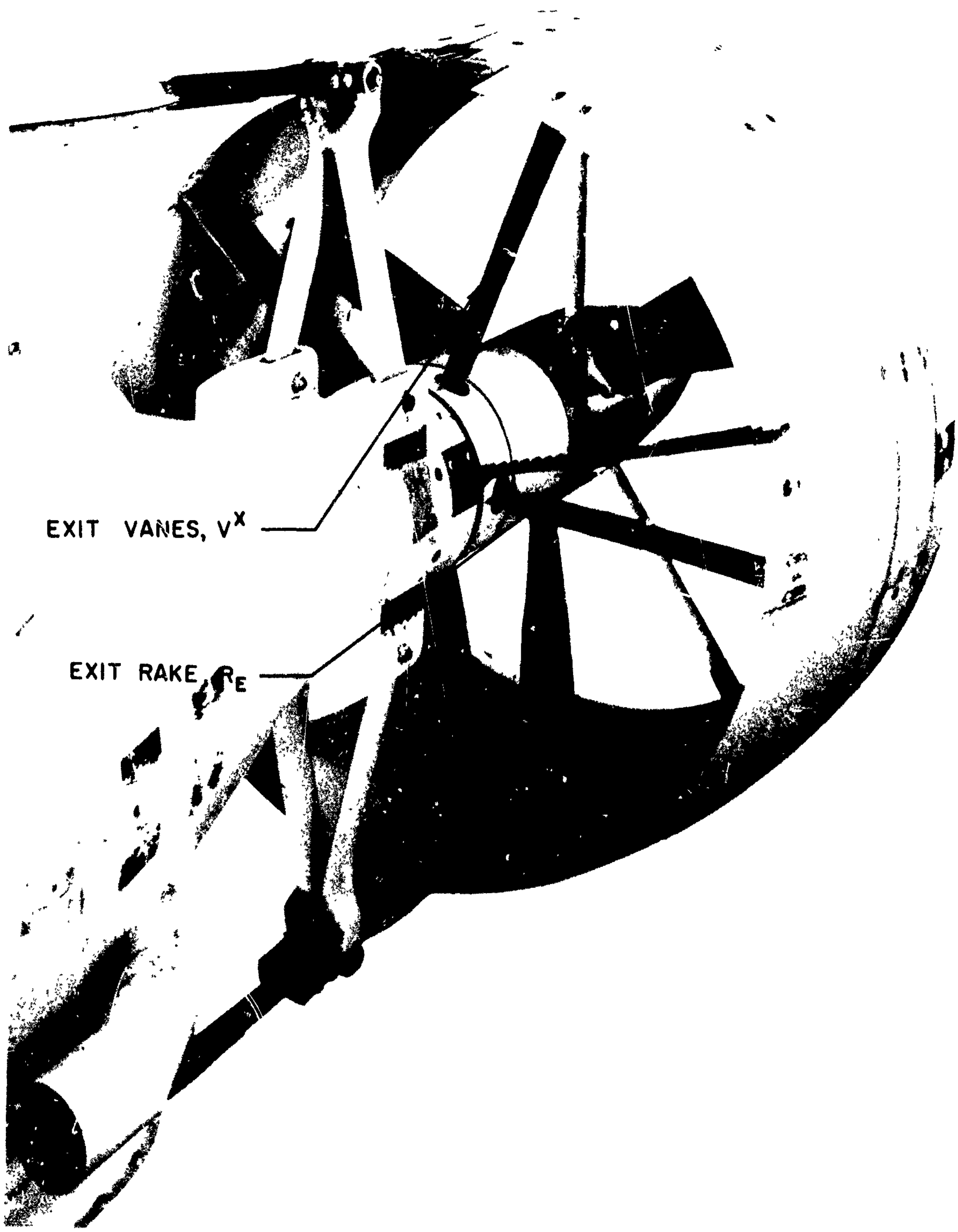

HSD SHROUDED PROPELLER TEST

PROPELLER TEST BLADES

3-WAY	3-WAY	3-WAY	4-WAY
RECTANGULAR, P_R	WIDE TIP, P_{WT}	NARROW TIP, P_{NT}	NARROW TIP, P_{NT}

HSD SHROUDED PROPELLER TEST

RECTANGULAR BLADES INSTALLED IN 3-WAY HUB

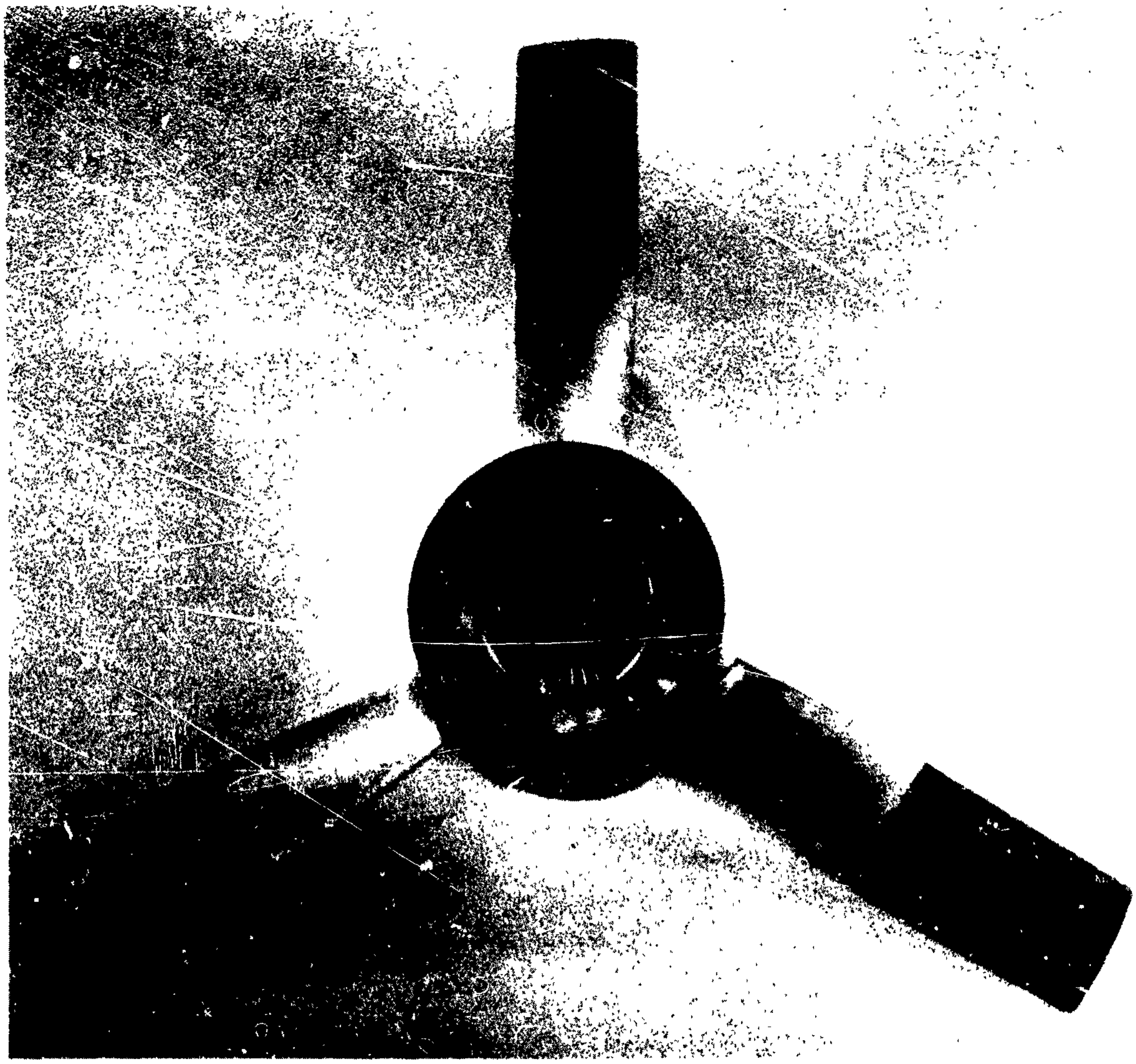

HSD SHROUDED PROPELLER TEST

NARROW TIP BLADES WITH STRAIN GAGE INSTRUMENTATION INSTALLED IN 4-WAY HUB

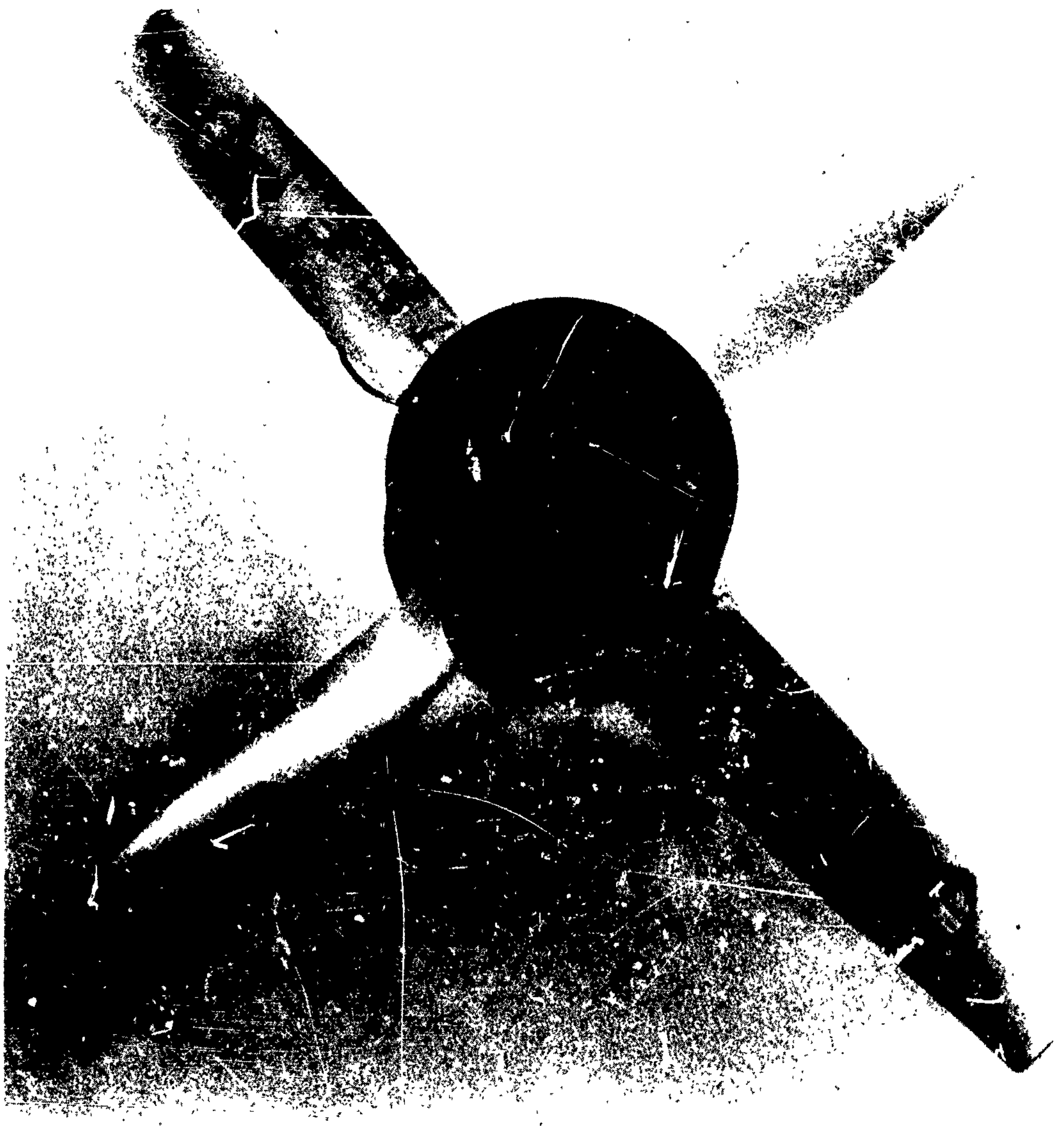

E330590-1

FIG. 17

HSD SHROUDED PROPELLER TEST

COMPARISON OF DATA REPEATABILITY IN 18-FT TEST SECTION

SYM	RUN NO.	MACH NO.	CONFIGURATION	$\theta_{3/4}$
○	94	0.02	$L_1 C_1 E_3 B_3 P_{WT} T_1 R_1 R_E$	30
△	102			
⊡	126		E_4	35
◇	129			

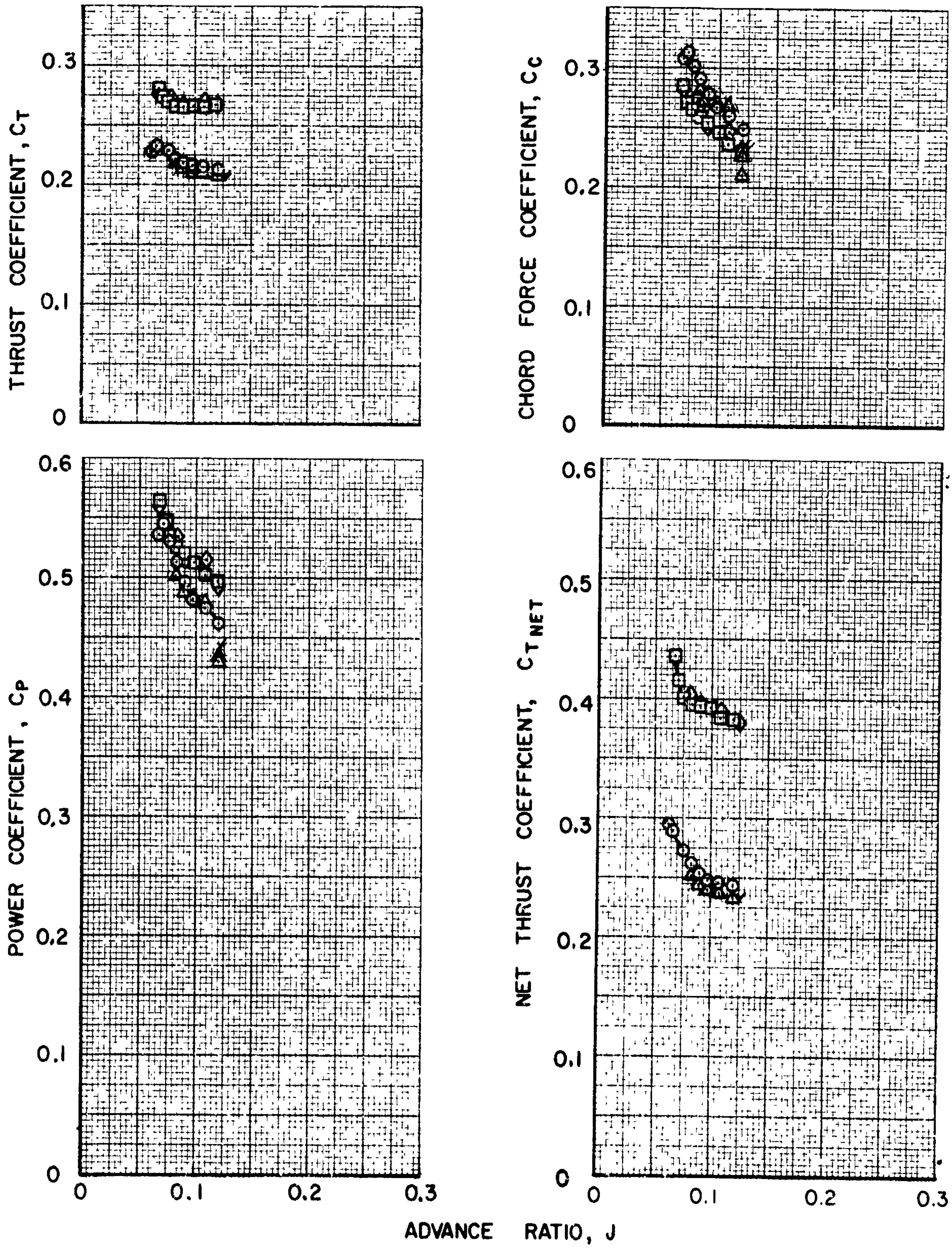

HSD SHROUDED PROPELLER TEST

COMPARISON OF DATA REPEATABILITY IN 18-FT TEST SECTION

SYM	RUN NO.	MACH NO.	CONFIGURATION	$\theta_{3/4}$
⊙	19	0.10	$L_1C_1E_1B_3P_{WT}T_1R_1$	30
△	21	↓	↓	↓
⊡	95	↓	E_3 R_E	↓
◇	103	↓	↓	↓

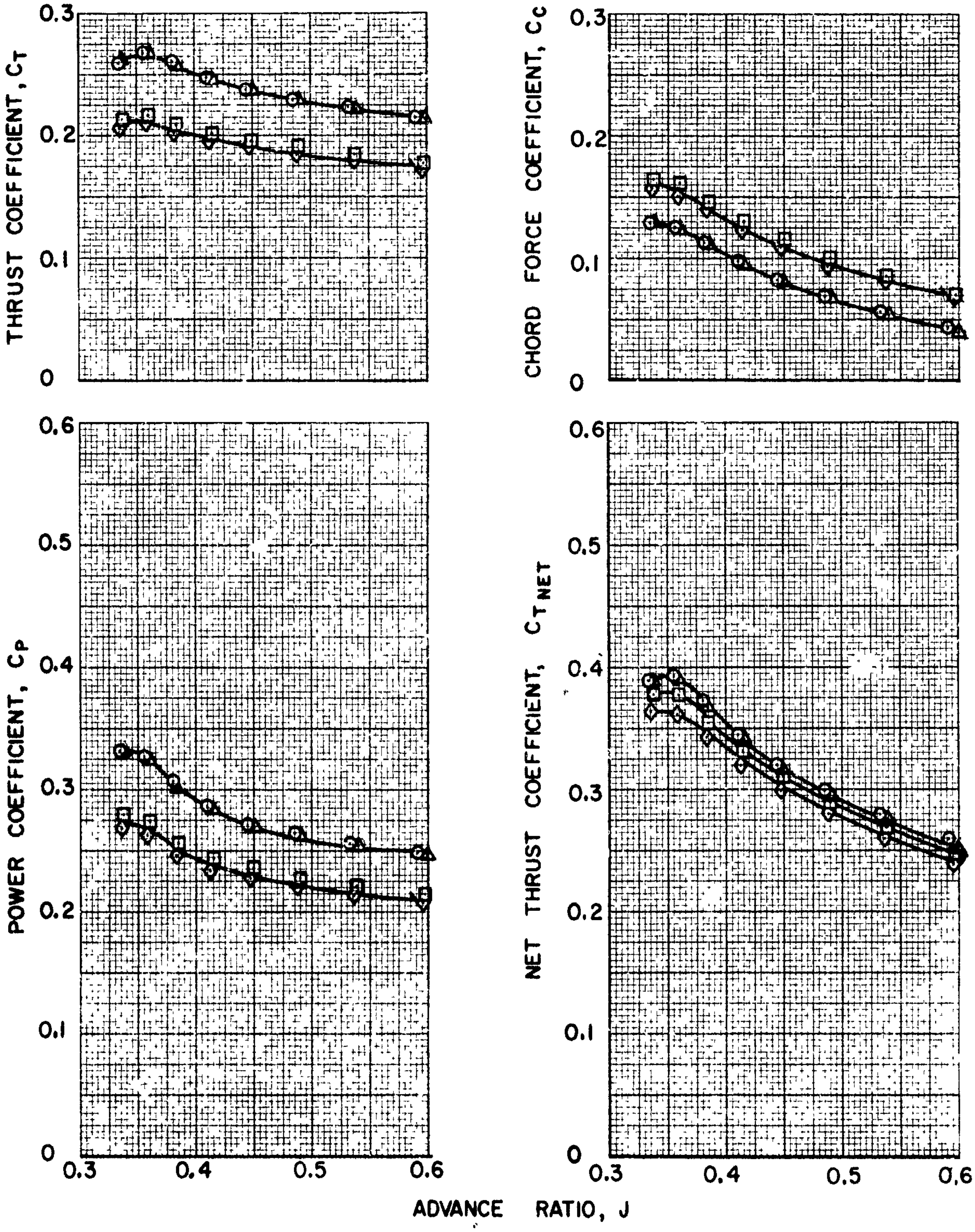

E330590-1

FIG. 19

HSD SHROUDED PROPELLER TEST

COMPARISON OF DATA REPEATABILITY IN 18-FT TEST SECTION

SYM	RUN NO.	MACH NO.	CONFIGURATION	$\theta_{3/4}$
⊙	73	0.20	$L_2 C_1 E, B_3 P_{WT} T_1 R_1 R_E$	25
△	74	↓	↓	↓
⊡	20		L_1	30
◇	34	↓	↓	↓

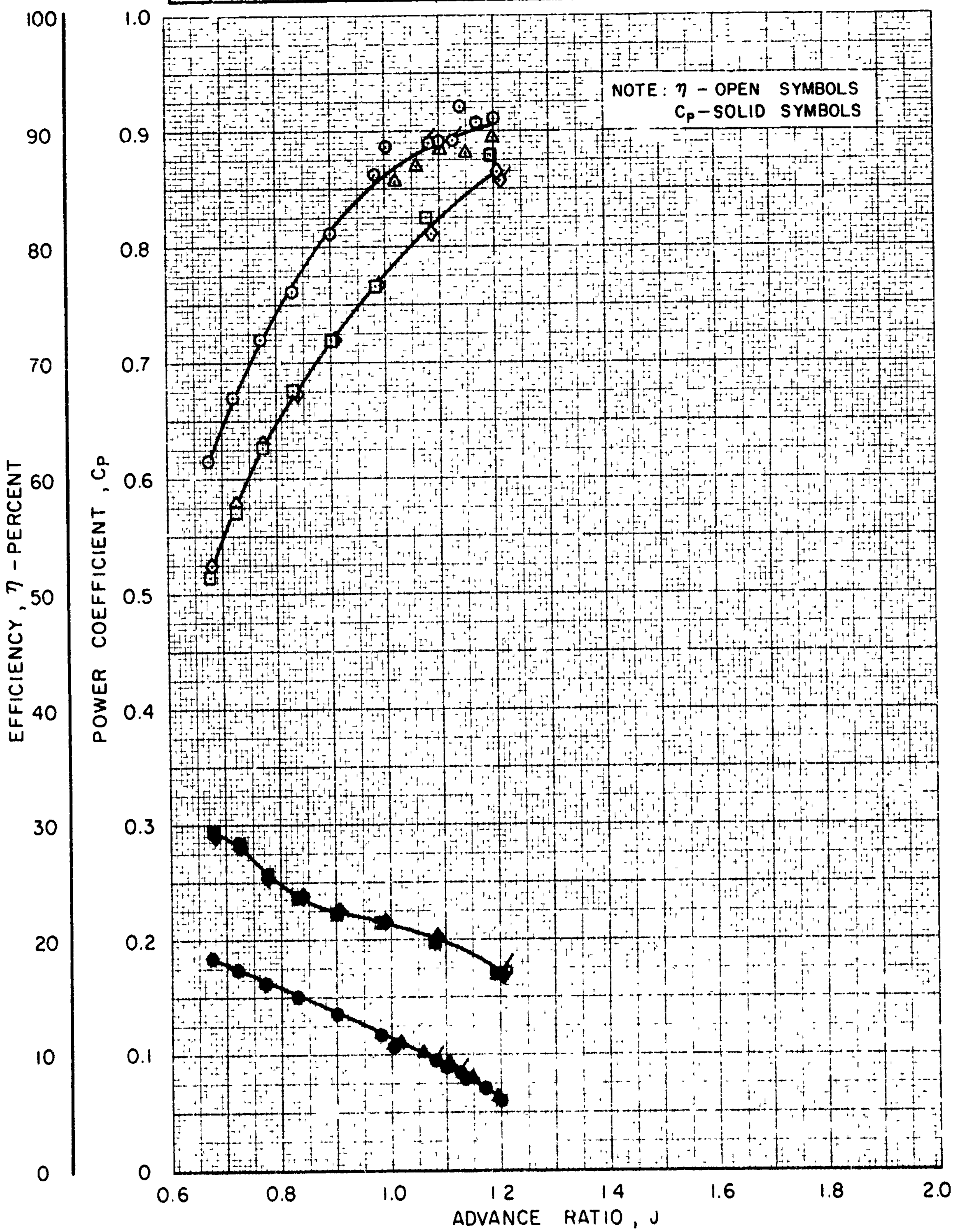

HSD SHROUDED PROPELLER TEST

COMPARISON OF DATA REPEATABILITY IN 18-FT TEST SECTION

SYM	RUN NO.	MACH NO.	CONFIGURATION	$\theta_{3/4}$
○	73	0.20	$L_2 C_1 E_1 B_3 P_{WT} T_1 R_1 R_E$	25
△	74	↓	↓	↓
⊡	20		L_1	30
◇	34	↓	↓	↓

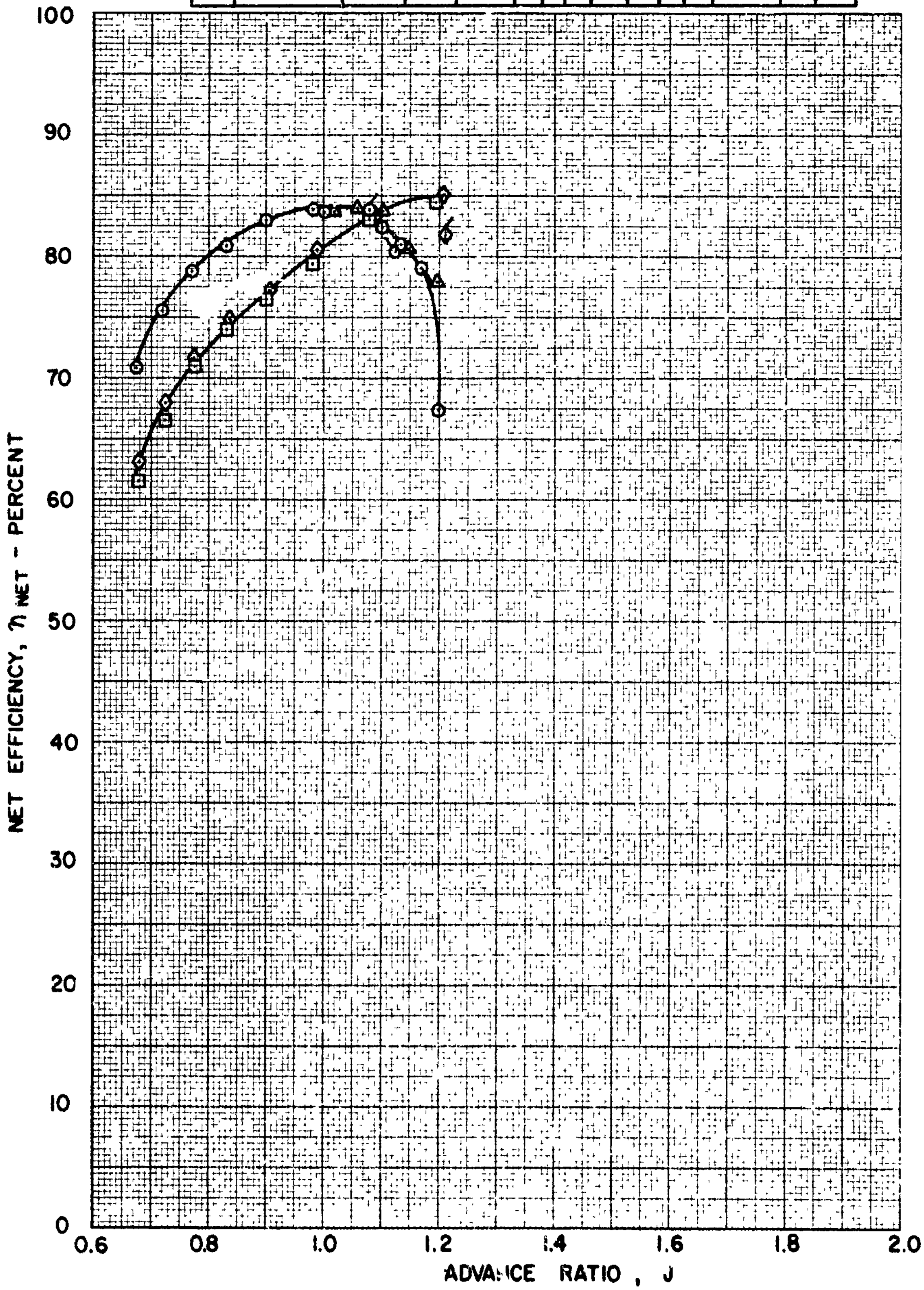

E330590-I

FIG. 21

HSD SHROUDED PROPELLER TEST

COMPARISON OF DATA IN 18- AND 8-FT TEST SECTIONS

SYM	RUN NO.	MACH NO.	CONFIGURATION	$\theta_{3/4}$
⊙	190 (18 FT)	0.20	$L_1 C_1 E_1 B_4 P_{NT} T_1 R_1 R_E$	20
△	434 (8 FT)	↓	↓ ↓ ↓ ↓ ↓ ↓ ↓ ↓	↓

NOTE: η - OPEN SYMBOLS C_P - SOLID SYMBOLS

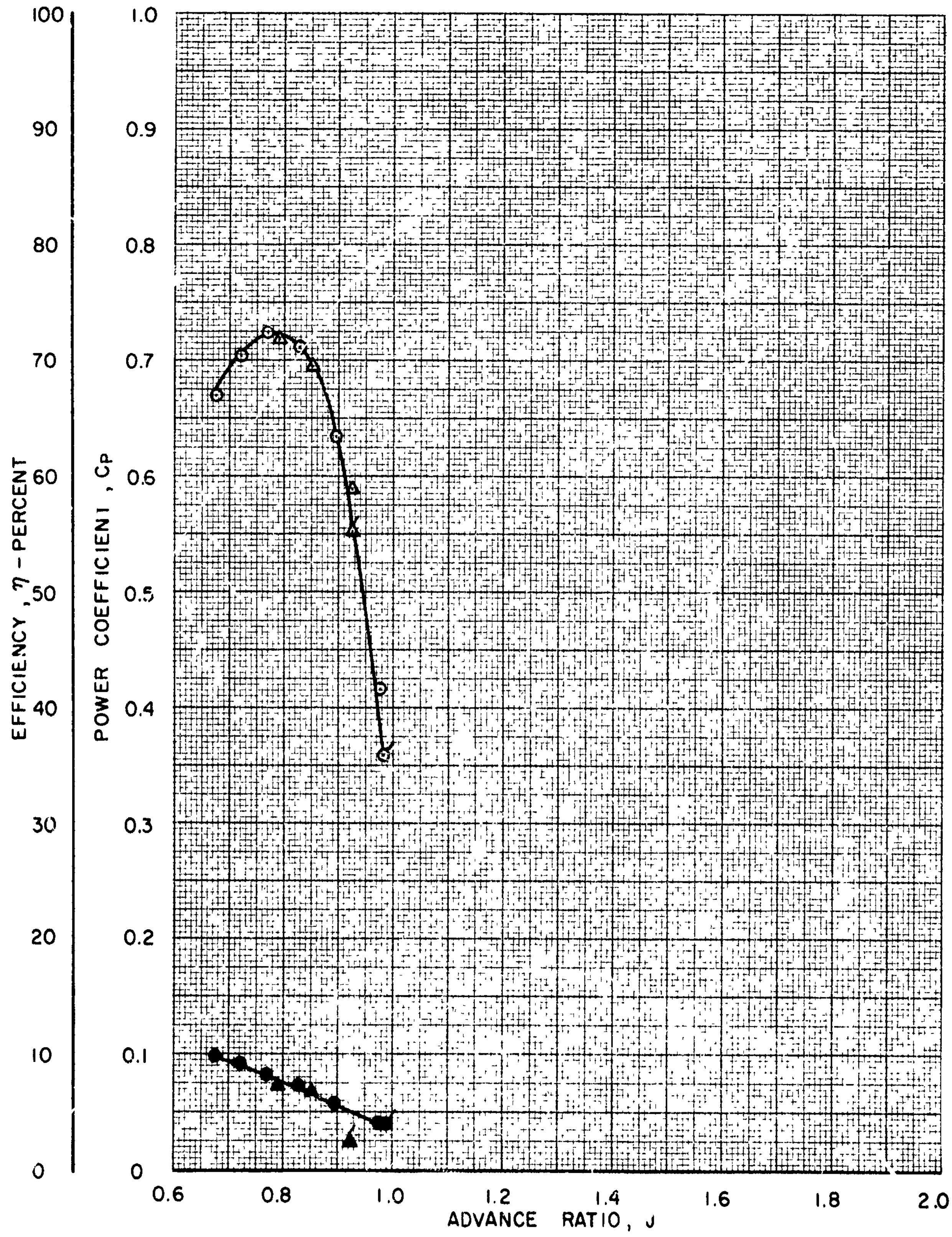

HSD SHROUDED PROPELLER TEST

COMPARISON OF DATA IN 18-AND 8-FT TEST SECTIONS

SYM	RUN NO.	MACH NO.	CONFIGURATION	$\theta_{3/4}$
O	190 (18 FT)	0.20	$L_1 C_1 E_1 B_4 P_{NT} T_1 R_1 R_E$	20
Δ	434 (8 FT)	↓	↓ ↓ ↓ ↓ ↓ ↓ ↓ ↓	↓

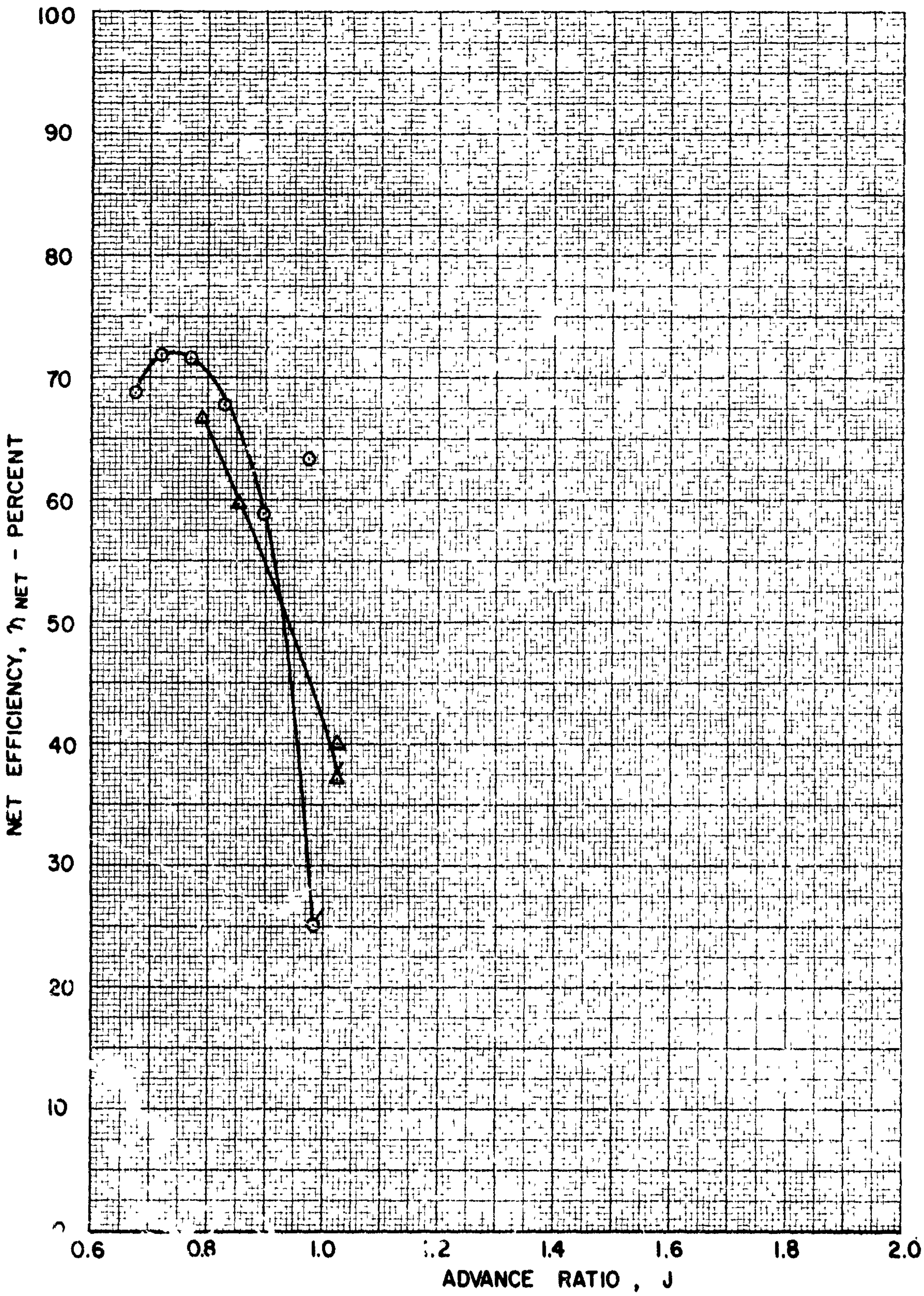

HSD SHROUDED PROPELLER TEST

COMPARISON OF DATA REPEATABILITY IN 8-FT TEST SECTION

SYM	RUN NO.	MACH NO.	CONFIGURATION	$\theta_{3/4}$
⊙	642	0.30	$L_1 C_1 E_1 B_3 P_R T_3 R_1 R_E$	34
△	648	↓	↓	↓

NOTE: η - OPEN SYMBOLS C_P - SOLID SYMBOLS

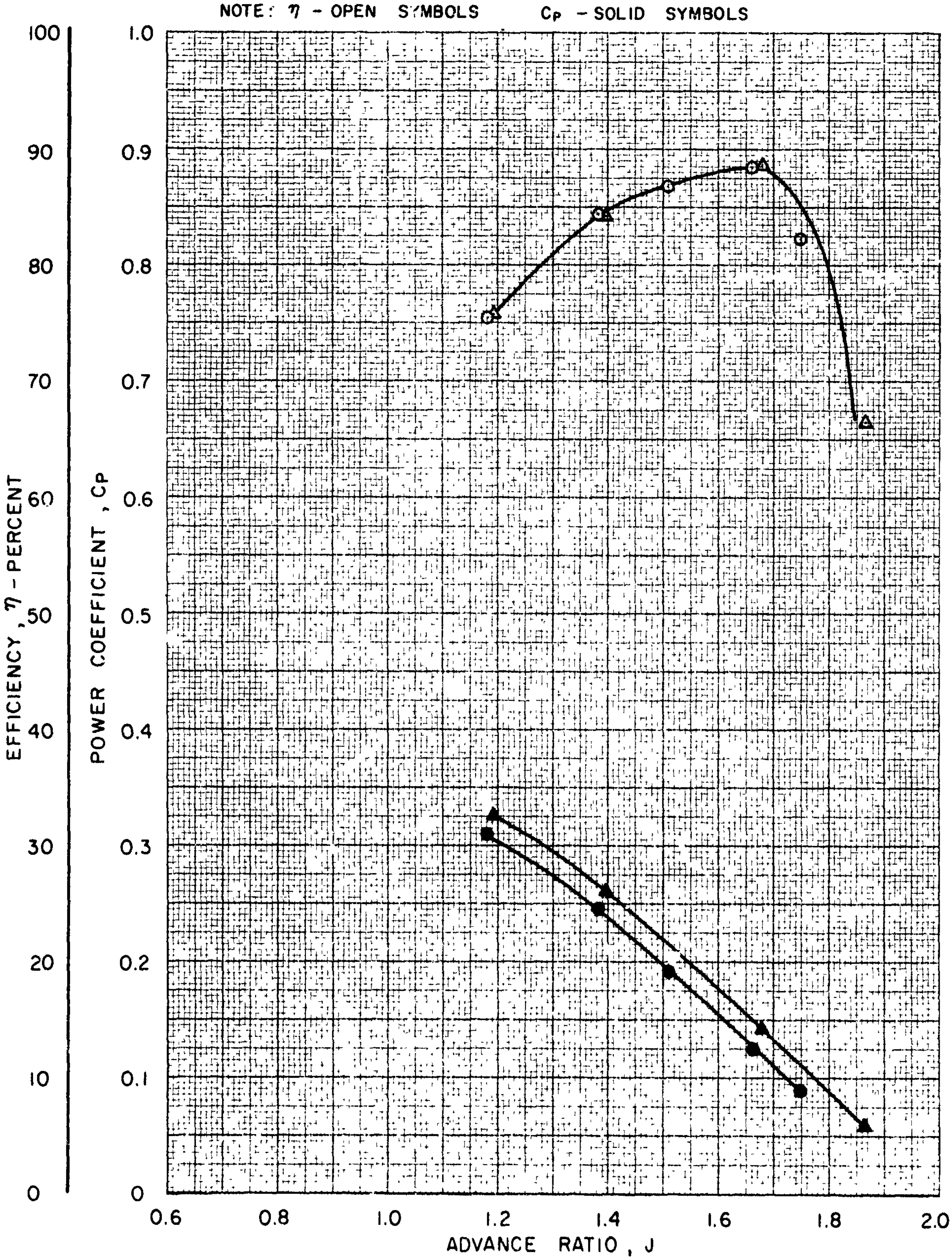

E330590-1

FIG. 24

HSD SHROUDED PROPELLER TEST

COMPARISON OF DATA REPEATABILITY IN 8-FT TEST SECTION

SYM	RUN NO.	MACH NO.	CONFIGURATION	$\theta_{3/4}$
⊙	642	0.30	$L_1 C_1 E_1 B_3 P_R T_3 R_1 R_E$	34
Δ	648	↓	↓ ↓ ↓ ↓ ↓ ↓ ↓ ↓	↓

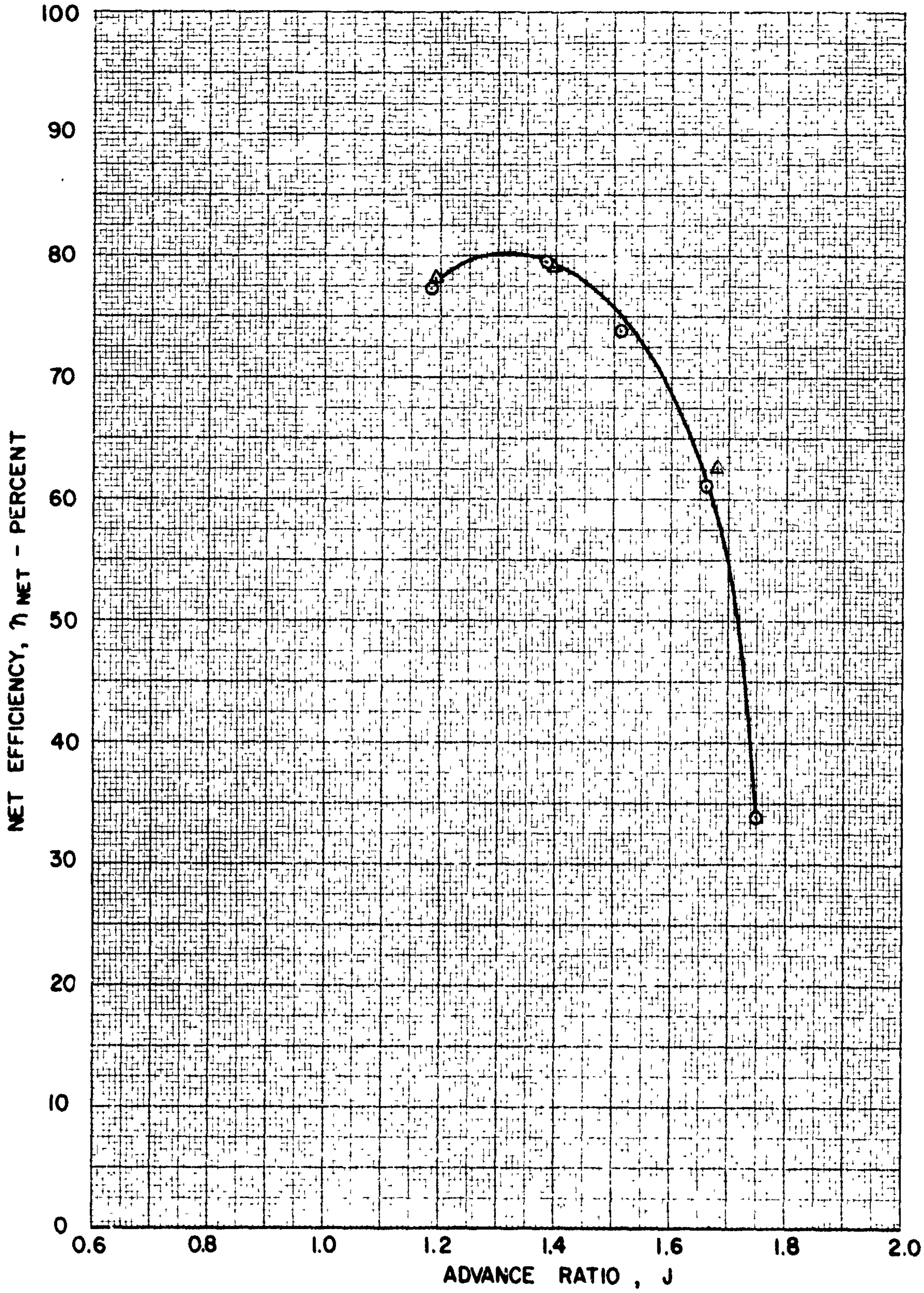

E330590-1 FIG. 25

HSD SHROUDED PROPELLER TEST

COMPARISON OF DATA REPEATABILITY IN 8 - FT TEST SECTION

SYM	RUN NO.	MACH NO.	CONFIGURATION	$\theta_{3/4}$
⊙	469	0.40	$L_1 C_1 E_1 B_3 P_{WT} T_1 R_1 R_E$	38
△	470	↓	↓	↓
⊡	479	↓	↓	50
◇	482	↓	↓	↓

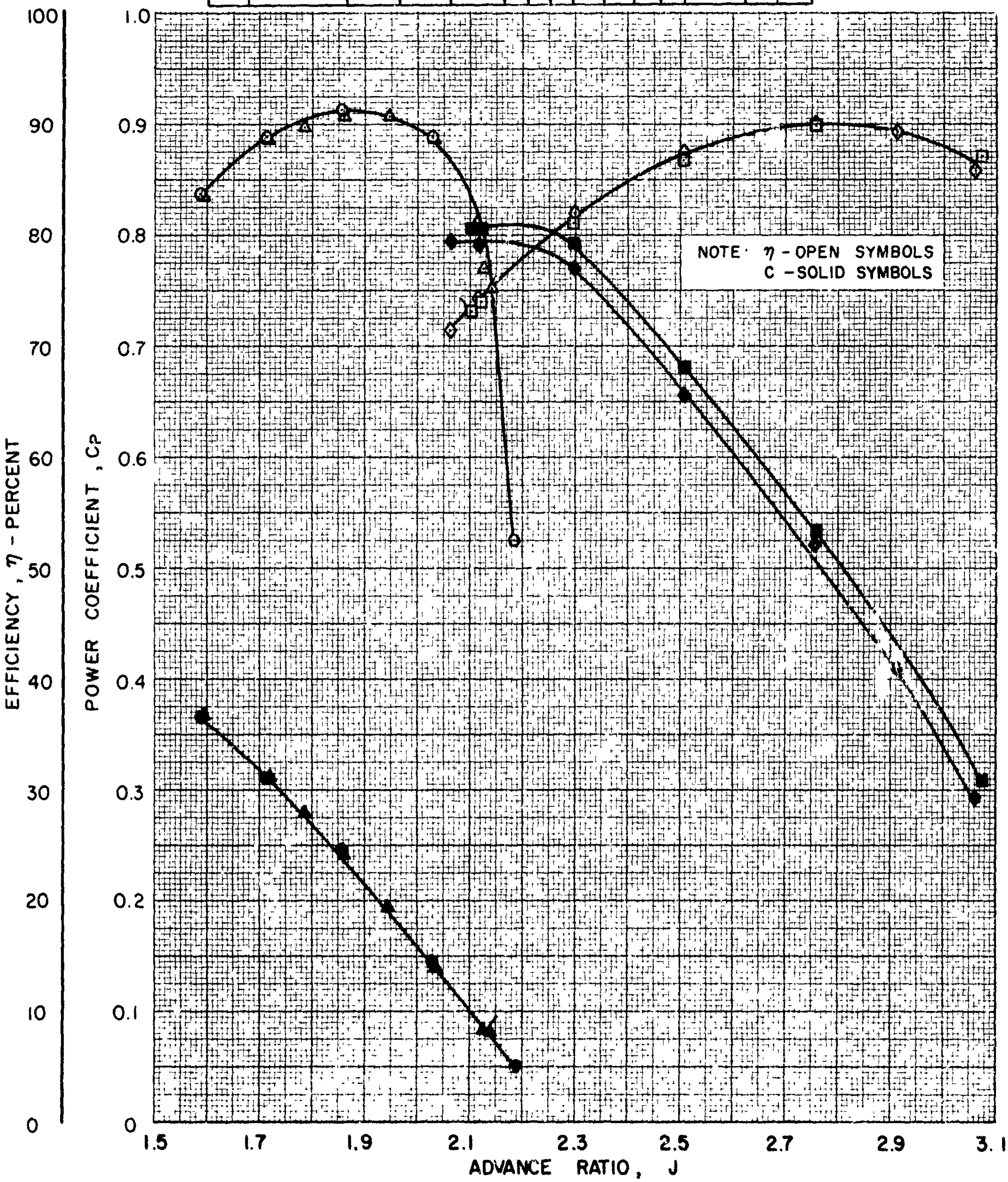

E330590-1 FIG. 26

HSD SHROUDED PROPELLER TEST

COMPARISON OF DATA REPEATABILITY IN 8 - FT TEST SECTION

SYM	RUN NO.	MACH NO.	CONFIGURATION	$\theta_{3/4}$
⊙	469	0.40	$L_1 C_1 E_1 B_3 P_{WT} T_1 R_1 R_E$	38
△	470	↓	↓	↓
⊡	479	↓	↓	50
◇	482	↓	↓	↓

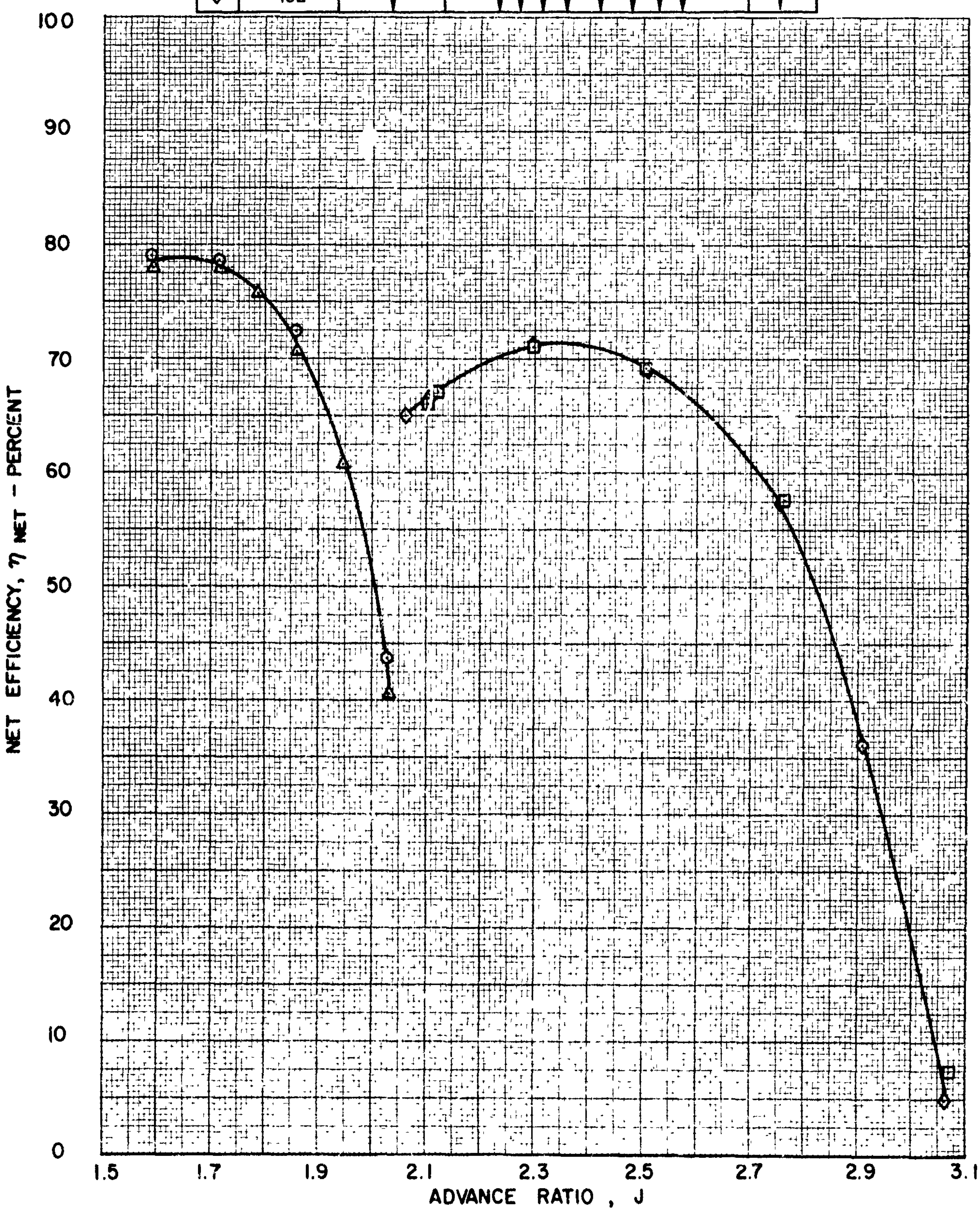

E330590-1

FIG. 27

HSD SHROUDED PROPELLER TEST

EFFECT OF BLADE ANGLE ON PROPELLER PERFORMANCE

SYM	RUN NO	MACH NO	CONFIGURATION	$\theta_{3/4}$
□	134, 133	0.05, 0.10	$B_3\ P_{WT}\ R_1\ R_E$	25
◇	132, 131	↓ ↓	↓ ↓ ↓ ↓	30

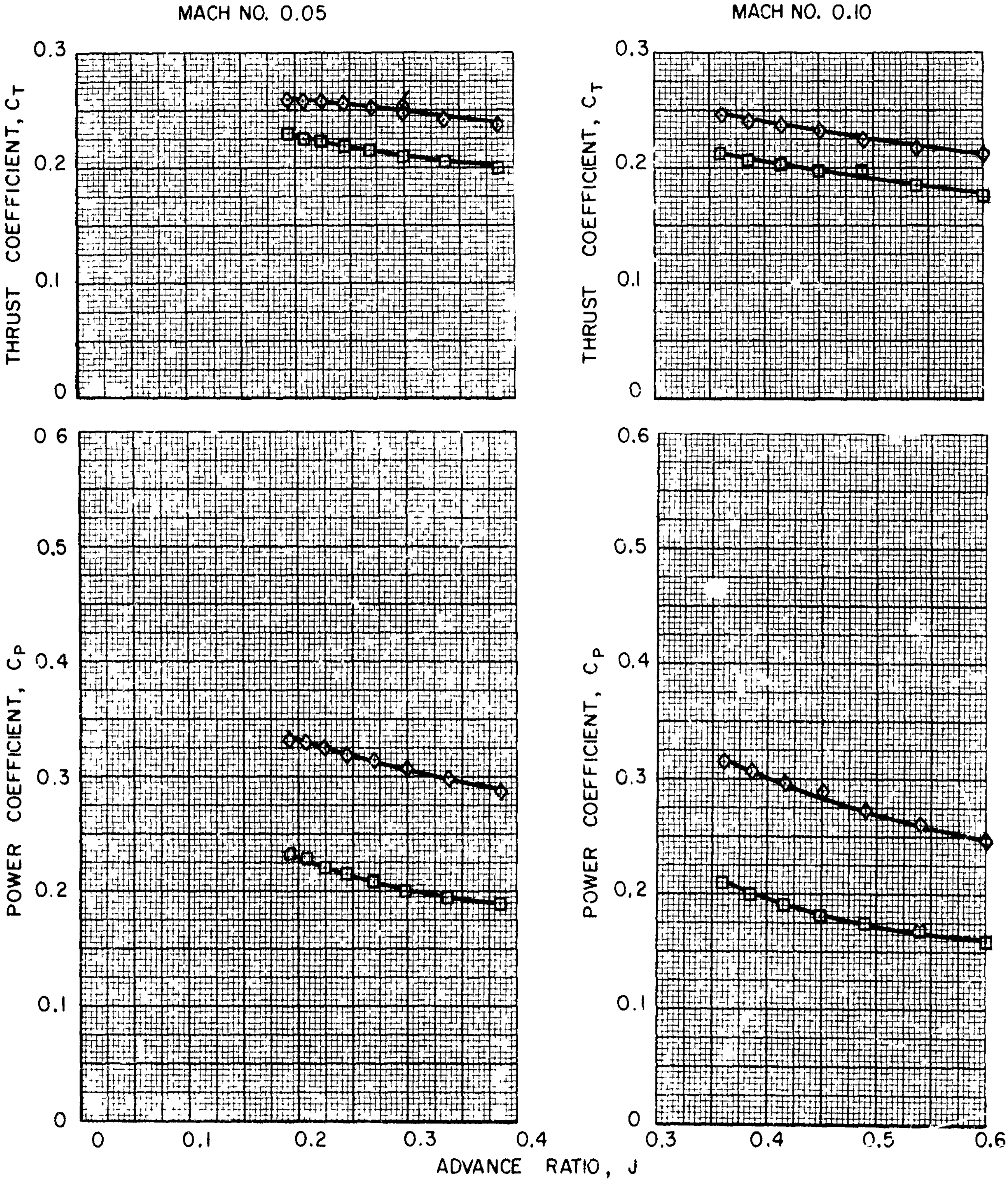

HSD SHROUDED PROPELLER TEST
EFFECT OF BLADE ANGLE ON SHROUDED PROPELLER PERFORMANCE

SYM	RUN NO	MACH NO	CONFIGURATION	$\theta_{3/4}$
⊙	260,261	0.02,0.05	$L_1 C_1 E_1 B_3 P_{WT} T_1 R_1 R_E, R_E$	15
△	263,36	↓	↓ , –	20
□	267,41	↓	↓ , R_E	25
◇	– ,32	↓	↓ , –	30
⊿	270,46	↓	↓ , R_E	35

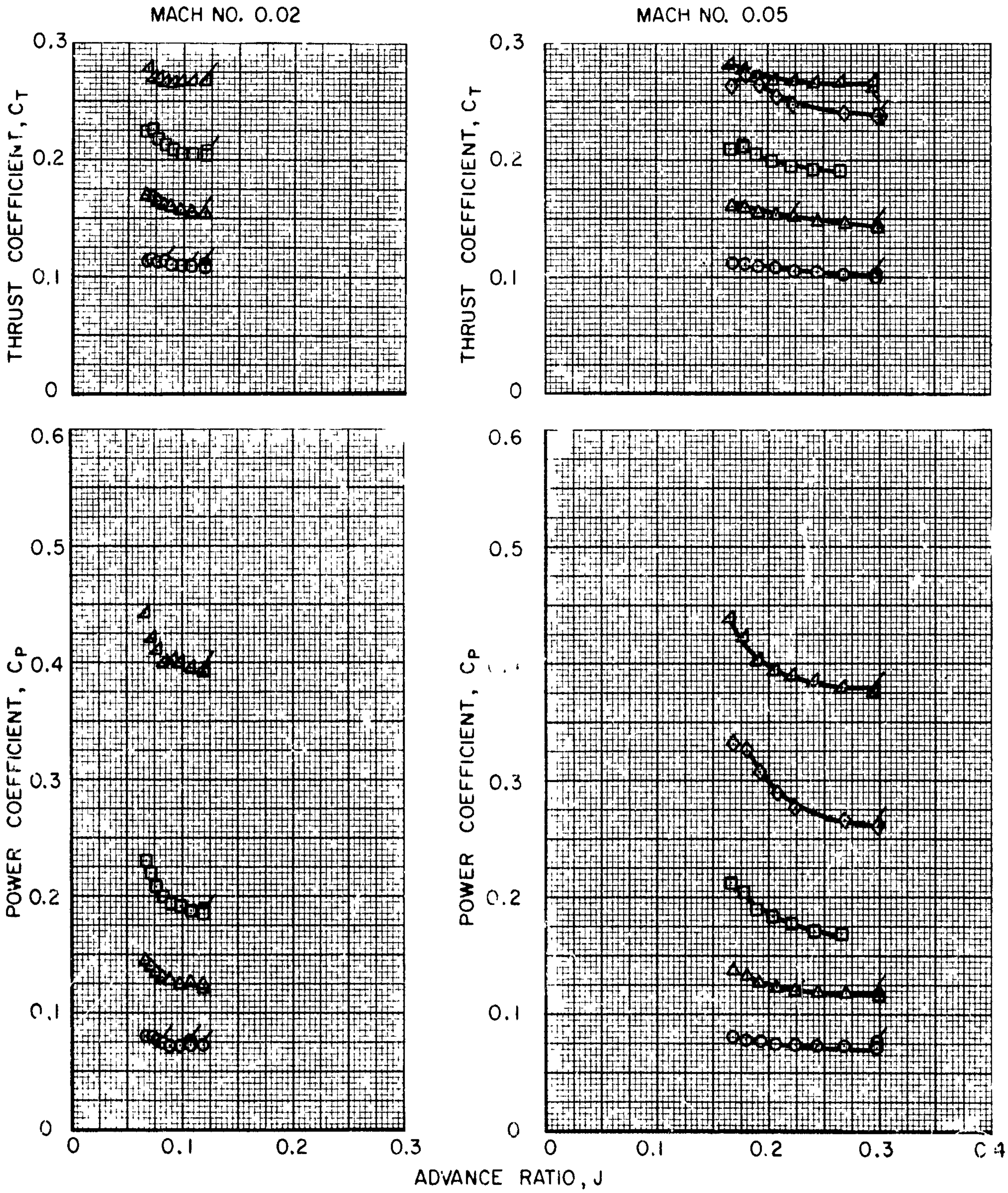

HSD SHROUDED PROPELLER TEST
EFFECT OF BLADE ANGLE ON SHROUDED PROPELLER PERFORMANCE

SYM	RUN NO	MACH NO.	CONFIGURATION	$\theta_{3/4}$
○	260,261	0.02,0.05	$L_1 C_1 E_1 B_3 P_{WT} T_1 R_1 R_E, R_E$	15
△	263,36	↓	↓ , —	20
□	267,41	↓	↓ , R_E	25
◇	— ,32	↓	↓ , —	30
⊿	270,46	↓	↓ , R_E	35

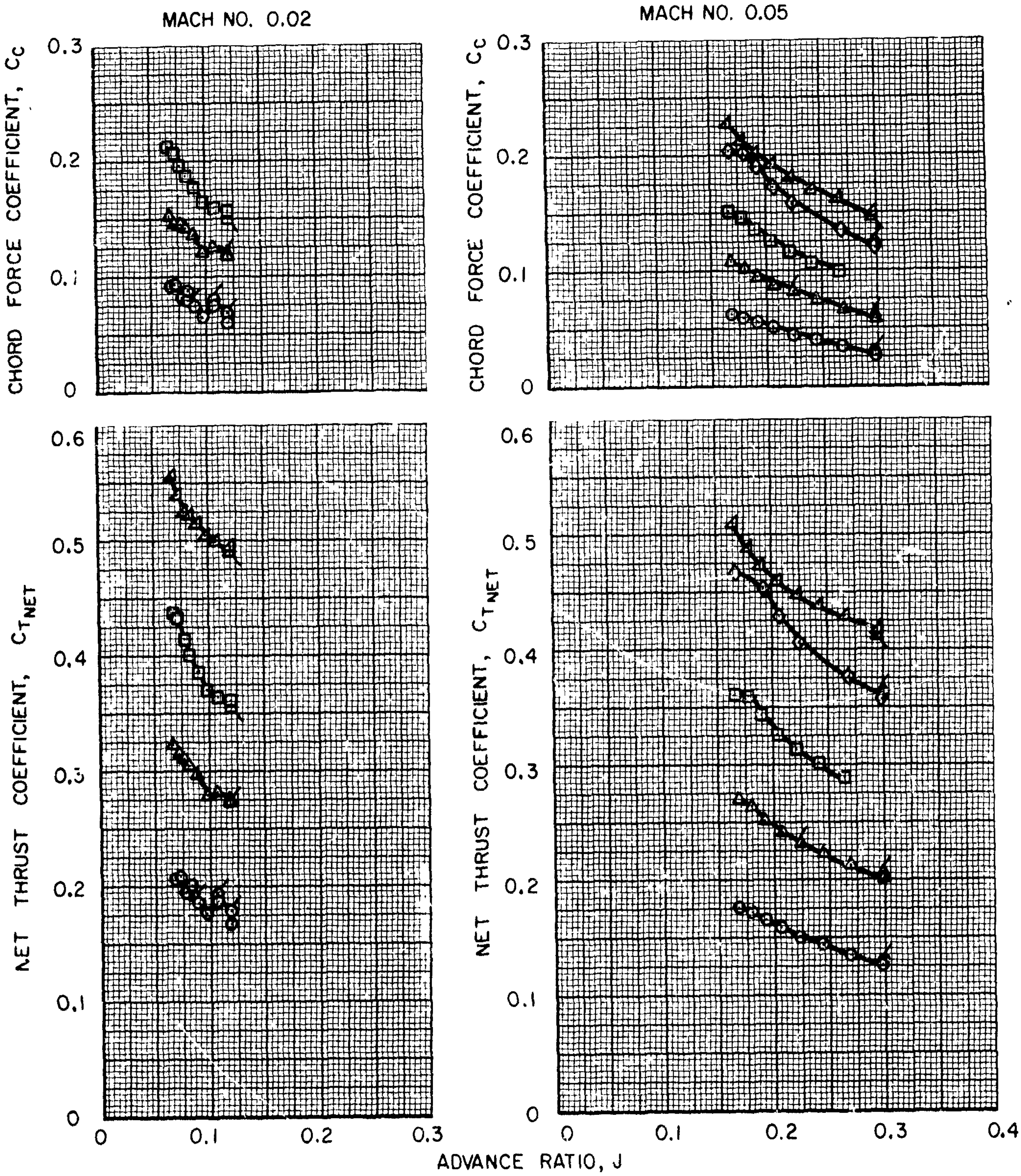

HSD SHROUDED PROPELLER TEST

EFFECT OF BLADE ANGLE ON SHROUDED PROPELLER PERFORMANCE

SYM	RUN NO	MACH NO.	CONFIGURATION	$\theta_{3/4}$
○	262, —	0.10, —	$L_1 C_1 E_1 B_3 P_{WT} T_1 R_1 R_E, R_E$	15
△	37, 264	0.15	—,	20
□	42, 266		R_E,	25
◇	33, 268		—,	30
⊿	45, 269		R_E,	35
▽	271, 272		R_E,	40

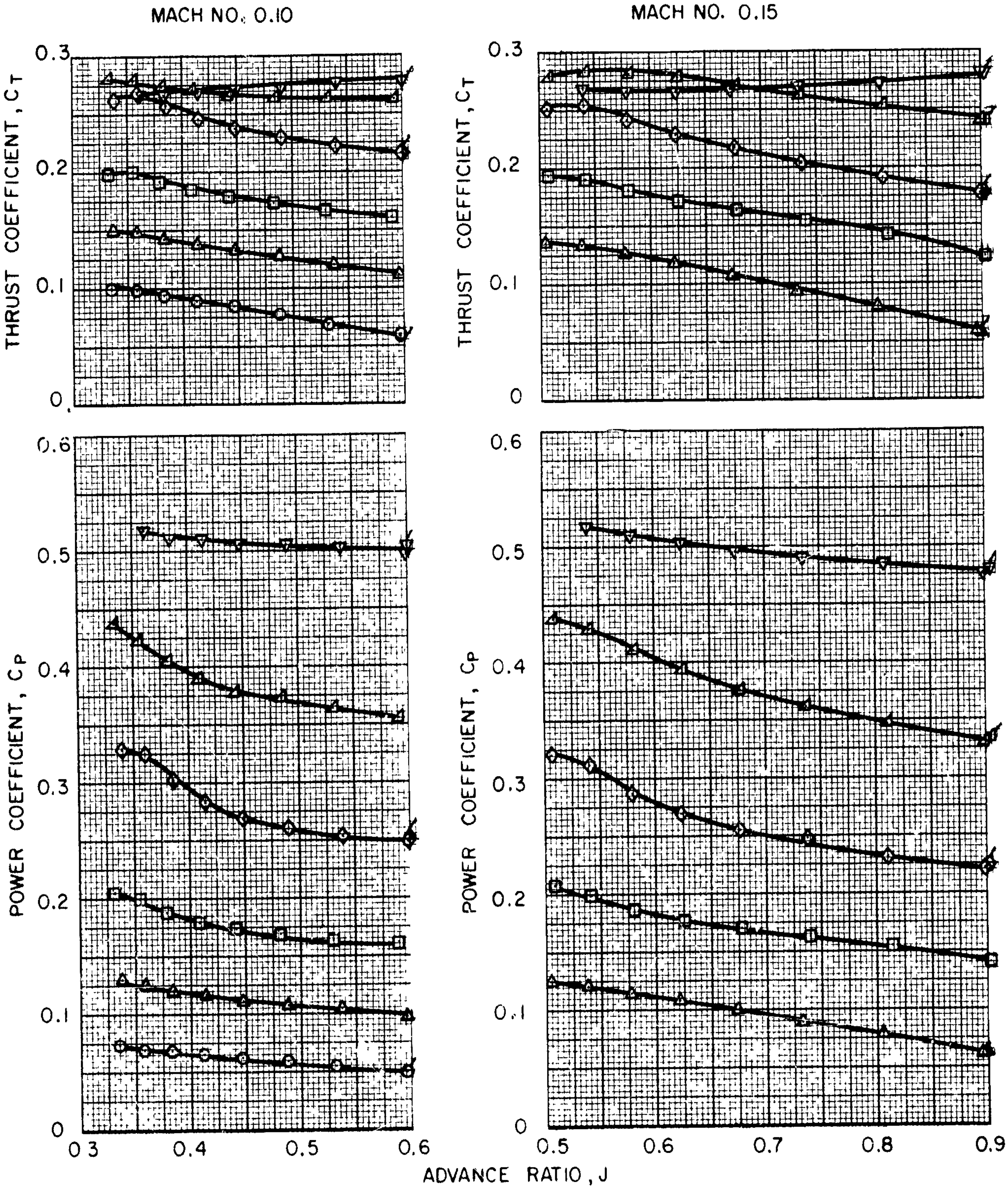

HSD SHROUDED PROPELLER TEST

EFFECT OF BLADE ANGLE ON SHROUDED PROPELLER PERFORMANCE

SYM	RUN NO	MACH NO	CONFIGURATION	$\theta_{3/4}$
○	262, —	0.10, —	$L_1C_1E_1B_3P_{WT}T_1R_1R_E, R_E$	15
△	37, 264	0.15	—,	20
□	42, 266		R_E,	25
◇	33, 268		—,	30
⊿	45, 269		R_E,	35
▽	271, 272		R_E,	40

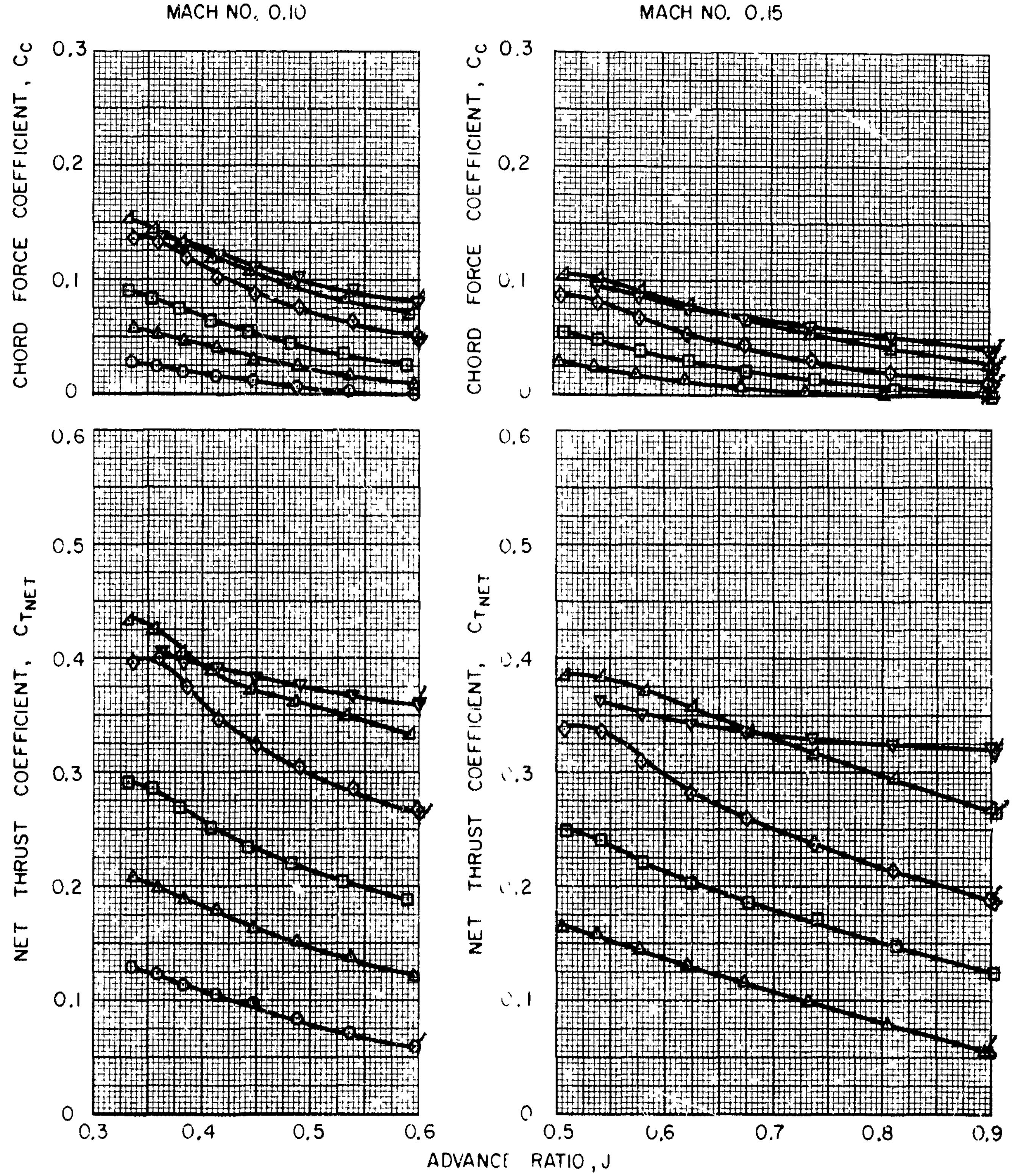

E330590-1

FIG. 32

HSD SHROUDED PROPELLER TEST

EFFECT OF BLADE ANGLE ON SHROUDED PROPELLER PERFORMANCE

SYM	RUN NO	MACH NO.	CONFIGURATION	$\theta_{3/4}$
△	265	0.20	$L_1 C_1 E_1 B_3 P_{WT} T_1 R_1 R_E$	20
□	43			25
◇	34			30
◺	44		R_E	35
▽	39			40

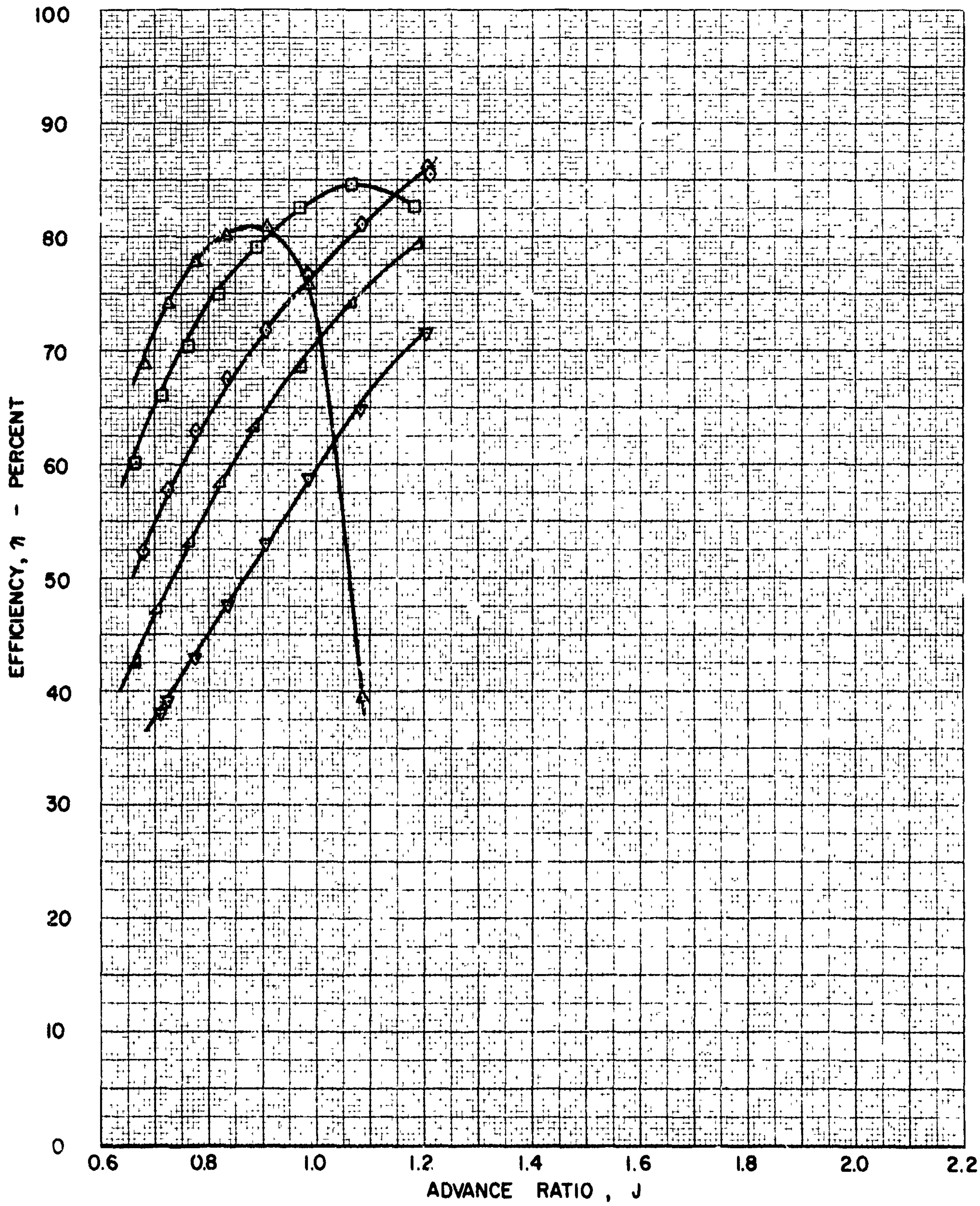

E330590-1 FIG.33

HSD SHROUDED PROPELLER TEST

EFFECT OF BLADE ANGLE ON SHROUDED PROPELLER PERFORMANCE

SYM	RUN NO	MACH NO	CONFIGURATION	$\theta_{3/4}$
△	265	0 20	$L_1 C_1 E_1 B_3 P_{WT} T_1 R_1 R_E$	20
⊡	43	↓	↓	25
◇	34	↓	↓	30
⊿	44	↓	R_E	35
▽	39	↓	↓	40

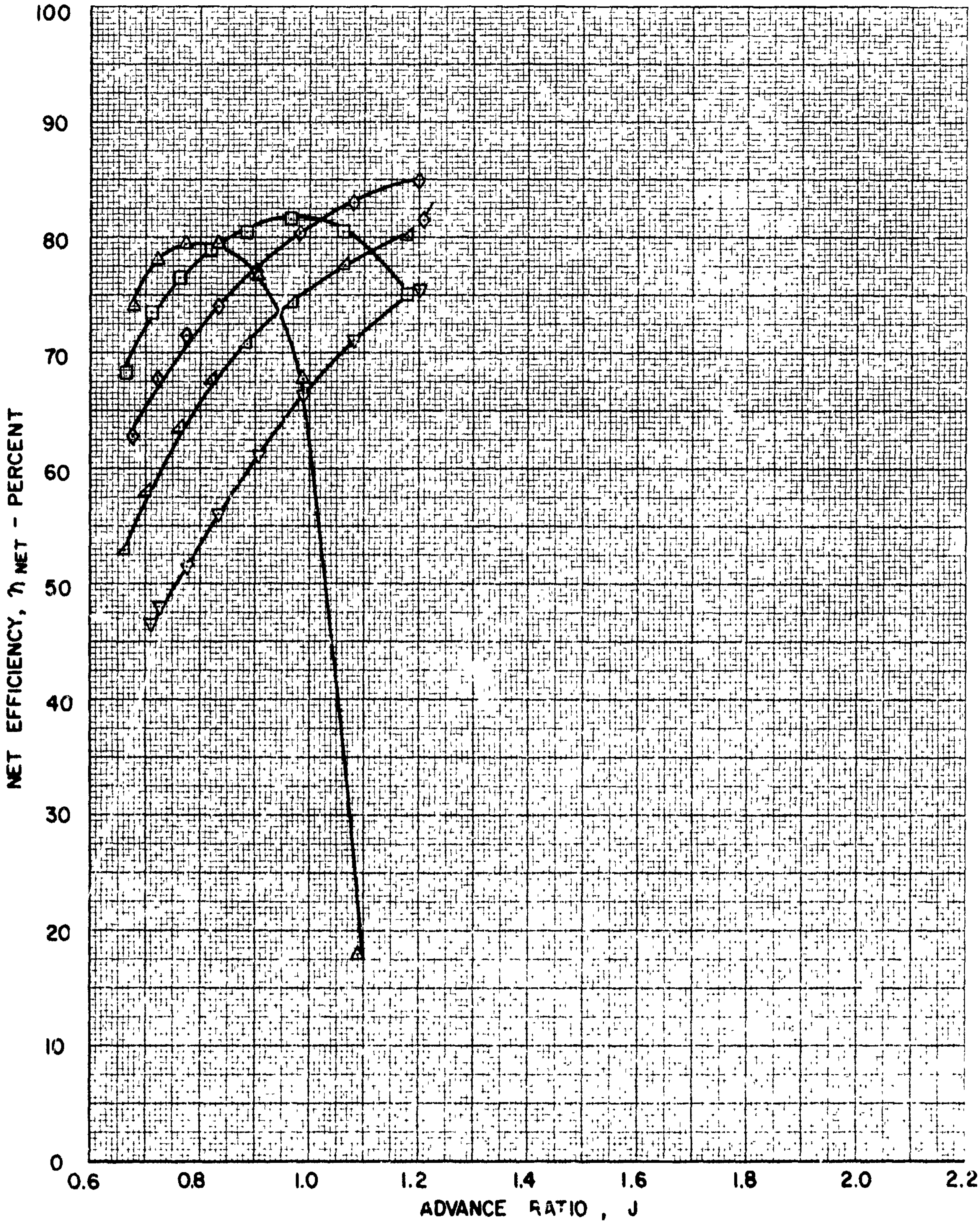

E330590-I

FIG. 34

HSD SHROUDED PROPELLER TEST

EFFECT OF BLADE ANGLE ON SHROUDED PROPELLER PERFORMANCE

SYM	RUN NO.	MACH NO.	CONFIGURATION	$\theta_{3/4}$
△	265	0.20	$L_1 C_1 E_1 B_3 P_{WT} T_1 R_1 R_E$	20
□	43			25
◇	34			30
◿	44		R_E	35
▽	39			40

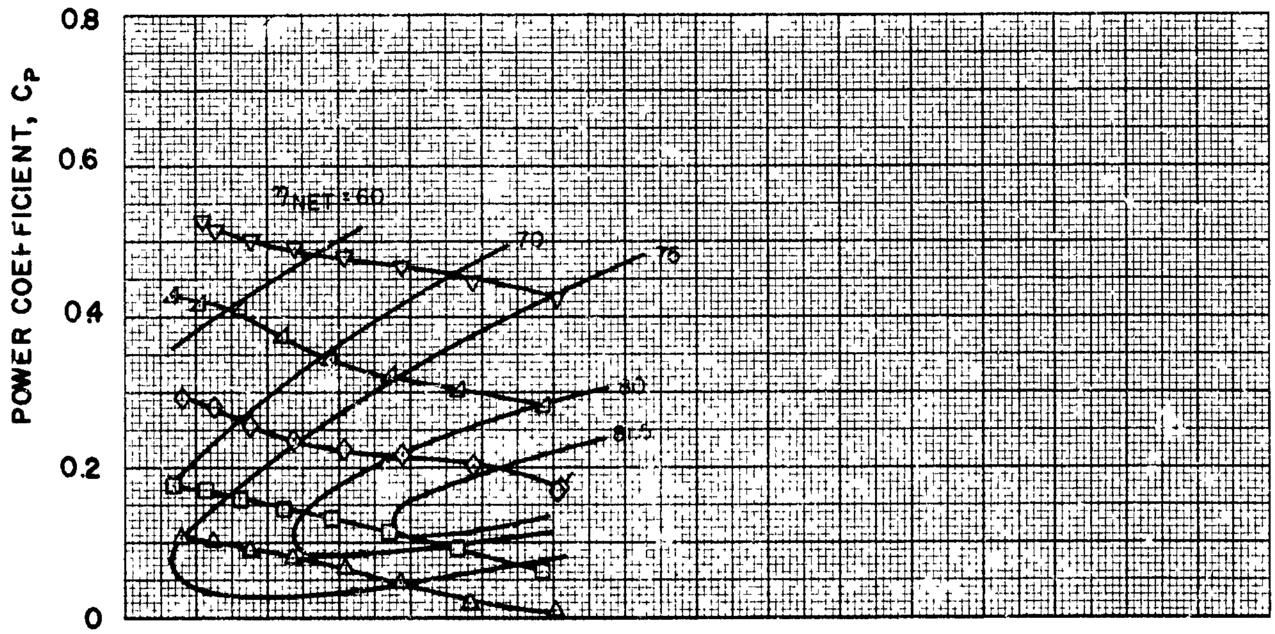

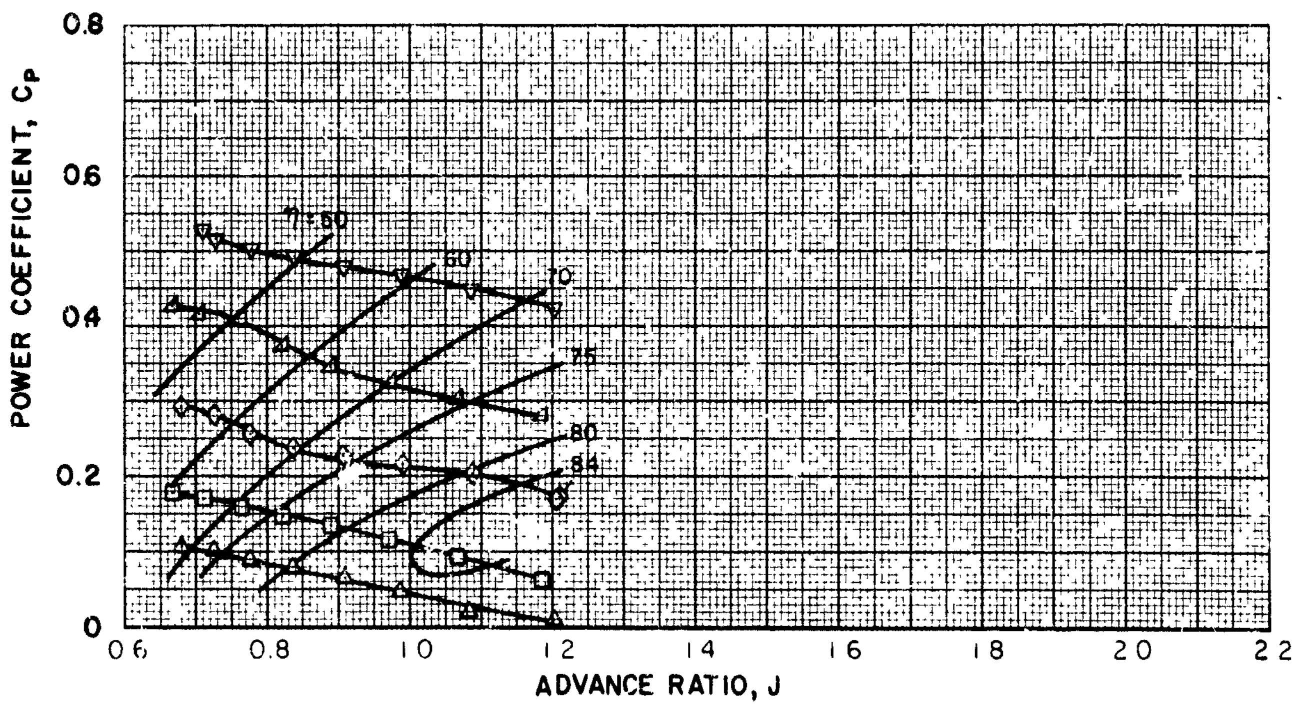

E330590-1

FIG. 35

HSD SHROUDED PROPELLER TEST

EFFECT OF BLADE ANGLE ON SHROUDED PROPELLER PERFORMANCE

SYM	RUN NO.	MACH NO.	CONFIGURATION	$\theta_{3/4}$
◇	465	0.30	$L_1 C_1 E_1 B_3 P_{WT} T_1 R_1 R_E$	30
⊿	466			34
▽	468			38
D	472			42

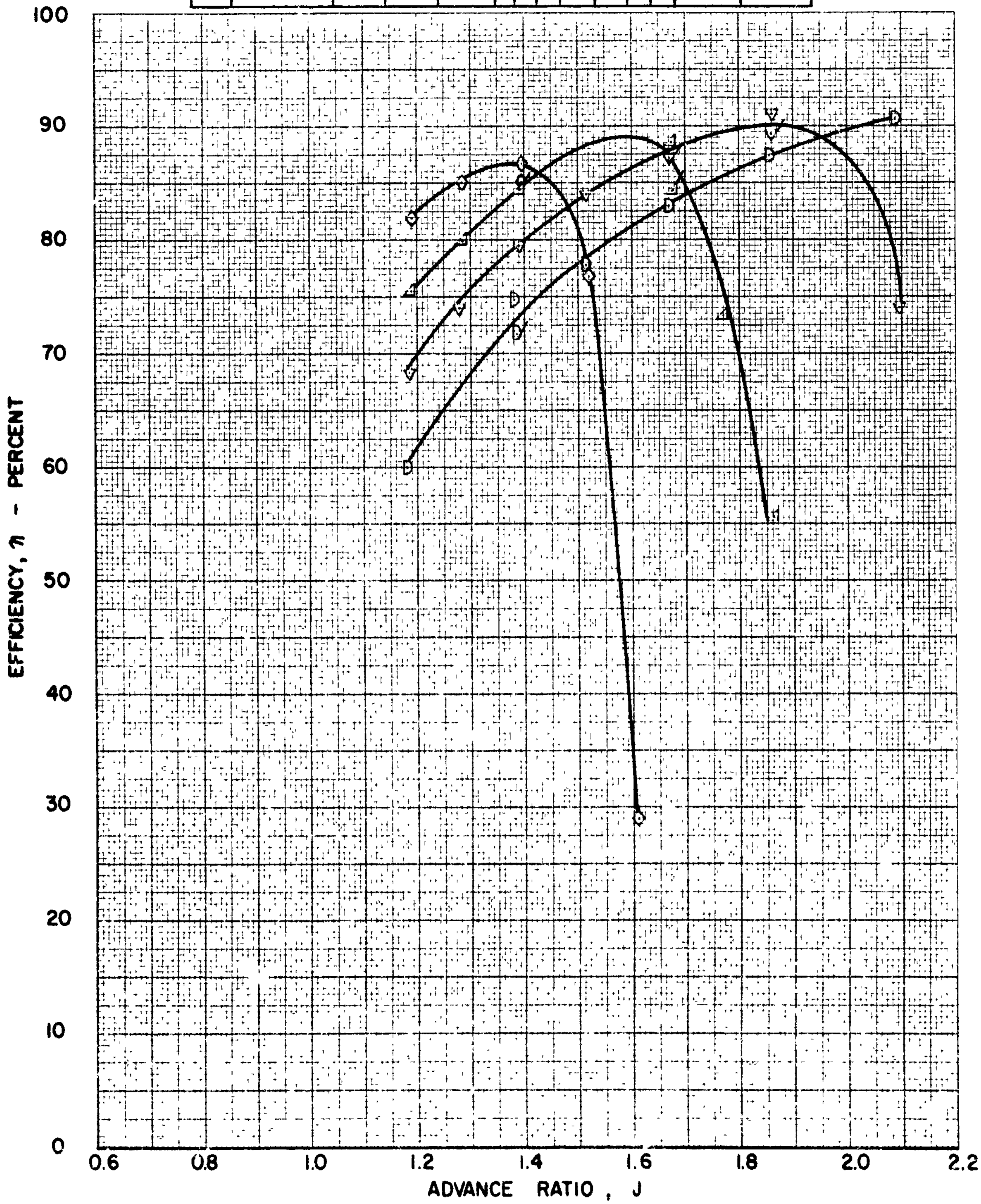

E330590-1

FIG. 36

HSD SHROUDED PROPELLER TEST

EFFECT OF BLADE ANGLE ON SHROUDED PROPELLER PERFORMANCE

SYM	RUN NO.	MACH NO.	CONFIGURATION	$\theta_{3/4}$
◇	465	0.30	$L_1 C_1 E_1 B_3 P_{WT} T_1 R_1 R_E$	30
◿	466	↓	↓	34
▽	468	↓	↓	38
D	472	↓	↓	42

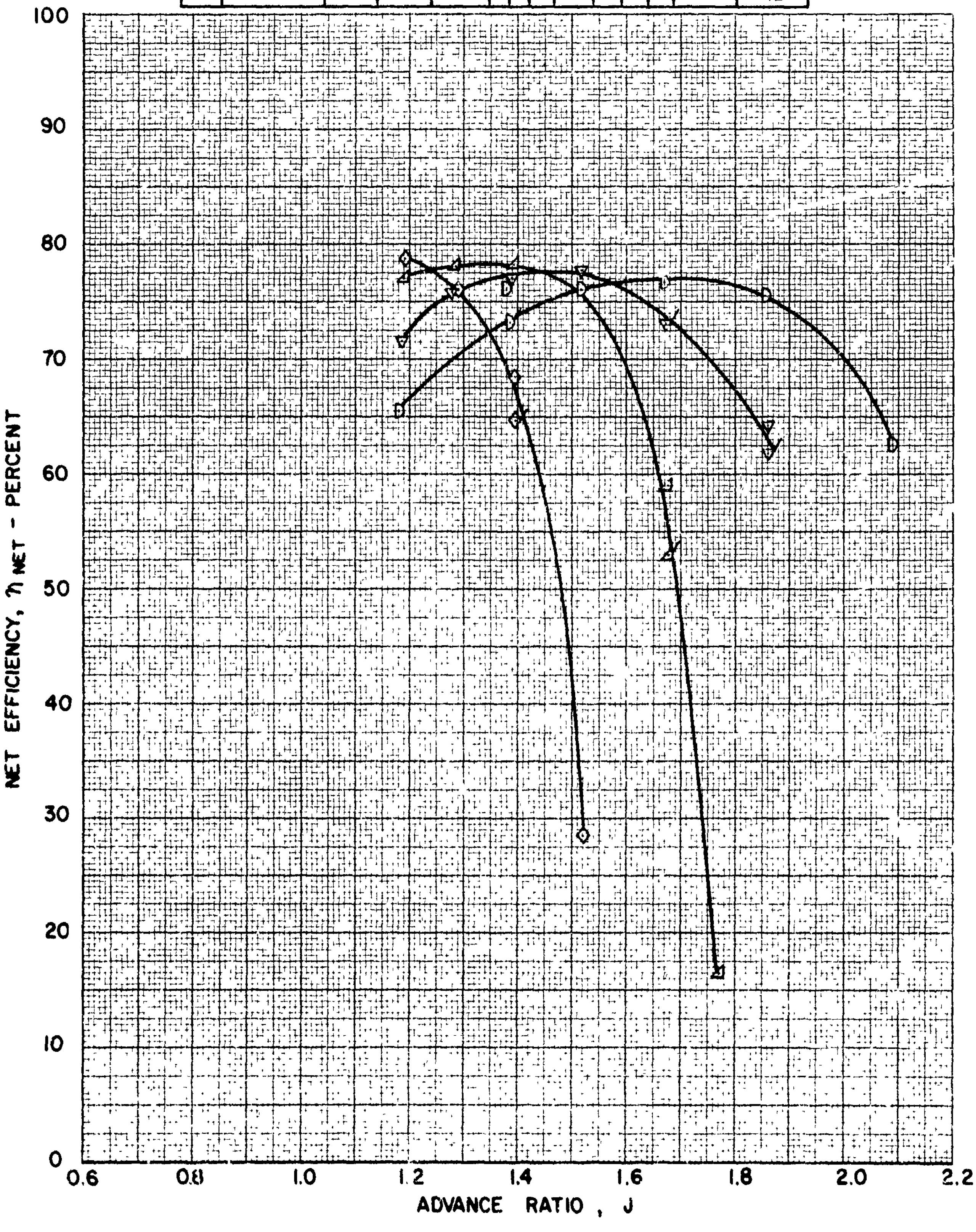

E330590-I

FIG.37

HSD SHROUDED PROPELLER TEST

EFFECT OF BLADE ANGLE ON SHROUDED PROPELLER PERFORMANCE

SYM	RUN NO.	MACH NO.	CONFIGURATION	$\theta_{3/4}$
◇	465	0.30	$L_1 C_1 E_1 B_3 P_{WT} T_1 R_1 R_E$	30
⊿	466	↓	↓	34
▽	468	↓	↓	38
D	472	↓	↓	42

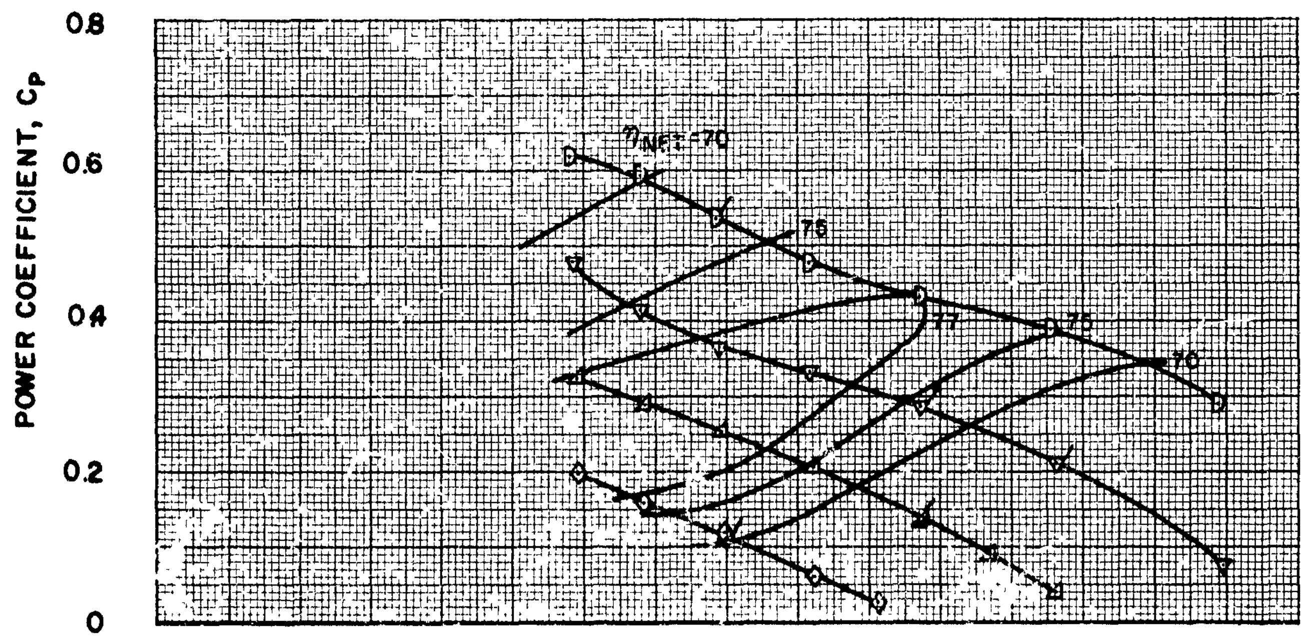

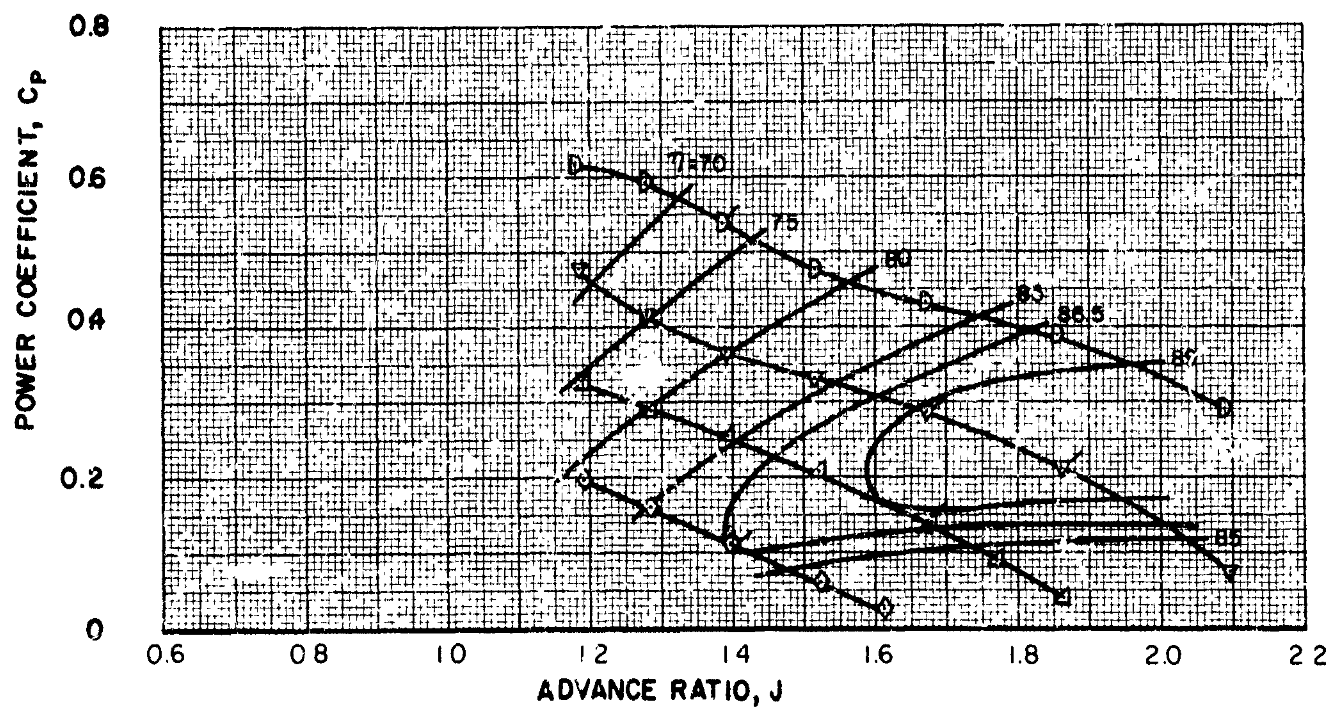

HSD SHROUDED PROPELLER TEST

EFFECT OF BLADE ANGLE ON SHROUDED PROPELLER PERFORMANCE

SYM	RUN NO.	MACH NO.	CONFIGURATION	$\theta_{3/4}$
▽	469	0.40	$L_1 C_1 E_1 B_3 P_{WT} T_1 R_1 R_E$	38
ᗞ	473	↓	↓	42
◺	475	↓	↓	46
ᗡ	478	↓	↓	50

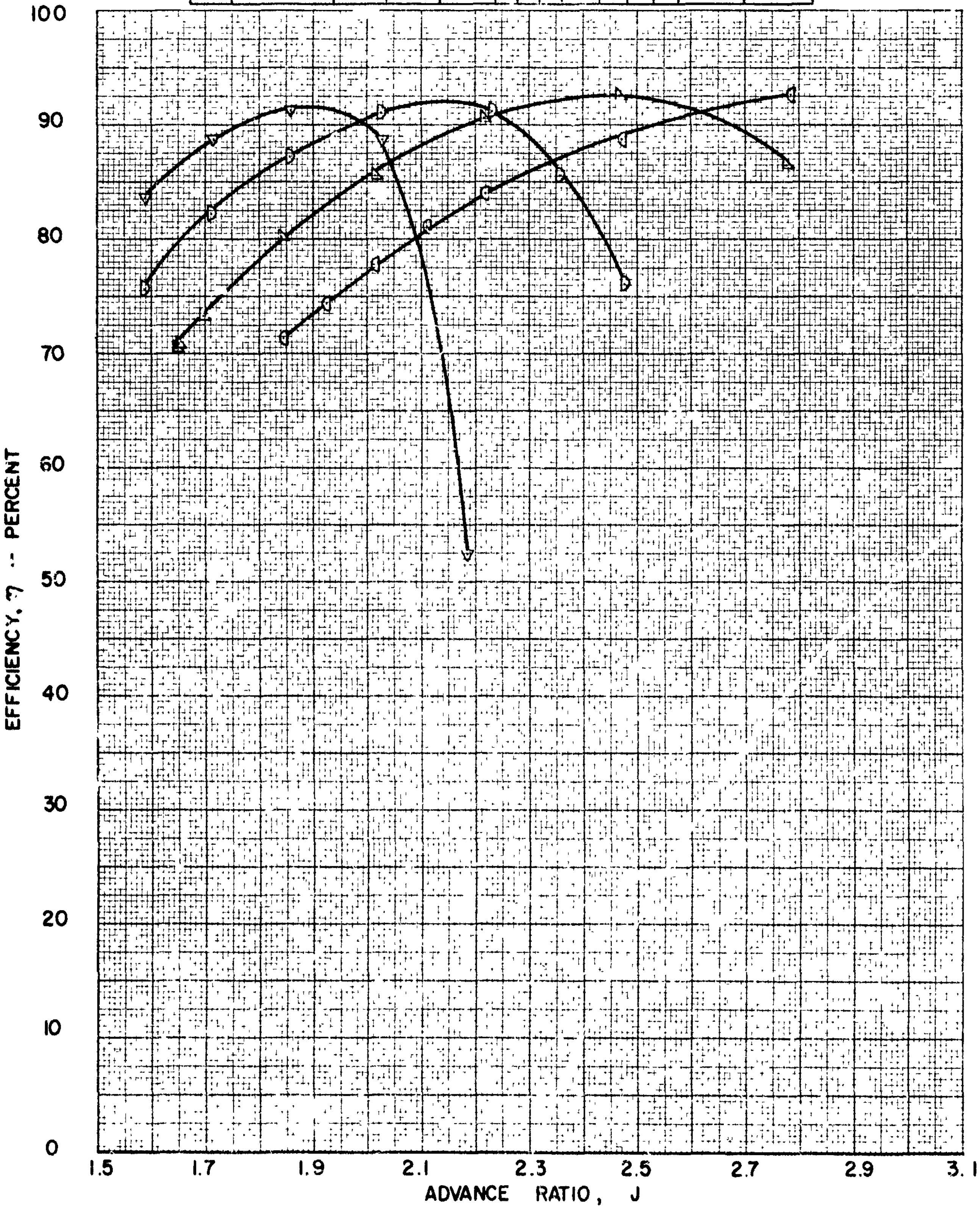

HSD SHROUDED PROPELLER TEST

EFFECT OF BLADE ANGLE ON SHROUDED PROPELLER PERFORMANCE

SYM	RUN NO.	MACH NO.	CONFIGURATION	$\theta_{3/4}$
▽	469	0.40	$L_1\ C_1\ E_1\ B_3\ P_{WT}\ T_1\ R_1\ R_E$	38
▷	473	↓	↓	42
△	475	↓	↓	46
◁	478	↓	↓	50

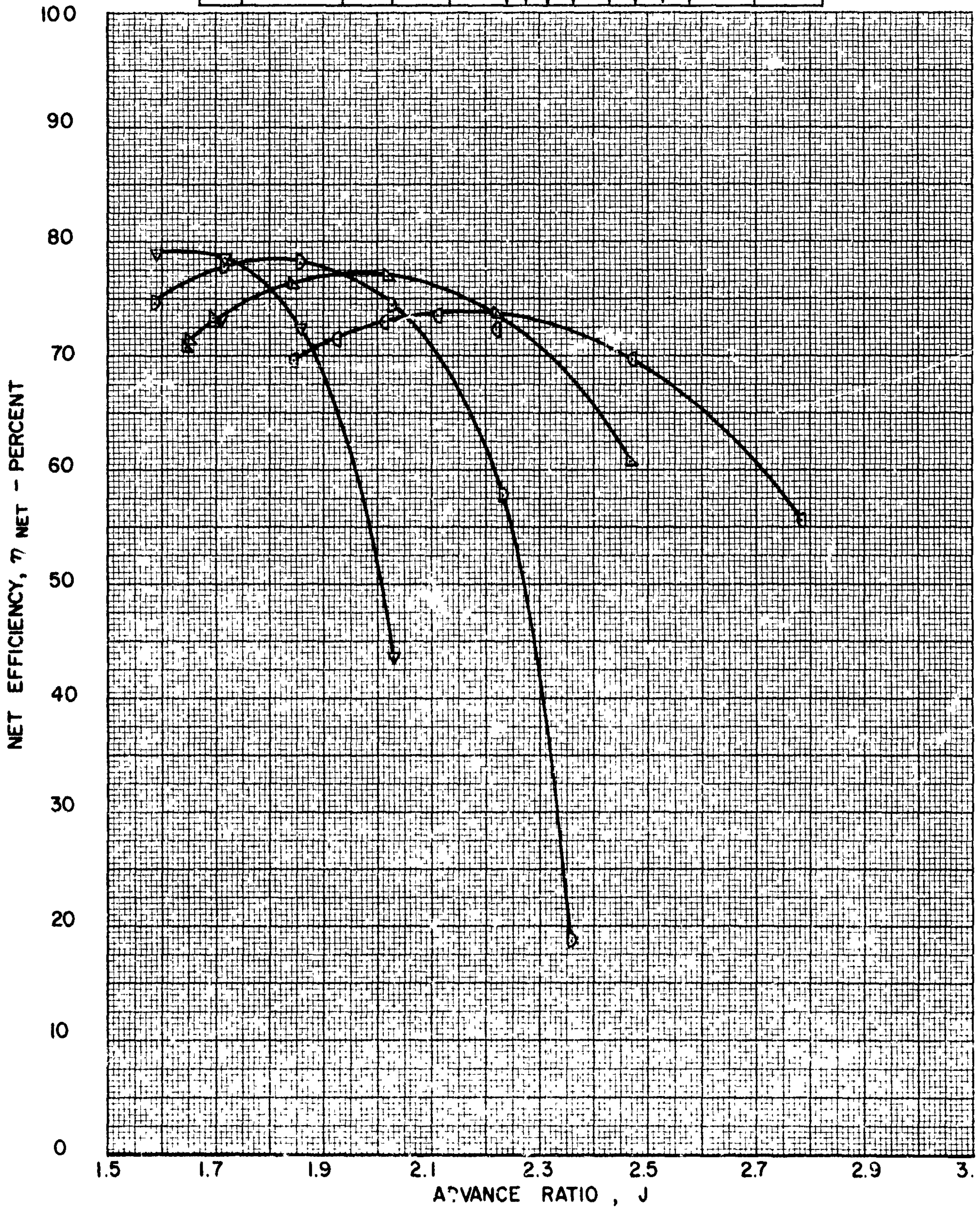

E330590-1

FIG. 40

HSD SHROUDED PROPELLER TEST

EFFECT OF BLADE ANGLE ON SHROUDED PROPELLER PERFORMANCE

SYM	RUN NO.	MACH NO.	CONFIGURATION	$\theta_{3/4}$
▽	469	0.40	$L_1 C_1 E_1 B_3 P_{WT} T_1 R_1 R_E$	38
D	473			42
◺	475			46
◖	478			50

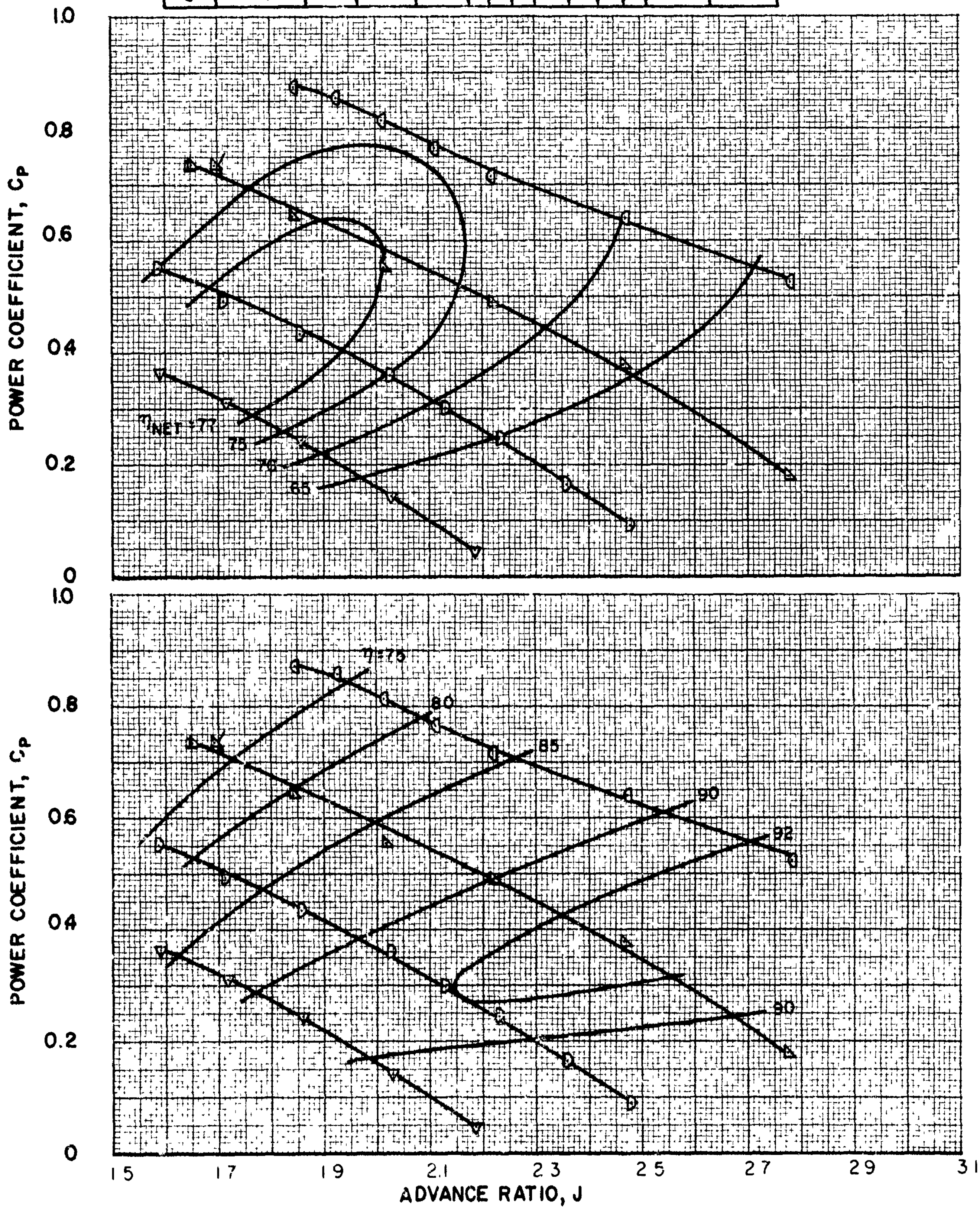

E330590-1

FIG. 41

HSD SHROUDED PROPELLER TEST

EFFECT OF BLADE ANGLE ON SHROUDED PROPELLER PERFORMANCE

SYM	RUN NO.	MACH NO.	CONFIGURATION	$\theta_{3/4}$
D	474	0.50	$L_1 C_1 E_1 B_3 P_{WT} T_1 R_1 R_E$	42
◺	476			46
◖	479			50
O	481			54

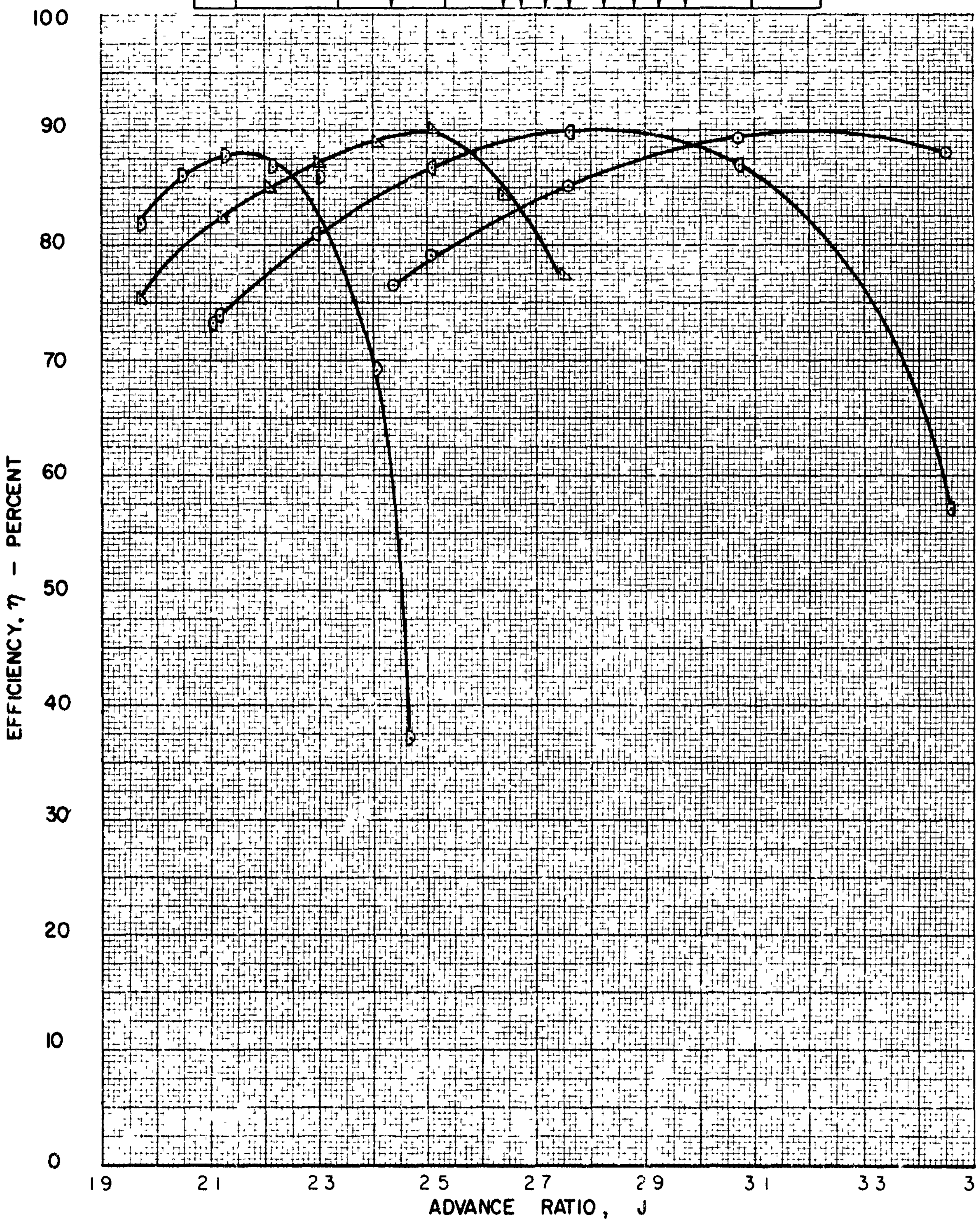

E330590-1

FIG. 42

HSD SHROUDED PROPELLER TEST

EFFECT OF BLADE ANGLE ON SHROUDED PROPELLER PERFORMANCE

SYM	RUN NO.	MACH NO.	CONFIGURATION	$\theta_{3/4}$
D	474	0.50	$L_1 C_1 E_1 B_3 P_{WT} T_1 R_1 R_E$	42
◺	476	↓	↓	46
◖	479	↓	↓	50
O	481	↓	↓	54

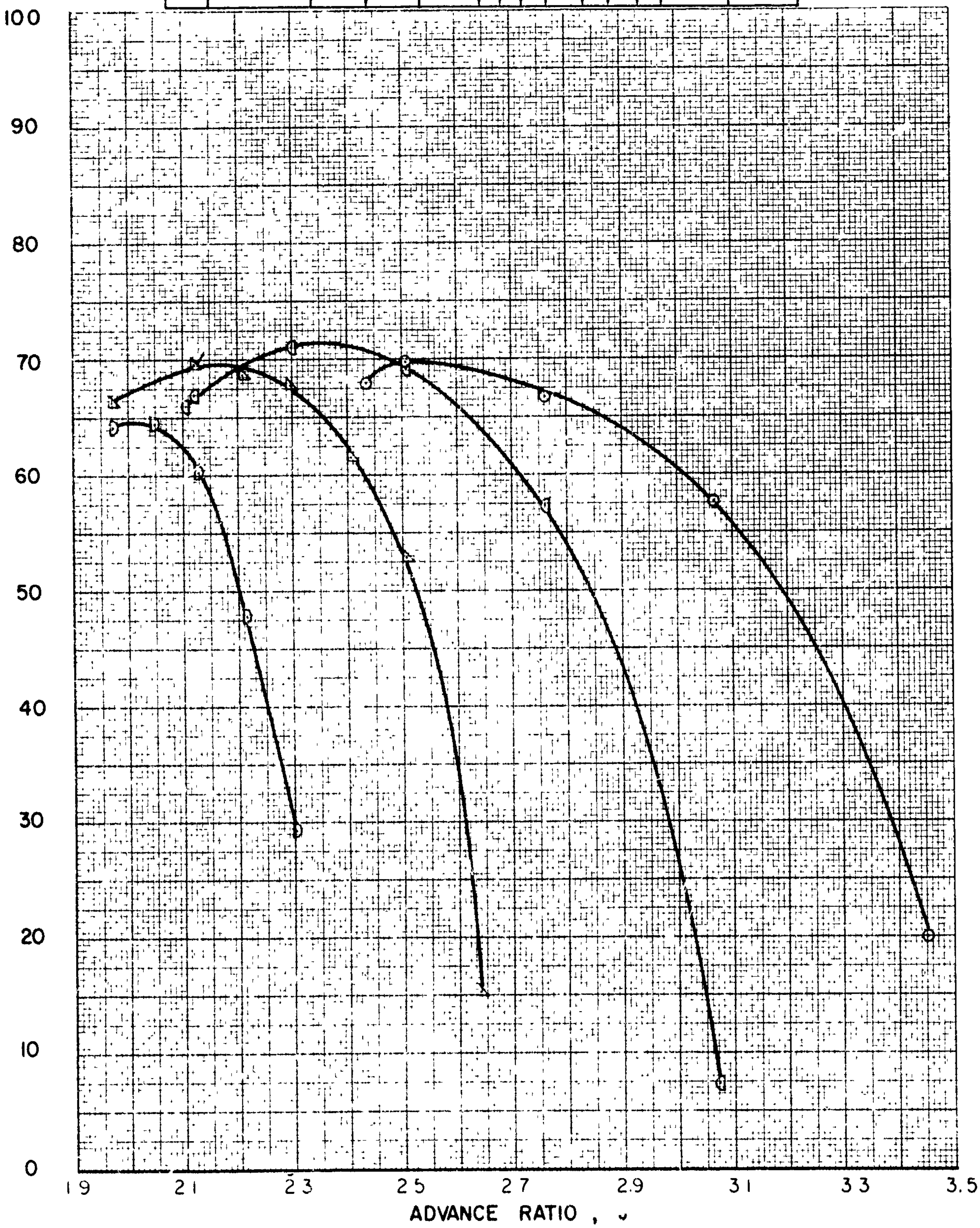

E330590-I

FIG. 43

HSD SHROUDED PROPELLER TEST

EFFECT OF BLADE ANGLE ON SHROUDED PROPELLER PERFORMANCE

SYM	RUN NO.	MACH NO.	CONFIGURATION	$\theta_{3/4}$
◻	474	0.50	$L_1 C_1 E_1 B_3 P_{WT} T_1 R_1 R_E$	42
△	476			46
◖	479			50
○	481			54

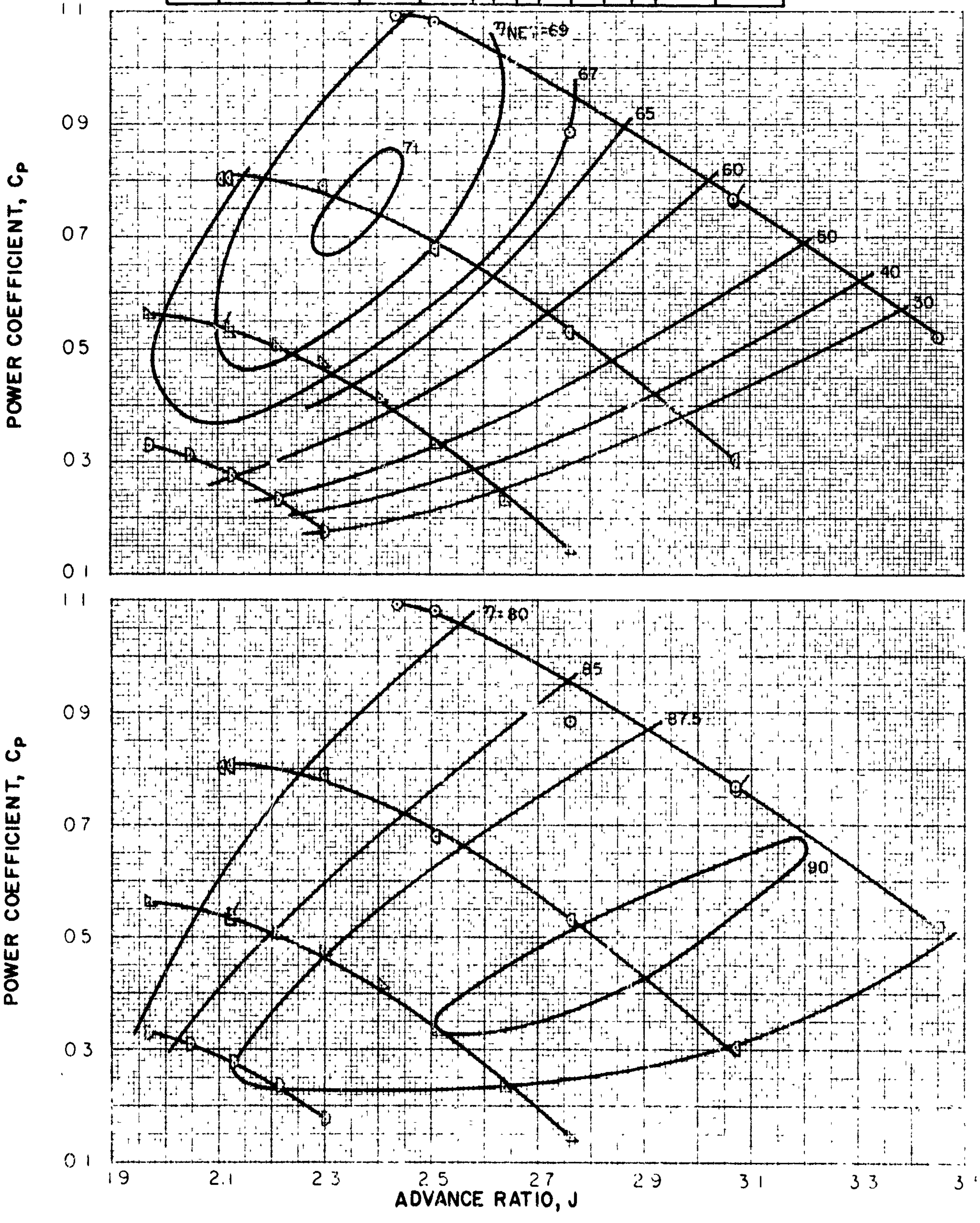

HSD SHROUDED PROPELLER TEST

EFFECT OF BLADE ANGLE ON SHROUDED PROPELLER PERFORMANCE

SYM	RUN NO.	MACH NO	CONFIGURATION	$\theta_{3/4}$
◺	477	0.60	$L_1 C_1 E_1 B_3 P_{WT} T_1 R_1 R_E$	46
◖	485	↓	↓	50
○	486	↓	↓	54
△	487	↓	↓	58

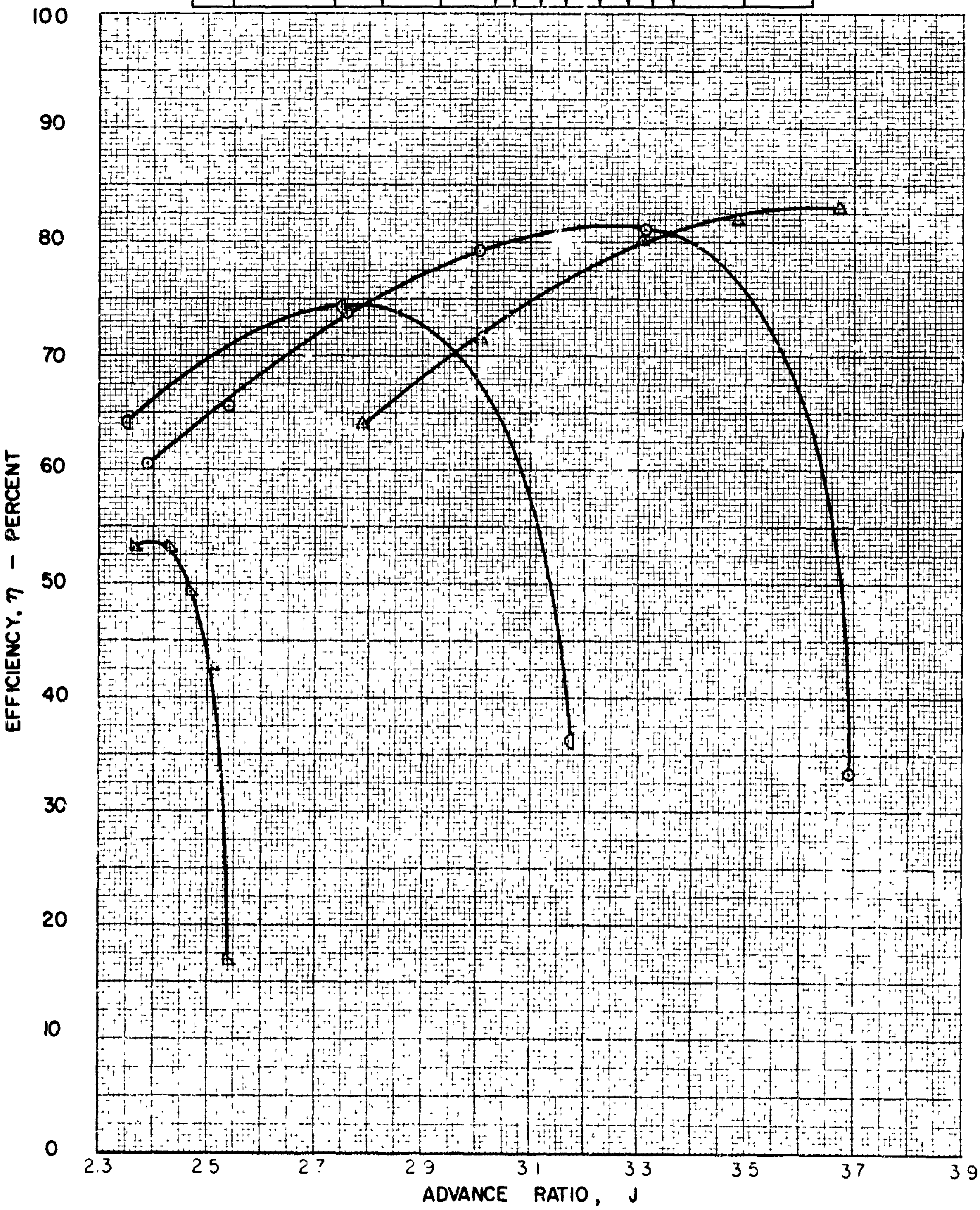

HSD SHROUDED PROPELLER TEST

EFFECT OF BLADE ANGLE ON SHROUDED PROPELLER PERFORMANCE

SYM	RUN NO.	MACH NO.	CONFIGURATION	$\theta_{3/4}$
◺	477	0.60	$L_1 C_1 E_1 B_3 P_{WT} T_1 R_1 R_E$	46
◖	485	↓	↓	50
⊙	486	↓	↓	54
△	487	↓	↓	58

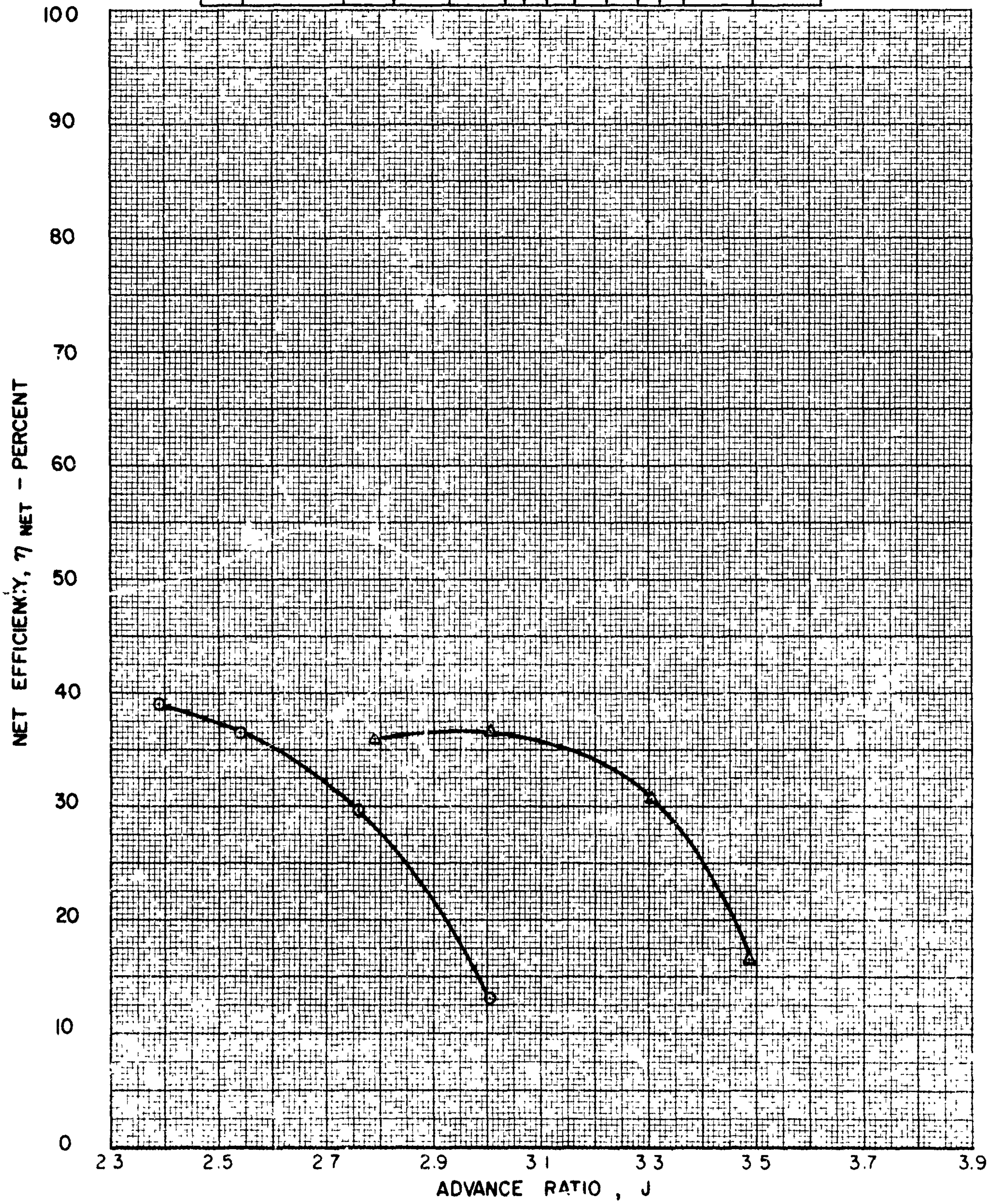

HSD SHROUDED PROPELLER TEST

EFFECT OF BLADE ANGLE ON SHROUDED PROPELLER PERFORMANCE

SYM	RUN NO.	MACH NO.	CONFIGURATION	$\theta_{3/4}$
◺	477	0.60	$L_1 C_1 E_1 B_3 P_{WT} T_1 R_1 R_E$	46
◖	485	↓	↓	50
○	486	↓	↓	54
△	487	↓	↓	58

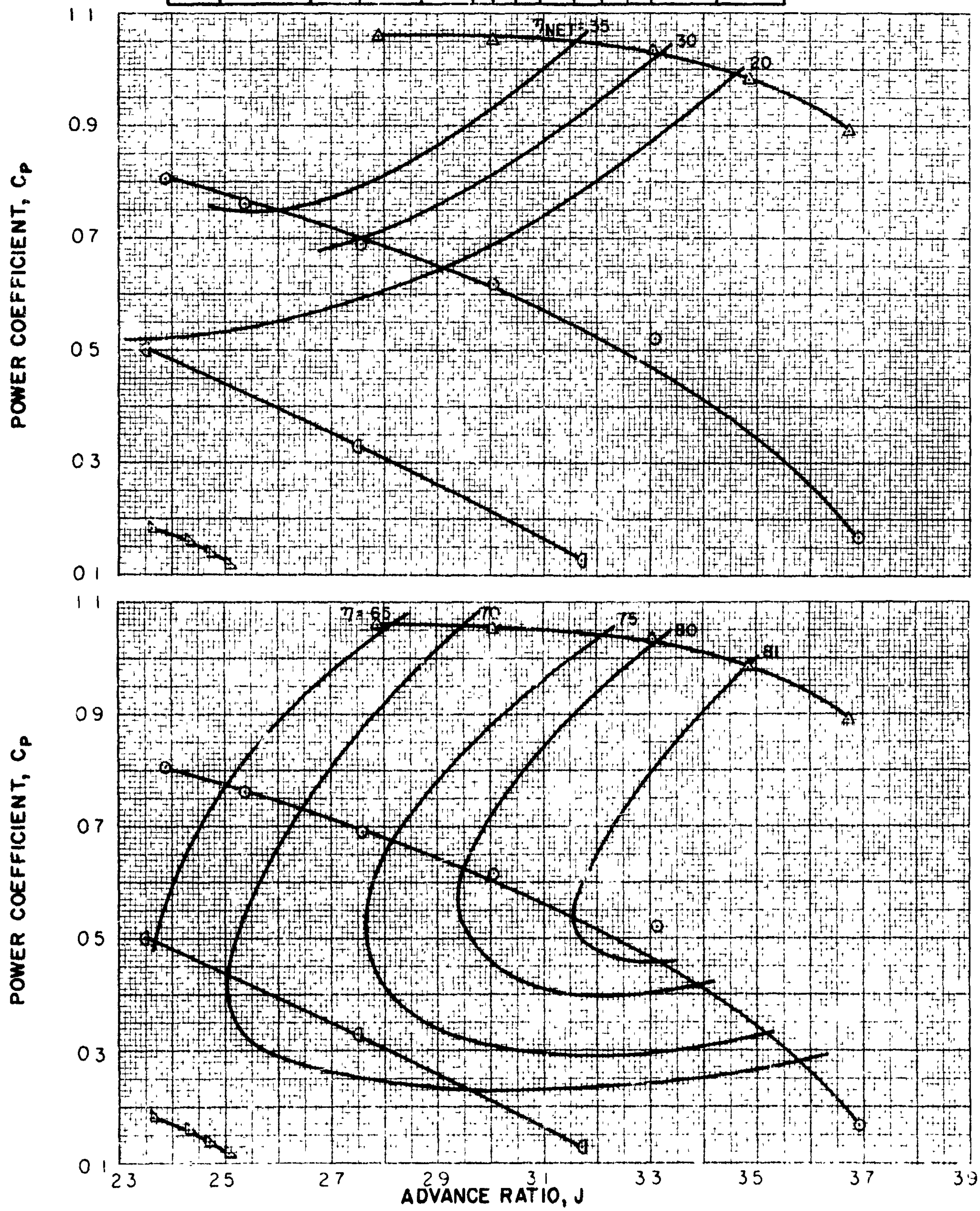

HSD SHROUDED PROPELLER TEST

EFFECT OF INLET LIP (L_2) ON SHROUDED PROPELLER PERFORMANCE

SYM	RUN NO	MACH NO.	CONFIGURATION	$\theta_{3/4}$
△	62, 61	0.05, 0.10	$L_2\ C_1\ E_1\ B_3\ P_{WT}\ T_1\ R_1\ R_E$	20
□	63, 64	↓	↓	25
◇	68, 67	↓	↓	30
⊿	69, 70	↓	↓	35

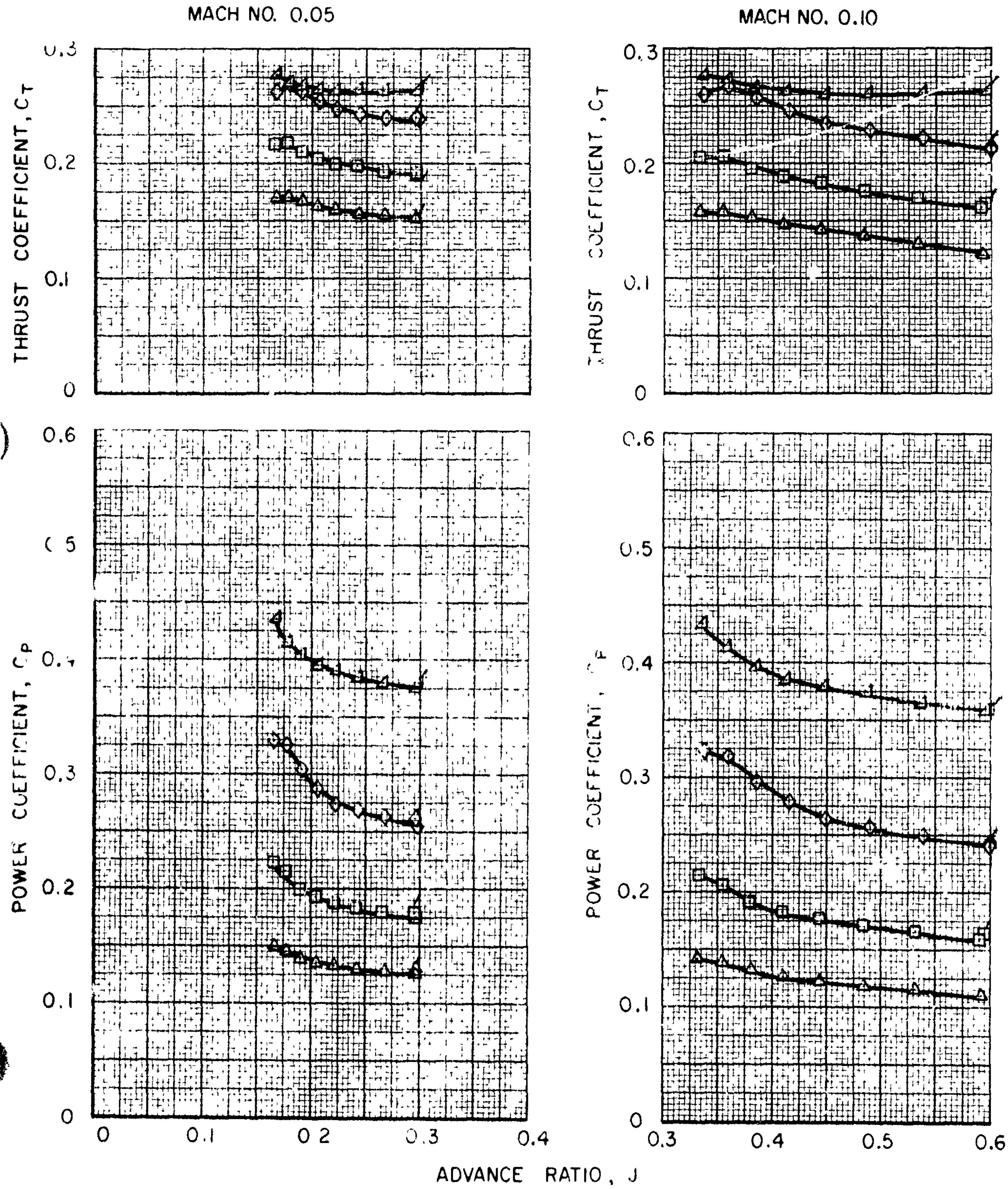

HSD SHROUDED PROPELLER TEST

EFFECT OF INLET LIP (L_2) ON SHROUDED PROPELLER PERFORMANCE

SYM	RUN NO	MACH NO	CONFIGURATION	$\theta_{3/4}$
△	62,61	0.05, 0.10	$L_2 C_1 E_1 B_3 P_{WT} T_1 R_1 R_E$	20
□	63,64	↓	↓	25
◇	68,67	↓	↓	30
⊿	69,70	↓	↓	35

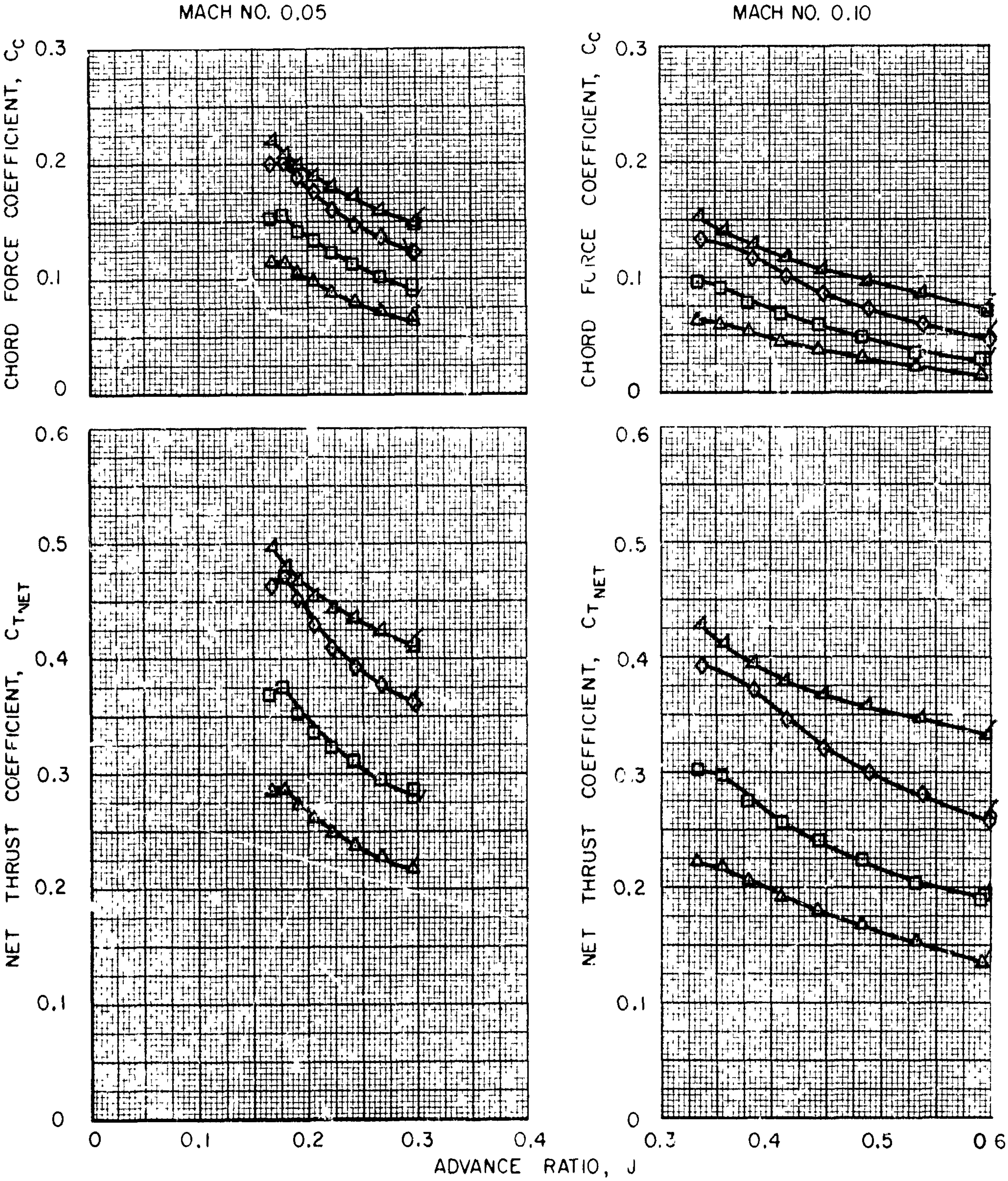

HSD SHROUDED PROPELLER TEST

EFFECT OF INLET LIP (L_2) ON SHROUDED PROPELLER PERFORMANCE

SYM	RUN NO.	MACH NO.	CONFIGURATION	$\theta_{3/4}$
⊡	65	0.20	$L_2 C_1 E_1 B_3 P_{WT} T_1 R_1 R_E$	25
◇	66	↓	↓	30
⊿	71	↓	↓	35
▽	72	↓	↓	40

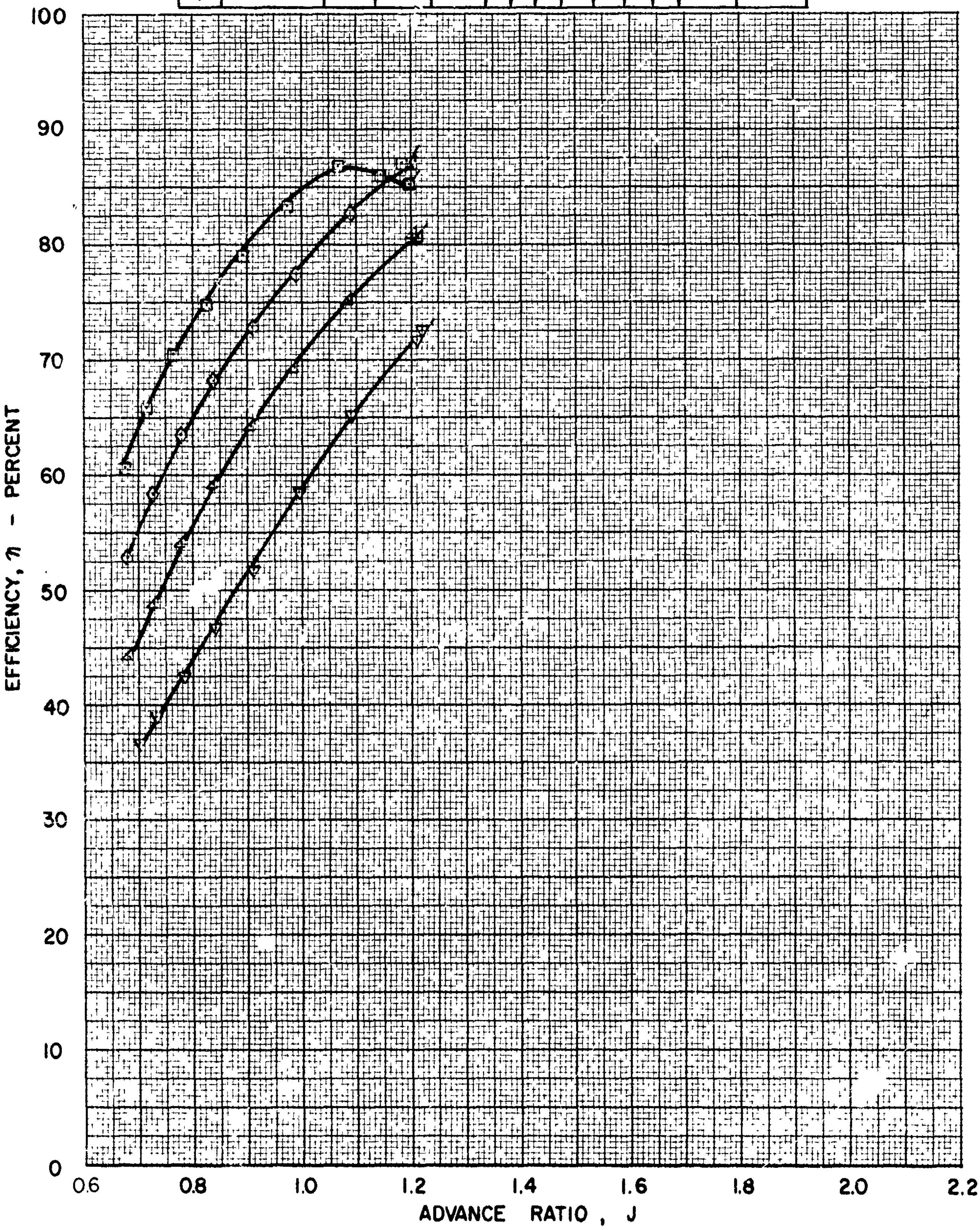

HSD SHROUDED PROPELLER TEST

EFFECT OF INLET LIP (L_2) ON SHROUDED PROPELLER PERFORMANCE

SYM	RUN NO.	MACH NO.	CONFIGURATION	$\theta_{3/4}$
□	65	0.20	$L_2 C_1 E_1 B_3 P_{WT} T_1 R_1 R_E$	25
◇	66	↓	↓	30
△	71	↓	↓	35
▽	72	↓	↓	40

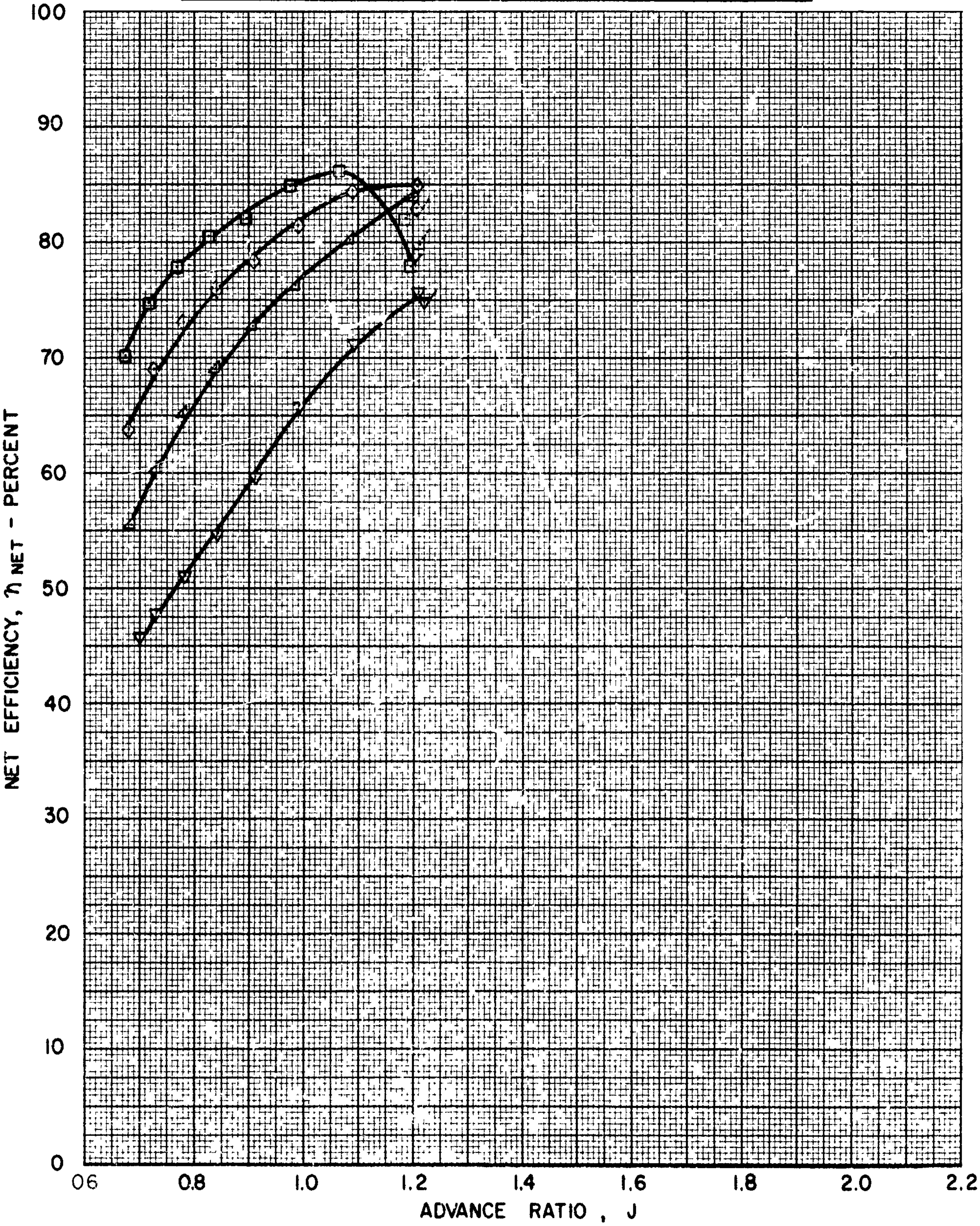

HSD SHROUDED PROPELLER TEST

EFFECT OF INLET LIP (L_2) ON SHROUDED PROPELLER PERFORMANCE

SYM	RUN NO.	MACH NO.	CONFIGURATION	$\theta_{3/4}$
□	65	0.20	$L_2 C_1 E_1 B_3 P_{WT} \Gamma_1 R_1 R_E$	25
◇	66	↓	↓	30
◿	71	↓	↓	35
▽	72	↓	↓	40

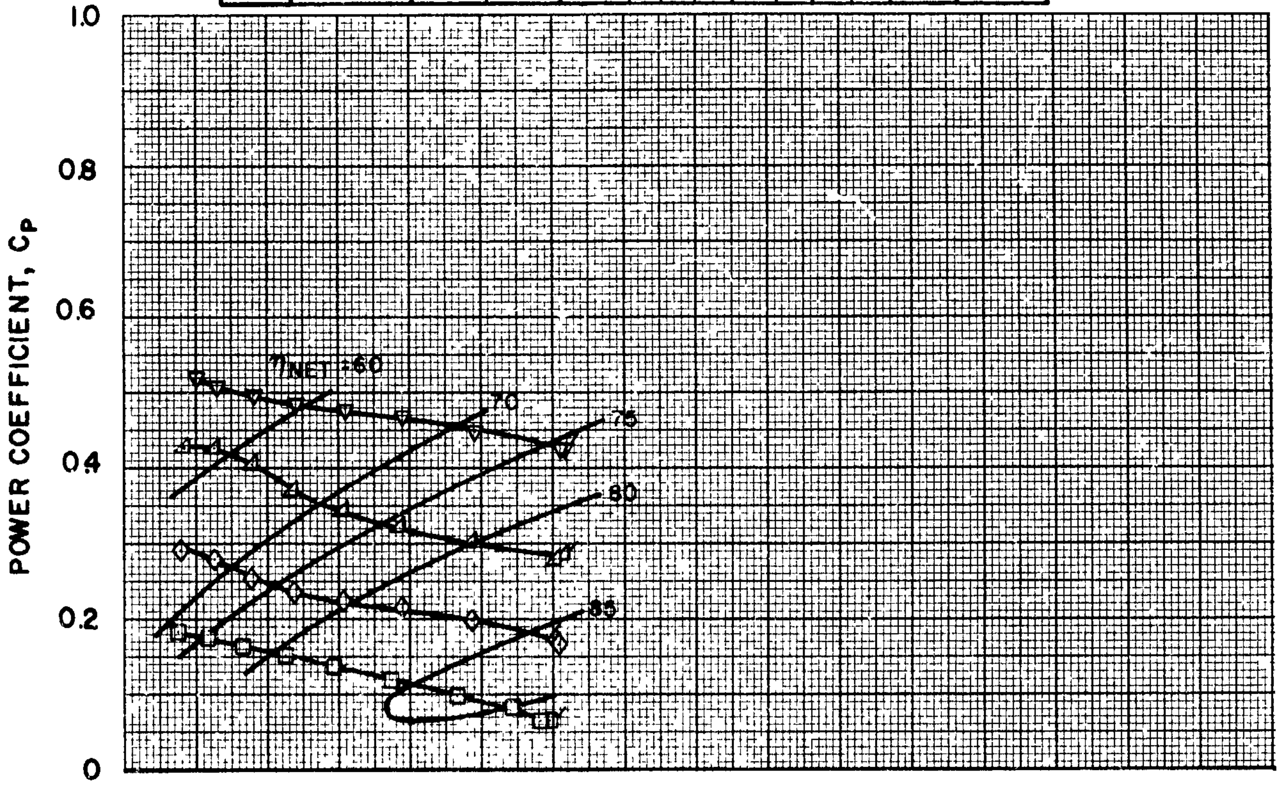

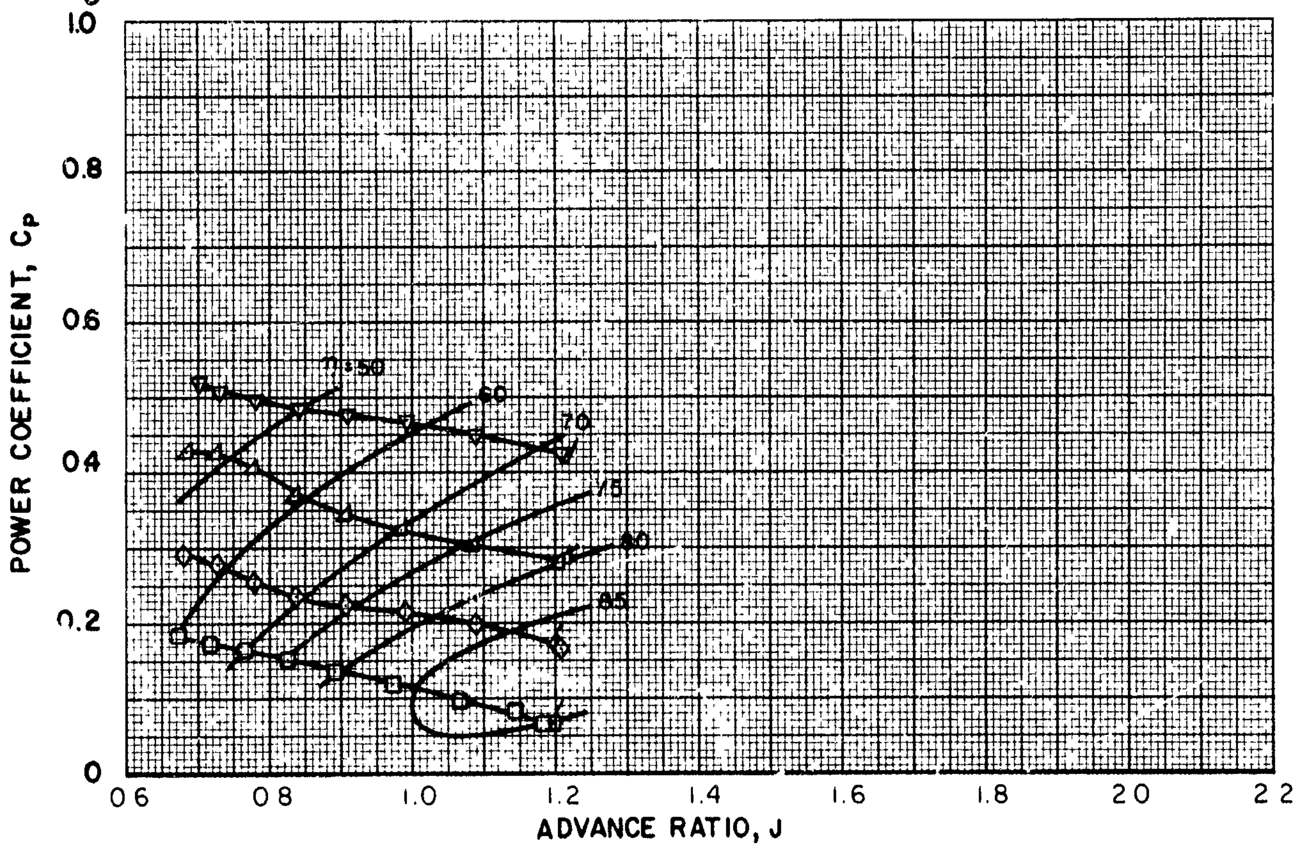

E330590-1

FIG. 52

HSD SHROUDED PROPELLER TEST

EFFECT OF INLET LIP (L_2) ON SHROUDED PROPELLER PERFORMANCE

SYM	RUN NO.	MACH NO.	CONFIGURATION	$\theta_{3/4}$
◇	552	0.31	$L_2 C_1 E_1 B_3 P_{WT} T_1 R_1 R_E$	30
⊿	553	↓	↓	34
▽	554	↓	↓	38
D	556	↓	↓	42

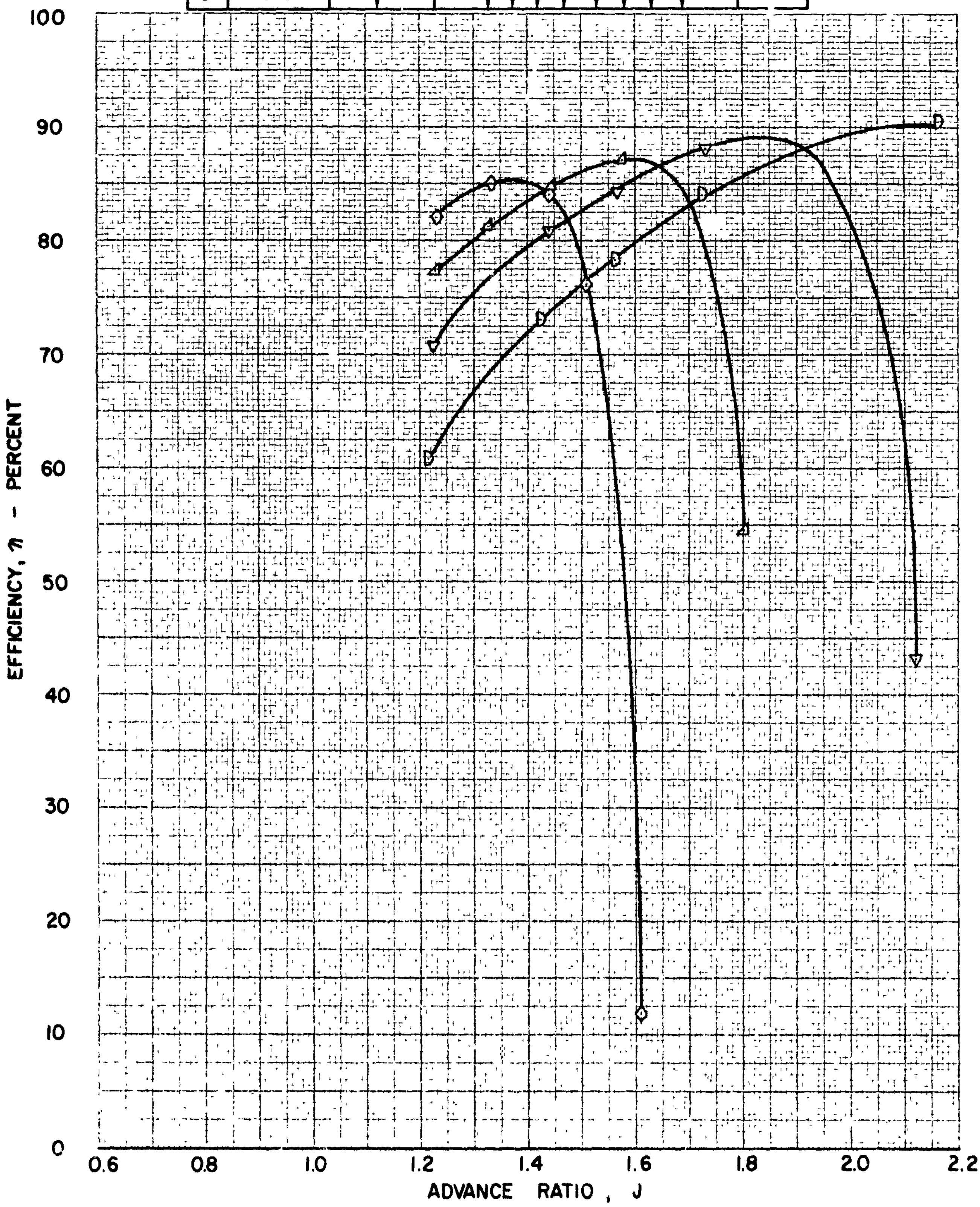

E330590-1

FIG. 53

HSD SHROUDED PROPELLER TEST

EFFECT OF INLET LIP (L_2) ON SHROUDED PROPELLER PERFORMANCE

SYM	RUN NO.	MACH NO.	CONFIGURATION	$\theta_{3/4}$
◇	552	0.31	$L_2 C_1 E_1 B_3 P_{WT} T_1 R_1 R_E$	30
⊿	553	↓	↓	34
▽	554	↓	↓	38
D	556	↓	↓	42

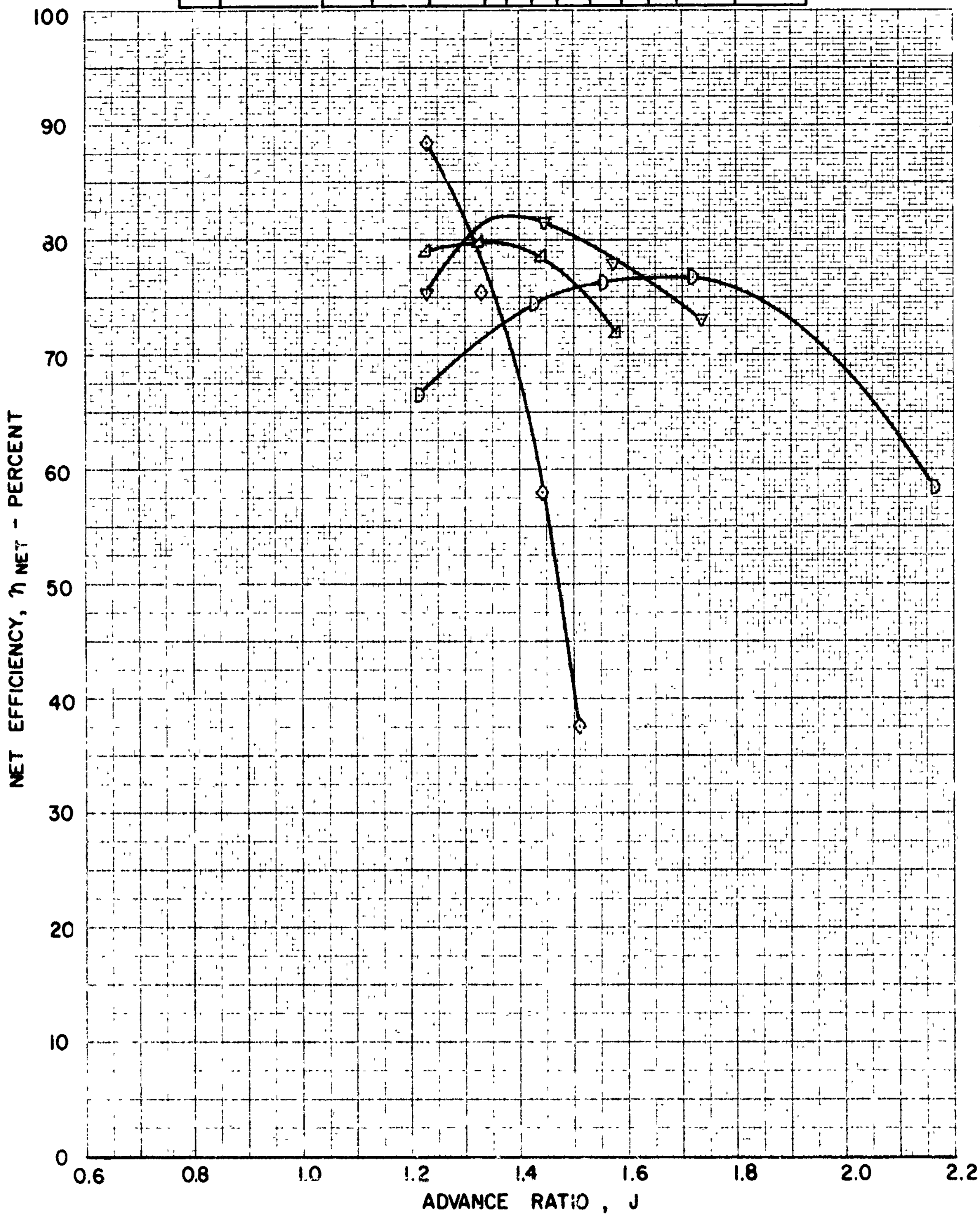

HSD SHROUDED PROPELLER TEST

EFFECT OF INLET LIP (L_2) ON SHROUDED PROPELLER PERFORMANCE

SYM	RUN NO.	MACH NO.	CONFIGURATION	$\theta_{3/4}$
◇	552	0.31	$L_2 C_1 E_1 B_3 P_{WT} T_1 R_1 R_E$	30
⊿	553			34
▽	554			38
D	556			42

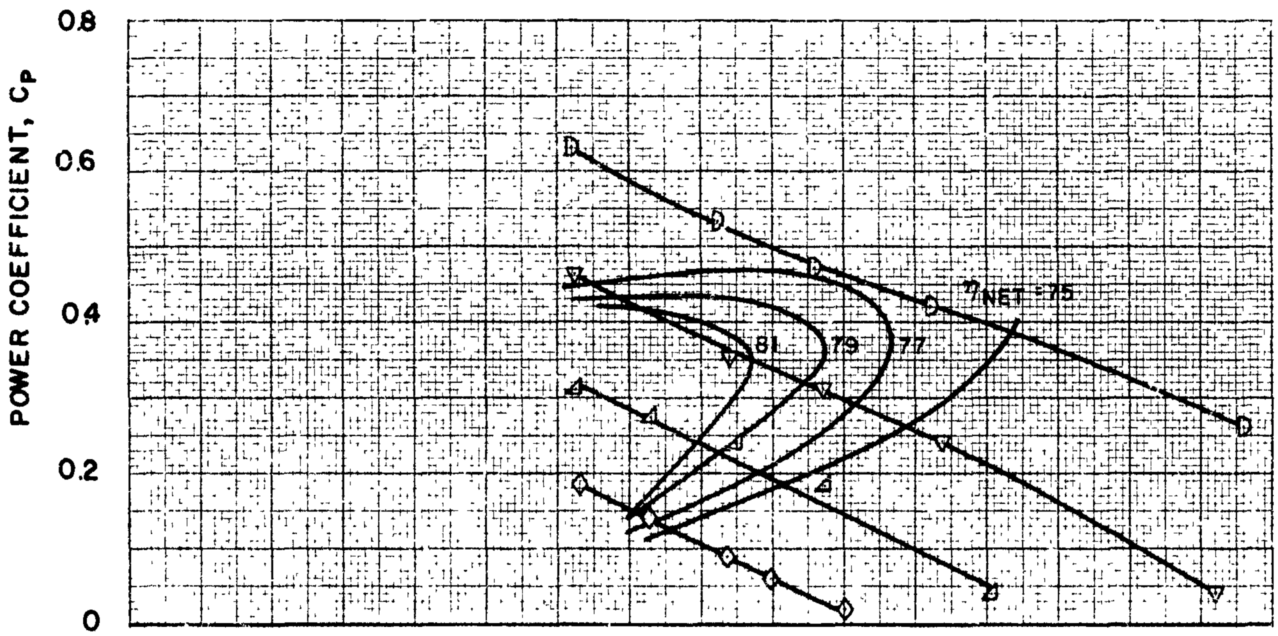

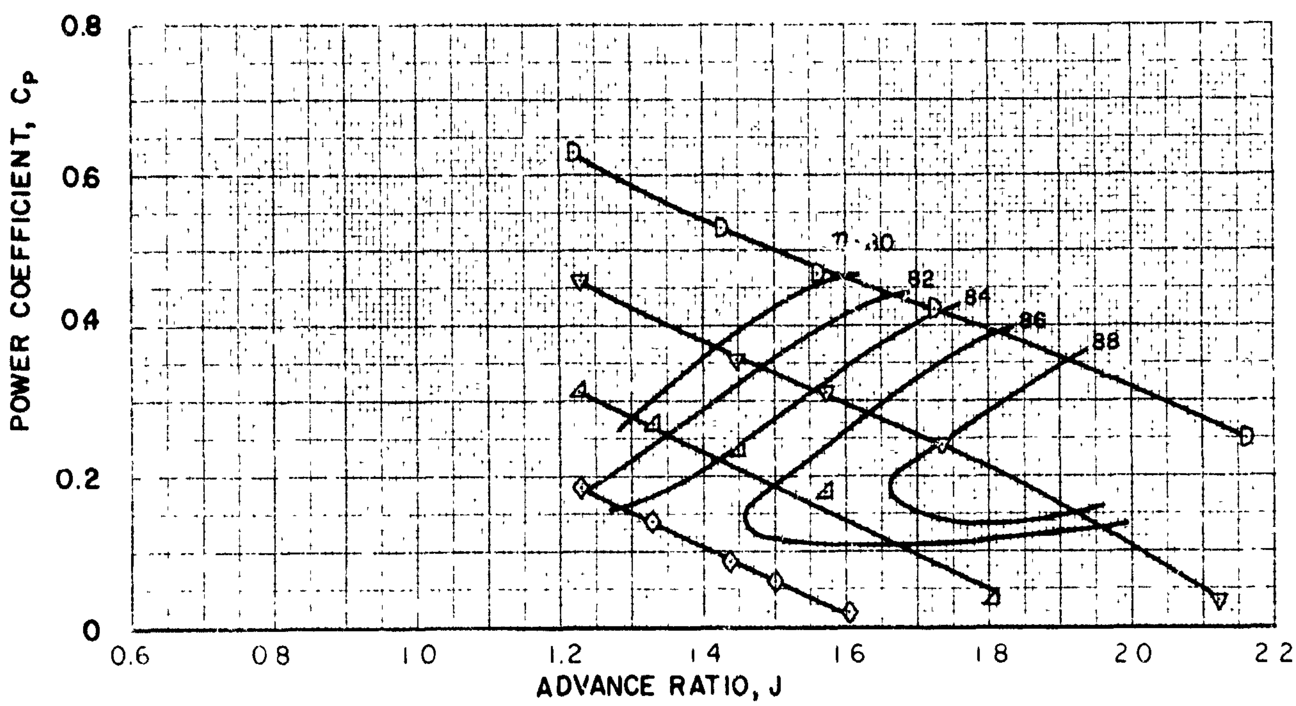

HSD SHROUDED PROPELLER TEST

EFFECT OF INLET LIP (L_2) ON SHROUDED PROPELLER PERFORMANCE

SYM	RUN NO.	MACH NO.	CONFIGURATION	$\theta_{3/4}$
▽	555	0.41	$L_2 C_1 E_1\ B_3\ P_{WT}\ T_1\ R_1\ R_E$	38
D	557			42
◺	559			46
◁	561			50

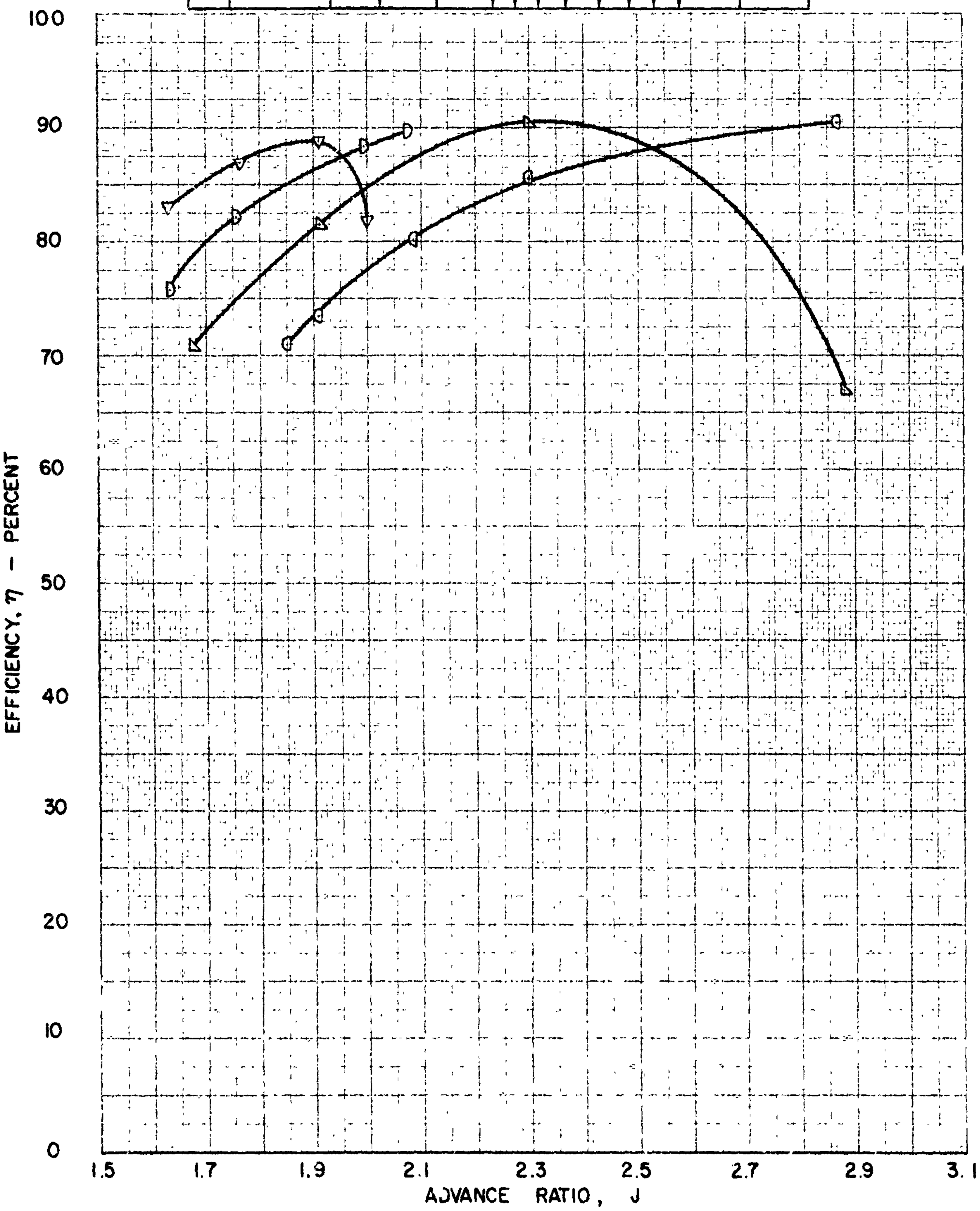

HSD SHROUDED PROPELLER TEST

EFFECT OF INLET LIP (L_2) ON SHROUDED PROPELLER PERFORMANCE

SYM	RUN NO.	MACH NO.	CONFIGURATION	$\theta_{3/4}$
▽	555	0.41	$L_2\ C_1\ E_1\ B_3\ P_{WT}\ T_1\ R_1\ R_E$	38
D	557			42
◺	559			46
◖	561			50

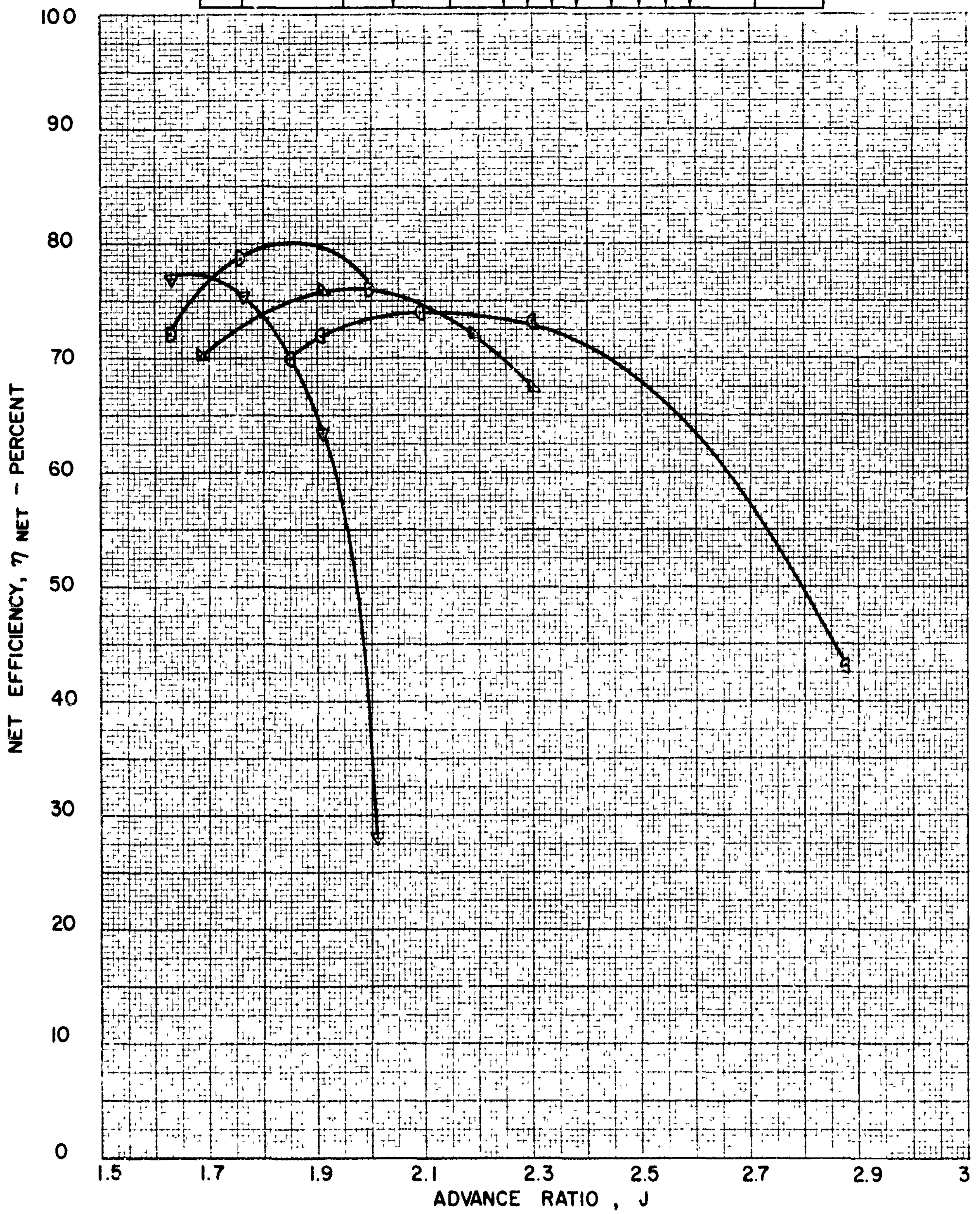

E330590-I

FIG. 57

HSD SHROUDED PROPELLER TEST

EFFECT OF INLET LIP (L_2) ON SHROUDED PROPELLER PERFORMANCE

SYM	RUN NO.	MACH NO.	CONFIGURATION	$\theta_{3/4}$
▽	555	0.41	$L_2 C_1 E_1 B_3 P_{WT} T_1 R_1 R_E$	38
D	557	↓	↓	42
◺	559	↓	↓	46
◖	561	↓	↓	50

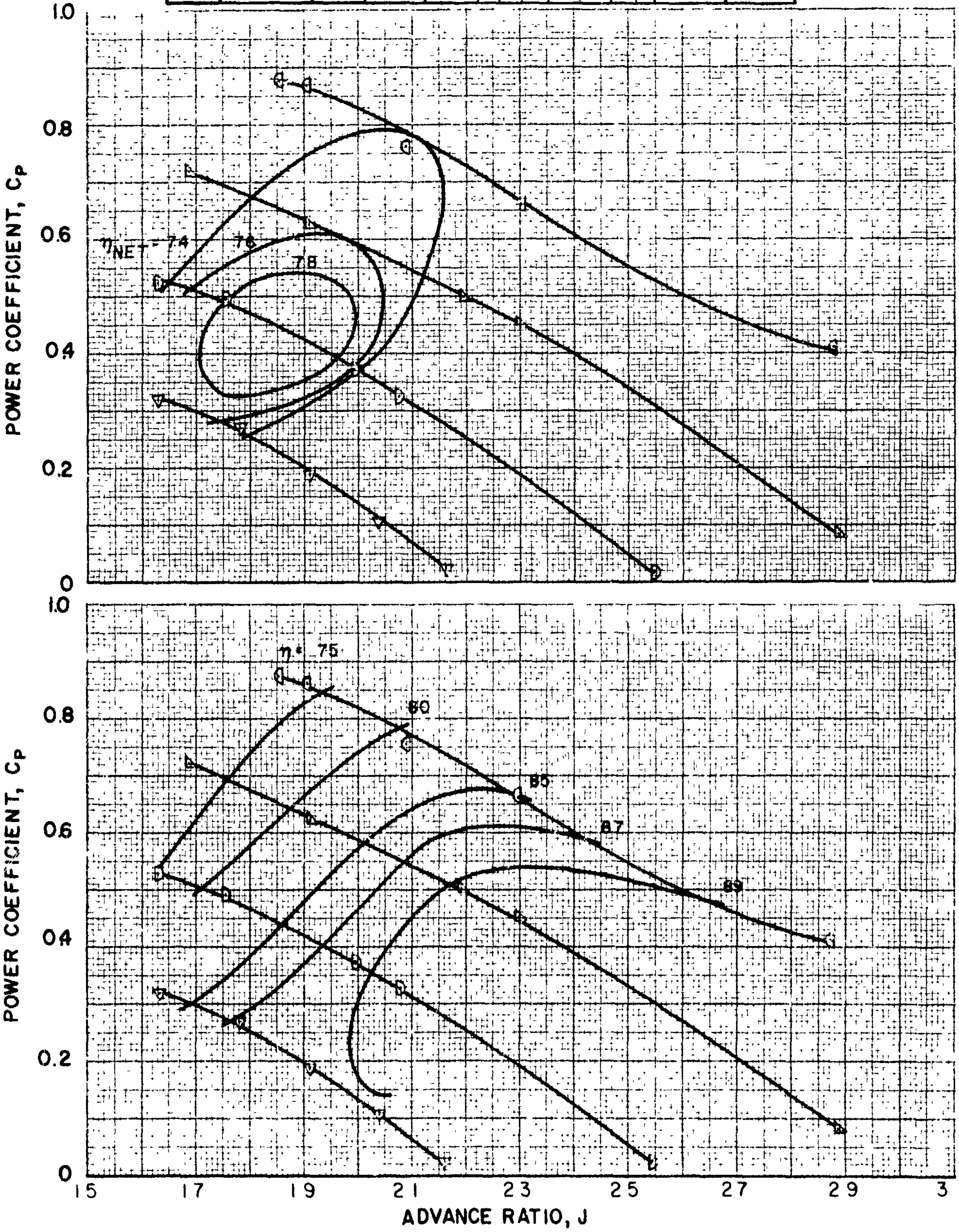

HSD SHROUDED PROPELLER TEST

EFFECT OF INLET LIP (L_2) ON SHROUDED PROPELLER PERFORMANCE

SYM	RUN NO.	MACH NO.	CONFIGURATION	$\theta_{3/4}$
◗	558	0.52	$L_2\ C_1\ E_1\ B_3\ P_{WT}\ T_1\ R_1\ R_E$	42
◺	560	↓	↓	46
◖	562	↓	↓	50
○	563	↓	↓	54

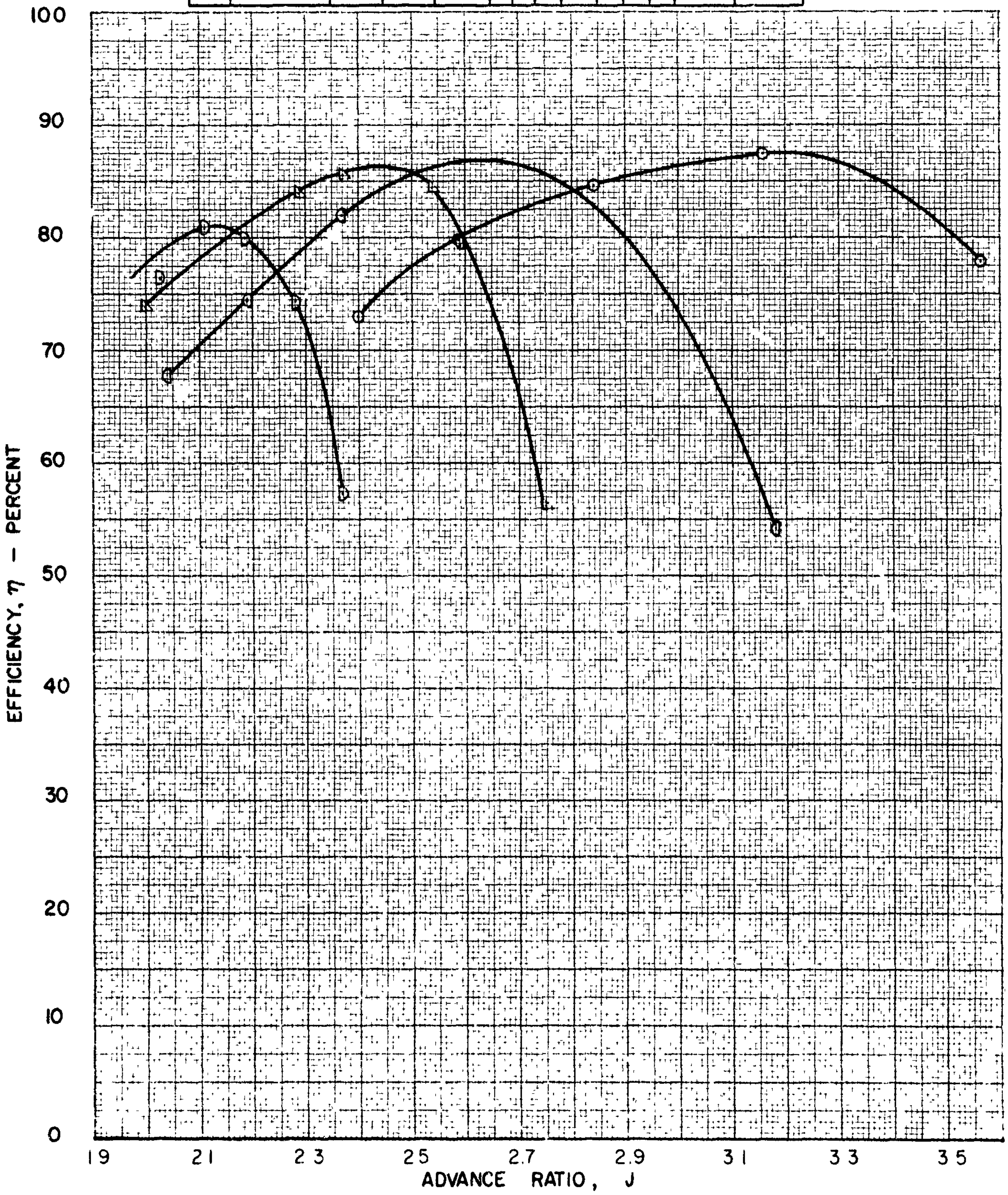

HSD SHROUDED PROPELLER TEST

EFFECT OF INLET LIP (L_2) ON SHROUDED PROPELLER PERFORMANCE

SYM	RUN NO	MACH NO.	CONFIGURATION	$\theta_{3/4}$
◻	558	0.52	L_2 C_1 E_1 B_3 P_{WT} T_1 R_1 R_E	42
◺	560			46
◐	562			50
○	563			54

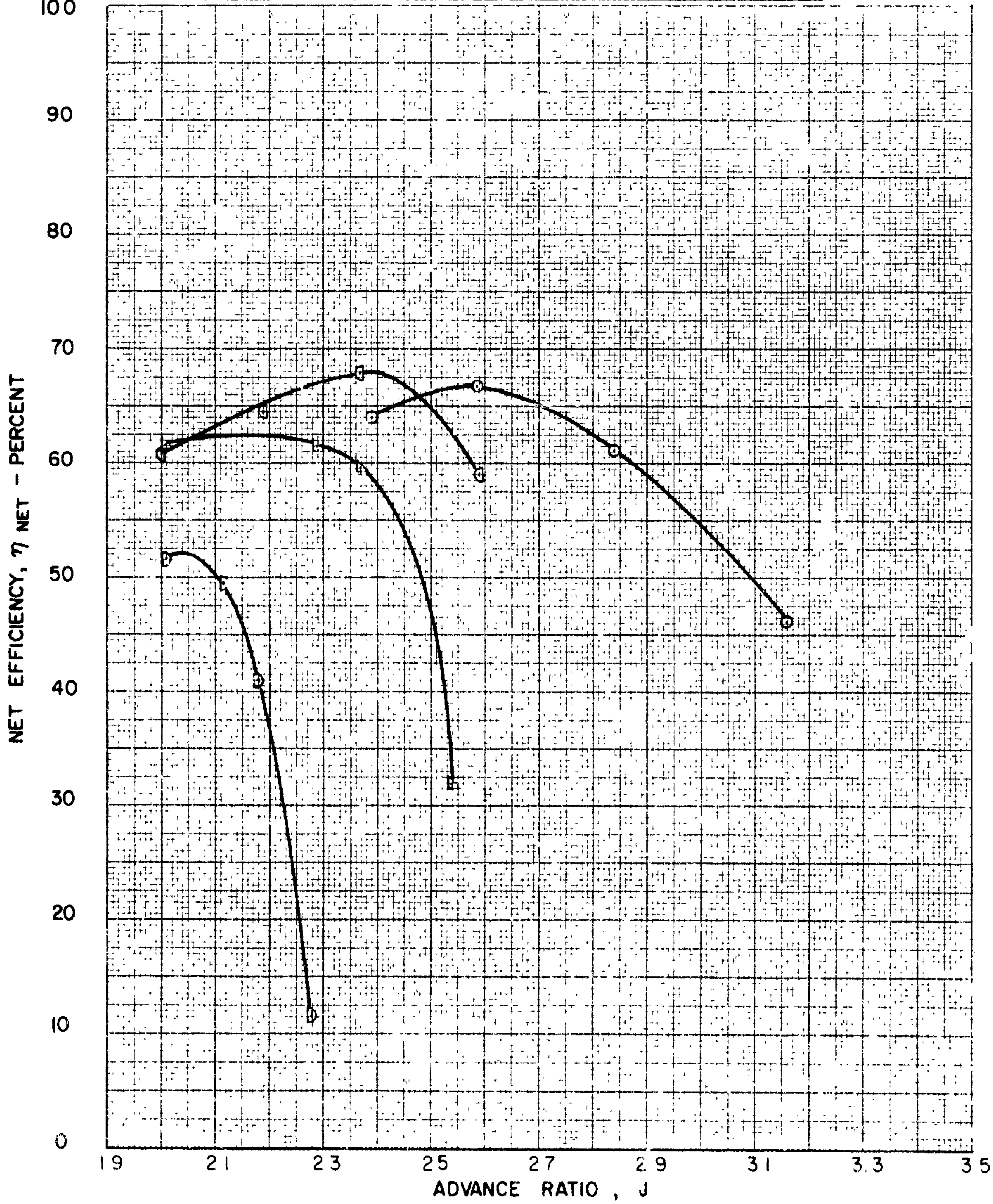

E330590-1

FIG. 60

HSD SHROUDED PROPELLER TEST

EFFECT OF INLET LIP (L_2) ON SHROUDED PROPELLER PERFORMANCE

SYM	RUN NO.	MACH NO.	CONFIGURATION	$\theta_{3/4}$
D	558	0.52	$L_2 C_1 E_1 B_3 P_{WT} T_1 R_1 R_E$	42
◺	560			46
◐	562			50
O	563			54

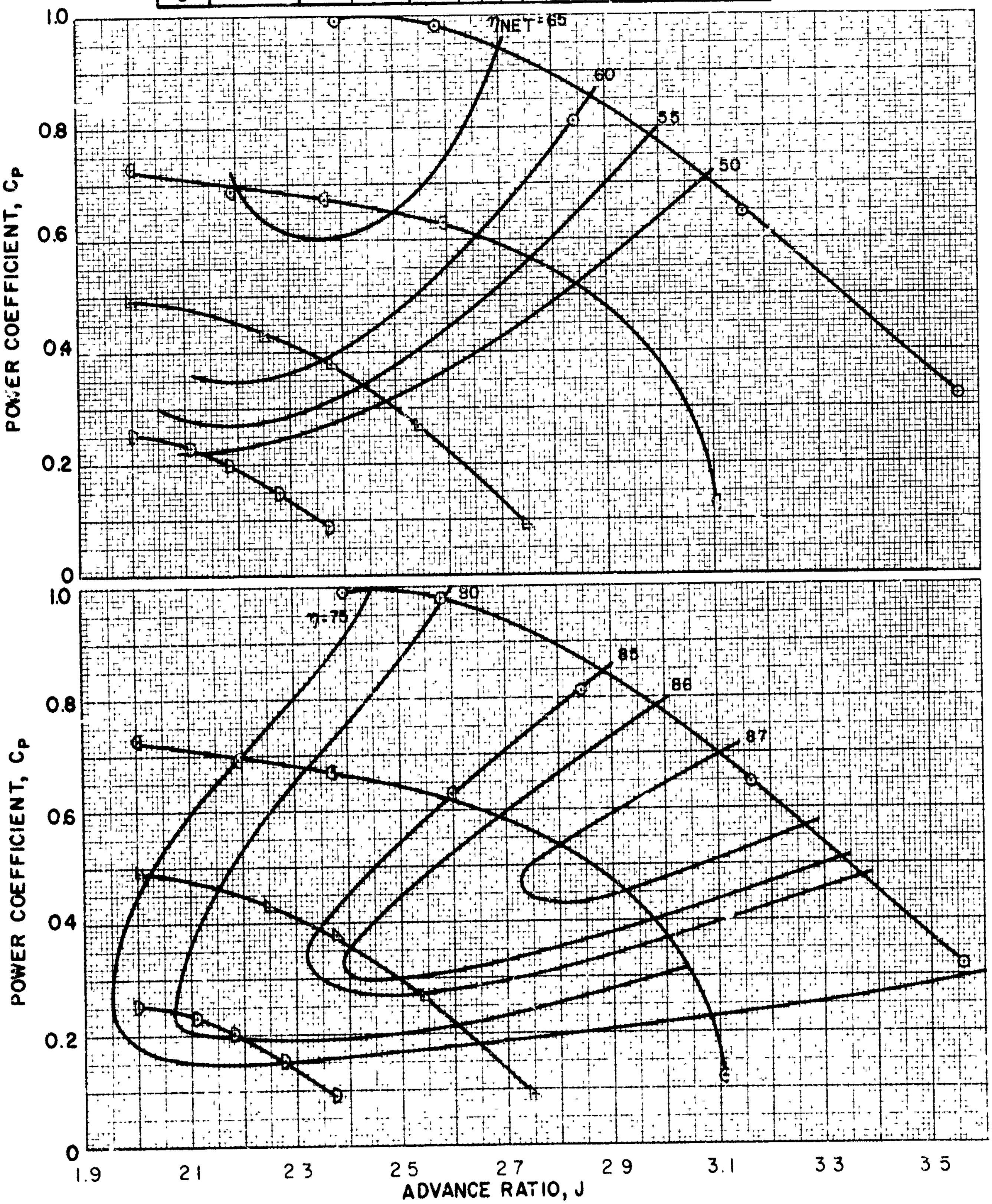

HSD SHROUDED PROPELLER TEST

EFFECT OF DIFFUSER (E_2) ON SHROUDED PROPELLER PERFORMANCE

SYM	RUN NO.	MACH NO.	CONFIGURATION	$\theta_{3/4}$
△	91, 78	0.02, 0.10	$L_1 C_1 E_2 B_3 P_{WT} T_1 R_1 R_E$ + TUFTS	20
□	90, 80	↓	↓	25
◇	84, 85	↓	↓	30
⊿	89, 88	↓	↓	35

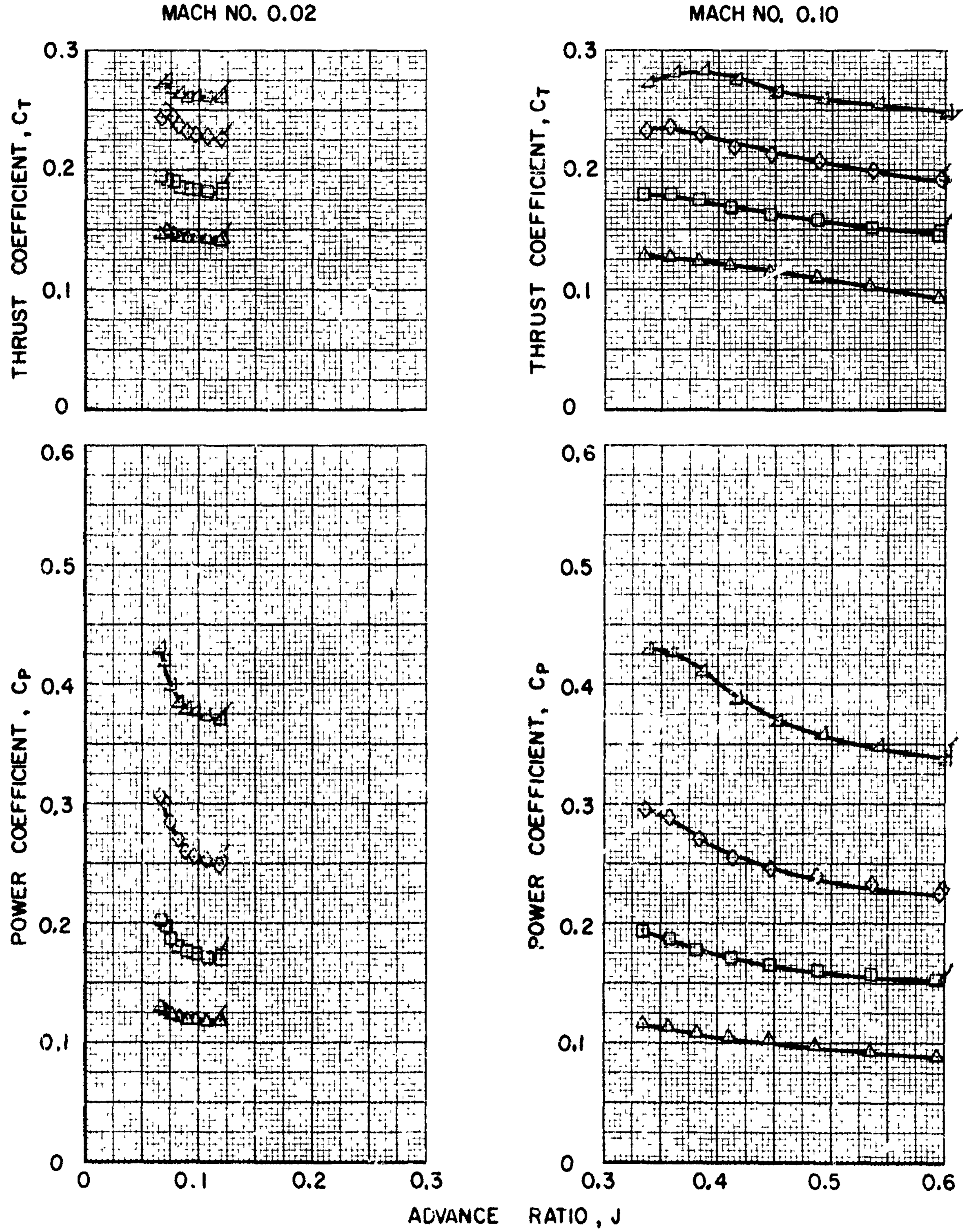

HSD SHROUDED PROPELLER TEST

EFFECT OF DIFFUSER (E_2) ON SHROUDED PROPELLER PERFORMANCE

SYM	RUN NO.	MACH NO.	CONFIGURATION	$\theta_{3/4}$
△	91 , 78	0.02 , 0.10	$L_1 C_1 E_2 B_3 P_{WT} T_1 R_1 R_E$ + TUFTS	20
⊡	90 , 80			25
◇	84 , 85			30
◿	89 , 88			35

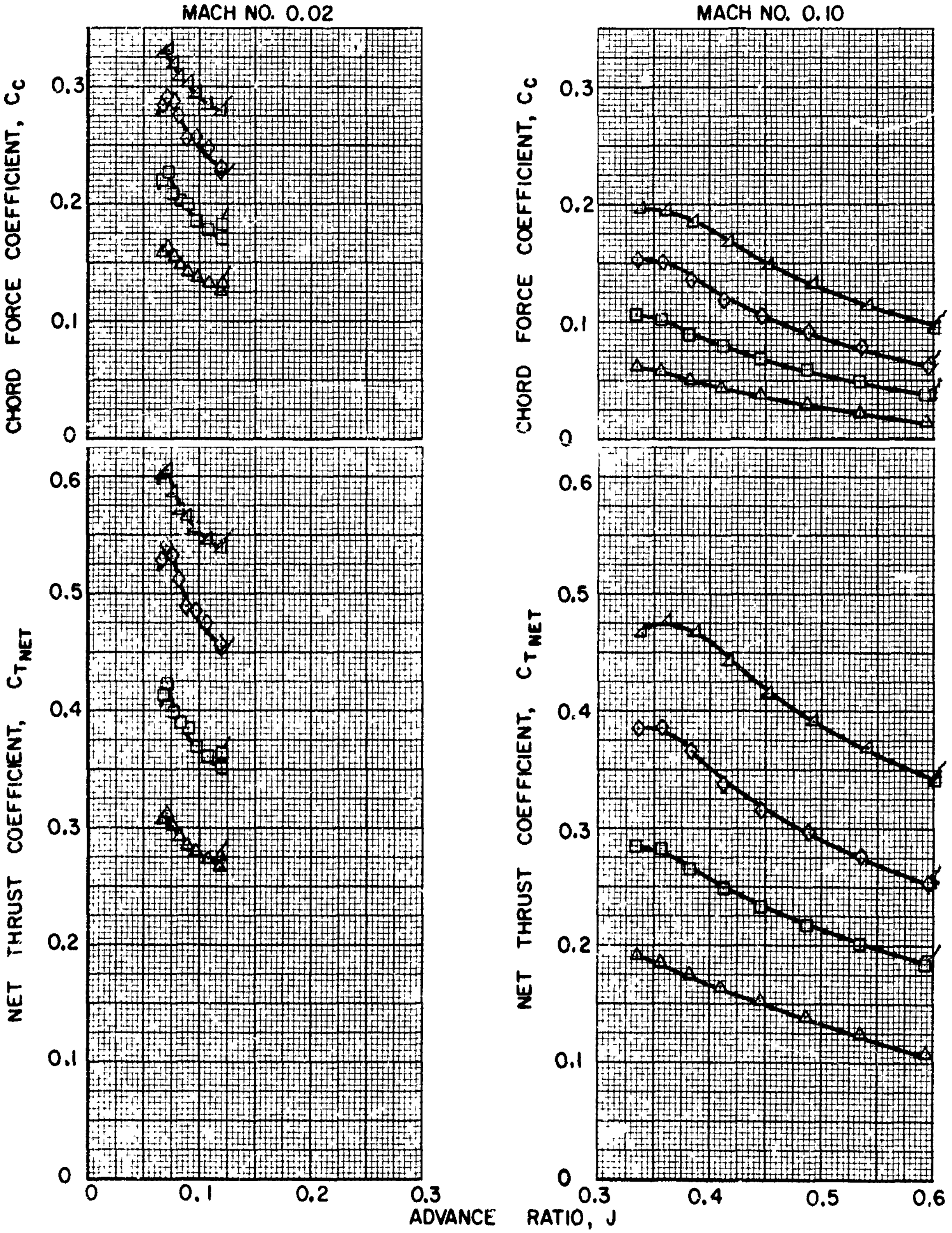

HSD SHROUDED PROPELLER TEST
EFFECT OF DIFFUSER (E_2) ON SHROUDED PROPELLER PERFORMANCE

SYM	RUN NO.	MACH NO.	CONFIGURATION	$\theta_{3/4}$
□	82	0.20	$L_1 C_1 E_2 B_3 P_{WT} T_1 R_1 R_E$	25
◇	86	↓	↓	30
◿	87	↓	↓	35
▽	92	↓	↓ + TUFTS	40

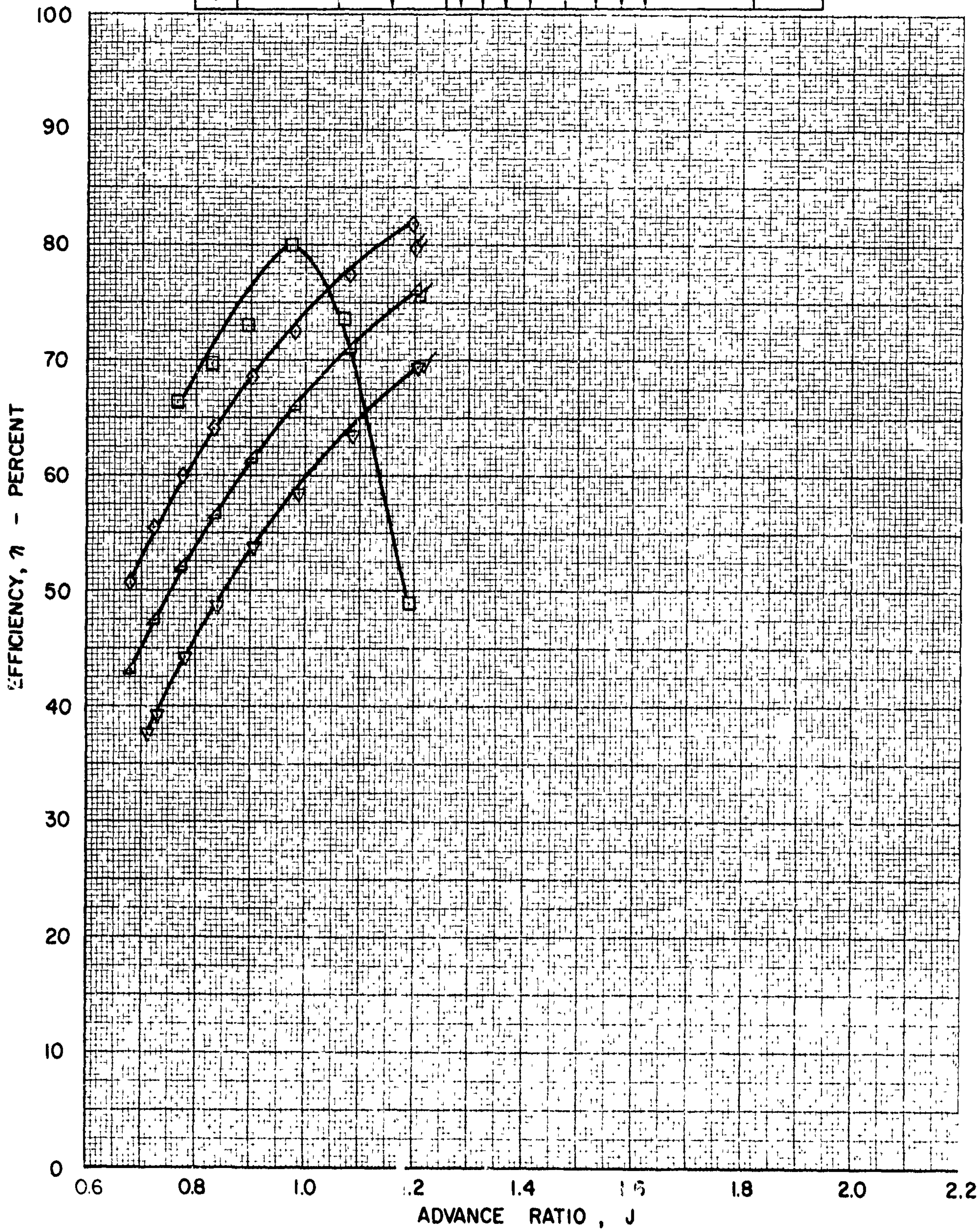

HSD SHROUDED PROPELLER TEST

EFFECT OF DIFFUSER (E_2) ON SHROUDED PROPELLER PERFORMANCE

SYM	RUN NO.	MACH NO.	CONFIGURATION	$\theta_{3/4}$
□	82	0.20	$L_1 C_1 E_2 B_3 P_{WT} T_1 R_1 R_E$	25
◇	86	↓	↓	30
◿	87	↓	↓	35
▽	92	↓	↓ + TUFTS	40

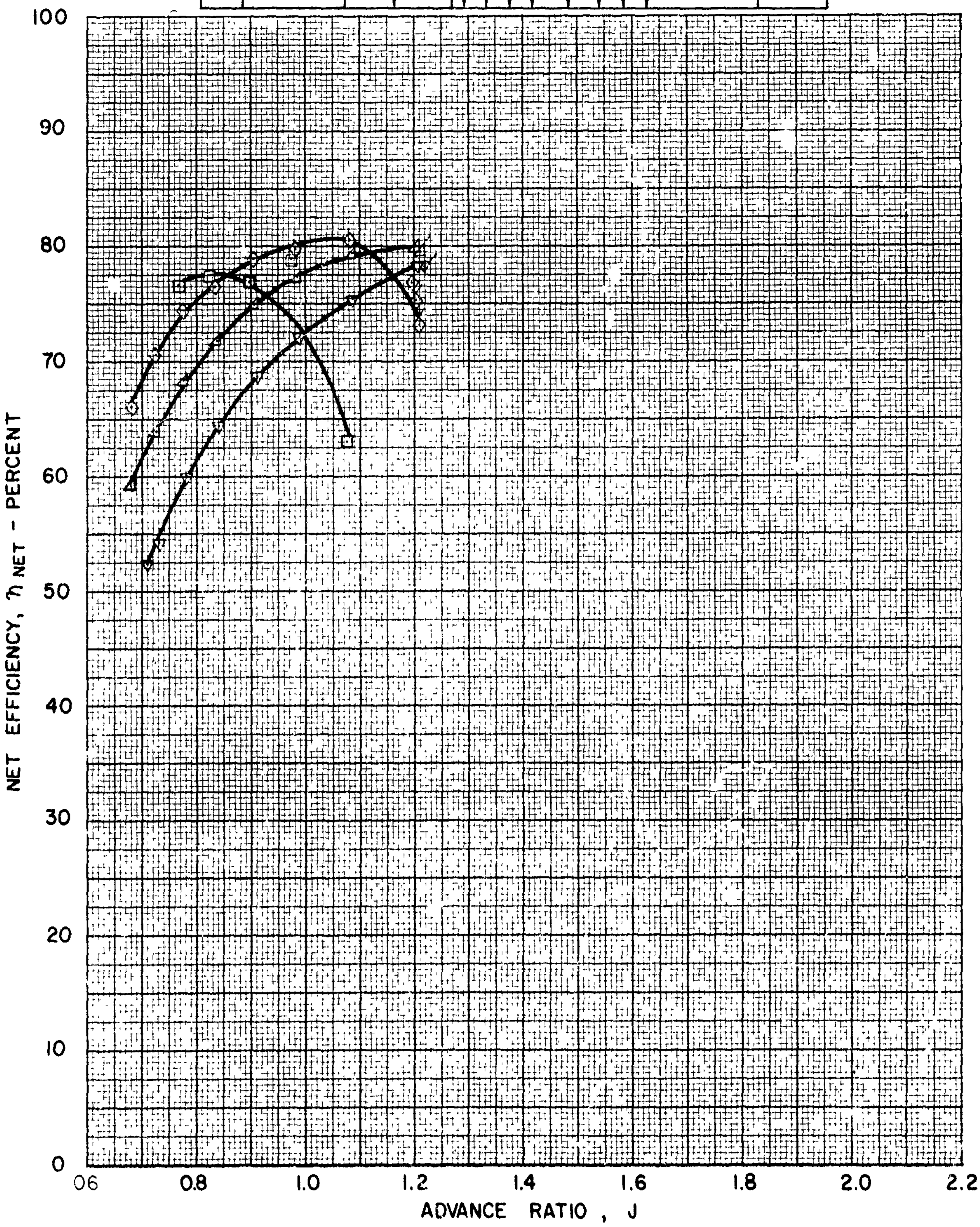

HSD SHROUDED PROPELLER TEST

EFFECT OF DIFFUSER (E_2) ON SHROUDED PROPELLER PERFORMANCE

SYM	RUN NO.	MACH NO.	CONFIGURATION	$\theta_{3/4}$
□	82	0.20	$L_1 C_1 E_2 B_3 P_{WT} T_1 R_1 R_E$	25
◇	86	↓	↓	30
△	87	↓	↓	35
▽	92	↓	↓ + TUFTS	40

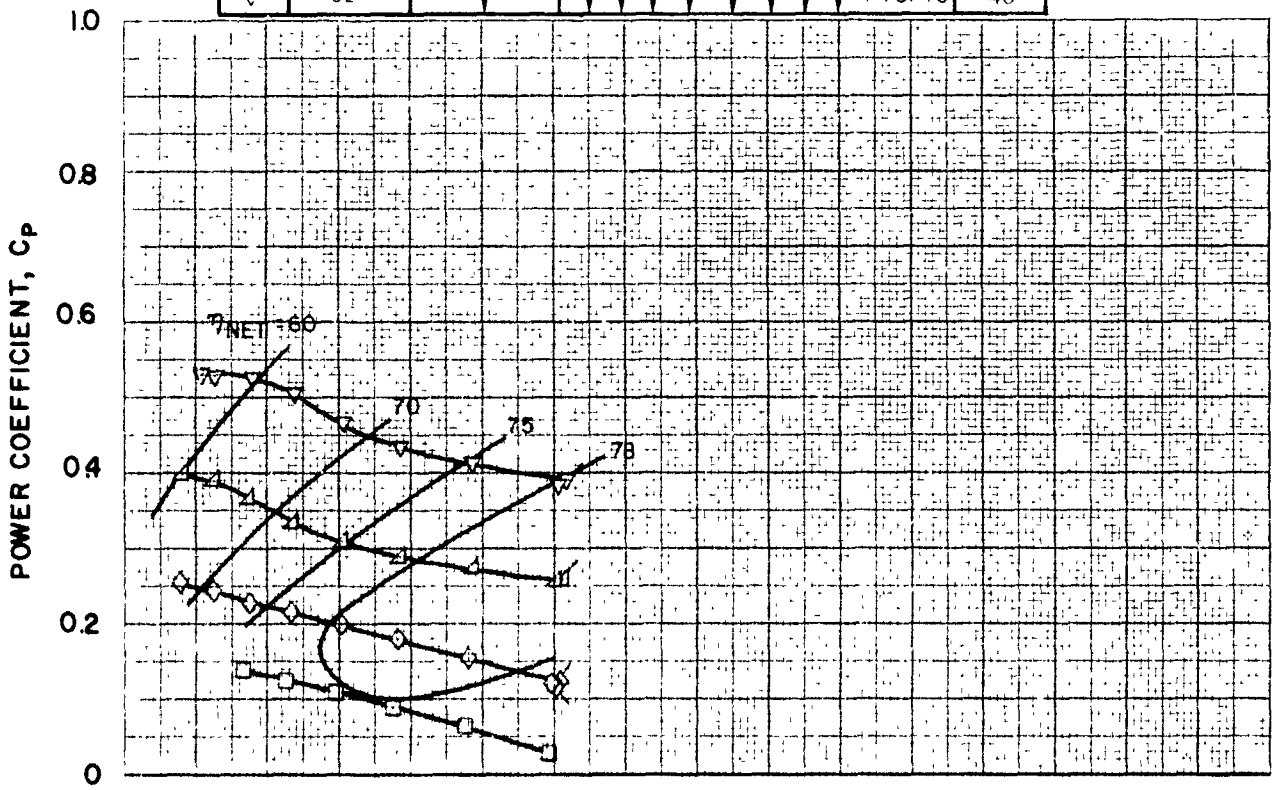

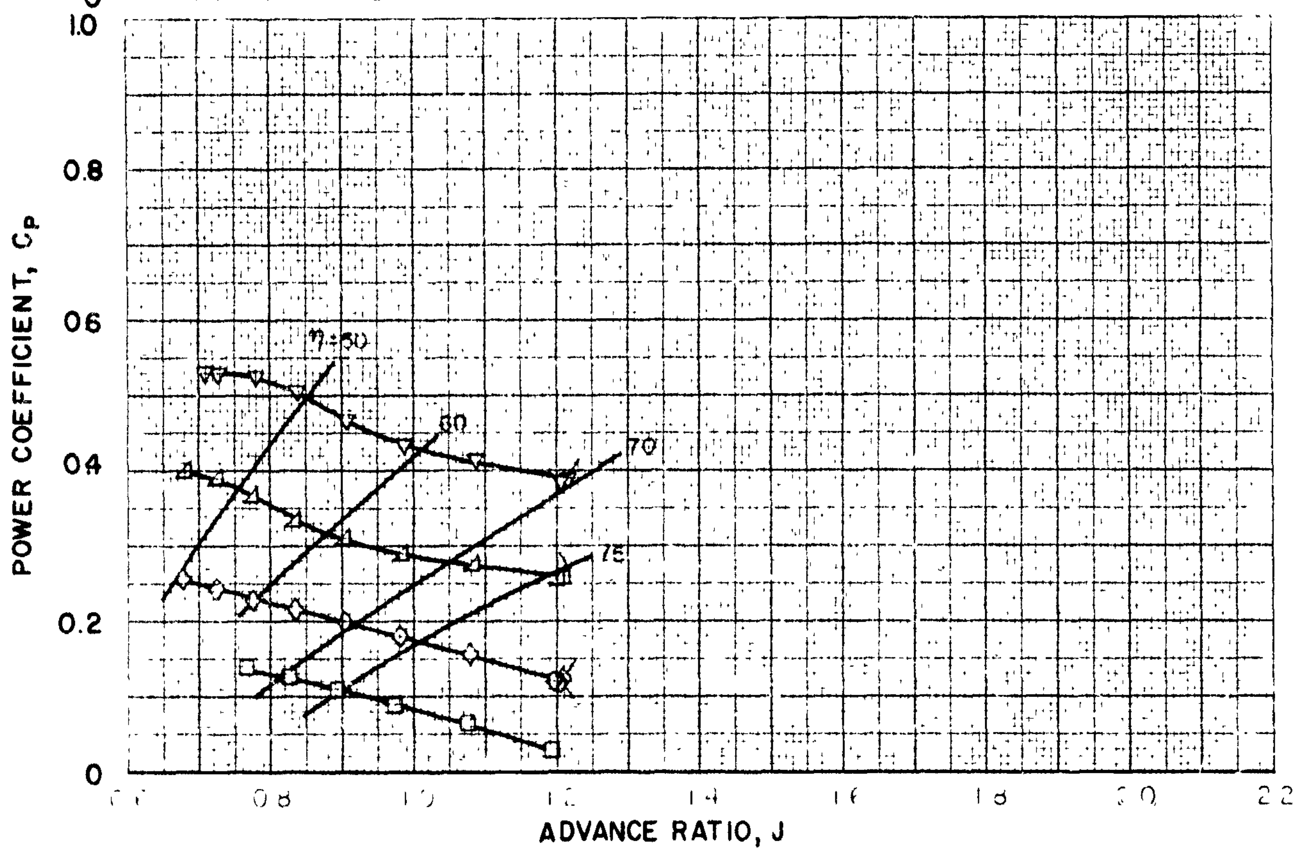

E330590-1

FIG. 66

HSD SHROUDED PROPELLER TEST

EFFECT OF DIFFUSER (E_2) ON SHROUDED PROPELLER PERFORMANCE

SYM	RUN NO.	MACH NO.	CONFIGURATION	$\theta_{3/4}$
◇	509	0.30	$L_1 C_1 E_2 B_3 P_{WT} T_1 R_1 R_E$	30
◁	510	↓	↓	34
▽	511	↓	↓	38
D	513	↓	↓	42

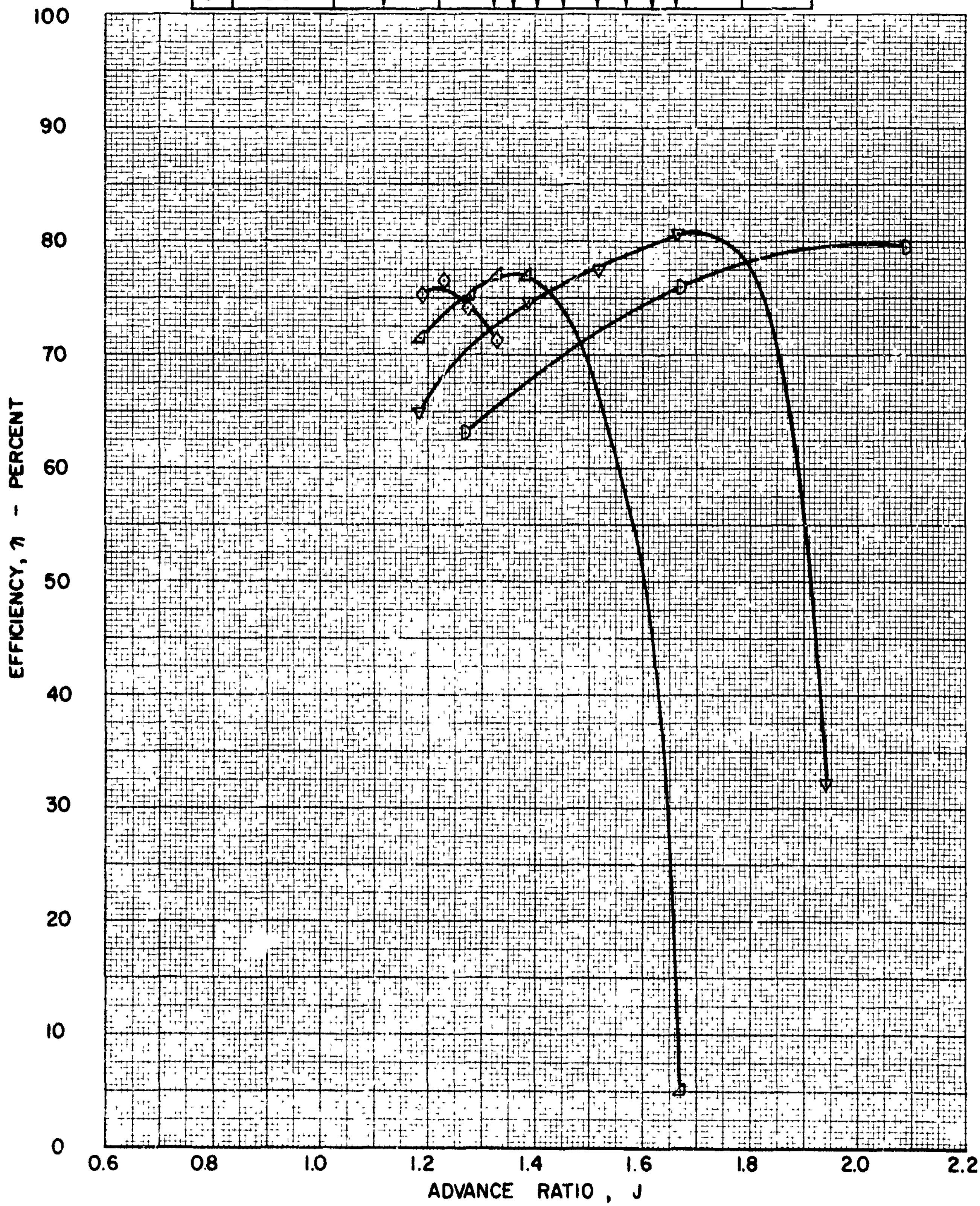

E330590-1

FIG. 67

HSD SHROUDED PROPF'.LER TEST

EFFECT OF DIFFUSER (E_2) ON SHROUDED PROPELLER PERFORMANCE

SYM	RUN NO.	MACH NO.	CONFIGURATION	$\theta_{3/4}$
◇	509	0.30	$L_1 C_1 E_2 B_3 P_{WT} T_1 R_1 R_E$	30
⊿	510	↓	↓	34
▽	511	↓	↓	38
D	513	↓	↓	42

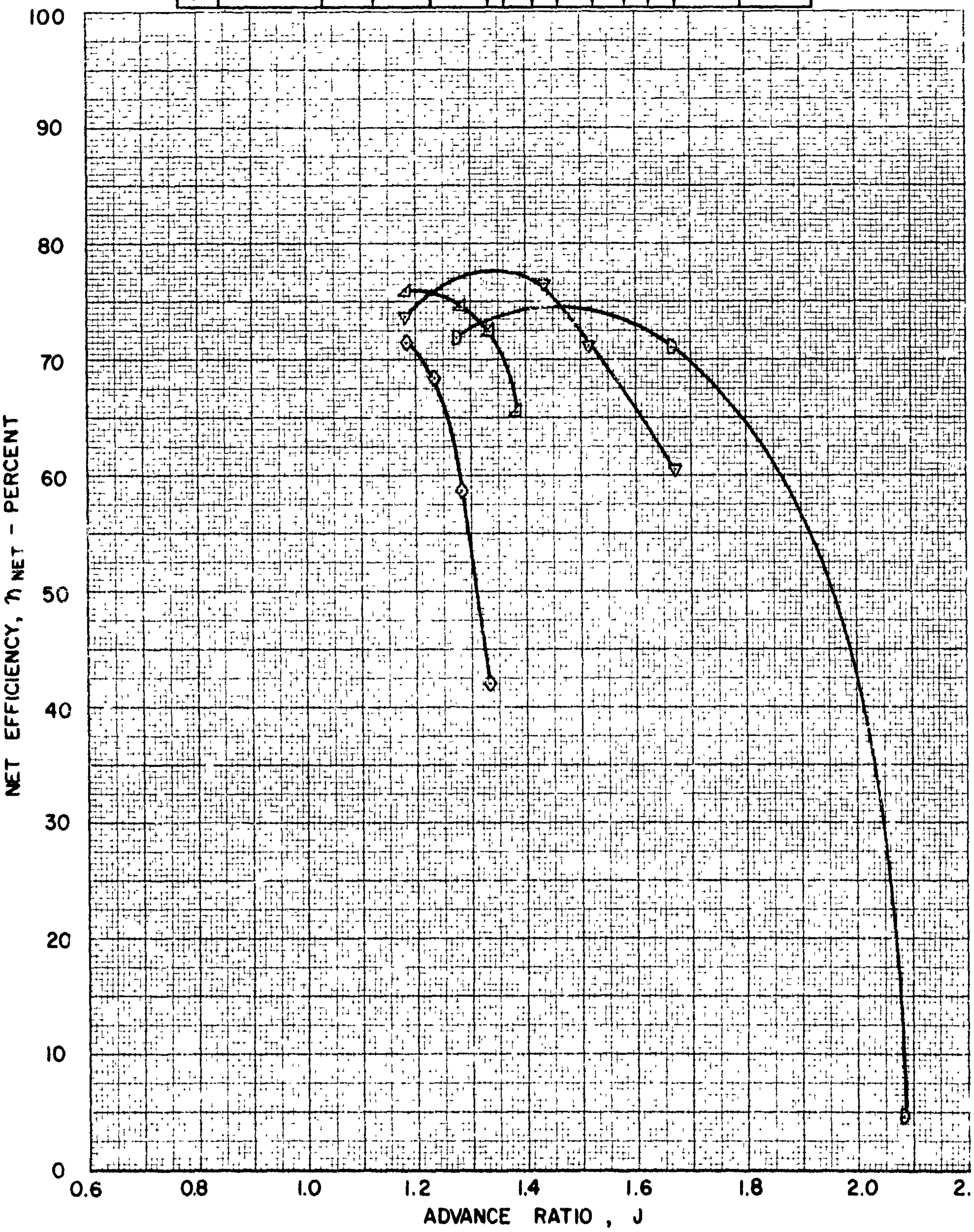

HSD SHROUDED PROPELLER TEST

EFFECT OF DIFFUSER (E2) ON SHROUDED PROPELLER PERFORMANCE

SYM	RUN NO.	MACH NO.	CONFIGURATION	θ 3/4
◇	509	0.30	I, C1 E2 B3 PWT T1 R1 RE	30
⊿	510			34
▽	511			38
D	513			42

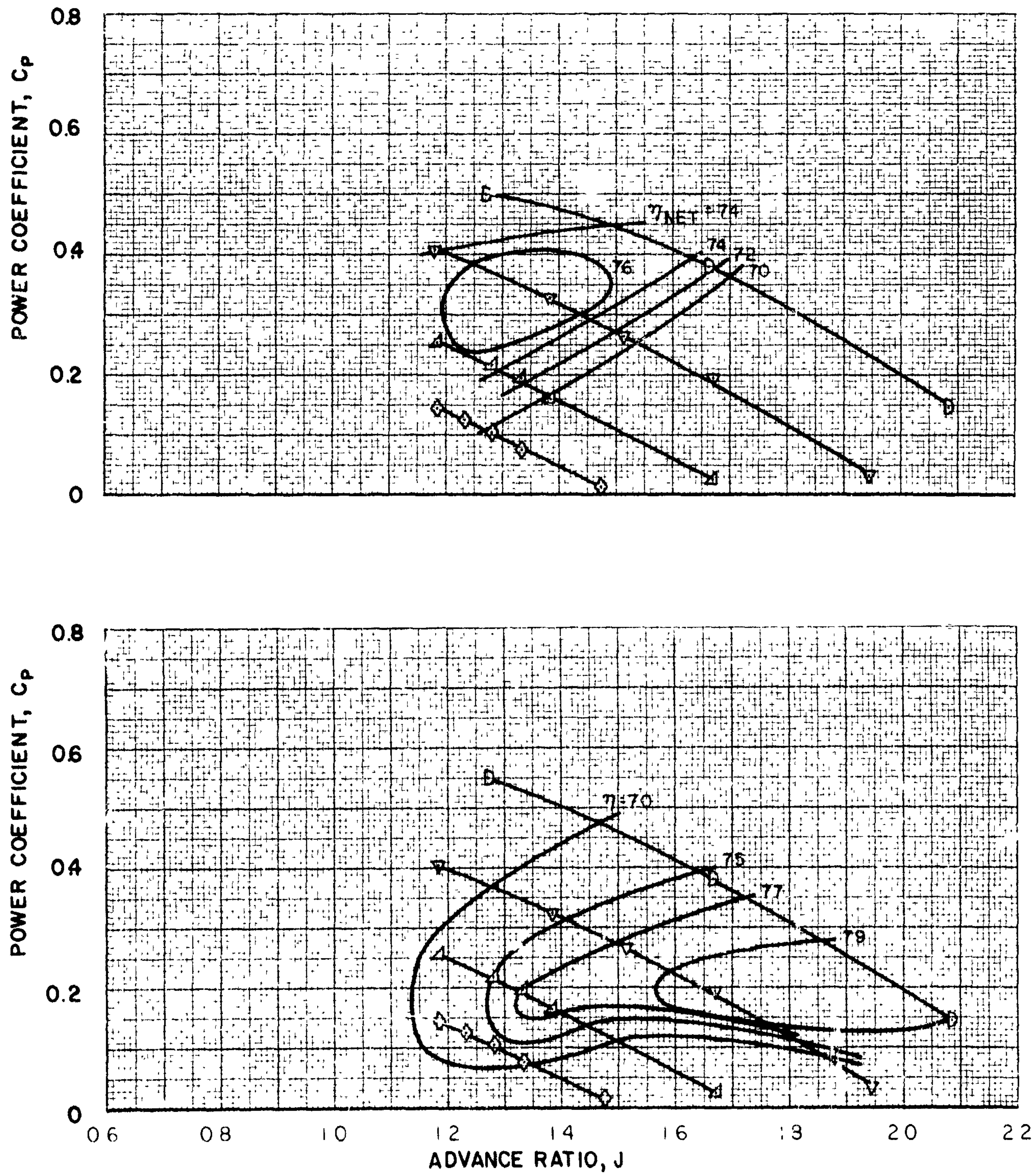

HSD SHROUDED PROPELLER TEST

EFFECT OF DIFFUSER (E_2) ON SHROUDED PROPELLER PERFORMANCE

SYM	RUN NO.	MACH NO.	CONFIGURATION	$\theta_{3/4}$
▽	512	0.40	$L_1 C_1 E_2 B_3 P_{WT} T_1 R_1 R_E$	38
D	514	↓	↓	42
◺	516	↓	↓	46
ɑ	518	↓	↓	50

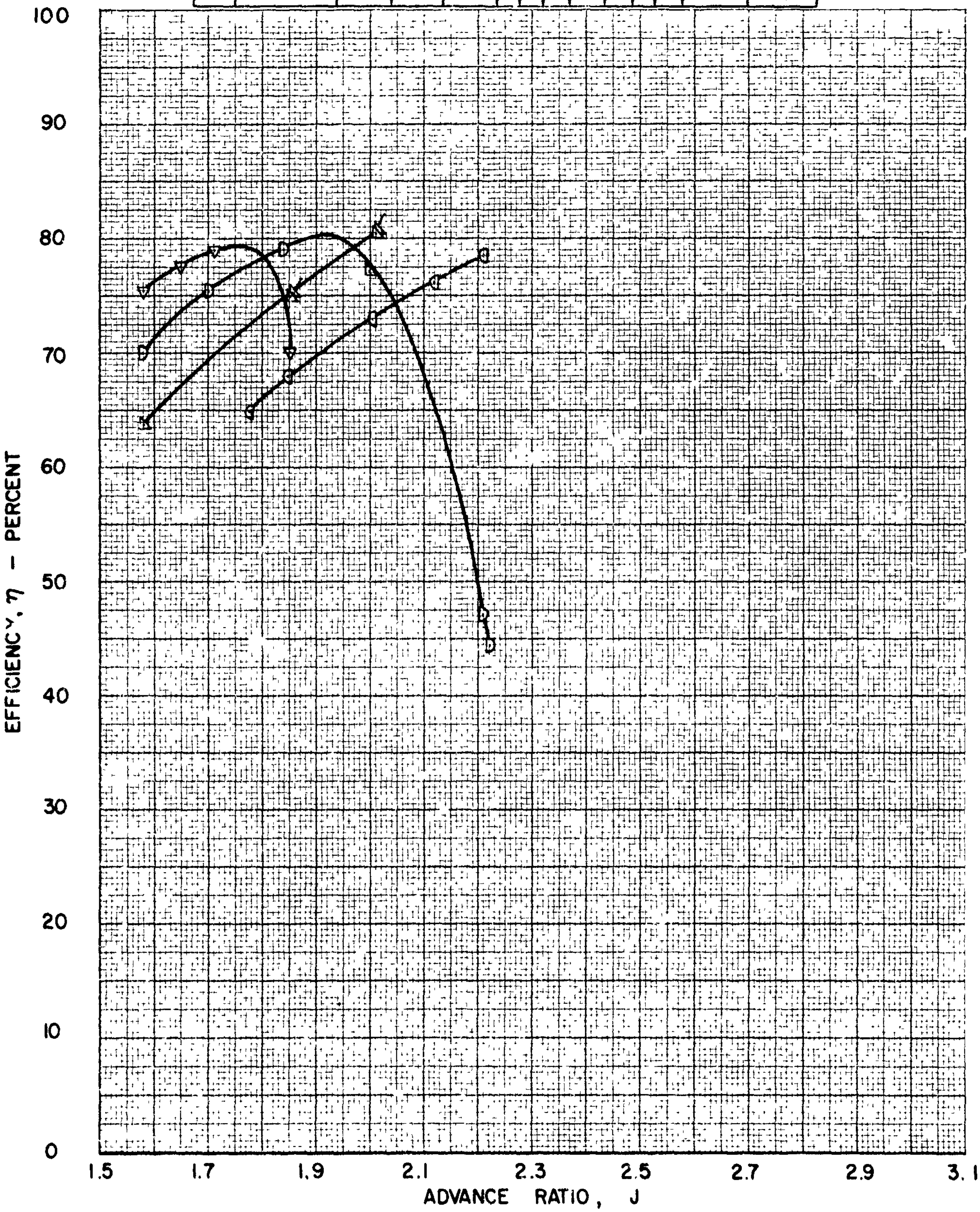

E330590-1

FIG. 70

HSD SHROUDED PROPELLER TEST

EFFECT OF DIFFUSER (E_2) ON SHROUDED PROPELLER PERFORMANCE

SYM	RUN NO.	MACH NO.	CONFIGURATION	$\theta_{3/4}$
▽	512	0.40	$L_1 C_1 E_2 B_3 P_{WT} T_1 R_1 R_E$	38
D	514	↓	↓	42
◺	516	↓	↓	46
C	518	↓	↓	50

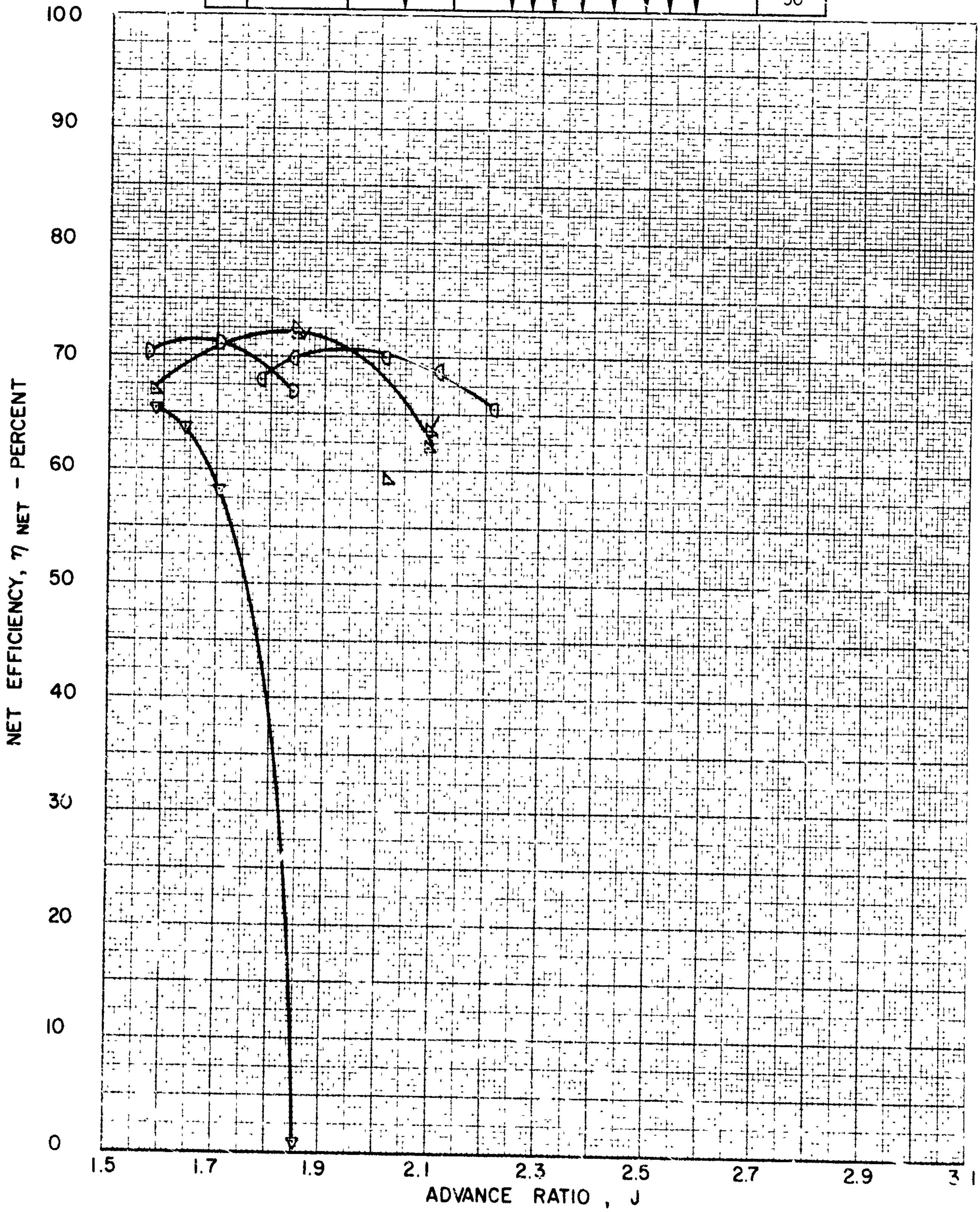

E330590-I

FIG.71

HSD SHROUDED PROPELLER TEST

EFFECT OF DIFFUSER (E_2) ON SHROUDED PROPELLER PERFORMANCE

SYM	RUN NO.	MACH NO.	CONFIGURATION	$\theta_{3/4}$
▽	512	0 40	$L_1C_1E_2B_3P_{WT}T_1R_1R_E$	38
D	514	↓	↓	42
◺	516	↓	↓	46
◖	518	↓	↓	50

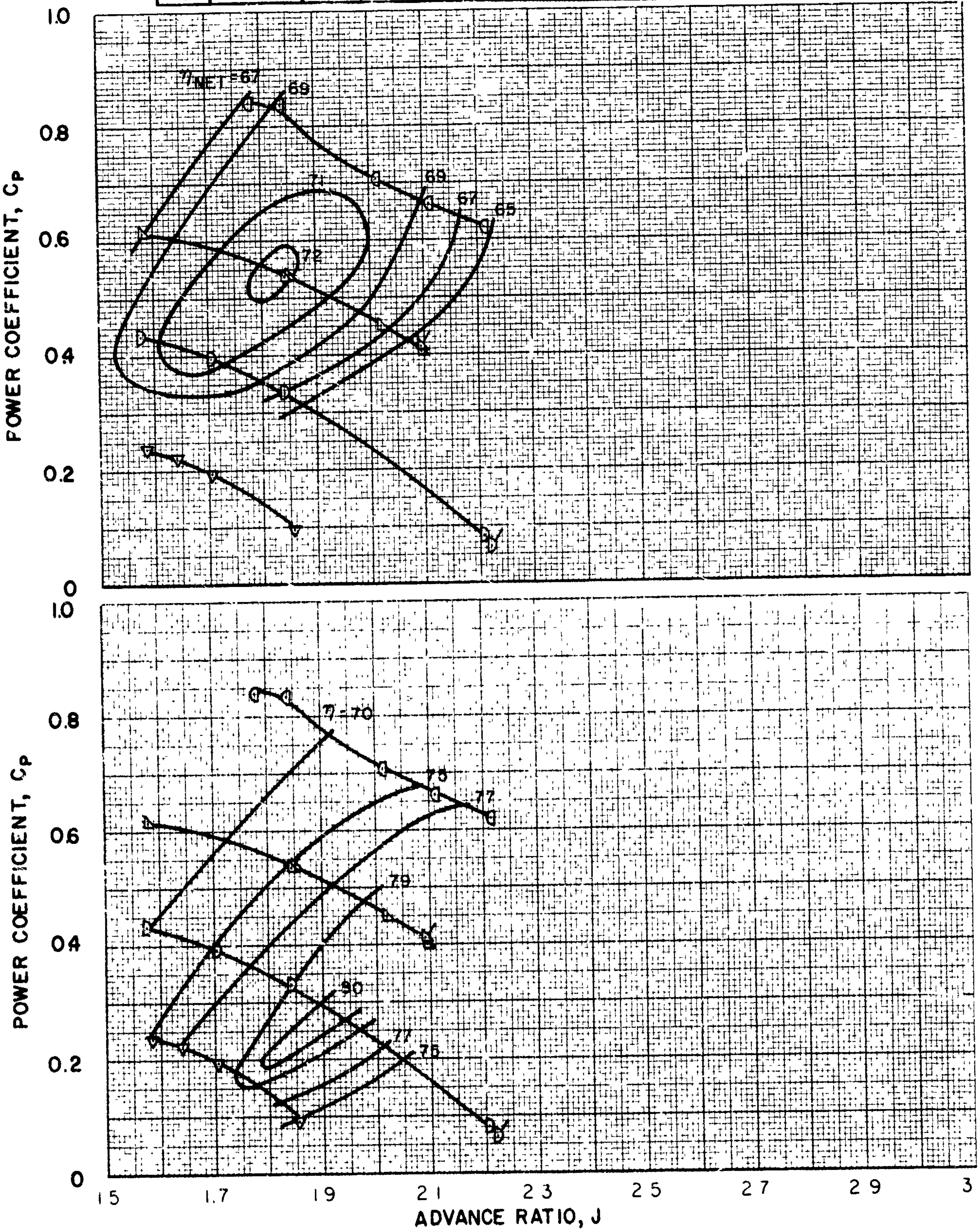

E330590-1

FIG. 72

HSD SHROUDED PROPELLER TEST

EFFECT OF DIFFUSER (E_2) ON SHROUDED PROPELLER PERFORMANCE

SYM	RUN NO.	MACH NO.	CONFIGURATION	$\theta_{3/4}$
◸	515	0.50	$L_1 C_1 E_2 B_3 P_{WT} T_1 R_1 R_E$	42
◺	517	↓	↓	46
◖	519	↓	↓	50
⊙	520	↓	↓	54

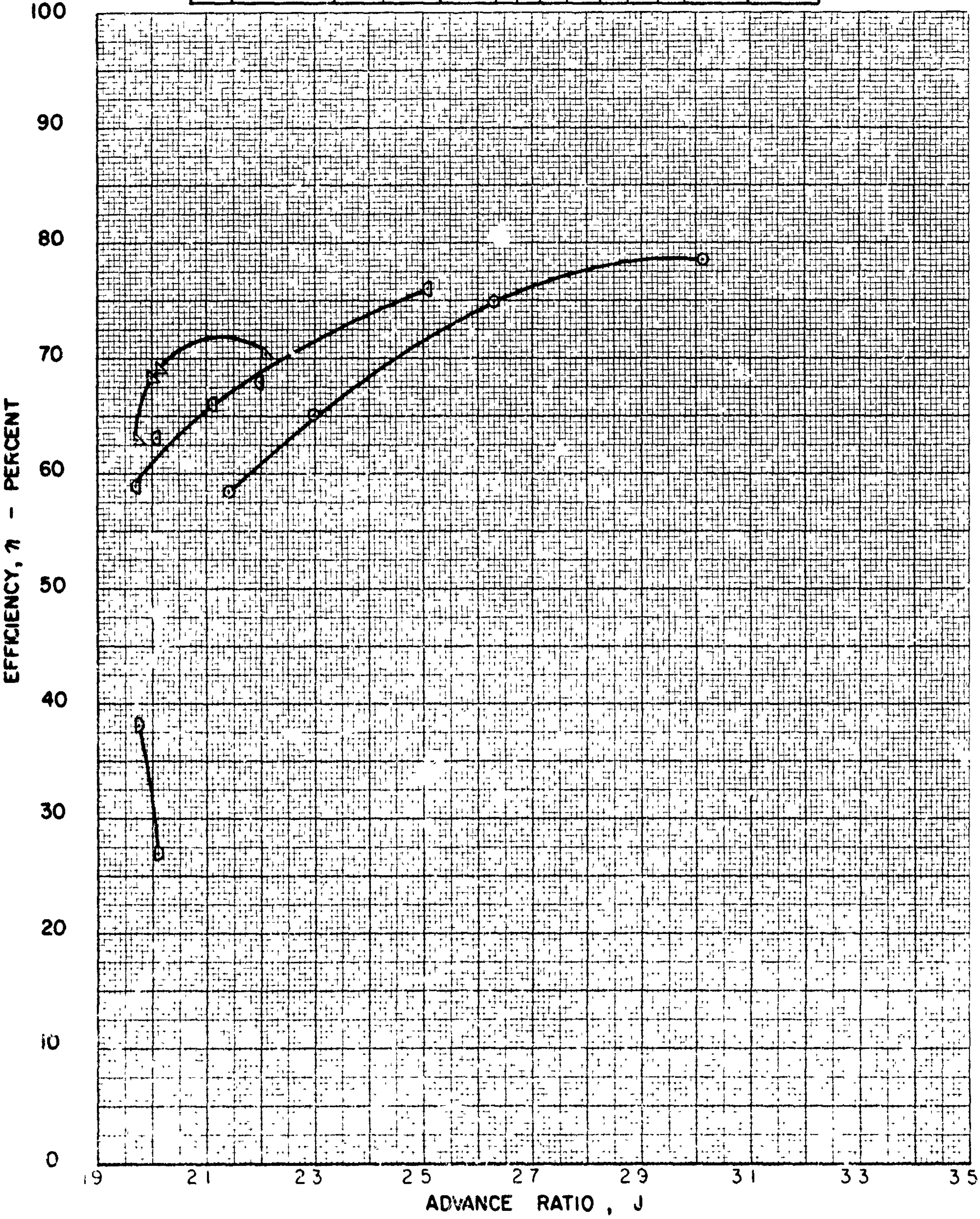

E330590-I

FIG. 73

HSD SHROUDED PROPELLER TEST

EFFECT OF DIFFUSER (E_2) ON SHROUDED PROPELLER PERFORMANCE

SYM	RUN NO.	MACH NO.	CONFIGURATION	$\theta_{3/4}$
□	515	0.50	$L_1 C_1 E_2 B_3 P_{WT} T_1 R_1 R_E$	42
△	517	↓	↓	46
◁	519	↓	↓	50
○	520	↓	↓	54

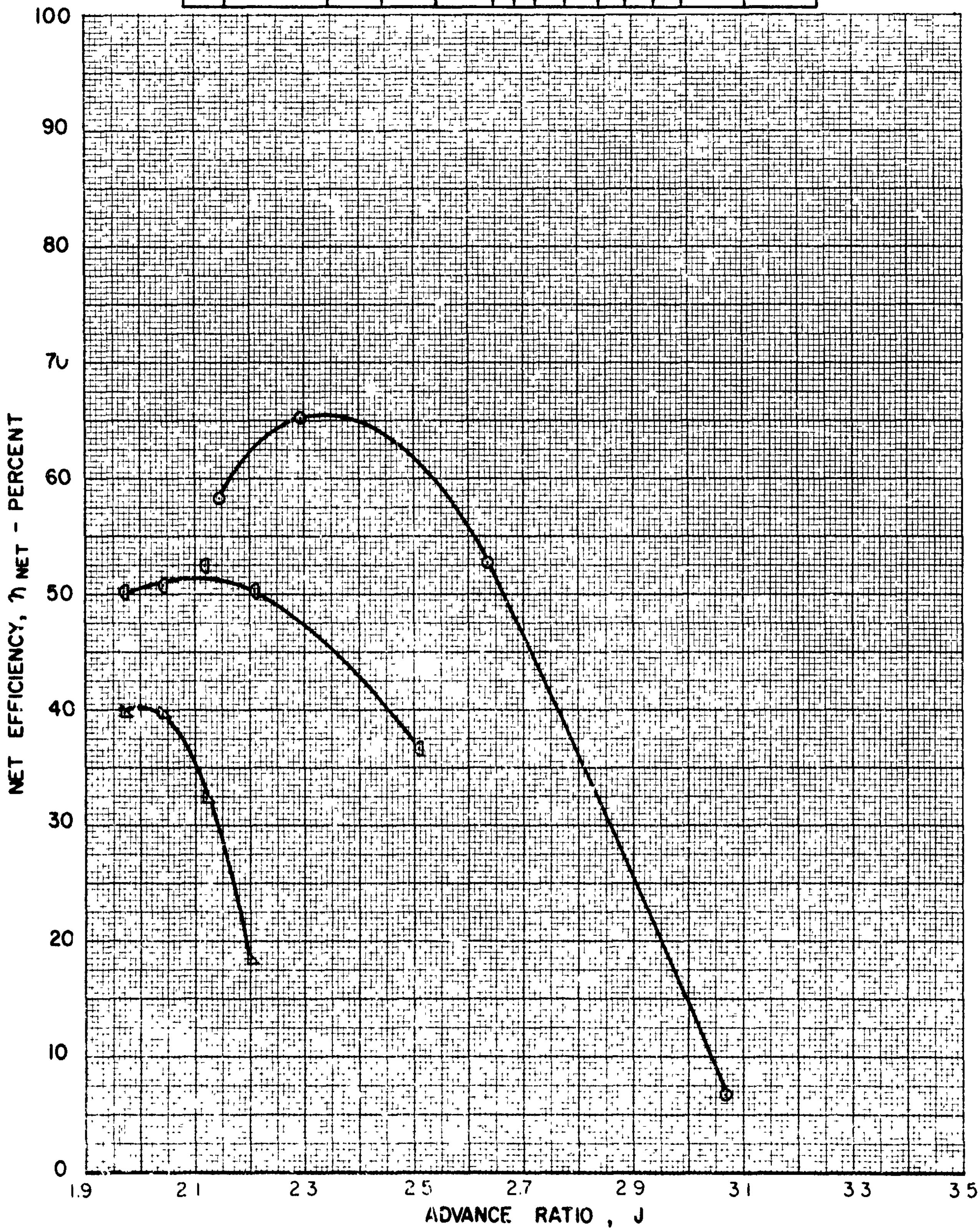

E330590-I

FIG. 74

HSD SHROUDED PROPELLER TEST

EFFECT OF DIFFUSER (E_2) ON SHROUDED PROPELLER PERFORMANCE

SYM	RUN NO.	MACH NO.	CONFIGURATION	$\theta_{3/4}$
D	515	0.50	$L_1 C_1 E_2 B_3 P_{WT} T_1 R_1 R_E$	42
Δ	517	↓	↓	46
ɑ	519	↓	↓	50
O	520	↓	↓	54

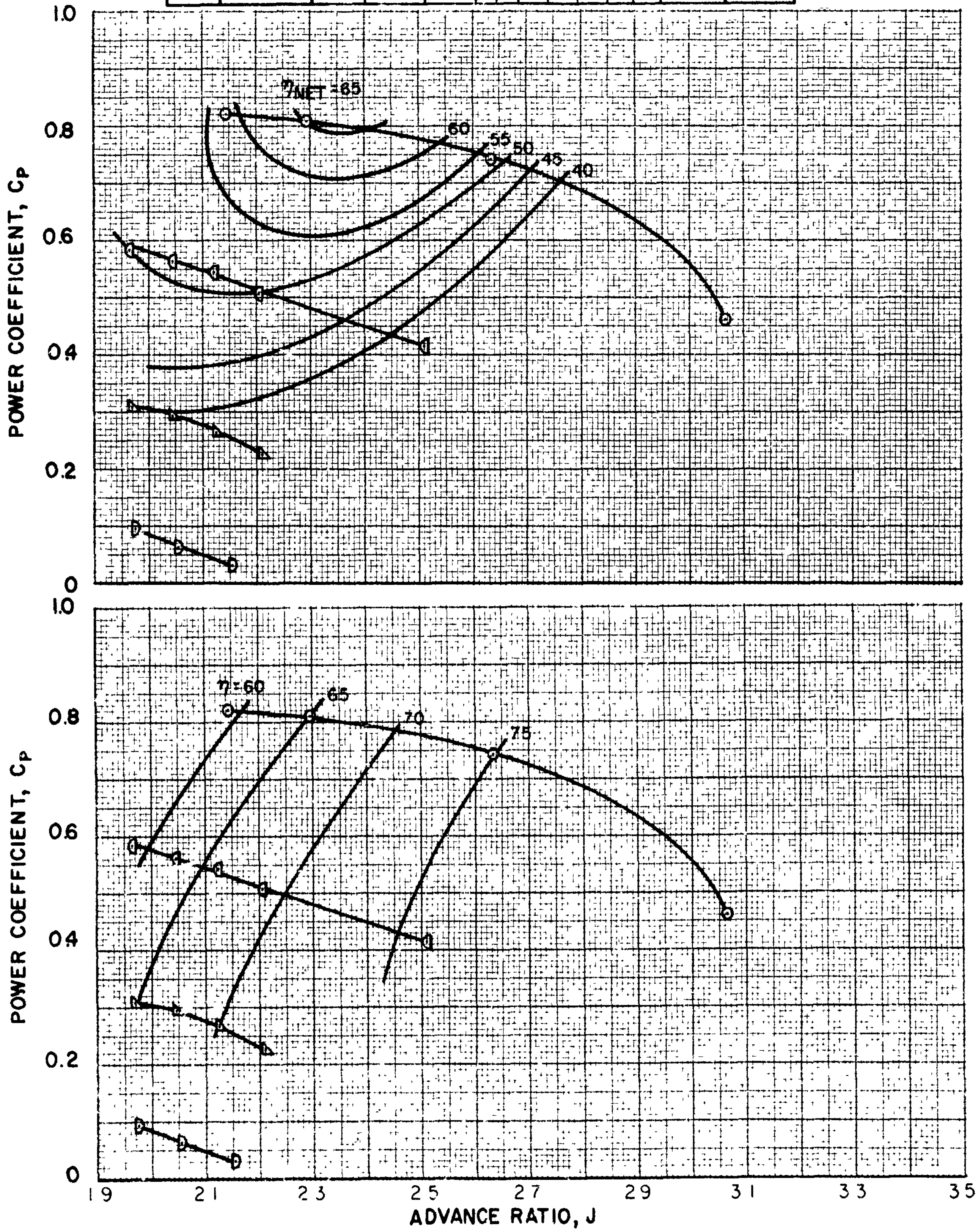

HSD SHROUDED PROPELLER TEST

EFFECT OF DIFFUSER (E_3) ON SHROUDED PROPELLER PERFORMANCE

SYM	RUN NO.	MACH NO.	CONFIGURATION	$\theta_{3/4}$
△	93 ,107	0.02 ,0.10	$L_1 C_1 E_3 B_3 P_{WT} T_1 R_1 R_E$	20
⊡	108 ,110	↓	↓	25
◇	102 ,95	↓	↓	30
◿	115 ,113	↓	↓	35

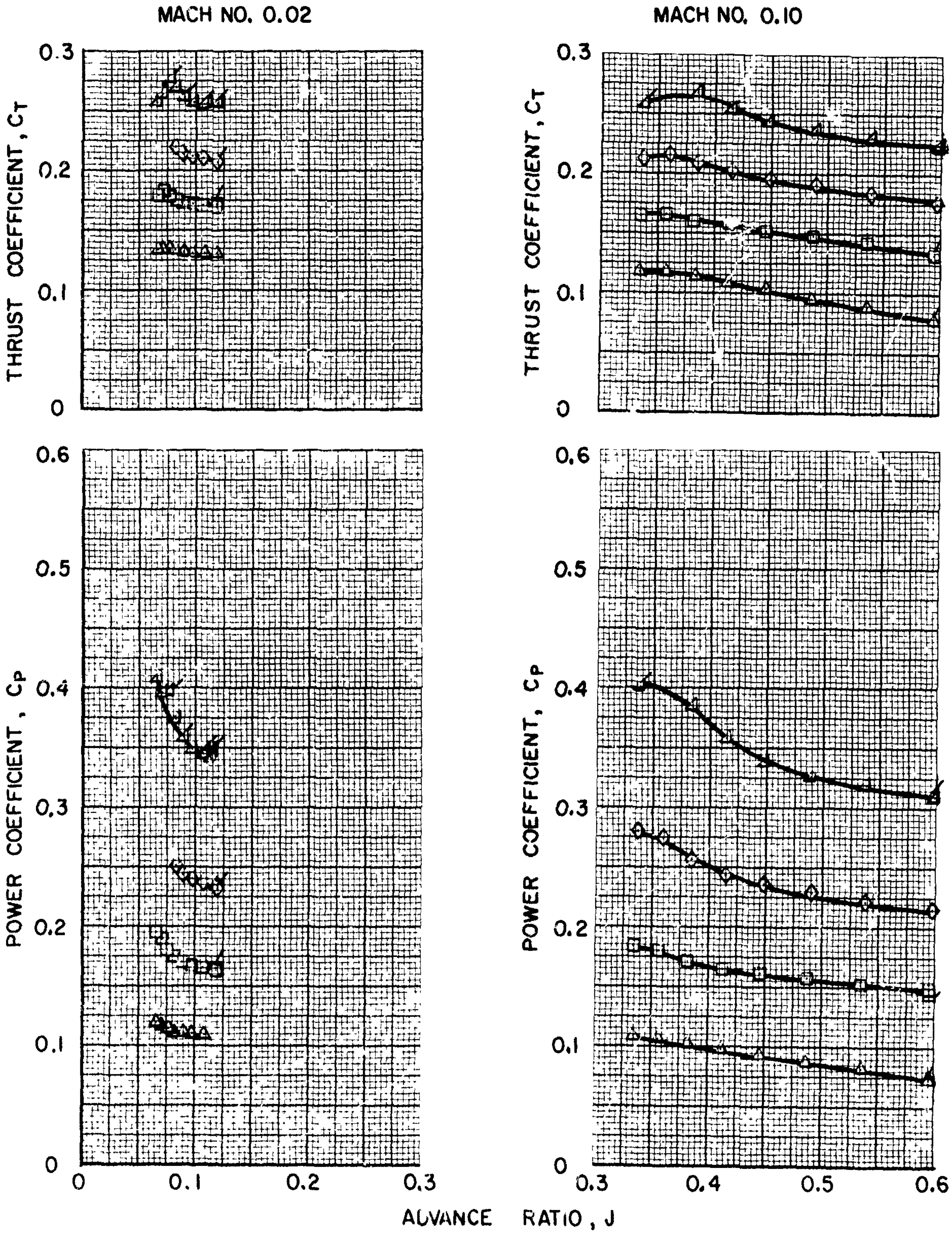

HSD SHROUDED PROPELLER TEST

EFFECT OF DIFFUSER (E_3) ON SHROUDED PROPELLER PERFORMANCE

SYM	RUN NO.	MACH NO.	CONFIGURATION	$\theta_{3/4}$
△	93 ,107	0.02 ,0.10	$L_1 C_1 E_3 B_3 P_{WT} T_1 R_1 R_E$	20
⊡	108 ,110	↓	↓	25
◇	102 , 95	↓	↓	30
⊿	115 ,113	↓	↓	35

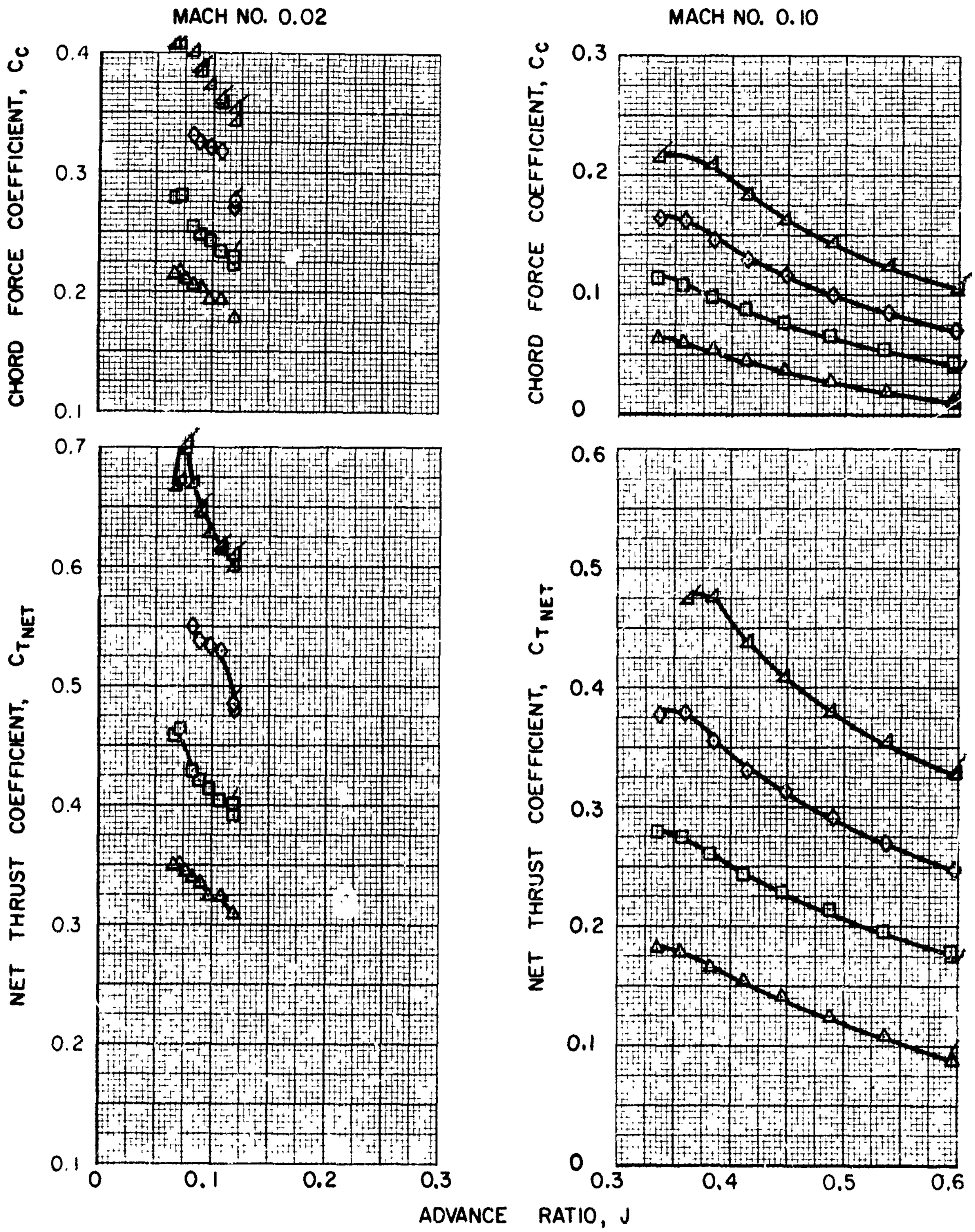

HSD SHROUDED PROPELLER TEST

EFFECT OF DIFFUSER (E_3) ON SHROUDED PROPELLER PERFORMANCE

SYM	RUN NO.	MACH NO.	CONFIGURATION	$\theta_{3/4}$
□	111	0 20	$L_1 C_1 E_3 B_3 P_{WT} T_1 R_1 R_E$	25
◇	96	↓	↓	30
◿	112	↓	↓	35
▽	116	↓	↓	40

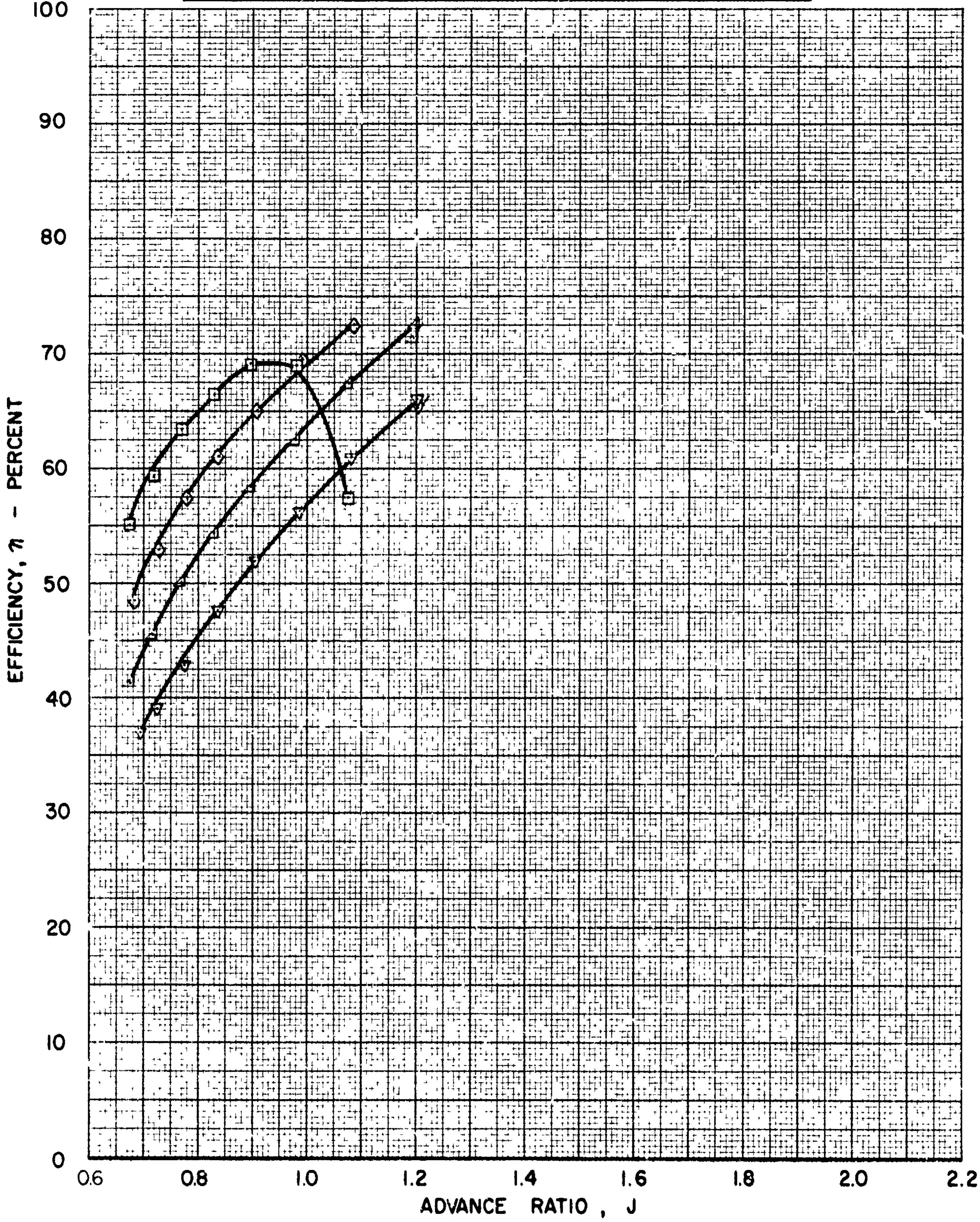

HSD SHROUDED PROPELLER TEST

EFFECT OF DIFFUSER (E_3) ON SHROUDED PROPELLER PERFORMANCE

SYM	RUN NO.	MACH NO.	CONFIGURATION	$\theta_{3/4}$
□	111	0.20	$L_1 C_1 E_3 B_3 P_{WT} T_1 R_1 R_E$	25
◇	96	↓	↓	30
◿	112	↓	↓	35
▽	116	↓	↓	40

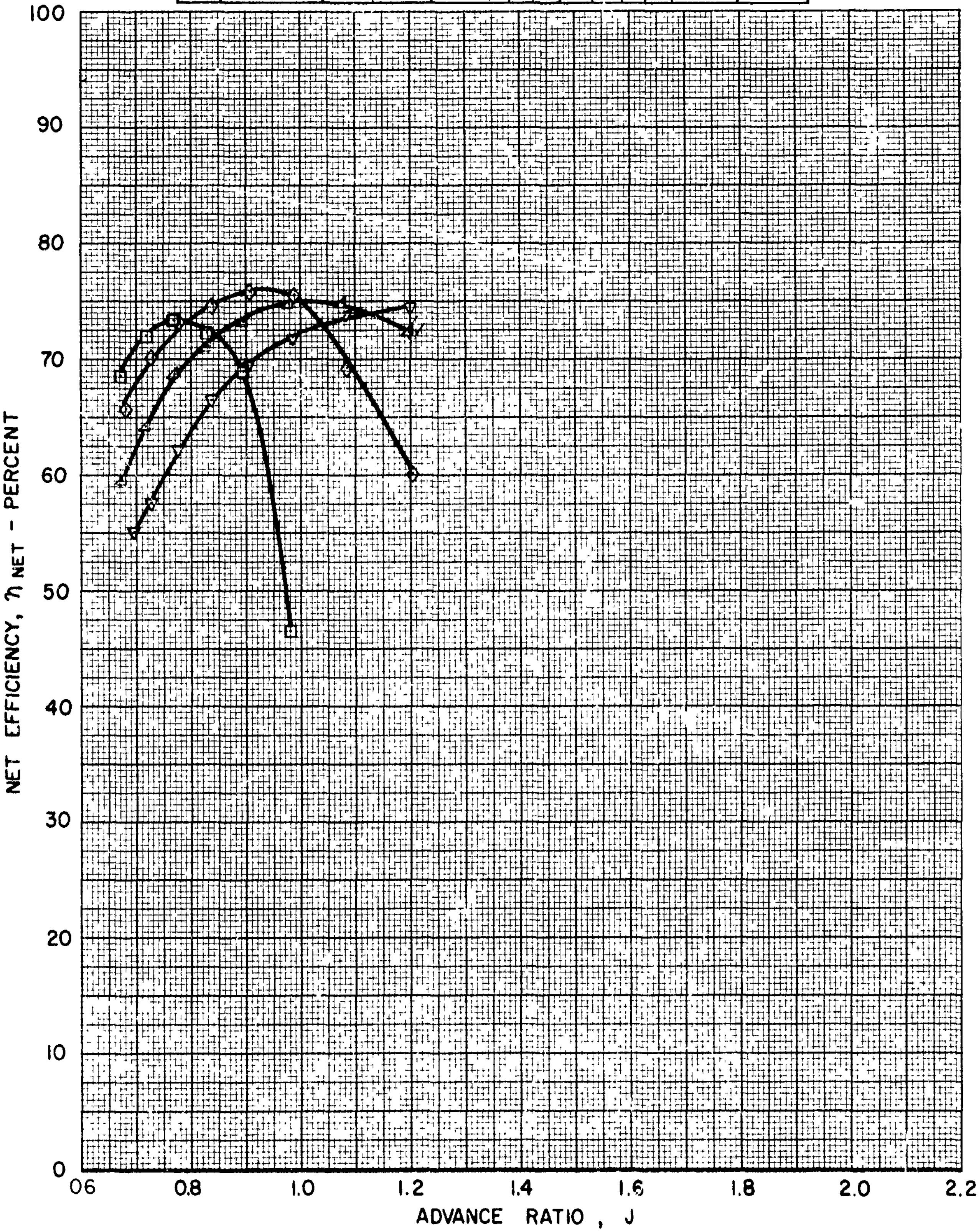

E330590-I

FIG.79

HSD SHROUDED PROPELLER TEST

EFFECT OF DIFFUSER (E_3) ON SHROUDED PROPELLER PERFORMANCE

SYM	RUN NO.	MACH NO.	CONFIGURATION	$\beta_{3/4}$
⊡	111	0.20	$L_1 C_1 E_3 B_3 P_{WT} T_1 R_1 R_E$	25
◇	96	↓	↓	30
△	112	↓	↓	35
▽	116	↓	↓	40

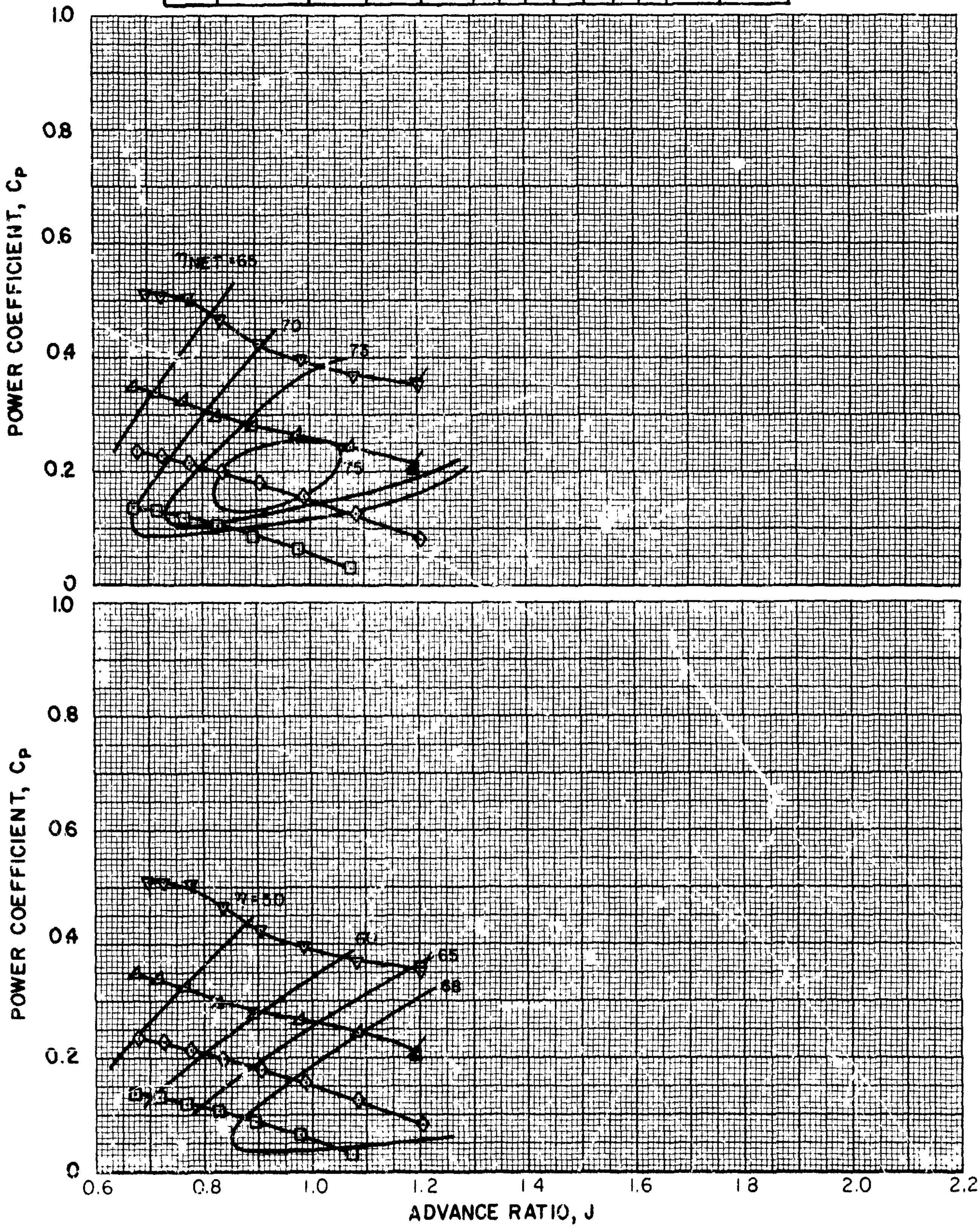

E330590-1

FIG.80

HSD SHROUDED PROPELLER TEST

EFFECT OF DIFFUSER (E_3) ON SHROUDED PROPELLER PERFORMANCE

SYM	RUN NO.	MACH NO.	CONFIGURATION	$\theta_{3/4}$
⊿	522	0.30	$L_1 C_1 E_3 B_3 P_{WT} T_1 R_1 R_E$	34
▽	523	↓	↓	38
D	524	↓	↓	42
◺	526	↓	↓	46

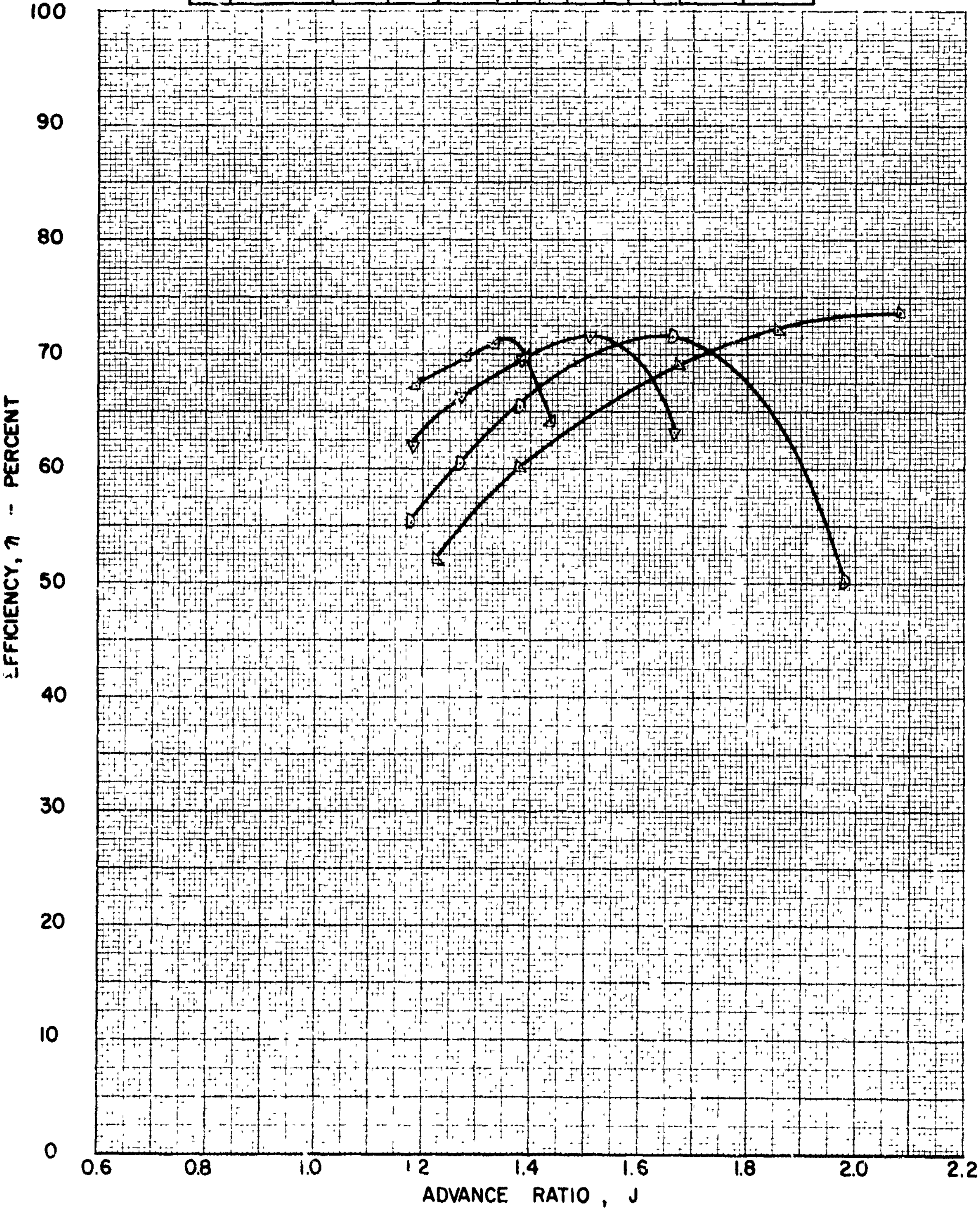

E330590-1 FIG. 81

HSD SHROUDED PROPELLER TEST

EFFECT OF DIFFUSER (E_3) ON SHROUDED PROPELLER PERFORMANCE

SYM	RUN NO.	MACH NO.	CONFIGURATION	$\theta_{3/4}$
⊿	522	0 30	$L_1 C_1 E_3 B_3 P_{WT} T_1 R_1 R_E$	34
▽	523	↓	↓	38
D	524	↓	↓	42
◺	526	↓	↓	46

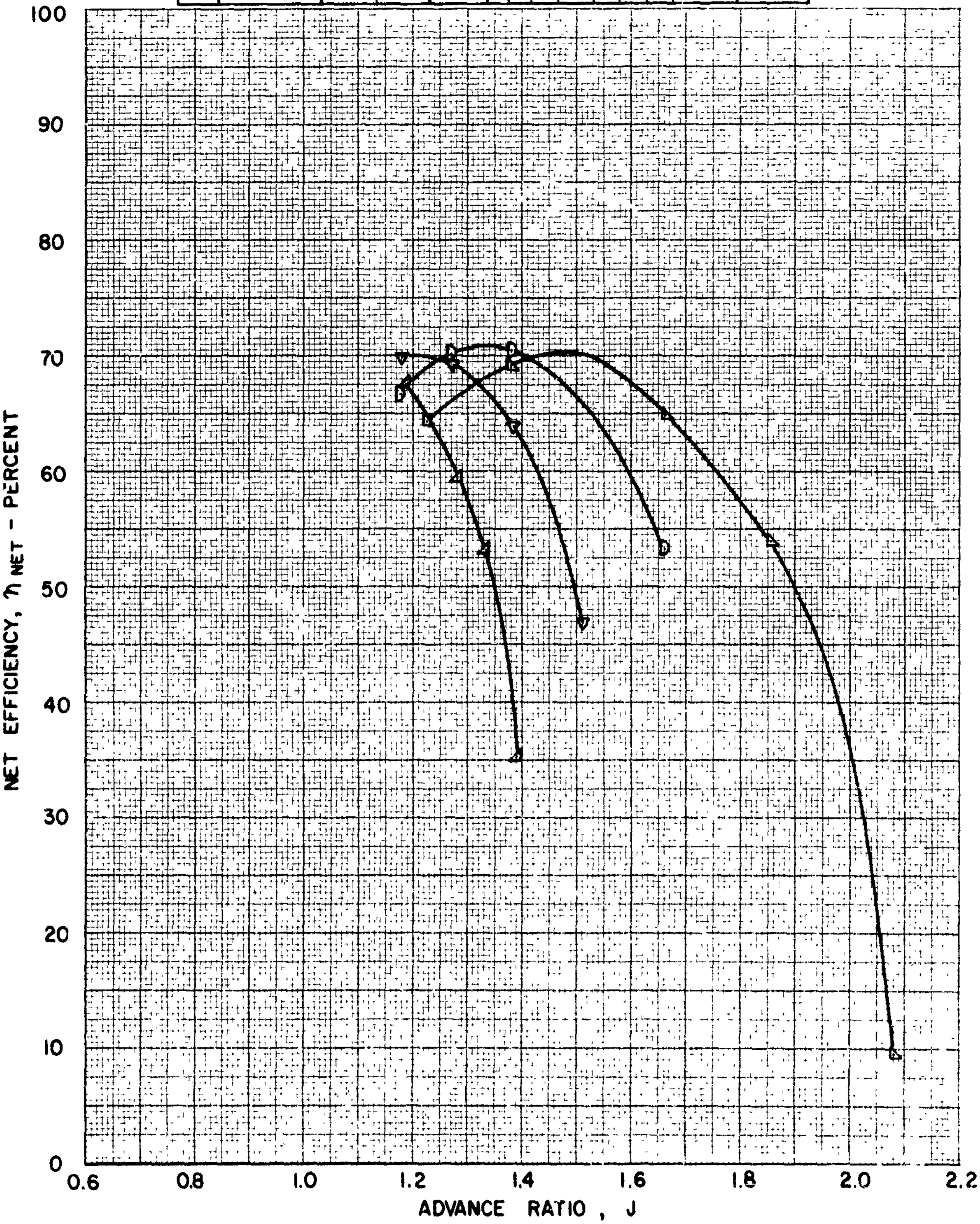

HSD SHROUDED PROPELLER TEST

EFFECT OF DIFFUSER (E_3) ON SHROUDED PROPELLER PERFORMANCE

SYM	RUN NO.	MACH NO.	CONFIGURATION	$\theta_{3/4}$
⊿	522	0.30	$L_1 C_1 E_3 B_3 P_{WT} T_1 R_1 R_E$	34
▽	523	↓	↓	38
D	524	↓	↓	42
◺	526	↓	↓	46

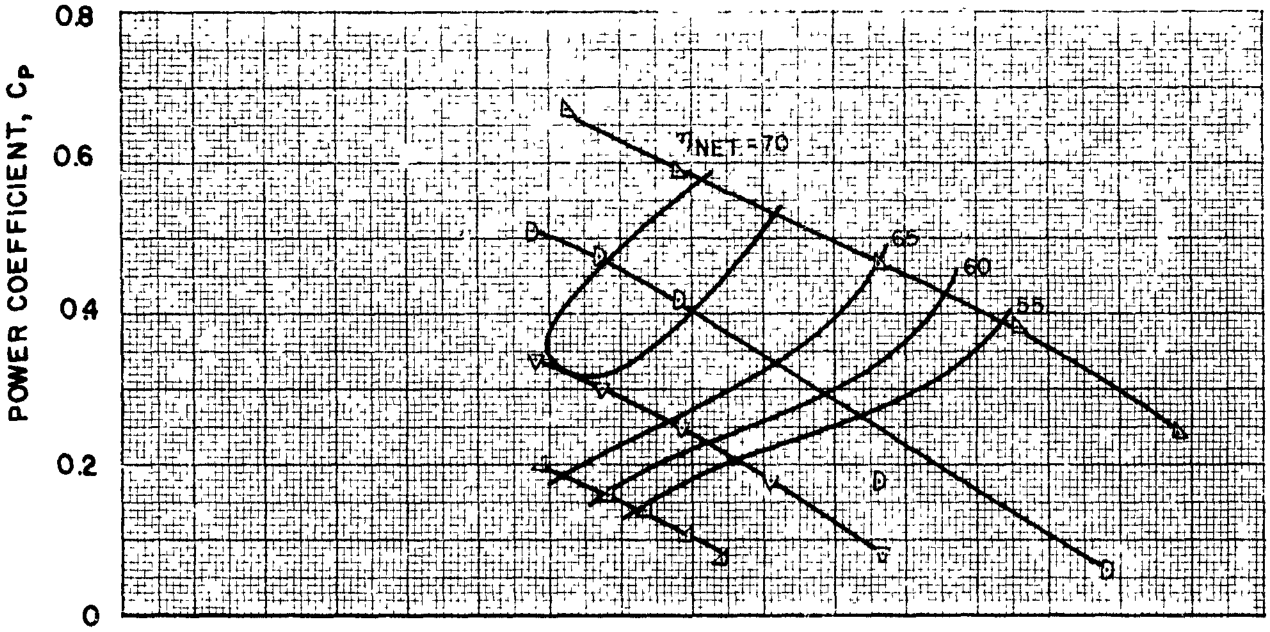

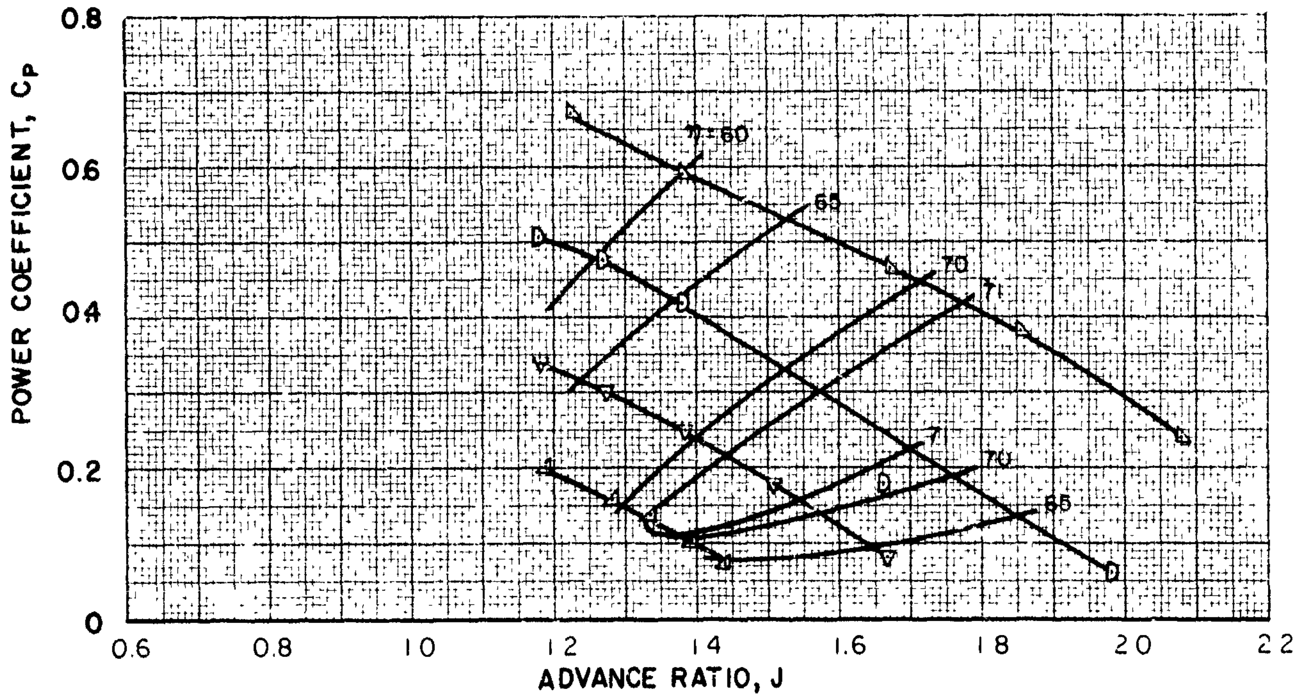

HSD SHROUDED PROPELLER TEST

EFFECT OF DIFFUSER (E_3) ON SHROUDED PROPELLER PERFORMANCE

SYM	RUN NO.	MACH NO.	CONFIGURATION	$\theta_{3/4}$
D	525	0.40	$L_1 C_1 E_3 B_3 P_{WT} T_1 R_1 R_E$	42
◁	527	↓	↓	46
◐	529	↓	↓	50
O	533	↓	↓	54

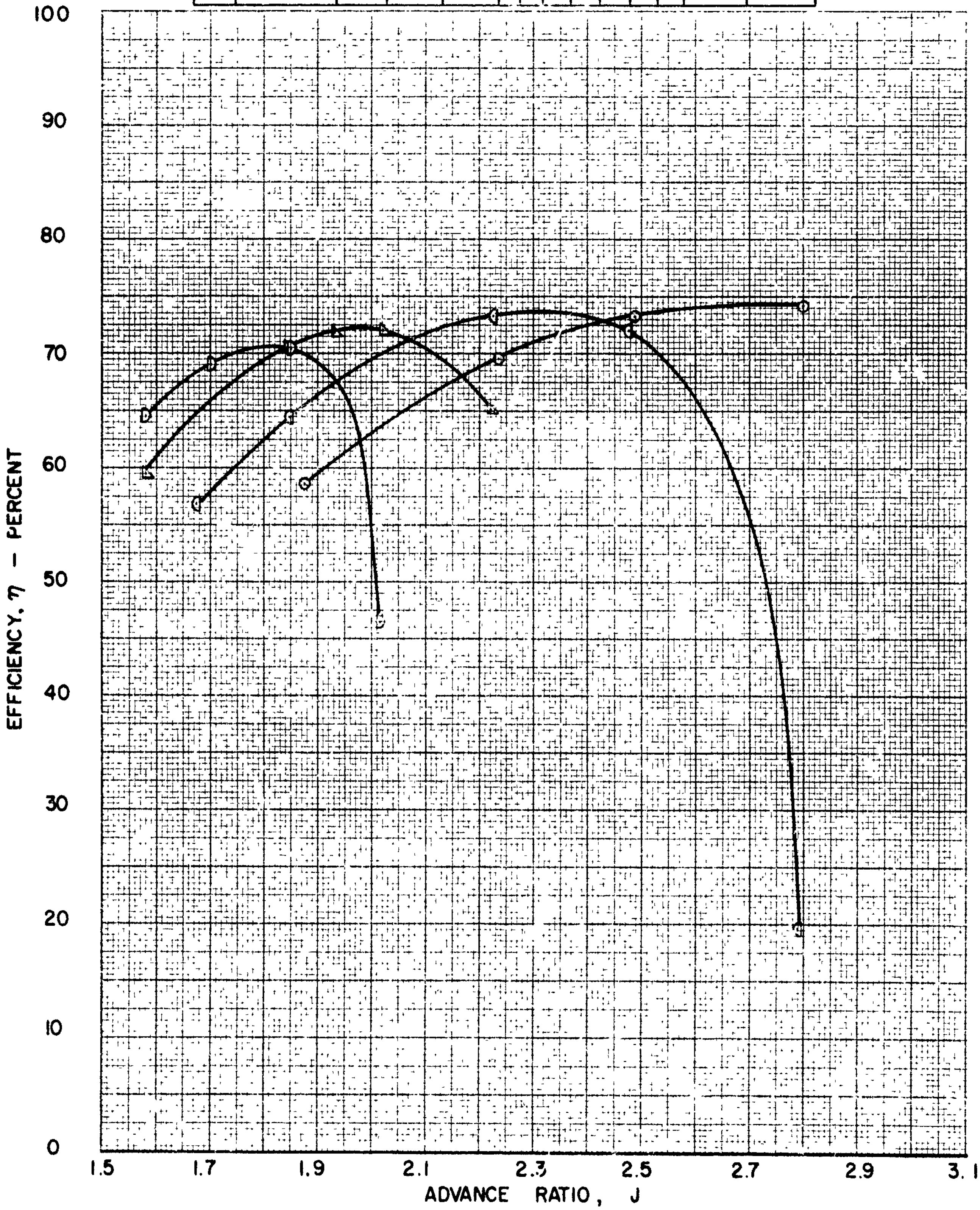

HSD SHROUDED PROPELLER TEST

EFFECT OF DIFFUSER (E_3) ON SHROUDED PROPELLER PERFORMANCE

SYM	RUN NO.	MACH NO.	CONFIGURATION	$\theta_{3/4}$
D	525	0.40	$L_1 C_1 E_3 B_3 P_{WT} T_1 R_1 R_E$	42
◺	527	↓	↓	46
◐	529	↓	↓	50
O	533	↓	↓	54

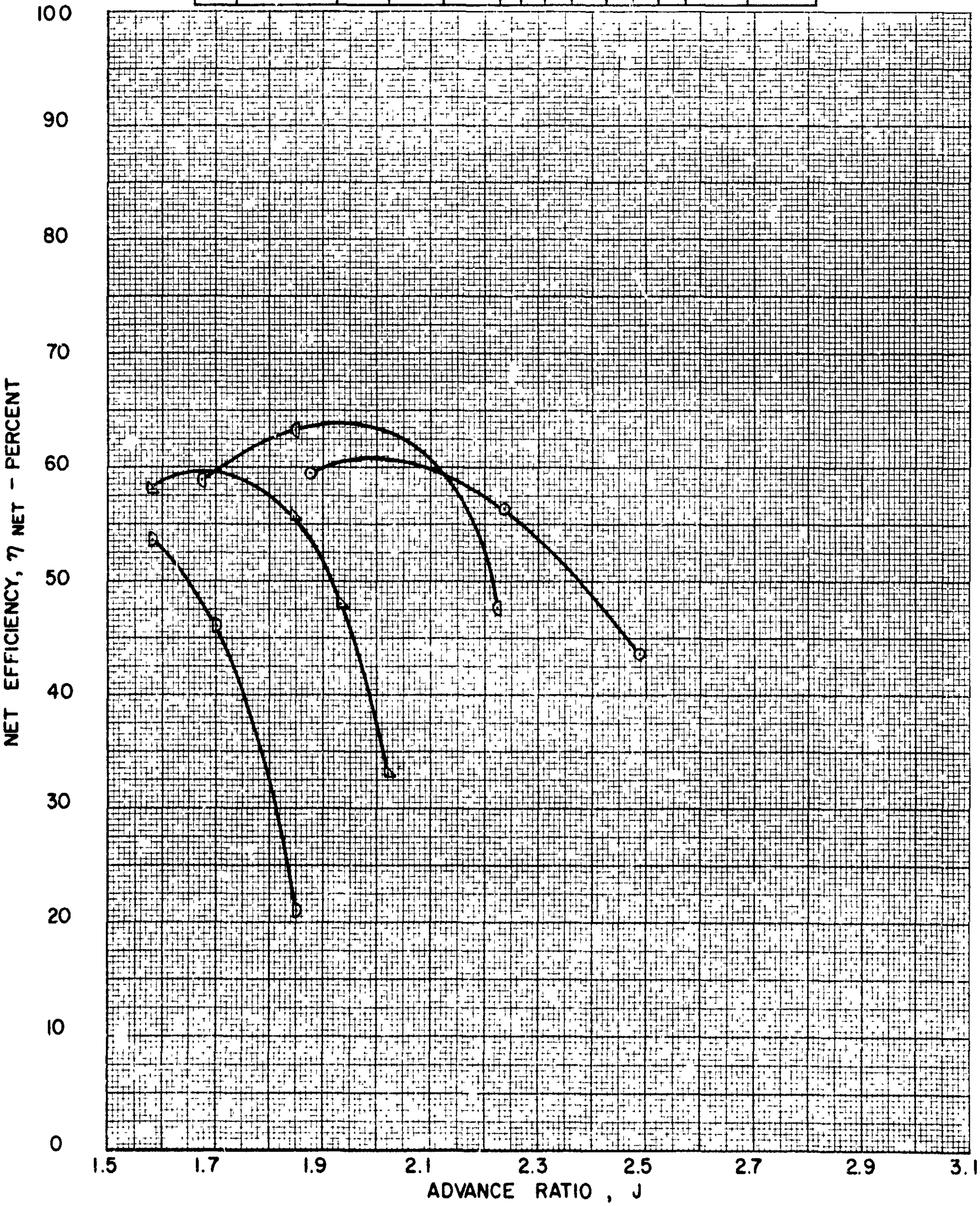

HSD SHROUDED PROPELLER TEST

EFFECT OF DIFFUSER (E_3) ON SHROUDED PROPELLER PERFORMANCE

SYM	RUN NO.	MACH NO.	CONFIGURATION	$\theta_{3/4}$
◻	525	0.40	$L_1 C_1 E_3 B_3 P_{WT} T_1 R_1 R_E$	42
△	527	↓	↓	46
◖	529	↓	↓	50
○	533	↓	↓	54

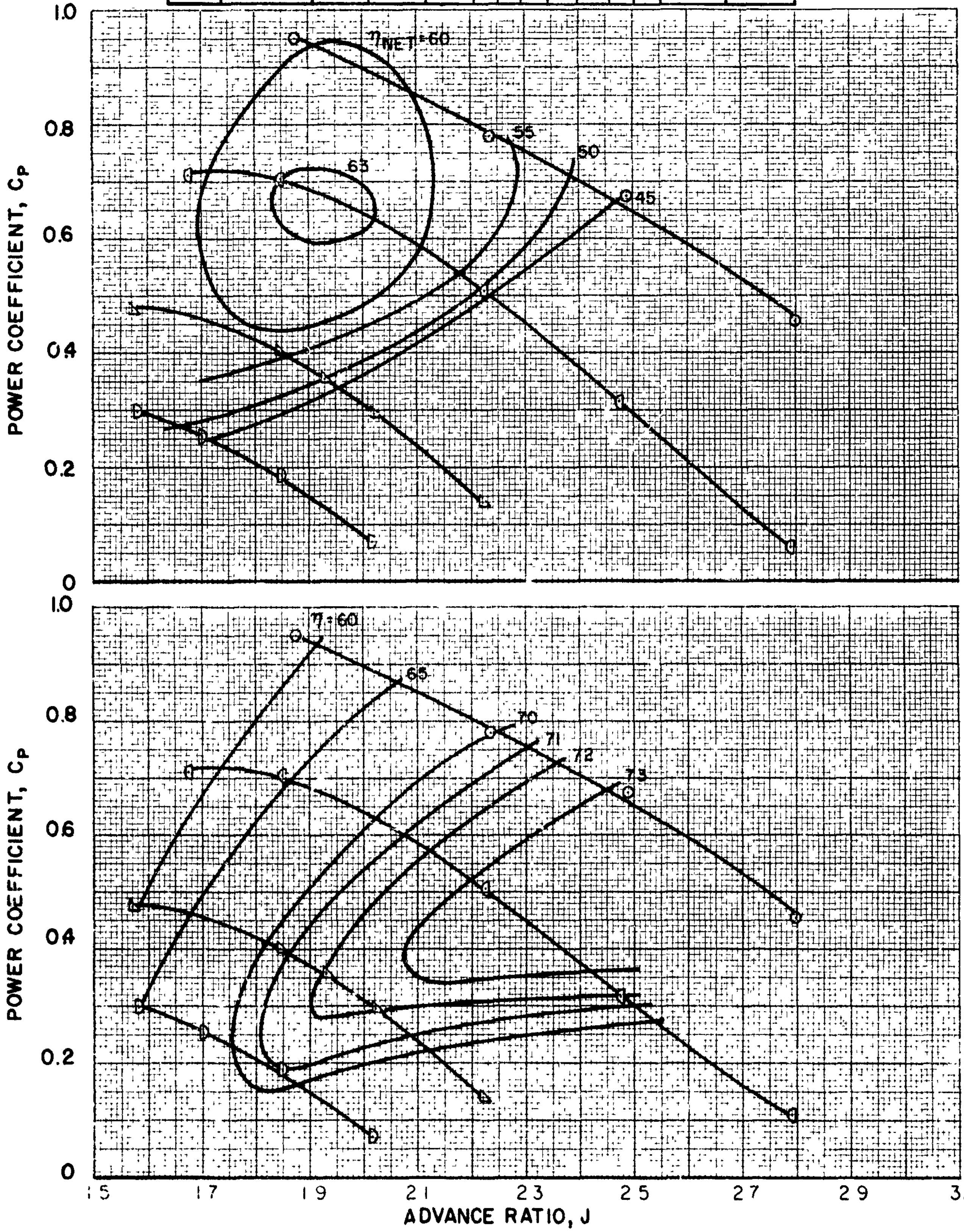

E330590-1 FIG. 86

HSD SHROUDED PROPELLER TEST

EFFECT OF DIFFUSER (E_3) ON SHROUDED PROPELLER PERFORMANCE

SYM	RUN NO.	MACH NO.	CONFIGURATION	$\theta_{3/4}$
◯	530	0.50	$L_1 C_1 E_3 B_3 P_{WT} T_1 R_1 R_E$	50
Δ	532	↓	↓ ↓ ↓ ↓ ↓ ↓ ↓ ↓	53

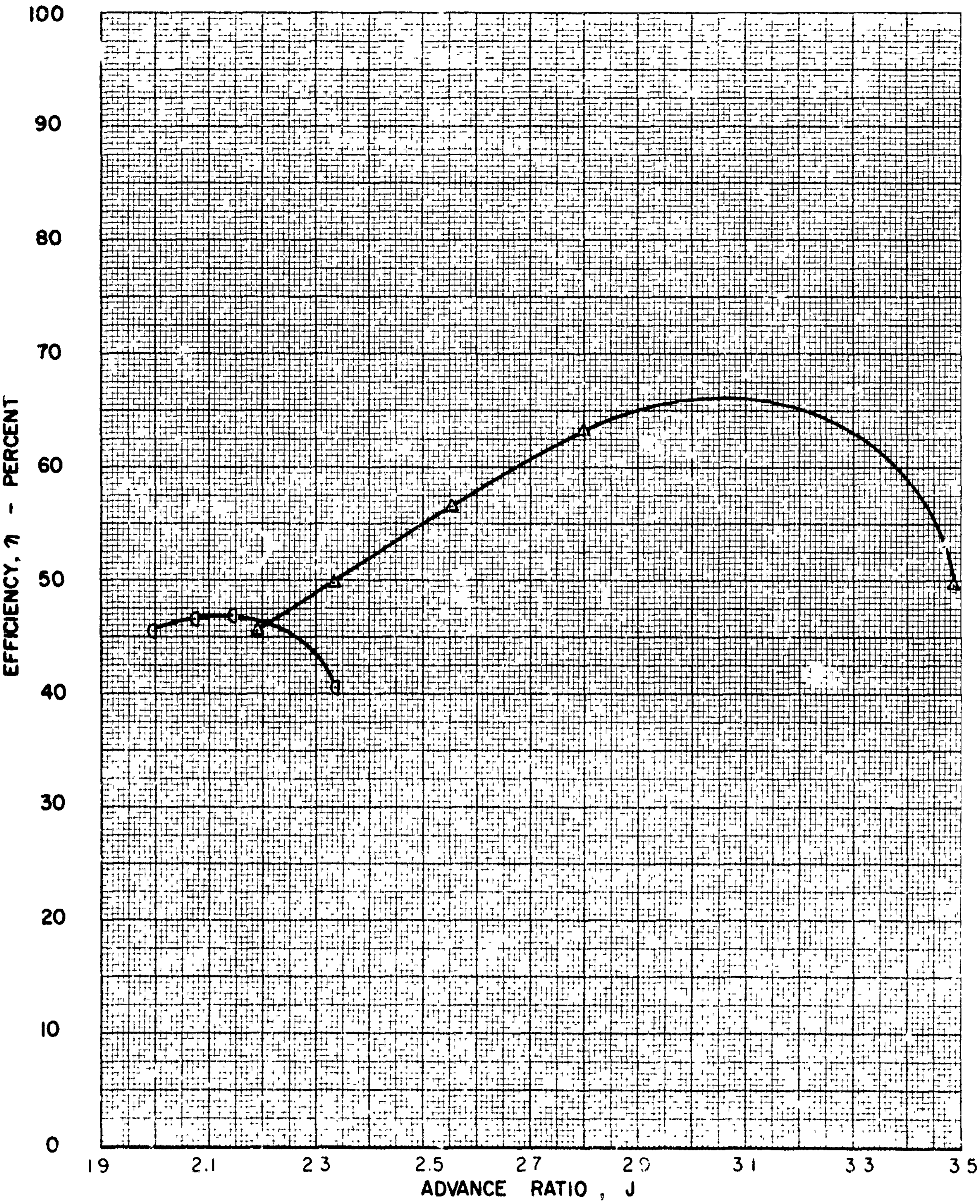

E330590-1

FIG.87

HSD SHROUDED PROPELLER TEST

EFFECT OF DIFFUSER (E_3) ON SHROUDED PROPELLER PERFORMANCE

SYM	RUN NO.	MACH NO.	CONFIGURATION	$\theta_{3/4}$
◐	530	0.50	$L_1 C_1 E_3 B_3 P_{WT} T_1 R_1 R_E$	50
△	532	↓	↓ ↓ ↓ ↓ ↓ ↓ ↓ ↓	58

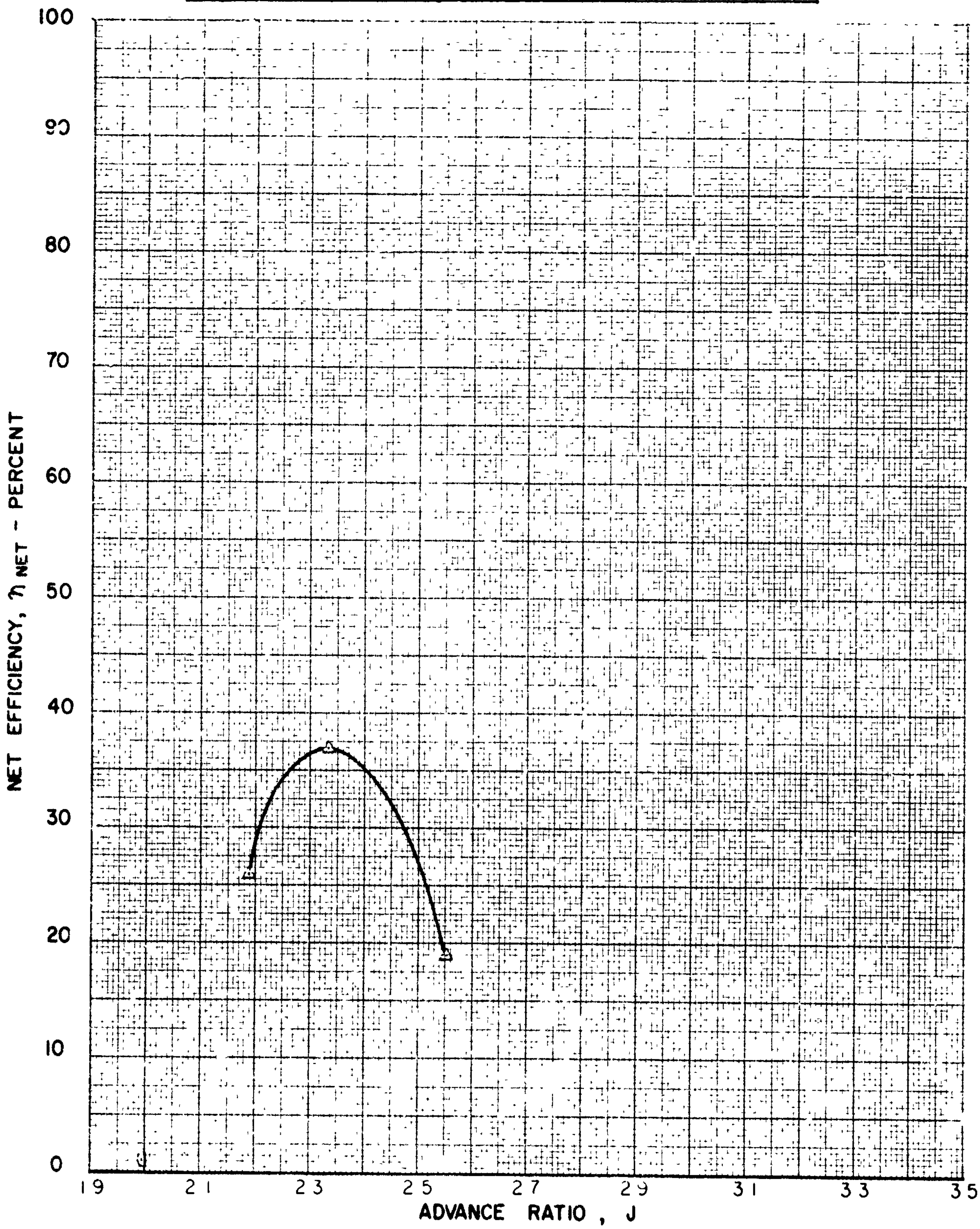

HSD SHROUDED PROPELLER TEST

EFFECT OF DIFFUSER (E_3) ON SHROUDED PROPELLER PERFORMANCE

SYM	RUN NO.	MACH NO.	CONFIGURATION	$\theta_{3/4}$
◁	530	0.50	$L_1 C_1 E_3 B_3 P_{WT} T_1 R_1 R_E$	50
△	532	↓	↓ ↓ ↓ ↓ ↓ ↓ ↓ ↓	58

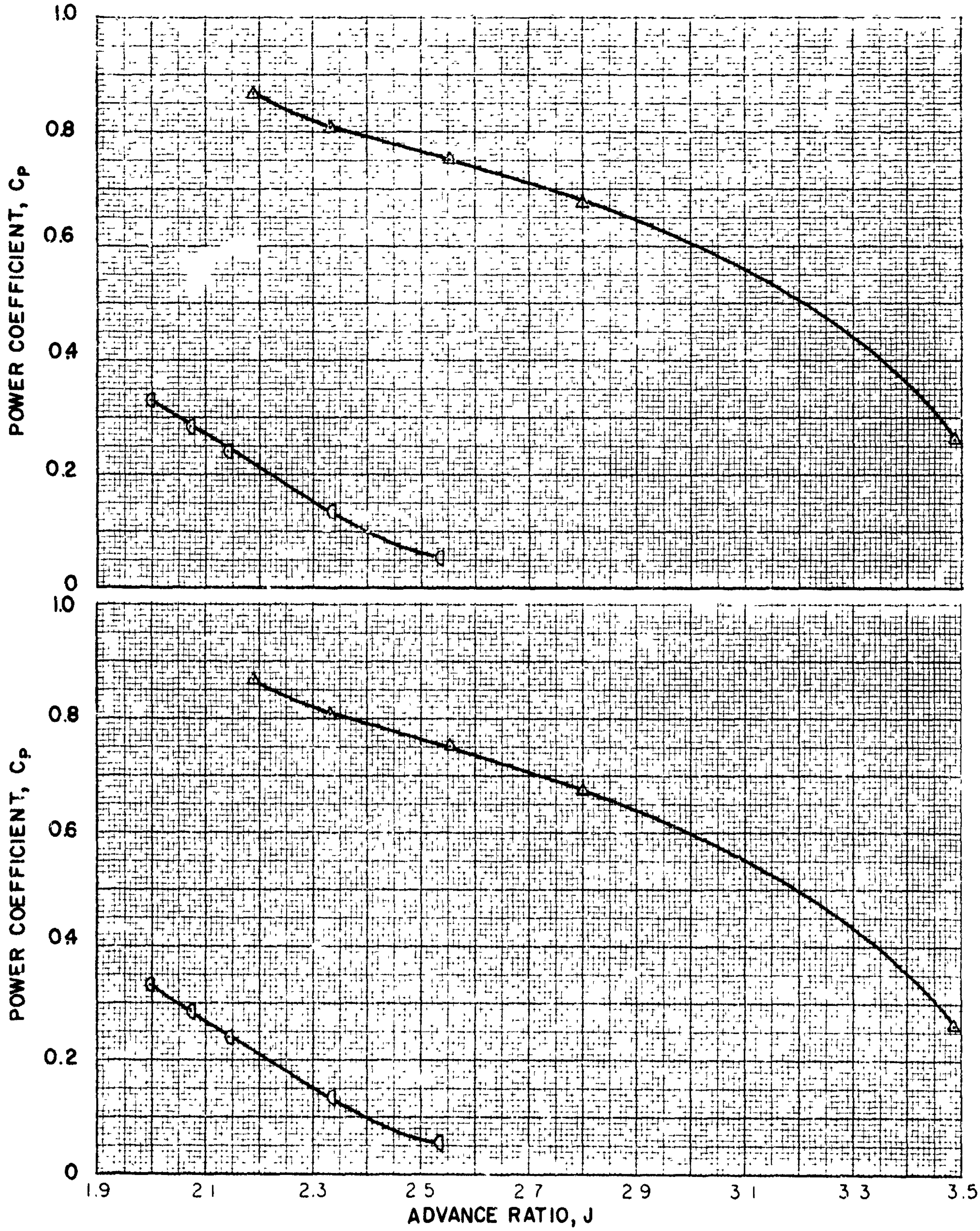

HSD SHROUDED PROPELLER TEST

EFFECT OF DIFFUSER (E_4) ON SHROUDED PROPELLER PERFORMANCE

SYM	RUN NO.	MACH NO.	CONFIGURATION	$\theta_{3/4}$
△	119 , 118	0.02 , 0.10	$L_1C_1E_4B_3P_{WT}T_1R_1R_E$	20
□	120 , 121			25
◇	125 , 124			30
⊿	126 , 127			35

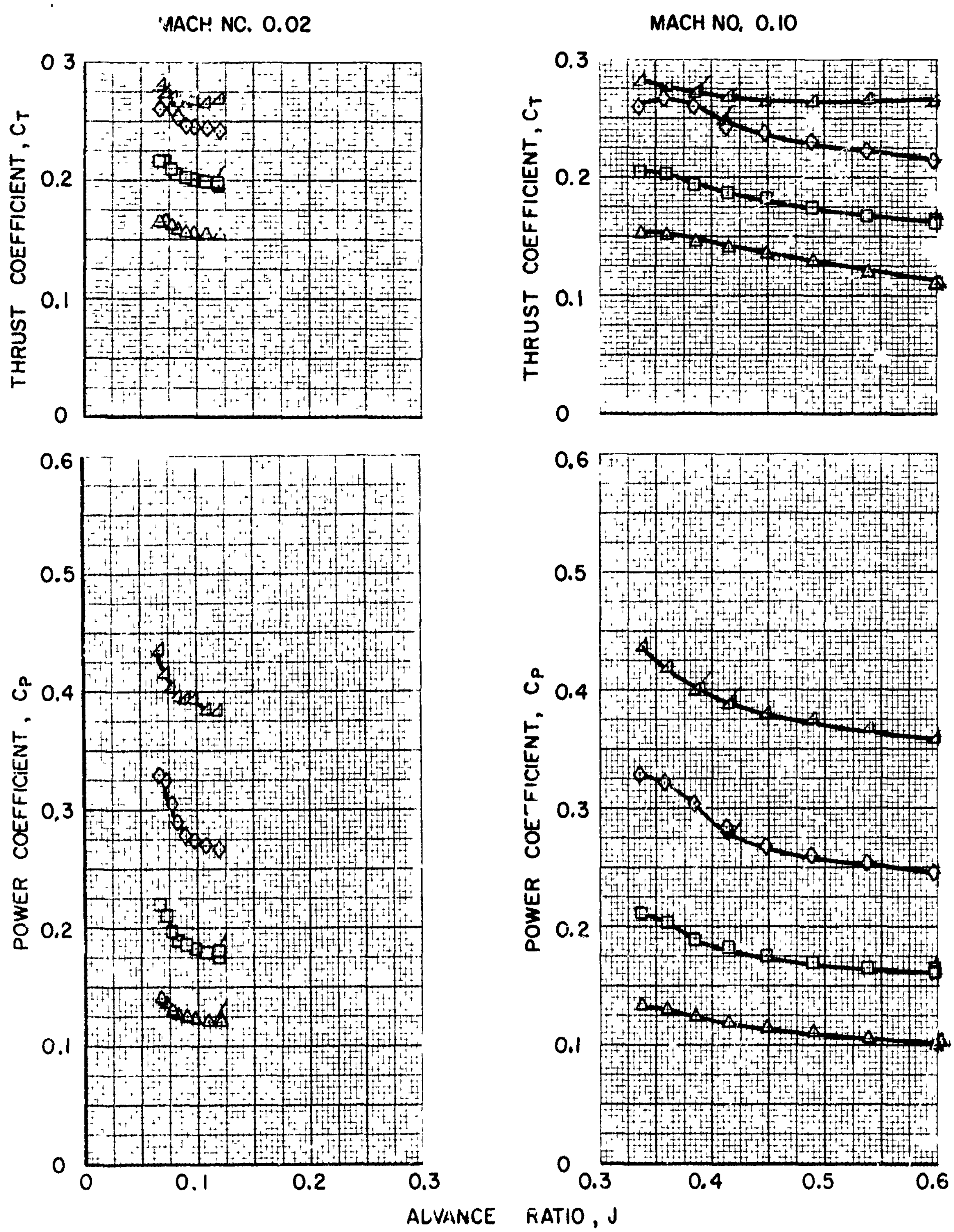

E330590-I FIG. 90

HSD SHROUDED PROPELLER TEST

EFFECT OF DIFFUSER (E_4) ON SHROUDED PROPELLER PERFORMANCE

SYM	RUN NO.	MACH NO.	CONFIGURATION	$\theta_{3/4}$
△	119, 118	0.02, 0.10	$L_1 C_1 E_4 B_3 P_{WT} T_1 R_1 R_E$	20
◻	120, 121	↓	↓	25
◇	125, 124	↓	↓	30
⊿	126, 127	↓	↓	35

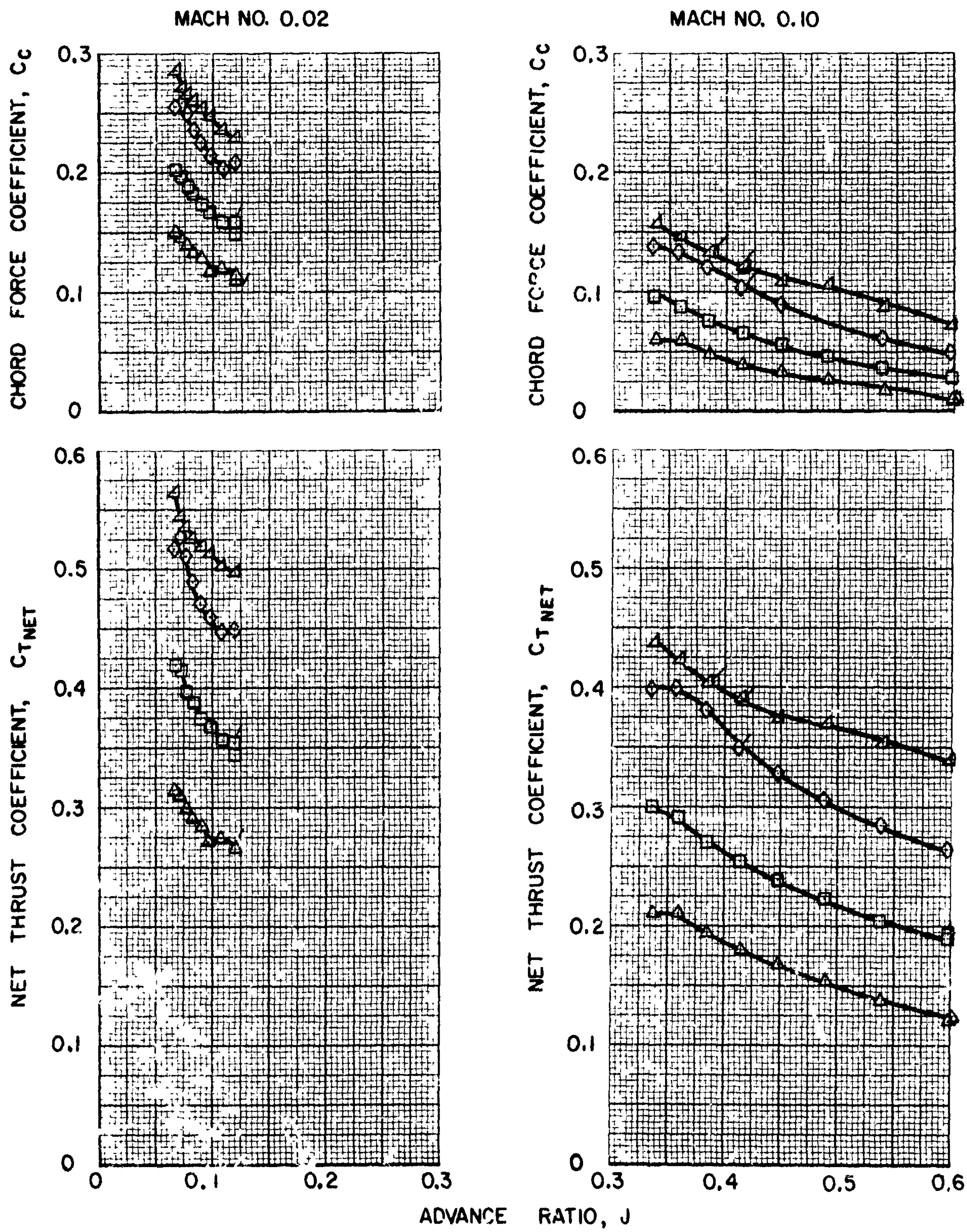

HSD SHROUDED PROPELLER TEST

EFFECT OF DIFFUSER (E_4) ON SHROUDED PROPELLER PERFORMANCE

SYM	RUN NO.	MACH NO.	CONFIGURATION	$\theta_{3/4}$
□	122	0.20	$L_1 C_1 E_4 B_3 P_{WT} T_1 R_1 R_E$	25
◇	123	↓	↓	30
◁	128	↓	↓	35
▽	117	↓	↓	40

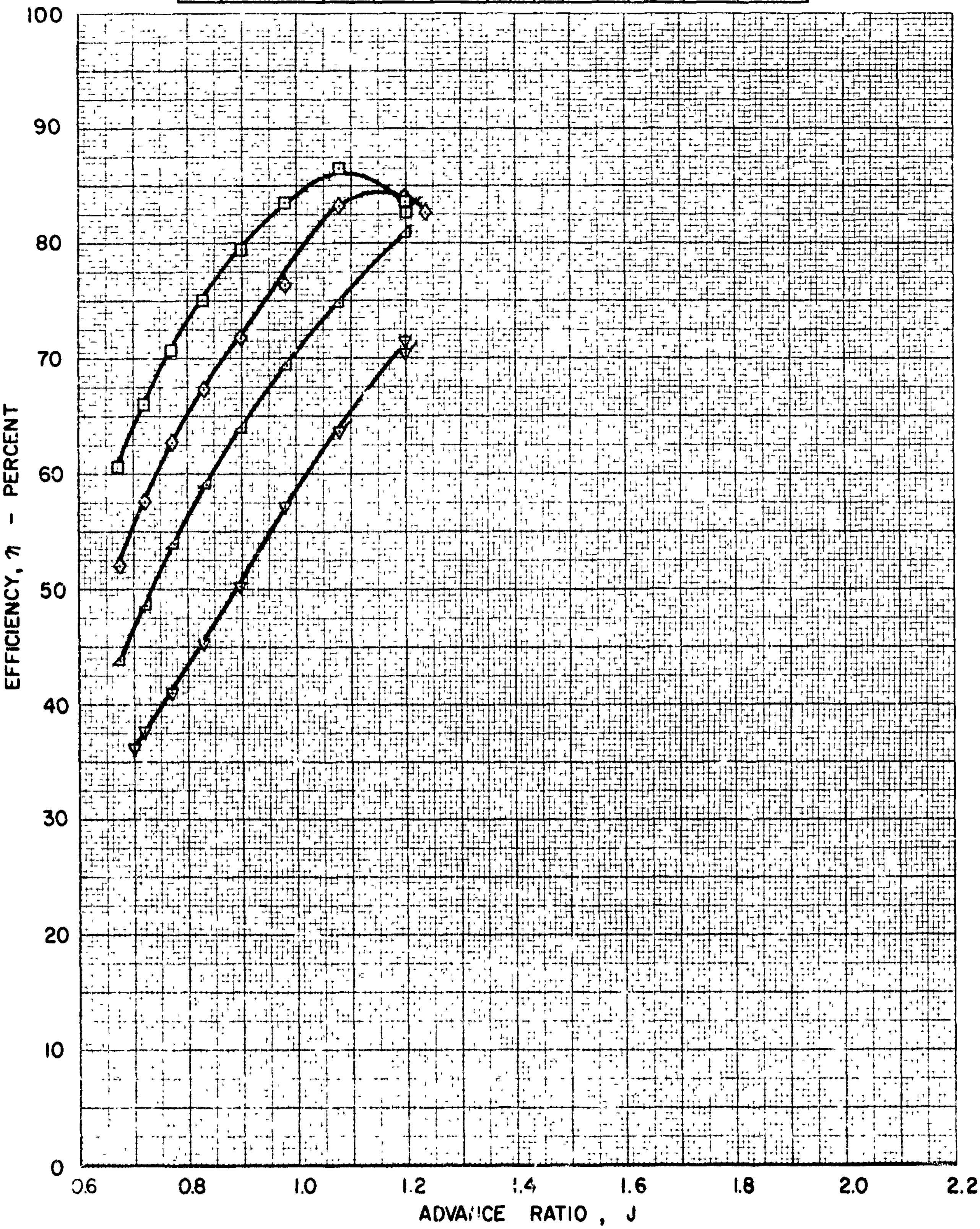

HSD SHROUDED PROPELLER TEST

EFFECT OF DIFFUSER (E_4) ON SHROUDED PROPELLER PERFORMANCE

SYM	RUN NO.	MACH NO.	CONFIGURATION	$\theta_{3/4}$
□	122	0.20	$L_1\ C_1\ E_4\ B_3\ P_{WT}\ T_1\ R_1\ R_E$	25
◇	123	↓	↓	30
⊿	128	↓	↓	35
▽	117	↓	↓	40

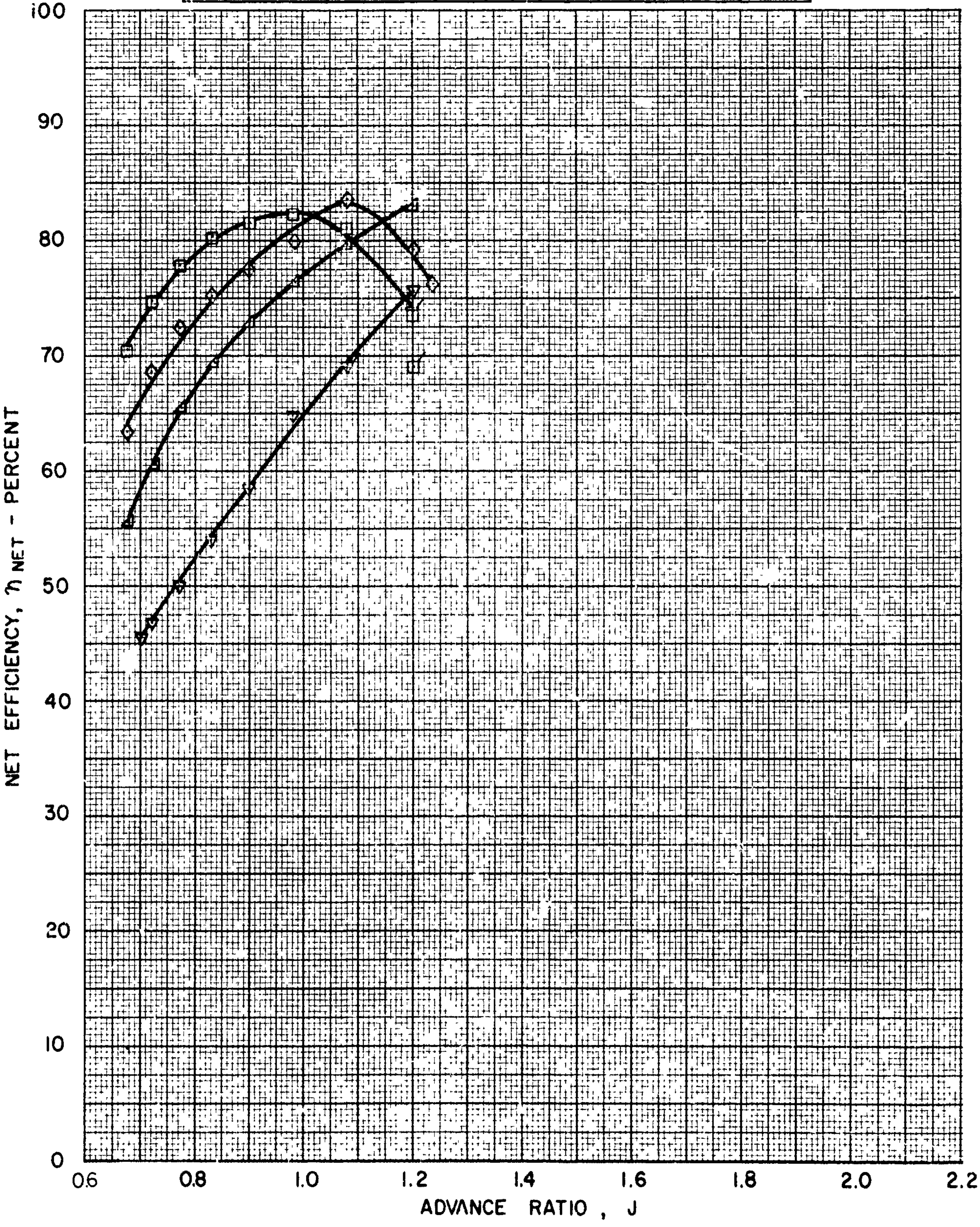

E330590-I

FIG.93

HSD SHROUDED PROPELLER TEST

EFFECT OF DIFFUSER (E_4) ON SHROUDED PROPELLER PERFORMANCE

SYM	RUN NO.	MACH NO.	CONFIGURATION	$\theta_{3/4}$
□	122	0.20	$L_1 C_1 E_4 B_3 P_{WT} T_1 R_1 R_E$	25
◇	123	↓	↓	30
◿	128	↓	↓	35
▽	117	↓	↓	40

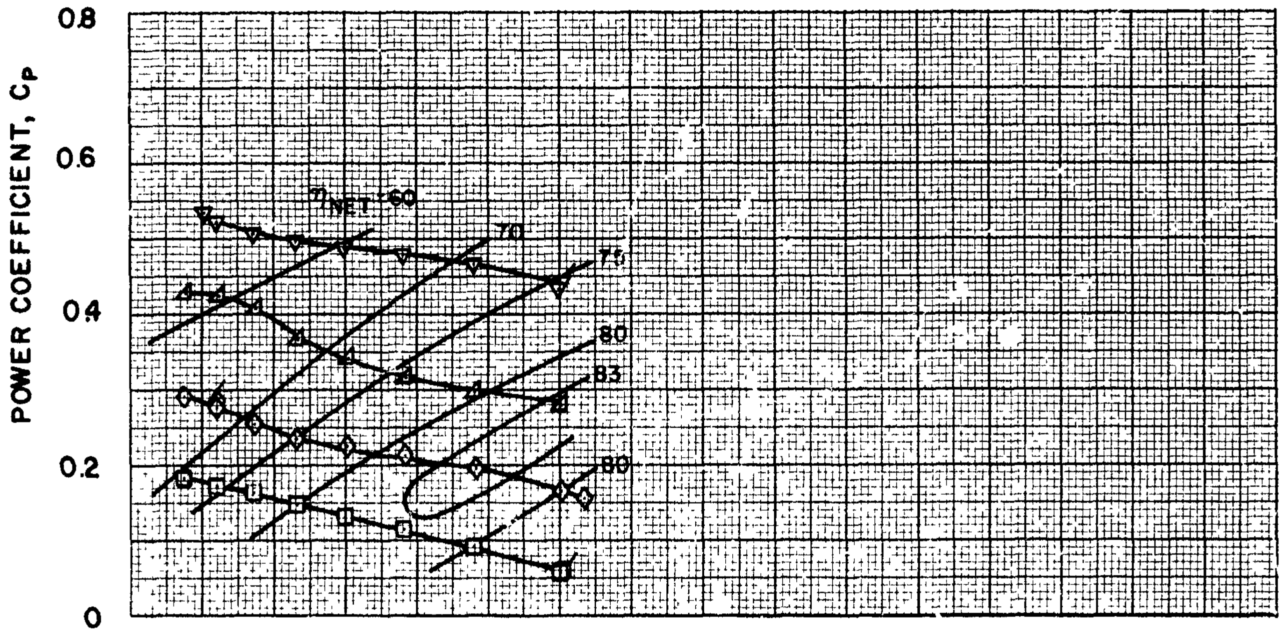

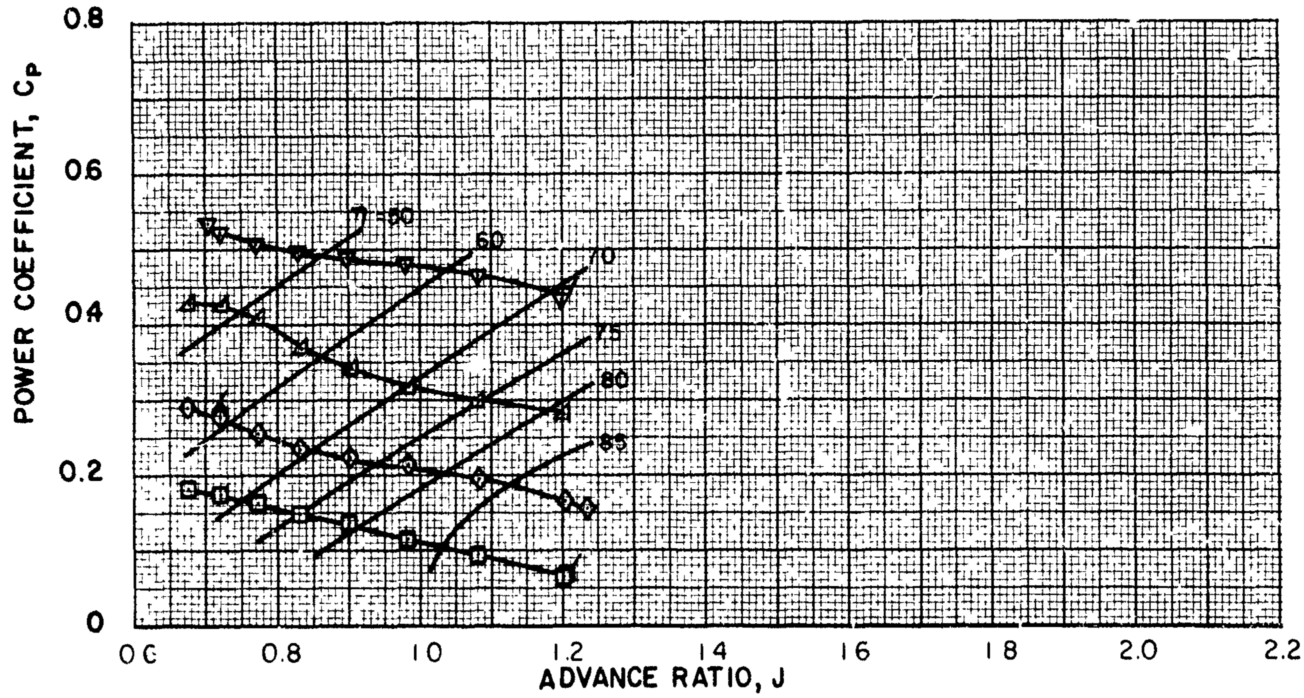

HSD SHROUDED PROPELLER TEST

EFFECT OF DIFFUSER (E_4) ON SHROUDED PROPELLER PERFORMANCE

SYM	RUN NO.	MACH NO.	CONFIGURATION	$\theta_{3/4}$
◇	539	0.30	$L_1 C_1 E_4 B_3 P_{WT} T_1 R_1 R_E$	30
⊿	540			34
▽	541			38
D	543			42

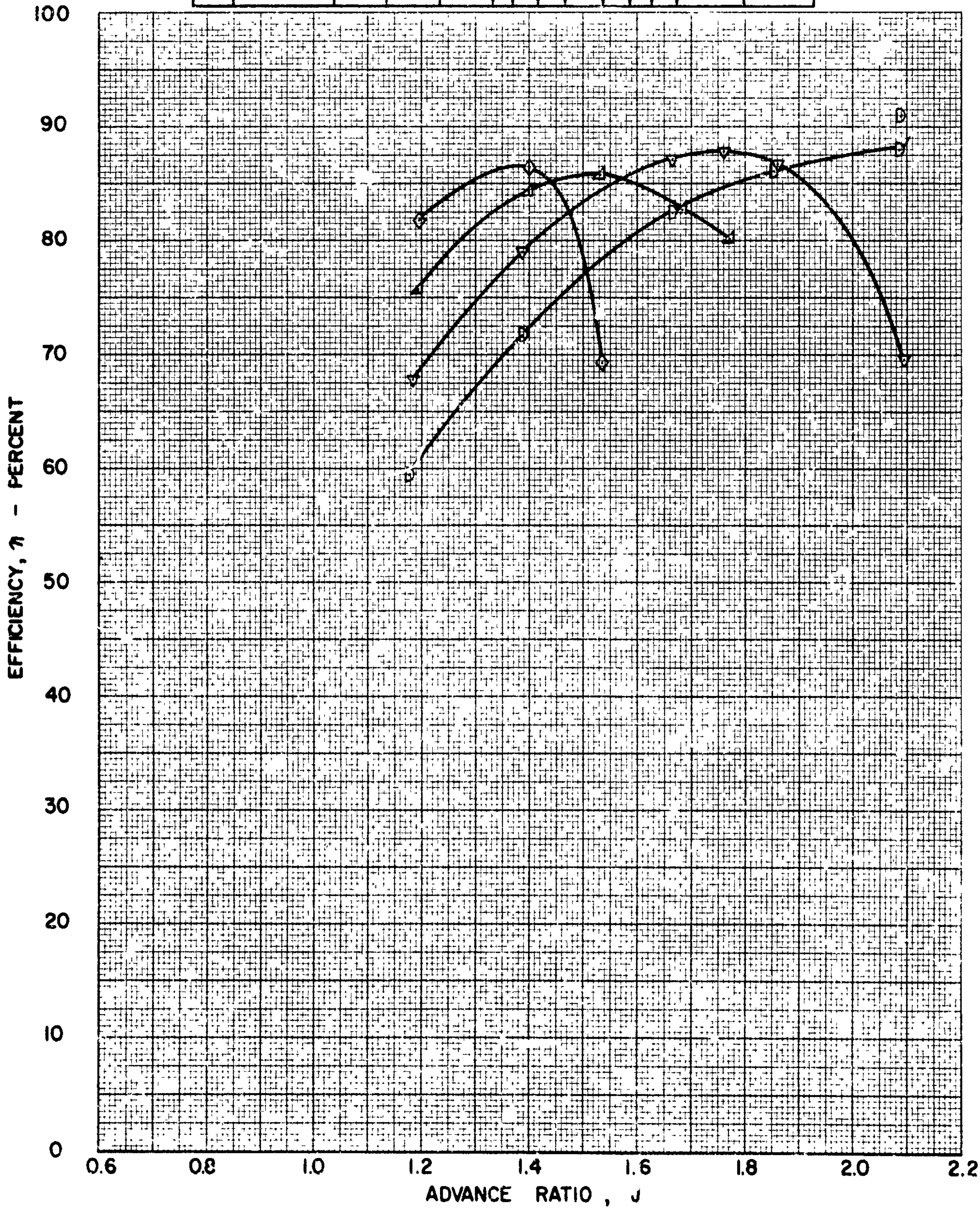

E330590-1

FIG.95

HSD SHROUDED PROPELLER TEST

EFFECT OF DIFFUSER (E_4) ON SHROUDED PROPELLER PERFORMANCE

SYM	RUN NO.	MACH NO.	CONFIGURATION	$\theta_{3/4}$
◇	539	0.30	$L_1 C_1 E_4 B_3 P_{WT} T_1 R_1 R_E$	30
⊿	540	↓	↓	34
▽	541	↓	↓	38
D	543	↓	↓	42

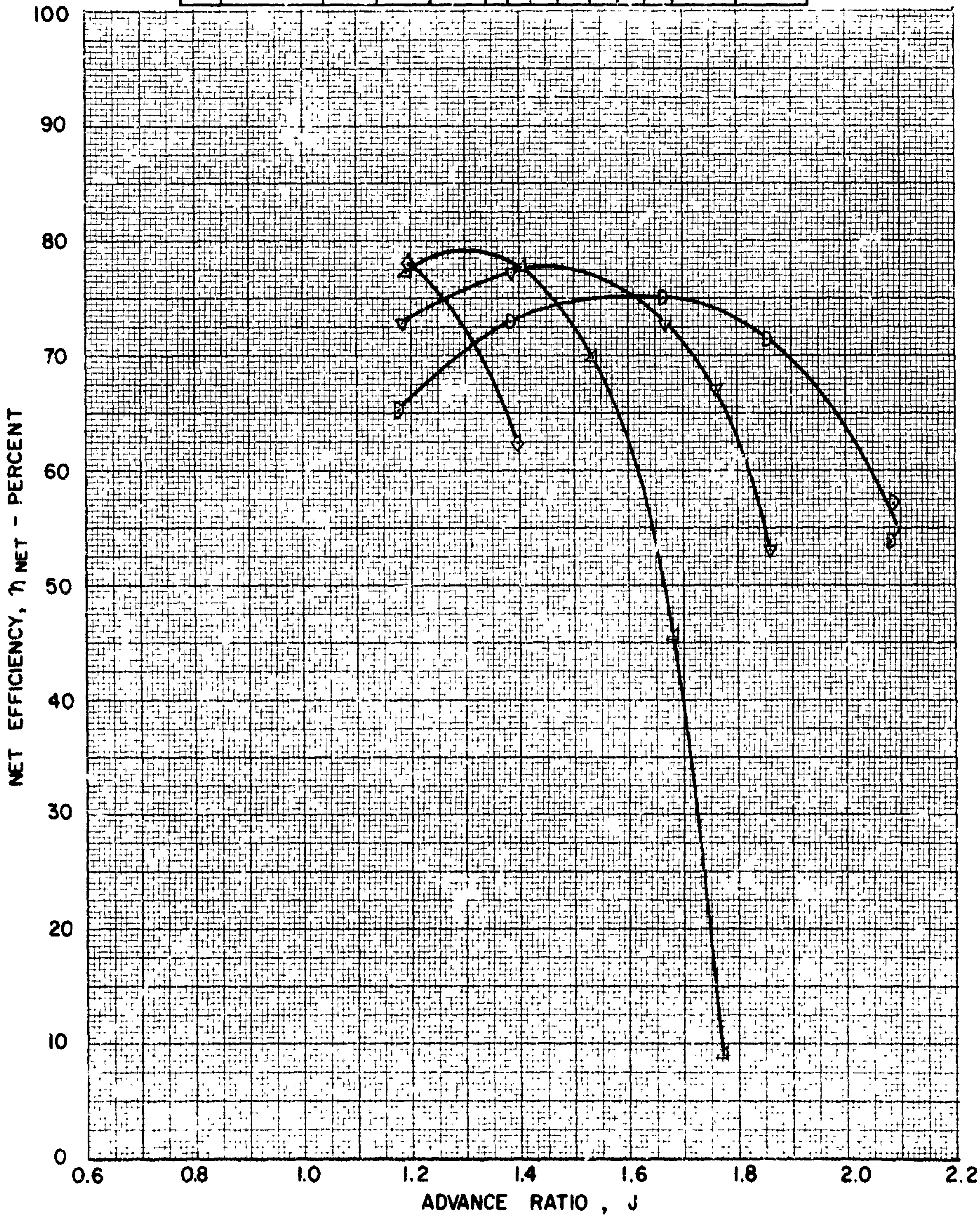

E330590-I

FIG. 96

HSD SHROUDED PROPELLER TEST

EFFECT OF DIFFUSER (E_4) ON SHROUDED PROPELLER PERFORMANCE

SYM	RUN NO.	MACH NO.	CONFIGURATION	$\theta_{3/4}$
◇	539	0.30	$L_1 C_1 E_4 B_3 P_{WT} T_1 R_1 R_E$	30
⊿	540			34
▽	541			38
D	543			42

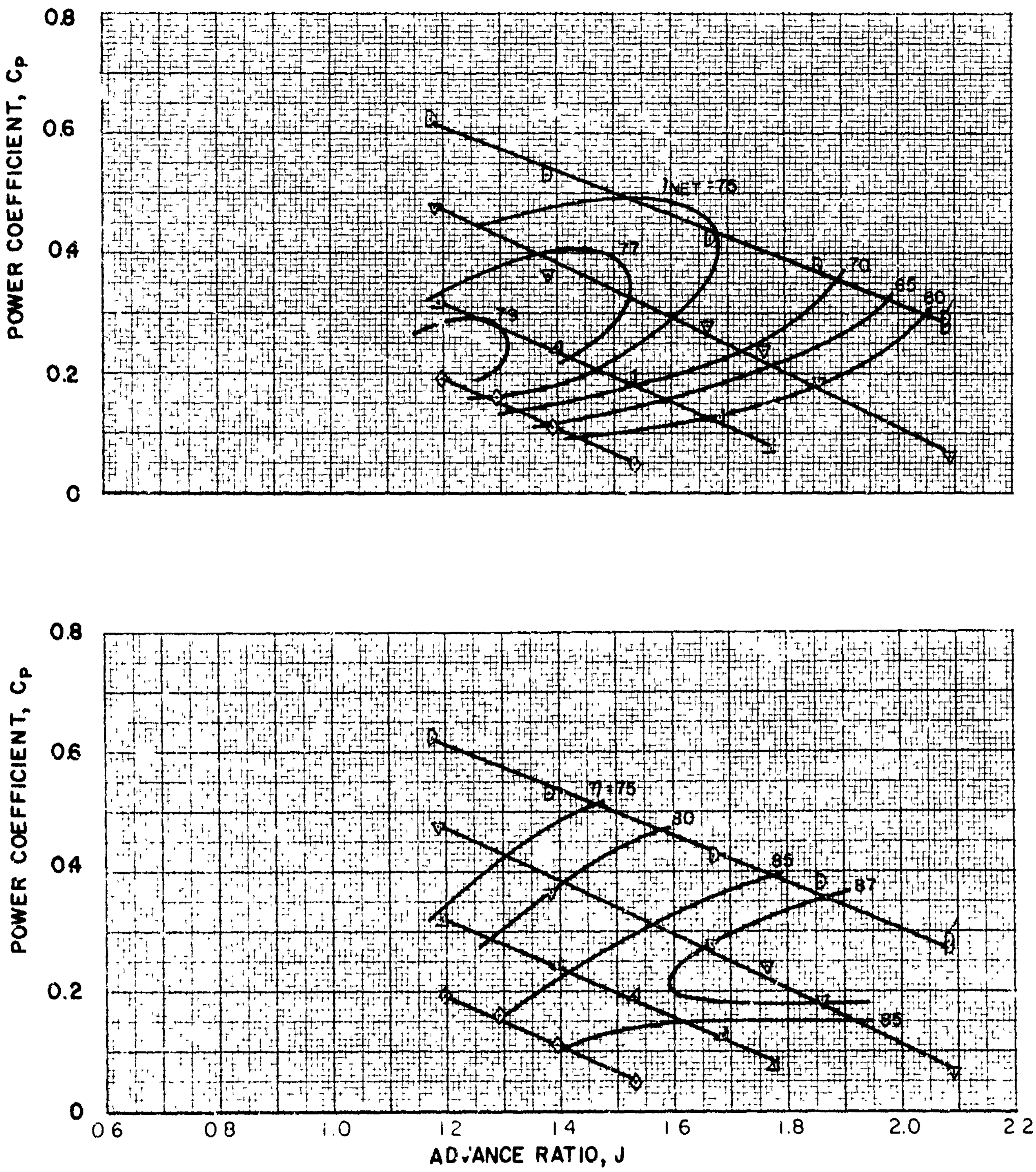

HSD SHROUDED PROPELLER TEST

EFFECT OF DIFFUSER (E_4) ON SHROUDED PROPELLER PERFORMANCE

SYM	RUN NO.	MACH NO.	CONFIGURATION	$\theta_{3/4}$
▽	542	0.40	$L_1 C_1 E_4 B_3 P_{WT} T_1 R_1 R_E$	38
D	544	↓	↓	42
◺	546	↓	↓	46
Q	548	↓	↓	50

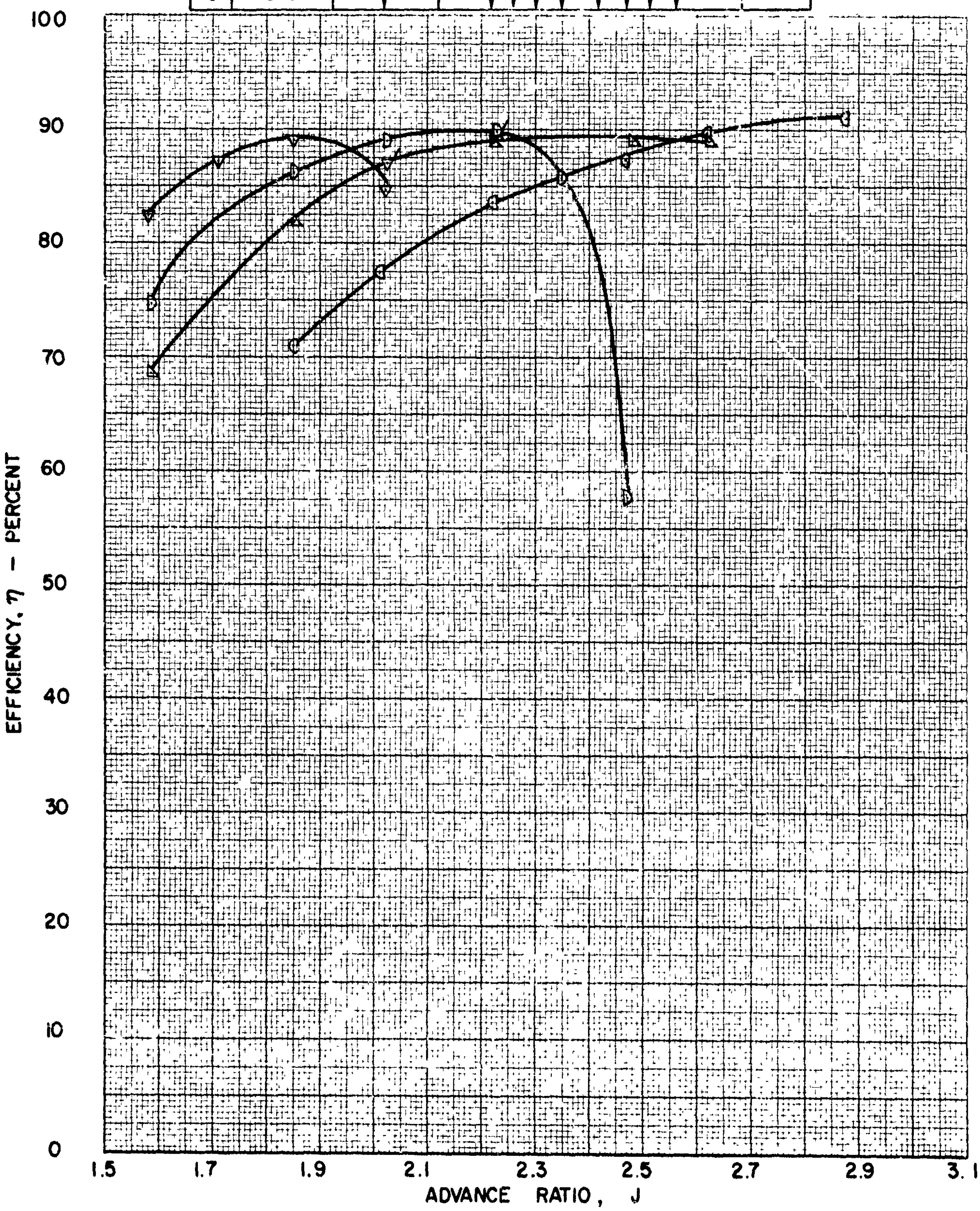

HSD SHROUDED PROPELLER TEST

EFFECT OF DIFFUSER (E_4) ON SHROUDED PROPELLER PERFORMANCE

SYM	RUN NO.	MACH NO.	CONFIGURATION	$\theta_{3/4}$
▽	542	0.40	$L_1 C_1 E_4 B_3 P_{WT} T_1 R_1 R_E$	38
D	544	↓	↓	42
◺	546	↓	↓	46
Ɑ	548	↓	↓	50

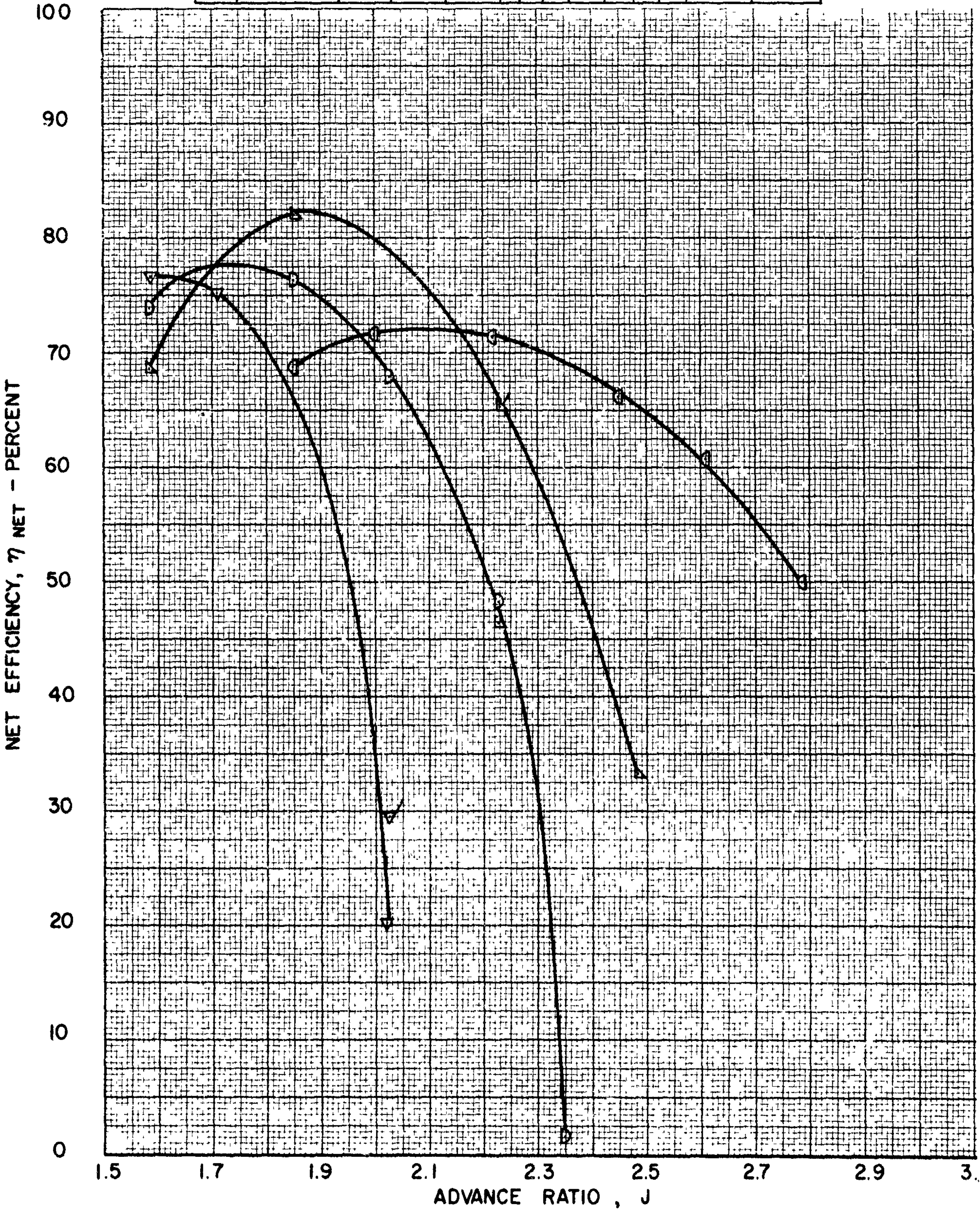

HSD SHROUDED PROPELLER TEST

EFFECT OF DIFFUSER (E_4) ON SHROUDED PROPELLER PERFORMANCE

SYM	RUN NO.	MACH NO.	CONFIGURATION	$\theta_{3/4}$
▽	542	0 40	$L_1 C_1 E_4 B_3 P_{WT} T_1 R_1 R_E$	38
D	544	↓	↓	42
◺	546	↓	↓	46
◑	548	↓	↓	50

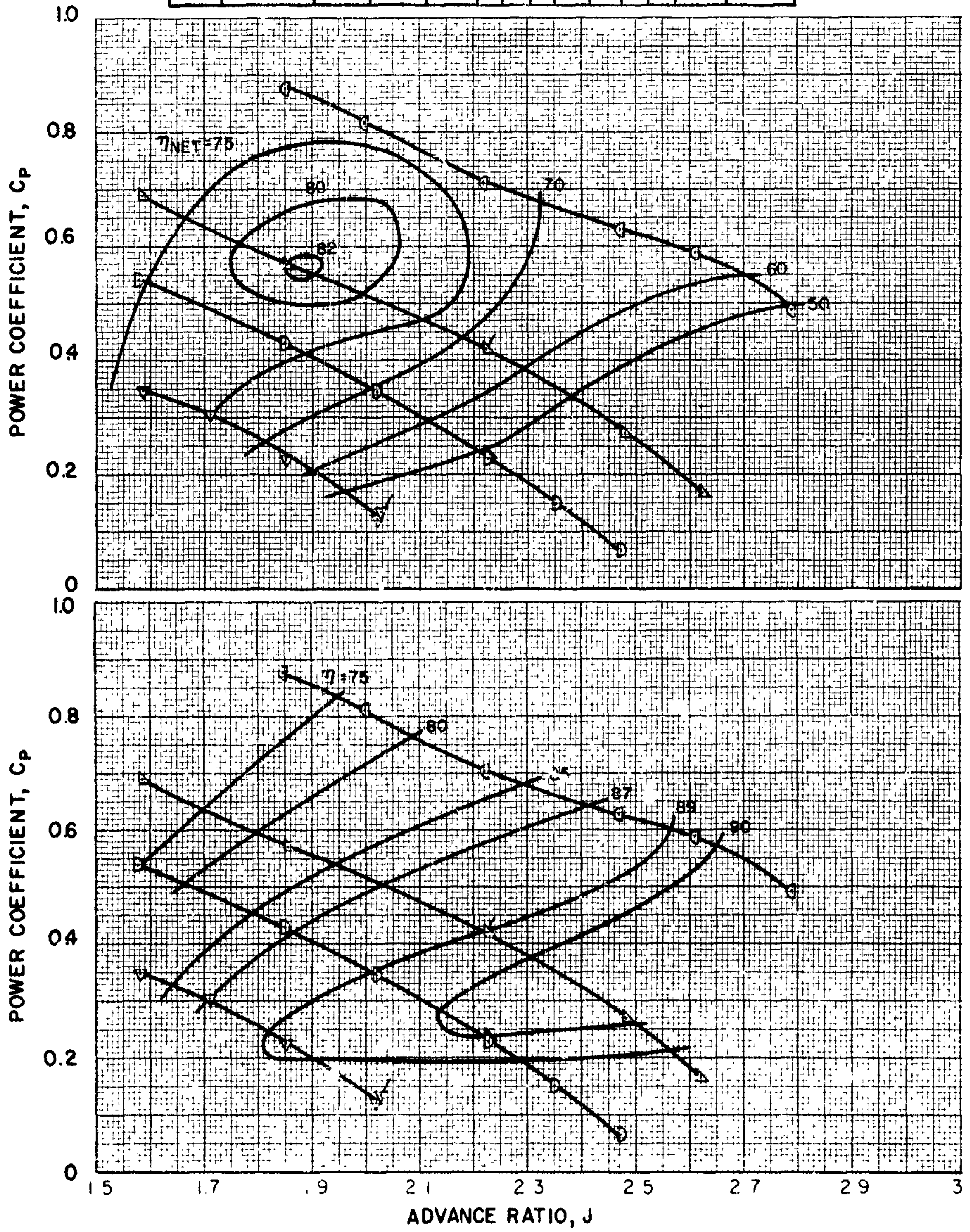

HSD SHROUDED PROPELLER TEST

EFFECT OF DIFFUSER (E_4) ON SHROUDED PROPELLER PERFORMANCE

SYM	RUN NO.	MACH NO.	CONFIGURATION	$\theta_{3/4}$
D	545	0.50	$L_1 C_1 E_4 B_3 P_{WT} T_1 R_1 R_E$	42
◺	547	↓	↓	46
ᗡ	549	↓	↓	50
○	550	↓	↓	54

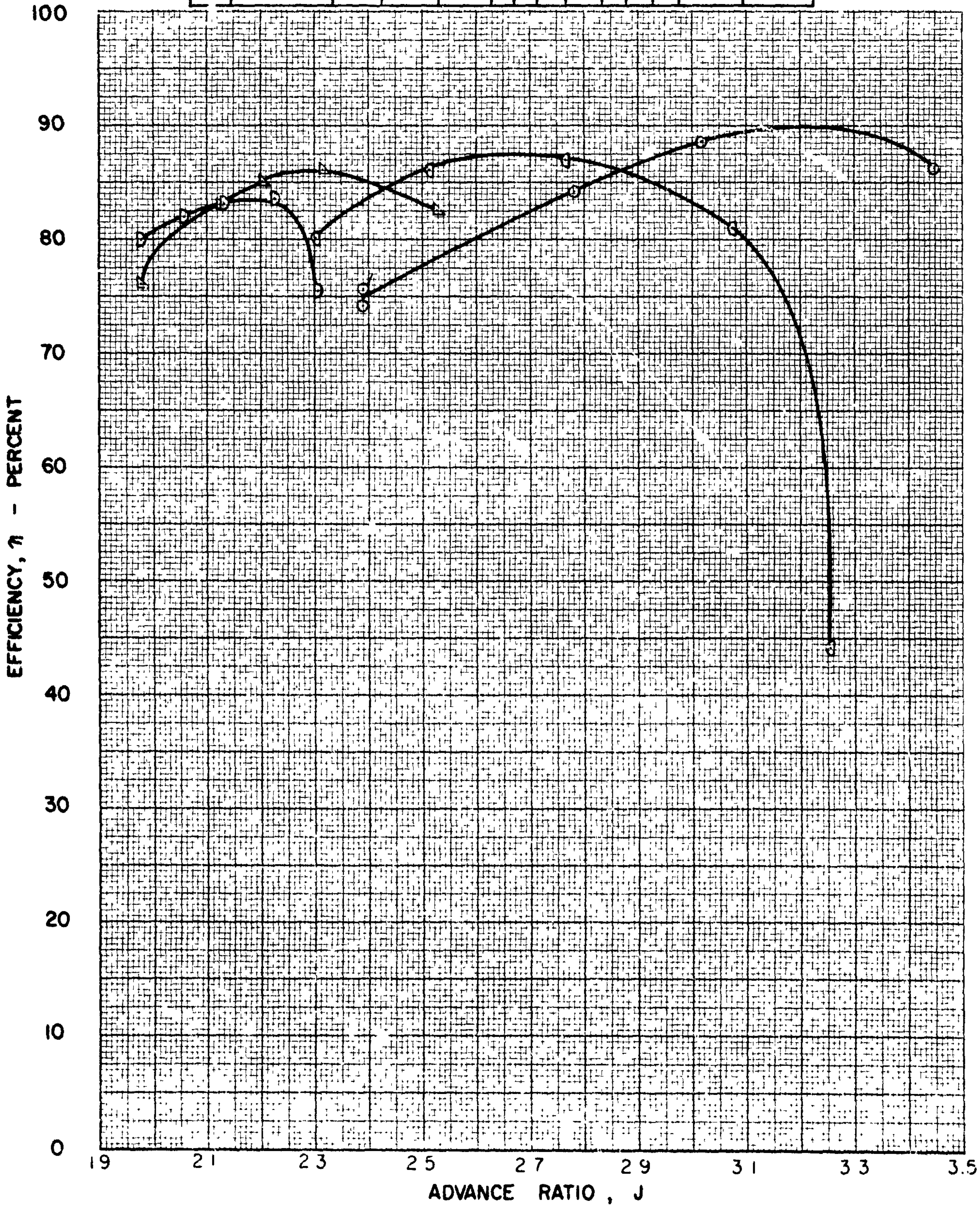

E330590-1

FIG. 101

HSD SHROUDED PROPELLER TEST

EFFECT OF DIFFUSER (E_4) ON SHROUDED PROPELLER PERFORMANCE

SYM	RUN NO.	MACH NO.	CONFIGURATION	$\theta_{3/4}$
D	545	0.50	$L_1 C_1 E_4 B_3 P_{WT} T_1 R_1 R_E$	42
◺	547	↓	↓	46
◖	549	↓	↓	50
O	550	↓	↓	54

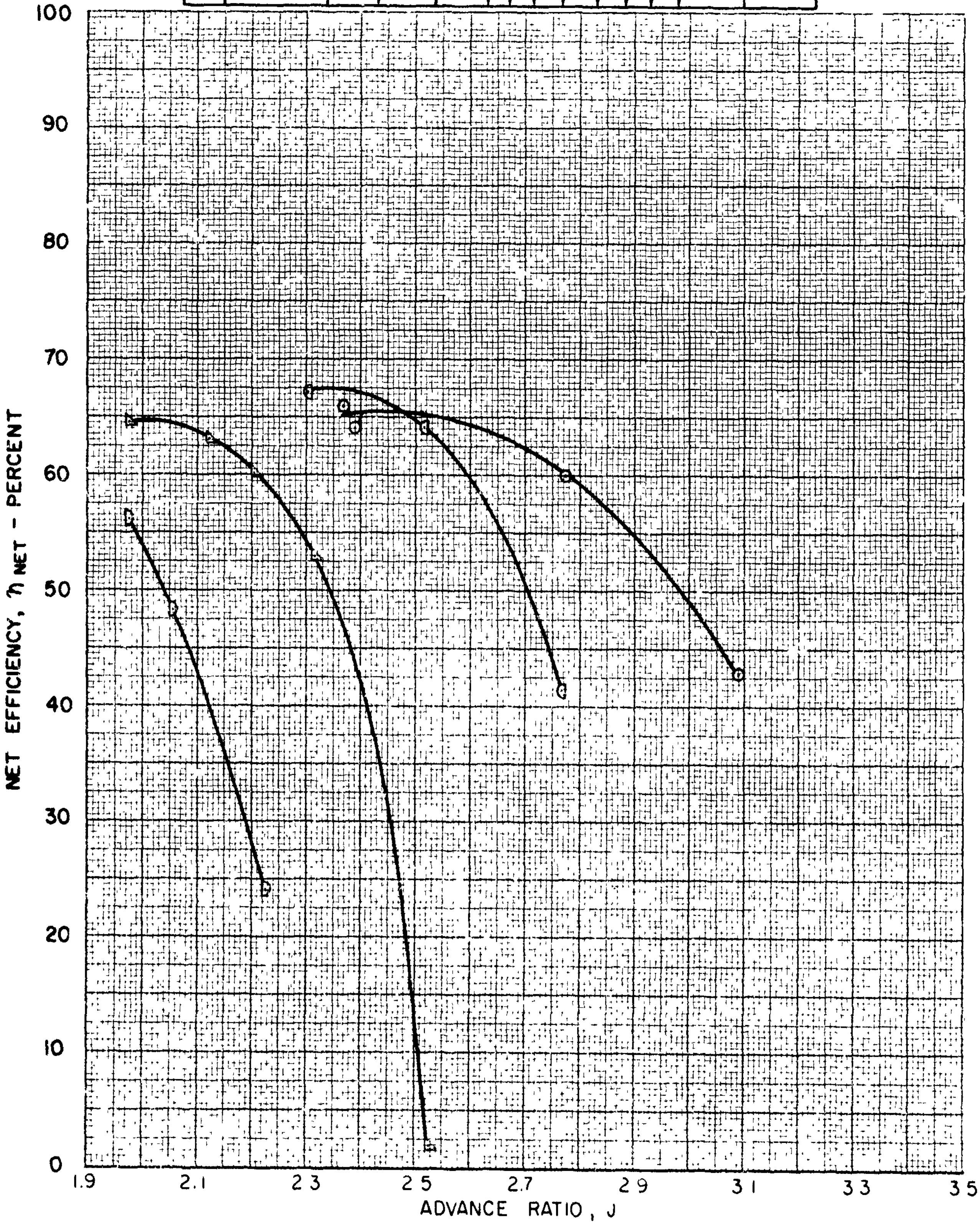

HSD SHROUDED PROPELLER TEST

EFFECT OF DIFFUSER (E_4) ON SHROUDED PROPELLER PERFORMANCE

SYM	RUN NO.	MACH NO.	CONFIGURATION	$\theta_{3/4}$
D	545	0.50	$L_1 C_1 E_4 B_3 P_{WT} T_1 R_1 R_E$	42
Δ	547	↓	↓	46
◁	549	↓	↓	50
O	550	↓	↓	54

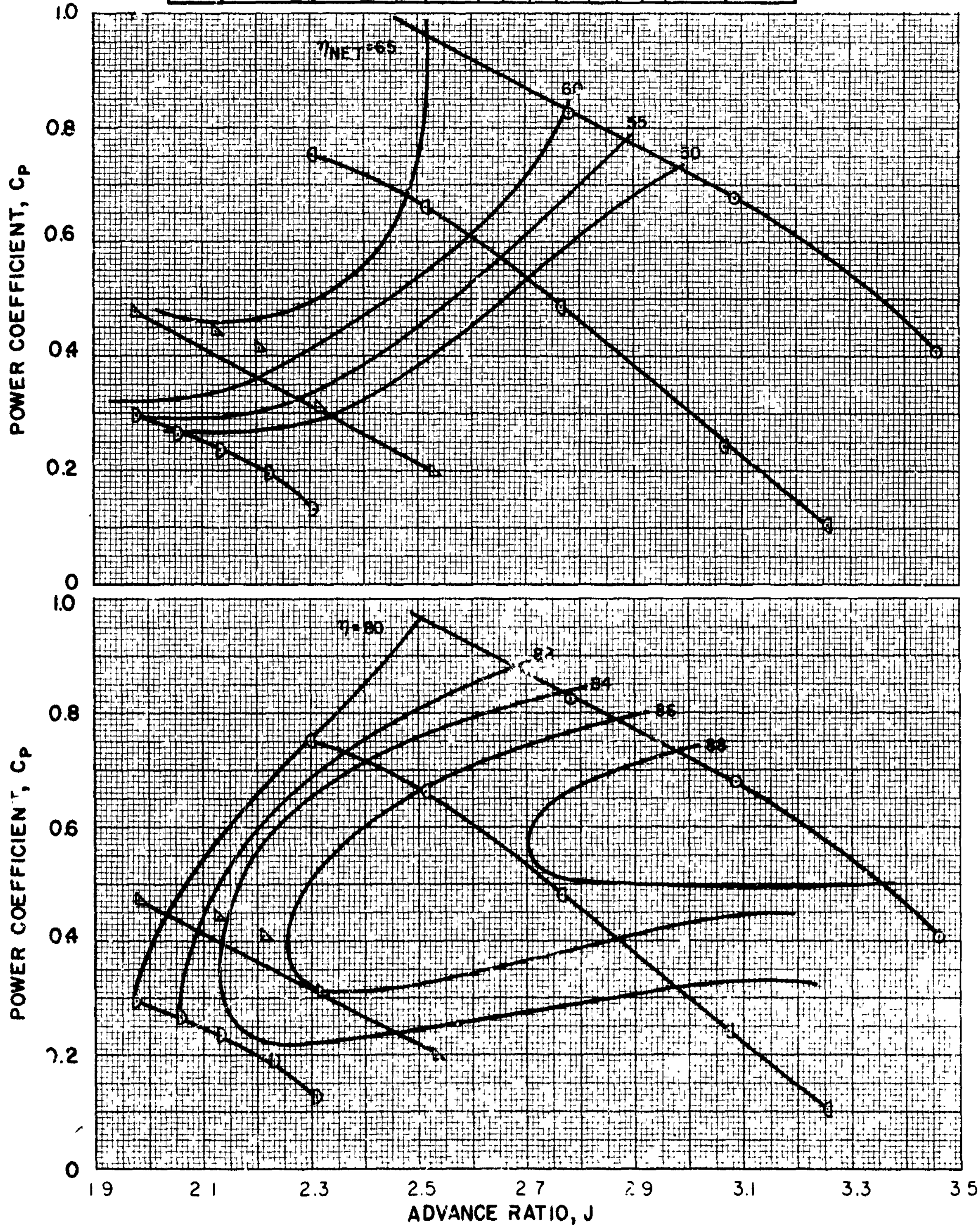

HSD SHROUDED PROPELLER TEST

EFFECT OF PROPELLER LOCATION ON SHROUDED PROPELLER PERFORMANCE

SYM	RUN NO.	MACH NO.	CONFIGURATION	$\theta_{3/4}$
△	283,282	0.02, 0.10	$L_1 C_2 E_1 B_3 P_{WT} T_1 R_1 R_E$	20
⊡	284,285	↓	↓	25
◇	278,279	↓	↓	30
◿	290,289	↓	↓	35

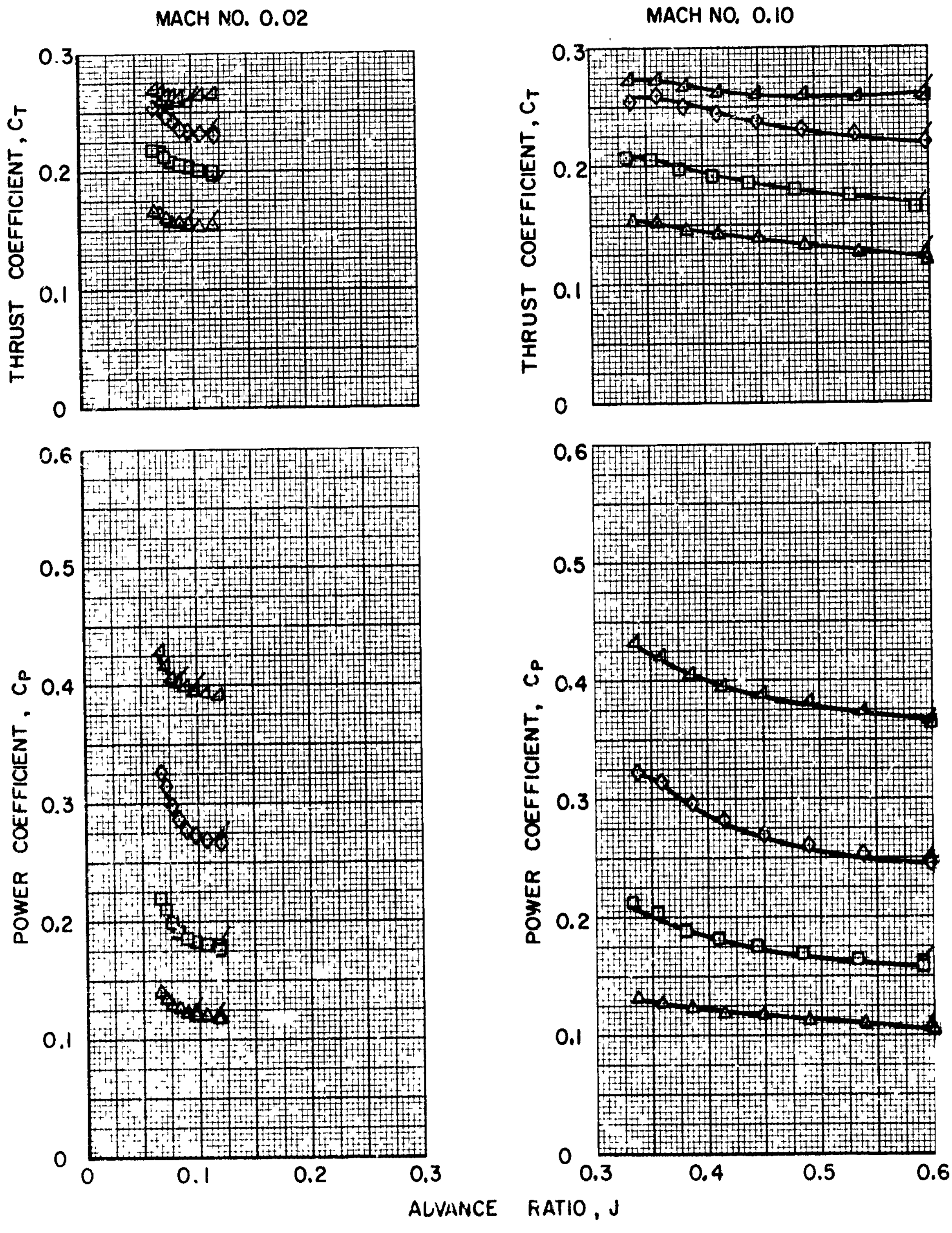

HSD SHROUDED PROPELLER TEST

EFFECT OF PROPELLER LOCATION ON SHROUDED PROPELLER PERFORMANCE

SYM	RUN NO.	MACH NO.	CONFIGURATION	$\theta_{3/4}$
△	283,282	0.02, 0.10	$L_1 C_2 E_1 B_3 P_{WT} T_1 R_1 R_E$	20
□	284,285	↓	↓	25
◇	278,279	↓	↓	30
◿	290,289	↓	↓	35

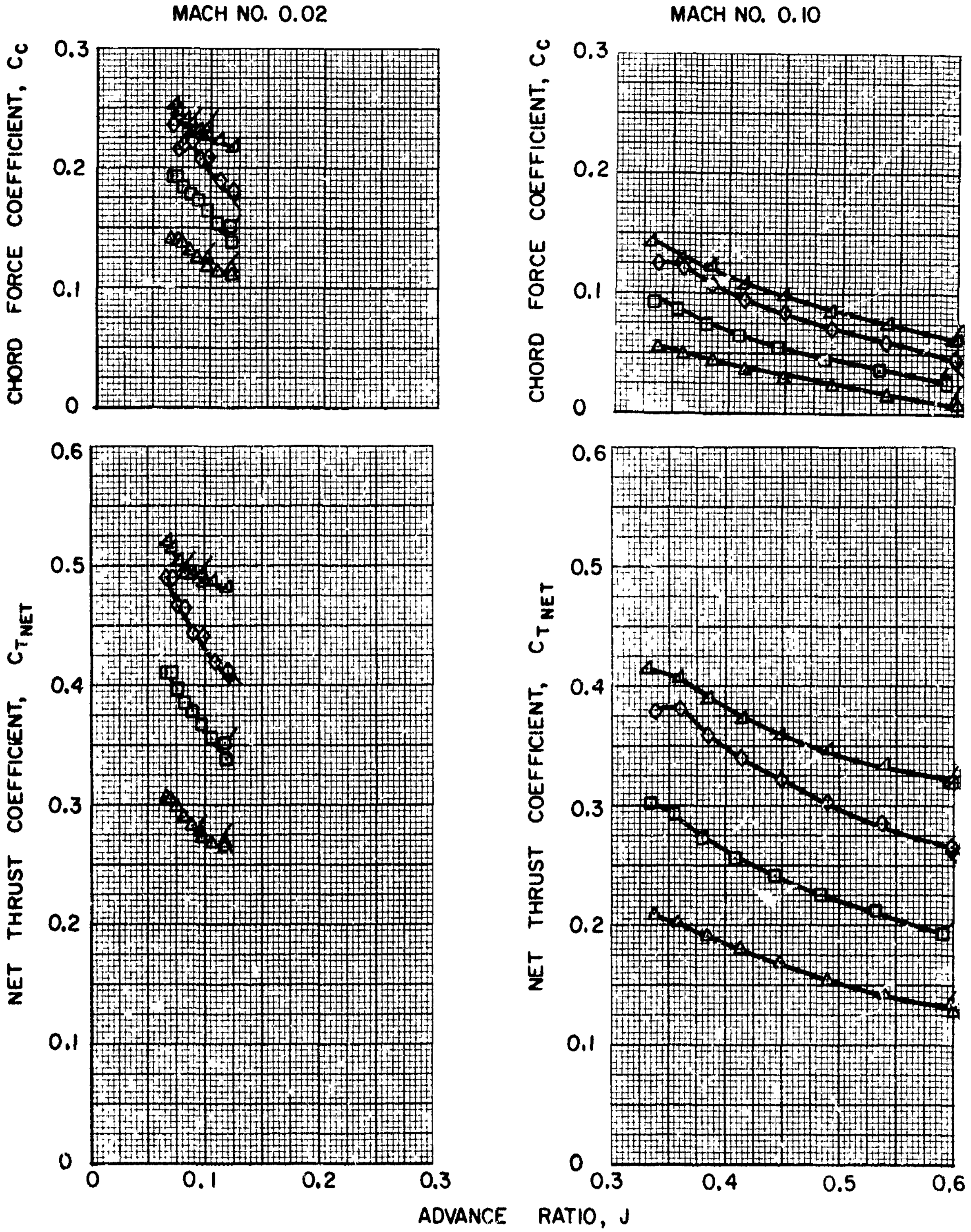

HSD SHROUDED PROPELLER TEST

EFFECT OF PROPELLER LOCATION ON SHROUDED PROPELLER PERFORMANCE

SYM	RUN NO.	MACH NO.	CONFIGURATION	$\theta_{3/4}$
△	281	0.20	$L_1\ C_2\ E_1\ B_3\ P_{WT}\ T_1\ R_1\ R_E$	20
□	287	↓	↓	25
◇	280	↓	↓	30
⊿	288	↓	↓	35

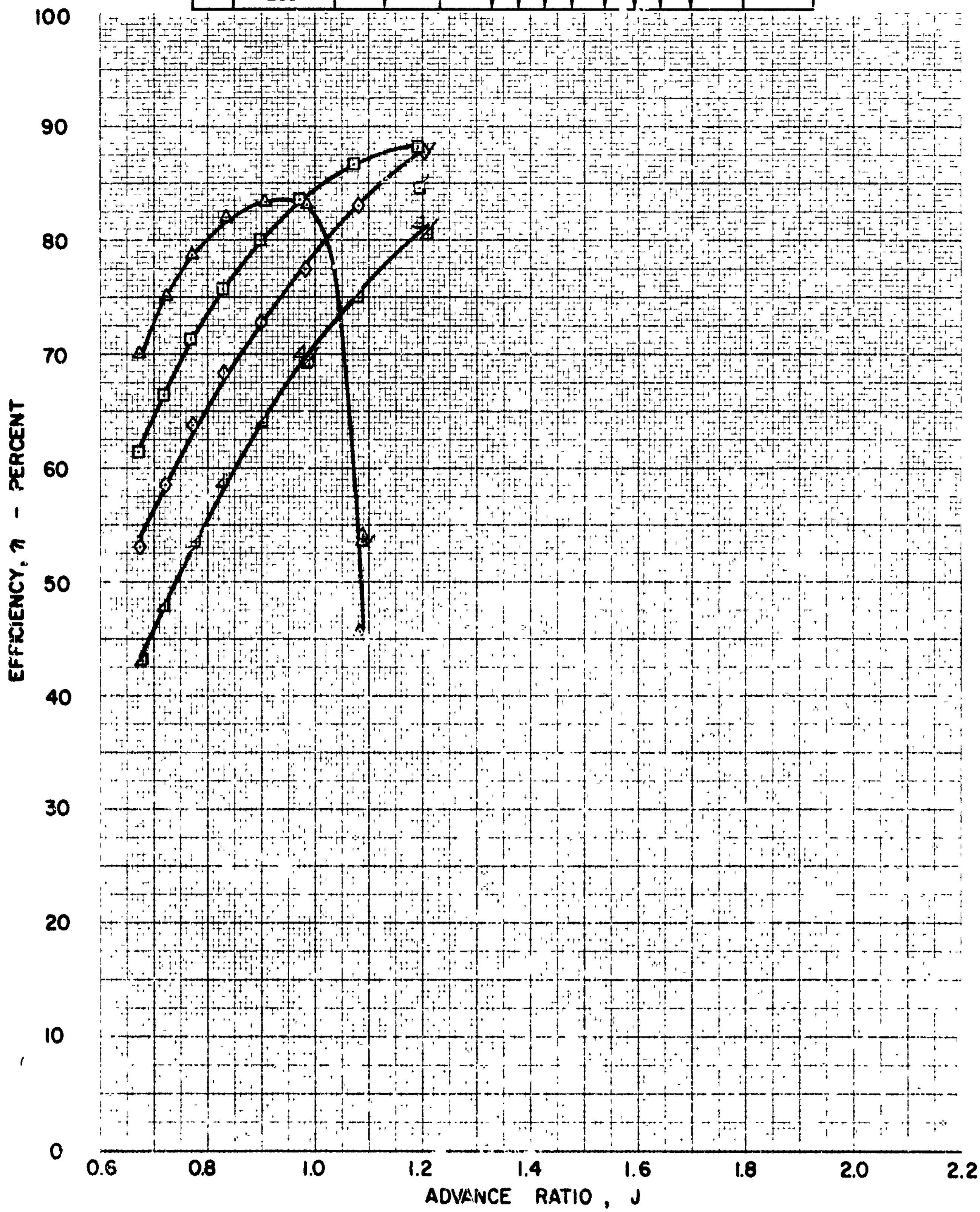

HSD SHROUDED PROPELLER TEST

EFFECT OF PROPELLER LOCATION ON SHROUDED PROPELLER PERFORMANCE

SYM	RUN NO.	MACH NO.	CONFIGURATION	$\theta_{3/4}$
△	281	0.20	$L_1 C_2 E_1 B_3 P_{WT} T_1 R_1 R_E$	20
□	287	↓	↓	25
◇	280	↓	↓	30
⊿	288	↓	↓	35

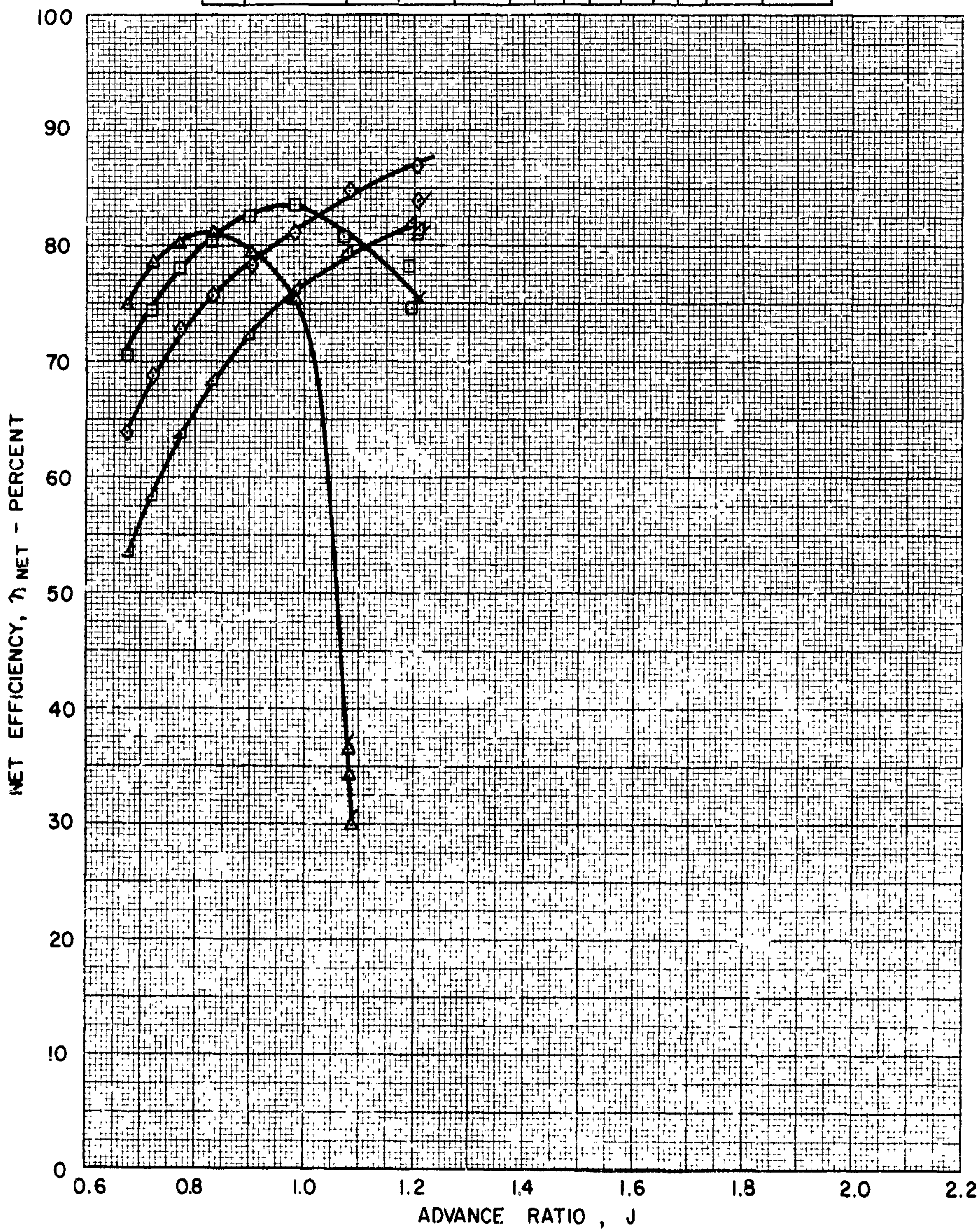

E330590-I

FIG.107

HSD SHROUDED PROPELLER TEST

EFFECT OF PROPELLER LOCATION ON SHROUDED PROPELLER PERFORMANCE

SYM	RUN NO.	MACH NO.	CONFIGURATION	$\theta_{3/4}$
△	281	0.20	$L_1 C_2 E_1 B_3 P_{WT} T_1 R_1 R_E$	20
□	287	↓	↓	25
◇	280	↓	↓	30
◺	288	↓	↓	35

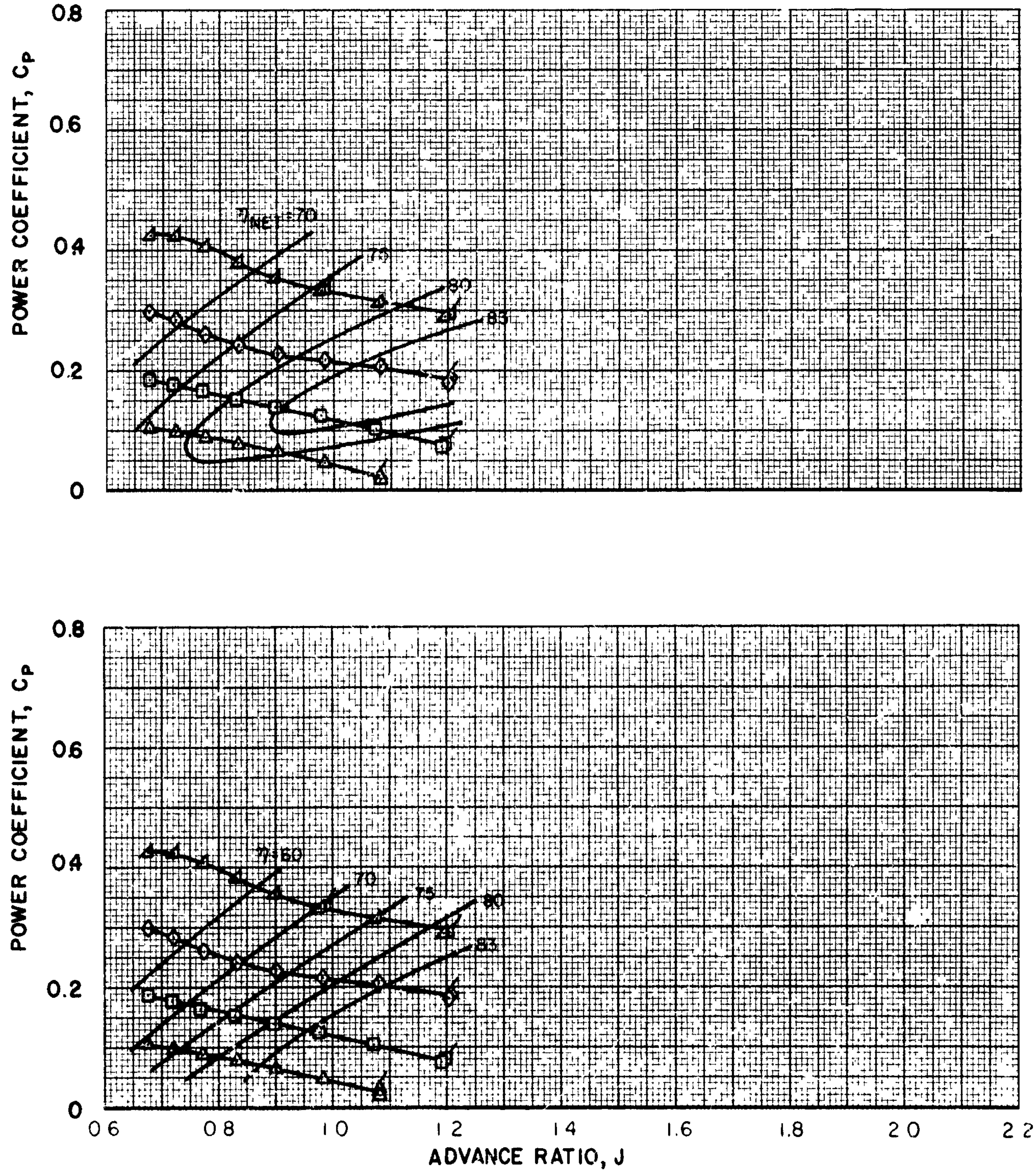

E330590-1

FIG.108

HSD SHROUDED PROPELLER TEST

EFFECT OF PROPELLER LOCATION ON SHROUDED PROPELLER PERFORMANCE

SYM	RUN NO.	MACH NO.	CONFIGURATION	$\theta_{3/4}$
◇	566	0.31	$L_1 C_2 E_1 B_3 P_{WT} T_1 R_1 R_E$	30
⊿	567	↓	↓	34
▽	568	↓	↓	38
D	570	↓	↓	42

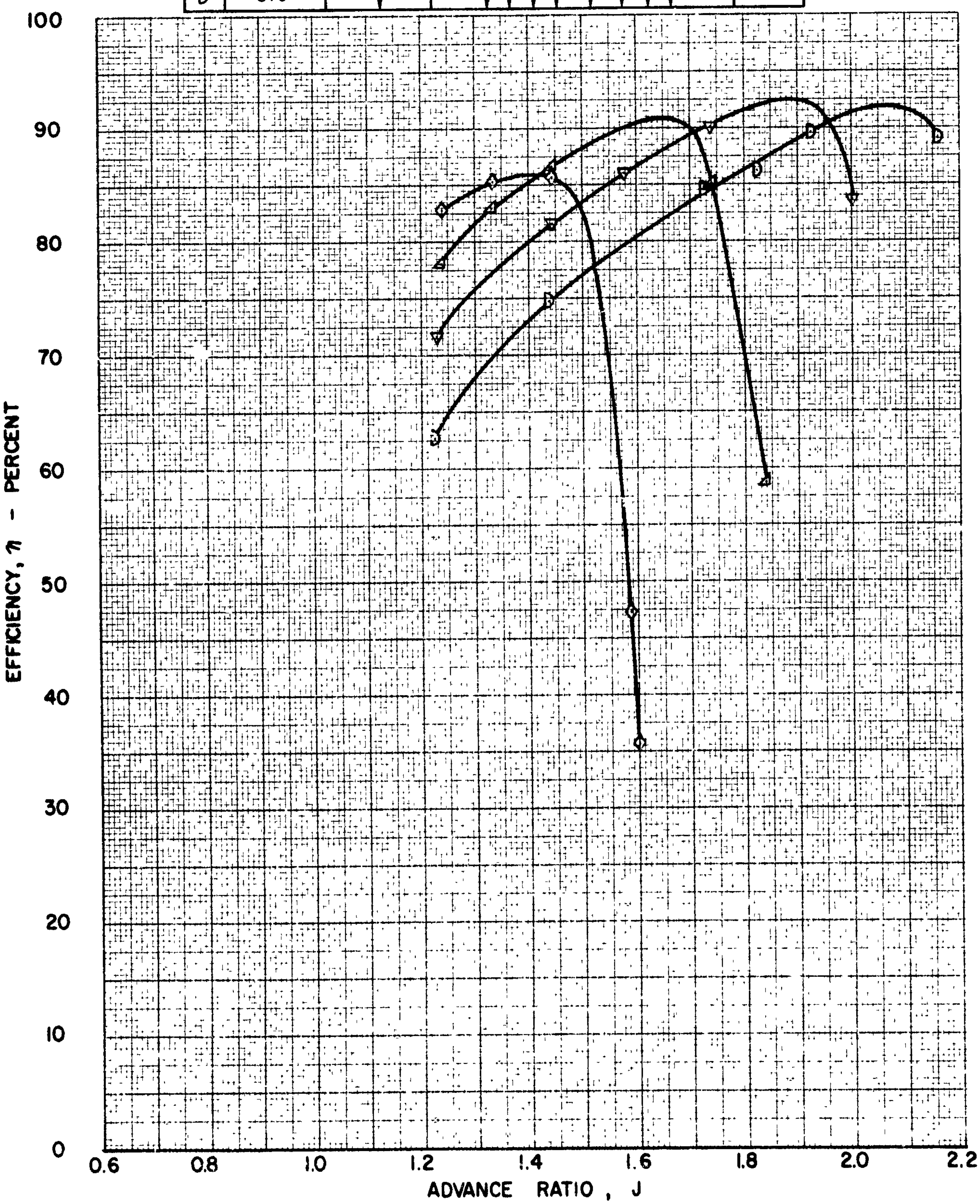

E330590-1

FIG.109

HSD SHROUDED PROPELLER TEST

EFFECT OF PROPELLER LOCATION ON SHROUDED PROPELLER PERFORMANCE

SYM	RUN NO.	MACH NO.	CONFIGURATION	$\theta_{3/4}$
◇	566	0.31	$L_1 C_2 E_1 B_3 P_{WT} T_1 R_1 R_E$	30
◁	567	↓	↓	34
▽	568	↓	↓	38
D	570	↓	↓	42

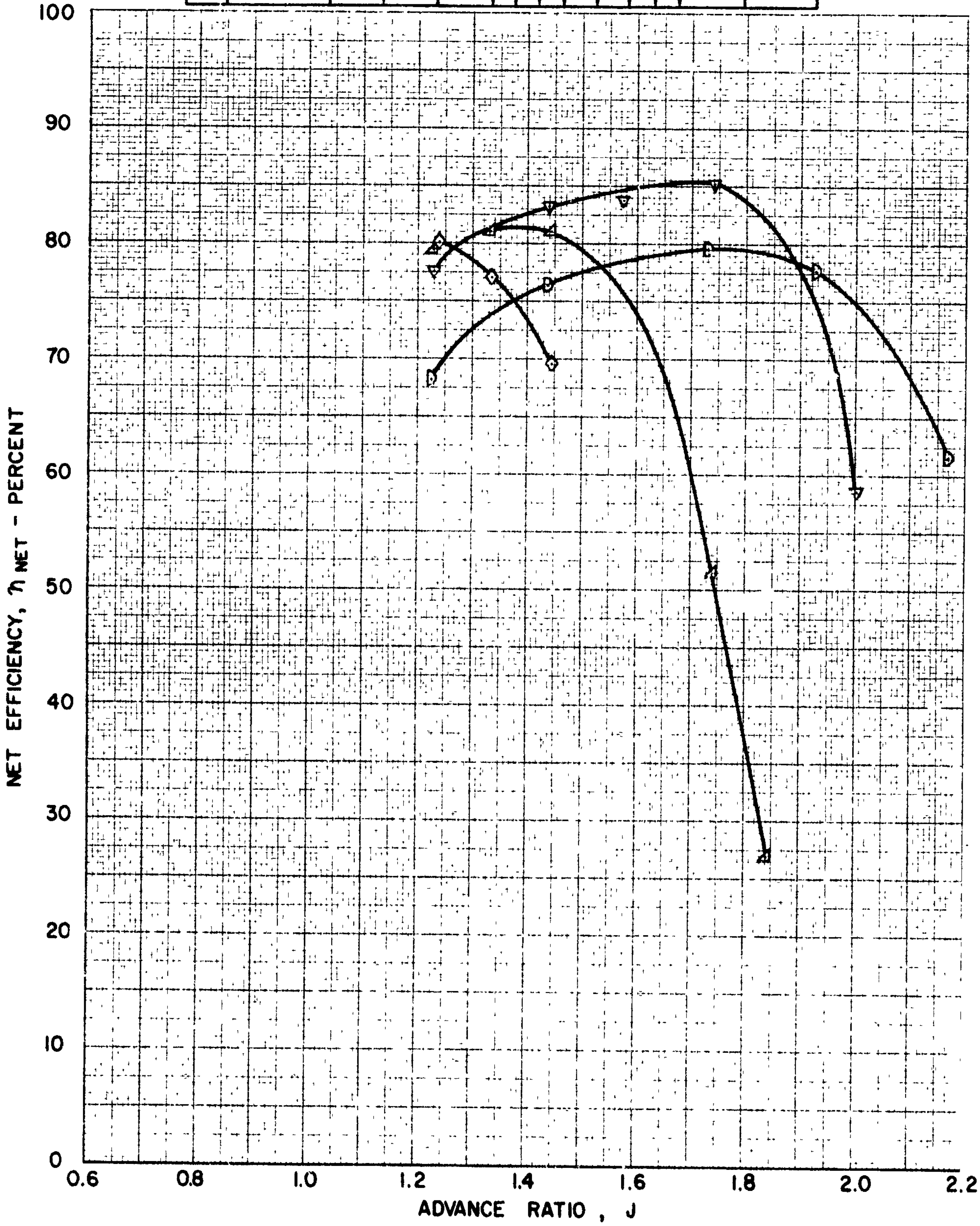

E330590-1

FIG. 110

HSD SHROUDED PROPELLER TEST

EFFECT OF PROPELLER LOCATION ON SHROUDED PROPELLER PERFORMANCE

SYM	RUN NO.	MACH NO.	CONFIGURATION	$\theta_{3/4}$
◊	566	0.31	$L_1 C_2 E_1 B_3 P_{WT} T_1 R_1 R_E$	30
⊿	567			34
▽	568			38
D	570			42

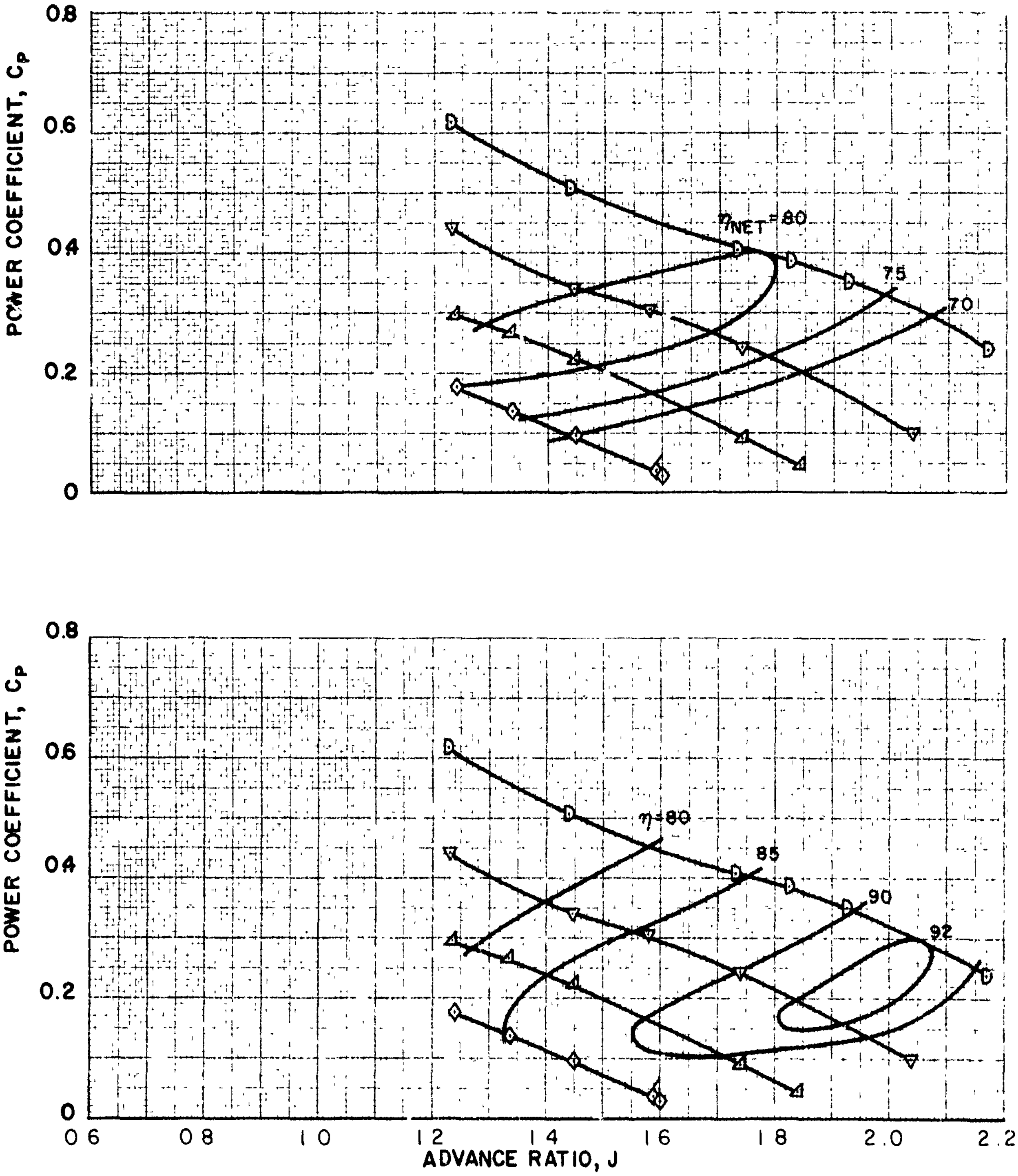

HSD SHROUDED PROPELLER TEST

EFFECT OF PROPELLER LOCATION ON SHROUDED PROPELLER PERFORMANCE

SYM	RUN NO.	MACH NO.	CONFIGURATION	$\theta_{3/4}$
▽	569	0.41	$L_1 C_2 E_1 B_3 P_{WT} T_1 R_1 R_E$	38
D	571	↓	↓	42
◺	573	↓	↓	46
◁	575	↓	↓	50

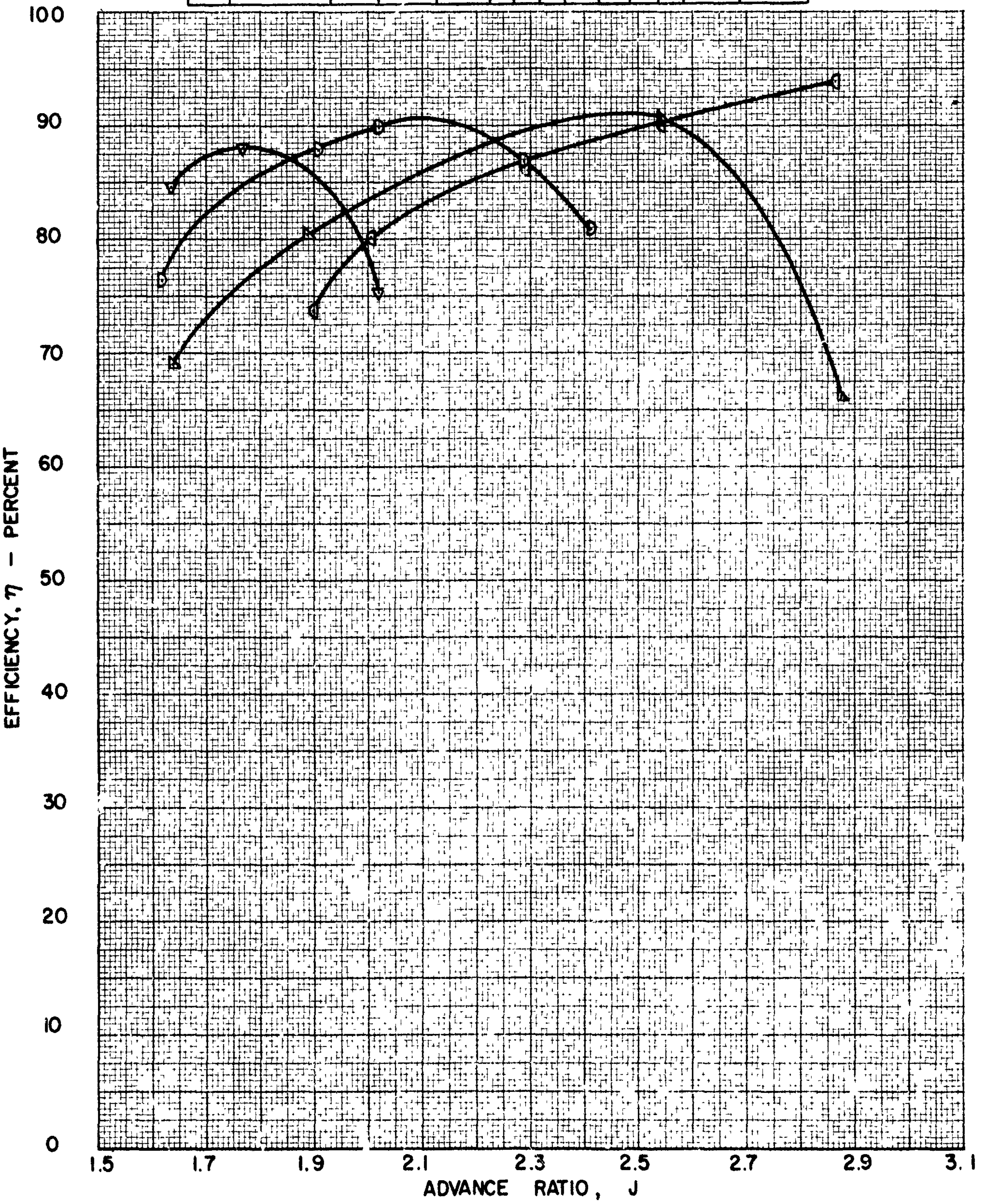

E330590-1

FIG. 112

HSD SHROUDED PROPELLER TEST

EFFECT OF PROPELLER LOCATION ON SHROUDED PROPELLER PERFORMANCE

SYM	RUN NO.	MACH NO.	CONFIGURATION	$\theta_{3/4}$
▽	569	0.41	$L_1 C_2 E_1 B_3 P_{WT} T_1 R_1 R_E$	38
D	571			42
◺	573			46
◖	575			50

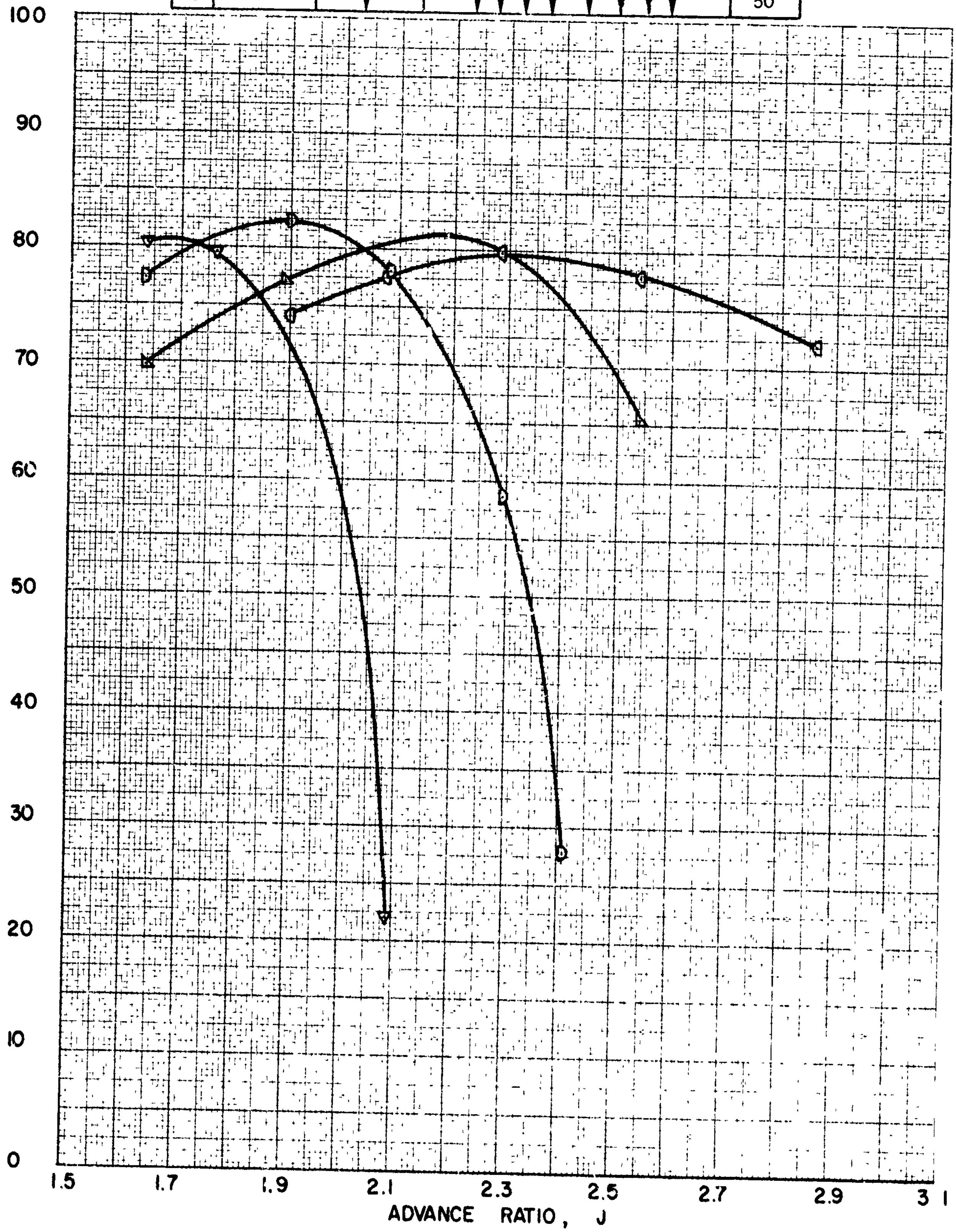

E330590-1

FIG. 113

HSD SHROUDED PROPELLER TEST

EFFECT OF PROPELLER LOCATION ON SHROUDED PROPELLER PERFORMANCE

SYM	RUN NO.	MACH NO.	CONFIGURATION	$\theta_{3/4}$
▽	569	0.41	$L_1 C_2 E_1 B_3 P_{WT} T_1 R_1 R_E$	38
D	571			42
◺	573			46
◁	575			50

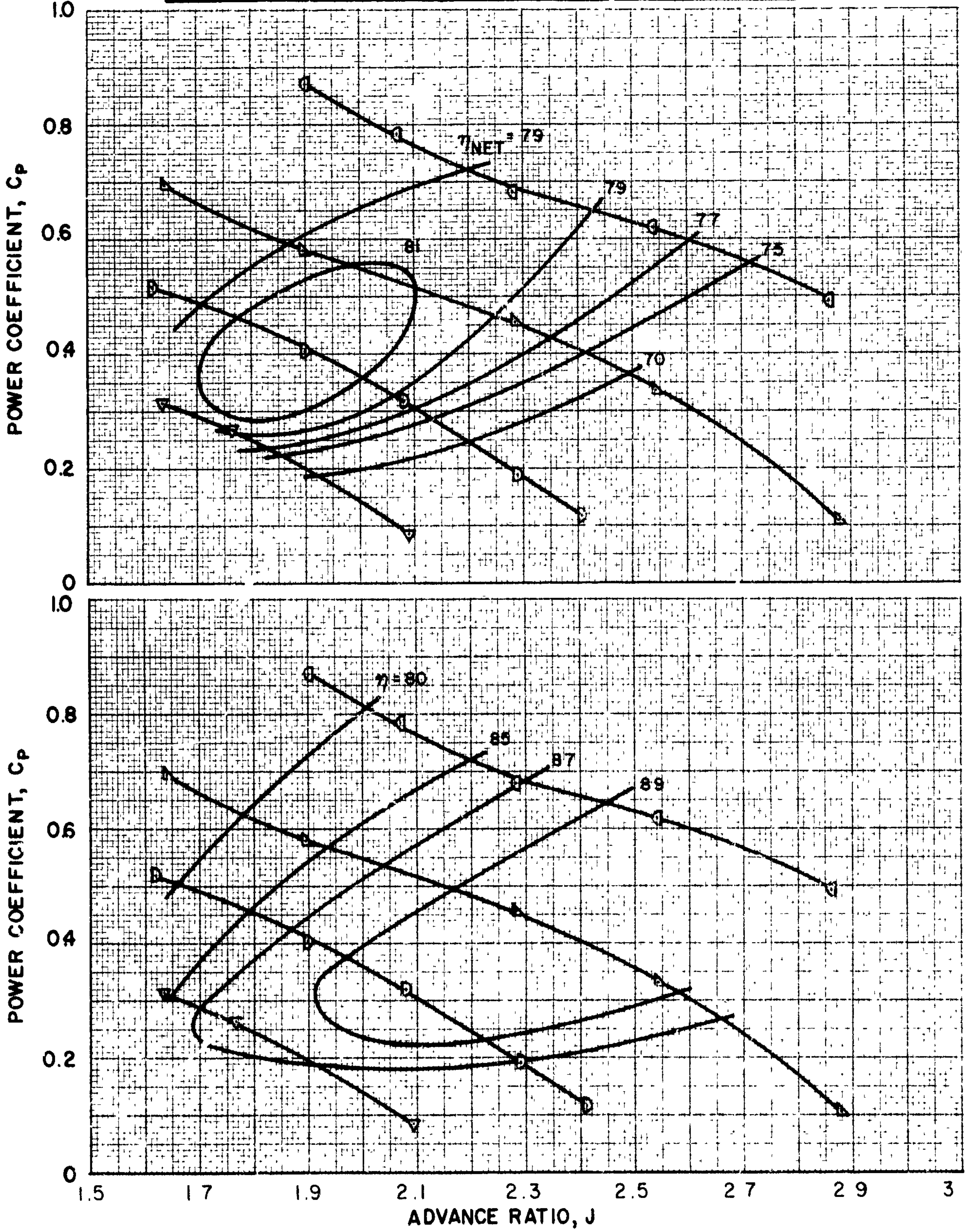

HSD SHROUDED PROPELLER TEST

EFFECT OF PROPELLER LOCATION ON SHROUDED PROPELLER PERFORMANCE

SYM	RUN NO.	MACH NO.	CONFIGURATION	$\theta_{3/4}$
D	572	0.52	$L_1 C_2 E_1 B_3 P_{WT} T_1 R_1 R_E$	42
◺	574	↓	↓	46
◖	576	↓	↓	50
⊙	577	↓	↓	54

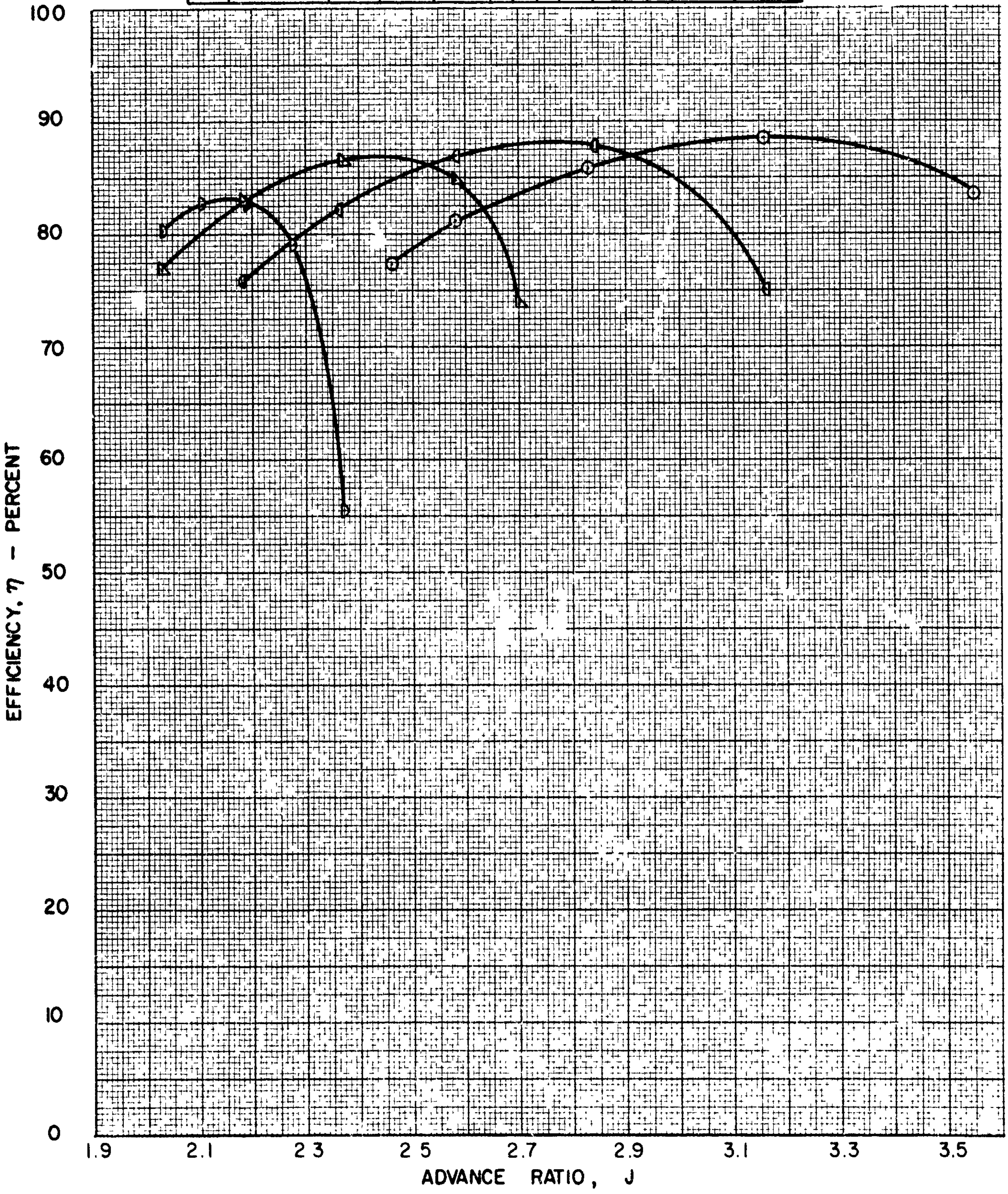

HSD SHROUDED PROPELLER TEST

EFFECT OF PROPELLER LOCATION ON SHROUDED PROPELLER PERFORMANCE

SYM	RUN NO.	MACH NO.	CONFIGURATION	$\theta_{3/4}$
◗	572	0.52	$L_1 C_2 E_1 B_3 P_{WT} T_1 R_1 R_E$	42
◺	574	↓	↓	46
◖	576	↓	↓	50
⊙	577	↓	↓	54

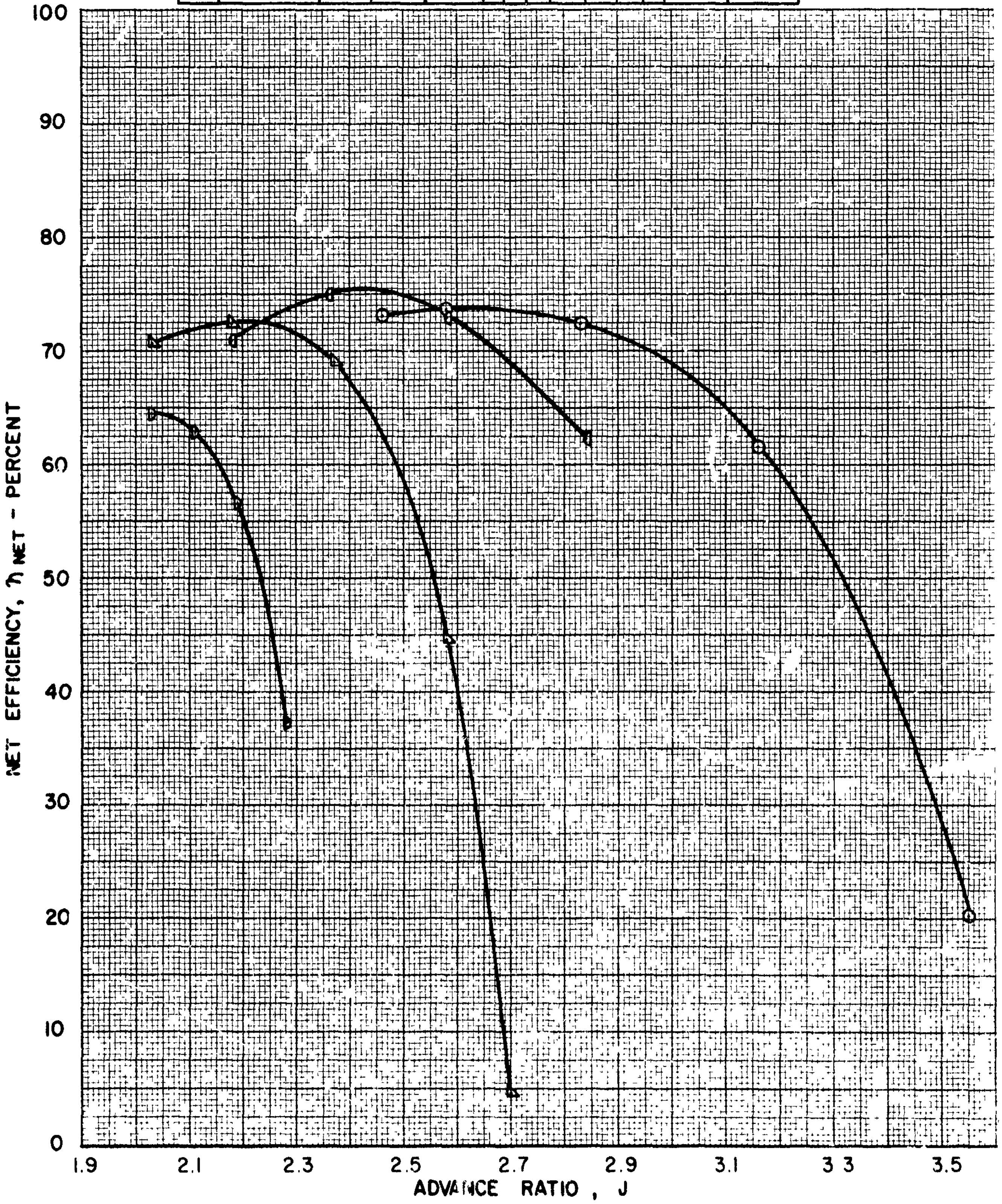

HSD SHROUDED PROPELLER TEST

EFFECT OF PROPELLER LOCATION ON SHROUDED PROPELLER PERFORMANCE

SYM	RUN NO.	MACH NO.	CONFIGURATION	$\theta_{3/4}$
◻	572	0.52	$L_1 C_2 E_1 B_3 P_{WT} T_1 R_1 R_E$	42
◺	574	↓	↓	46
◐	576	↓	↓	50
⊙	577	↓	↓	54

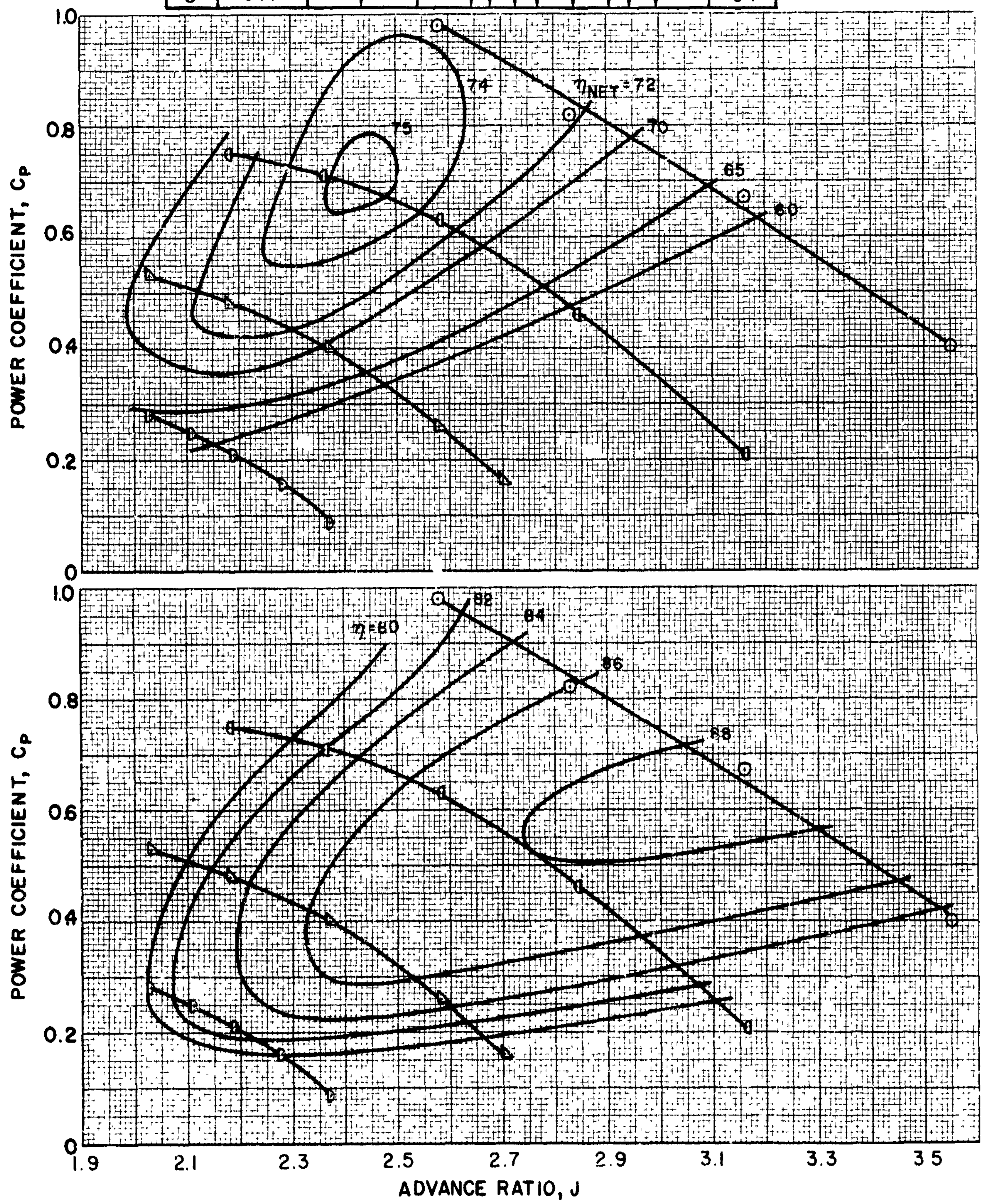

E330590-1

FIG. 117

HSD SHROUDED PROPELLER TEST

EFFECT OF CHORD LENGTH ON SHROUDED PROPELLER PERFORMANCE

SYM	RUN NO.	MACH NO.	CONFIGURATION	$\theta_{3/4}$
△	237,238	0.02, 0.10	L_{1SC} C_{1SC} E_{SC} B_3 P_{NT} T_1 R_1 R_E	20
⊡	240,241	↓	↓	25
◇	233,235	↓	↓	30
⊿	232,231	↓	↓	35

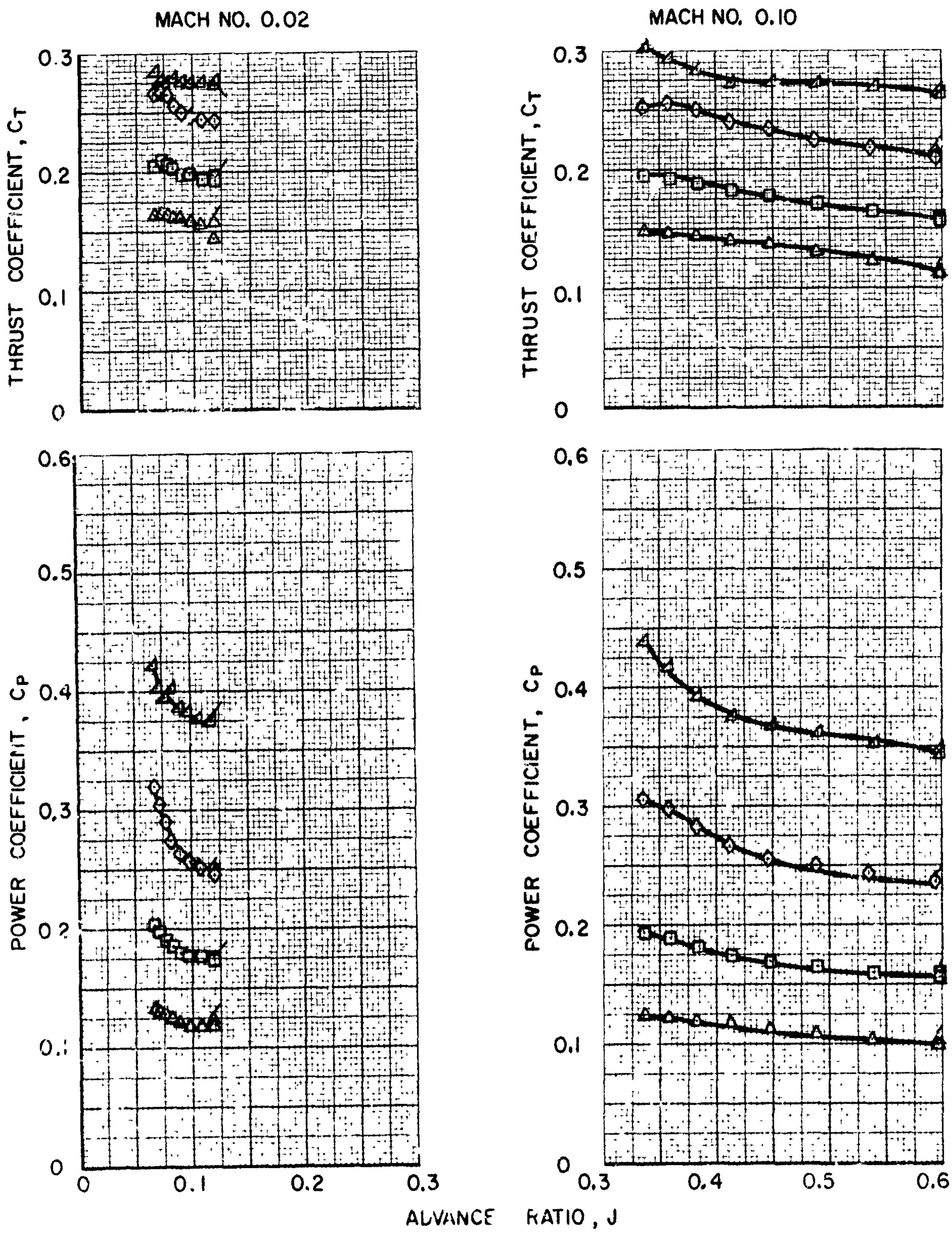

E330590-1

FIG. 118

HSD SHROUDED PROPELLER TEST

EFFECT OF CHORD LENGTH ON SHROUDED PROPELLER PERFORMANCE

SYM	RUN NO.	MACH NO.	CONFIGURATION	$\theta_{3/4}$
△	237,238	0.02, 0.10	L_{1SC} C_{1SC} E_{1SC} θ_3 P_{NT} T_1 R_1 R_E	20
⊡	240,241			25
◇	233,235			30
⊿	232,231			35

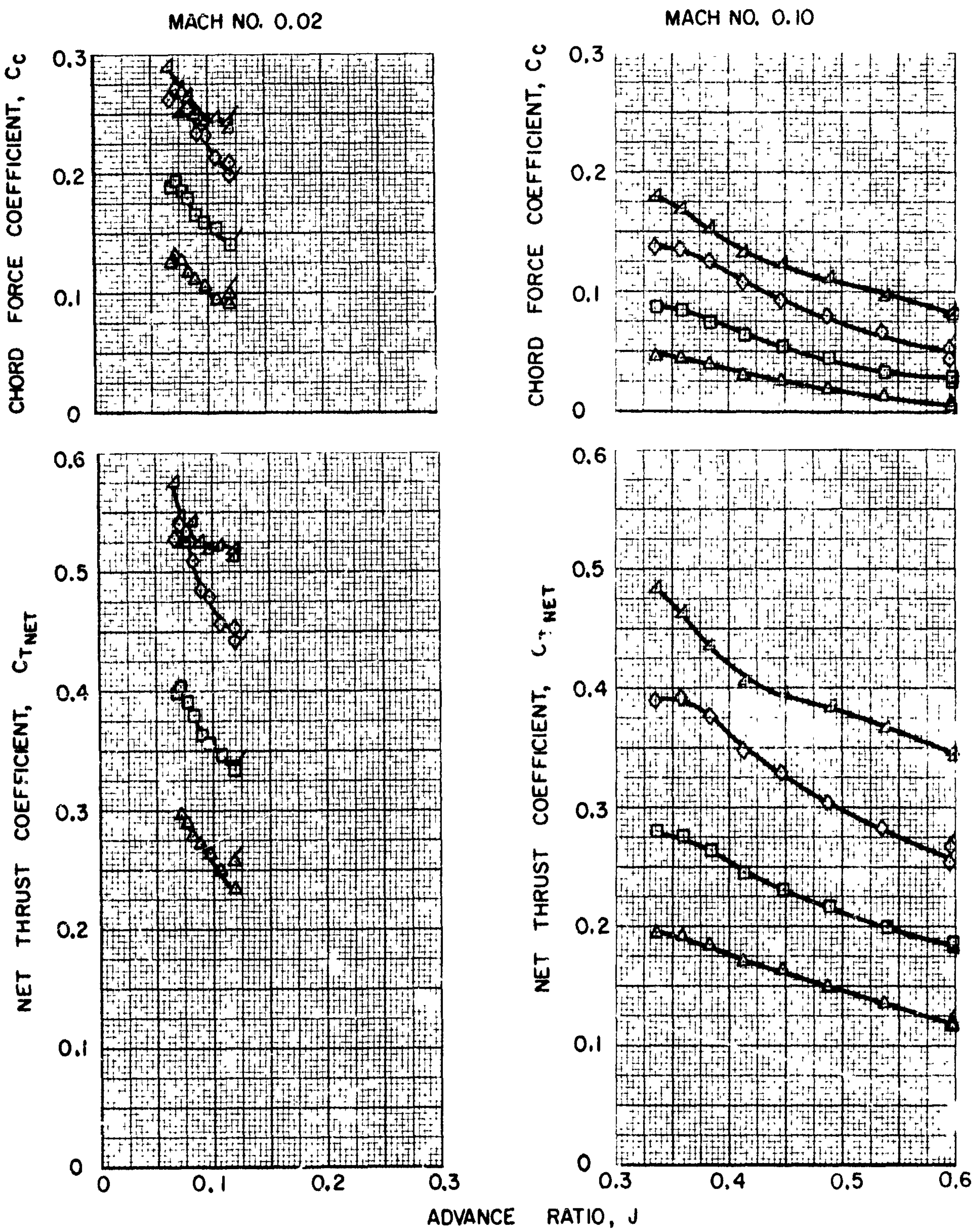

HSD SHROUDED PROPELLER TEST

EFFECT OF CHORD LENGTH ON SHROUDED PROPELLER PERFORMANCE

SYM	RUN NO	MACH NO.	CONFIGURATION	$\theta_{3/4}$
△	239	0.20	L_{ISC} C_{ISC} E_{ISC} B_3 P_{NT} T_1 R_1 R_E	20
⊡	242	↓	↓	25
◇	236	↓	↓	30
⊿	230	↓	↓	35

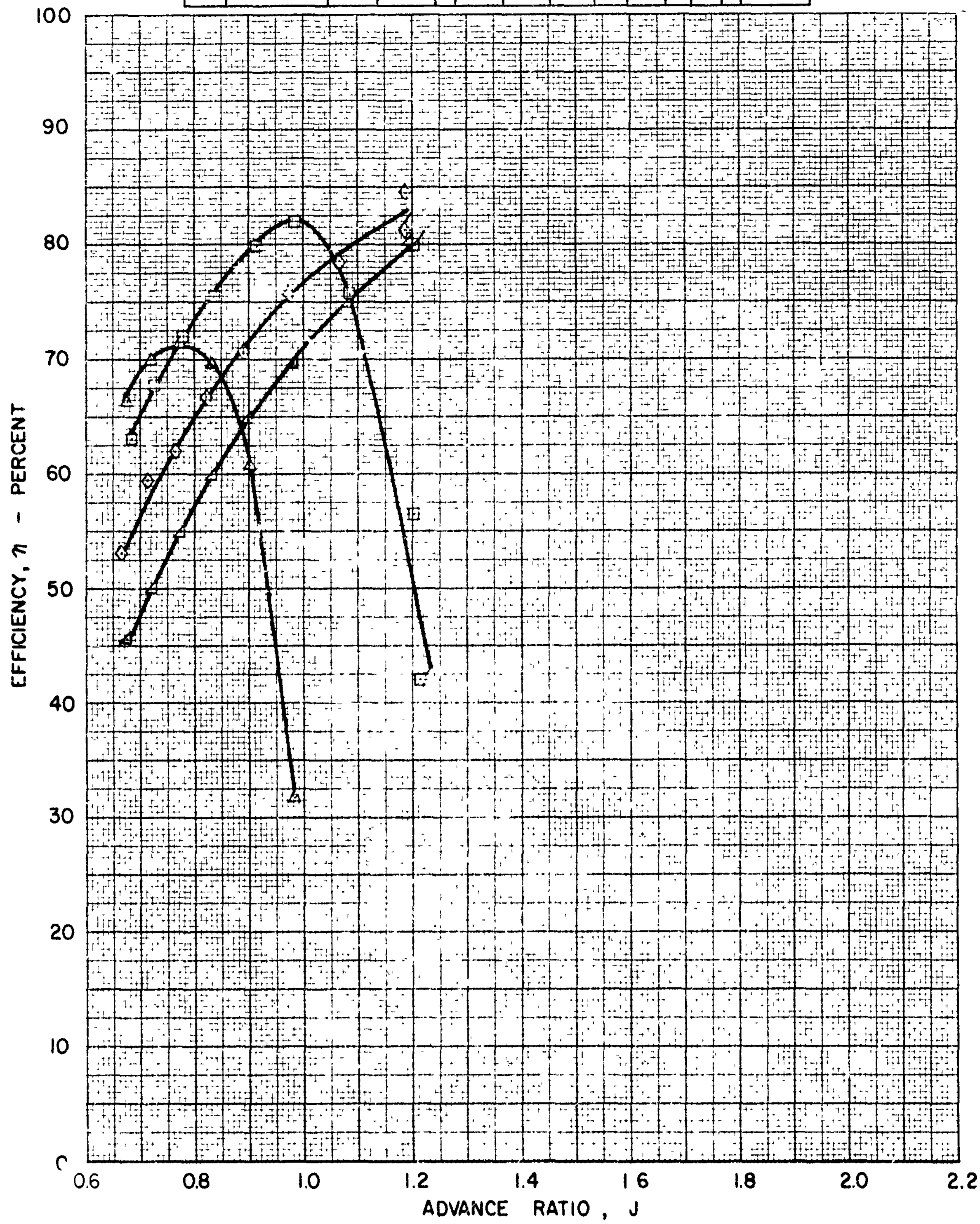

HSD SHROUDED PROPELLER TEST

EFFECT OF CHORD LENGTH ON SHROUDED PROPELLER PERFORMANCE

SYM	RUN NO.	MACH NO.	CONFIGURATION	$\theta_{3/4}$
△	239	0.20	L_{1SC} C_{1SC} E_{1SC} B_3 P_{NT} T_1 R_1 R_E	20
⊡	242	↓	↓	25
◇	236	↓	↓	30
⊿	230	↓	↓	35

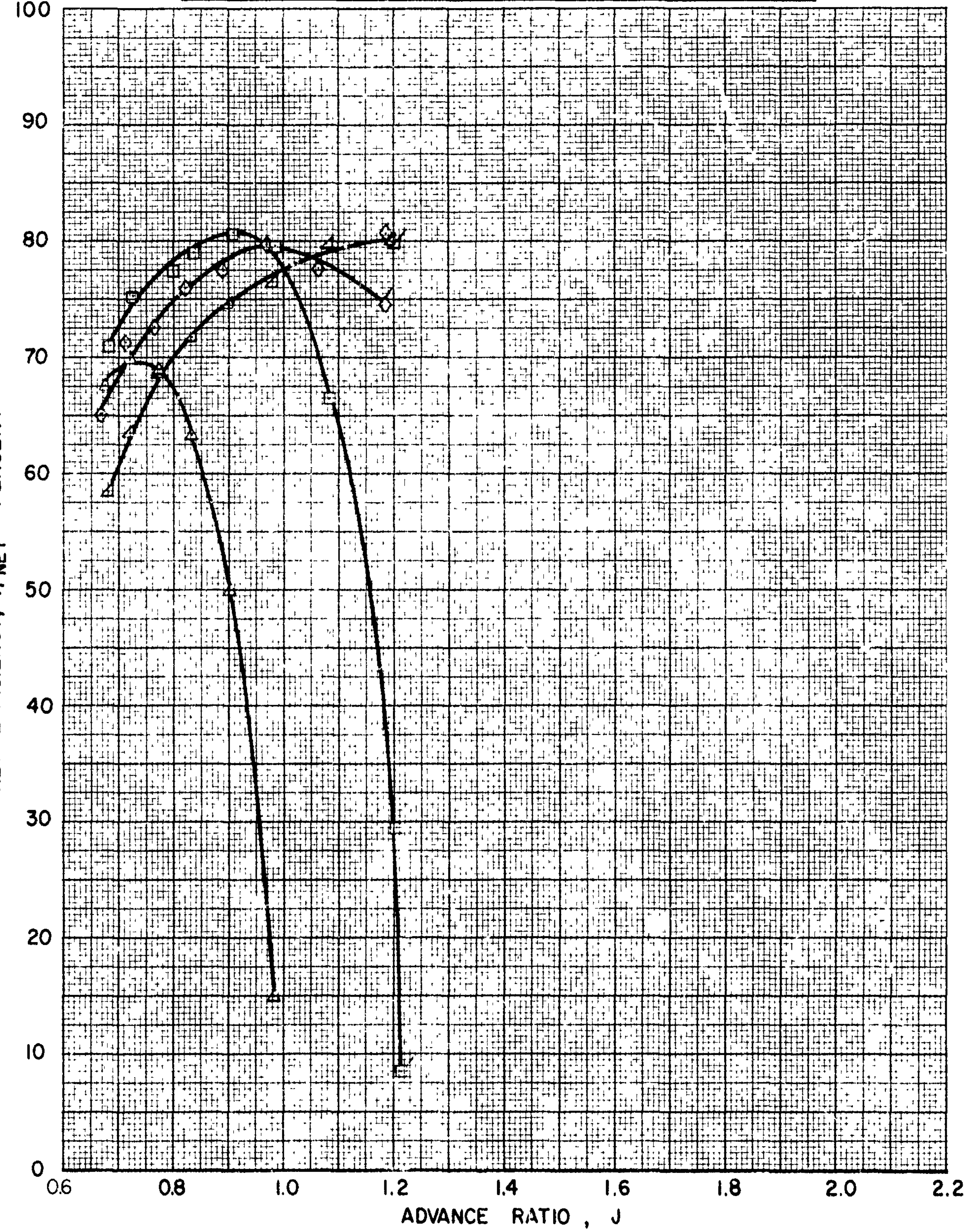

E330590-I

FIG. 121

HSD SHROUDED PROPELLER TEST

EFFECT OF CHORD LENGTH ON SHROUDED PROPELLER PERFORMANCE

SYM	RUN NO.	MACH NO.	CONFIGURATION	$\theta_{3/4}$
△	239	0.20	$L_{1SC}\ C_{1SC}\ E_{1SC}\ B_3\ P_{NT}\ T_1\ R_1\ R_E$	20
□	242	↓	↓	25
◇	236	↓	↓	30
⊿	230	↓	↓	35

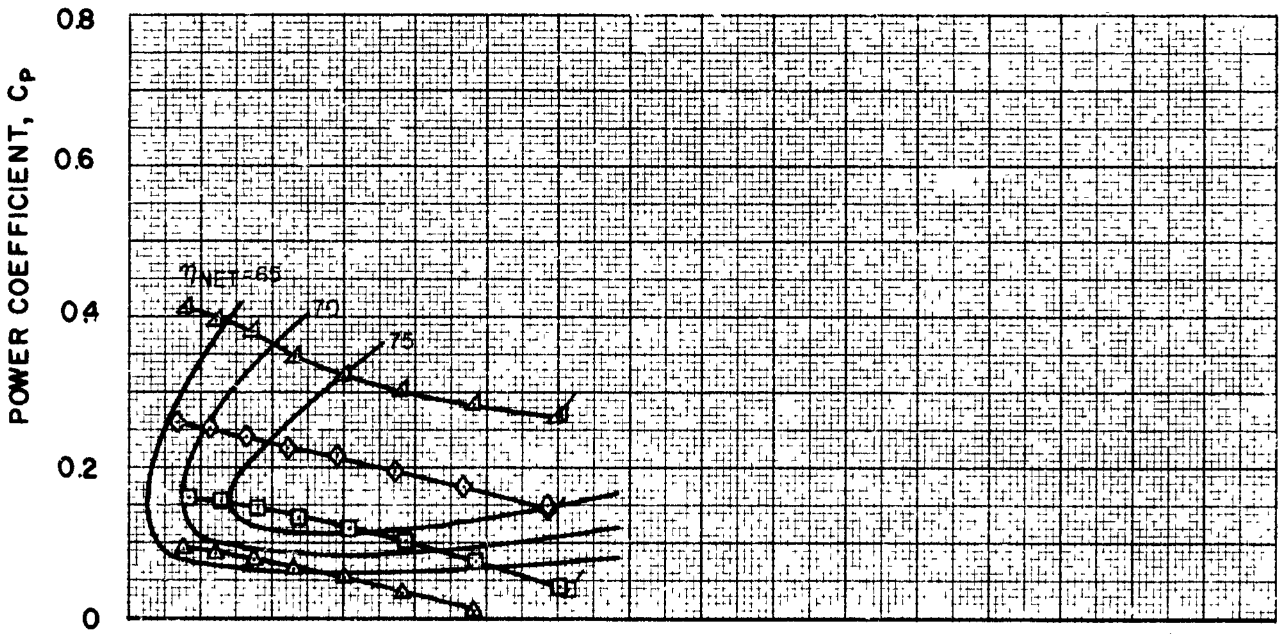

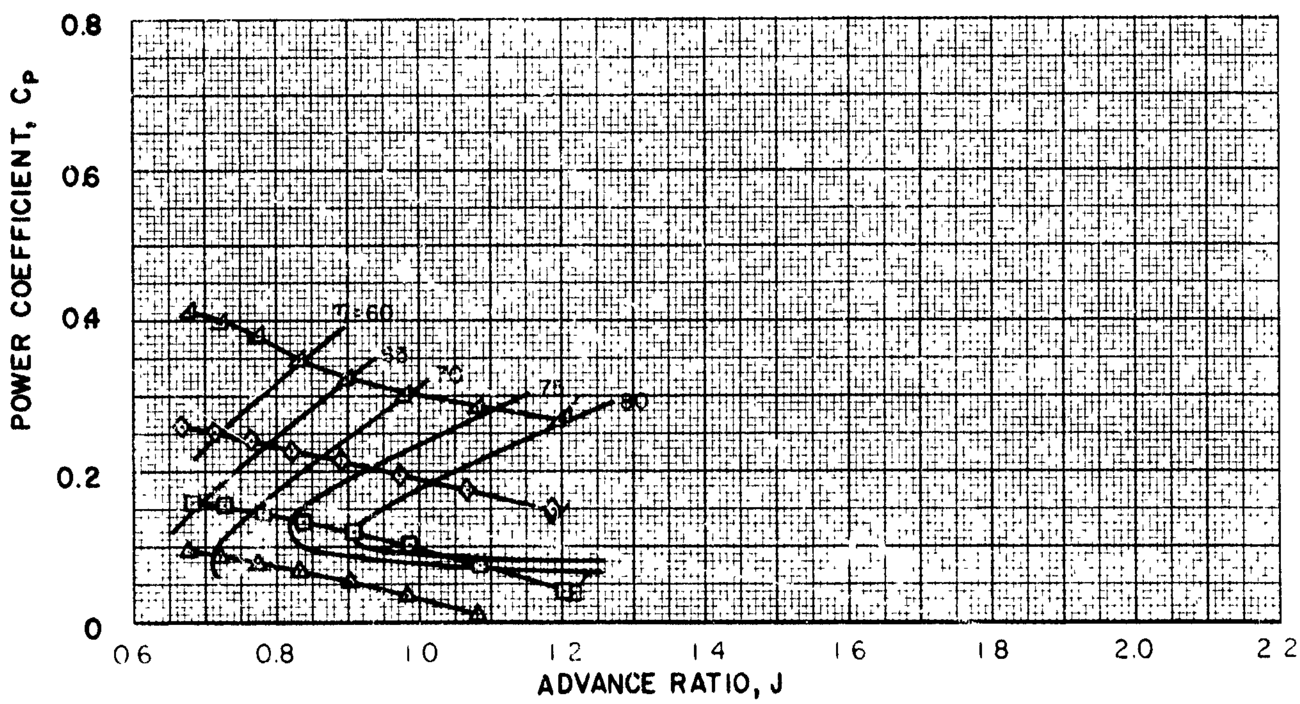

E330590-1

FIG. 122

HSD SHROUDED PROPELLER TEST

EFFECT OF CHORD LENGTH ON SHROUDED PROPELLER PERFORMANCE

SYM	RUN NO.	MACH NO.	CONFIGURATION	$\theta_{3/4}$
◇	585	0.31	L_{1SC} C_{1SC} E_{13C} B_3 P_{NT} T_1 R_1 R_E	30
⊿	586	↓	↓	34
▽	587	↓	↓	38
D	589	↓	↓	42

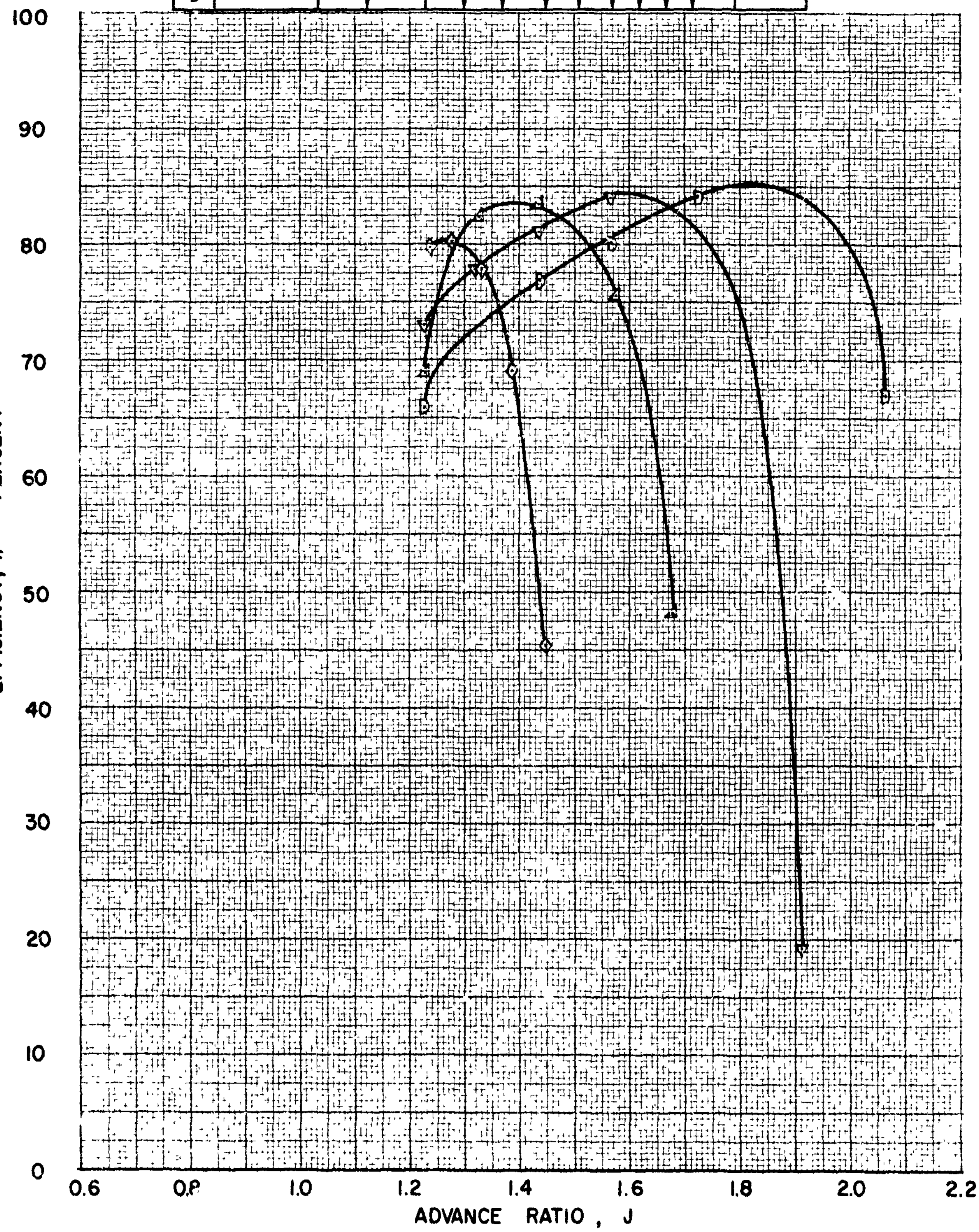

E330590-1

FIG.123

HSD SHROUDED PROPELLER TEST

EFFECT OF CHORD LENGTH ON SHROUDED PROPELLER PERFORMANCE

SYM	RUN NO.	MACH NO.	CONFIGURATION	$\theta_{3/4}$
◇	585	0.31	L_{ISC} C_{ISC} E_{ISC} B_3 P_{NT} T_1 R_1 R_E	30
⊿	586	↓	↓	34
▽	587	↓	↓	38
D	589	↓	↓	42

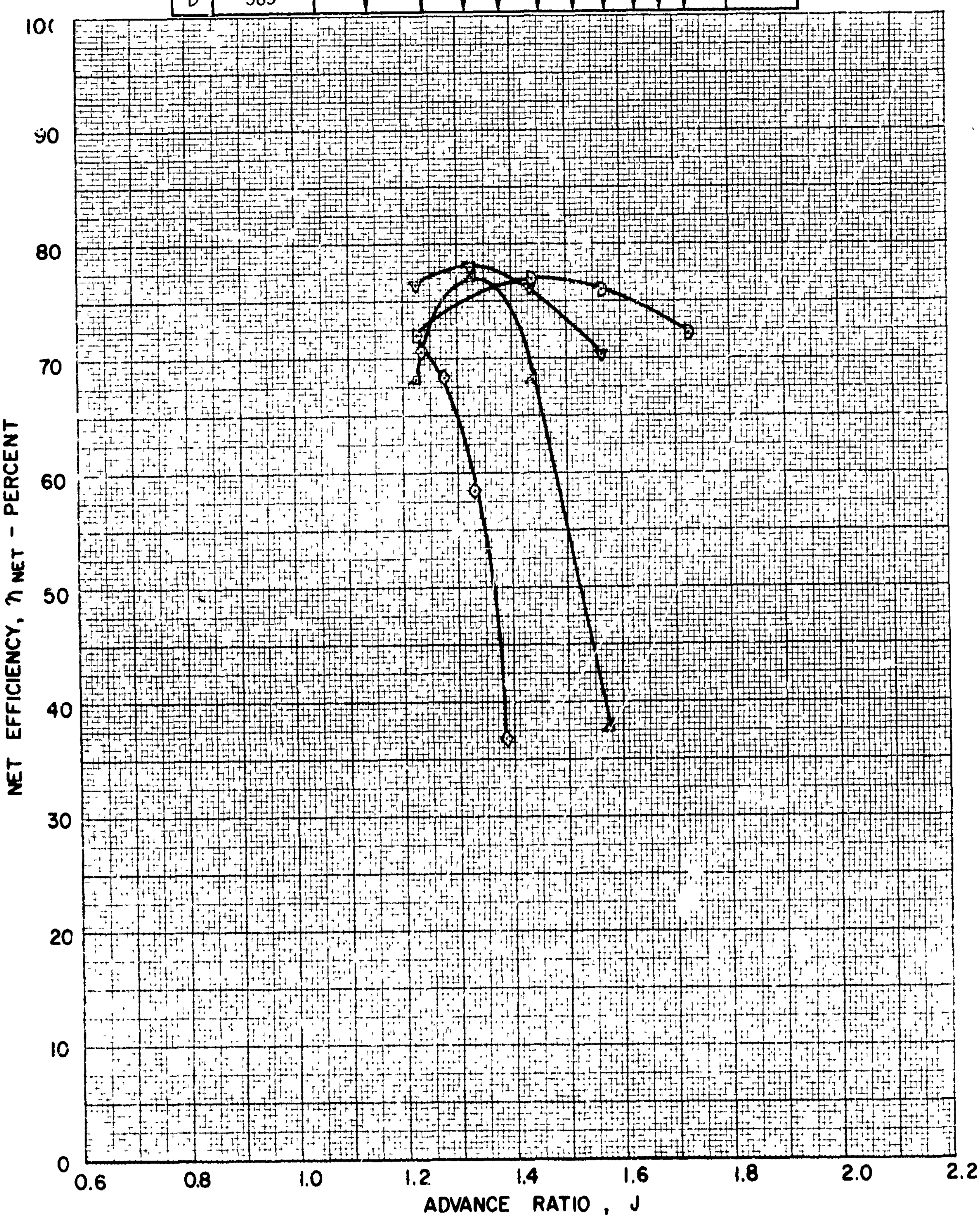

E330590-I

FIG. 124

HSD SHROUDED PROPELLER TEST

EFFECT OF CHORD LENGTH ON SHROUDED PROPELLER PERFORMANCE

SYM	RUN NO.	MACH NO.	CONFIGURATION	$\theta_{3/4}$
◇	585	0.31	L_{ISC} C_{ISC} E_{ISC} B_3 P_{NT} T_1 R_1 R_E	30
⊿	586			34
▽	587			38
D	589			42

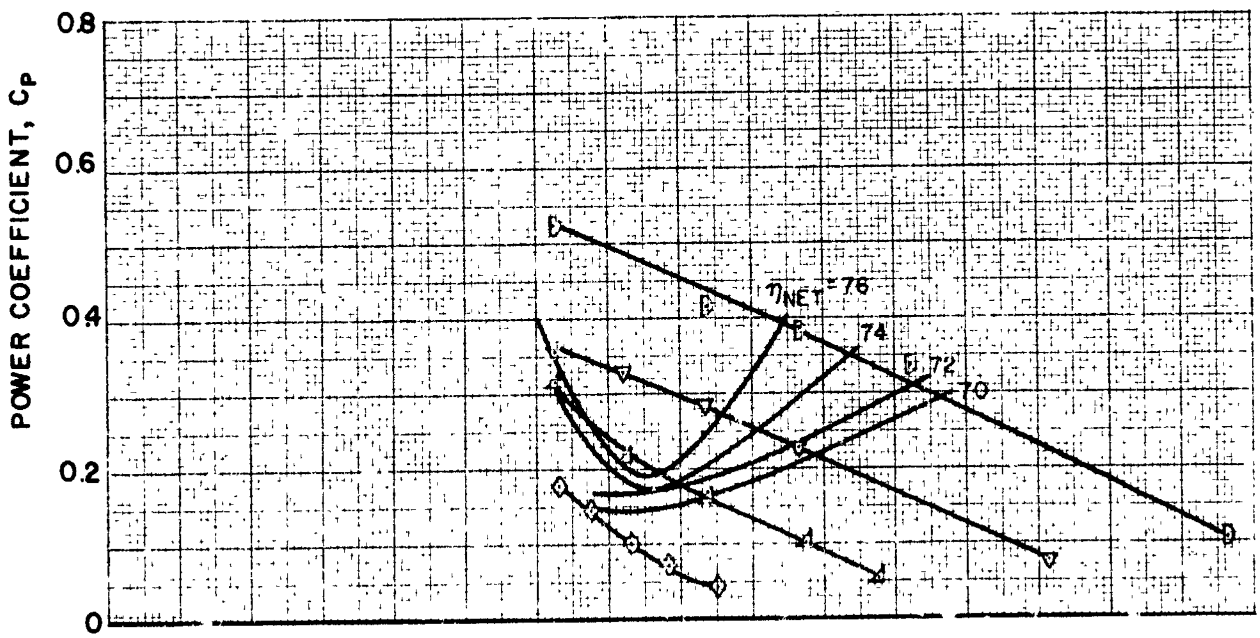

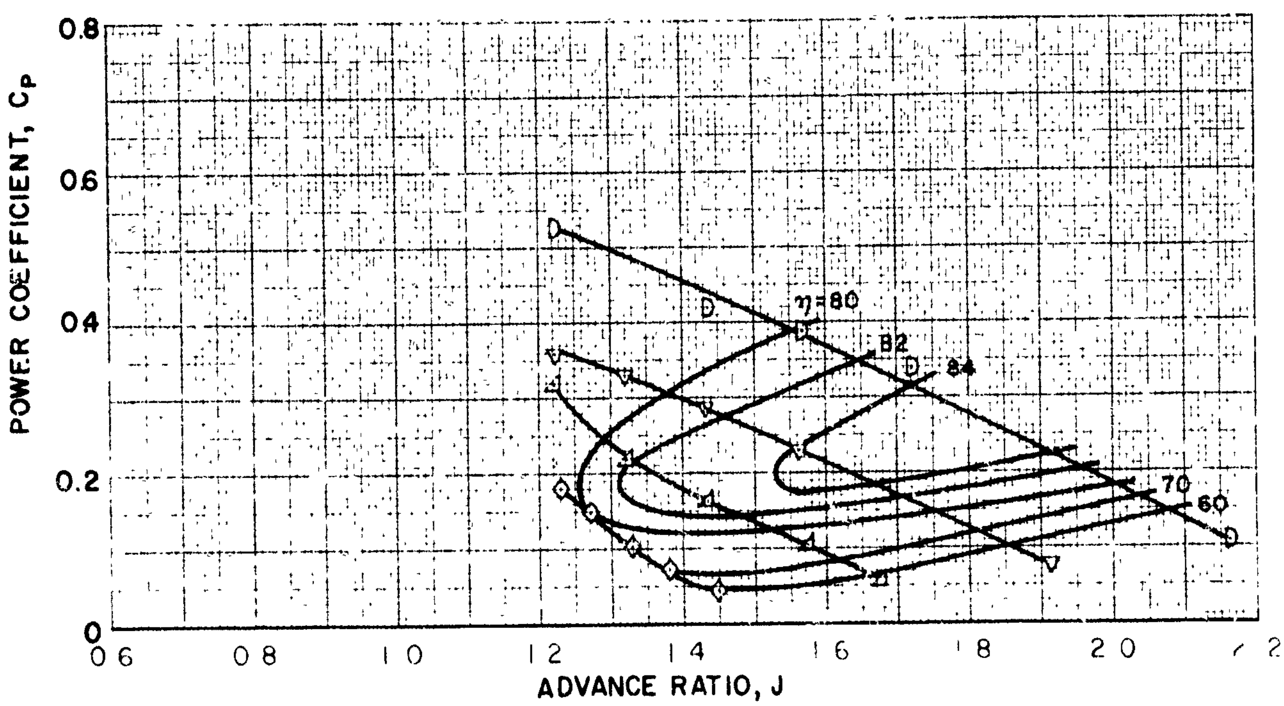

HSD SHROUDED PROPELLER TEST

EFFECT OF CHORD LENGTH ON SHROUDED PROPELLER PERFORMANCE

SYM	RUN NO.	MACH NO.	CONFIGURATION	$\theta_{3/4}$
▽	588	0.41	L_{ISC} C_{ISC} E_{ISC} B_3 P_{NT} T_1 R_1 R_E	38
◺	594	↓	↓	46
◁	596	↓	↓	50

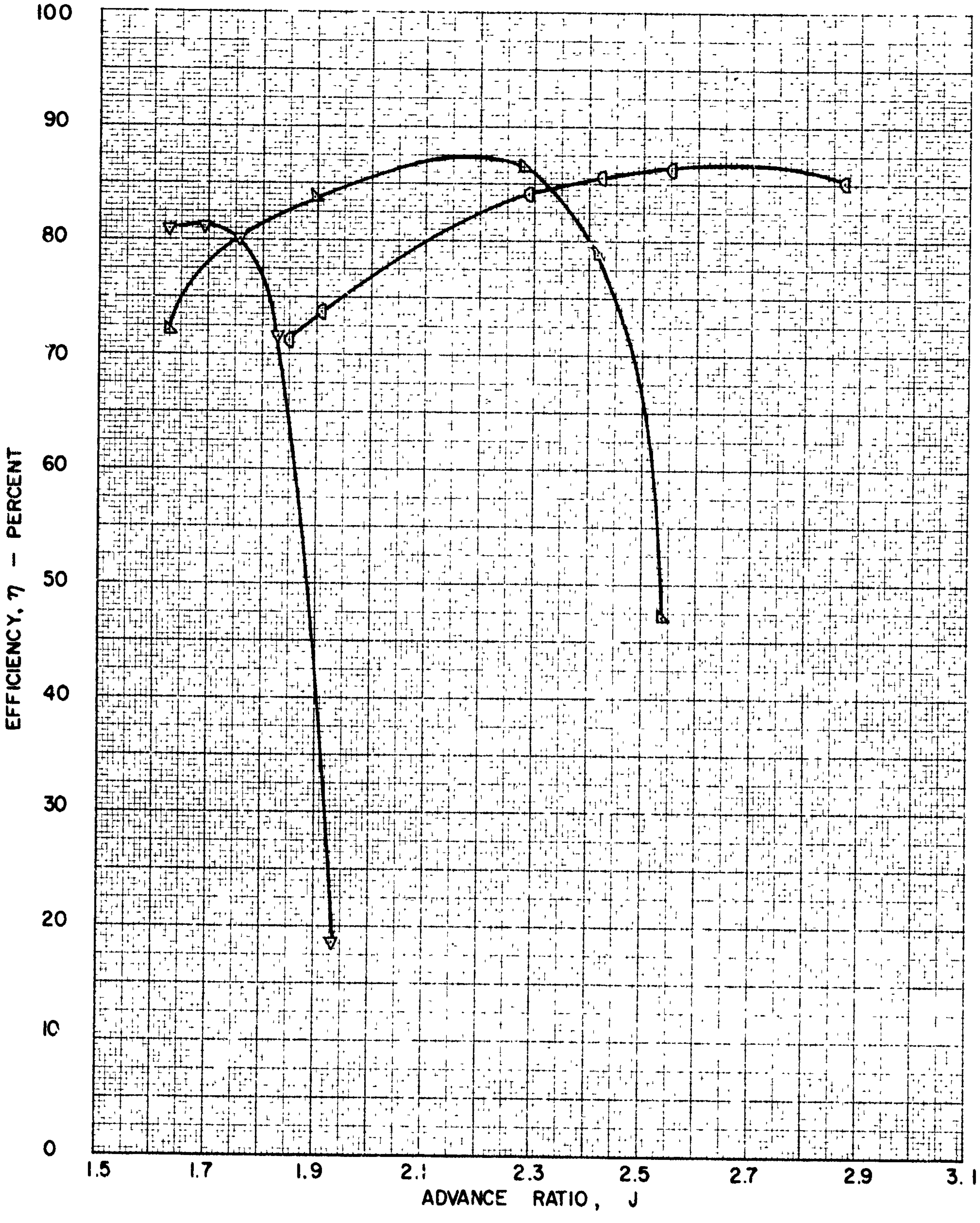

E330590-1

FIG. 126

HSD SHROUDED PROPELLER TEST

EFFECT OF CHORD LENGTH ON SHROUDED PROPELLER PERFORMANCE

SYM	RUN NO.	MACH NO.	CONFIGURATION	$\theta_{3/4}$
▽	588	0 41	$L_{1SC}\,C_{1SC}\,E_{1SC}\,B_3\,P_{NT}\,T_1\,R_1\,R_E$	38
◺	594			46
◖	596			50

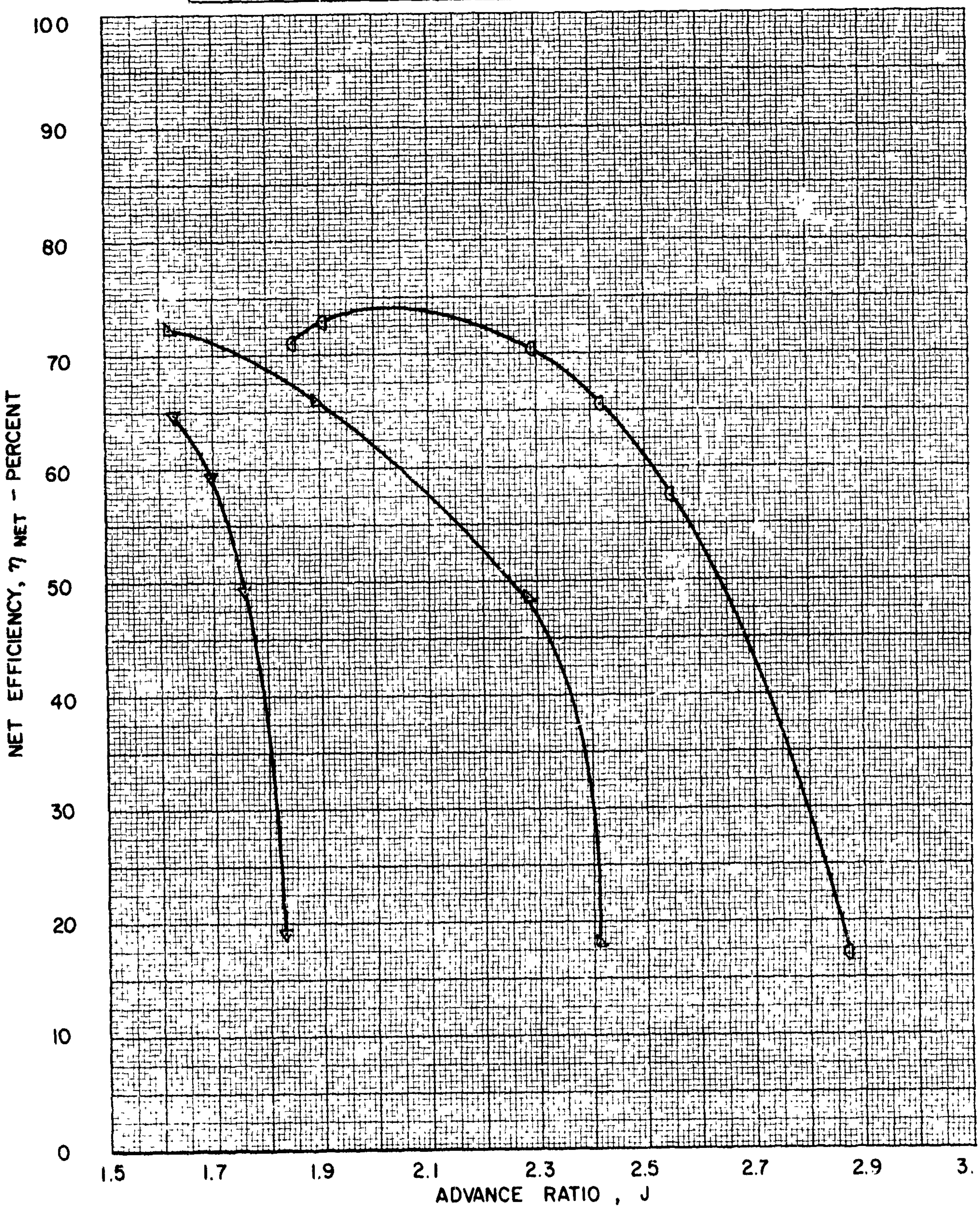

E330590-I FIG. 127

HSD SHROUDED PROPELLER TEST

EFFECT OF CHORD LENGTH ON SHROUDED PROPELLER PERFORMANCE

SYM	RUN NO.	MACH NO.	CONFIGURATION	θ 3/4
▽	588	0.41	$L_{1SC}\ C_{1SC}\ E_{1SC}\ B_3\ P_{NT}\ T_1\ R_1 R_E$	38
◺	594	↓	↓	46
◫	596	↓	↓	50

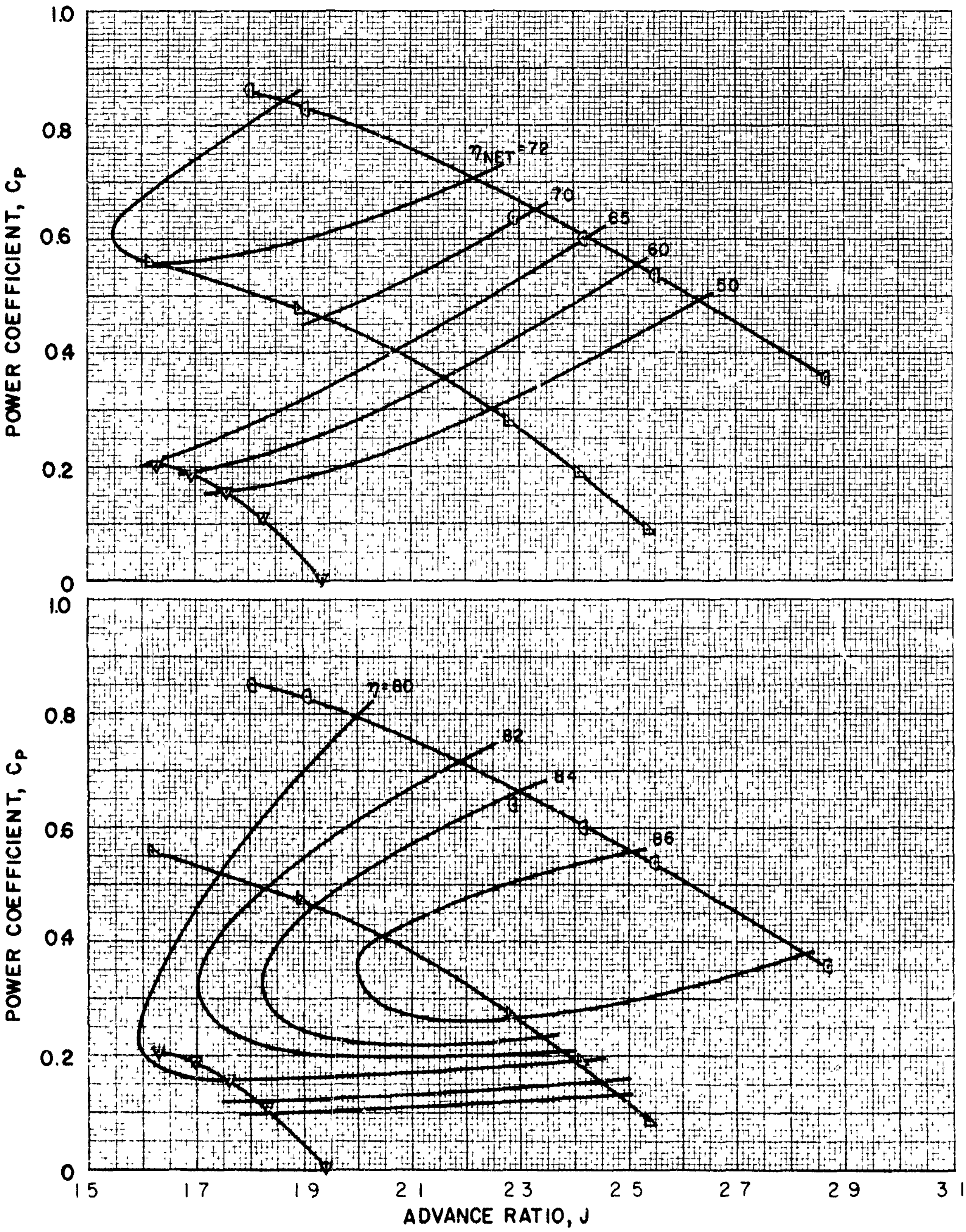

E330590-1

FIG.128

HSD SHROUDED PROPELLER TEST

EFFECT OF CHORD LENGTH ON SHROUDED PROPELLER PERFORMANCE

SYM	RUN NO.	MACH NO.	CONFIGURATION	$\beta_{3/4}$
△	595	0.52	$L_{1SC}\ C_{1SC}\ E_{1SC}\ B_3\ P_{WT} T_1\ R_1\ R_E$	46
◖	597	↓	↓	50
○	598	↓	↓	54

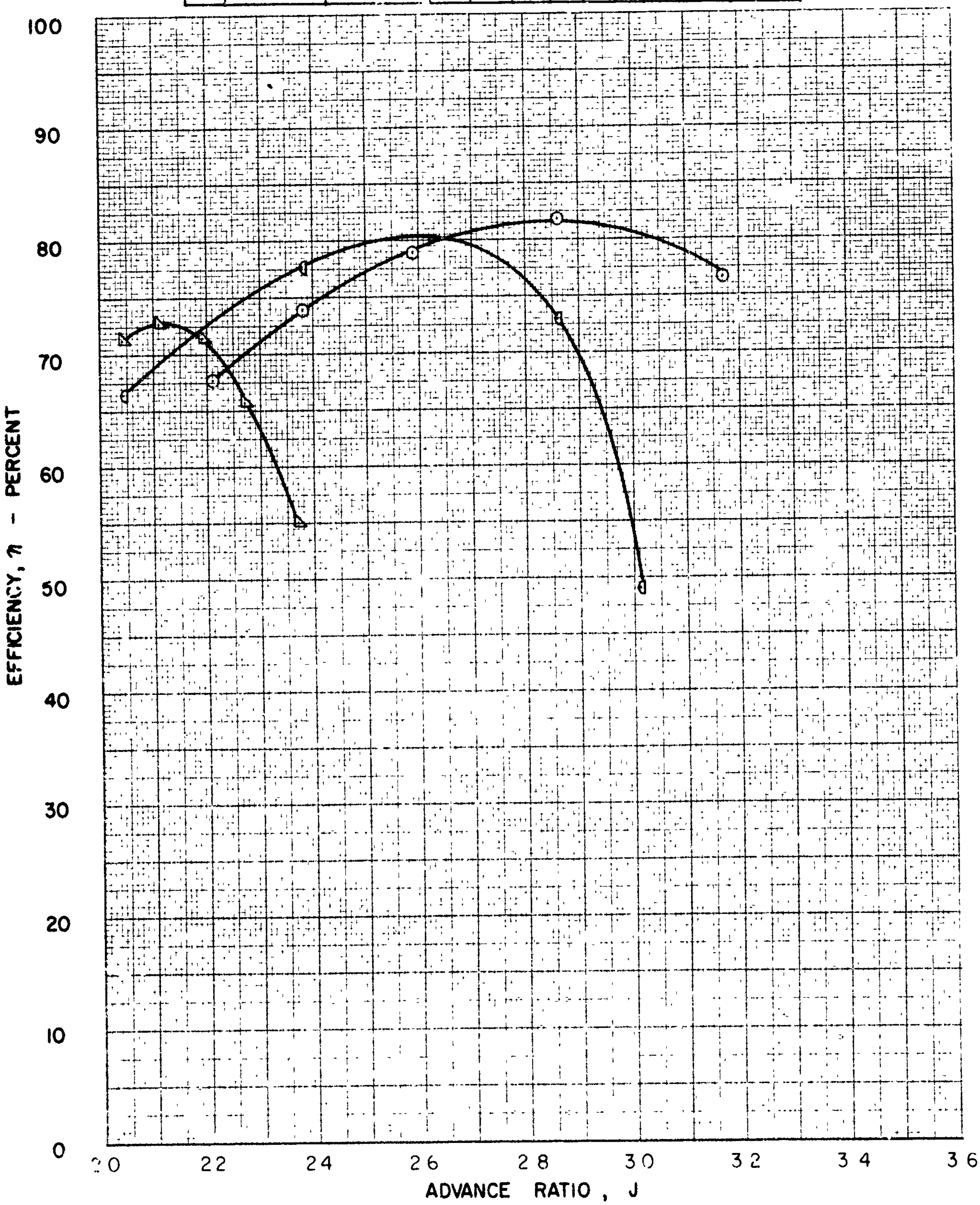

E330590-1

FIG. 129

HSD SHROUDED PROPELLER TEST

EFFECT OF CHORD LENGTH ON SHROUDED PROPELLER PERFORMANCE

SYM	RUN NO.	MACH NO.	CONFIGURATION	$\theta_{3/4}$
△	595	0.52	L_{ISC} C_{ISC} F_{ISC} B_3 P_{WT-1} R_1 R_E	46
◐	597	↓	↓	50
○	598	↓	↓	54

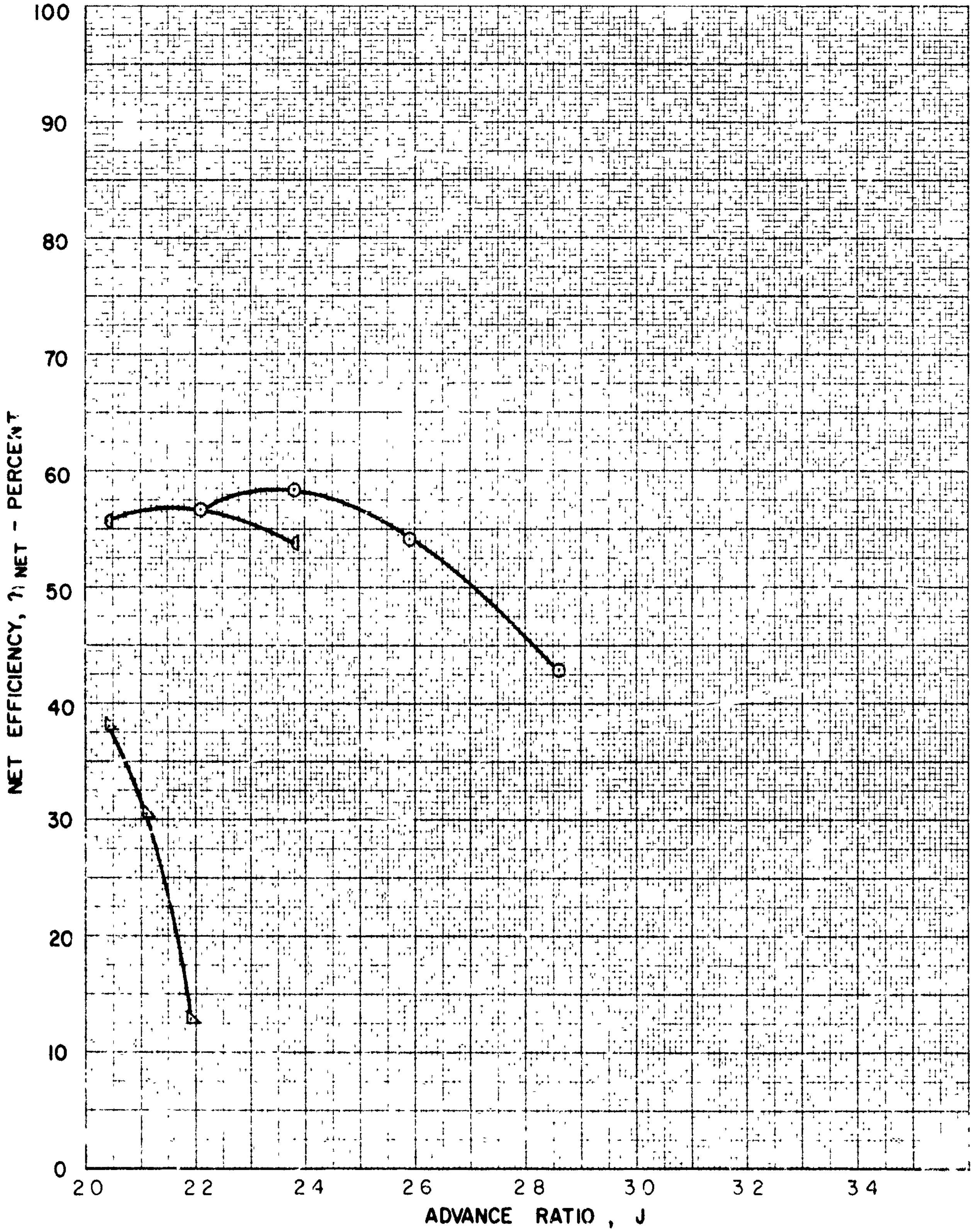

E330590-I FIG. 130

HSD SHROUDED PROPELLER TEST

EFFECT OF CHORD LENGTH ON SHROUDED PROPELLER PERFORMANCE

SYM	RUN NO.	MACH NO.	CONFIGURATION	$\theta_{3/4}$
△	595	0.52	L_{1SC} C_{1SC} E_{1SC} B_3 P_{WT} T_1 R_1 R_E	46
◻	597	↓	↓	50
○	598	↓	↓	54

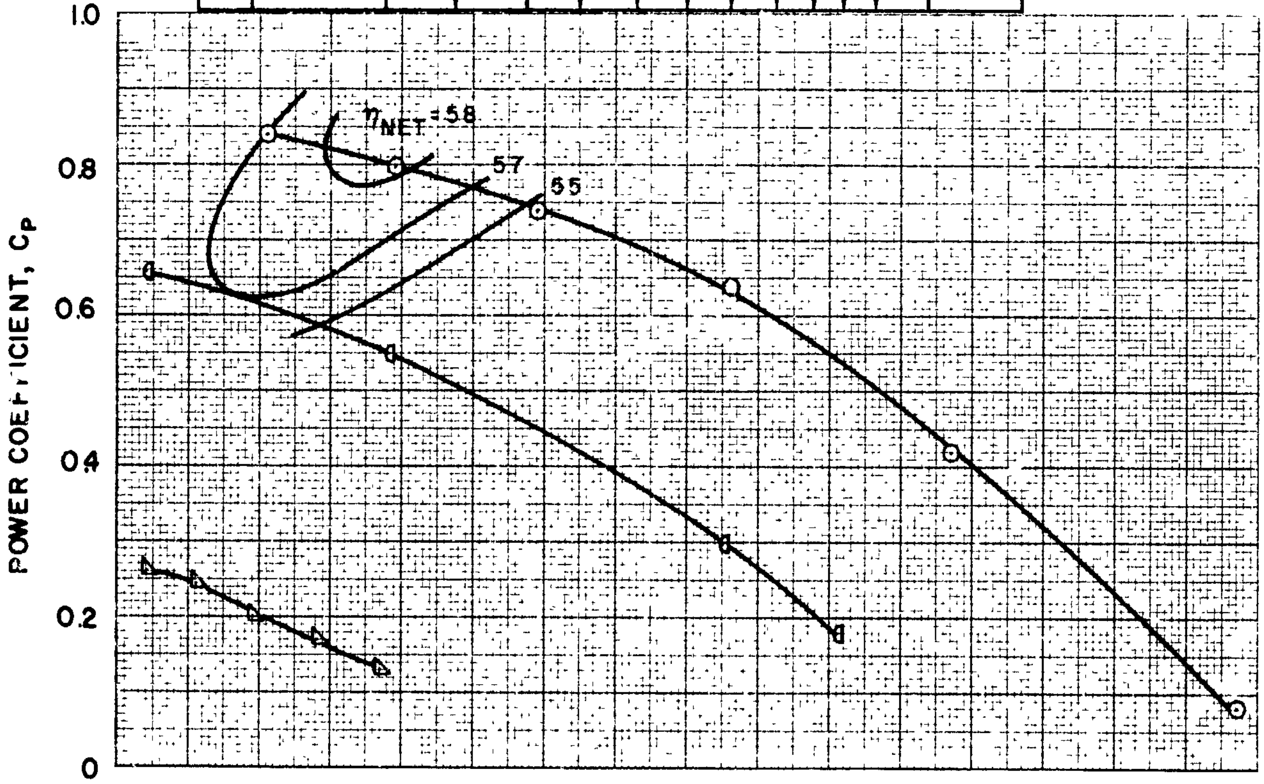

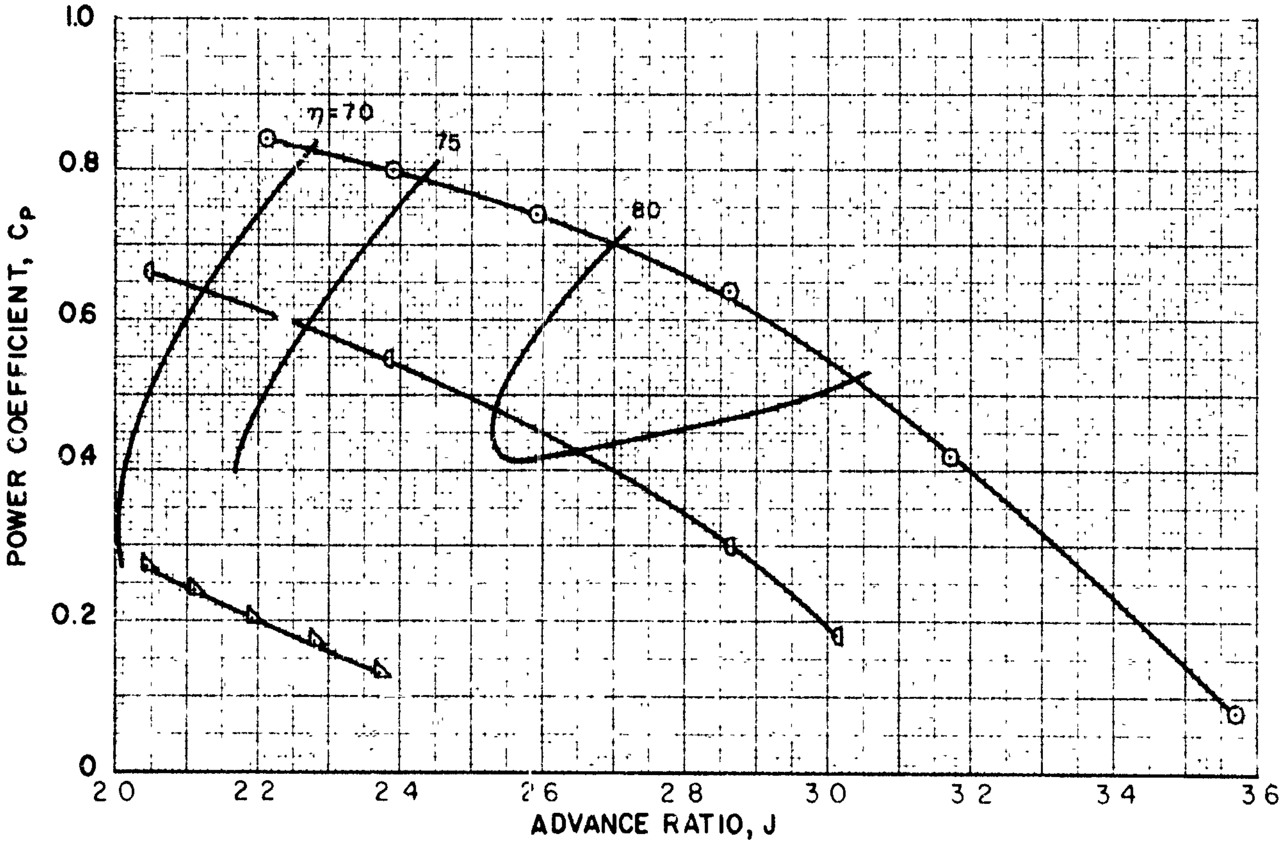

HSD SHROUDED PROPELLER TEST

EFFECT OF INLET VANES ON SHROUDED PROPELLER PERFORMANCE

SYM	RUN NO.	MACH NO.	CONFIGURATION	$\theta_{3/4}$
⊡	306	0.20	$L_1 C_1 E_1 B_3 P_{WT} T_1 R_1 R_E I^0$	25
⊿	305	↓	↓	35
▽	723	0.30	↓	38
D	729	↓	↓	42

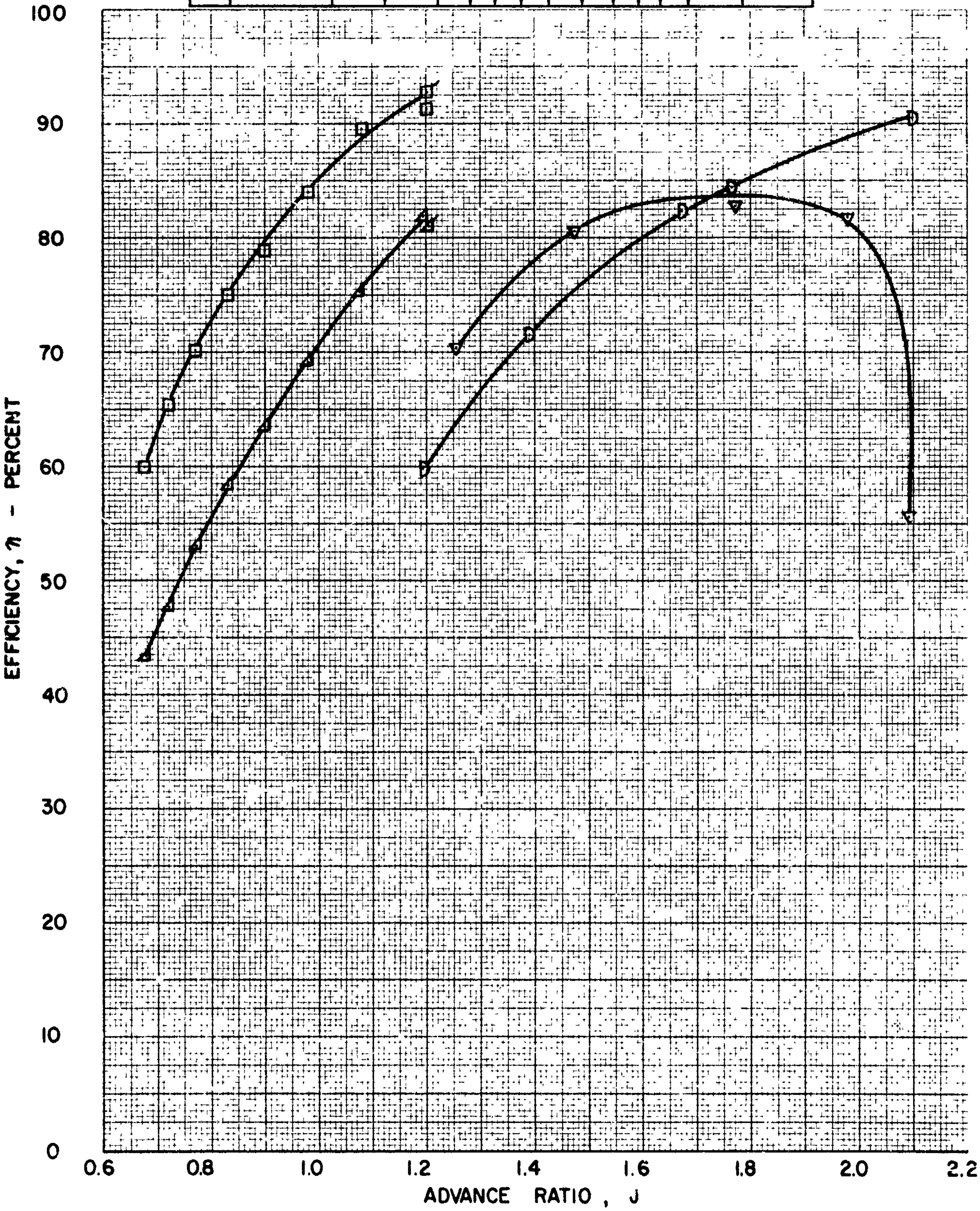

E330590-1

FIG.132

HSD SHROUDED PROPELLER TEST

EFFECT OF INLET VANES ON SHROUDED PROPELLER PERFORMANCE

SYM	RUN NO.	MACH NO.	CONFIGURATION	$\theta_{3/4}$
⊡	306	0.20	$L_1 C_1 E_1 B_3 P_{WT} T_1 R_1 R_E I^0$	25
⊿	305	↓	↓	35
▽	723	0.30	↓	38
D	729	↓	↓	42

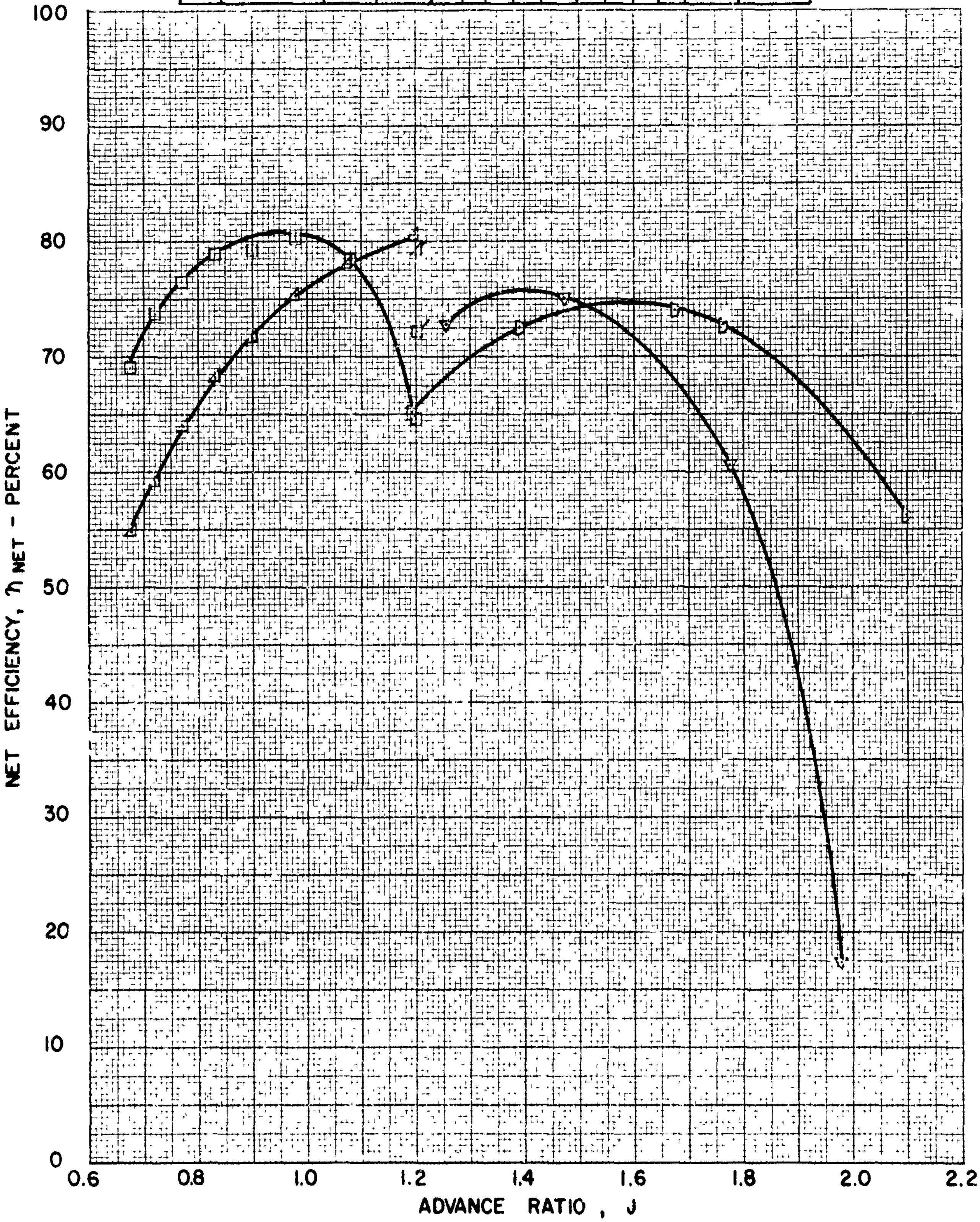

HSD SHROUDED PROPELLER TEST

EFFECT OF INLET VANES ON SHROUDED PROPELLER PERFORMANCE

SYM	RUN NO.	MACH NO.	CONFIGURATION	$\theta_{3/4}$
□	306	0.20	$L_1 C_1 E_1 B_3 P_{WT} T_1 R_1 R_E I^0$	25
◿	305	↓		35
▽	723	0.30		38
D	729	↓	↓ ↓ ↓ ↓ ↓ ↓ ↓ ↓ ↓	42

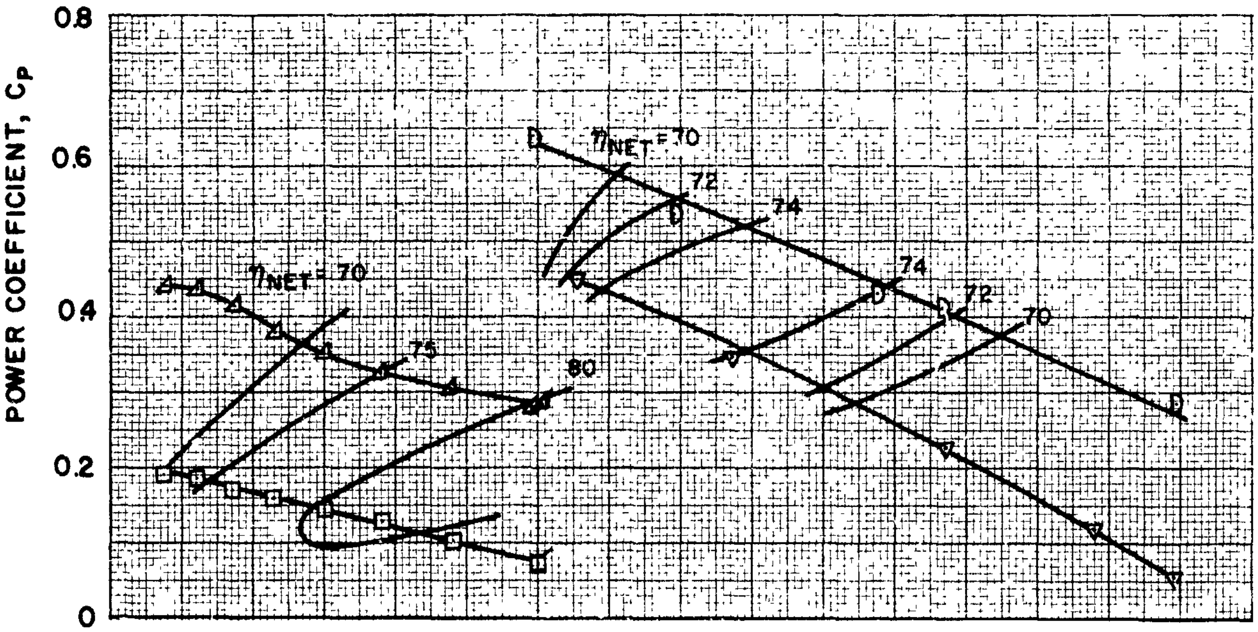

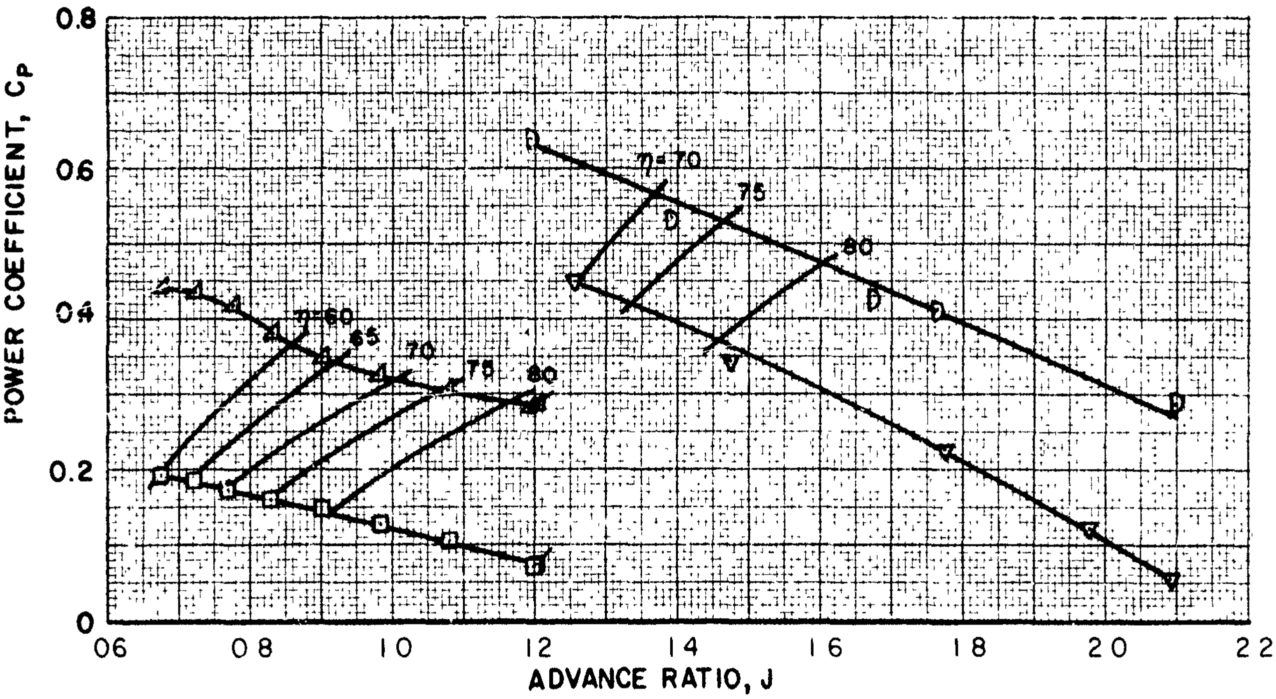

HSD SHROUDED PROPELLER TEST

EFFECT OF INLET VANES ON SHROUDED PROPELLER PERFORMANCE

SYM	RUN NO.	MACH NO.	CONFIGURATION	$\theta_{3/4}$
D	501	0.40	$L_1 C_1 E_1 B_3 P_{WT} T_1 R_1 R_E I^0$	42
△	502	↓	↓	46
C	504	0.50	↓	50
O	728	↓	↓	54

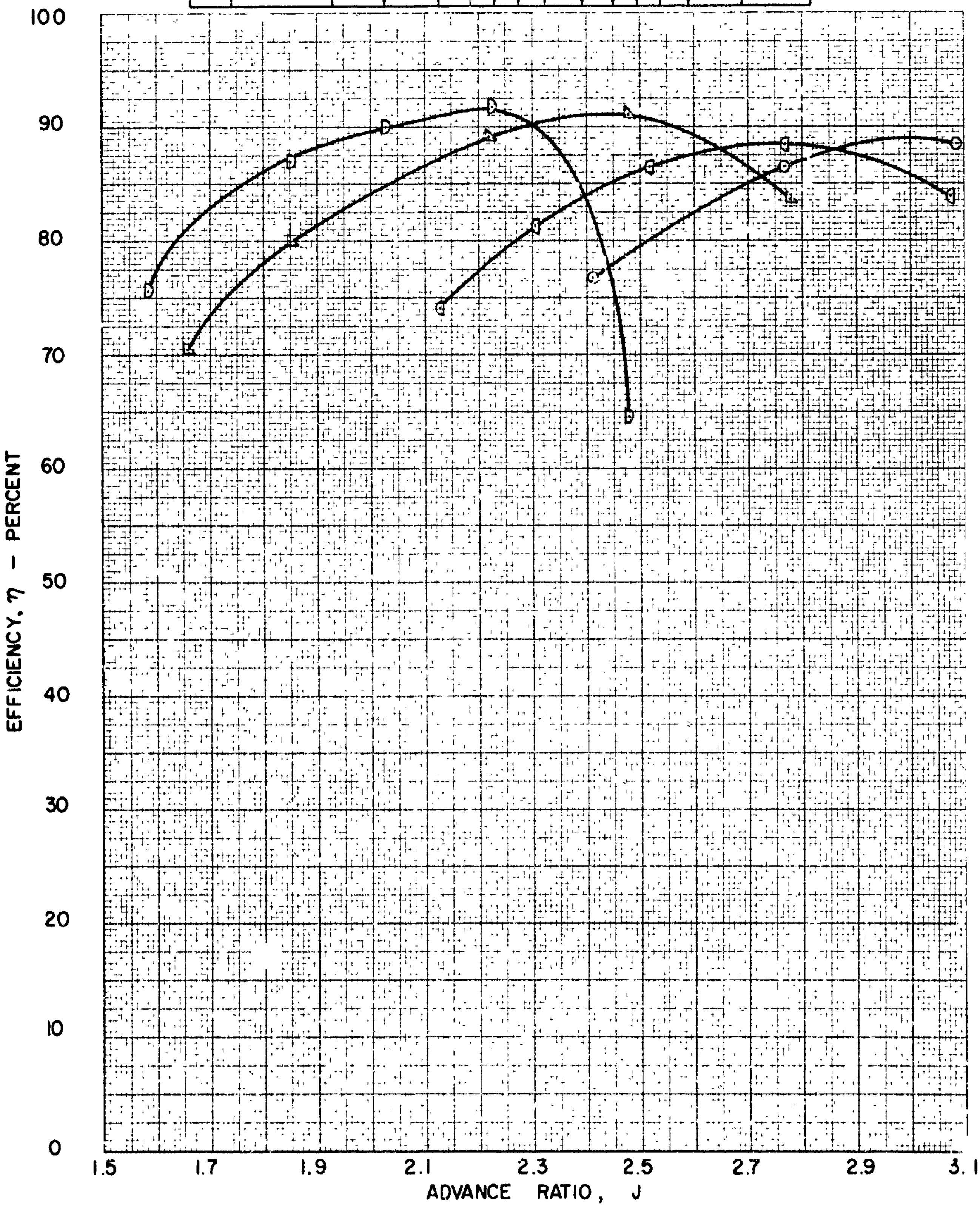

FIG.135

E330590-1

HSD SHROUDED PROPELLER TEST

EFFECT OF INLET VANES ON SHROUDED PROPELLER PERFORMANCE

SYM	RUN NO.	MACH NO.	CONFIGURATION	$\theta_{3/4}$
D	501	0.40	$L_1 C_1 E_1 B_3 P_{WT} T_1 R_1 R_E I^0$	42
◺	502	↓	↓	46
C	504	0.50	↓	50
O	728	↓	↓	54

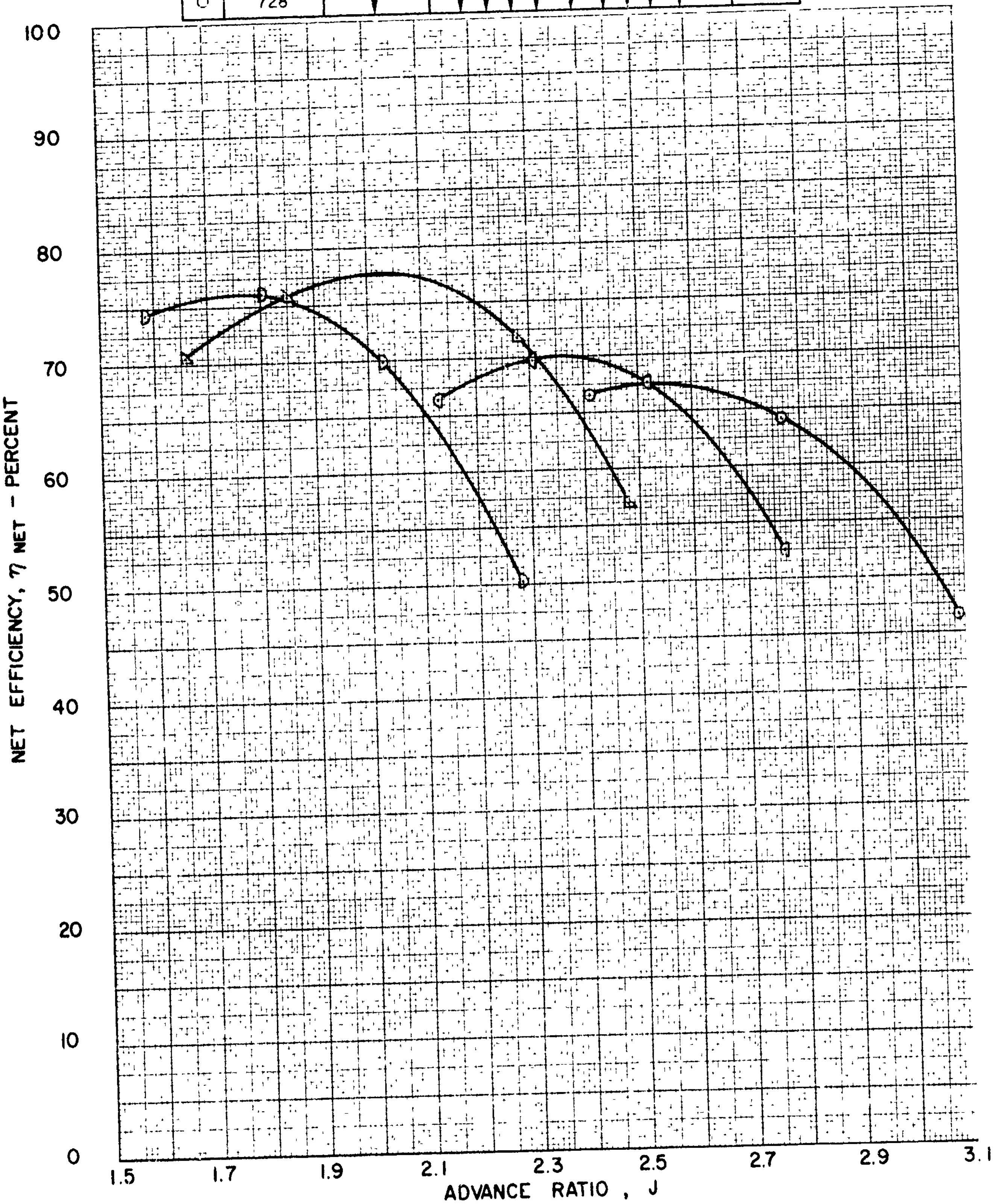

E330590-1 FIG. 136

HSD SHROUDED PROPELLER TEST

EFFECT OF INLET VANES ON SHROUDED PROPELLER PERFORMANCE

SYM	RUN NO.	MACH NO.	CONFIGURATION	$\theta_{3/4}$
D	501	0.40	$L_1C_1E_1B_3P_{WT}T_1R_1R_EI^0$	42
◺	502	↓		46
◖	504	0.50		50
O	728	↓	↓	54

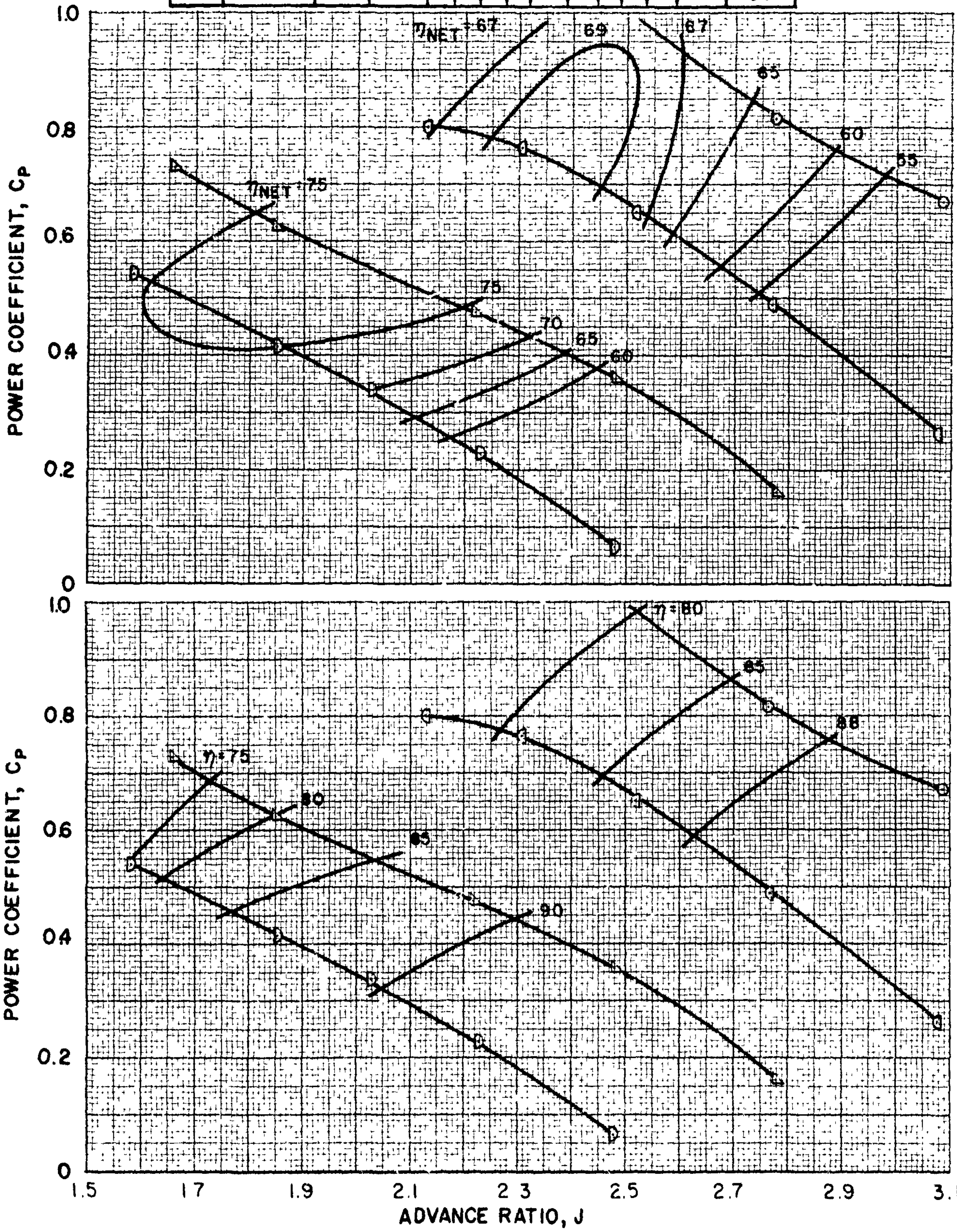

HSD SHROUDED PROPELLER TEST

EFFECT OF INLET VANE ANGLE ON SHROUDED PROPELLER PERFORMANCE

SYM	RUN NO.	MACH NO.	CONFIGURATION	$\theta_{3/4}$
○	314, 312	0.05	$L_1 C_1 E_1 B_3 P_{WT} T_1 R_1 R_E I^{-10}$	25, 35
△	307, 304	↓	↓ I^{0}	↓
□	308, 311	↓	↓ I^{10}	↓

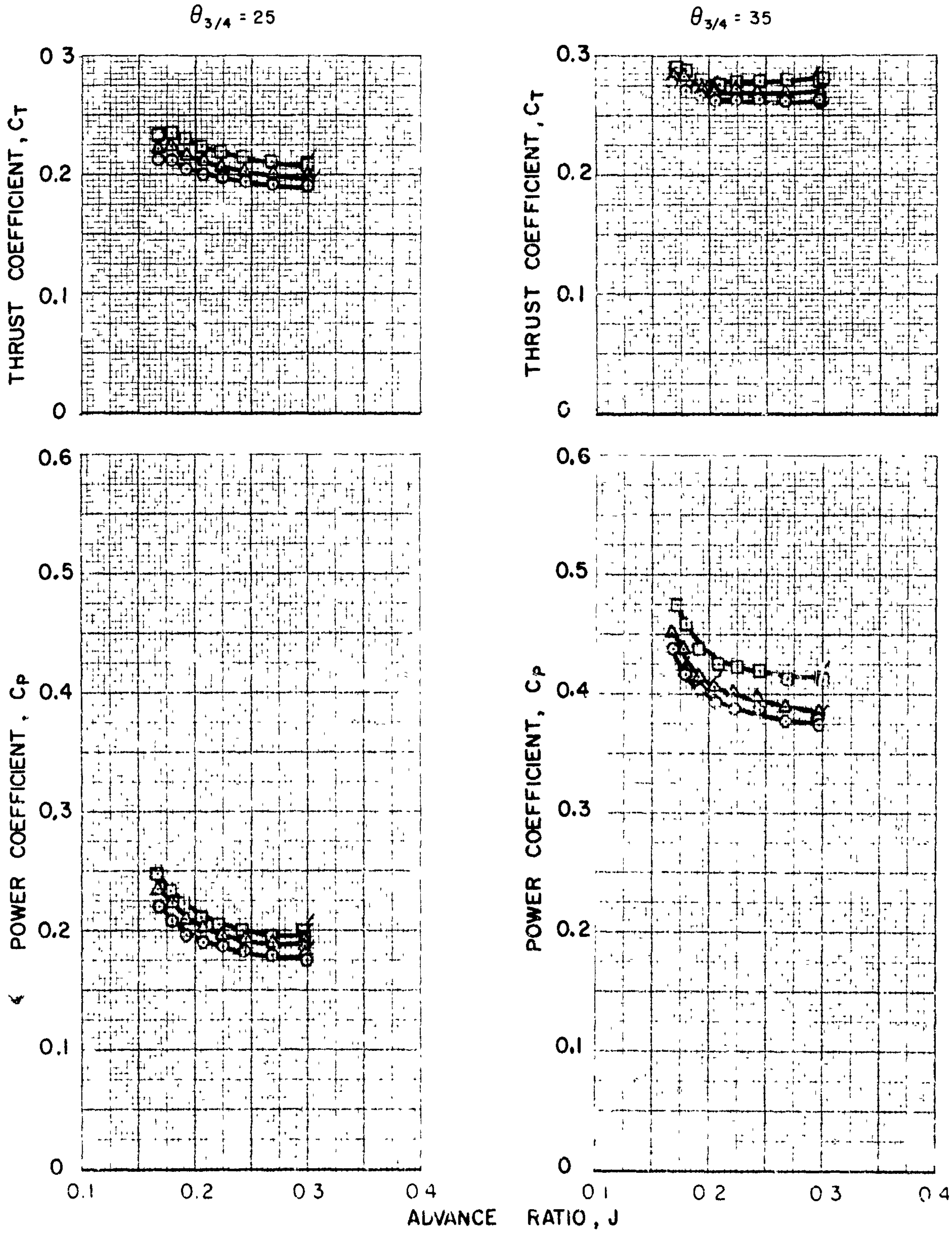

HSD SHROUDED PROPELLER TEST

EFFECT OF INLET VANE ANGLE ON SHROUDED PROPELLER PERFORMANCE

SYM	RUN NO.	MACH NO.	CONFIGURATION	$\theta_{3/4}$
○	314, 312	0.05	$L_1 C_1 E_1 B_3 P_{WT} T_1 R_1 R_E\ I^{-10}$	25, 35
△	307, 304	↓	I^{0}	↓
□	308, 311	↓	I^{10}	↓

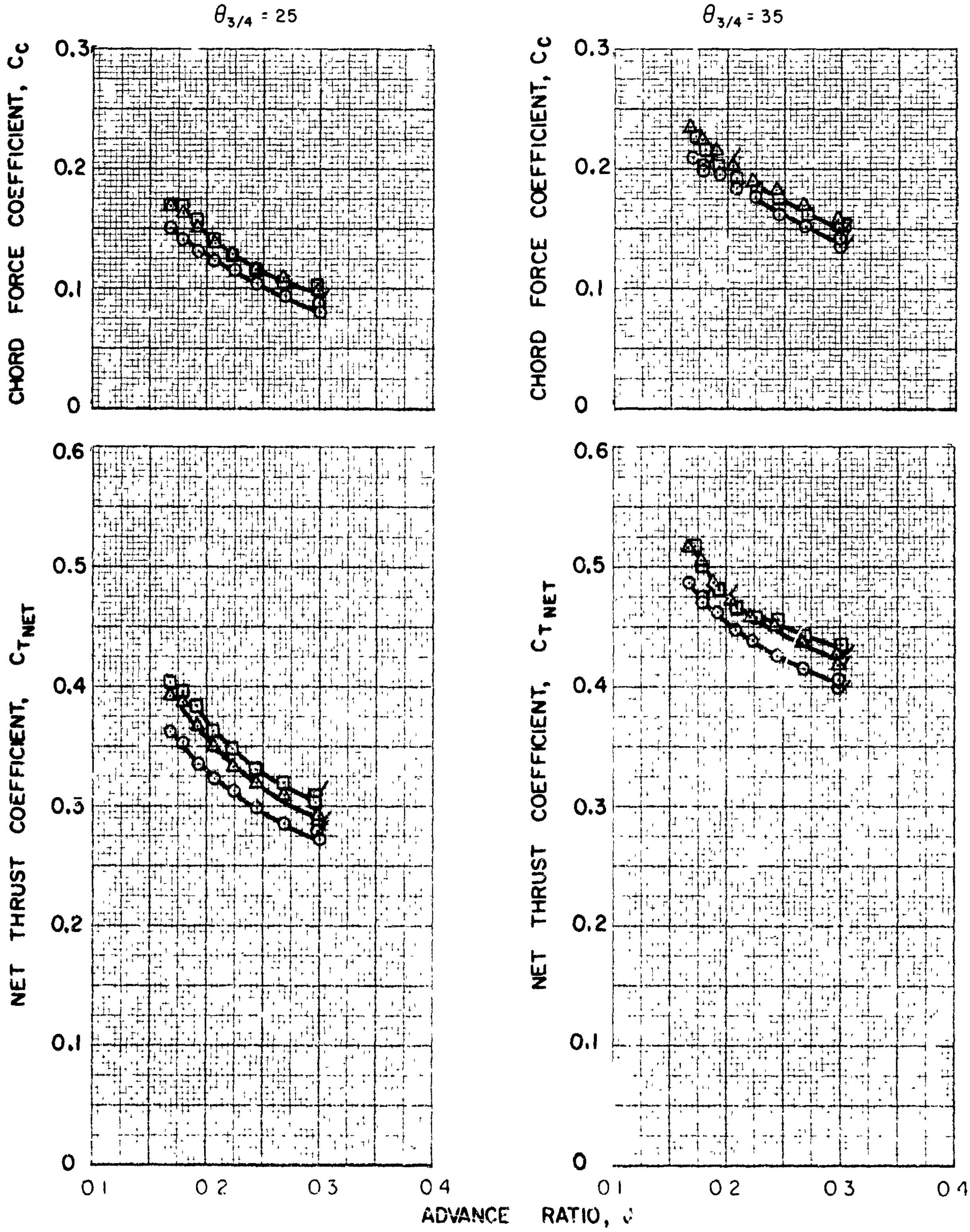

E330590-I

FIG. 139

HSD SHROUDED PROPELLER TEST

EFFECT OF INLET VANE ANGLE ON SHROUDED PROPELLER PERFORMANCE

SYM	RUN NO.	MACH NO.	CONFIGURATION	$\theta_{3/4}$
⊙	315	0.20	$L_1 C_1 E_1 B_3 P_{WT} T_1 R_1 R_E I^{-10}$	25
△	306	↓	↓ I^{0}	↓
⊡	309	↓	↓ I^{10}	↓

NOTE η - OPEN SYMBOLS C_P - SOLID SYMBOLS

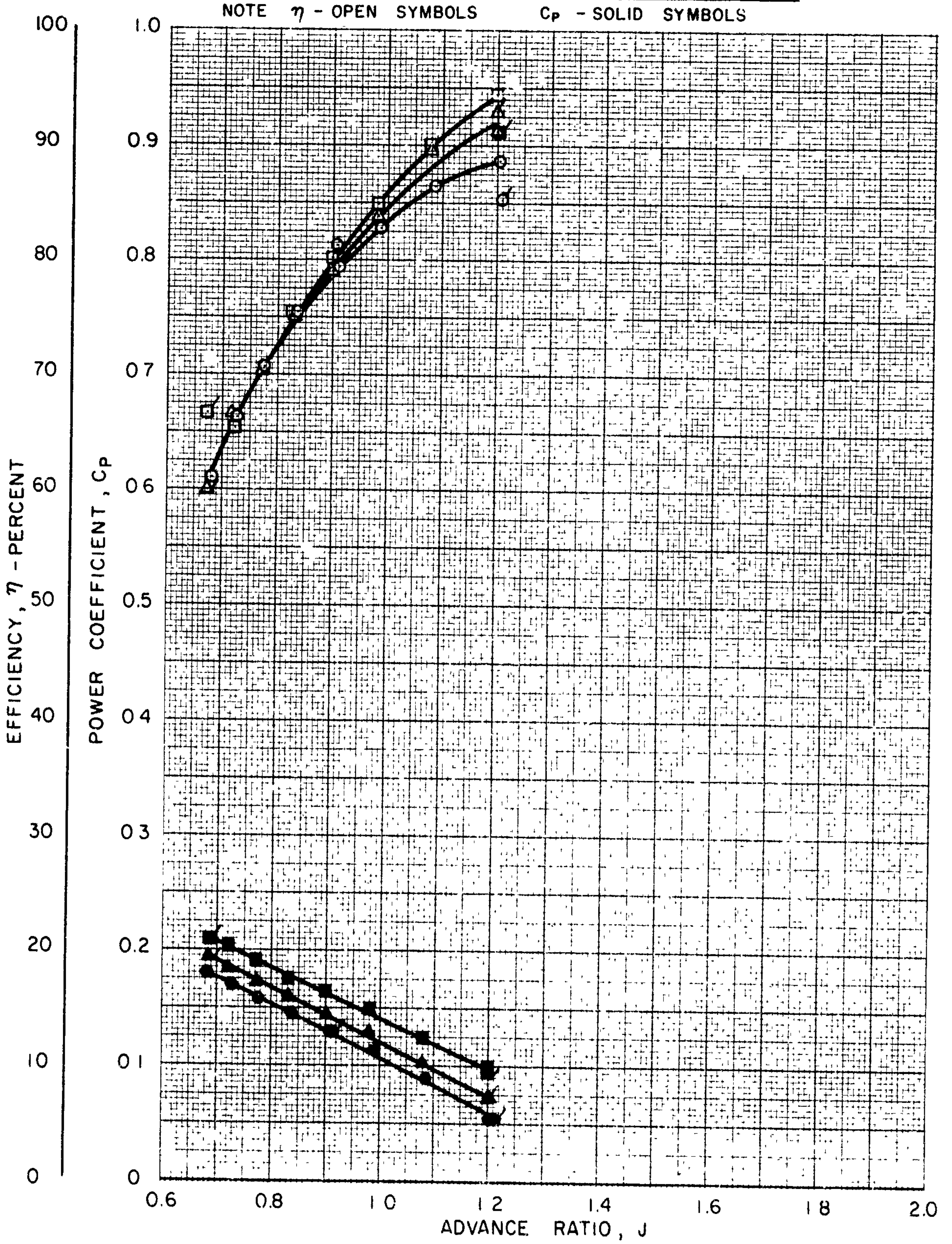

E330590-I FIG. 140

HSD SHROUDED PROPELLER TEST

EFFECT OF INLET VANE ANGLE ON SHROUDED PROPELLER PERFORMANCE

SYM	RUN NO.	MACH NO.	CONFIGURATION	$\theta_{.75}$
⊙	315	0.20	$L_1\ C_1\ E_1\ B_3\ P_{WT}\ T_1\ R_1\ R_E\ I^{-10}$	25
△	306	↓	↓ ↓ ↓ ↓ ↓ ↓ ↓ ↓ I^{0}	↓
⊡	309	↓	↓ ↓ ↓ ↓ ↓ ↓ ↓ ↓ I^{10}	↓

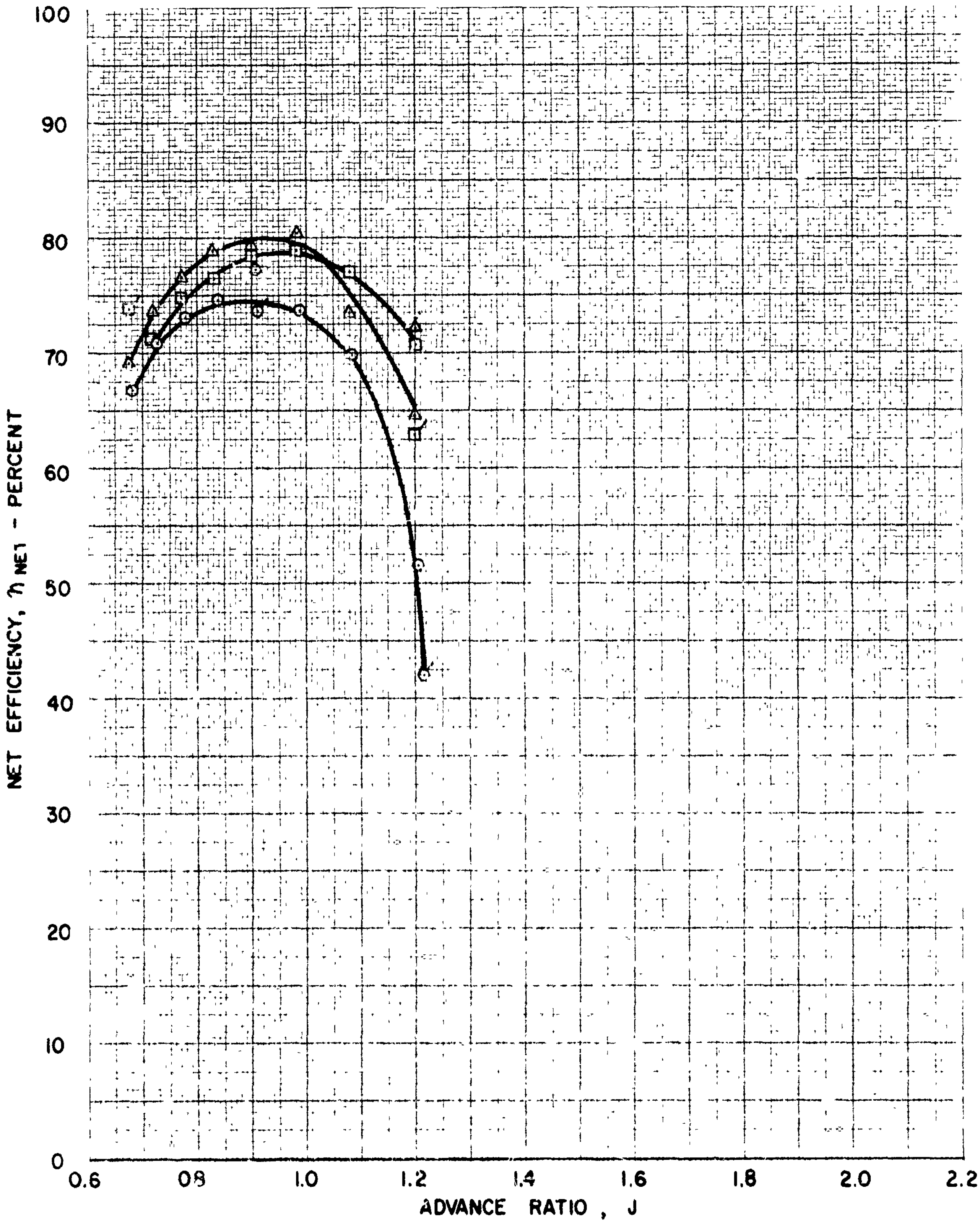

E330590-I

FIG.141

HSD SHROUDED PROPELLER TEST

EFFECT OF INLET VANE ANGLE ON SHROUDED PROPELLER PERFORMANCE

SYM	RUN NO.	MACH NO.	CONFIGURATION	$\theta_{3/4}$
○	313	0.20	$L_1 C_1 E_1 B_3 P_{WT} T_1 R_1 R_E I^{-10}$	35
△	305	↓	↓ I^{0}	↓
⊡	310	↓	↓ I^{10}	↓

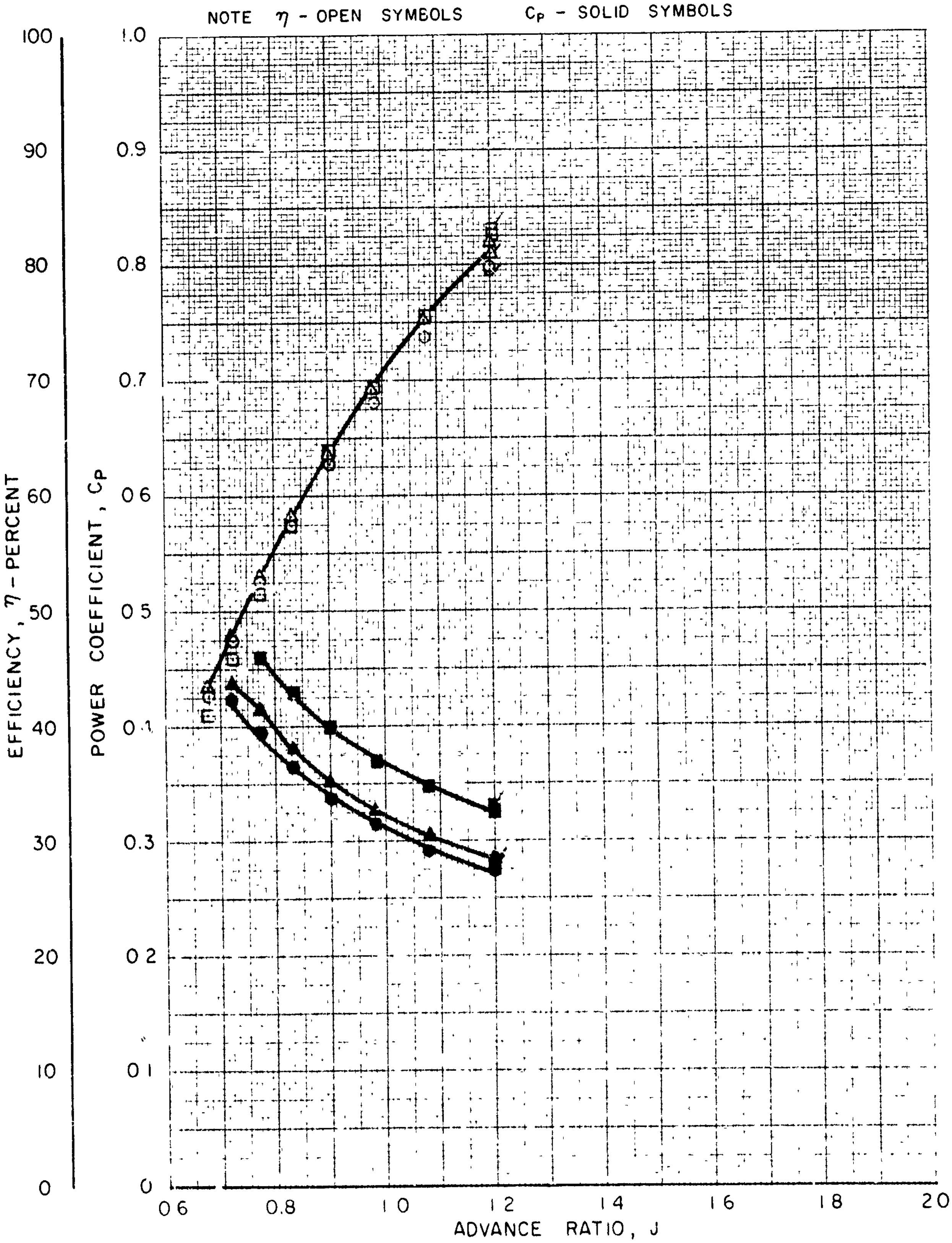

E330590-I

FIG. 142

HSD SHROUDED PROPELLER TEST

EFFECT OF INLET VANE ANGLE ON SHROUDED PROPELLER PERFORMANCE

SYM	RUN NO.	MACH NO.	CONFIGURATION	$\theta_{3/4}$
○	313	0.20	$L_1 C_1 E_1 B_3 P_{WT} T_1 R_1 R_E I^{-10}$	35
△	305	↓	↓ I^{0}	↓
□	310	↓	↓ I^{10}	↓

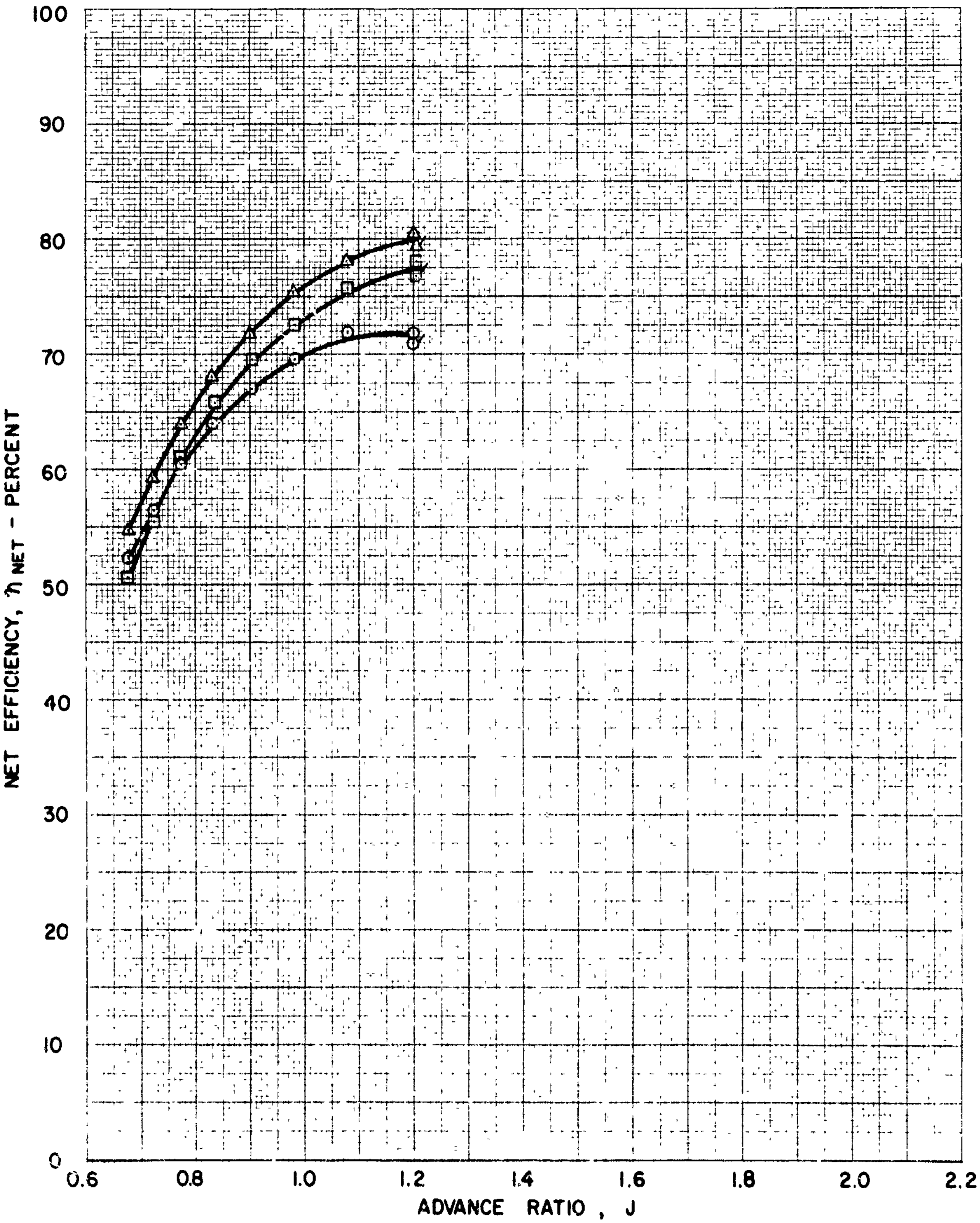

E330590-1

FIG.143

HSD SHROUDED PROPELLER TEST

EFFECT OF EXIT VANES ON SHROUDED PROPELLER PERFORMANCE

SYM	RUN NO.	MACH NO.	CONFIGURATION	$\theta_{3/4}$
□	293	0.20	$L_1 C_1 E_1 B_3 P_{WT} T_1 R_1 R_E V^0$	25
△	292	↓	↓ ↓ ↓ ↓ ↓ ↓ ↓ ↓ ↓	35

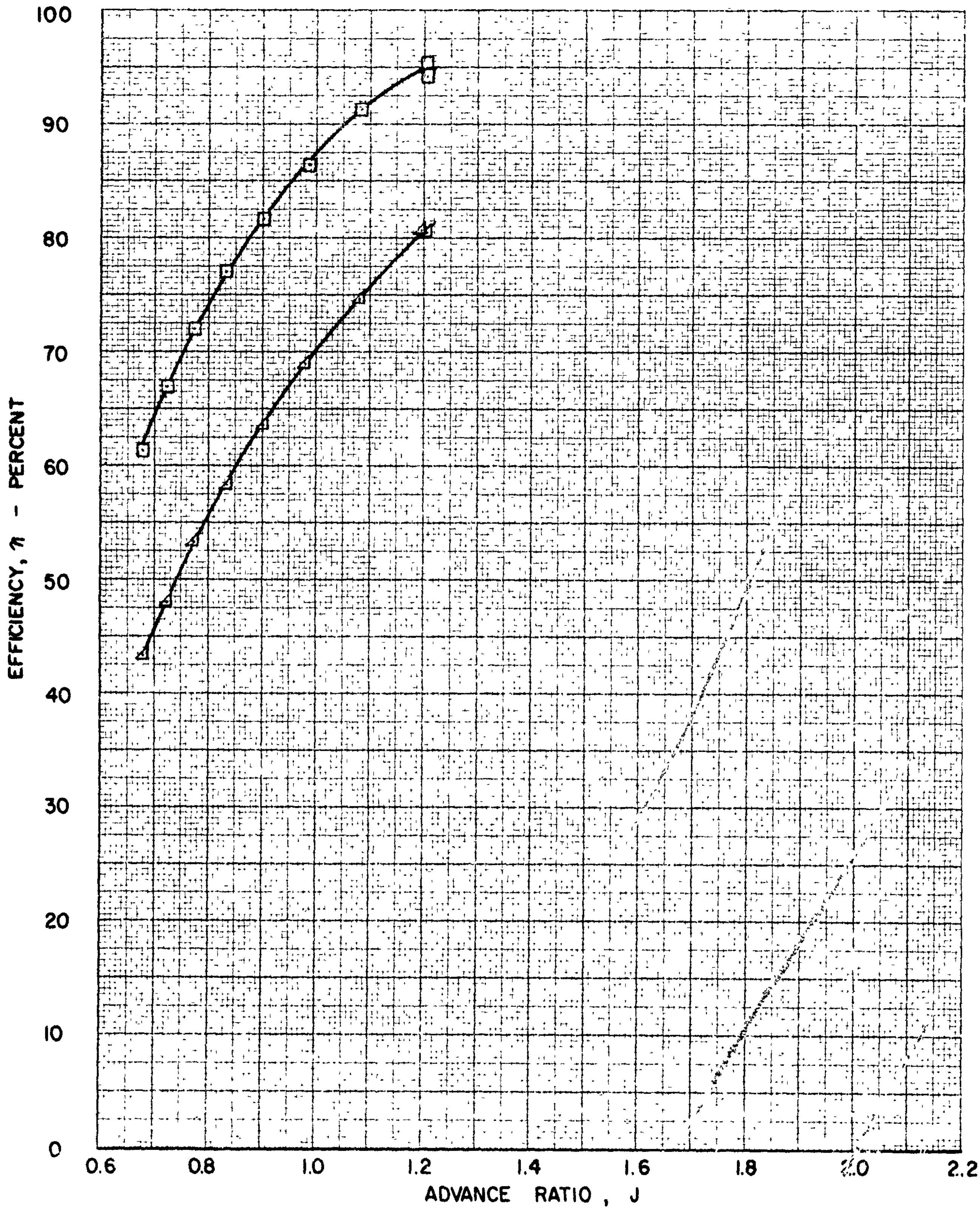

HSD SHROUDED PROPELLER TEST

EFFECT OF EXIT VANES ON SHROUDED PROPELLER PERFORMANCE

SYM	RUN NO.	MACH NO.	CONFIGURATION	$\theta_{3/4}$
⊡	293	0.20	$L_1 C_1 E_1 B_3 P_{WT} T_1 R_1 R_E V^0$	25
△	292	↓	↓ ↓ ↓ ↓ ↓ ↓ ↓ ↓ ↓	35

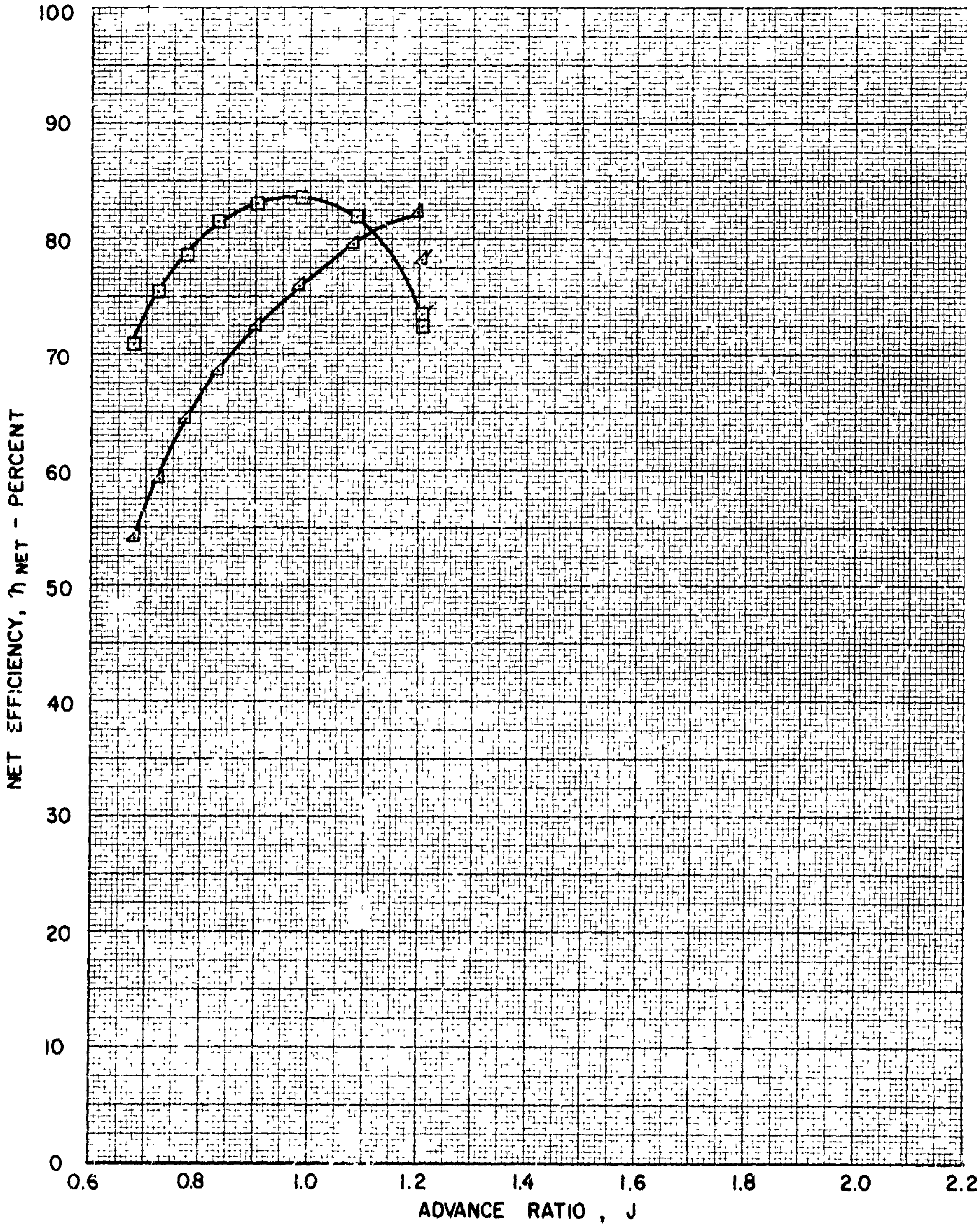

HSD SHROUDED PROPELLER TEST

EFFECT OF EXIT VANES ON SHROUDED PROPELLER PERFORMANCE

SYM	RUN NO.	MACH NO.	CONFIGURATION	$\beta_{3/4}$
⊡	293	0.20	$L_1 C_1 E_1 B_3 P_{WT} T_1 R_1 R_E V^0$	25
⊿	292	↓	↓ ↓ ↓ ↓ ↓ ↓ ↓ ↓ ↓	35

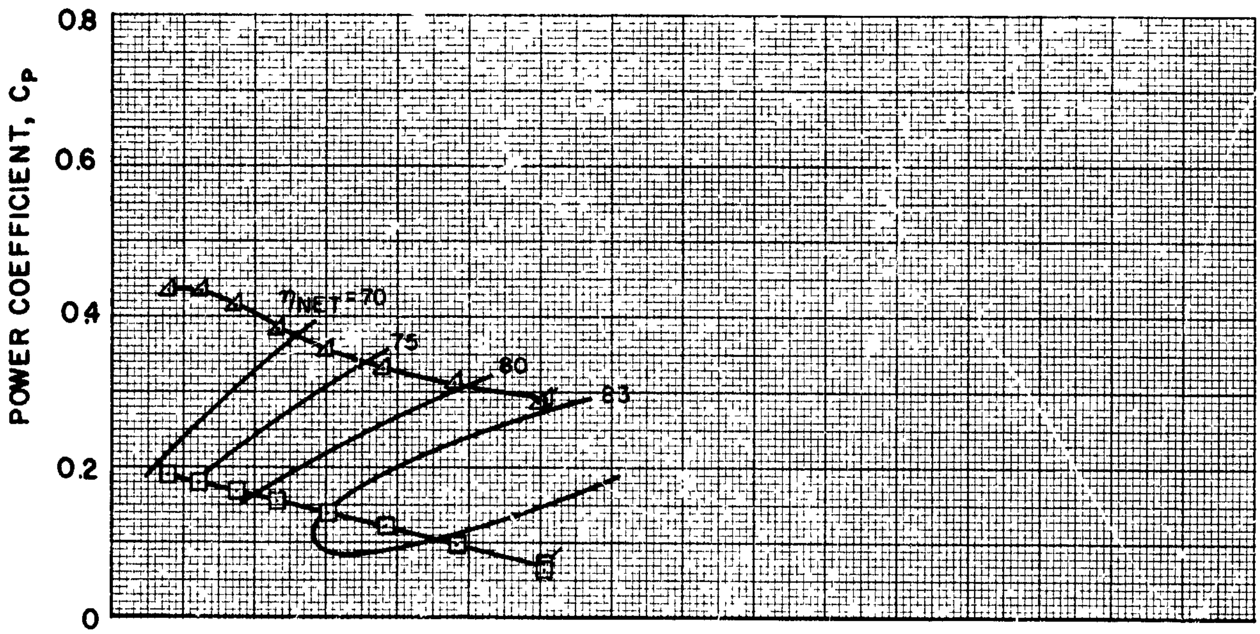

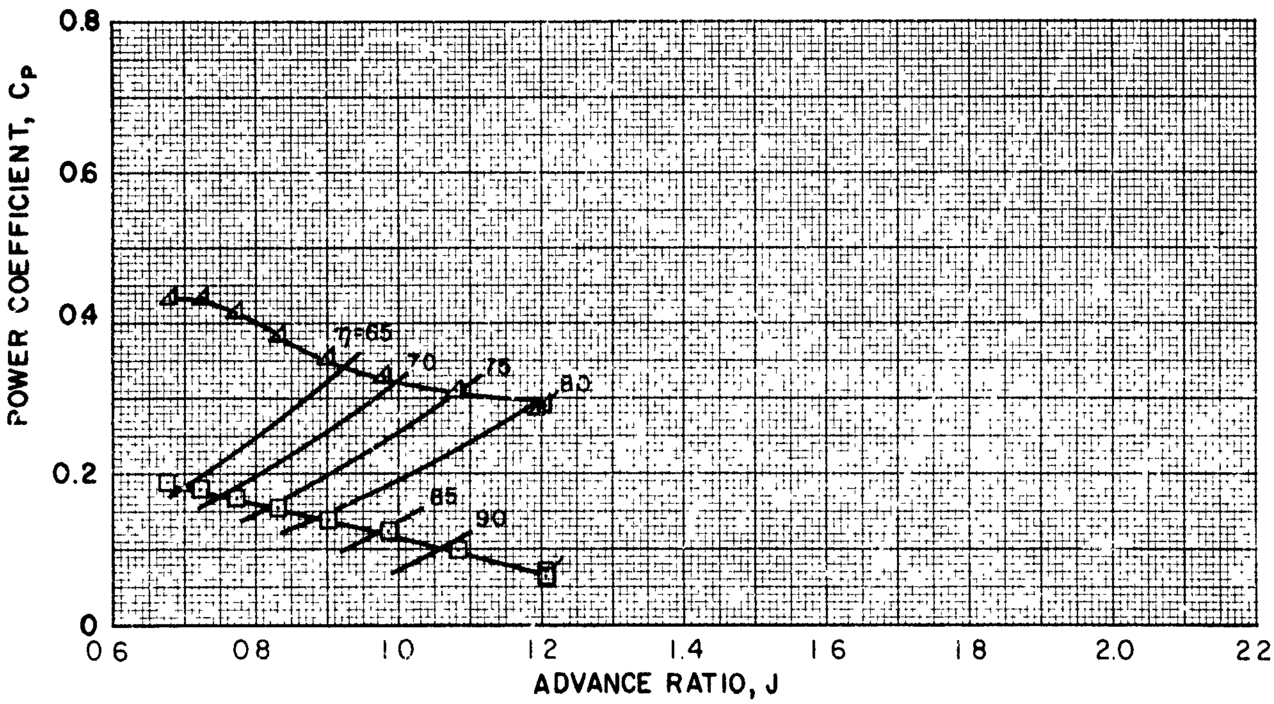

HSD SHROUDED PROPELLER TEST

EFFECT OF EXIT VANES ON SHROUDED PROPELLER PERFORMANCE

SYM	RUN NO.	MACH NO.	CONFIGURATION	$\theta_{3/4}$
D	506	0.40	$L_1\ C_1\ E_1\ B_3\ P_{WT}\ T_1\ R_1\ R_E\ V^0$	42
◬	507	↓	↓ ↓ ↓ ↓ ↓ ↓ ↓ ↓ ↓	46

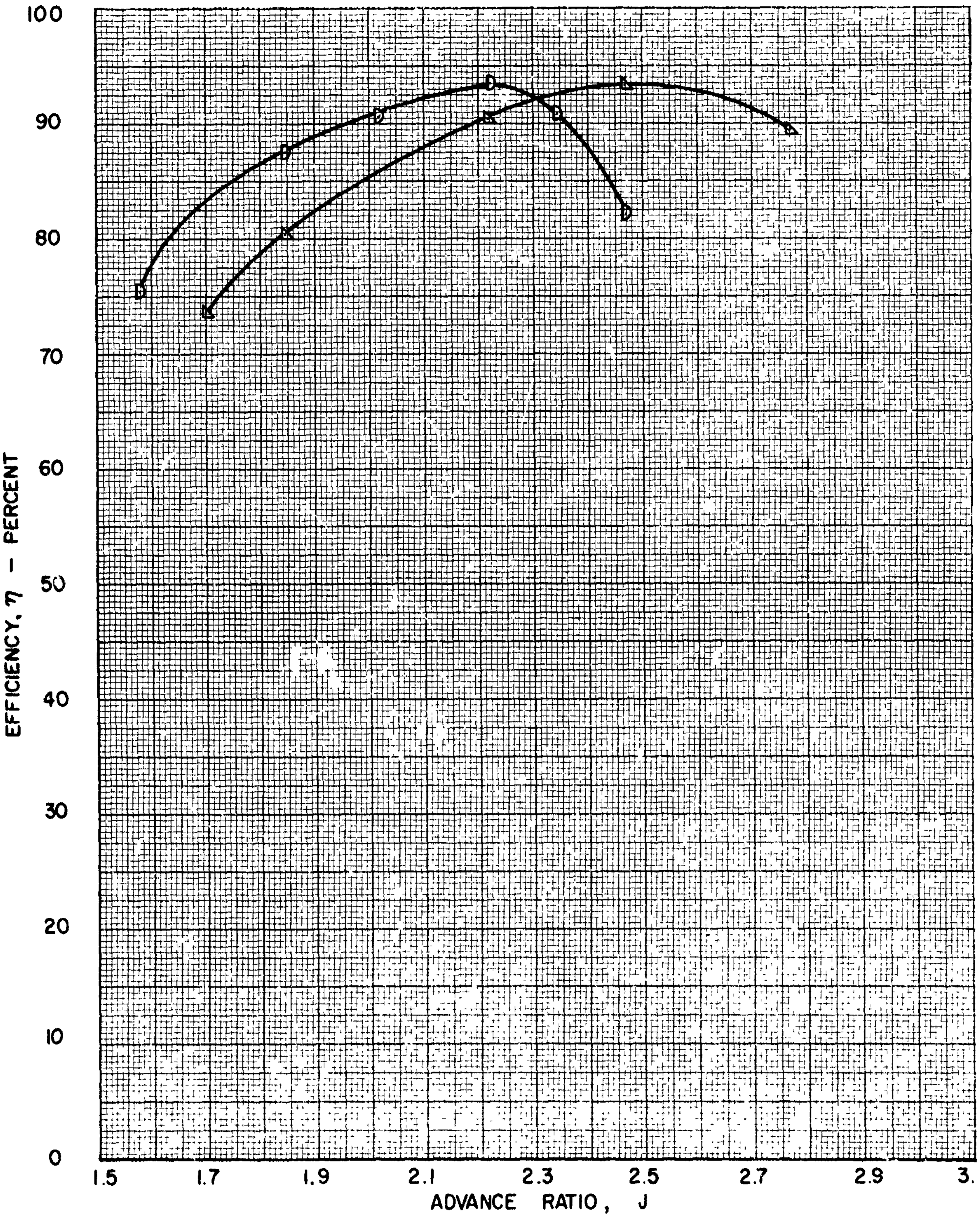

HSD SHROUDED PROPELLER TEST

EFFECT OF EXIT VANES ON SHROUDED PROPELLER PERFORMANCE

SYM	RUN NO.	MACH NO.	CONFIGURATION	$\theta_{3/4}$
D	506	0.40	$L_1 C_1 E_1 B_3 P_{WT} T_1 R_1 R_E V^0$	42
◺	507	↓	↓ ↓ ↓ ↓ ↓ ↓ ↓ ↓ ↓	46

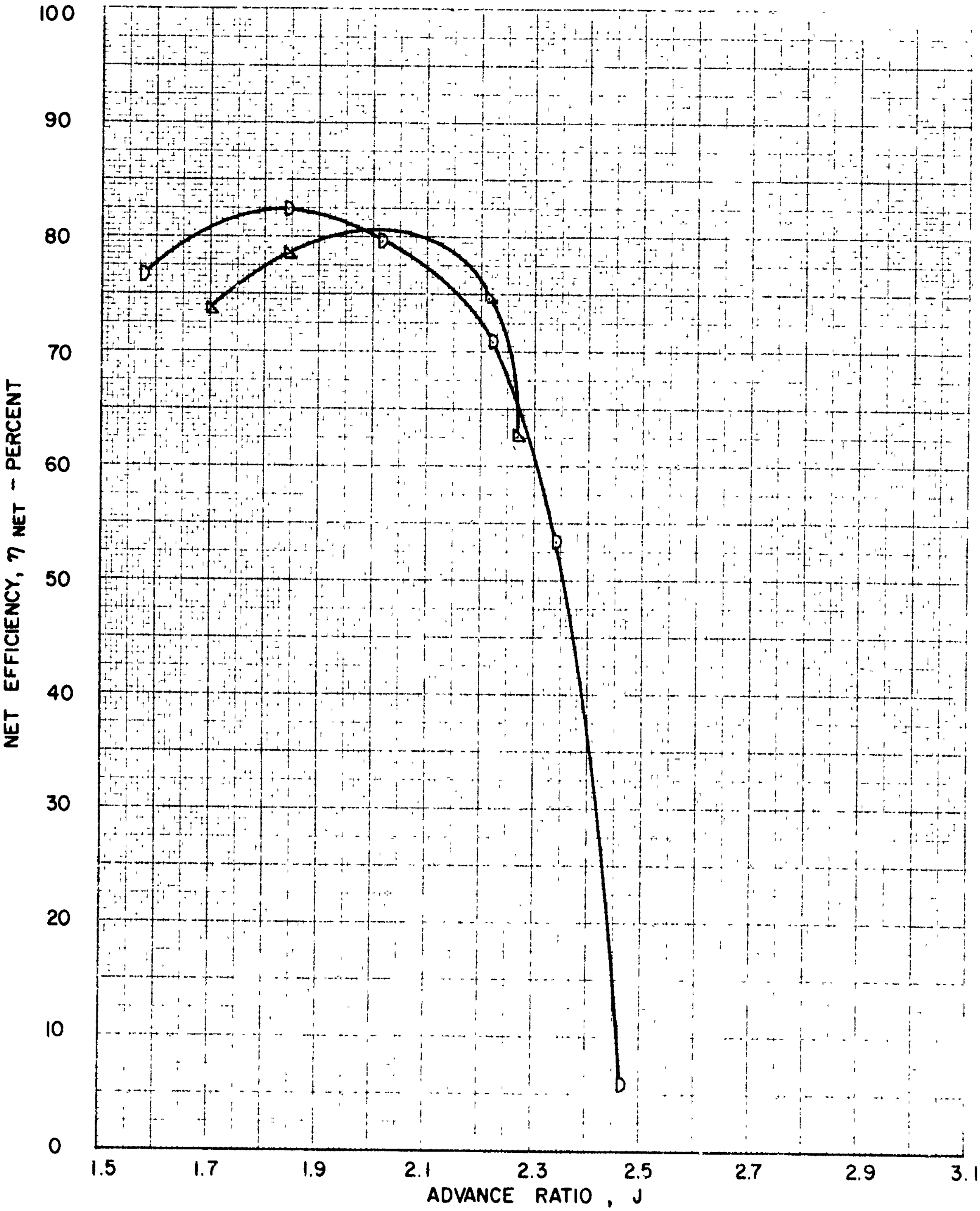

HSD SHROUDED PROPELLER TEST

EFFECT OF EXIT VANES ON SHROUDED PROPELLER PERFORMANCE

SYM	RUN NO.	MACH NO.	CONFIGURATION	$\theta_{3/4}$
D	506	0.40	$L_1 C_1 E_1 B_3 P_{WT} T_1 R_1 R_E V^0$	42
◺	507	↓	↓ ↓ ↓ ↓ ↓ ↓ ↓ ↓ ↓	46

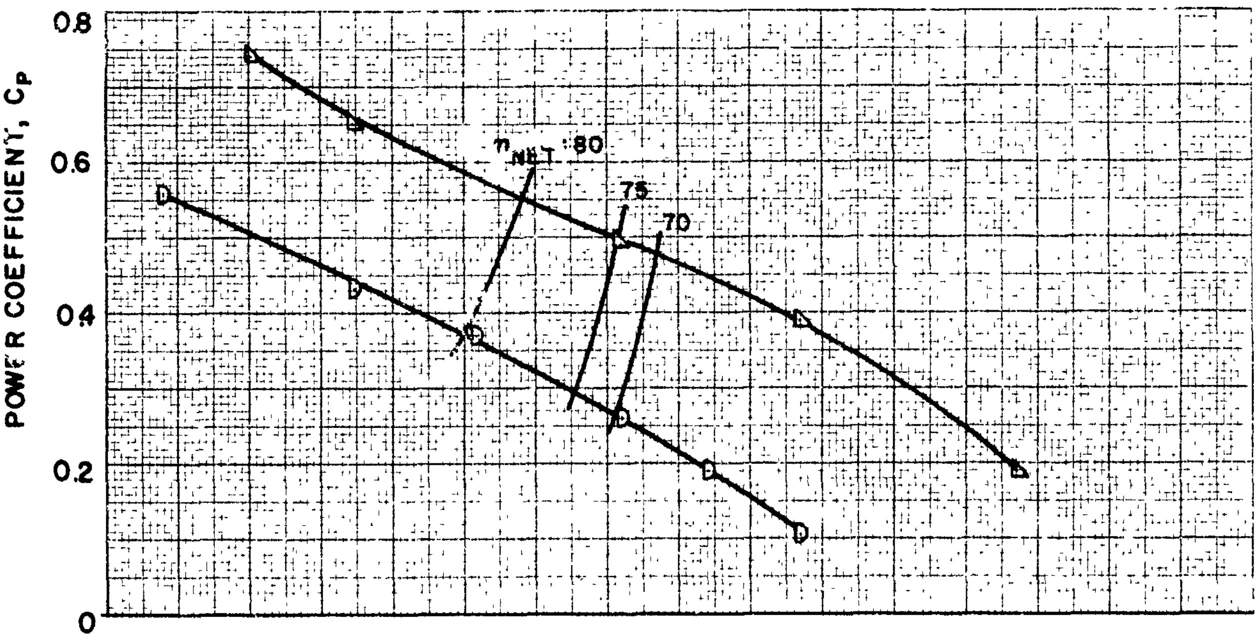

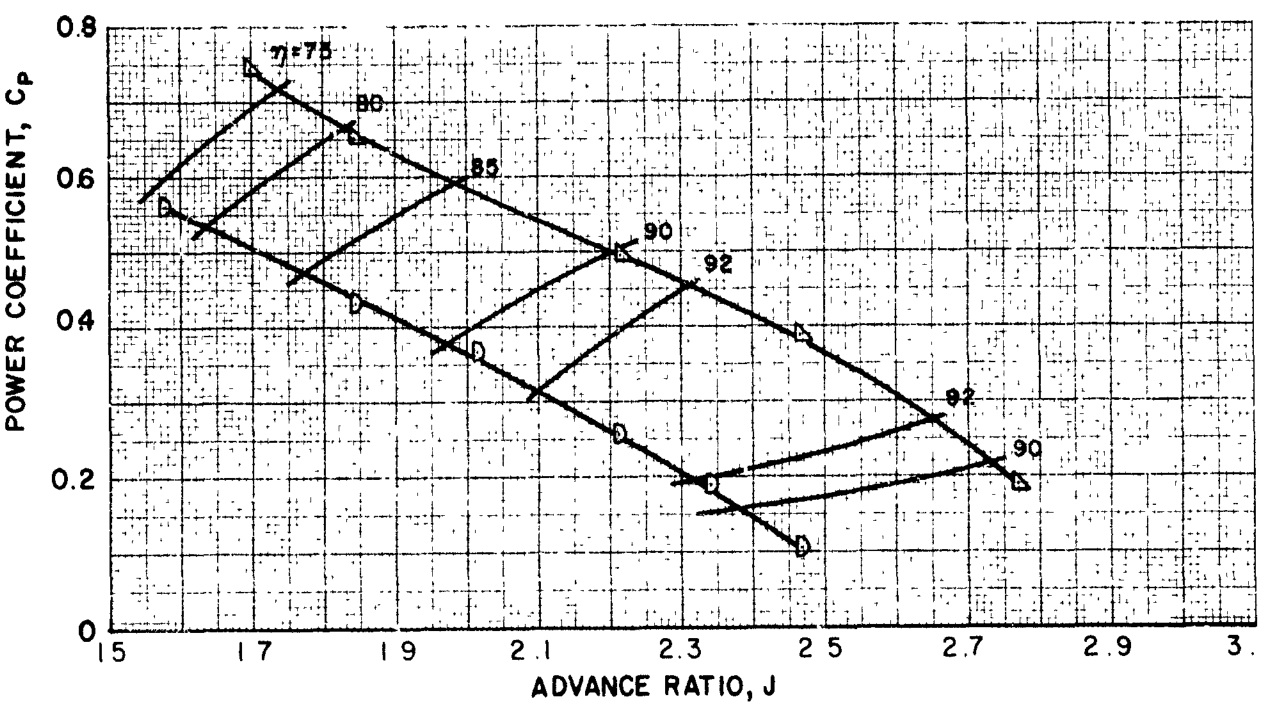

E330590-I FIG.149

HSD SHROUDED PROPELLER TEST

EFFECT OF EXIT VANES ON SHROUDED PROPELLER PERFORMANCE

SYM	RUN NO.	MACH NO.	CONFIGURATION	$\theta_{3/4}$
◺	508	0.50	$L_1 C_1 E_1 B_3 P_{WT} T_1 R_1 R_E V^0$	46
◁	505	↓	↓ ↓ ↓ ↓ ↓ ↓ ↓ ↓ ↓	50

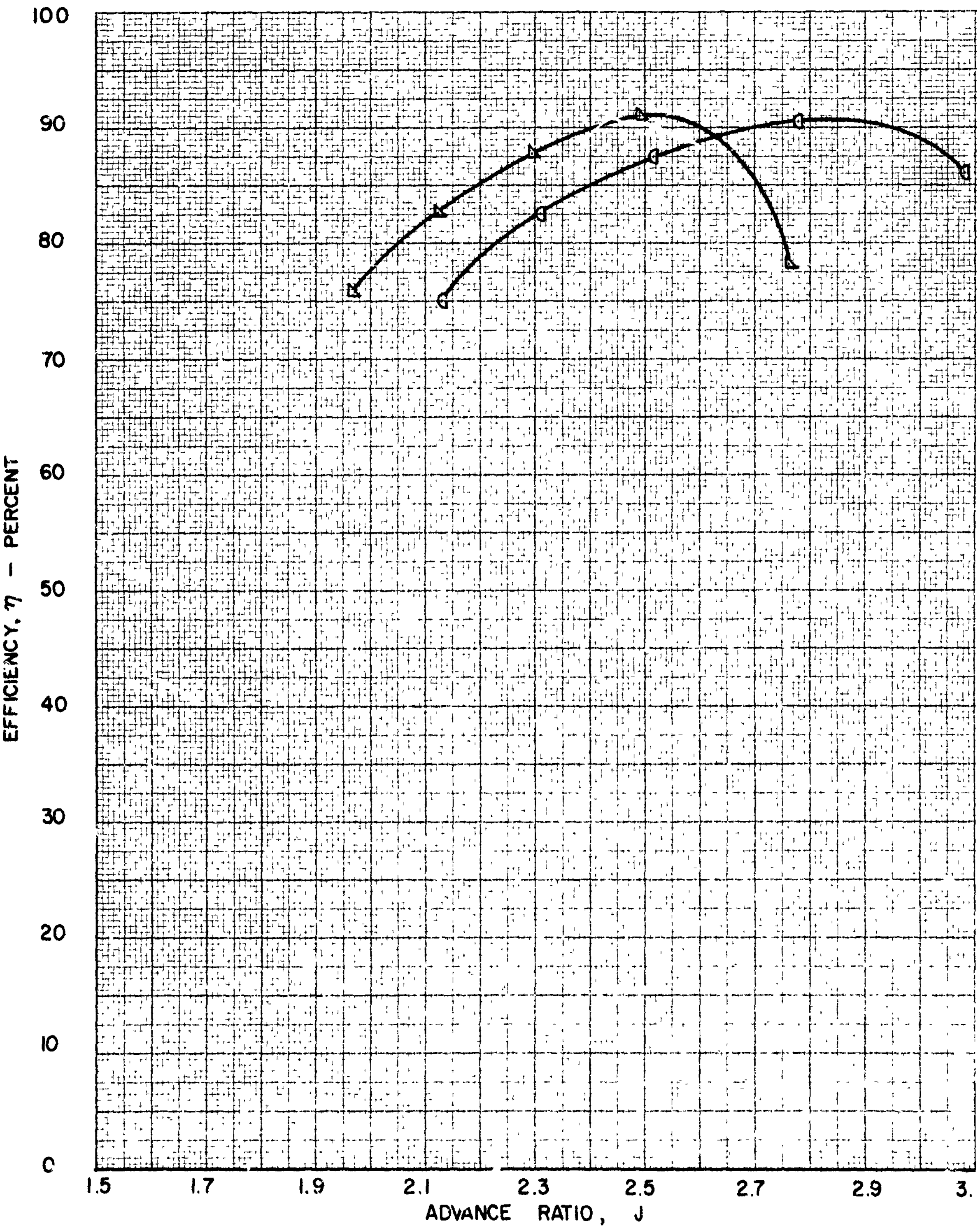

HSD SHROUDED PROPELLER TEST

EFFECT OF EXIT VANES ON SHROUDED PROPELLER PERFORMANCE

SYM	RUN NO.	MACH NO.	CONFIGURATION	$\theta_{3/4}$
△	508	0.50	$L_1 C_1 E_1 B_3 P_{WT} T_1 R_1 R_E V^0$	46
◁	505	↓	↓ ↓ ↓ ↓ ↓ ↓ ↓ ↓ ↓	50

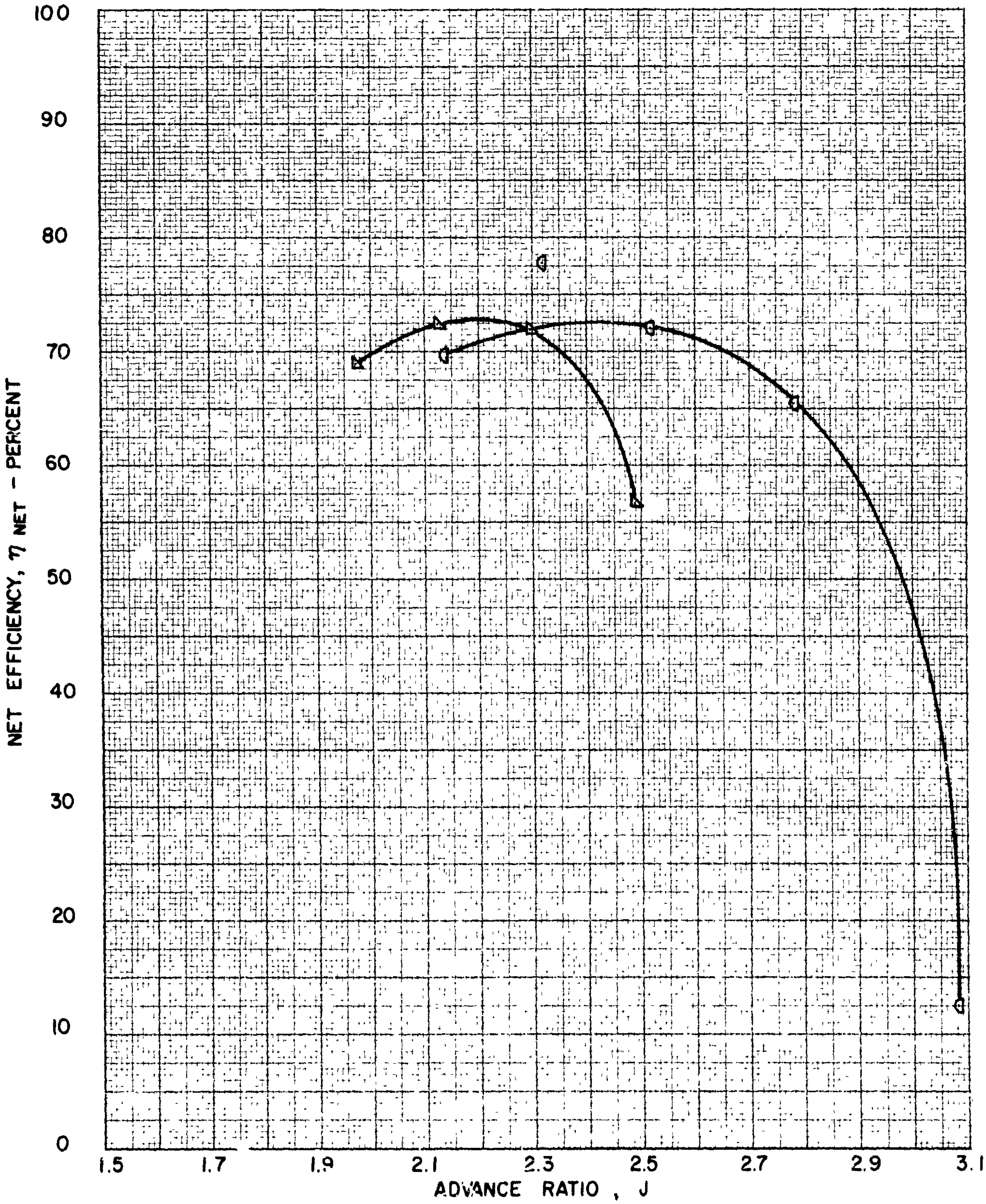

E330590-1

FIG. 151

HSD SHROUDED PROPELLER TEST

EFFECT OF EXIT VANES ON SHROUDED PROPELLER PERFORMANCE

SYM	RUN NO.	MACH NO.	CONFIGURATION	$\theta_{3/4}$
△	508	0.50	$L_1 C_1 E_1 B_3 P_{WT} T_1 R_1 R_E V^0$	46
◁	505	↓	↓ ↓ ↓ ↓ ↓ ↓ ↓ ↓ ↓	50

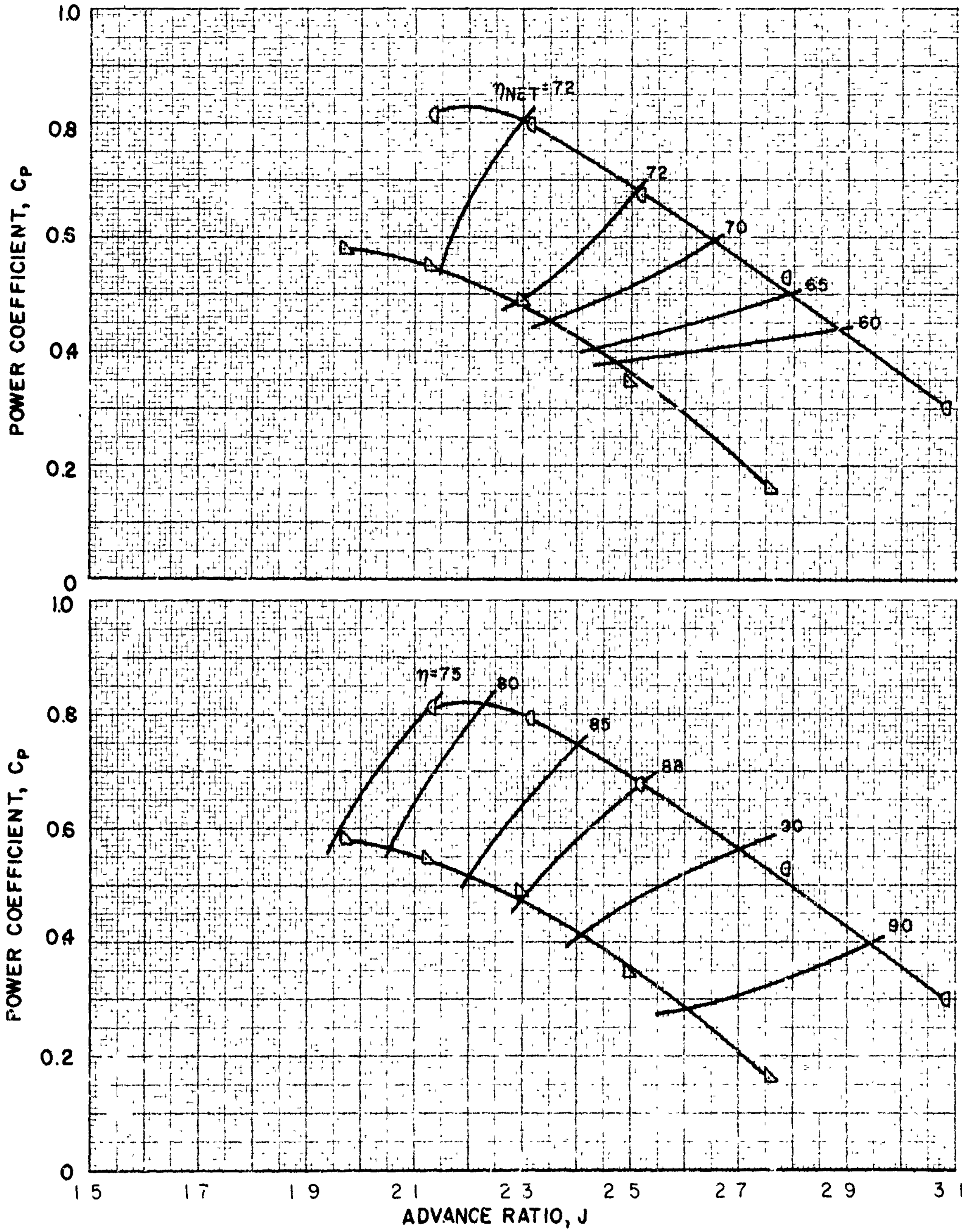

HSD SHROUDED PROPELLER TEST

EFFECT OF EXIT VANE ANGLE ON SHROUDED PROPELLER PERFORMANCE

SYM	RUN NO.	MACH NO.	CONFIGURATION	$\theta_{3/4}$
O	300,303	0.05	$L_1 C_1 E_1 B_3 P_{WT} T_1 R_1 R_E V^{-5}$	25,35
Δ	294,291	↓	↓ V^0	↓
⊡	295,298	↓	↓ V^{10}	↓

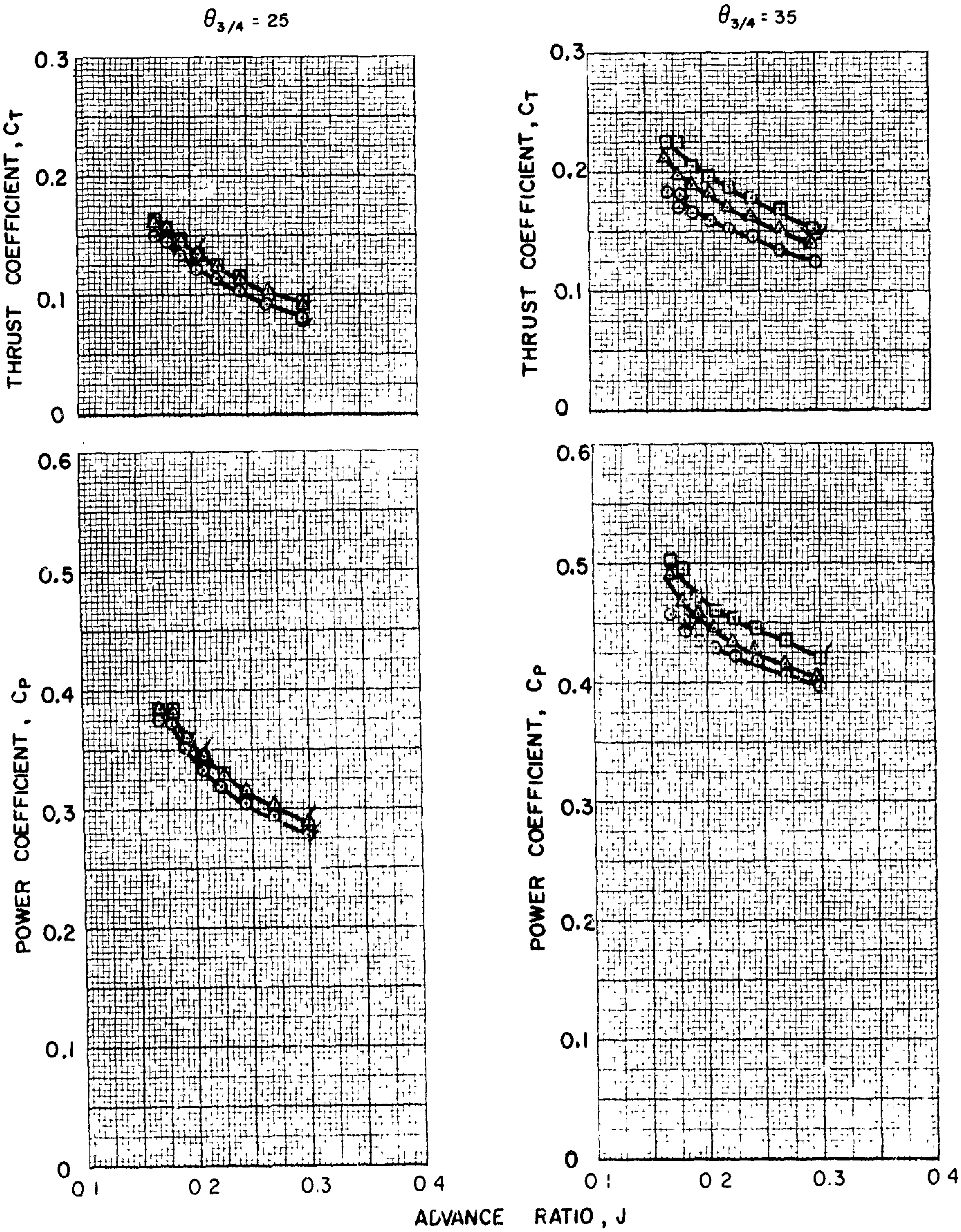

HSD SHROUDED PROPELLER TEST

EFFECT OF EXIT VANE ANGLE ON SHROUDED PROPELLER PERFORMANCE

SYM	RUN NO.	MACH NO.	CONFIGURATION	$\theta_{3/4}$
○	300,303	0.05	$L_1 C_1 E_1 B_3 P_{WT} T_1 R_1 R_E$ V^{-5}	25,35
△	294,291	↓	↓ V^0	↓
□	295,298	↓	↓ V^{10}	↓

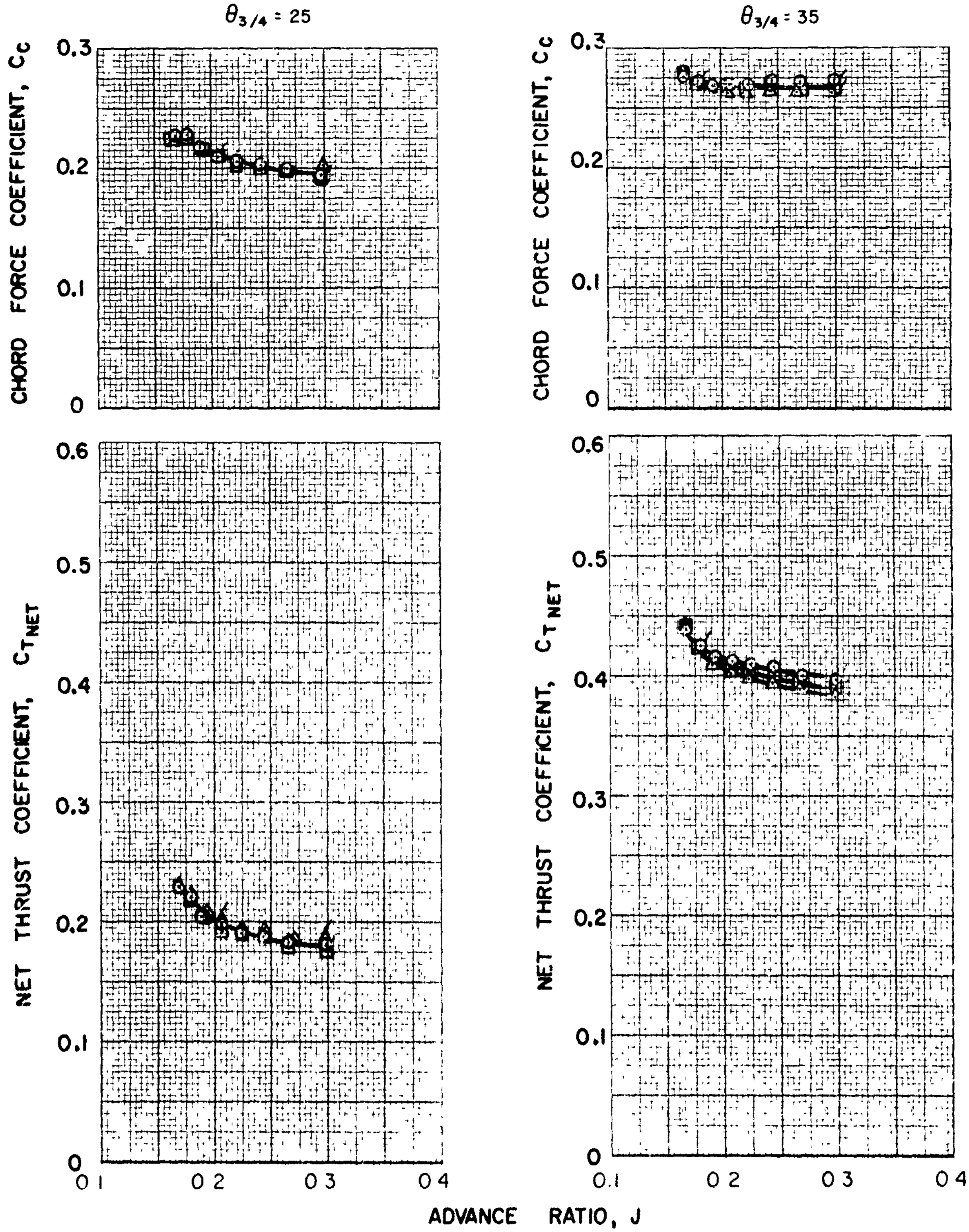

HSD SHROUDED PROPELLER TEST

EFFECT OF EXIT VANE ANGLE ON SHROUDED PROPELLER PERFORMANCE

SYM	RUN NO.	MACH NO.	CONFIGURATION	$\theta_{3/4}$
○	301	0.20	$L_1 C_1 E_1 B_3 P_{WT} T_1 R_1 R_E V^{-5}$	25
△	293	↓	↓ ↓ ↓ ↓ ↓ ↓ ↓ ↓ V^0	↓
□	296	↓	↓ ↓ ↓ ↓ ↓ ↓ ↓ ↓ V^{10}	↓

NOTE: η - OPEN SYMBOLS C_P - SOLID SYMBOLS

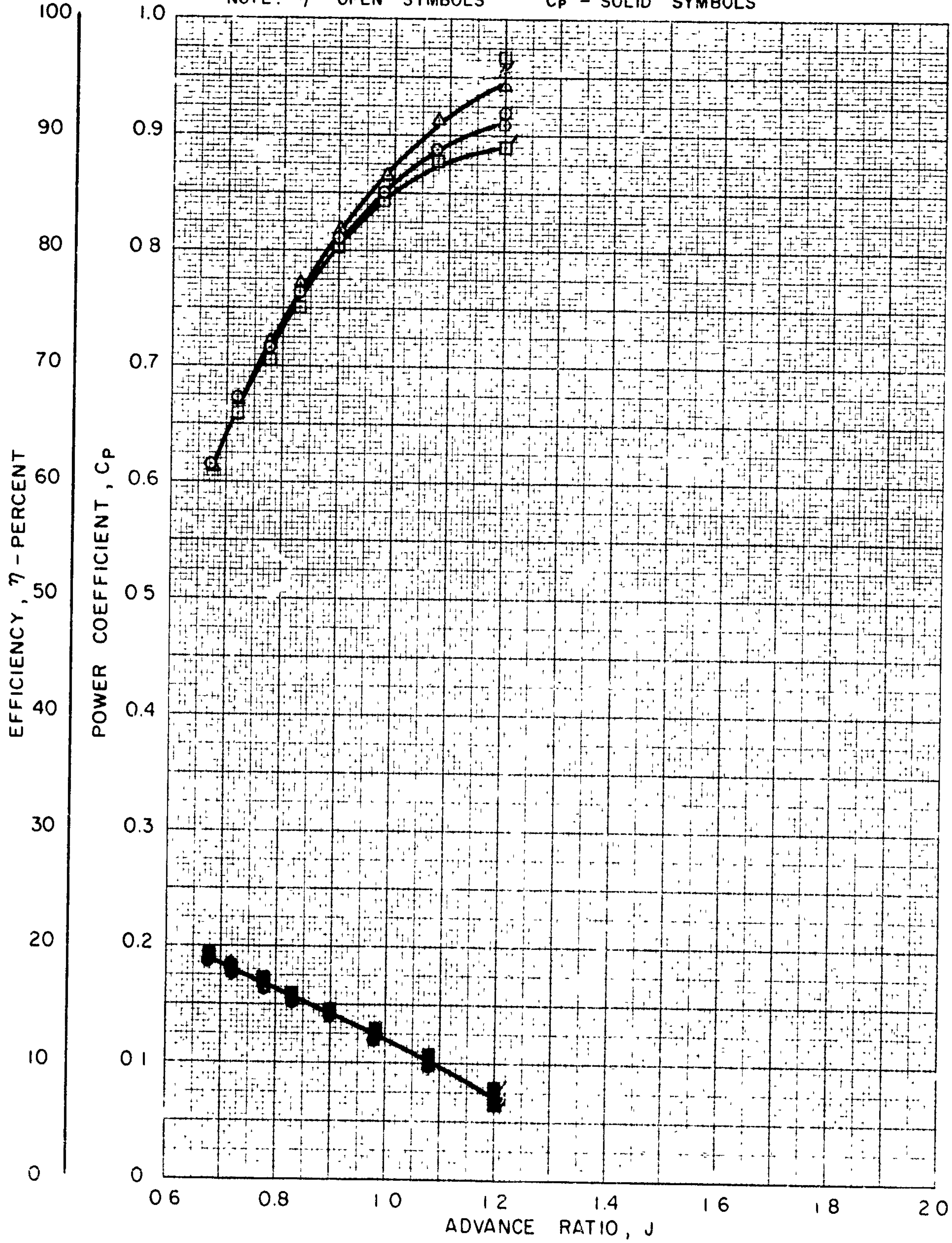

HSD SHROUDED PROPELLER TEST

EFFECT OF EXIT VANE ANGLE ON SHROUDED PROPELLER PERFORMANCE

SYM	RUN NO.	MACH NO.	CONFIGURATION	$\theta_{3/4}$
○	301	0.20	$L_1\ C_1\ E_1\ B_3\ P_{WT}T_1\ R_1\ R_E\ V^{-5}$	25
△	293	↓	↓ V^{0}	↓
□	296	↓	↓ V^{10}	↓

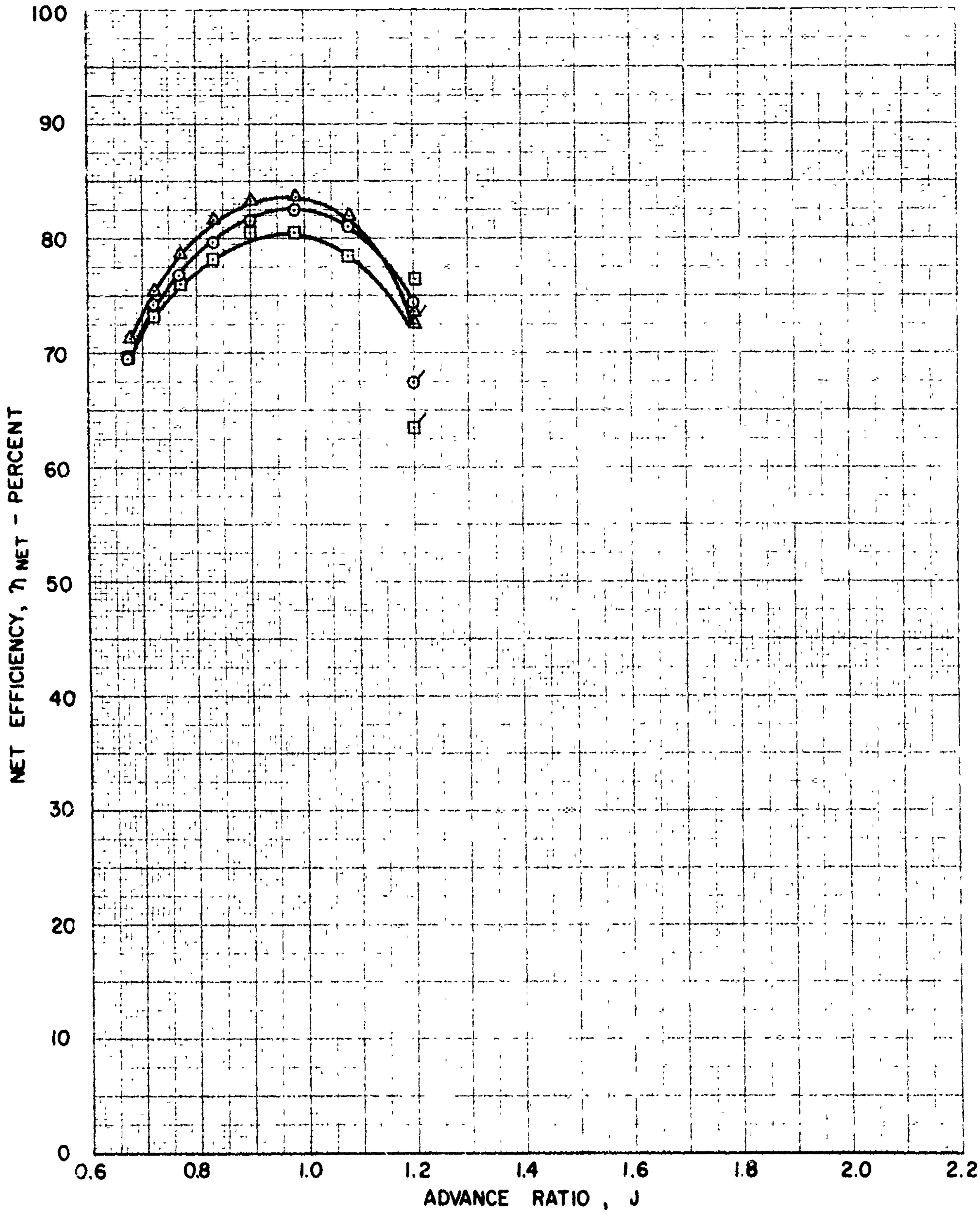

HSD SHROUDED PROPELLER TEST

EFFECT OF EXIT VANE ANGLE ON SHROUDED PROPELLER PERFORMANCE

SYM	RUN NO.	MACH NO.	CONFIGURATION	$\theta_{3/4}$
○	302	0.20	$L_1 C_1 E_1 B_3 P_{WT} T_1 R_1 R_E V^{-5}$	35
△	292	↓	↓ V^{0}	↓
□	297	↓	↓ V^{10}	↓

NOTE: η – OPEN SYMBOLS C_P – SOLID SYMBOLS

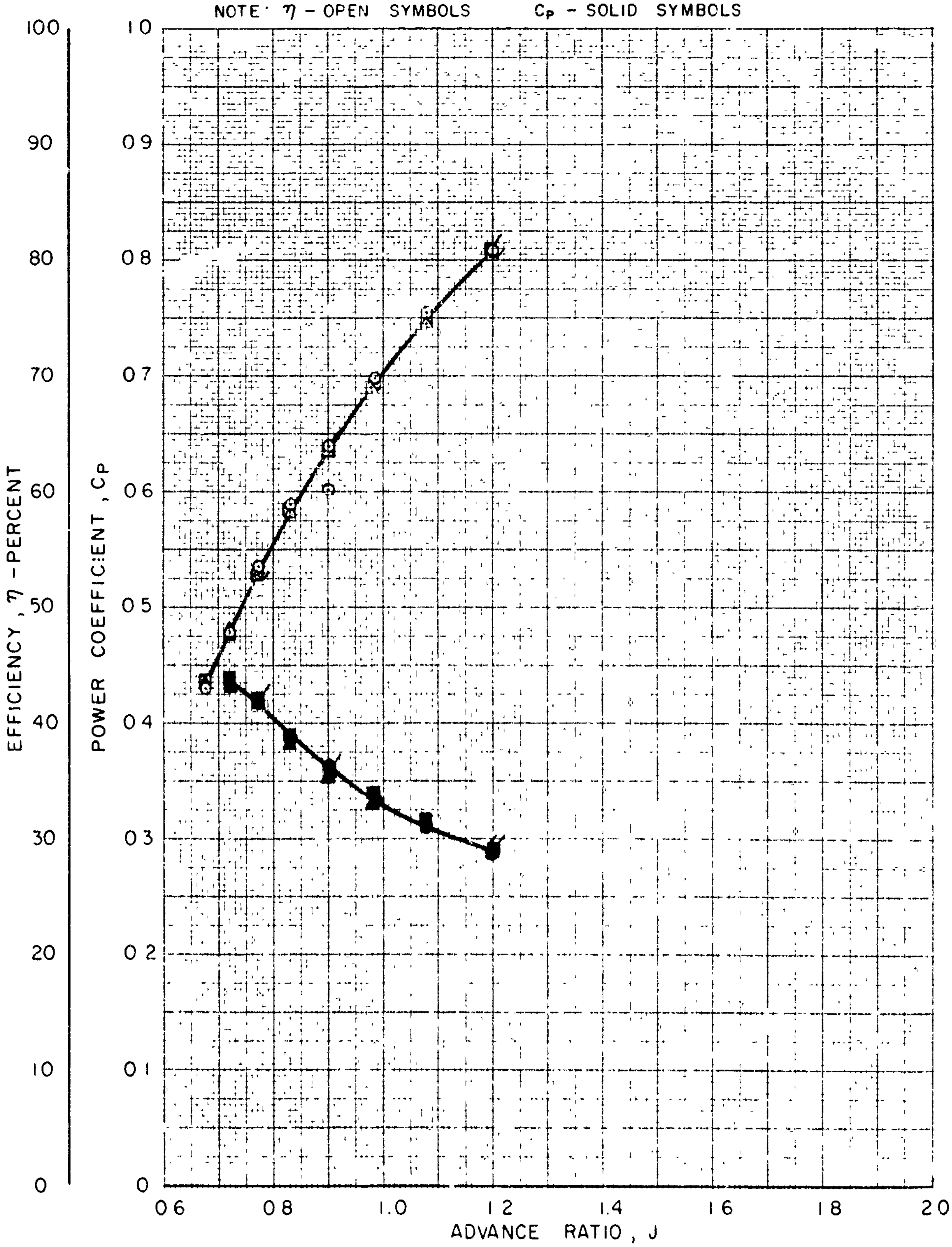

E330590-1

FIG.157

HSD SHROUDED PROPELLER TEST

EFFECT OF EXIT VANE ANGLE ON SHROUDED PROPELLER PERFORMANCE

SYM	RUN NO.	MACH NO	CONFIGURATION	$\theta_{3/4}$
○	302	0.20	$L_1\ C_1\ E_1\ B_3\ P_{WT}\ T_1\ R_1\ R_E\ V^{-5}$	35
△	292	↓	↓ ↓ ↓ ↓ ↓ ↓ ↓ ↓ V^{0}	↓
□	297	↓	↓ ↓ ↓ ↓ ↓ ↓ ↓ ↓ V^{10}	↓

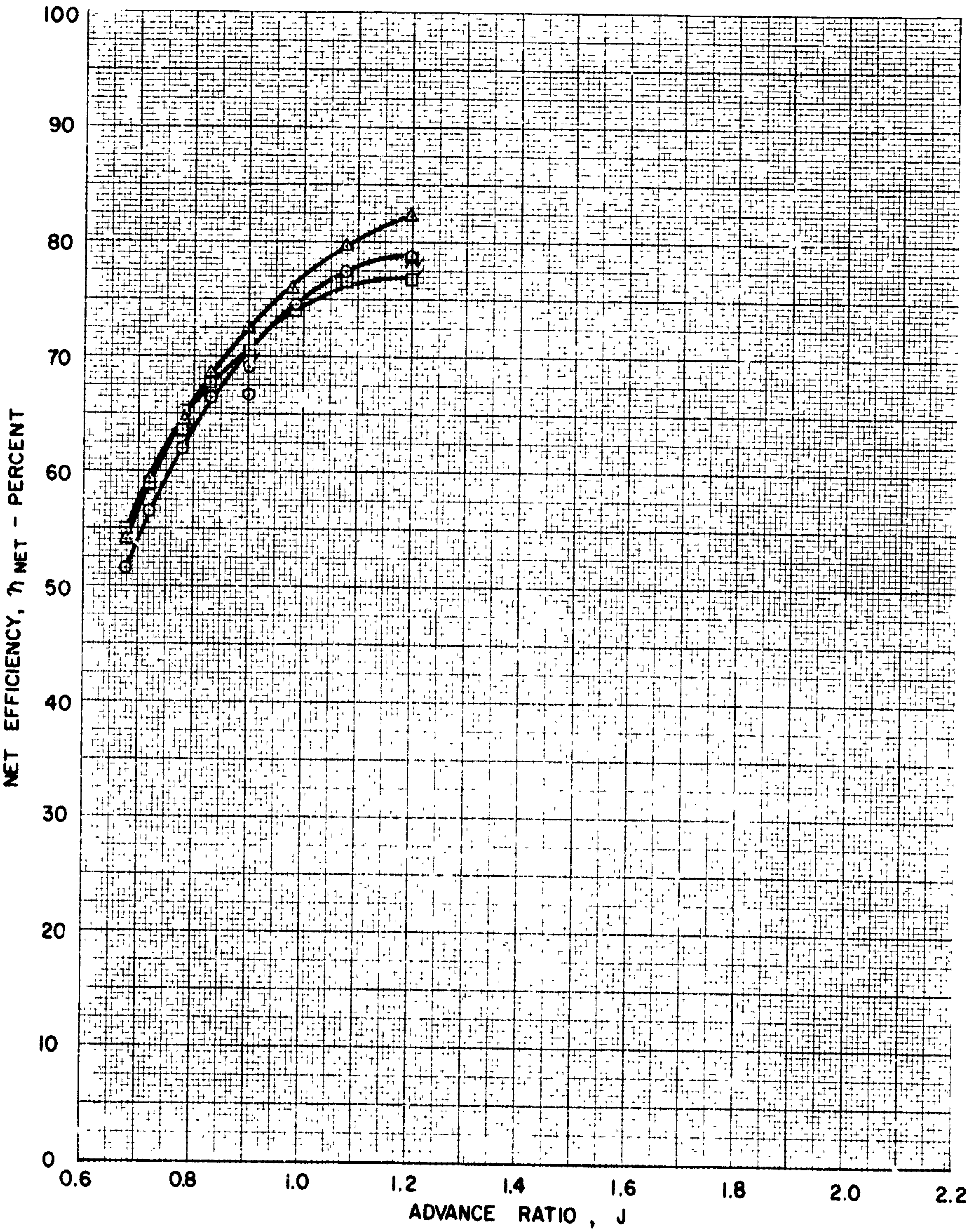

E330590-1 FIG. 158

HSD SHROUDED PROPELLER TEST

EFFECT OF BLADE PLANFORM ON SHROUDED PROPELLER PERFORMANCE

SYM	RUN NO.	MACH NO.	CONFIGURATION	$\theta_{3/4}$
△	175, 176	0.02, 0.10	$L_1 C_1 E_1 B_3 P_R T_1 R_1 R_E$	20
□	177, 178	↓	↓	25
◇	183, 182	↓	↓	30
⊿	184, 185	↓	↓	35

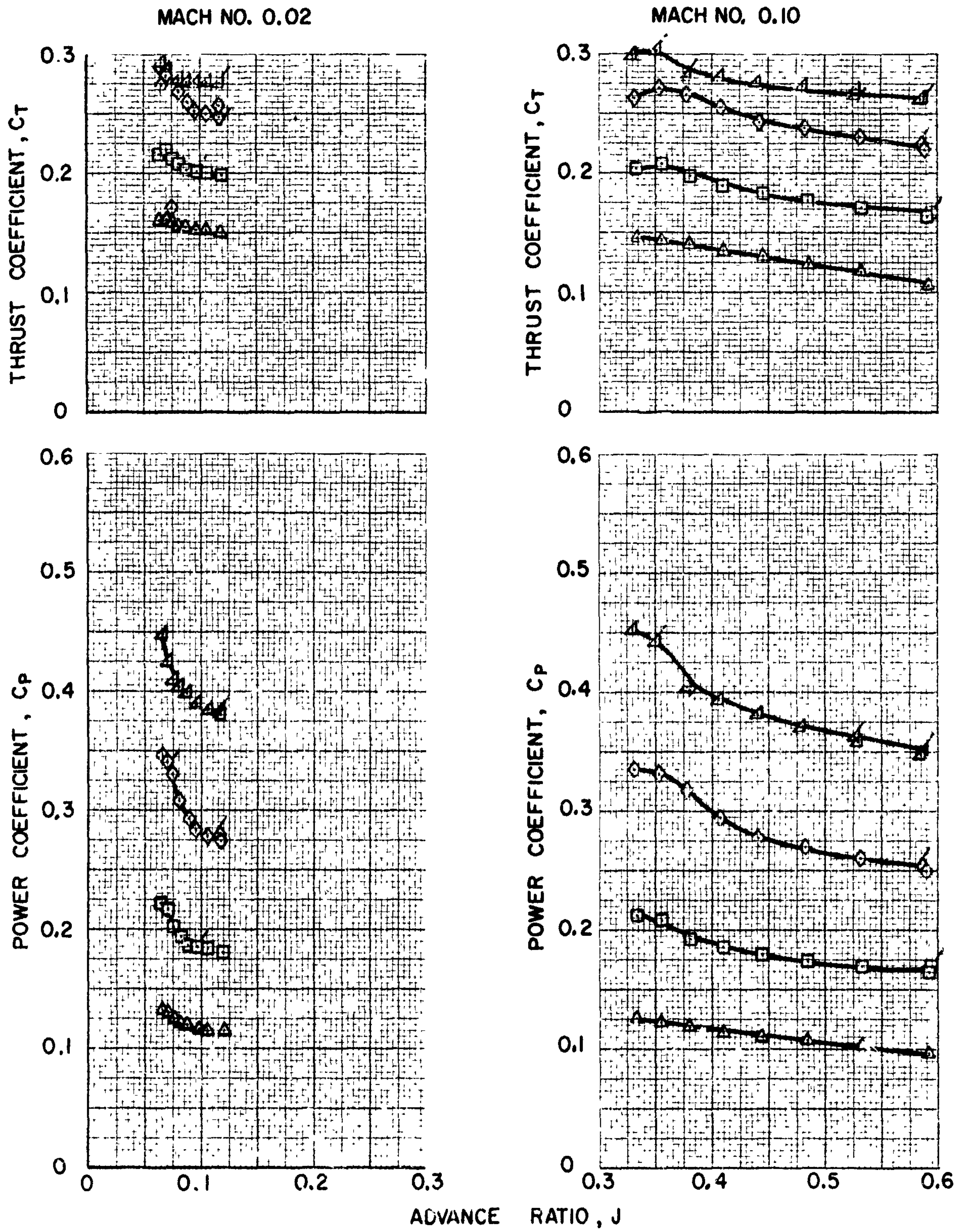

HSD SHROUDED PROPELLER TEST

EFFECT OF BLADE PLANFORM ON SHROUDED PROPELLER PERFORMANCE

SYM	RUN NO.	MACH NO.	CONFIGURATION	$\theta_{3/4}$
△	175,176	0.02, 0.10	$L_1 C_1 E_1 B_3 P_R T_1 R_1 R_E$	20
⊡	177,178	↓	↓	25
◇	183,182	↓	↓	30
⊿	184,185	↓	↓	35

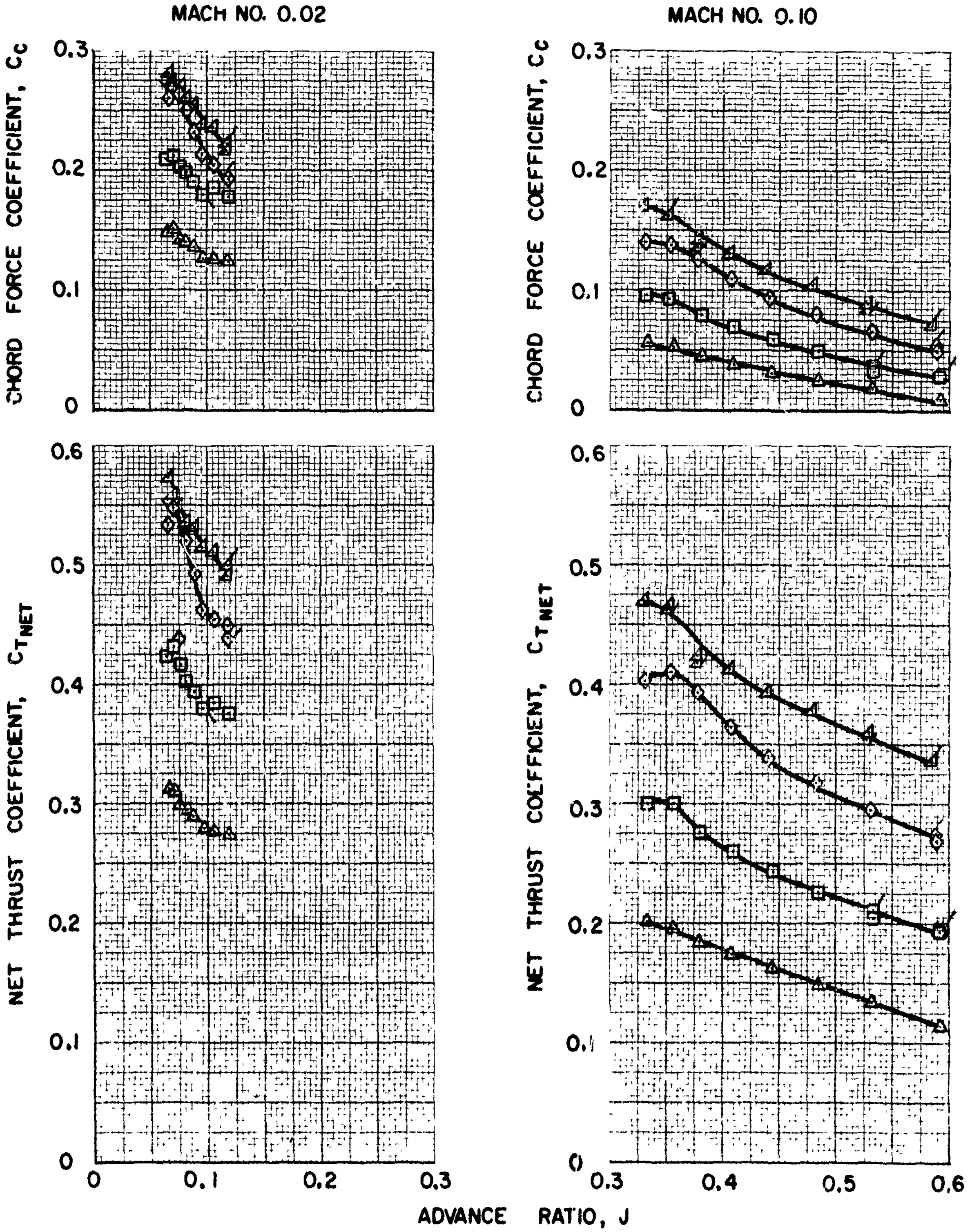

E330590-1 FIG. 160

HSD SHROUDED PROPELLER TEST

EFFECT OF BLADE PLANFORM ON SHROUDED PROPELLER PERFORMANCE

SYM	RUN NO.	MACH NO.	CONFIGURATION	$\theta_{3/4}$
⊡	179	0.20	$L_1C_1E_1B_3P_RT_1R_1R_E$	25
◇	181	↓	↓	30
⊿	186	↓	↓	35

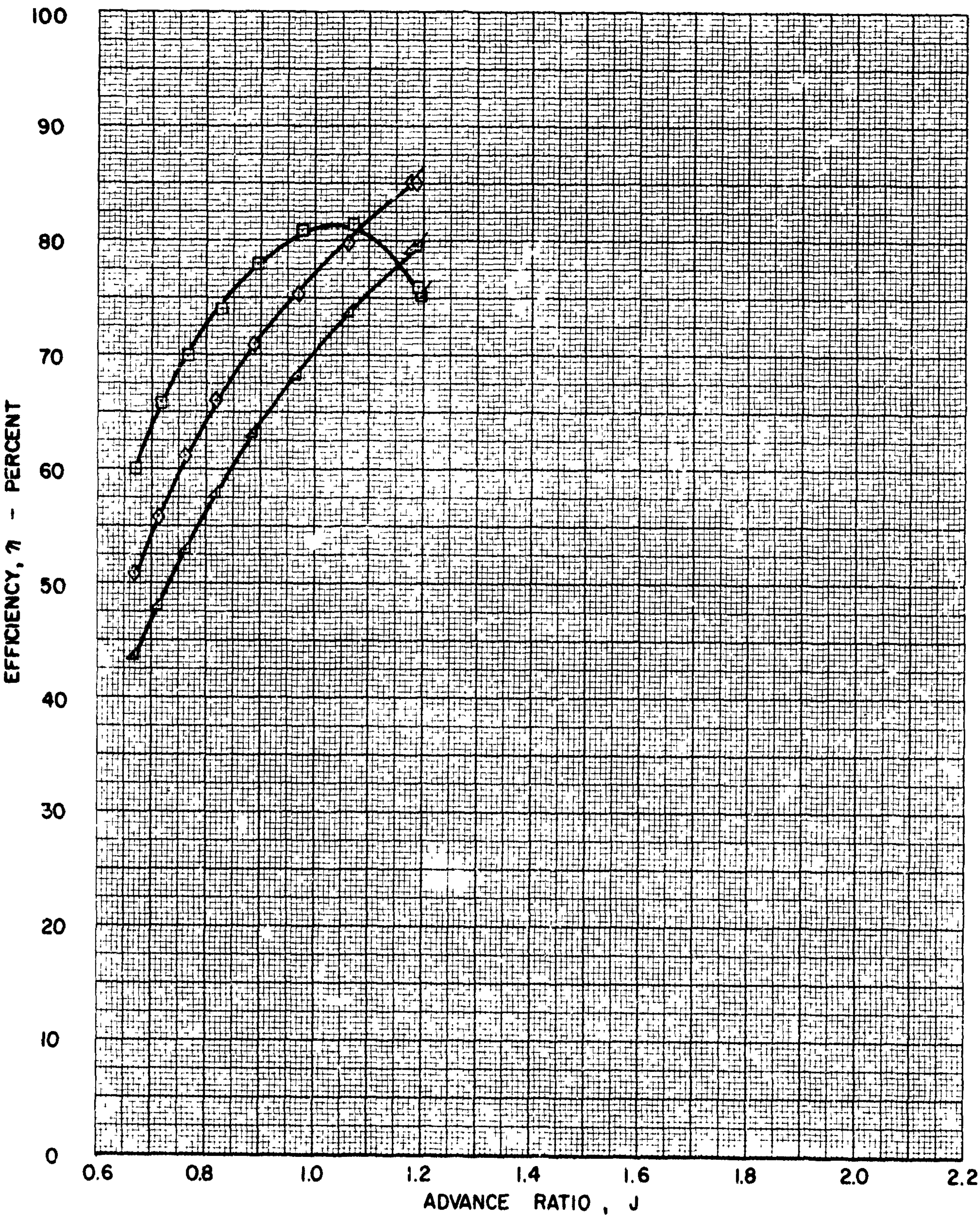

HSD SHROUDED PROPELLER TEST

EFFECT OF BLADE PLANFORM ON SHROUDED PROPELLER PERFORMANCE

SYM	RUN NO.	MACH NO.	CONFIGURATION	$\theta_{3/4}$
⊡	179	0.20	$L_1\ C_1\ E_1\ B_3\ P_R\ T_1\ R_1\ R_E$	25
◇	181	↓	↓	30
⊿	186	↓	↓	35

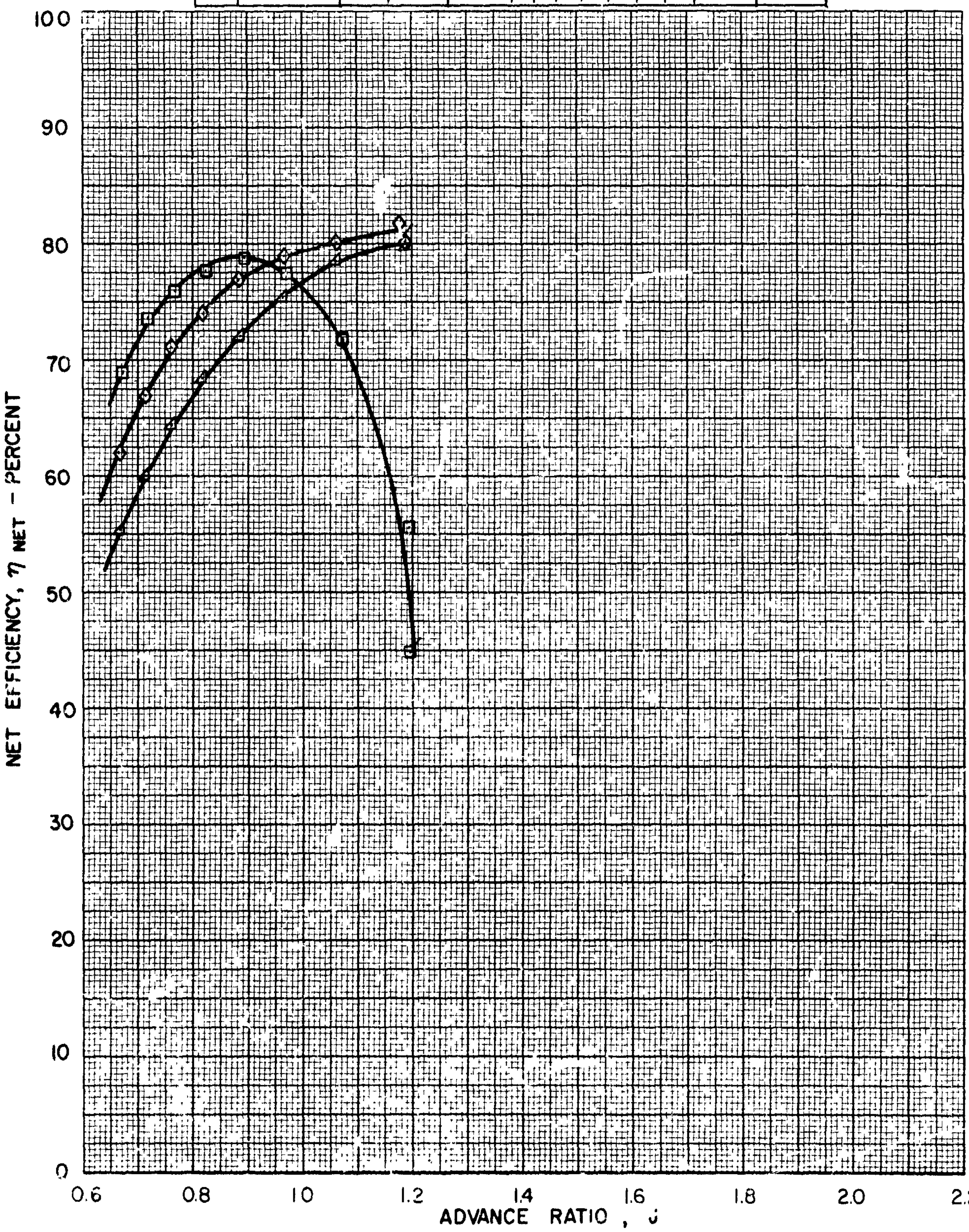

E330590-1 FIG.162

HSD SHROUDED PROPELLER TEST

EFFECT OF BLADE PLANFORM ON SHROUDED PROPELLER PERFORMANCE

SYM	RUN NO.	MACH NO.	CONFIGURATION	$\theta_{3/4}$
⊡	179	0.20	$L_1 C_1 E_1 B_3 P_R T_1 R_1 R_E$	25
◇	181	↓	↓	30
⊿	186	↓	↓	35

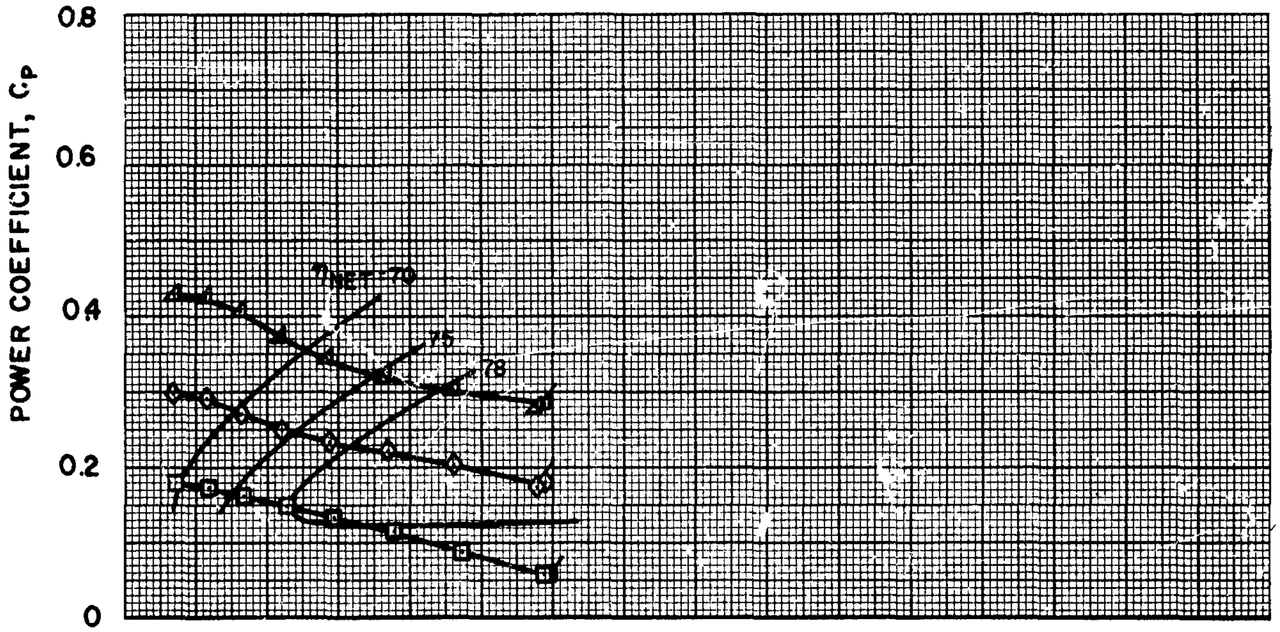

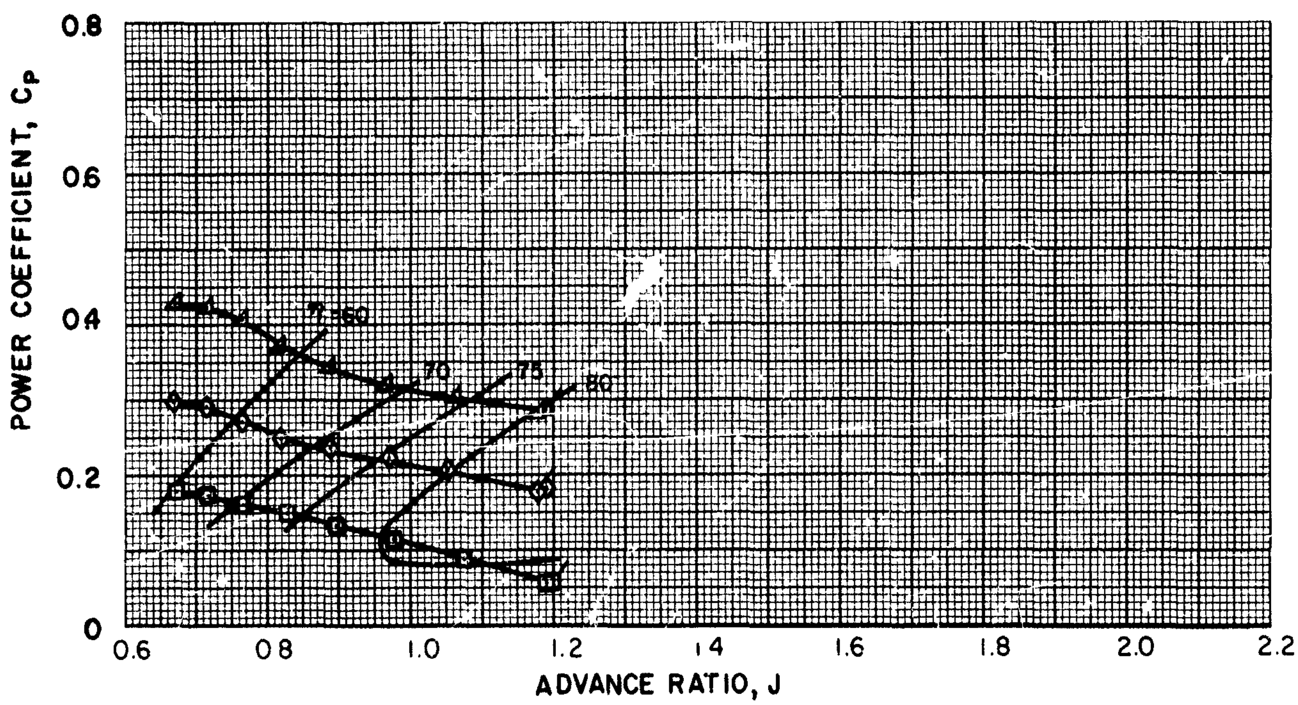

E330590-1

FIG. 163

HSD SHROUDED PROPELLER TEST

EFFECT OF BLADE PLANFORM ON SHROUDED PROPELLER PERFORMANCE

SYM	RUN NO.	MACH NO.	CONFIGURATION	$\theta_{3/4}$
◿	449	0.30	$L_1 C_1 E_1 B_3 P_R T_1 R_1 R_E$	34
▽	450	↓	↓	38
D	451	↓	↓	42
◺	453	↓	↓	46

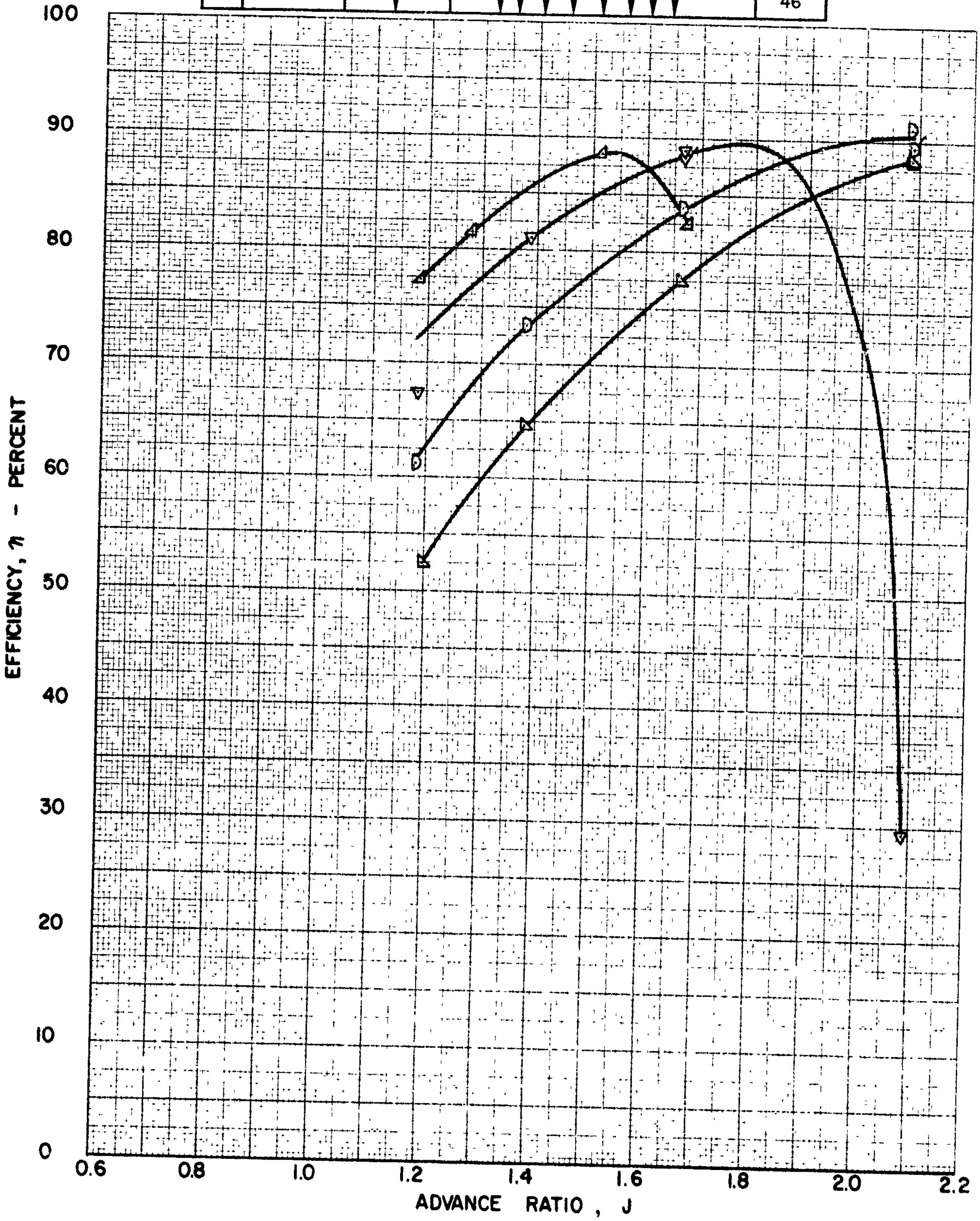

E330590-1

FIG. 164

HSD SHROUDED PROPELLER TEST

EFFECT OF BLADE PLANFORM ON SHROUDED PROPELLER PERFORMANCE

SYM	RUN NO.	MACH NO.	CONFIGURATION	$\theta_{3/4}$
◺	449	0.30	$L_1 C_1 E_1 B_3 P_R T_1 R_1 R_C$	34
▽	450	↓	↓	38
D	451	↓	↓	42
◺	453	↓	↓	46

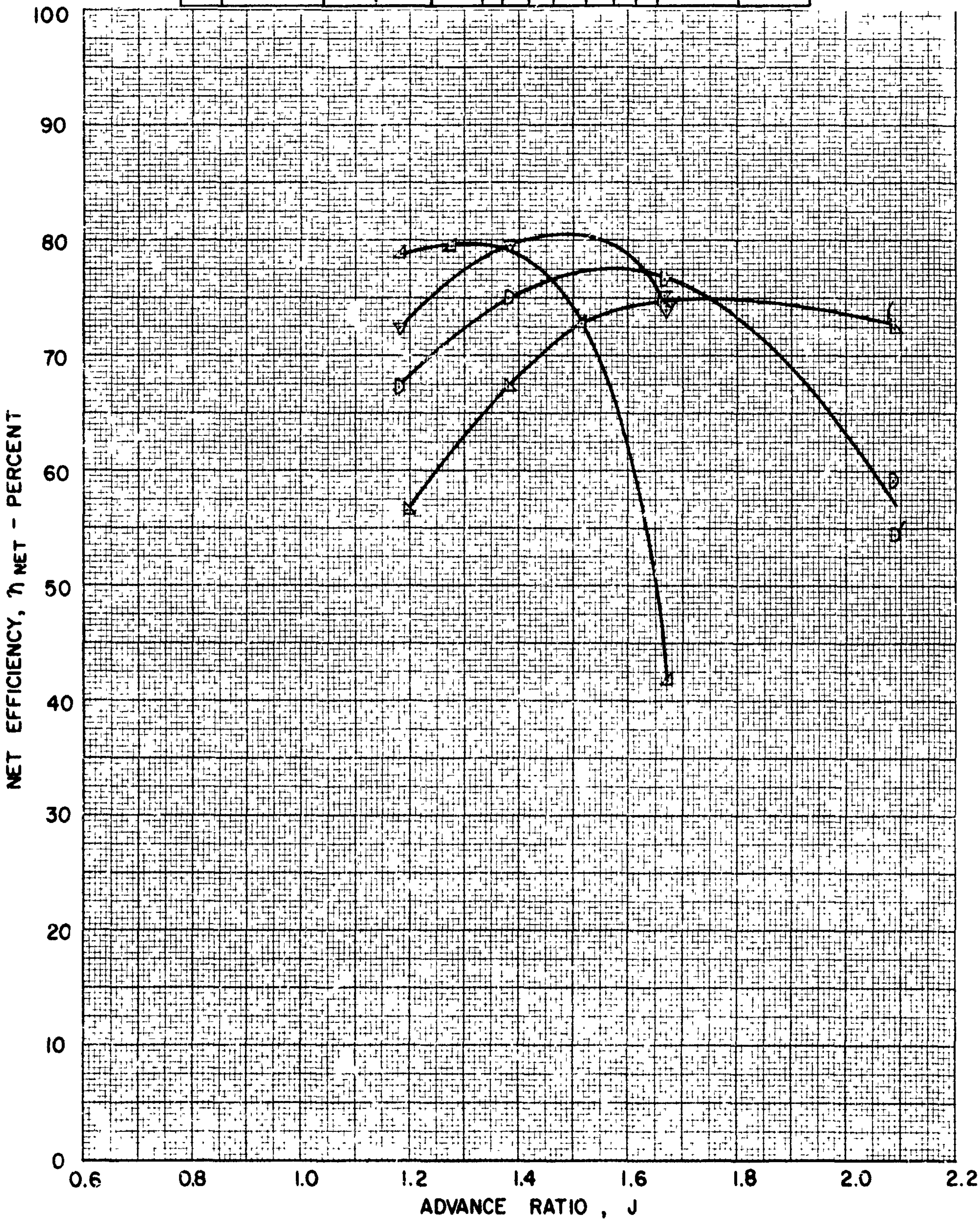

E330590-1

FIG.165

HSD SHROUDED PROPELLER TEST

EFFECT OF BLADE PLANFORM ON SHROUDED PROPELLER PERFORMANCE

SYM	RUN NO.	MACH NO.	CONFIGURATION	$\theta_{3/4}$
◿	449	0.30	$L_1 C_1 E_1 B_3 P_R T_1 R_1 R_E$	34
▽	450	↓	↓	38
D	451	↓	↓	42
◺	453	↓	↓	46

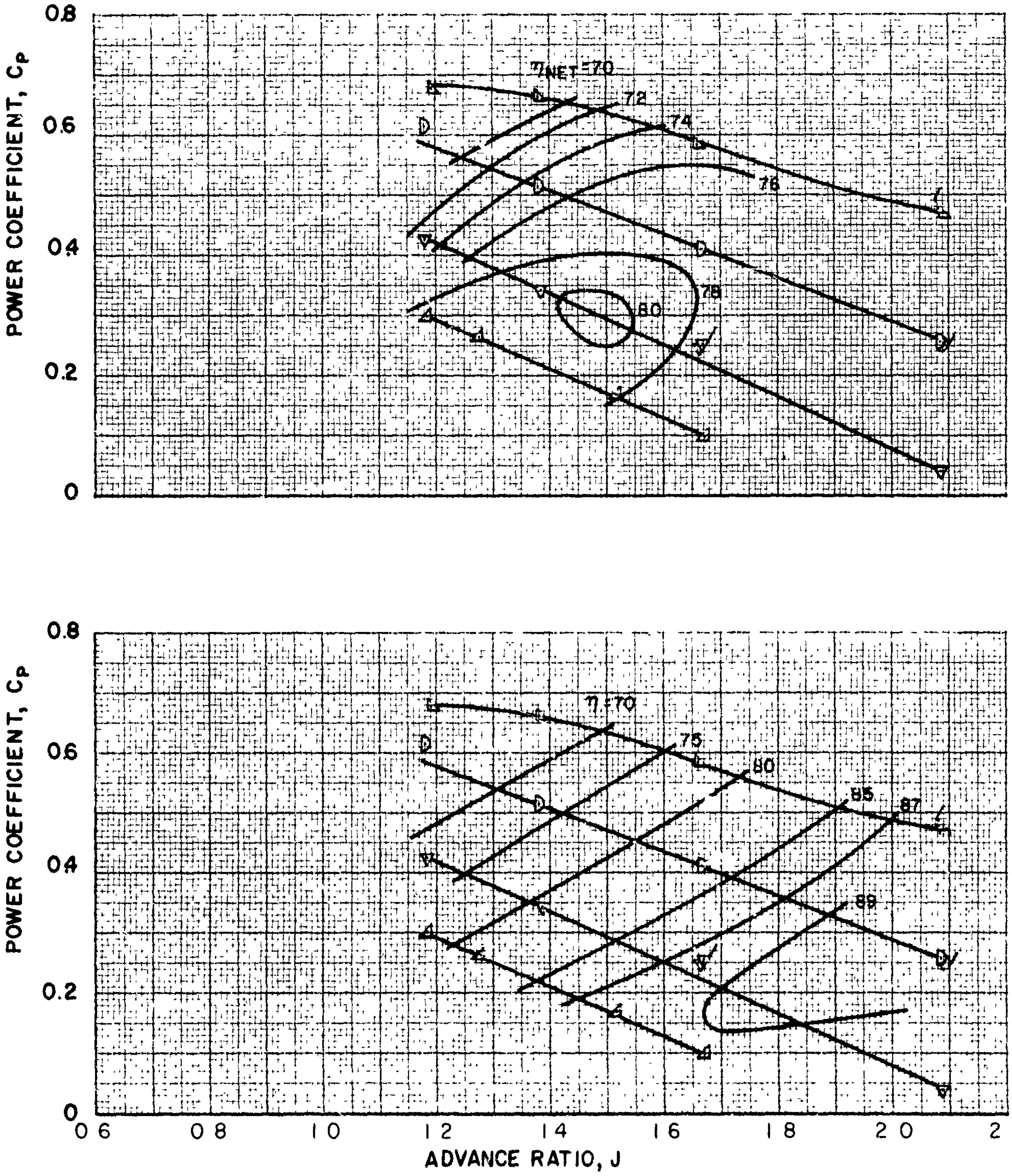

HSD SHROUDED PROPELLER TEST

EFFECT OF BLADE PLANFORM ON SHROUDED PROPELLER PERFORMANCE

SYM	RUN NO.	MACH NO.	CONFIGURATION	$\theta_{3/4}$
D	452	0.40	$L_1 C_1 E_1 B_3 P_R T_1 R_1 R_E$	42
◺	454	↓	↓	46
◖	456	↓	↓	50
⊙	458	↓	↓	54

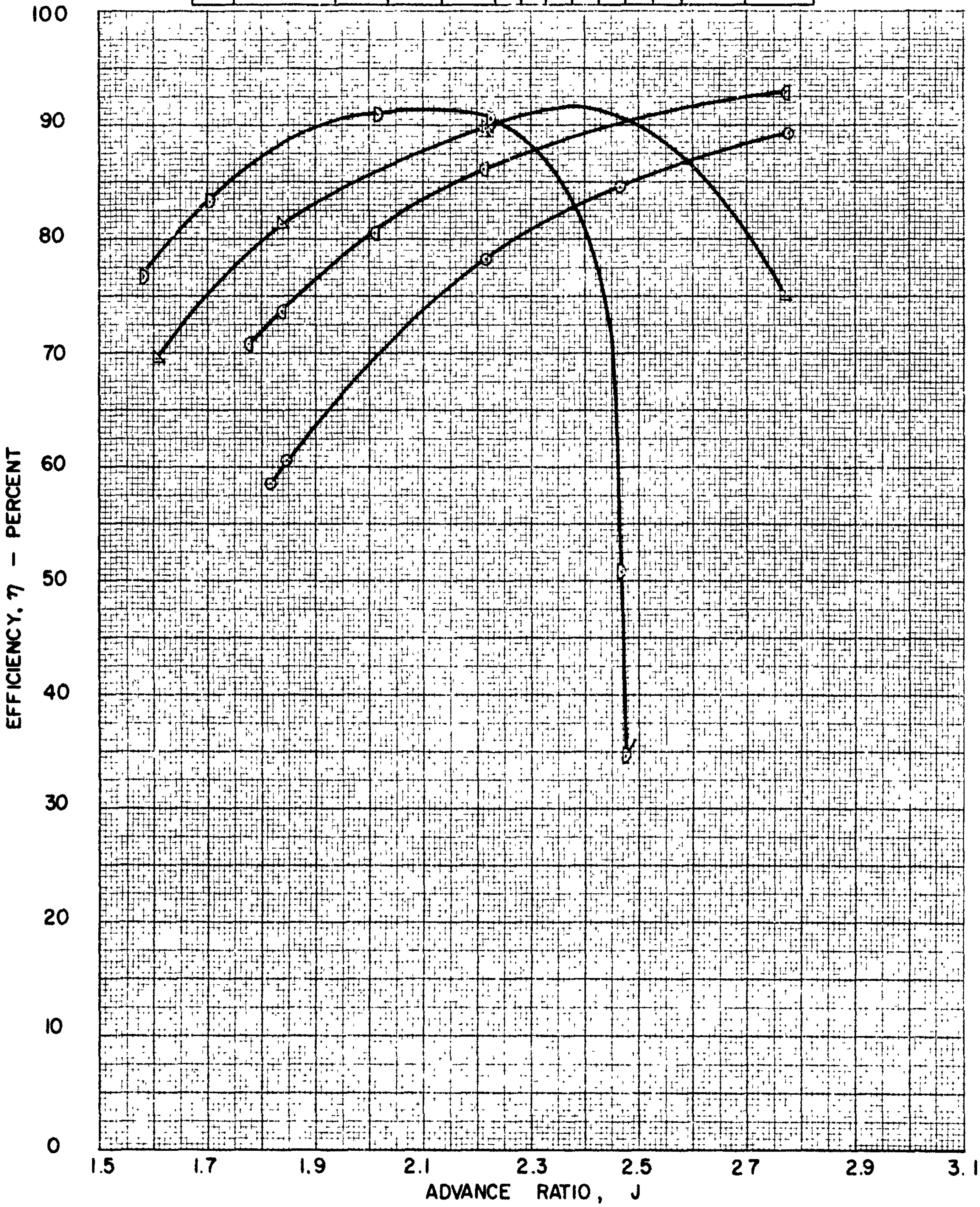

HSD SHROUDED PROPELLER TEST

EFFECT OF BLADE PLANFORM ON SHROUDED PROPELLER PERFORMANCE

SYM	RUN NO.	MACH NO.	CONFIGURATION	$\theta_{3/4}$
◗	452	0.40	$L_1 C_1 E_1 B_3 P_R T_1 R_1 R_E$	42
◺	454	↓	↓	46
◖	456	↓	↓	50
○	458	↓	↓	54

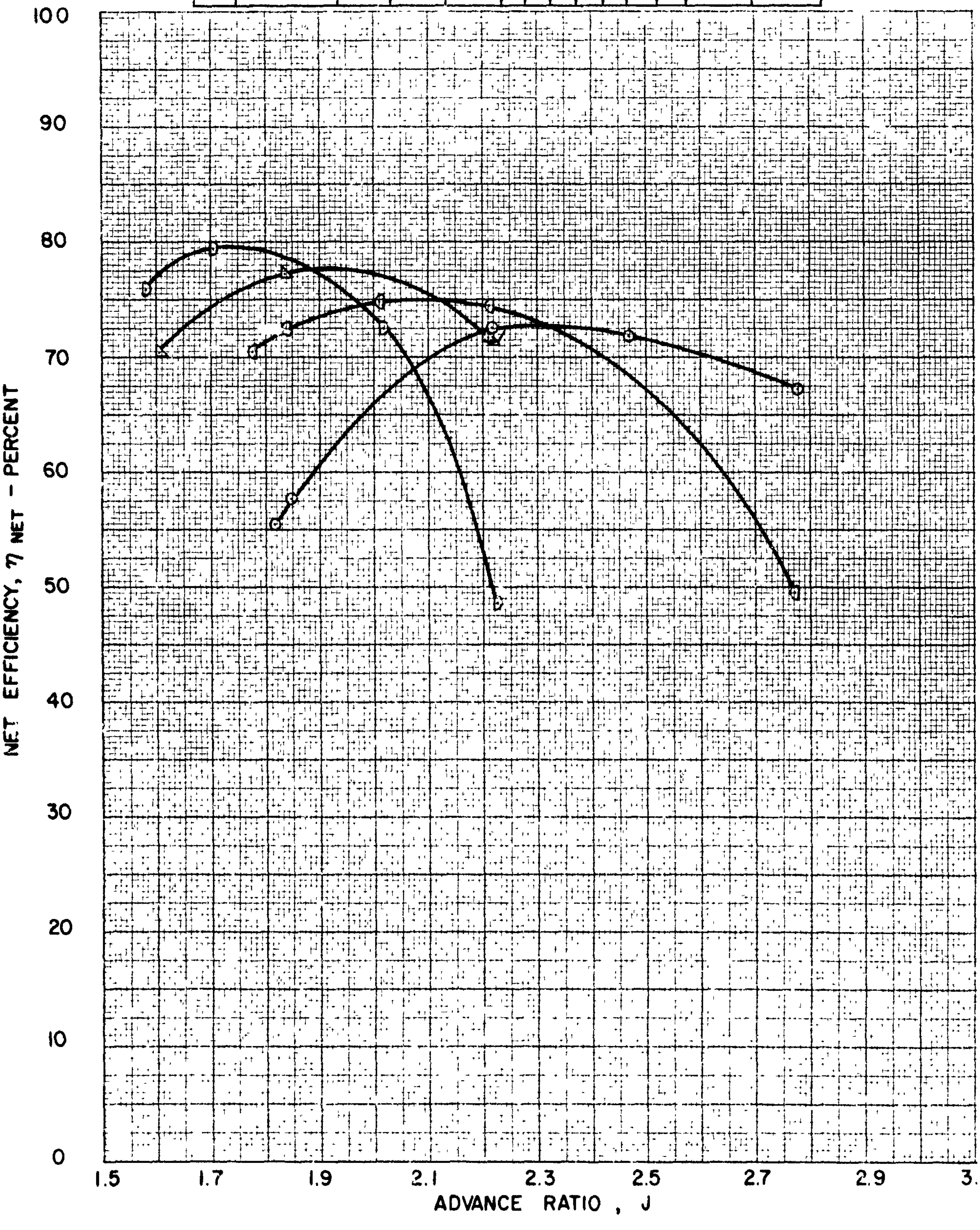

HSD SHROUDED PROPELLER TEST

EFFECT OF BLADE PLANFORM ON SHROUDED PROPELLER PERFORMANCE

SYM	RUN NO.	MACH NO.	CONFIGURATION	θ 3/4
D	452	0 40	$L_1 C_1 E_1 B_3 P_R T_1 R_1 R_E$	42
◺	454	↓	↓	46
◖	456	↓	↓	50
○	458	↓	↓	54

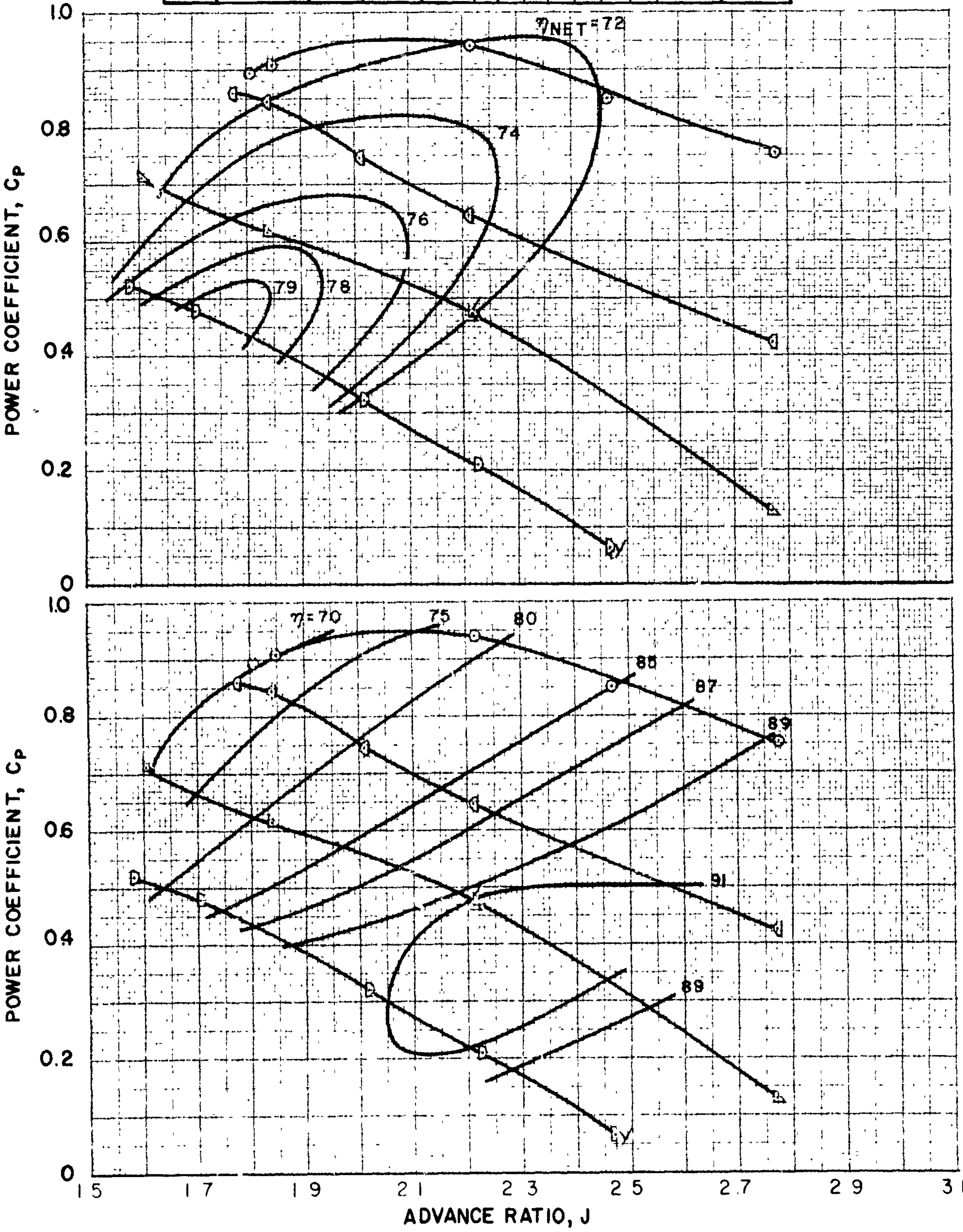

E330590-I

FIG. 169

HSD SHROUDED PROPELLER TEST

EFFECT OF BLADE PLANFORM ON SHROUDED PROPELLER PERFORMANCE

SYM	RUN NO.	MACH NO.	CONFIGURATION	$\theta_{3/4}$
D	461	0.50	$L_1 C_1 E_1 B_3 P_R T_1 R_1 R_E$	42
◁	455	↓	↓	46
◖	457	↓	↓	50
O	460	↓	↓	54

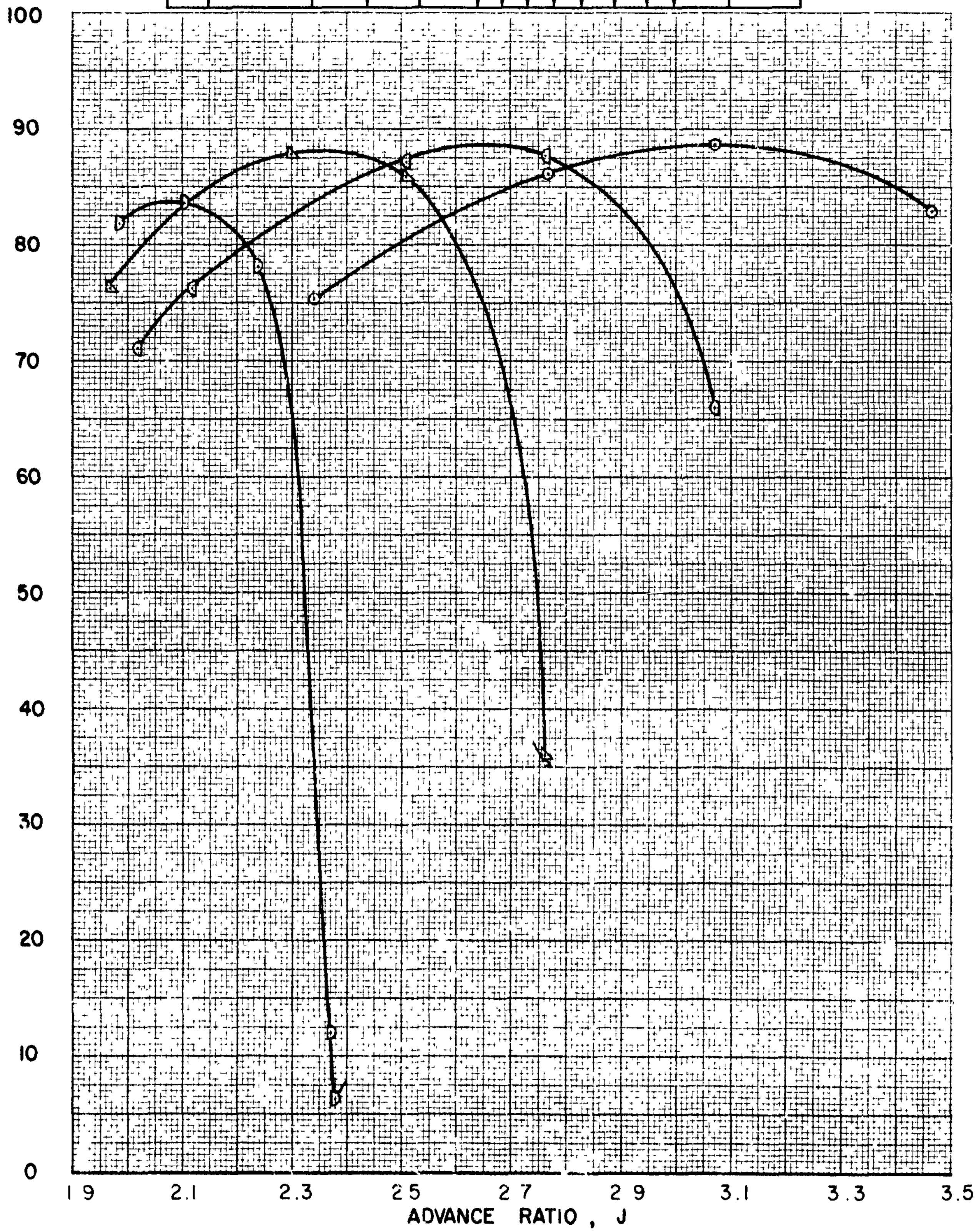

E330590-1

FIG. 170

HSD SHROUDED PROPELLER TEST

EFFECT OF BLADE PLANFORM ON SHROUDED PROPELLER PERFORMANCE

SYM	RUN NO.	MACH NO.	CONFIGURATION	$\theta_{3/4}$
◻	461	0.50	$L_1 C_1 E_1 B_3 P_R T_1 R_1 R_E$	42
◺	455	↓	↓	46
◖	457	↓	↓	50
⊙	460	↓	↓	54

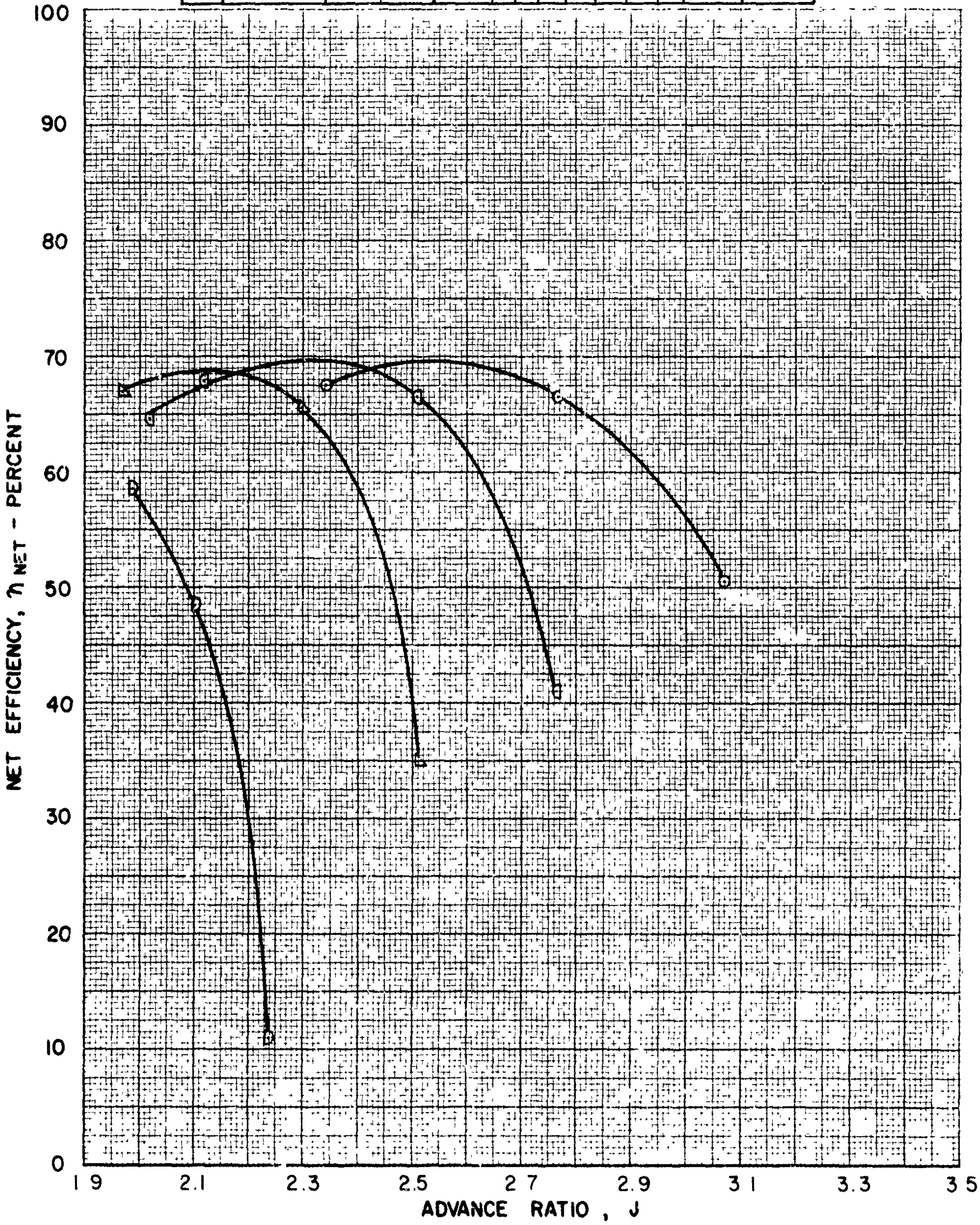

E330590-1 FIG. 171

HSD SHROUDED PROPELLER TEST

EFFECT OF BLADE PLANFORM ON SHROUDED PROPELLER PERFORMANCE

SYM	RUN NO.	MACH NO.	CONFIGURATION	$\theta_{3/4}$
D	461	0.50	$L_1C_1E_1B_3P_RT_1R_1R_E$	42
◺	455	↓	↓	46
◖	457	↓	↓	50
⊙	460	↓	↓	54

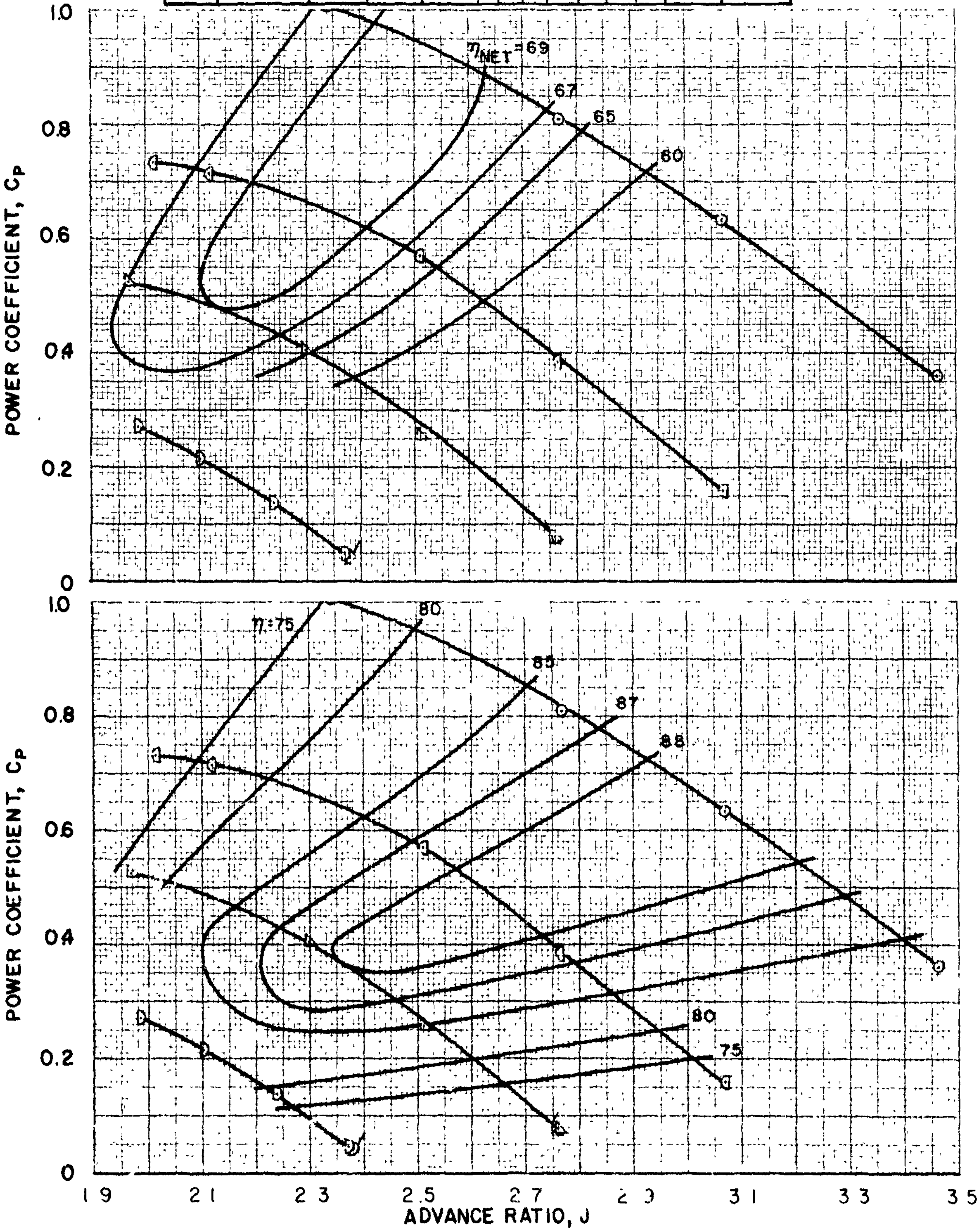

E330590-1

FIG. 172

HSD SHROUDED PROPELLER TEST

EFFECT OF BLADE PLANFORM ON SHROUDED PROPELLER PERFORMANCE

SYM	RUN NO.	MACH NO.	CONFIGURATION	$\theta_{3/4}$
△	213, 52	002, 010	$L_1\ C_1\ E_1\ B_3\ P_{NT}\ T_1\ R_1\ R_E$	20
⊡	214, 55	↓	↓	25
◇	215, 58	↓	↓	30
⊿	217, 219	↓	↓	35

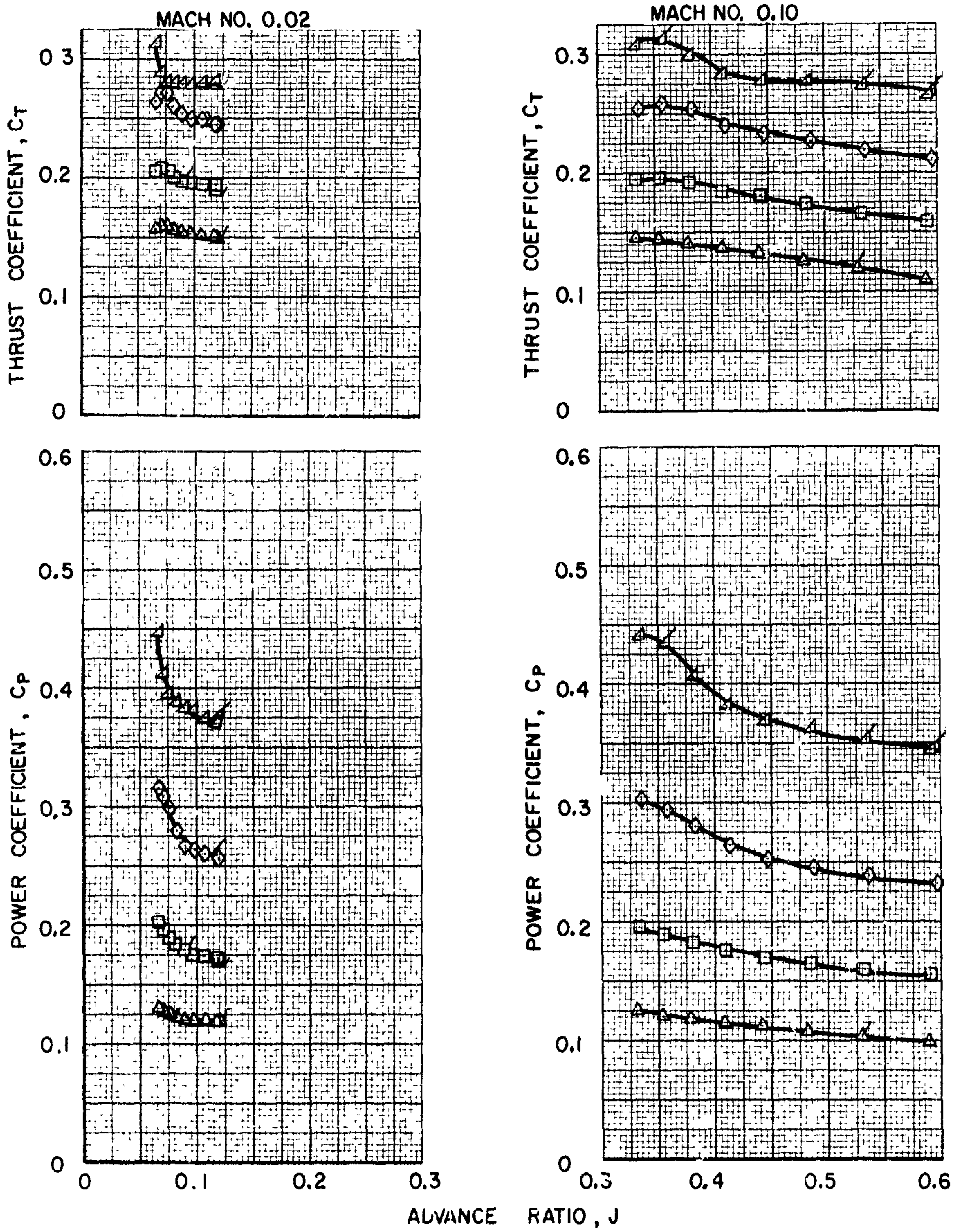

HSD SHROUDED PROPELLER TEST

EFFECT OF BLADE PLANFORM ON SHROUDED PROPELLER PERFORMANCE

SYM	RUN NO.	MACH NO.	CONFIGURATION	$\theta_{3/4}$
△	213 , 52	0.02, 0.10	$L_1\ C_1\ E_1\ B_3\ P_{NT}\ T_1\ R_1\ R_E$	20
□	214 , 5[illegible]	↓	↓	25
◇	215 , 58	↓	↓	30
⊿	217 , 219	↓	↓	35

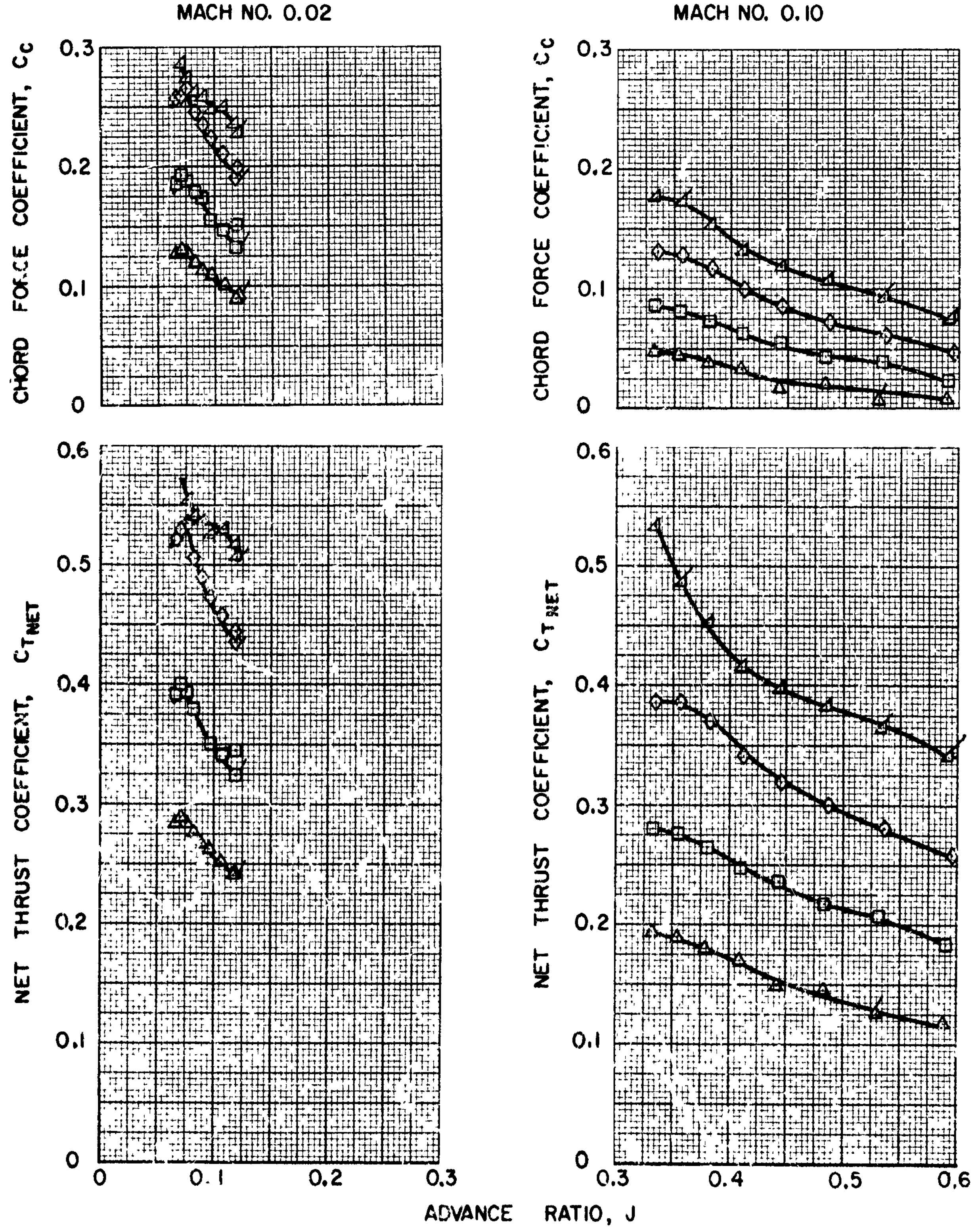

HSD SHROUDED PROPELLER TEST

EFFECT OF BLADE PLANFORM ON SHROUDED PROPELLER PERFORMANCE

SYM	RUN NO.	MACH NO.	CONFIGURATION	$\theta_{3/4}$
△	53	0.20	$L_1 C_1 E_1 B_3 P_{NT} T_1 R_1 R_E$	20
⊡	56	↓	↓	25
◇	57	↓	↓	30
⊿	220	↓	↓	35

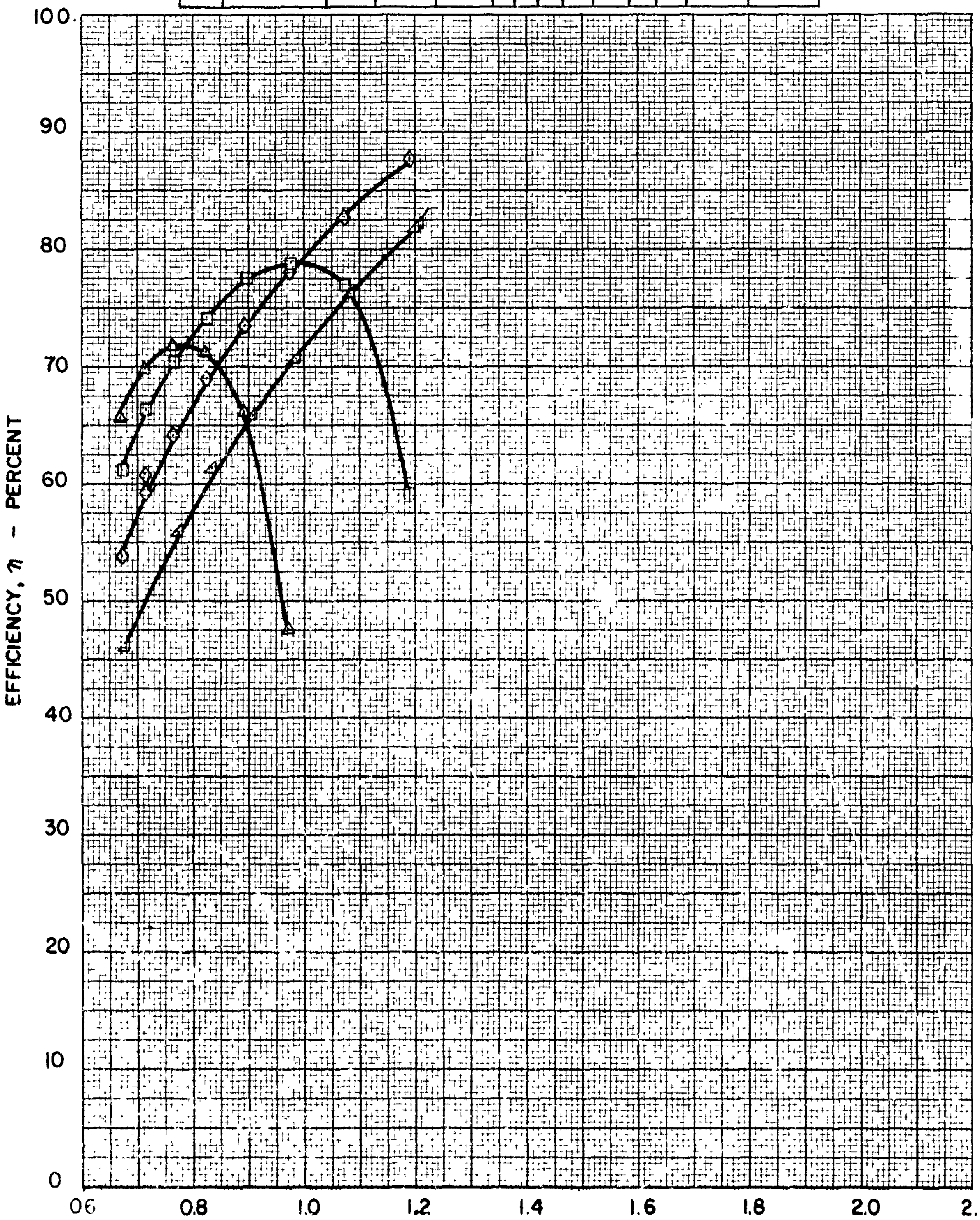

E330590-1

FIG.175

HSD SHROUDED PROPELLER TEST

EFFECT OF BLADE PLANFORM ON SHROUDED PROPELLER PERFORMANCE

SYM	RUN NO.	MACH NO.	CONFIGURATION	$\theta_{3/4}$
△	53	0 20	$L_1C_1E_1B_3P_{NT}\ T_1\ R_1\ R_E$	20
⊡	56			25
◇	57			30
⊿	220			35

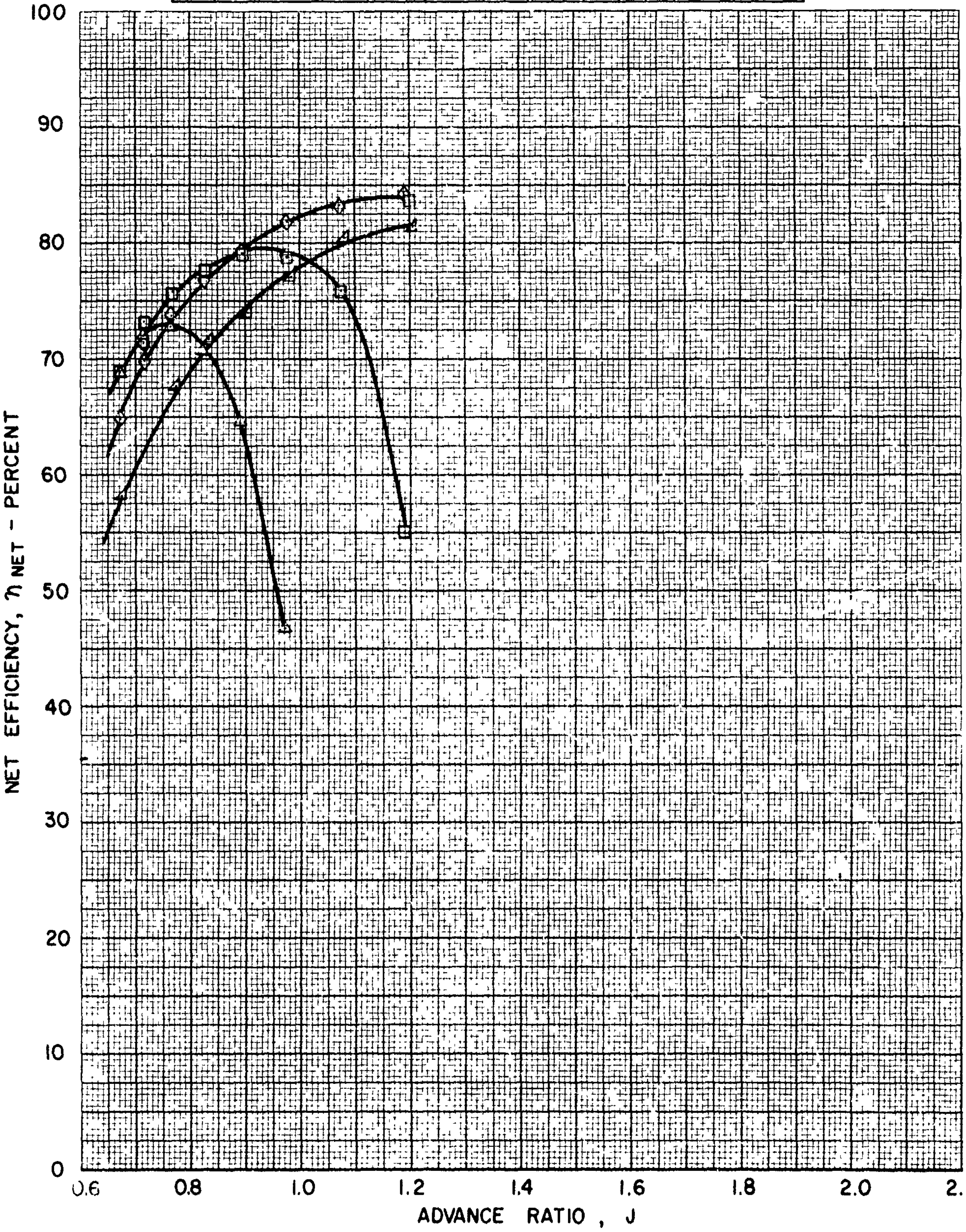

HSD SHROUDED PROPELLER TEST

EFFECT OF BLADE PLANFORM ON SHROUDED PROPELLER PERFORMANCE

SYM	RUN NO.	MACH NO.	CONFIGURATION	$\theta_{3/4}$
△	53	0.20	$L_1 C_1 E_1 B_3 P_{NT} T_1 R_1 R_E$	20
□	56			25
◇	57			30
⊿	220			35

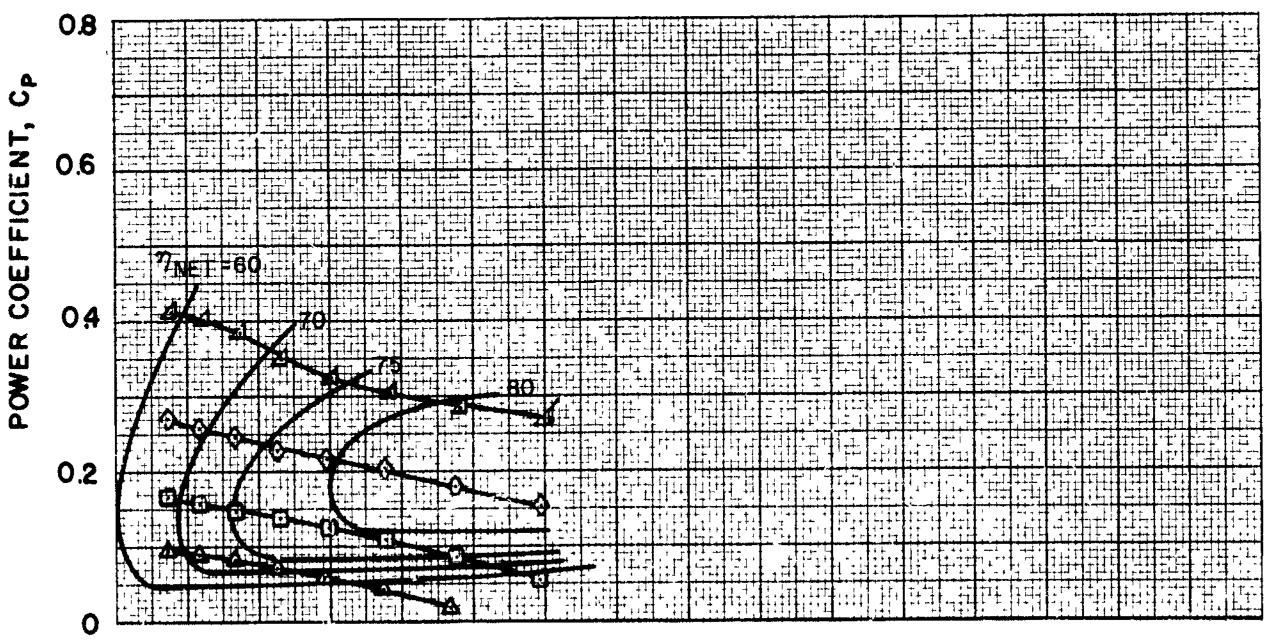

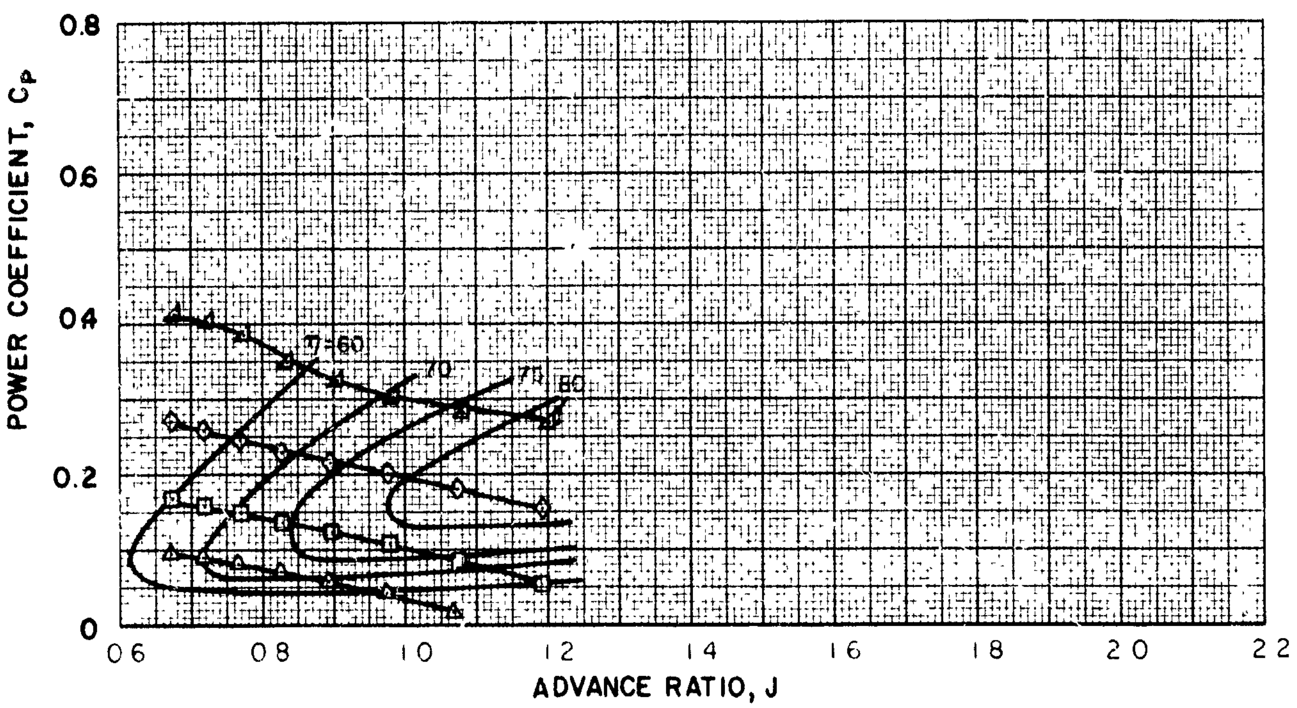

E330590-1 FIG. 177

HSD SHROUDED PROPELLER TEST

EFFECT OF BLADE PLANFORM ON SHROUDED PROPELLER PERFORMANCE

SYM	RUN NO.	MACH NO.	CONFIGURATION	$\theta_{3/4}$
◇	627	0.31	$L_1 C_1 E_1 B_3 P_{NT} T_1 R_1 R_E$	30
◿	628			34
▽	629			38
D	631			42

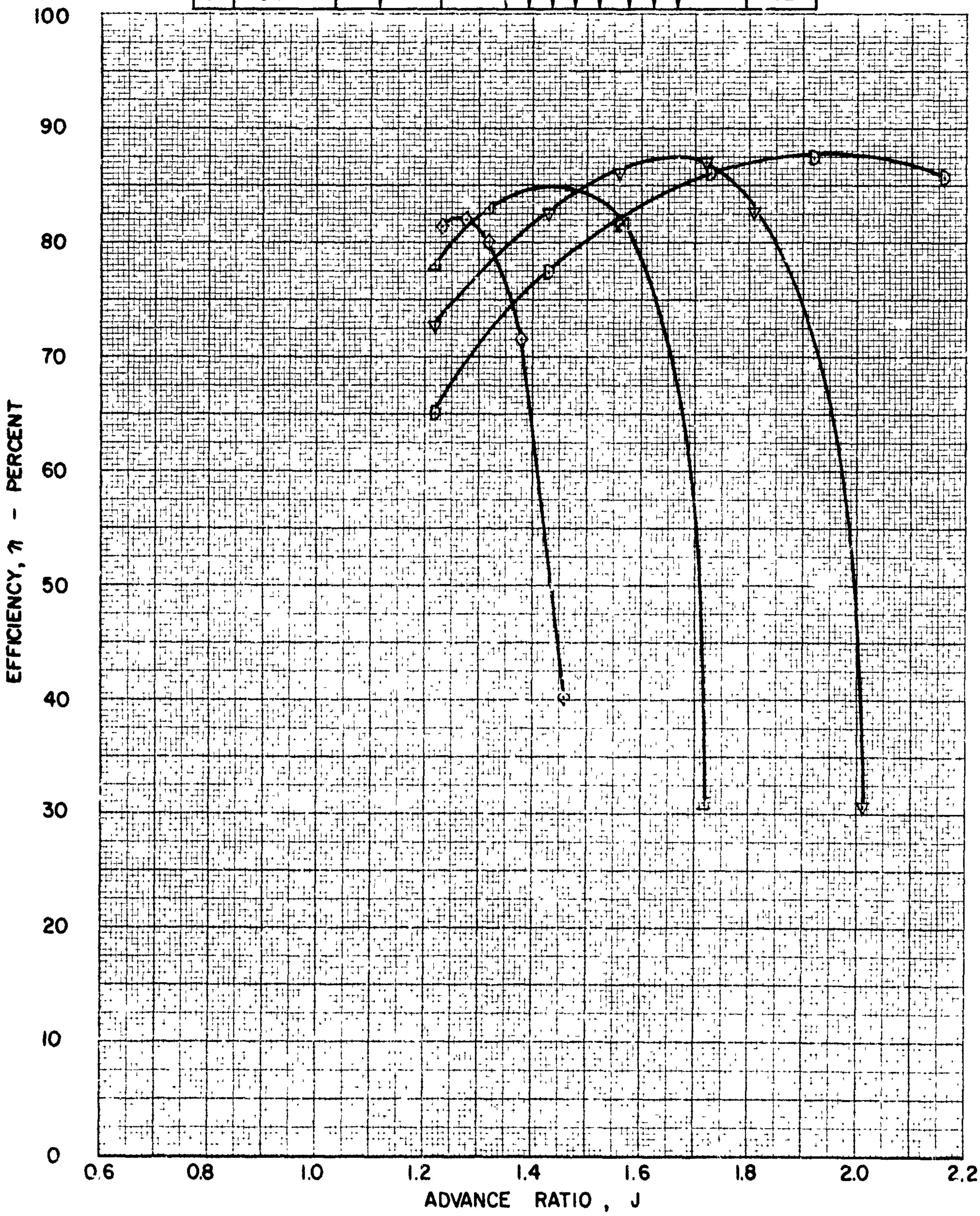

E330590-1 FIG. 178

HSD SHROUDED PROPELLER TEST

EFFECT OF BLADE PLANFORM ON SHROUDED PROPELLER PERFORMANCE

SYM	RUN NO.	MACH NO.	CONFIGURATION	$\theta_{3/4}$
◇	627	0.31	$L_1 C_1 E_1 B_3 P_{NT} T_1 R_1 R_E$	30
◿	628	↓	↓	34
▽	629	↓	↓	38
D	631	↓	↓	42

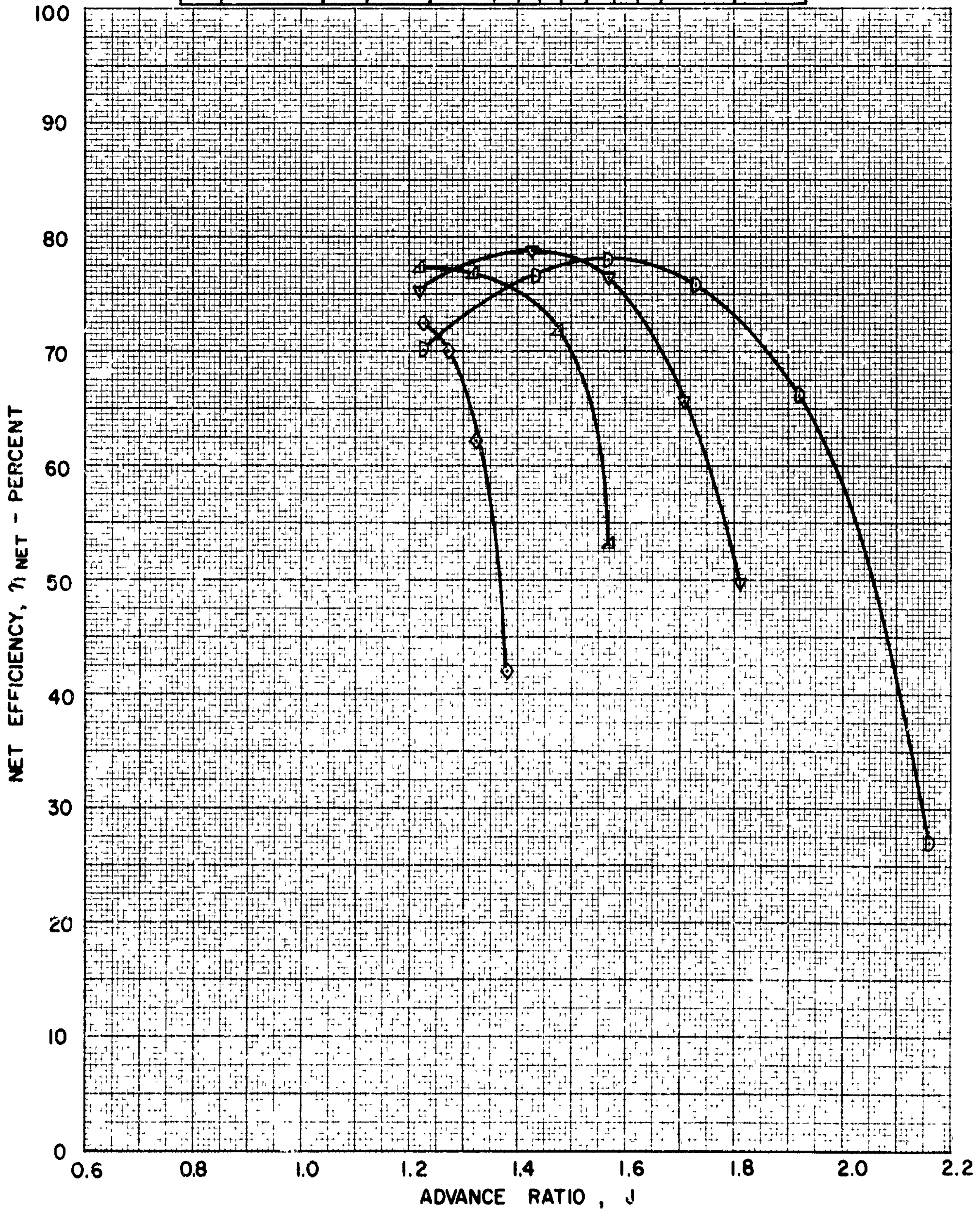

HSD SHROUDED PROPELLER TEST

EFFECT OF BLADE PLANFORM ON SHROUDED PROPELLER PERFORMANCE

SYM	RUN NO.	MACH NO.	CONFIGURATION	$\theta_{3/4}$
◇	627	0.31	$L_1 C_1 E_1 B_3 P_{NT} T_1 R_1 R_E$	30
◁	628	↓	↓	34
▽	629	↓	↓	38
D	631	↓	↓	42

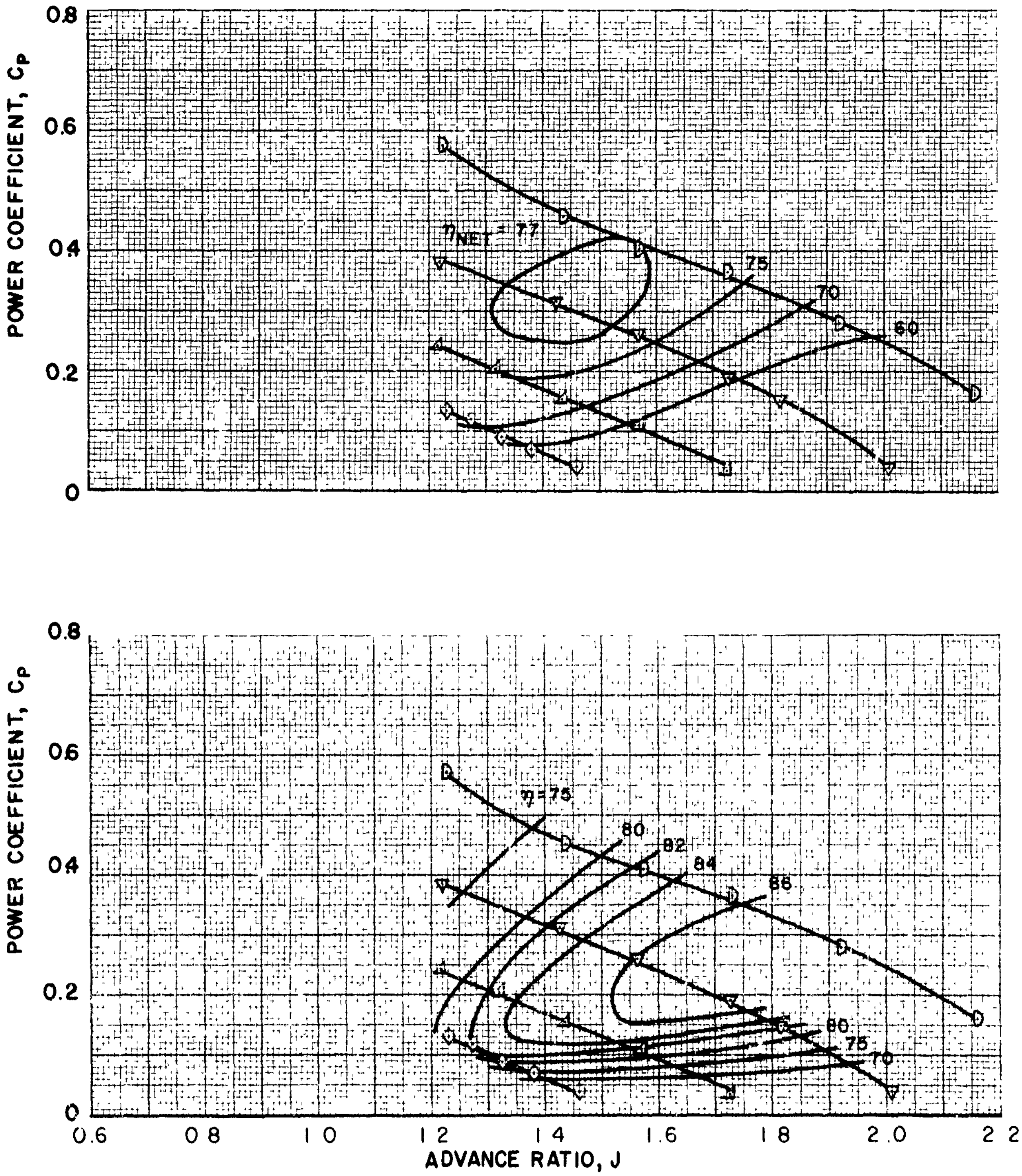

HSD SHROUDED PROPELLER TEST

EFFECT OF BLADE PLANFORM ON SHROUDED PROPELLER PERFORMANCE

SYM	RUN NO.	MACH NO.	CONFIGURATION	$\theta_{3/4}$
▽	630	0.41	$L_1 C_1 E_1 B_3 P_{NT} T_1 R_1 R_E$	38
D	632			42
◺	635			46
◖	637			50

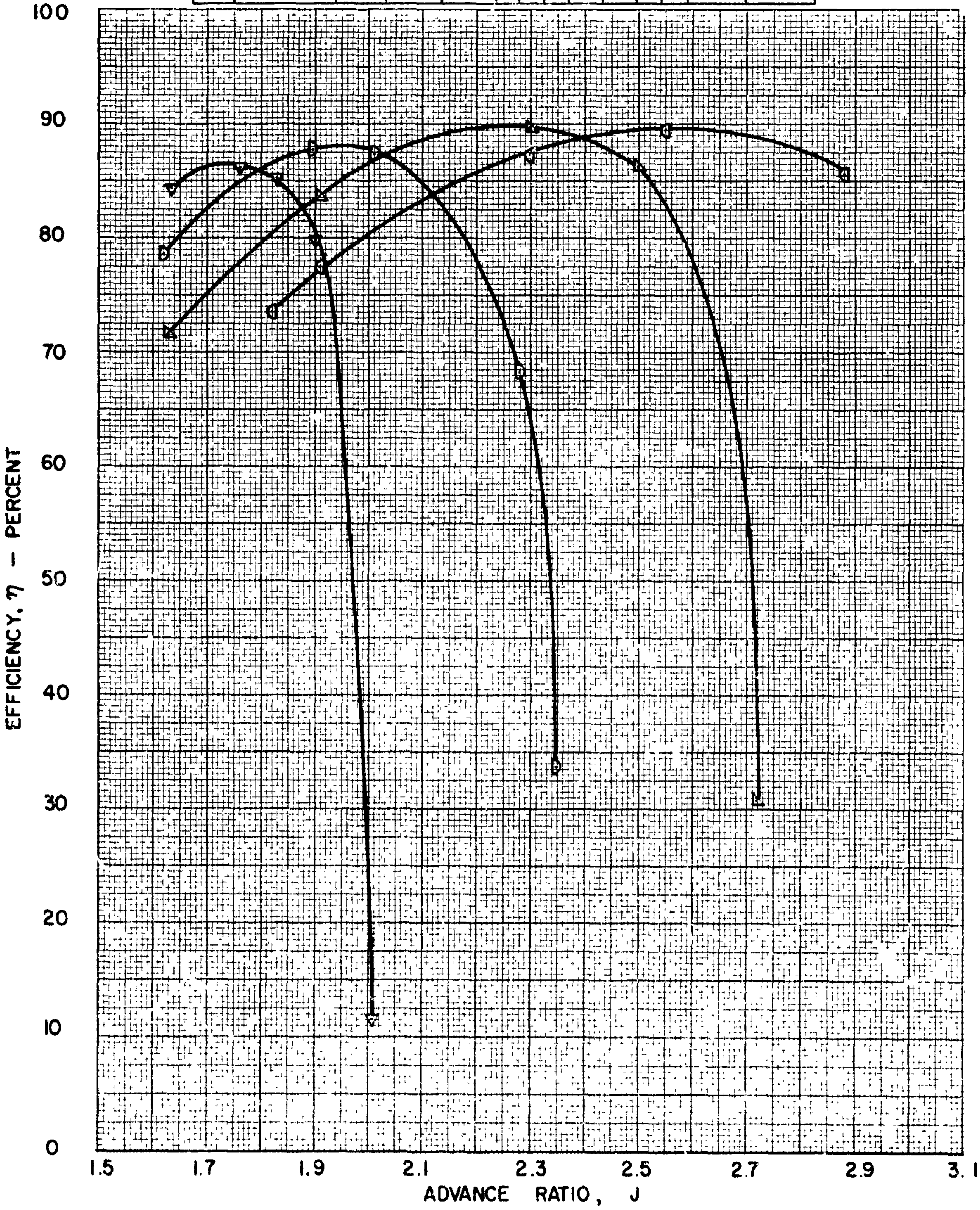

E330590-1

FIG. 181

HSD SHROUDED PROPELLER TEST

EFFECT OF BLADE PLANFORM ON SHROUDED PROPELLER PERFORMANCE

SYM	RUN NO.	MACH NO.	CONFIGURATION	$\beta_{3/4}$
▽	630	0.41	$L_1 C_1 F_1 B_3 P_{NT} T_1 R_1 R_E$	38
D	632			42
◺	635			46
C	637			50

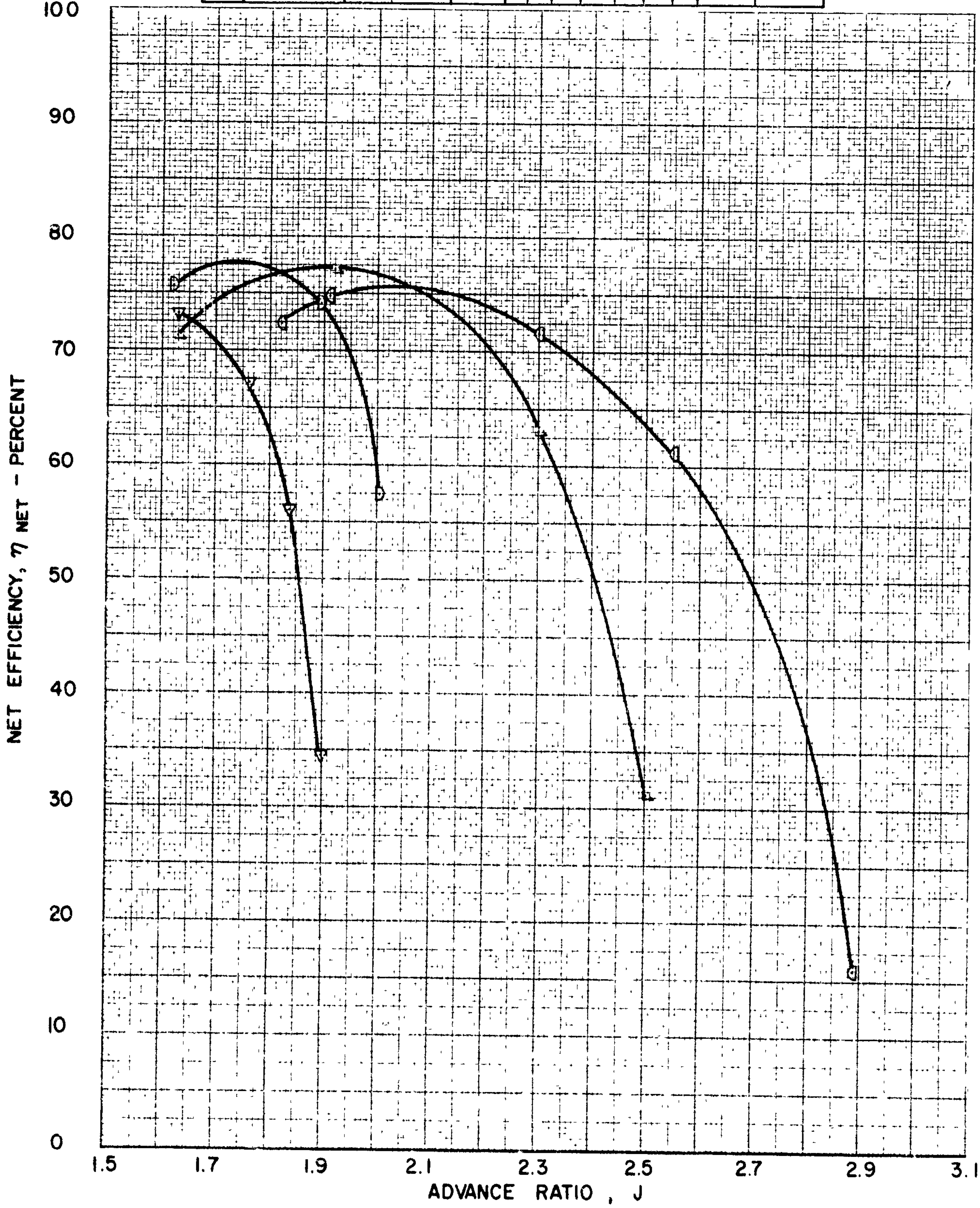

HSD SHROUDED PROPELLER TEST

EFFECT OF BLADE PLANFORM ON SHROUDED PROPELLER PERFORMANCE

SYM	RUN NO.	MACH NO.	CONFIGURATION	$\theta_{3/4}$
▽	630	0.41	$L_1 C_1 E_1 B_3 P_{NT} T_1 R_1 R_E$	38
D	632	↓	↓	42
◺	635	↓	↓	46
◖	637	↓	↓	50

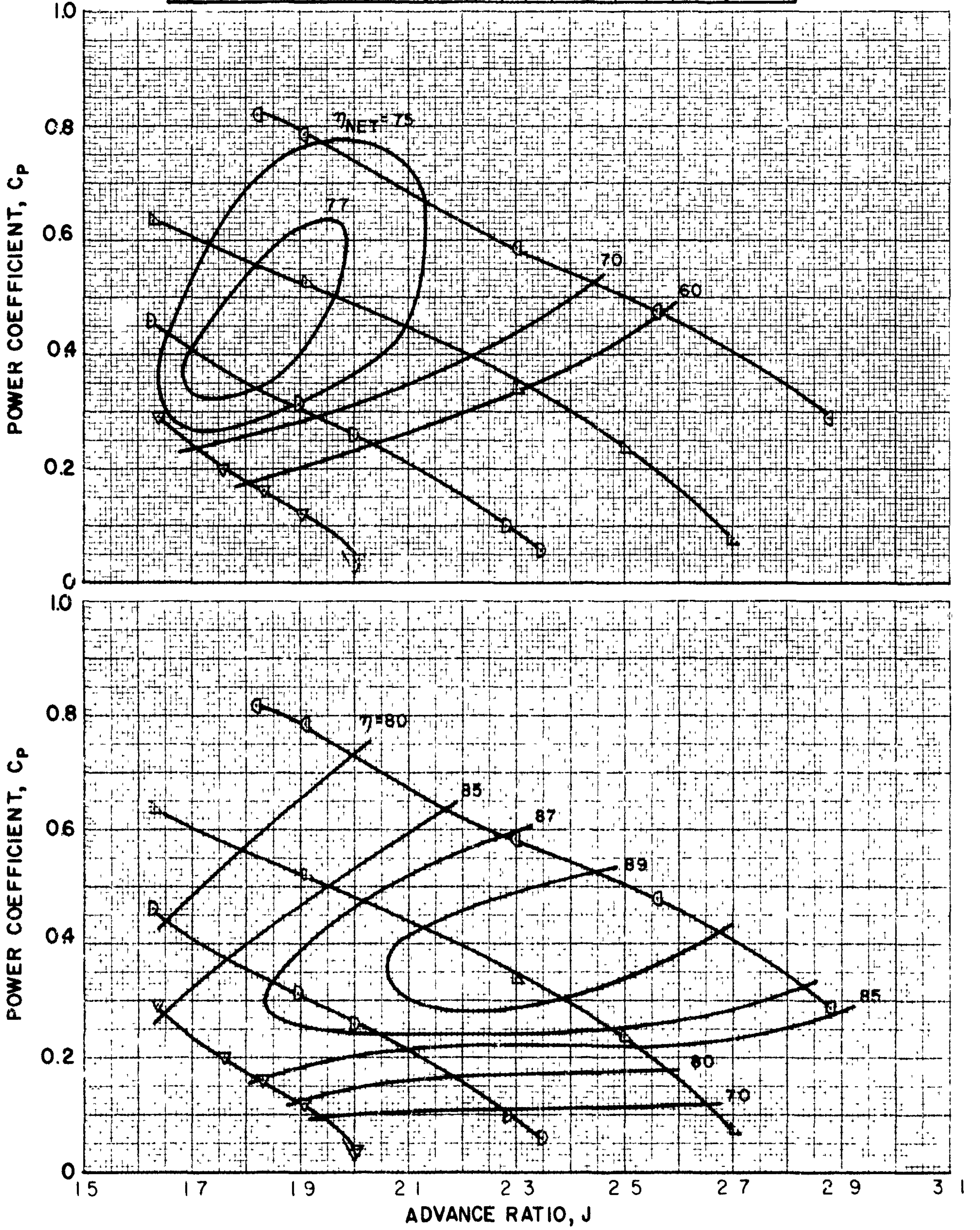

E330590-1

FIG. 183

HSD SHROUDED PROPELLER TEST

EFFECT OF BLADE PLANFORM ON SHROUDED PROPELLER PERFORMANCE

SYM	RUN NO.	MACH NO.	CONFIGURATION	$\theta_{3/4}$
△	636	0.52	$L_1 C_1 E_1 B_3 P_{NT} T_1 R_1 R_E$	46
◐	638	↓	↓	50
○	639	↓	↓	54

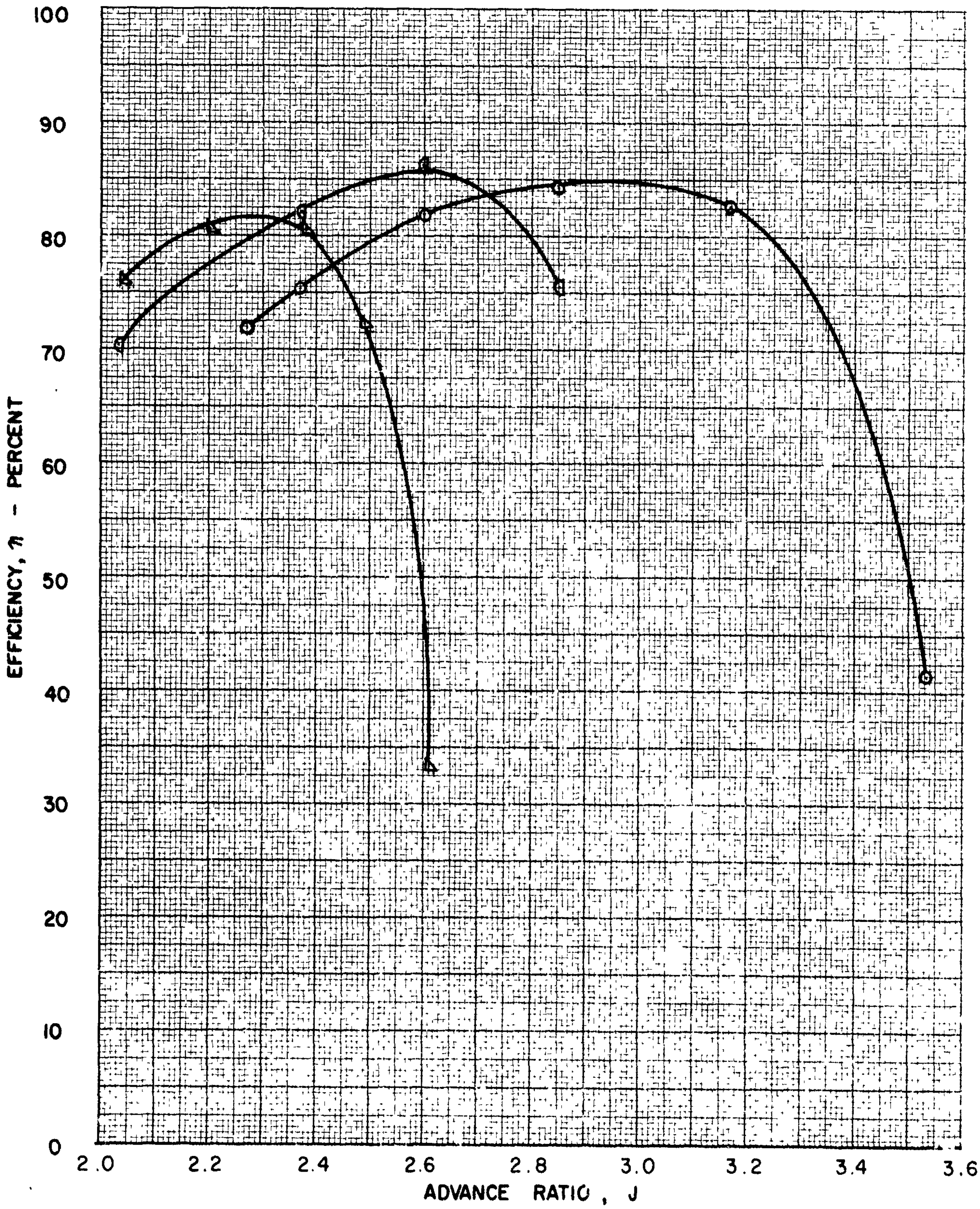

E330590-1

FIG. 184

HSD SHROUDED PROPELLER TEST

EFFECT OF BLADE PLANFORM ON SHROUDED PROPELLER PERFORMANCE

SYM	RUN NO.	MACH NO.	CONFIGURATION	$\theta_{3/4}$
△	636	0.52	$L_1 C_1 E_1 B_3 P_{NT} T_1 R_1 P_E$	46
◐	638	↓	↓	50
○	639	↓	↓	54

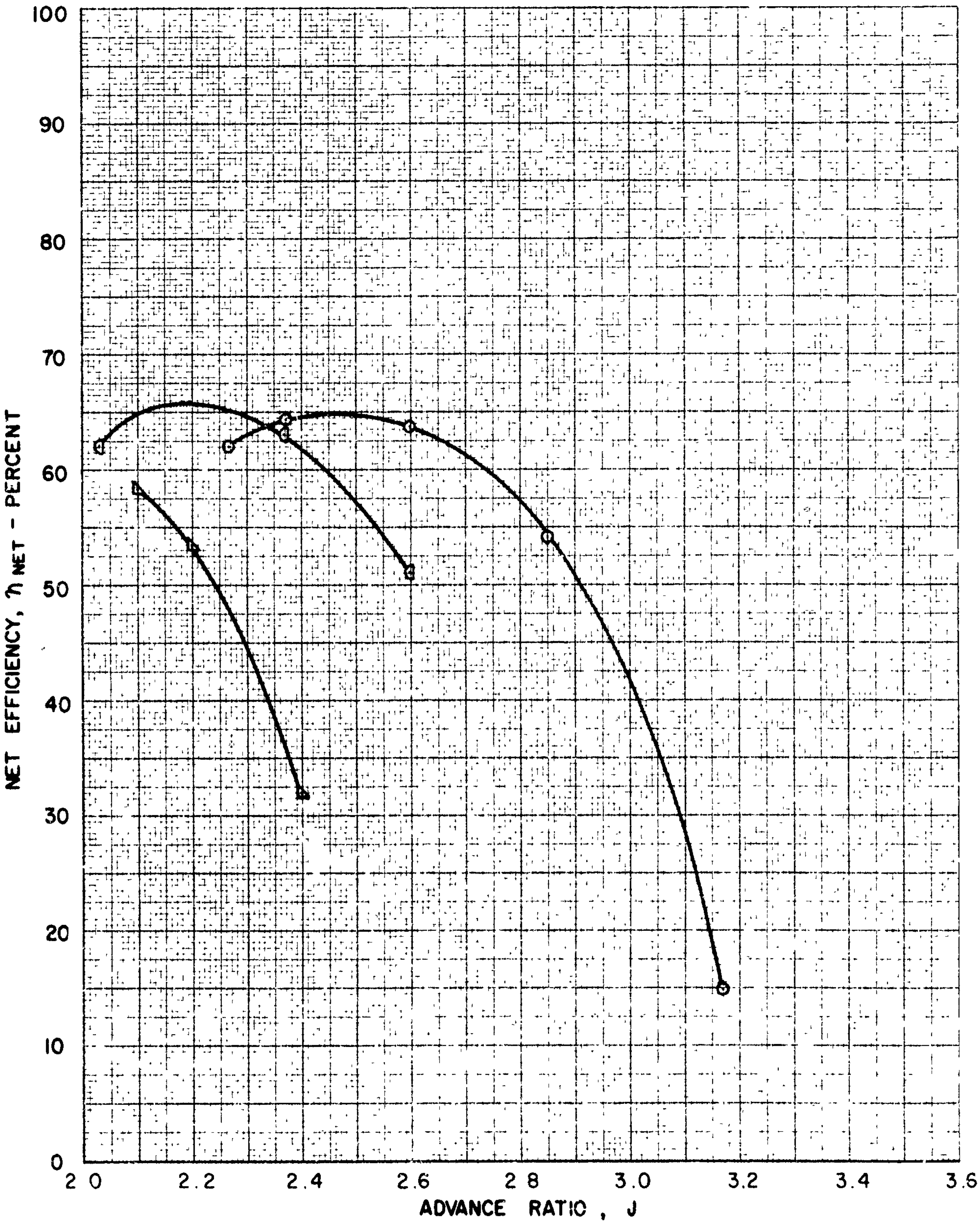

HSD SHROUDED PROPELLER TEST

EFFECT OF BLADE PLANFORM ON SHROUDED PROPELLER PERFORMANCE

SYM	RUN NO.	MACH NO.	CONFIGURATION	$\theta_{3/4}$
△	636	0.52	$L_1 C_1 E_1 B_3 P_{NT} T_1 R_1 R_E$	46
◁	638	↓	↓	50
○	639	↓	↓	54

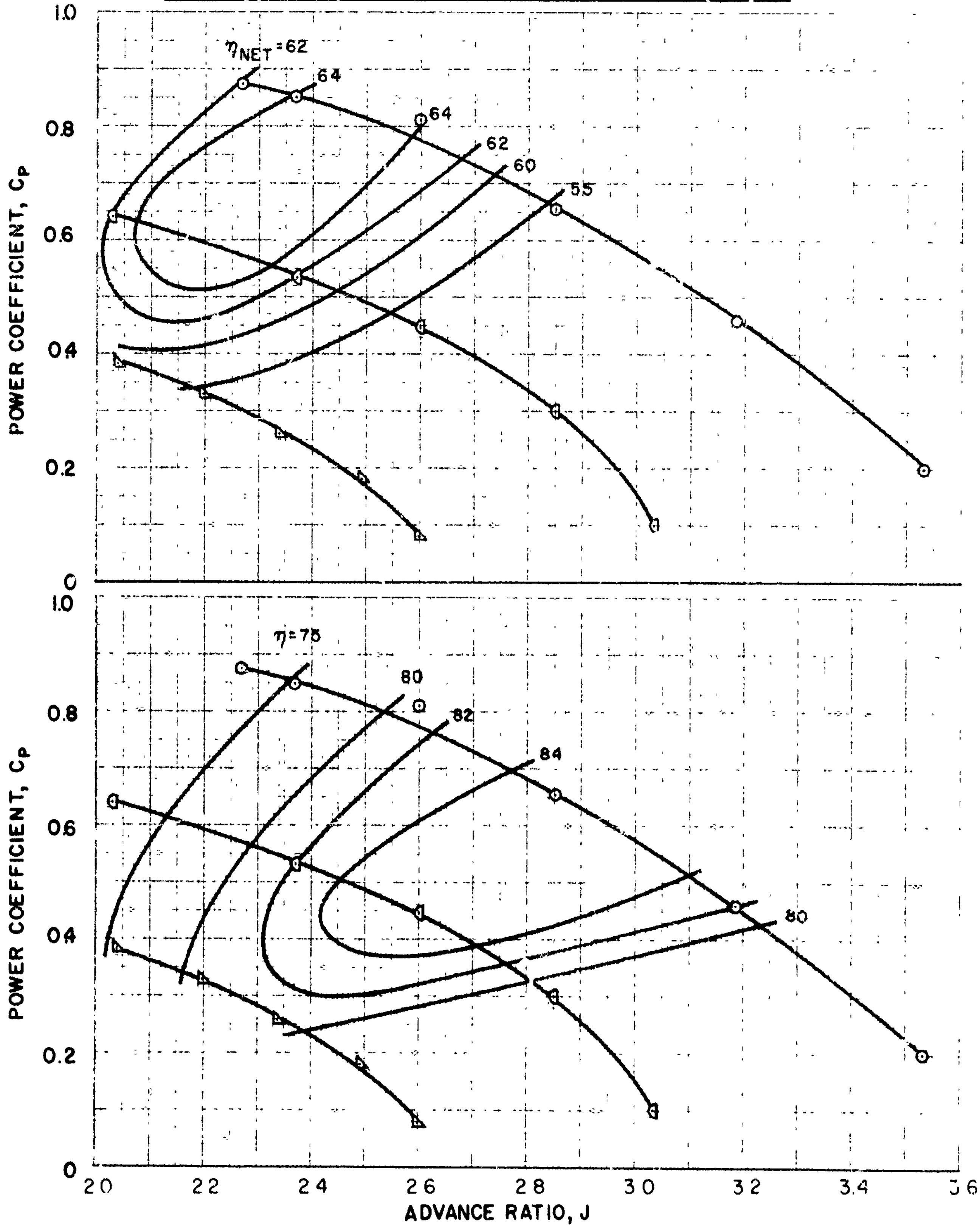

HSD SHROUDED PROPELLER TEST

EFFECT OF 4-WAY BLADES ON SHROUDED PROPELLER PERFORMANCE

SYM	RUN NO.	MACH NO.	CONFIGURATION	$\theta_{3/4}$
△	188, 189	0.02, 0.10	$L_1 C_1 E_1 B_4 P_{NT} T_1 R_1 R_E$	20
□	191, 192			25
◇	196, 195			30
⊿	'37, 198			35

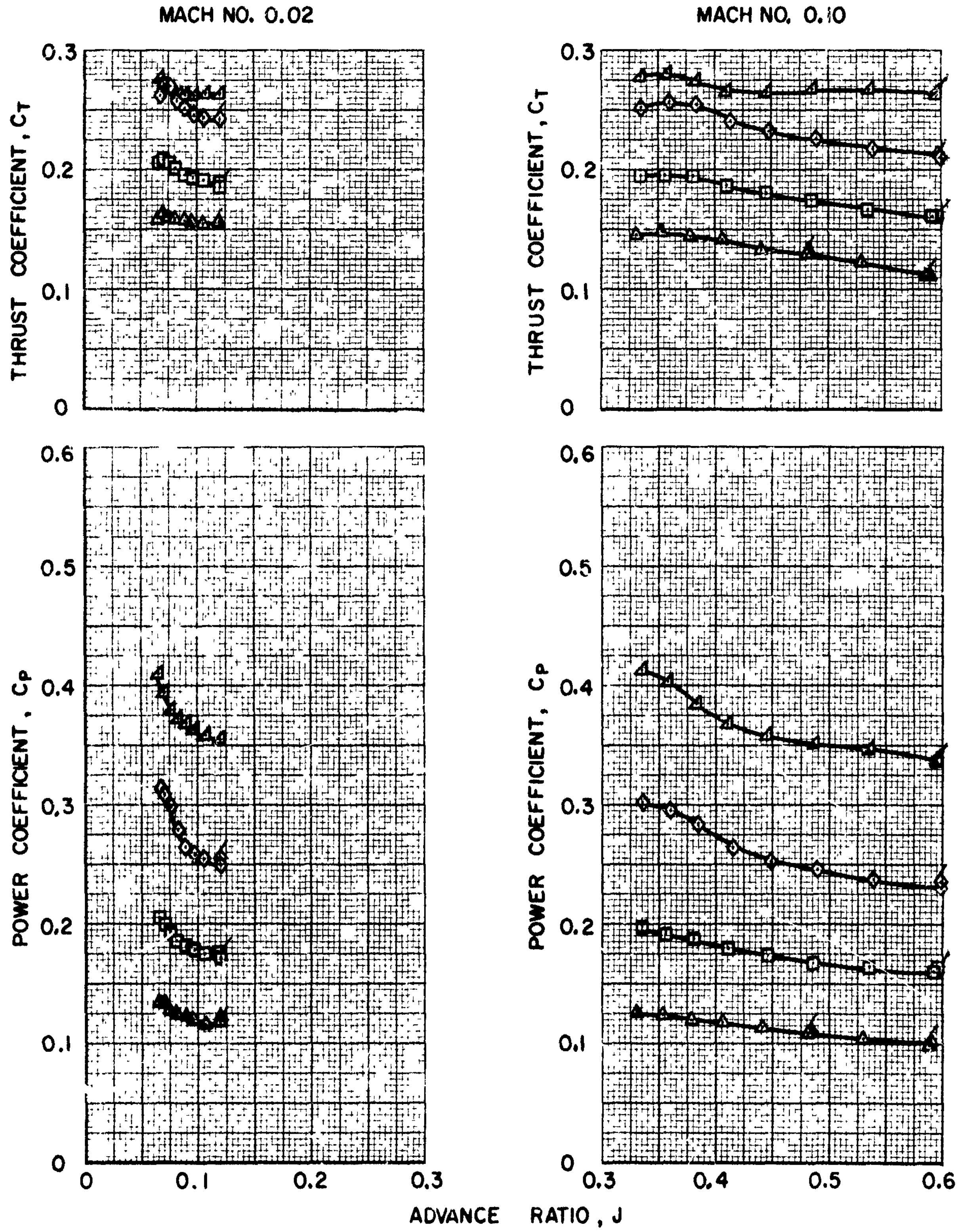

HSD SHROUDED PROPELLER TEST

EFFECT OF 4-WAY BLADES ON SHROUDED PROPELLER PERFORMANCE

SYM	RUN NO.	MACH NO.	CONFIGURATION	$\theta_{3/4}$
△	188, 189	0.02, 0.10	$L_1 C_1 E_1 B_4 P_{NT} T_1 R_1 R_E$	20
□	191, 192	↓	↓	25
◇	196, 195	↓	↓	30
⊿	197, 198	↓	↓	35

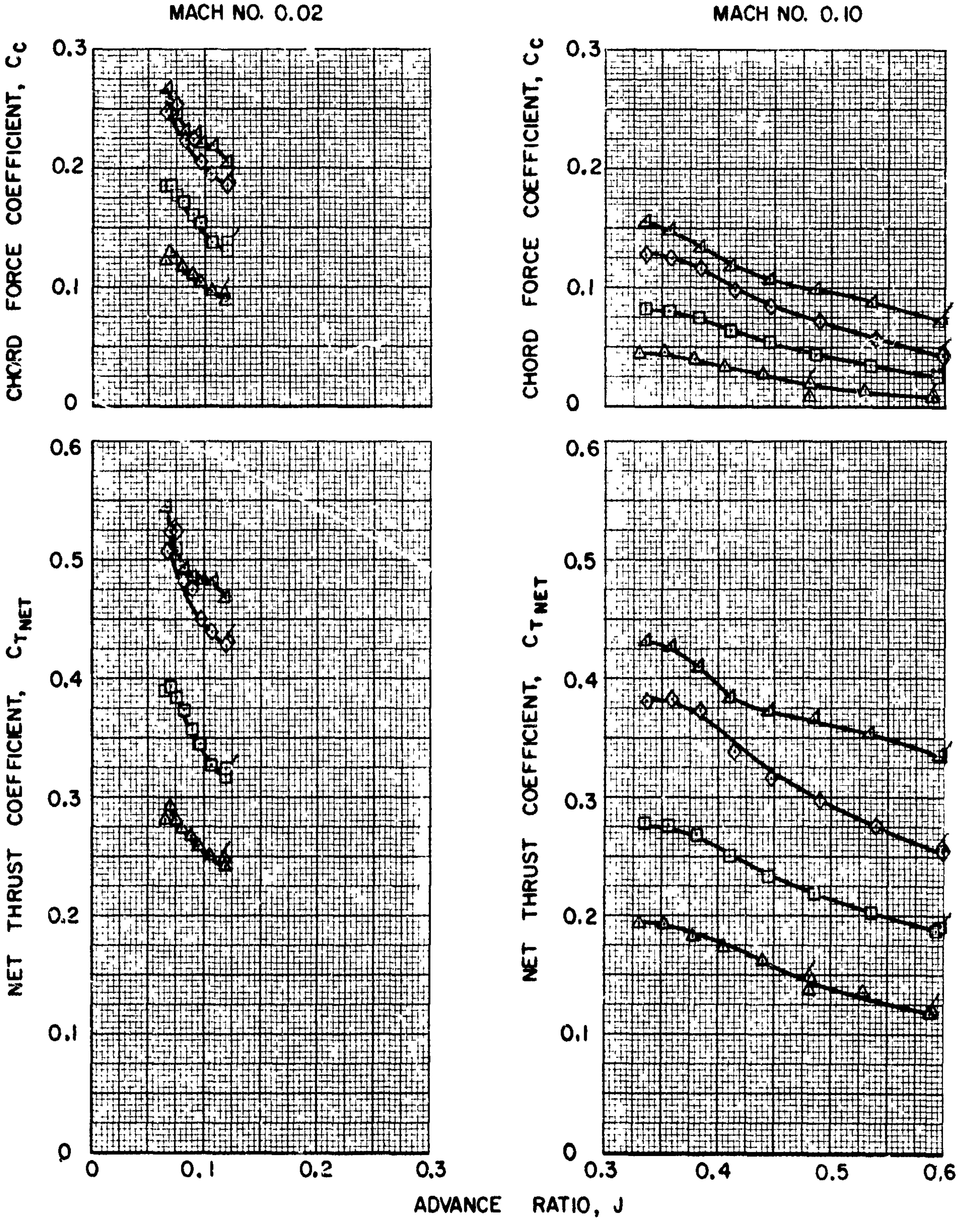

HSD SHROUDED PROPELLER TEST

EFFECT OF 4-WAY BLADES ON SHROUDED PROPELLER PERFORMANCE

SYM	RUN NO.	MACH NO.	CONFIGURATION	$\theta_{3/4}$
△	190	0.20	$L_1 C_1 E_1 B_4 P_{NT} T_1 R_1 R_E$	20
□	193	↓	↓	25
◇	194	↓	↓	30
⊿	199	↓	↓	35

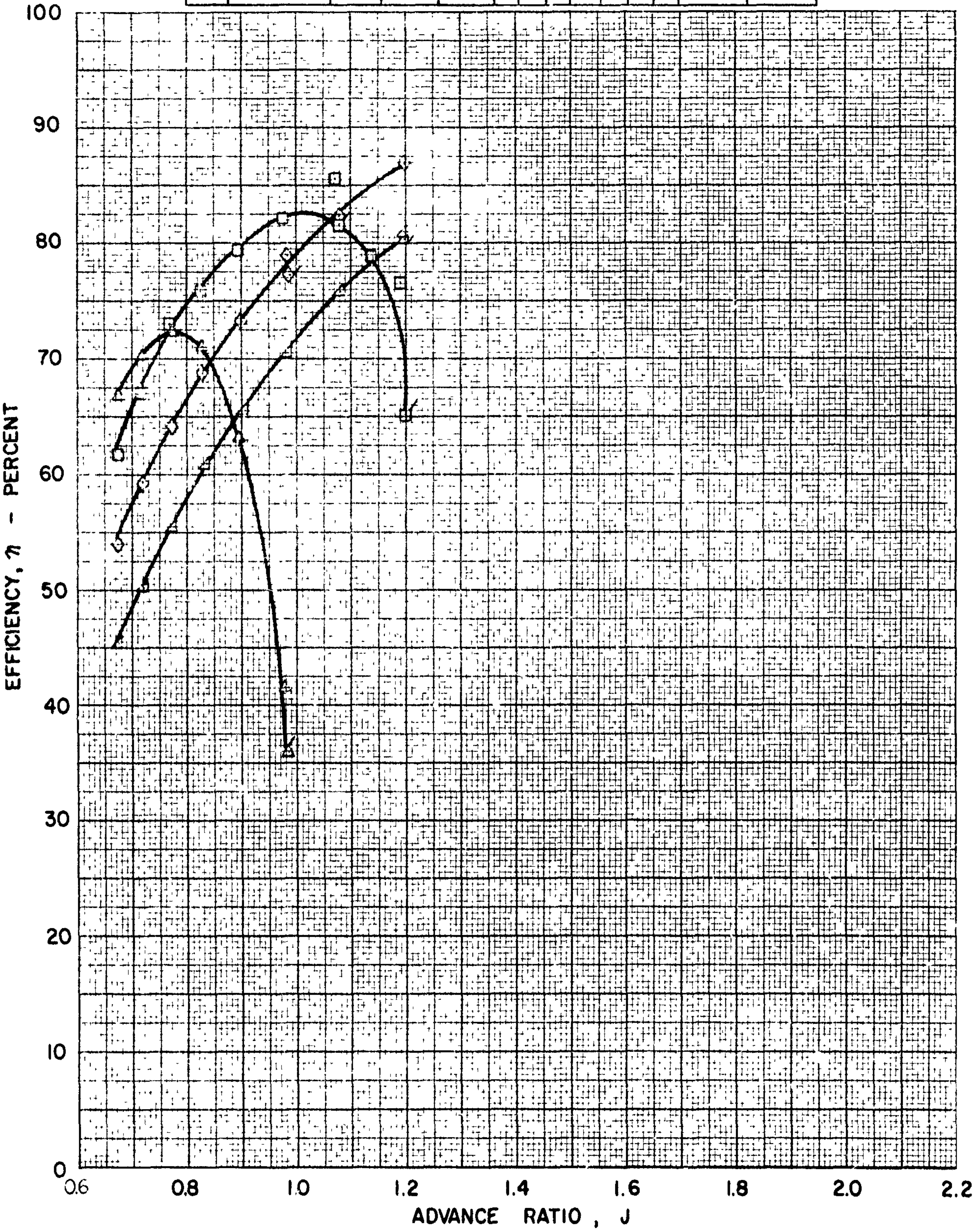

E330590-1

FIG. 189

HSD SHROUDED PROPELLER TEST

EFFECT OF 4-WAY BLADES ON SHROUDED PROPELLER PERFORMANCE

SYM	RUN NO.	MACH NO.	CONFIGURATION	$\theta_{3/4}$
△	190	0.20	$L_1 C_1 E_1 B_4 P_{NT} T_1 R_1 R_E$	20
□	193	↓	↓	25
◇	194	↓	↓	30
⊿	199	↓	↓	35

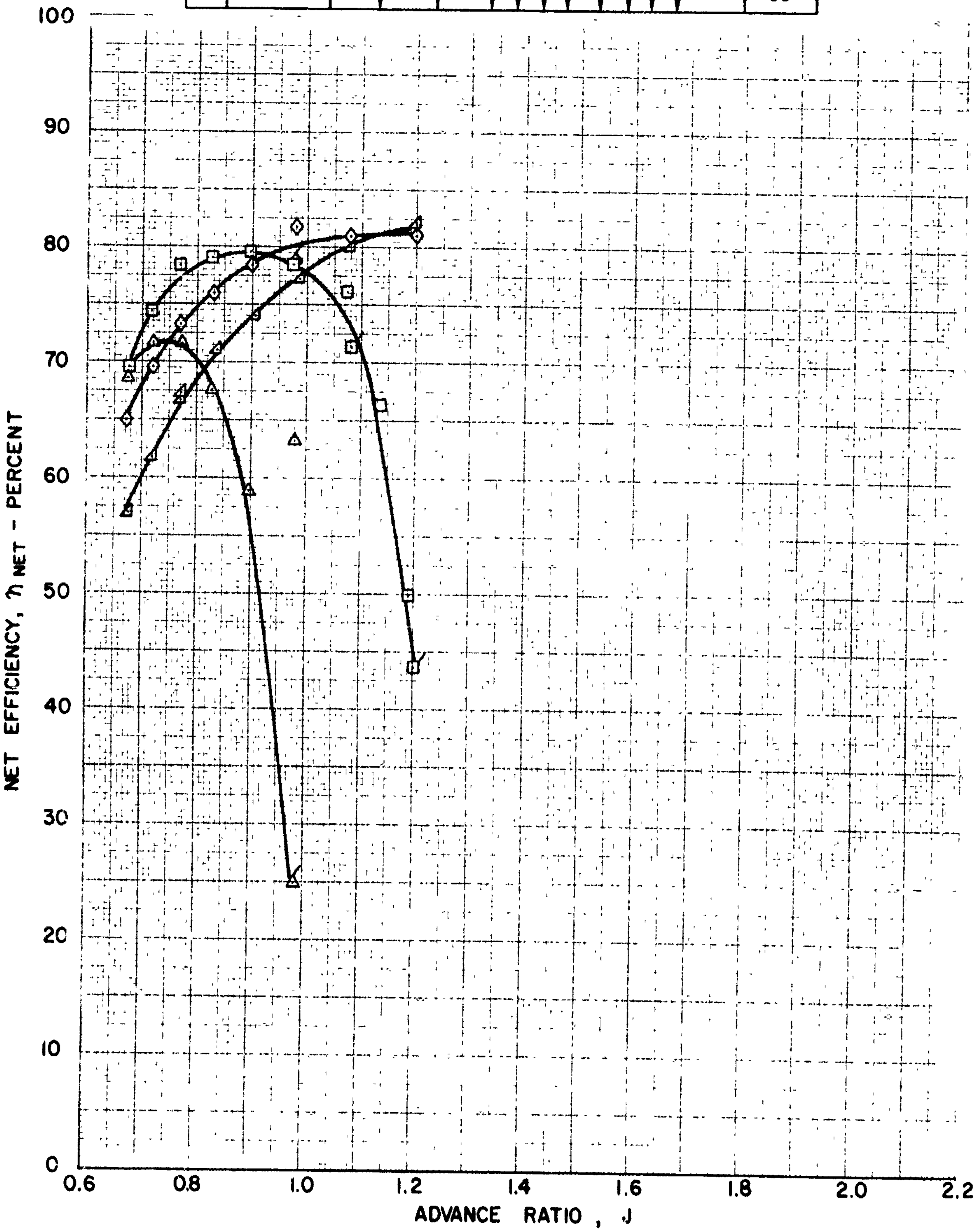

E330590-1

FIG.190

HSD SHROUDED PROPELLER TEST

EFFECT OF 4-WAY BLADE ON SHROUDED PROPELLER PERFORMANCE

SYM	RUN NO.	MACH NO.	CONFIGURATION	$\theta_{3/4}$
△	190	0.20	$L_1 C_1 E_1 B_4 P_{NT} T_1 R_1 R_E$	20
□	193			25
◇	194			30
◿	199			35

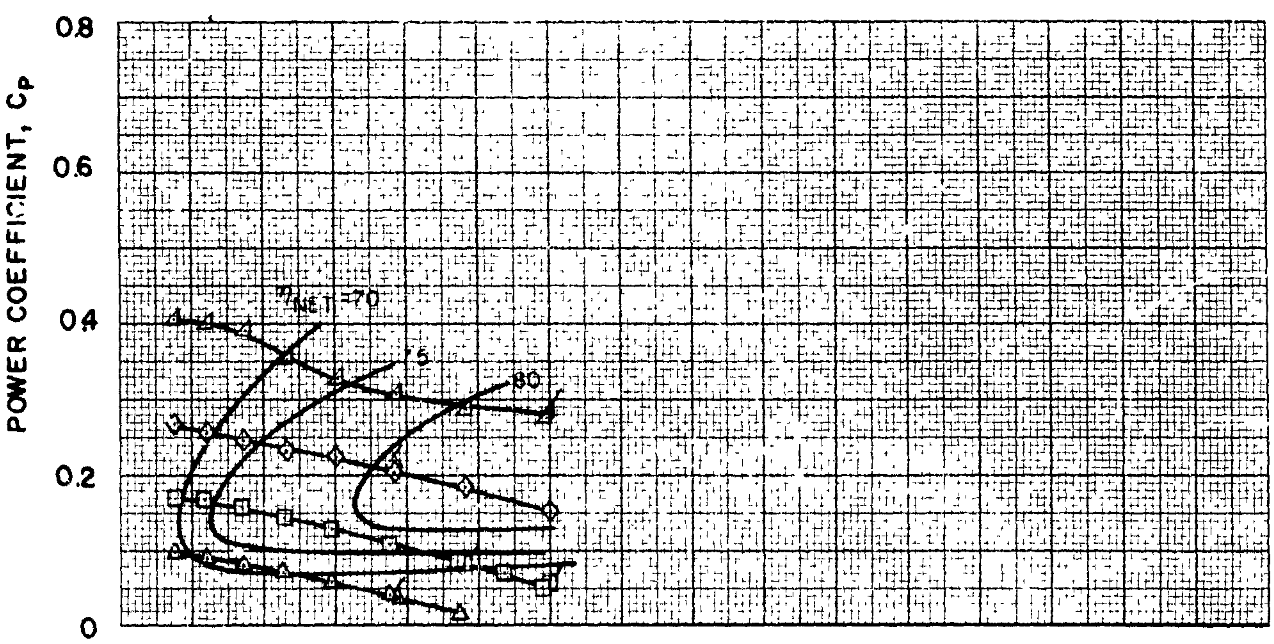

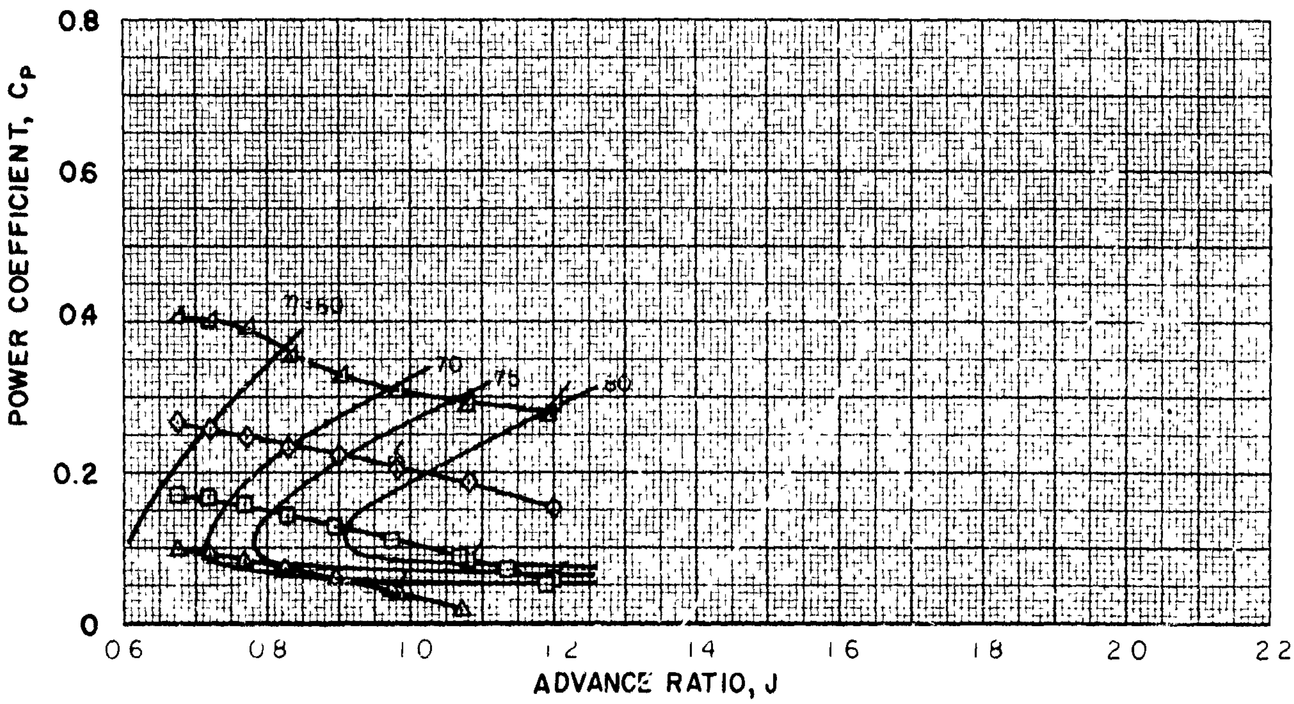

E330590-1

FIG. 191

HSD SHROUDED PROPELLER TEST

EFFECT OF 4-WAY BLADES ON SHROUDED PROPELLER PERFORMANCE

SYM	RUN NO.	MACH NO.	CONFIGURATION	$\theta_{3/4}$
◺	435	0.30	$L_1\ C_1\ E_1\ B_4\ P_{NT}\ T_1\ R_1\ R_E$	34
▽	436	↓	↓	38
D	437	↓	↓	42
◺	439	↓	↓	46

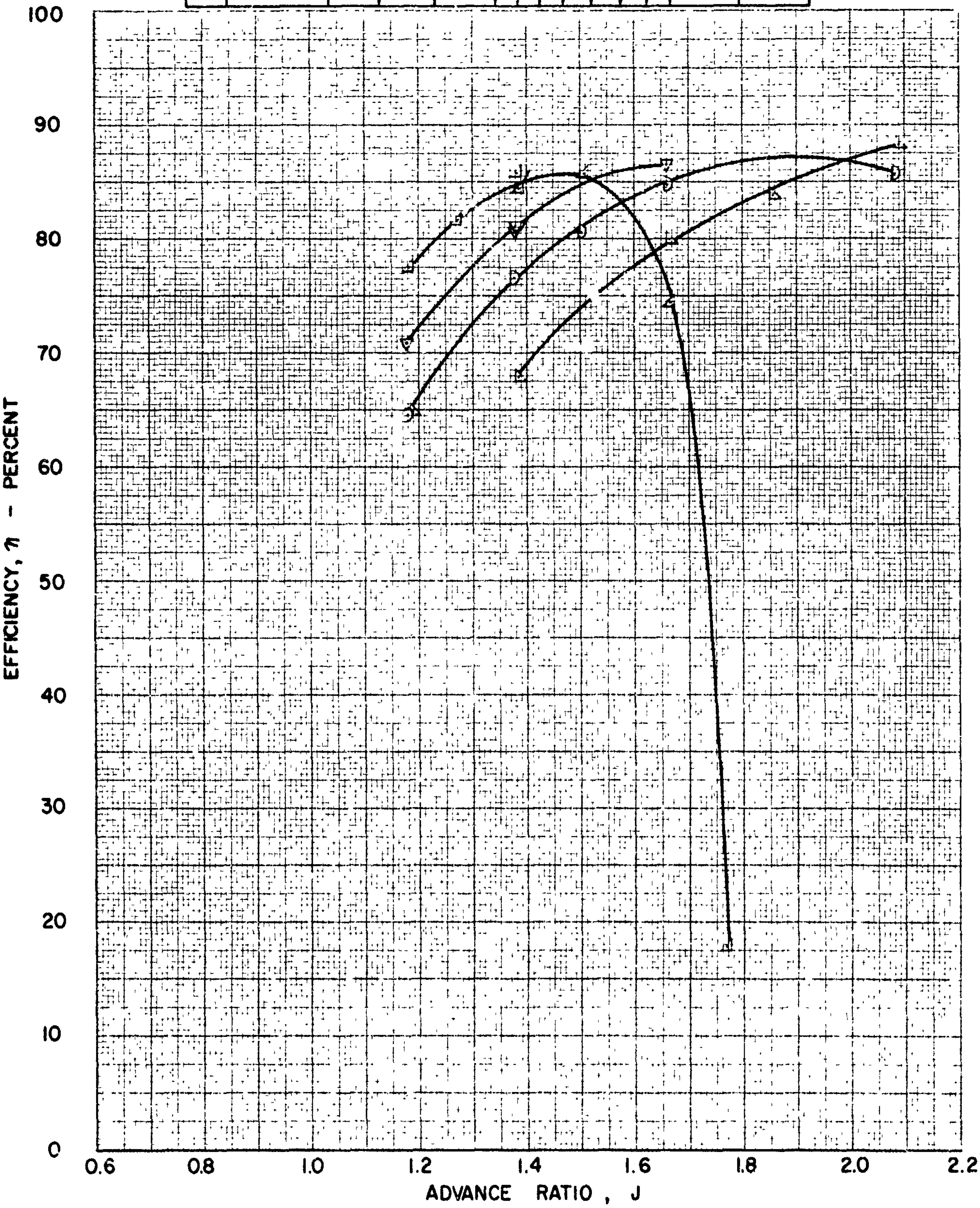

E330590-1

FIG. 192

HSD SHROUDED PROPELLER TEST

EFFECT OF 4-WAY BLADES ON SHROUDED PROPELLER PERFORMANCE

SYM	RUN NO.	MACH NO.	CONFIGURATION	$\theta_{3/4}$
◺	435	0.30	L_1 C_1 E_1 B_4 P_{NT} T_1 R_1 R_E	34
▽	436	↓	↓	38
D	437	↓	↓	42
◺	439	↓	↓	46

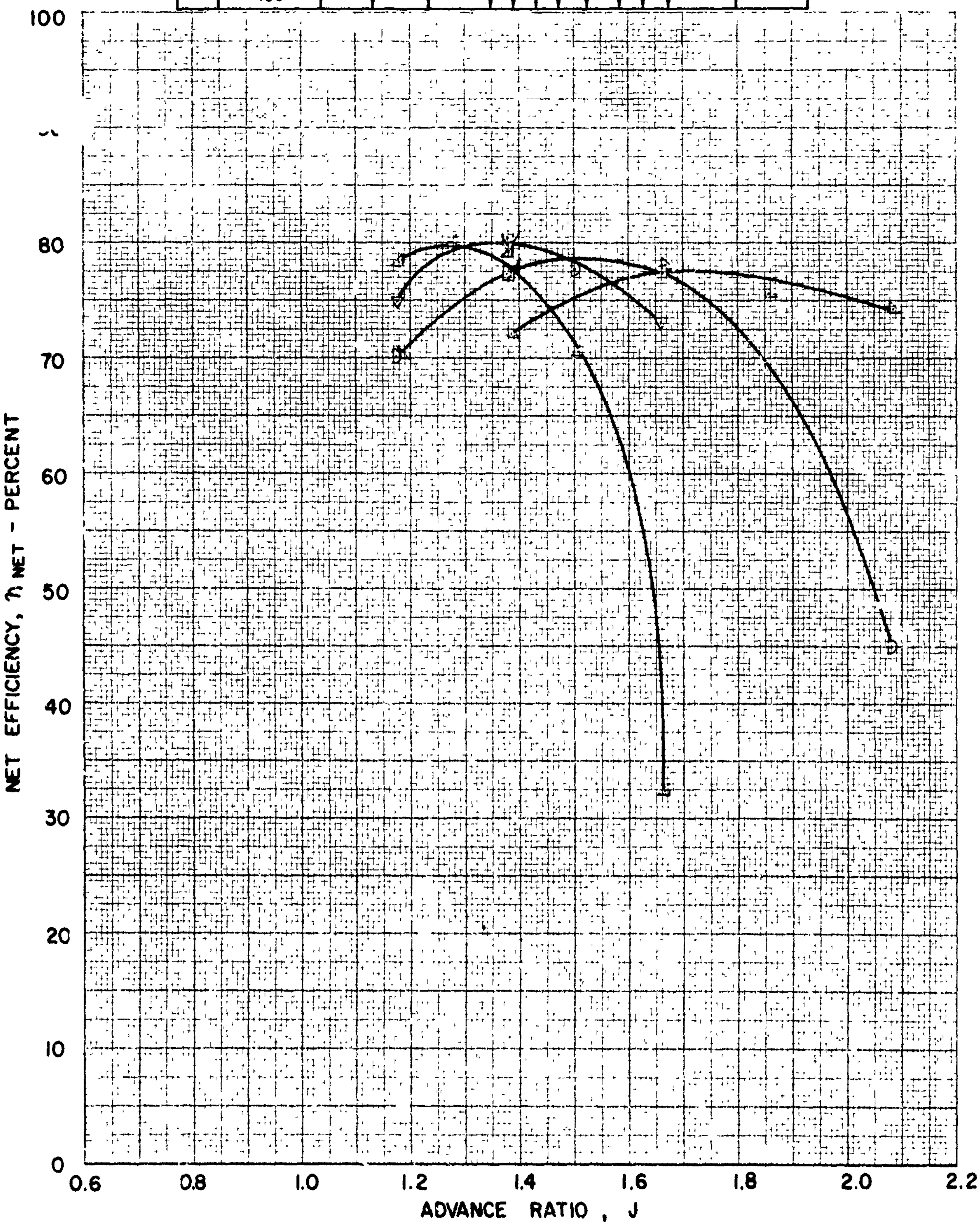

HSD SHROUDED PROPELLER TEST

EFFECT OF 4-WAY BLADES ON SHROUDED PROPELLER PERFORMANCE

SYM	RUN NO.	MACH NO.	CONFIGURATION	$\theta_{3/4}$
⊿	435	0.30	L_1 C_1 E_1 B_4 P_{NT} T_1 R_1 R_E	34
▽	436	↓	↓	38
D	437	↓	↓	42
◺	439	↓	↓	46

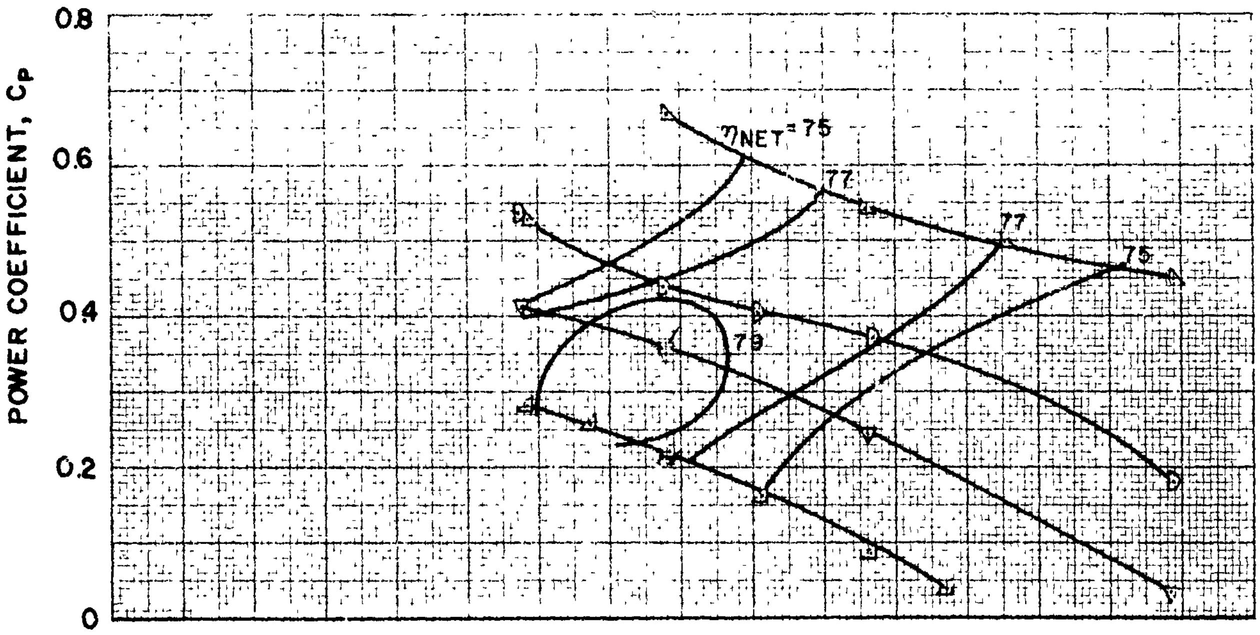

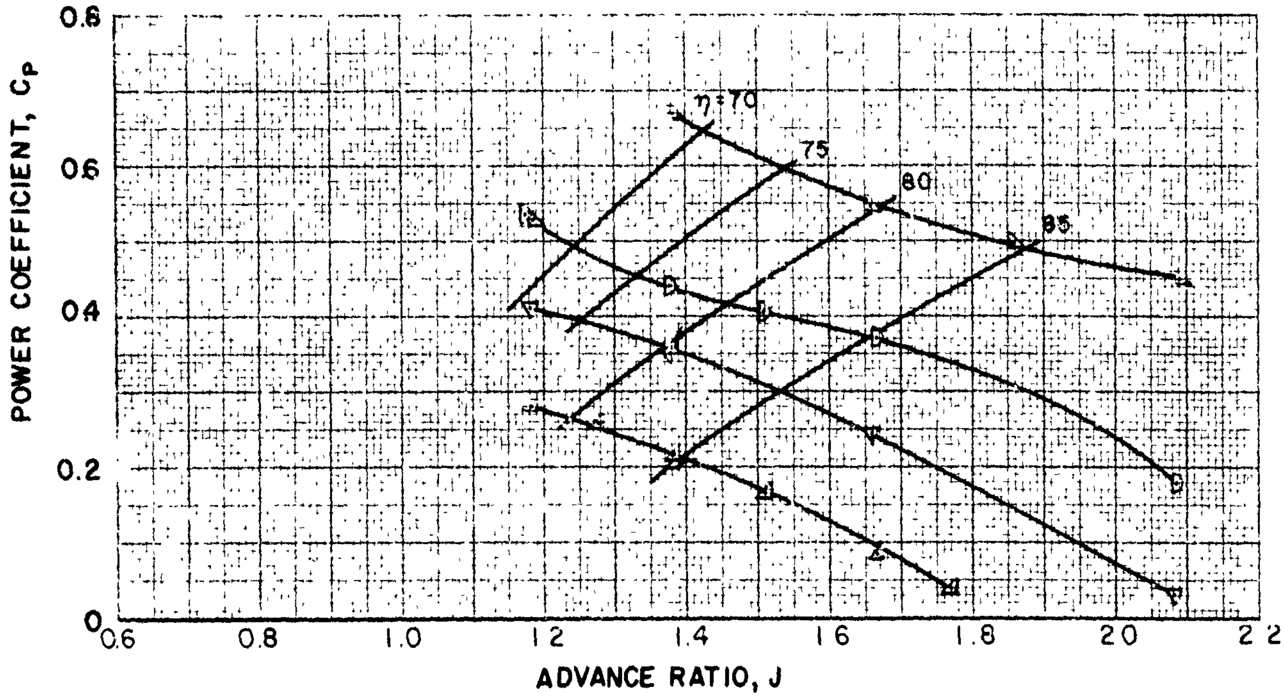

HSD SHROUDED PROPELLER TEST

EFFECT OF 4-WAY BLADES ON SHROUDED PROPELLER PERFORMANCE

SYM	RUN NO.	MACH NO.	CONFIGURATION	$\theta_{3/4}$
D	438	0.40	$L_1\ C_1\ E_1\ B_4\ P_{NT}\ T_1\ R_1\ R_E$	42
◺	440	↓	↓	46
◖	442	↓	↓	50
⊙	444	↓	↓	54

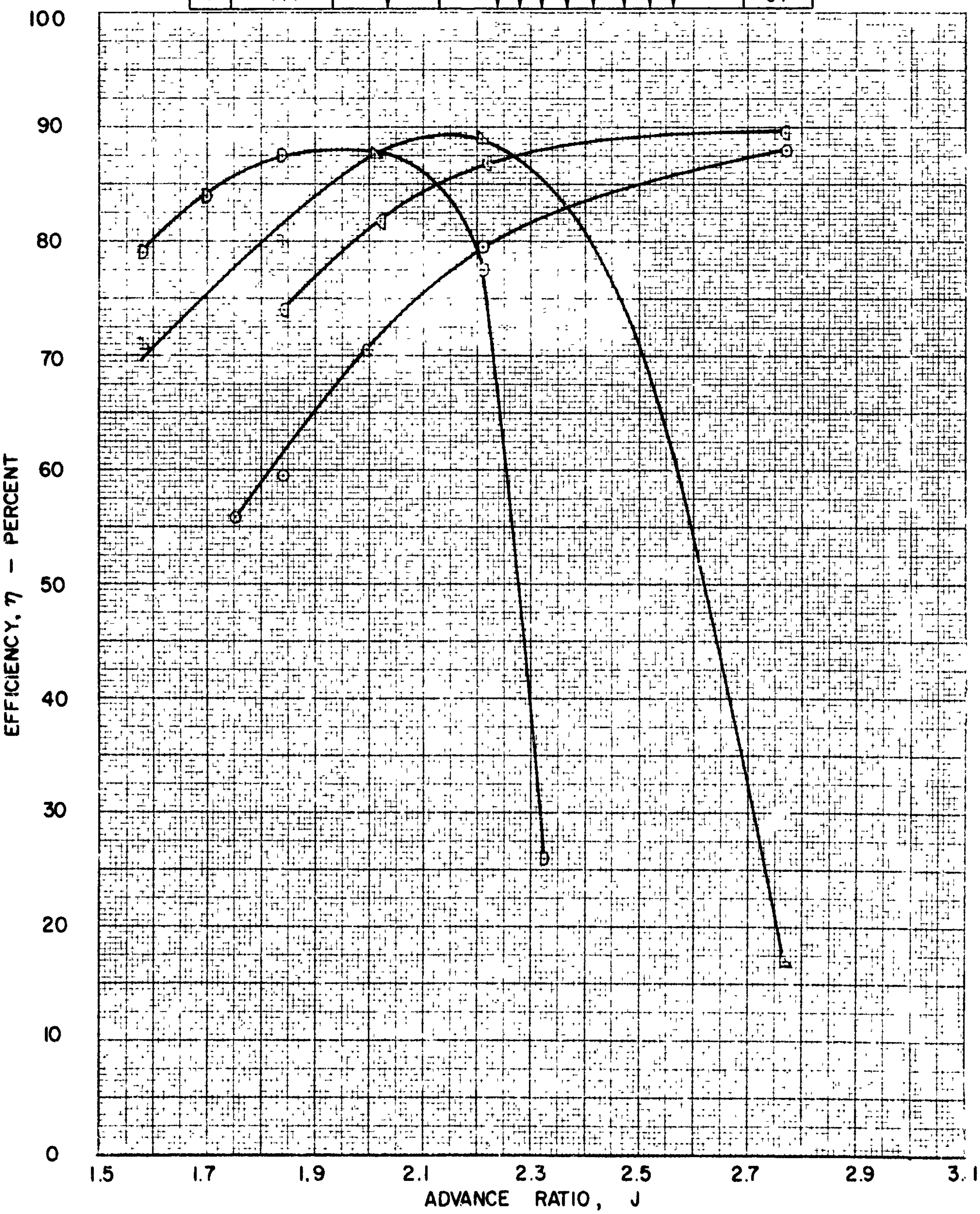

HSD SHROUDED PROPELLER TEST

EFFECT OF 4-WAY BLADES ON SHROUDED PROPELLER PERFORMANCE

SYM	RUN NO.	MACH NO.	CONFIGURATION	$\theta_{3/4}$
D	438	0.40	L_1 C_1 E_1 B_4 P_{NT} T_1 R_1 R_E	42
◺	440			46
◖	442			50
⊙	444			54

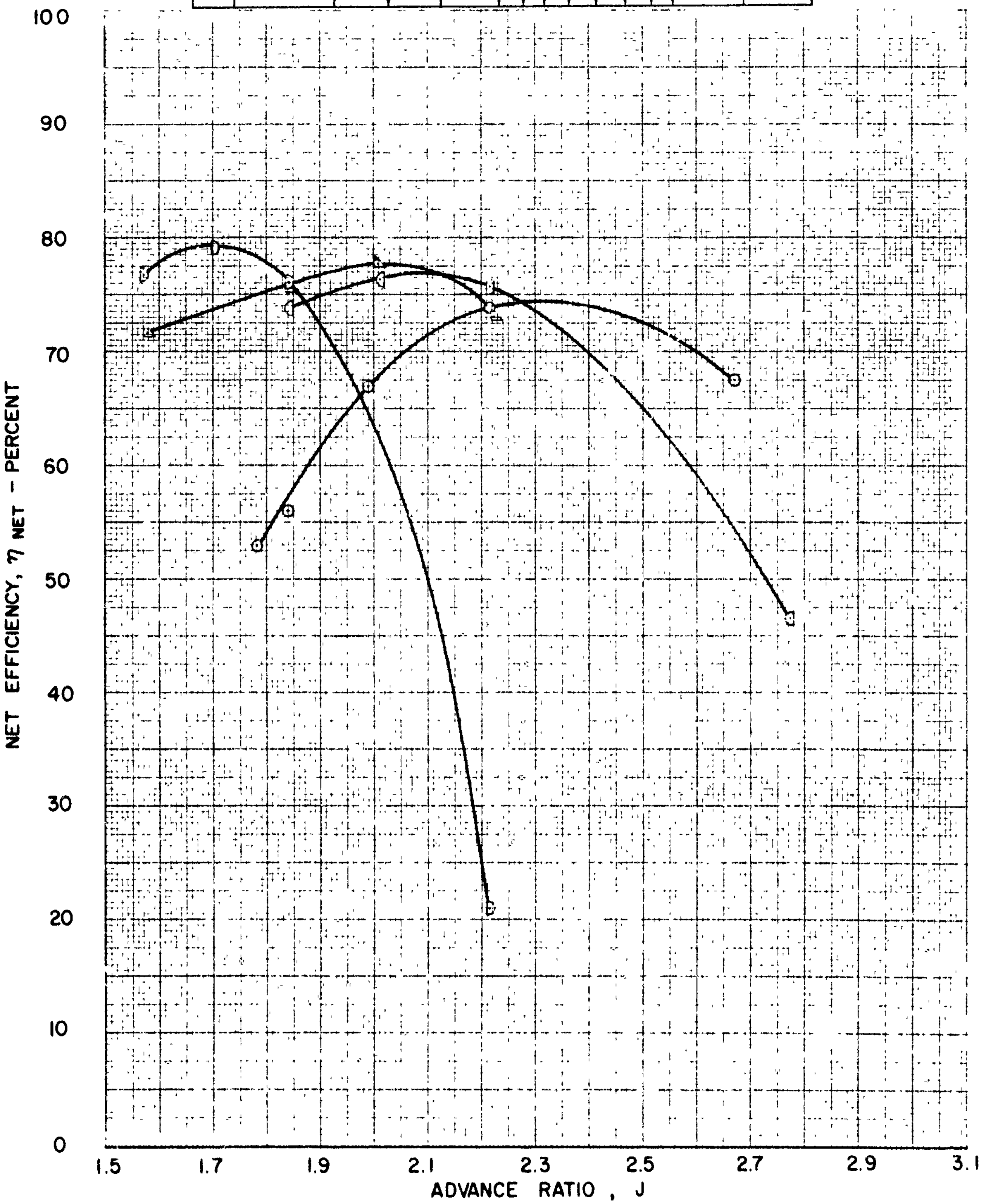

HSD SHROUDED PROPELLER TEST

EFFECT OF 4-WAY BLADES ON SHROUDED PROPELLER PERFORMANCE

SYM	RUN NO.	MACH NO.	CONFIGURATION	$\theta_{3/4}$
D	438	0.40	$L_1\ C_1\ E_1\ B_4\ P_{NT}\ T_1\ R_1\ R_E$	42
◺	440	↓	↓	46
◖	442	↓	↓	50
○	444	↓	↓	54

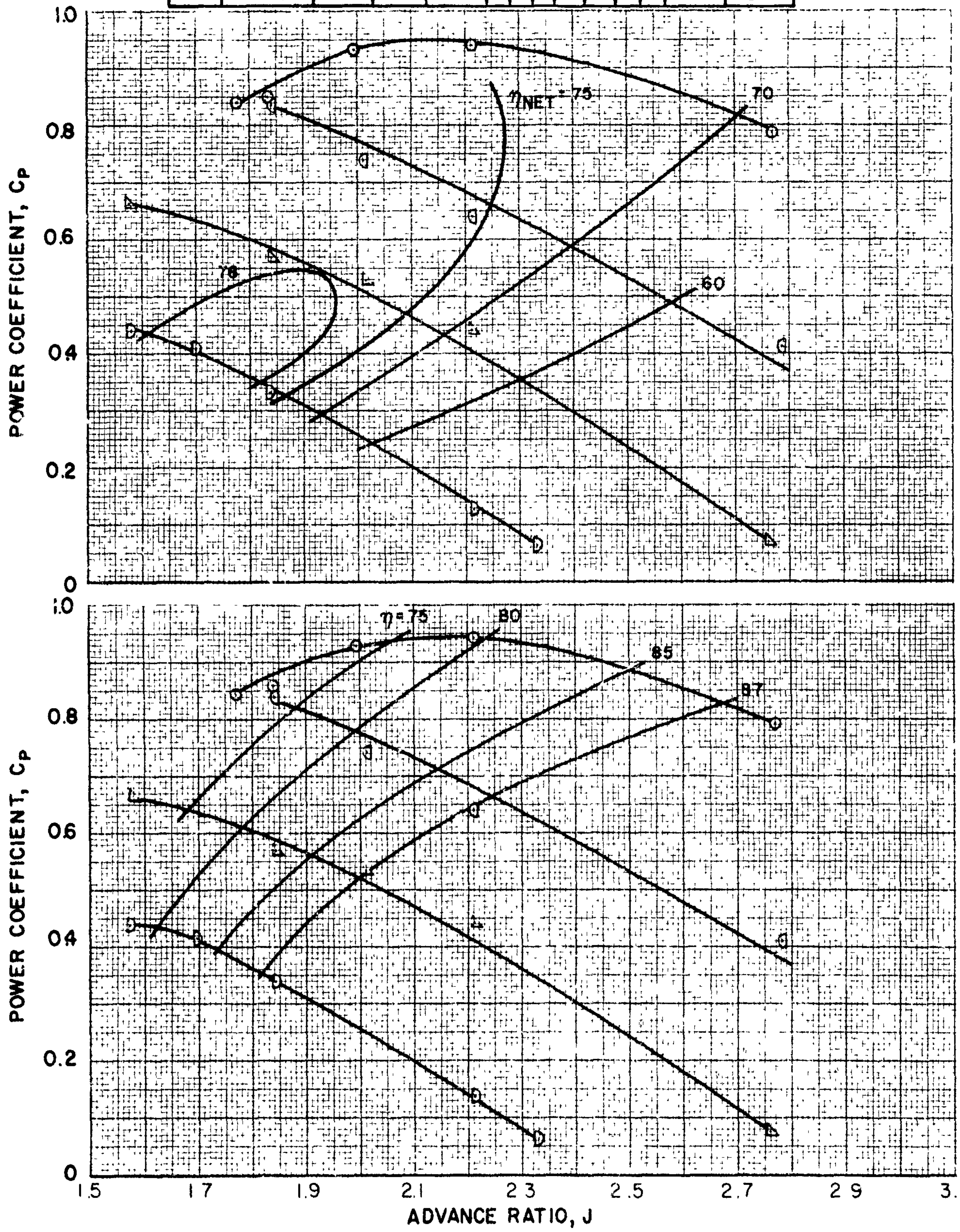

E330590-1 FIG. 197

HSD SHROUDED PROPELLER TEST

EFFECT OF 4-WAY BLADES ON SHROUDED PROPELLER PERFORMANCE

SYM	RUN NO.	MACH NO.	CONFIGURATION	$\theta_{3/4}$
△	441	0.50	$L_1\ C_1\ E_1\ B_4\ P_{NT}\ T_1\ R_1\ R_E$	46
◧	443	↓	↓	50
○	445	↓	↓	54

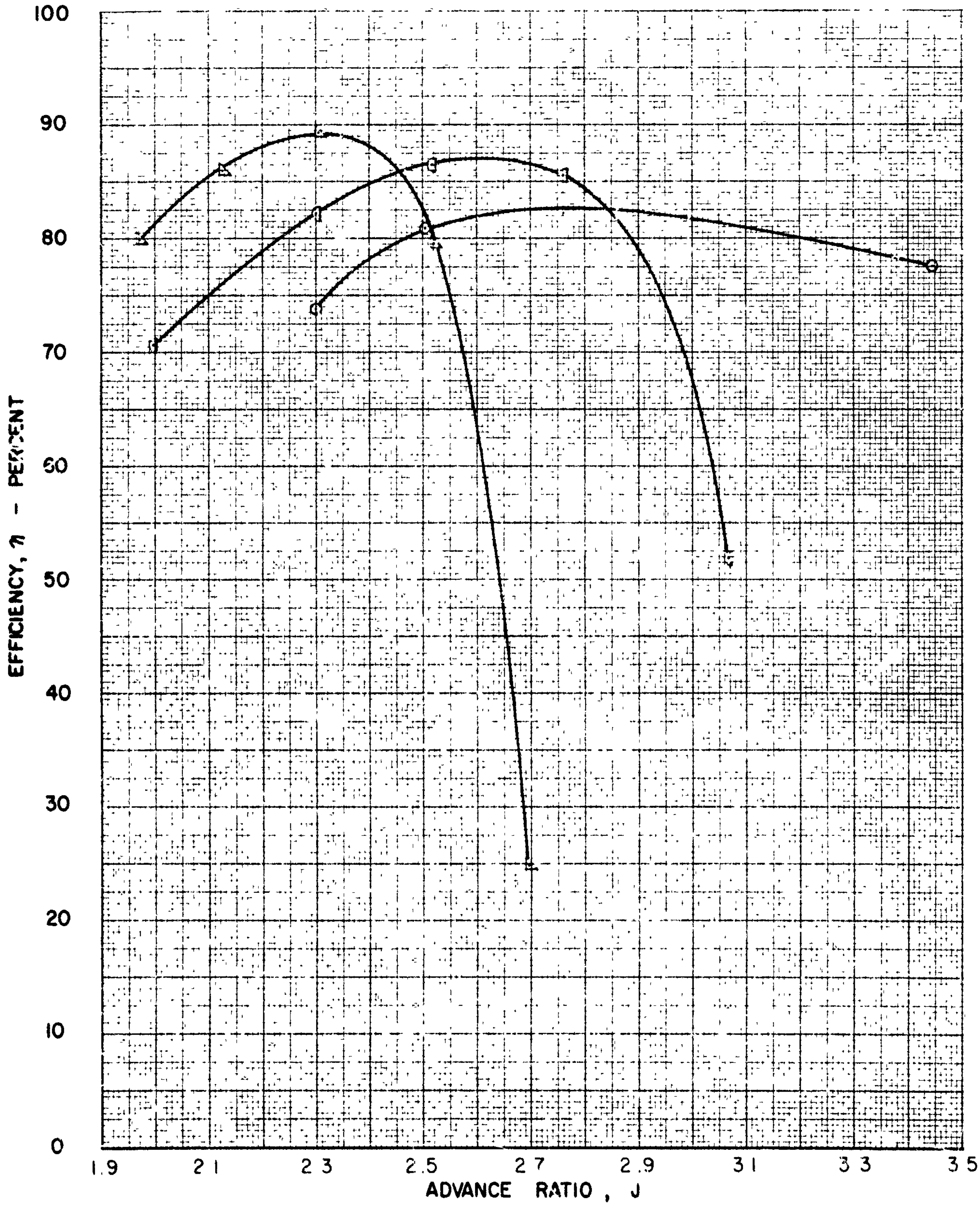

E330590-I

FIG. 198

HSD SHROUDED PROPELLER TEST

EFFECT OF 4-WAY BLADES ON SHROUDED PROPELLER PERFORMANCE

SYM	RUN NO.	MACH NO.	CONFIGURATION	$\theta_{3/4}$
◺	441	0.50	$L_1\ C_1\ E_1\ B_4\ P_{NT}\ T_1\ R_1\ R_E$	46
◖	443	↓	↓	50
○	445	↓	↓	54

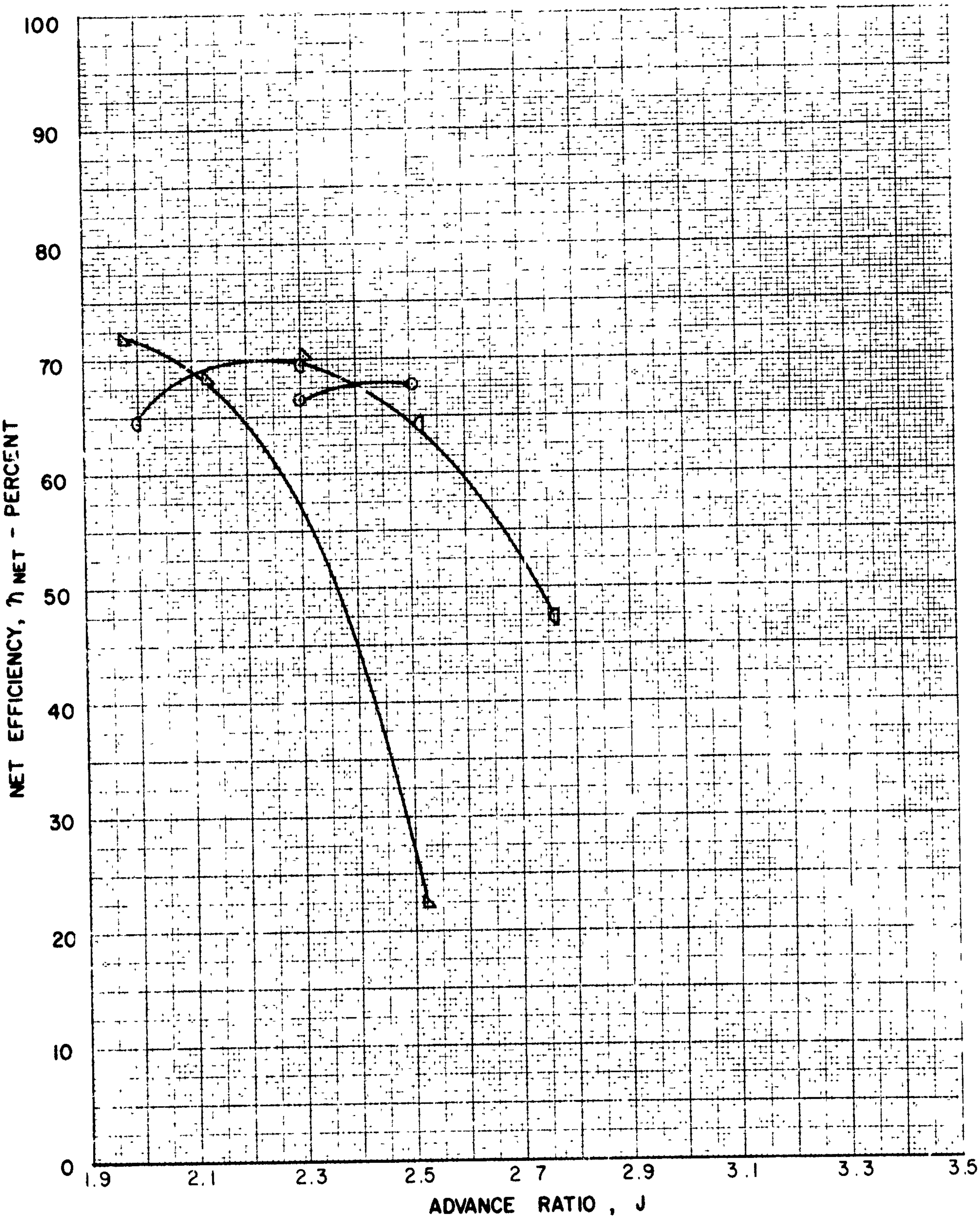

HSD SHROUDED PROPELLER TEST

EFFECT OF 4-WAY BLADES ON SHROUDED PROPELLER PERFORMANCE

SYM	RUN NO.	MACH NO.	CONFIGURATION	$\theta_{3/4}$
◺	441	0.50	$L_1\ C_1\ E_1\ B_4\ P_{NT}\ T_1\ R_1\ R_E$	46
◖	443	↓	↓	50
⊙	445	↓	↓	54

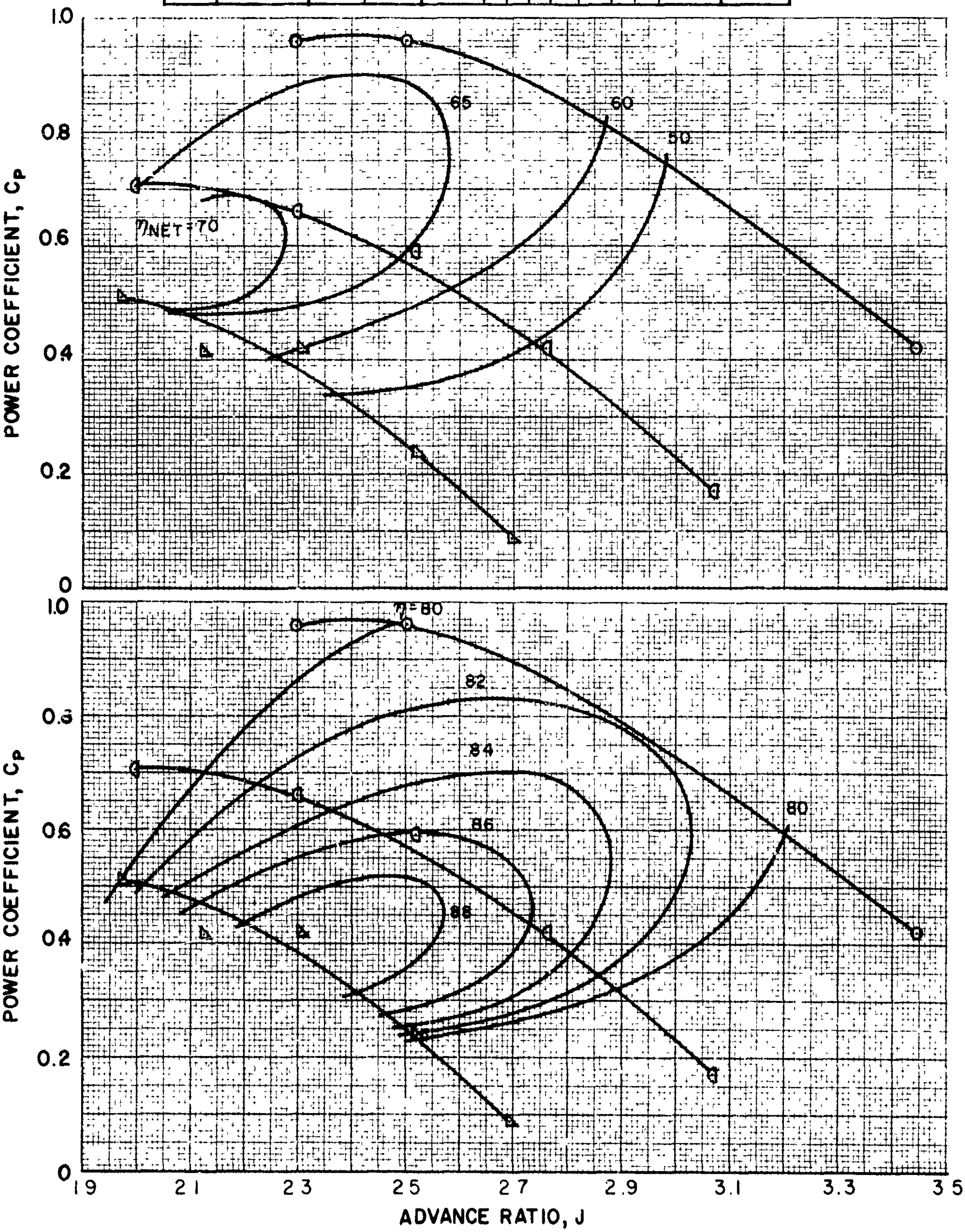

HSD SHROUDED PROPELLER TEST

EFFECT OF BLADE TIP CLEARANCE ON SHROUDED PROPELLER PERFORMANCE

SYM	RUN NO	MACH NO.	CONFIGURATION	$\theta_{3/4}$
△	201 ,202	0.02,0.10	$L_1\ C_1\ E_1\ B_3\ P_R\ T_2\ R_1\ R_E$	20
□	203 ,204	↓	↓	25
◇	208 ,207	↓	↓	30
⊿	209 ,210	↓	↓	35

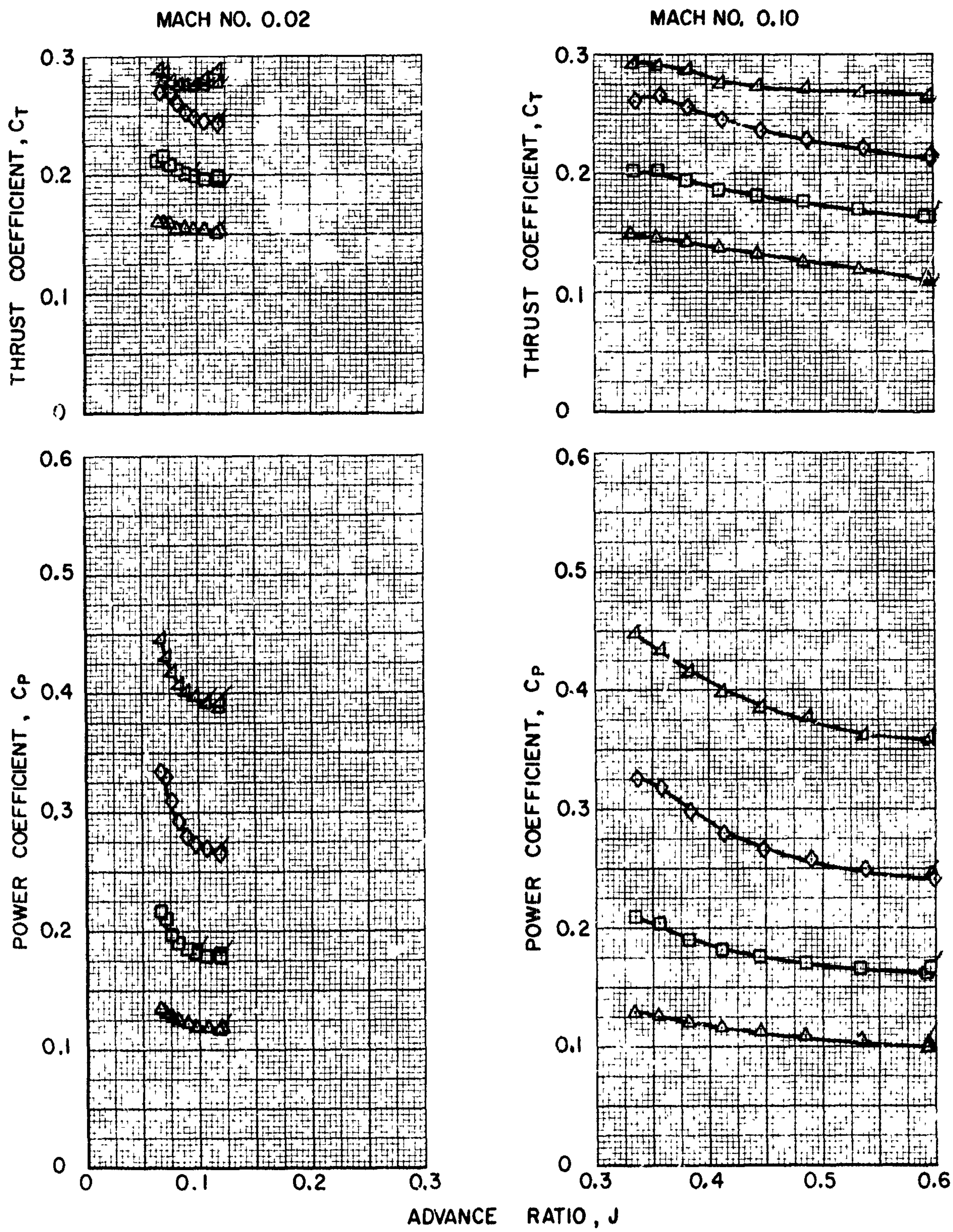

HSD SHROUDED PROPELLER TEST

EFFECT OF BLADE TIP CLEARANCE ON SHROUDED PROPELLER PERFORMANCE

SYM	RUN NO.	MACH NO.	CONFIGURATION	$\theta_{3/4}$
△	201 ,202	0.02,0.10	$L_1 C_1 E_1 B_3 P_R T_2 R_1 R_E$	20
□	203 ,204	↓	↓	25
◇	208 ,207	↓	↓	30
⊿	209 ,210	↓	↓	35

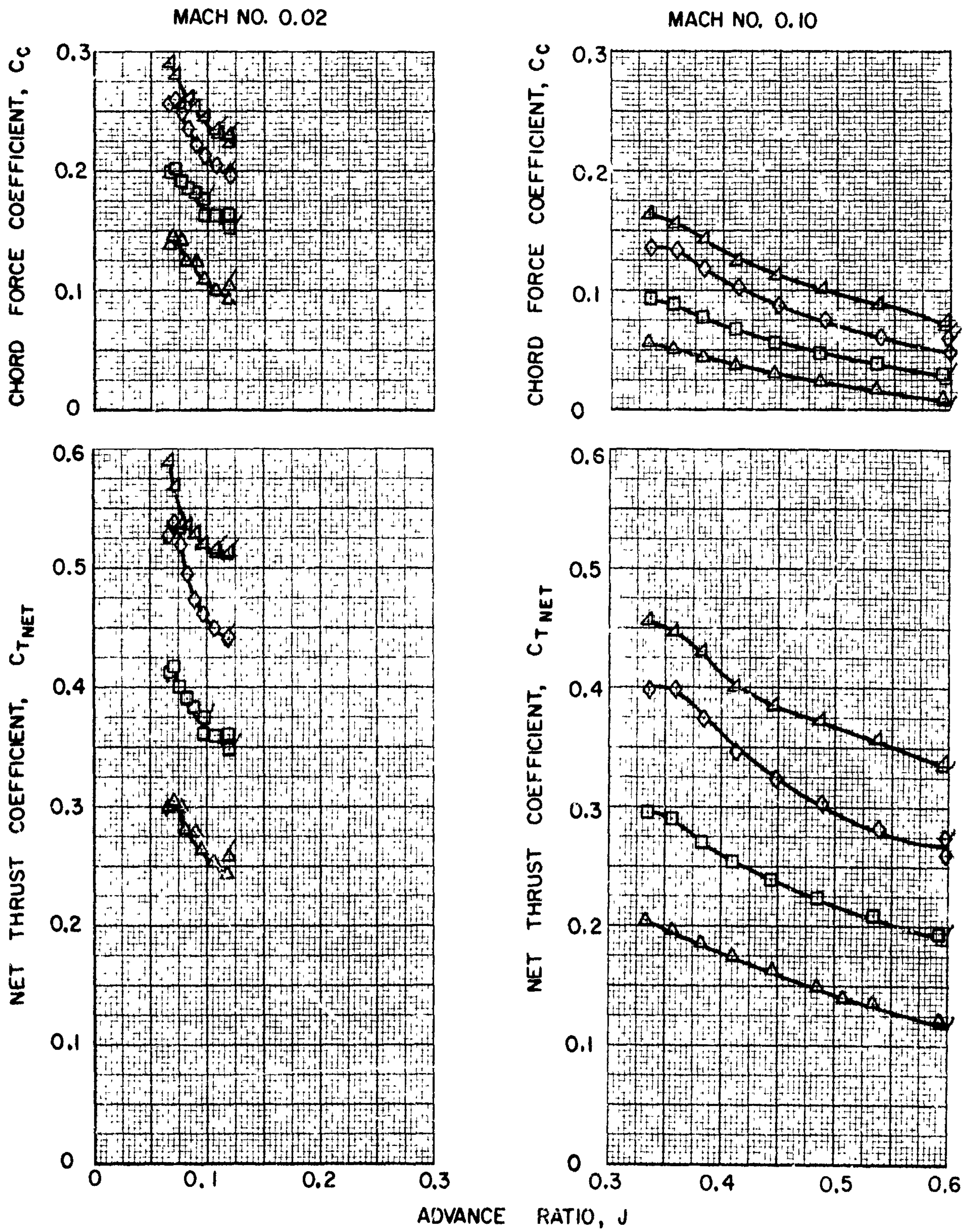

HSD SHROUDED PROPELLER TEST

EFFECT OF BLADE TIP CLEARANCE ON SHROUDED PROPELLER PERFORMANCE

SYM	RUN NO.	MACH NO	CONFIGURATION	$\theta_{3/4}$
□	205	0.20	$L_1 C_1 E_1 B_3 P_R T_2 R_1 R_E$	25
◇	206	↓	↓	30
△	211	↓	↓	35

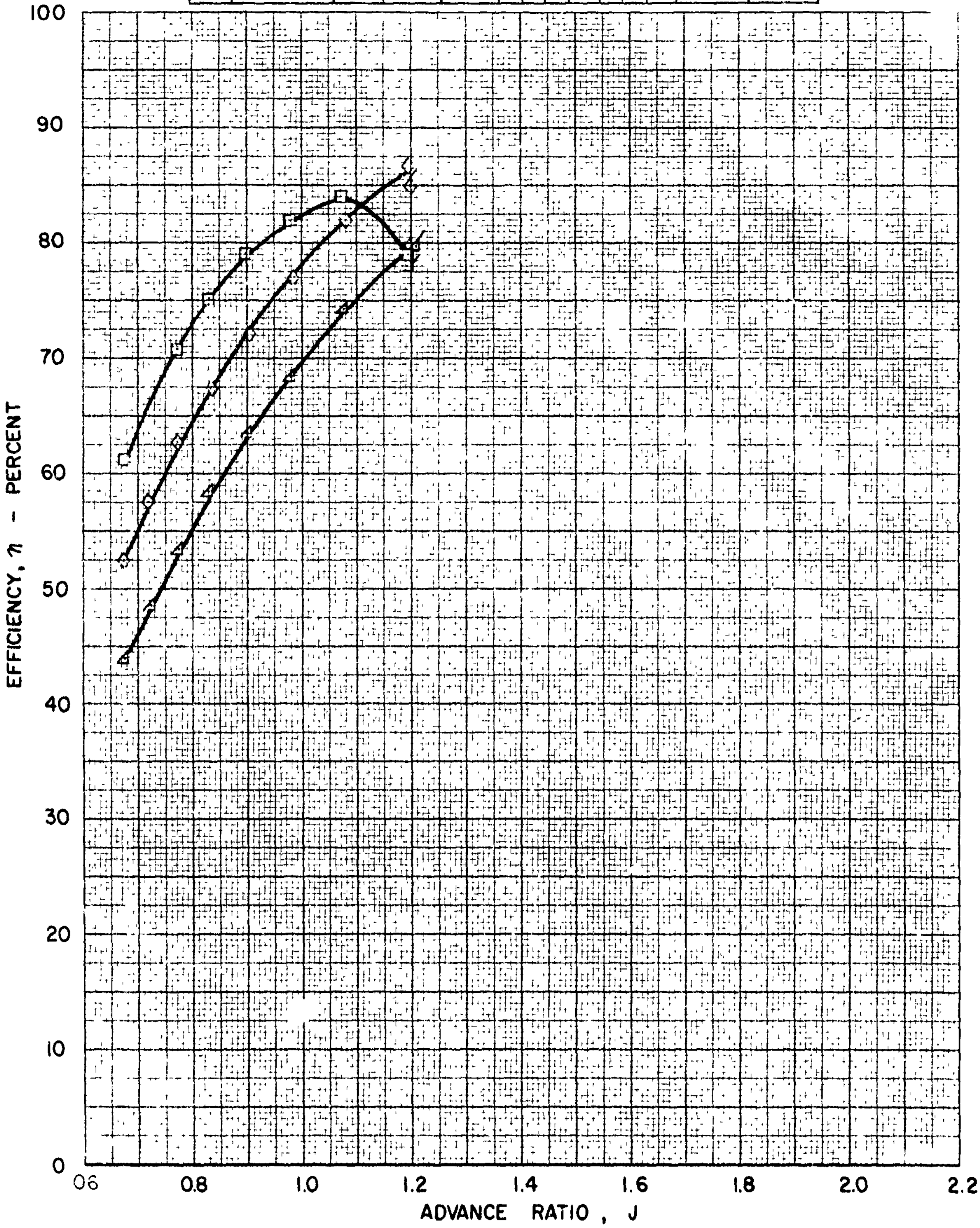

HSD SHROUDED PROPELLER TEST

EFFECT OF BLADE TIP CLEARANCE ON SHROUDED PROPELLER PERFORMANCE

SYM	RUN NO.	MACH NO.	CONFIGURATION	$\theta_{3/4}$
□	205	0.20	$L_1 C_1 E_1 B_3 P_R T_2 R_1 R_E$	25
◇	206	↓	↓	30
◿	211	↓	↓	35

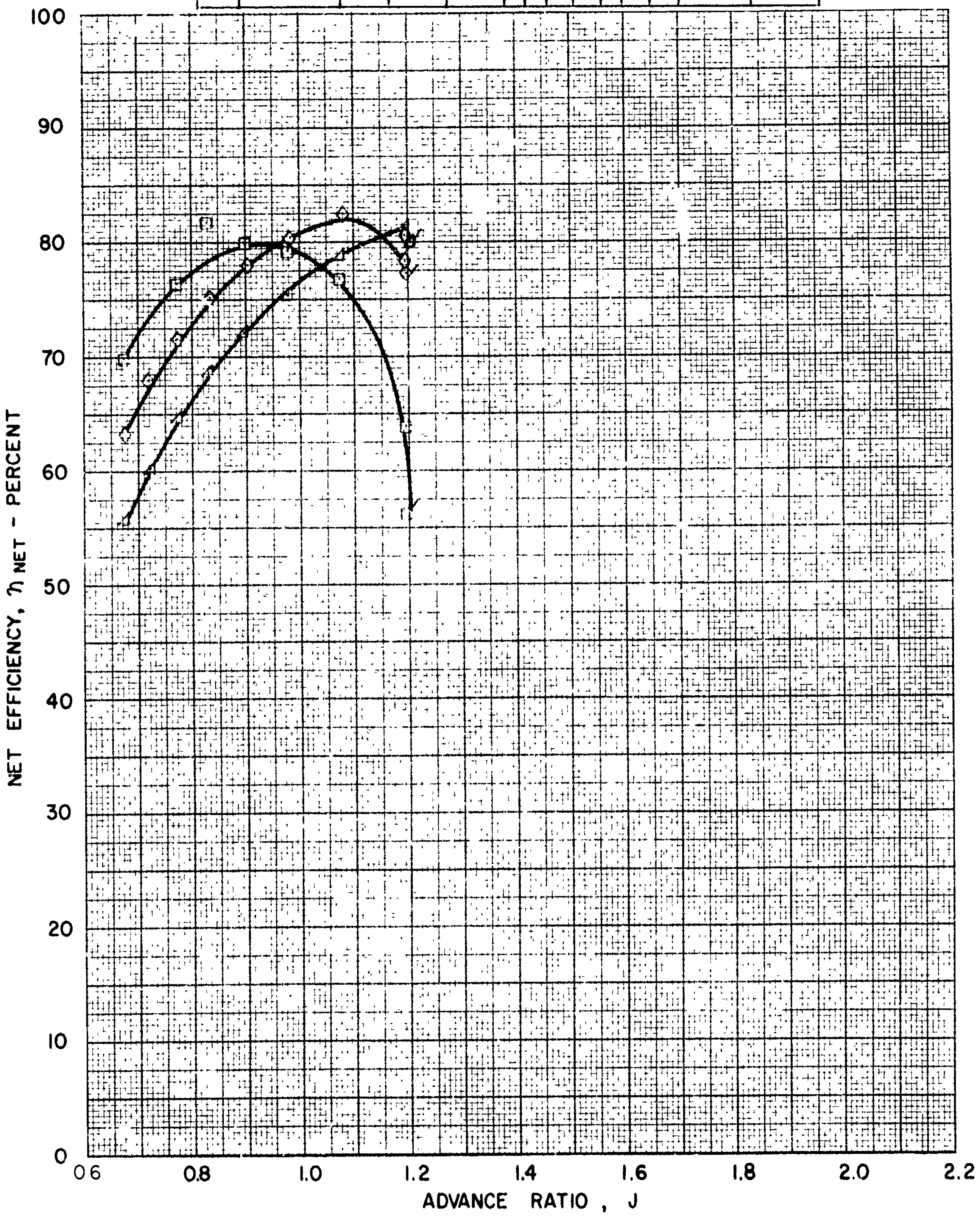

E330590-I

FIG.204

HSD SHROUDED PROPELLER TEST

EFFECT OF BLADE TIP CLEARANCE ON SHROUDED PROPELLER PERFORMANCE

SYM	RUN NO.	MACH NO.	CONFIGURATION	$\theta_{3/4}$
⊡	205	0.20	$L_1 C_1 E_1 B_3 P_R T_2 R_1 R_E$	25
◇	206	↓	↓	30
⊿	211	↓	↓	35

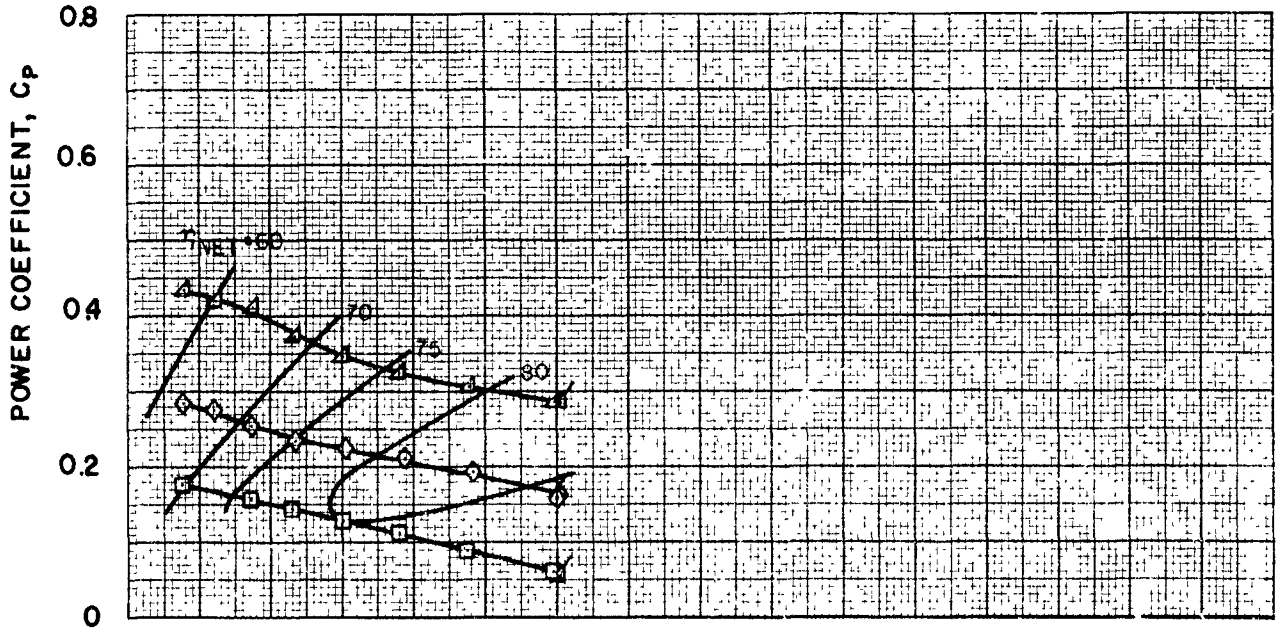

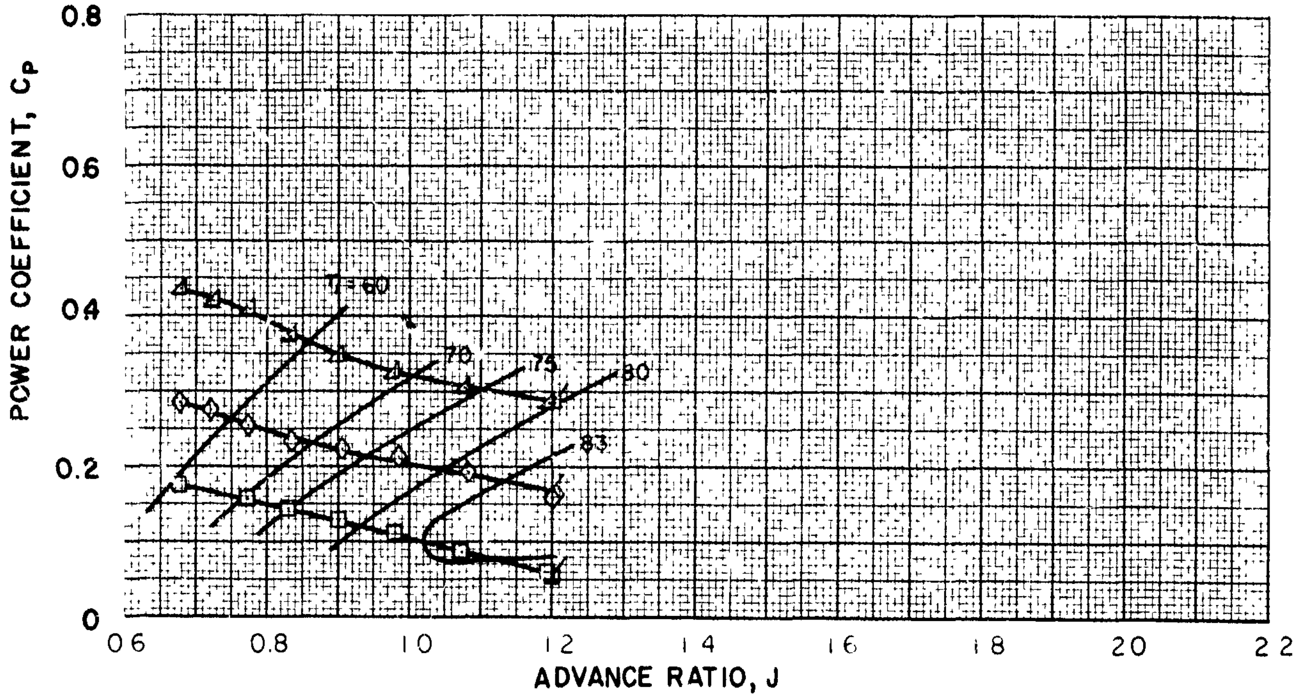

E330590-1

FIG. 205

HSD SHROUDED PROPELLER TEST

EFFECT OF BLADE TIP CLEARANCE ON SHROUDED PROPELLER PERFORMANCE

SYM	RUN NO.	MACH NO.	CONFIGURATION	$\theta_{3/4}$
◇	612	0.31	L_1 C_1 E_1 B_3 P_R T_2 R_1 R_E	30
◿	613	↓	↓	34
▽	614	↓	↓	38
◗	617	↓	↓	42

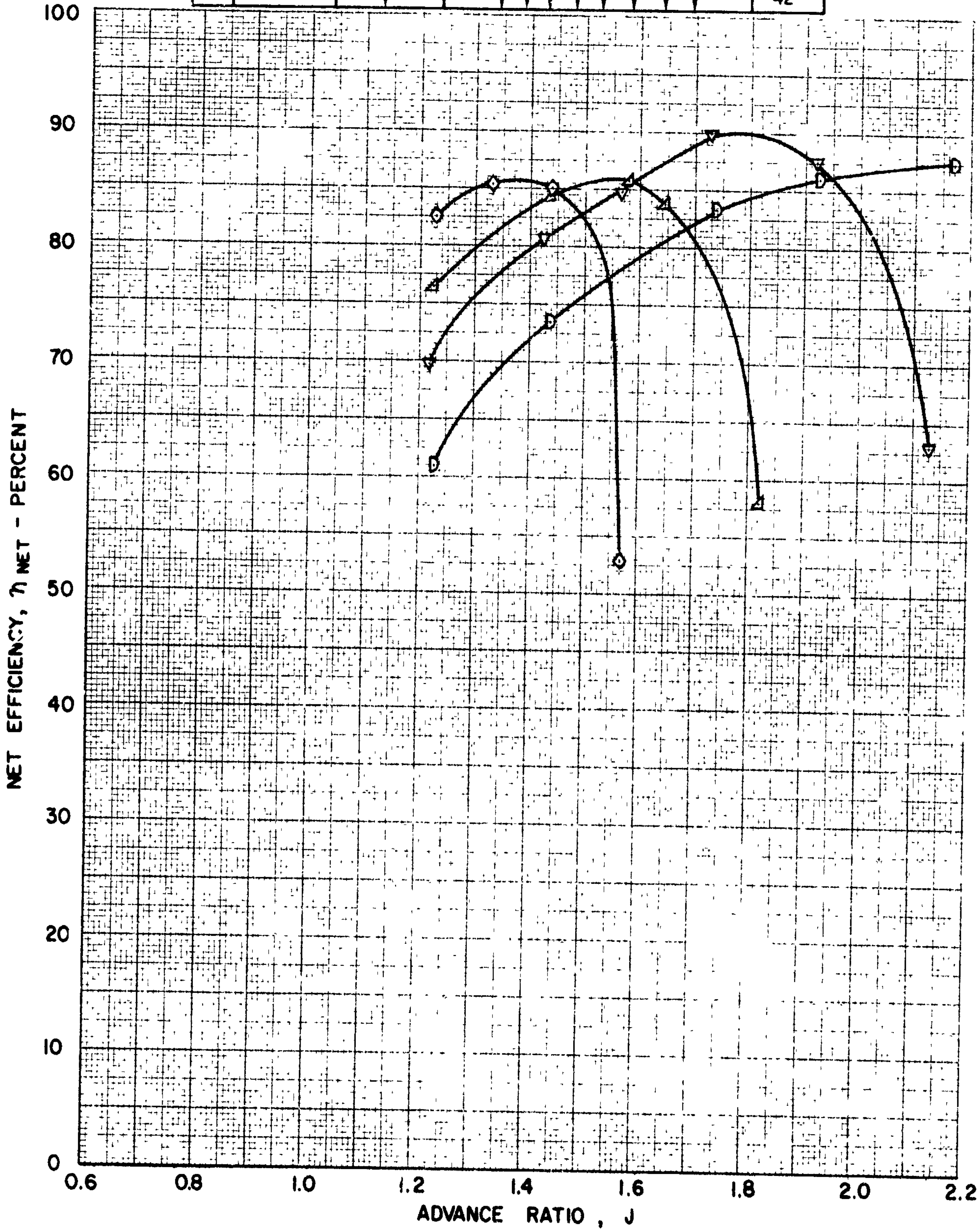

HSD SHROUDED PROPELLER TEST

EFFECT OF BLADE TIP CLEARANCE ON SHROUDED PROPELLER PERFORMANCE

SYM	RUN NO.	MACH NO.	CONFIGURATION	$\theta_{3/4}$
◇	612	0.31	L_1 C_1 E_1 B_3 P_R T_2 R_1 R_E	30
◿	613	↓	↓	34
▽	614	↓	↓	38
D	617	↓	↓	42

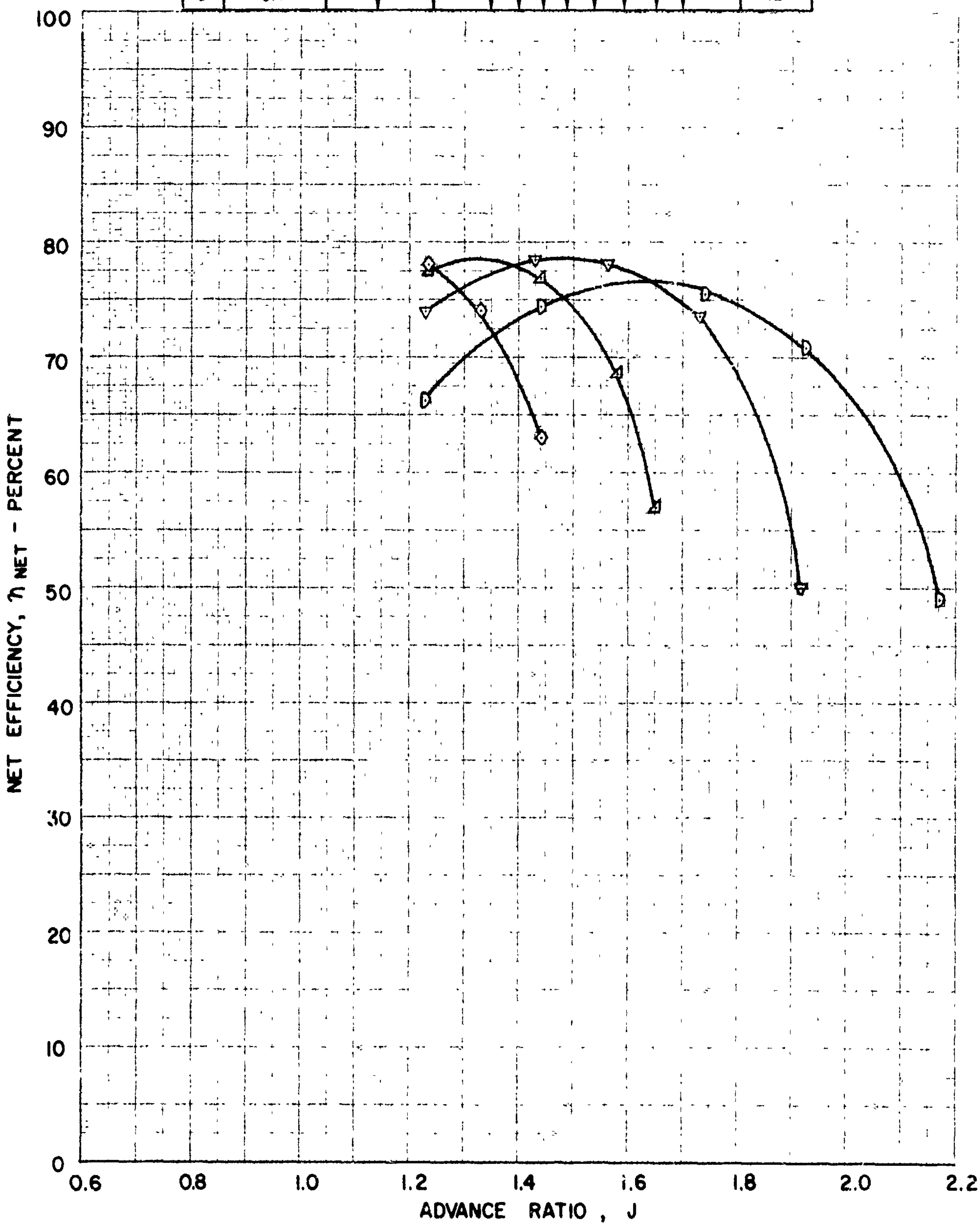

HSD SHROUDED PROPELLER TEST

EFFECT OF BLADE TIP CLEARANCE ON SHROUDED PROPELLER PERFORMANCE

SYM	RUN NO.	MACH NO.	CONFIGURATION	θ 3/4
◇	612	0.31	L_1 C_1 E_1 B_3 P_R T_2 R_1 R_E	30
⊿	613	↓	↓	34
▽	614	↓	↓	38
D	617	↓	↓	42

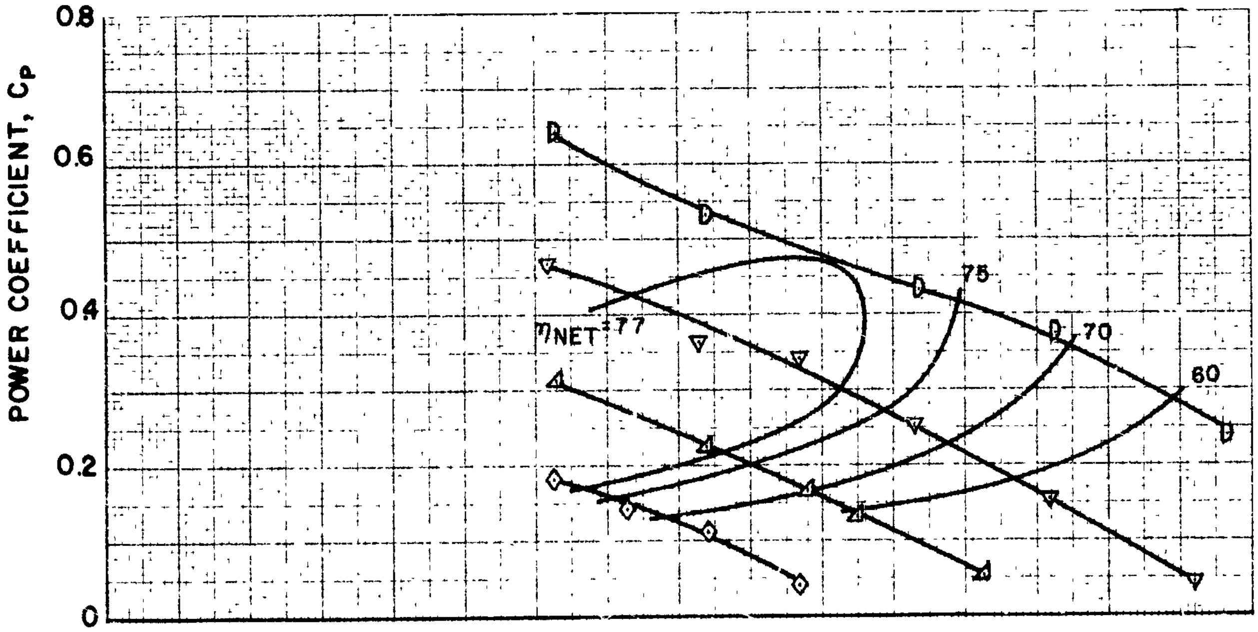

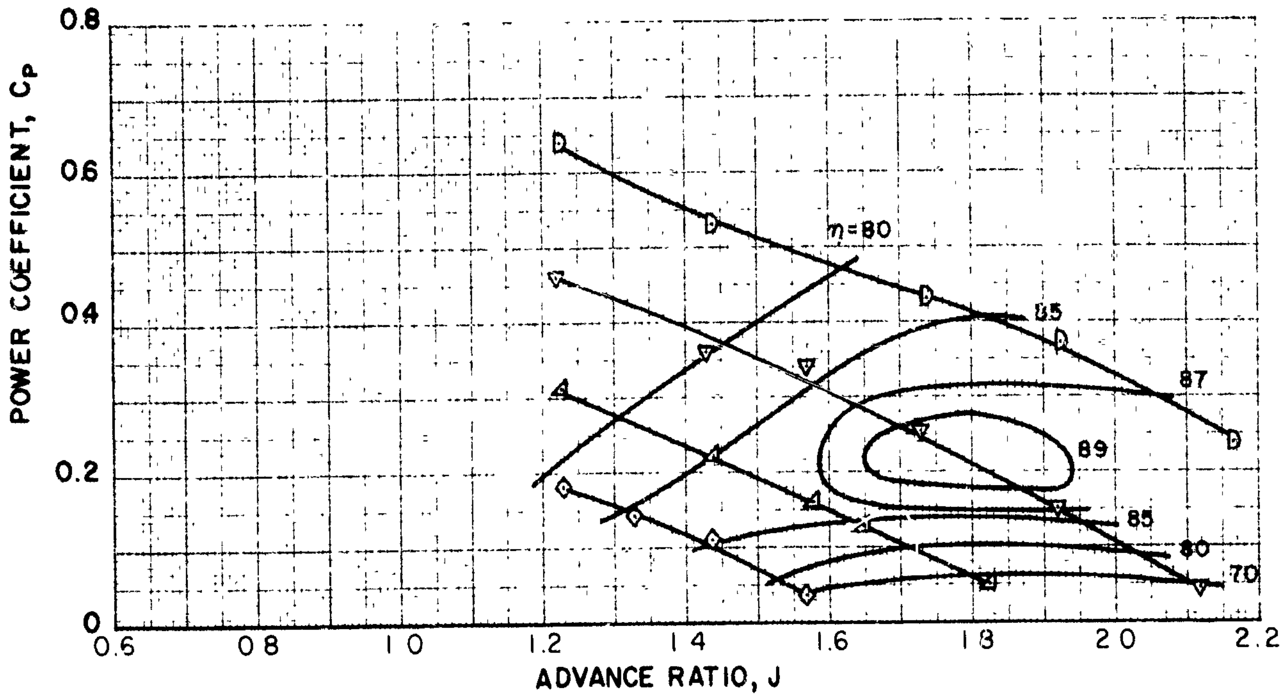

HSD SHROUDED PROPELLER TEST

EFFECT OF BLADE TIP CLEARANCE ON SHROUDED PROPELLER PERFORMANCE

SYM	RUN NO.	MACH NO.	CONFIGURATION	$\theta_{3/4}$
▽	616	0.41	L_1 C_1 E_1 B_3 P_R T_2 R_1 R_E	38
D	618	↓	↓	42
◺	620	↓	↓	46
◖	622	↓	↓	50

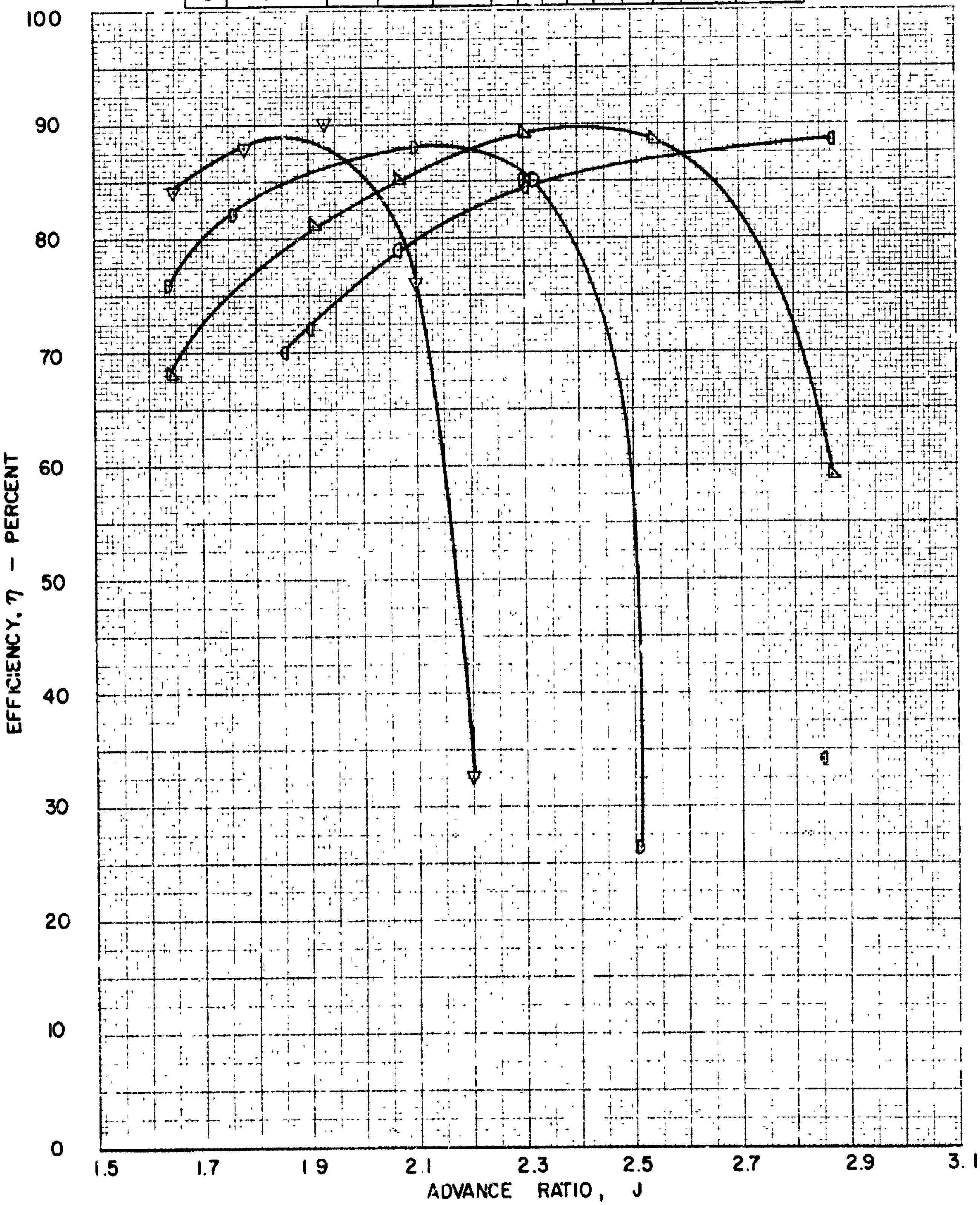

E330590-1

FIG.209

HSD SHROUDED PROPELLER TEST

EFFECT OF BLADE TIP CLEARANCE ON SHROUDED PROPELLER PERFORMANCE

SYM	RUN NO.	MACH NO.	CONFIGURATION	$\theta_{3/4}$
▽	616	0.41	$L_1\ C_1\ E_1\ B_3\ P_R\ T_2\ R_1\ R_E$	38
▷	618	↓	↓	42
◺	620	↓	↓	46
◁	622	↓	↓	50

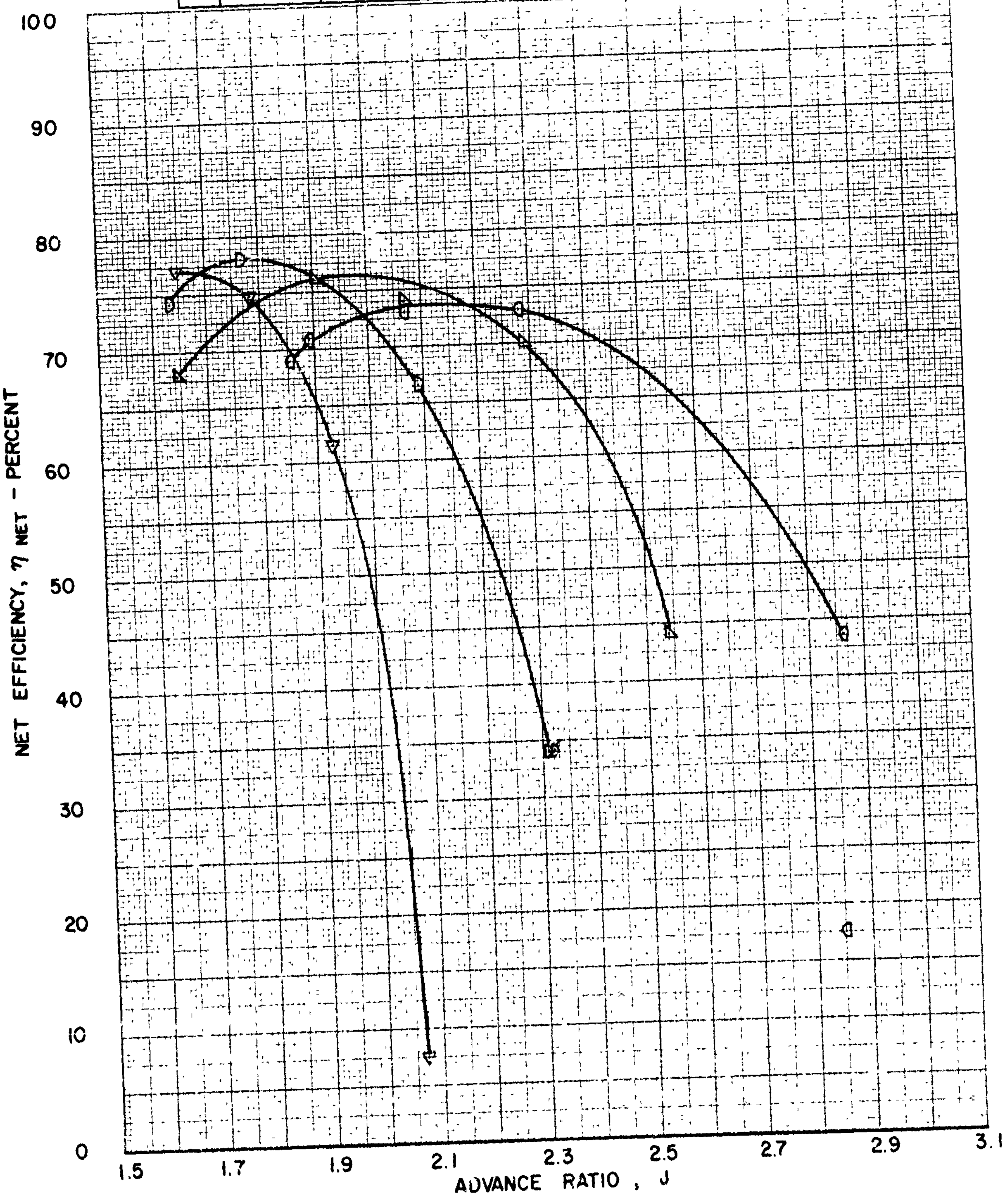

HSD SHROUDED PROPELLER TEST

EFFECT OF BLADE TIP CLEARANCE ON SHROUDED PROPELLER PERFORMANCE

SYM	RUN NO.	MACH NO.	CONFIGURATION	$\theta_{3/4}$
▽	616	0.41	$L_1\ C_1\ E_1\ B_3\ P_R\ T_2\ R_1\ R_E$	38
D	618	↓	↓	42
◺	620	↓	↓	46
Q	622	↓	↓	50

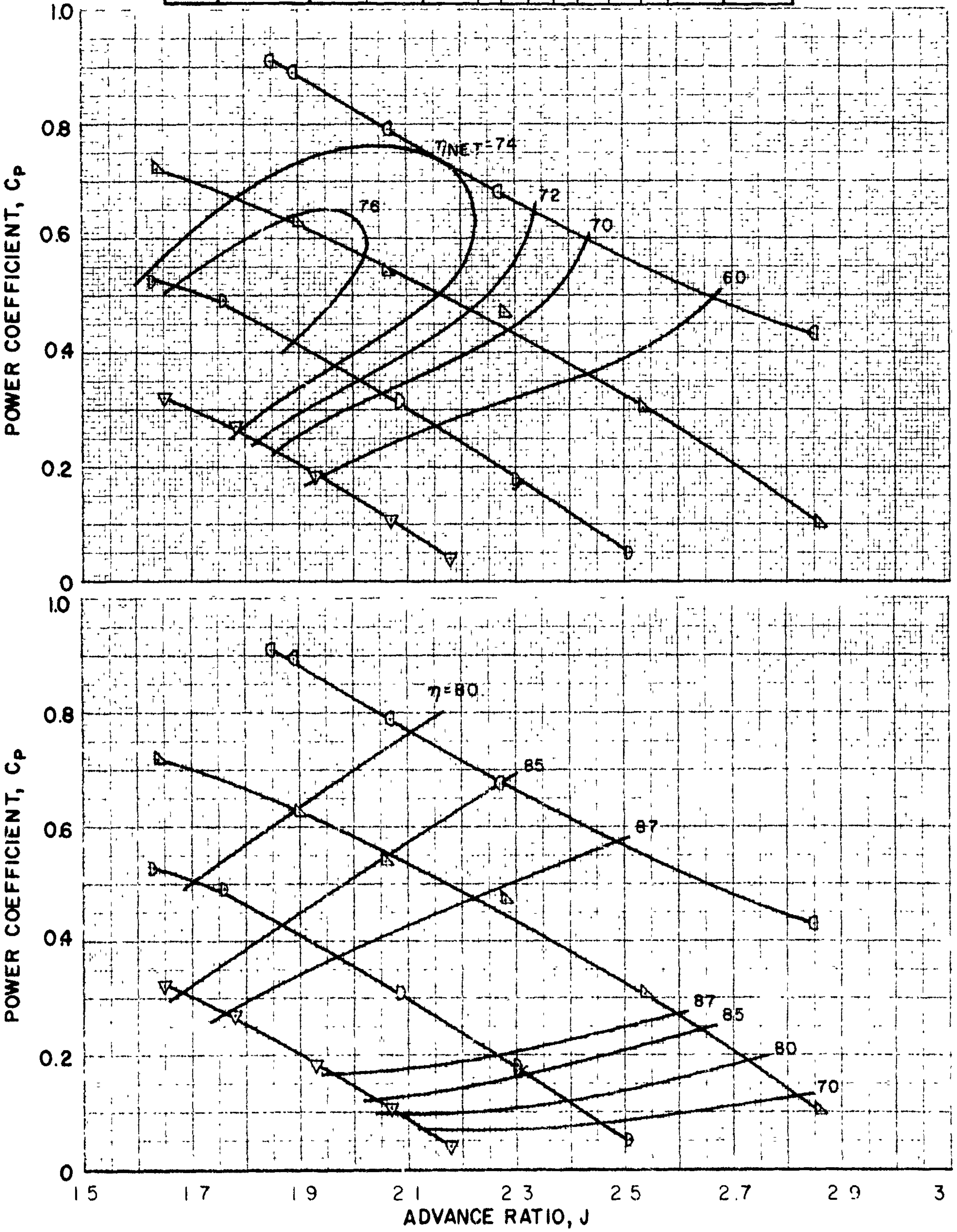

E330590-1

FIG. 211

HSD SHROUDED PROPELLER TEST

EFFECT OF BLADE TIP CLEARANCE ON SHROUDED PROPELLER PERFORMANCE

SYM	RUN NO.	MACH NO.	CONFIGURATION	$\theta_{3/4}$
D	619	052	L_1 C_1 E_1 B_3 P_R T_2 R_1 R_E	42
◺	621	↓	↓	46
◖	623	↓	↓	50
⊙	624	↓	↓	54

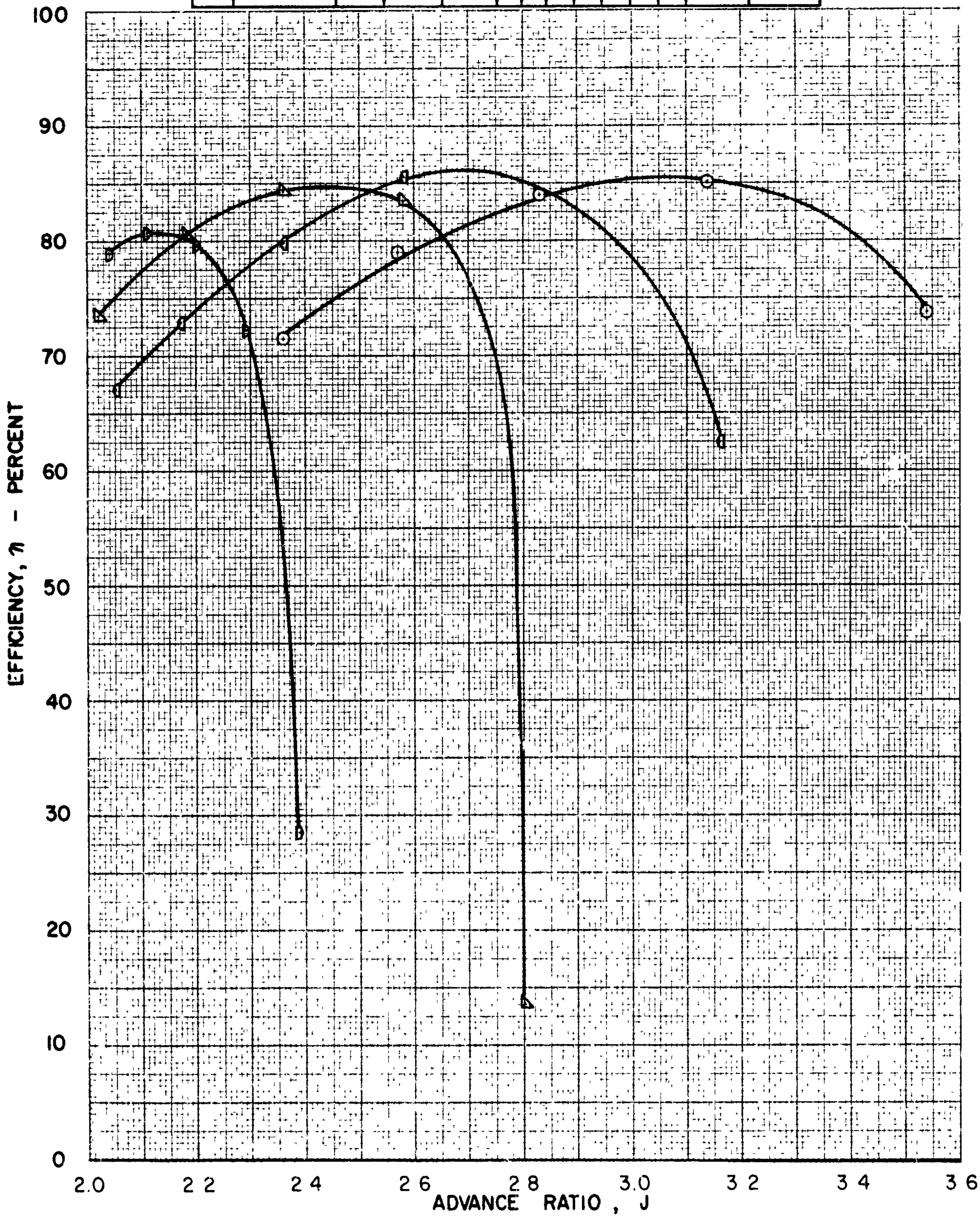

HSD SHROUDED PROPELLER TEST

EFFECT OF BLADE TIP CLEARANCE ON SHROUDED PROPELLER PERFORMANCE

SYM	RUN NO.	MACH NO.	CONFIGURATION	$\theta_{3/4}$
D	619	0.52	L_1 C_1 E_1 B_3 P_R T_2 R_1 R_E	42
◺	621	↓	↓	46
◖	623	↓	↓	50
O	624	↓	↓	54

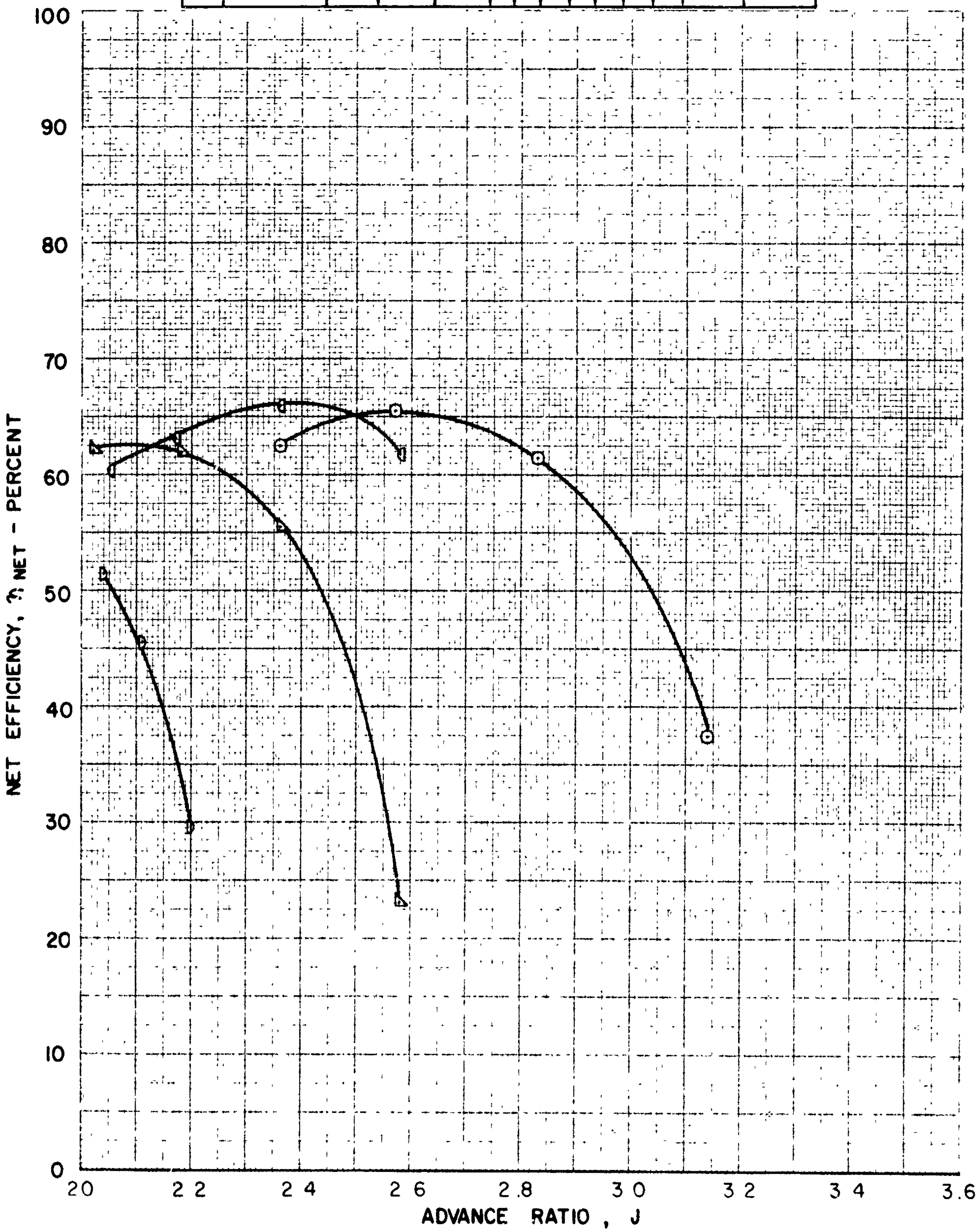

E330590-I

FIG. 213

HSD SHROUDED PROPELLER TEST

EFFECT OF BLADE TIP CLEARANCE ON SHROUDED PROPELLER PERFORMANCE

SYM	RUN NO.	MACH NO.	CONFIGURATION	$\theta_{3/4}$
D	619	0.52	$L_1\ C_1\ E_1\ B_3\ P_R\ T_2\ R_1\ R_E$	42
◺	621	↓	↓	46
◖	623	↓	↓	50
O	624	↓	↓	54

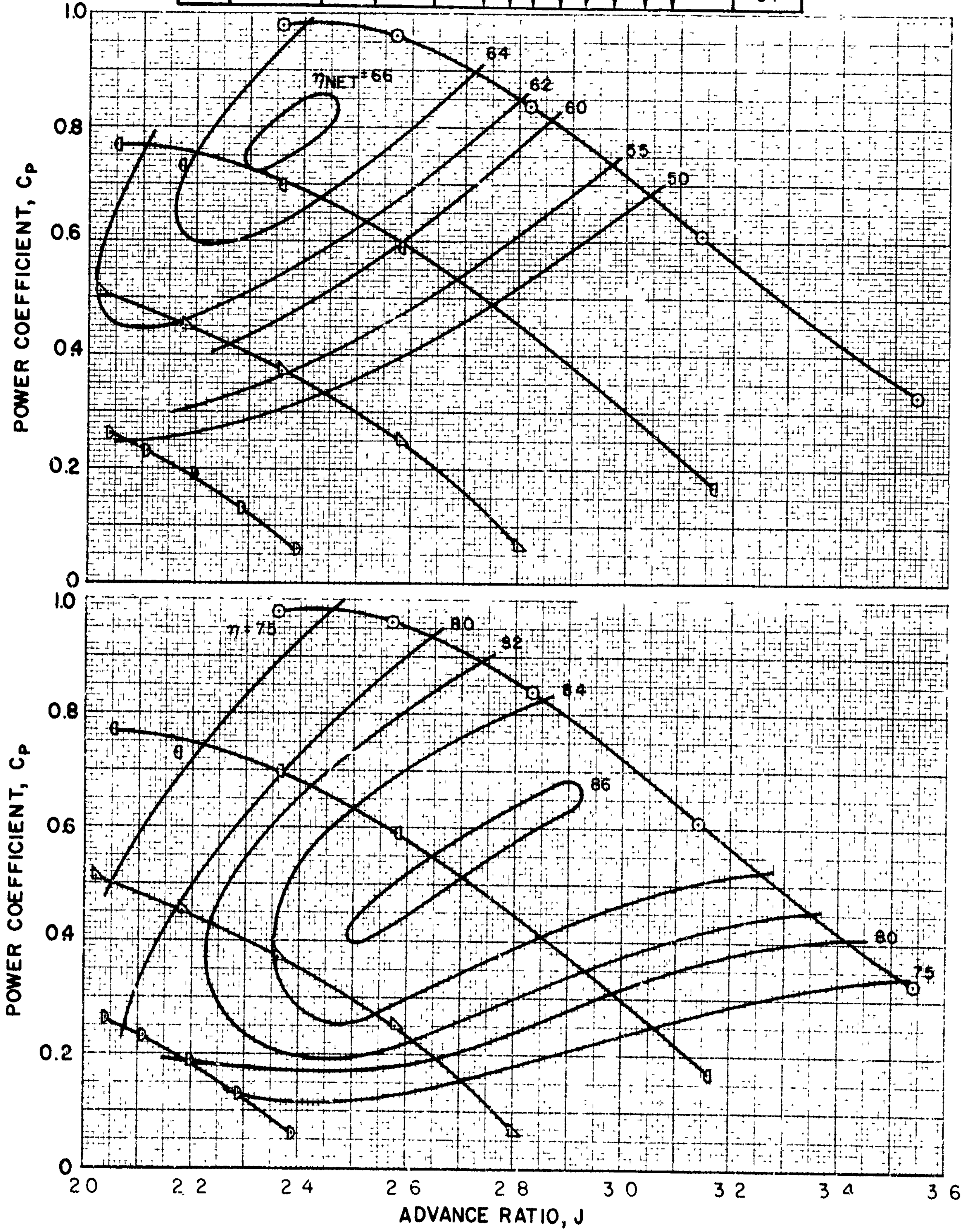

HSD SHROUDED PROPELLER TEST

EFFECT OF BLADE TIP CLEARANCE ON SHROUDED PROPELLER PERFORMANCE

SYM	RUN NO.	MACH NO.	CONFIGURATION	$\theta_{3/4}$
△	249 ,248	0.02,0.10	$L_1 C_1 E_1 B_3 P_R T_3 R_1 R_E$	20
□	250 ,251	↓	↓	25
◇	255 ,254	↓	↓	30
◿	256 ,257	↓	↓	35

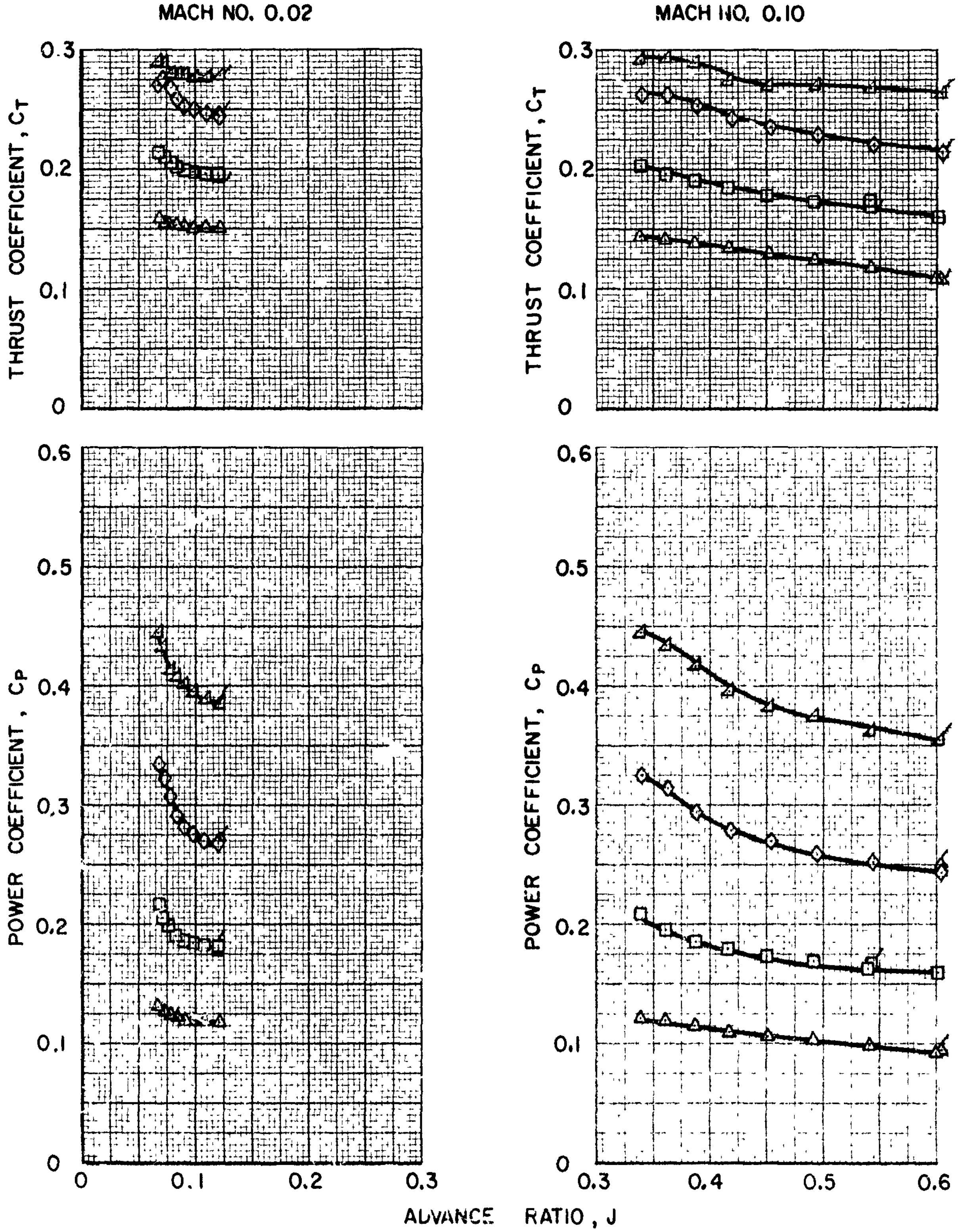

HSD SHROUDED PROPELLER TEST

EFFECT OF BLADE TIP CLEARANCE ON SHROUDED PROPELLER PERFORMANCE

SYM	RUN NO.	MACH NO.	CONFIGURATION	$\theta_{3/4}$
△	249, 248	002, 0.10	$L_1 C_1 E_1 B_3 P_R T_3 R_1 R_E$	20
□	250, 251	↓	↓	25
◇	255, 254	↓	↓	30
◺	256, 257	↓	↓	35

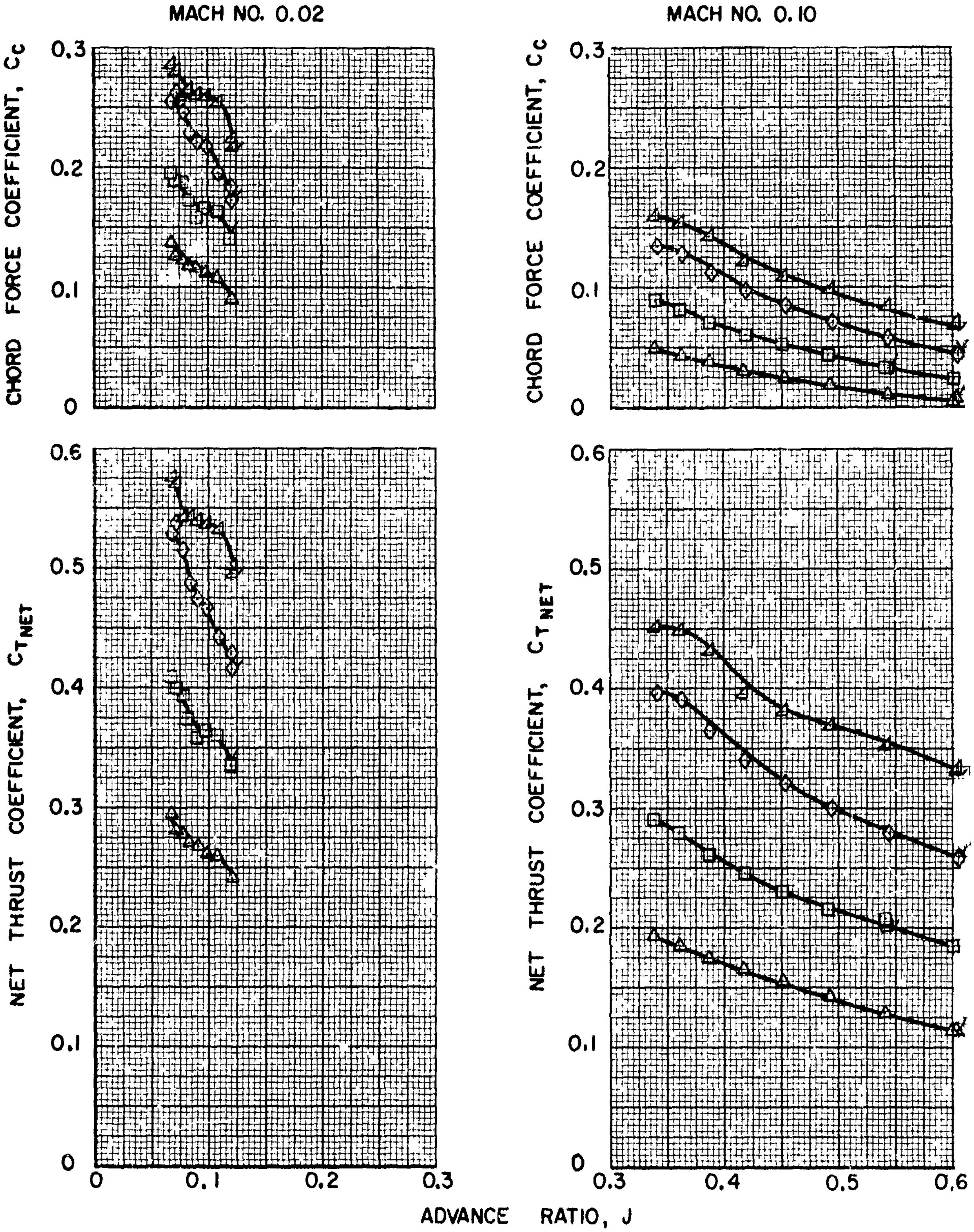

HSD SHROUDED PROPELLER TEST

EFFECT OF BLADE TIP CLEARANCE ON SHROUDED PROPELLER PERFORMANCE

SYM	RUN NO.	MACH NO.	CONFIGURATION	$\theta_{3/4}$
△	247	0.20	$L_1 C_1 E_1 B_3 P_R T_3 R_1 R_E$	20
□	252			25
◇	253			30
⊿	258			35

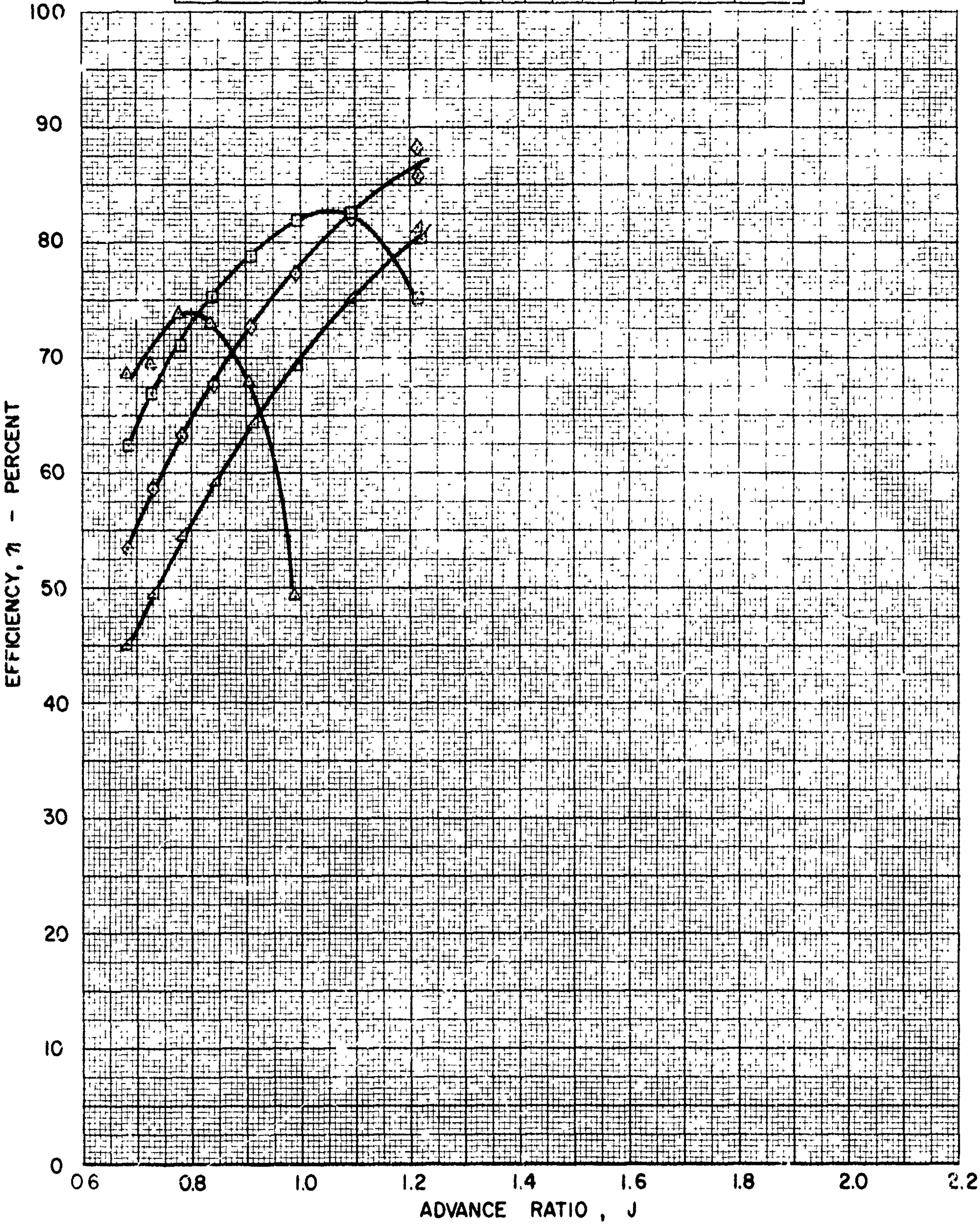

HSD SHROUDED PROPELLER TEST

EFFECT OF BLADE TIP CLEARANCE ON SHROUDED PROPELLER PERFORMANCE

SYM	RUN NO.	MACH NO.	CONFIGURATION	$\theta_{3/4}$
△	247	0.20	$L_1 C_1 E_1 B_3 P_R T_3 R_1 R_E$	20
⊡	252	↓	↓	25
◇	253	↓	↓	30
◿	258	↓	↓	35

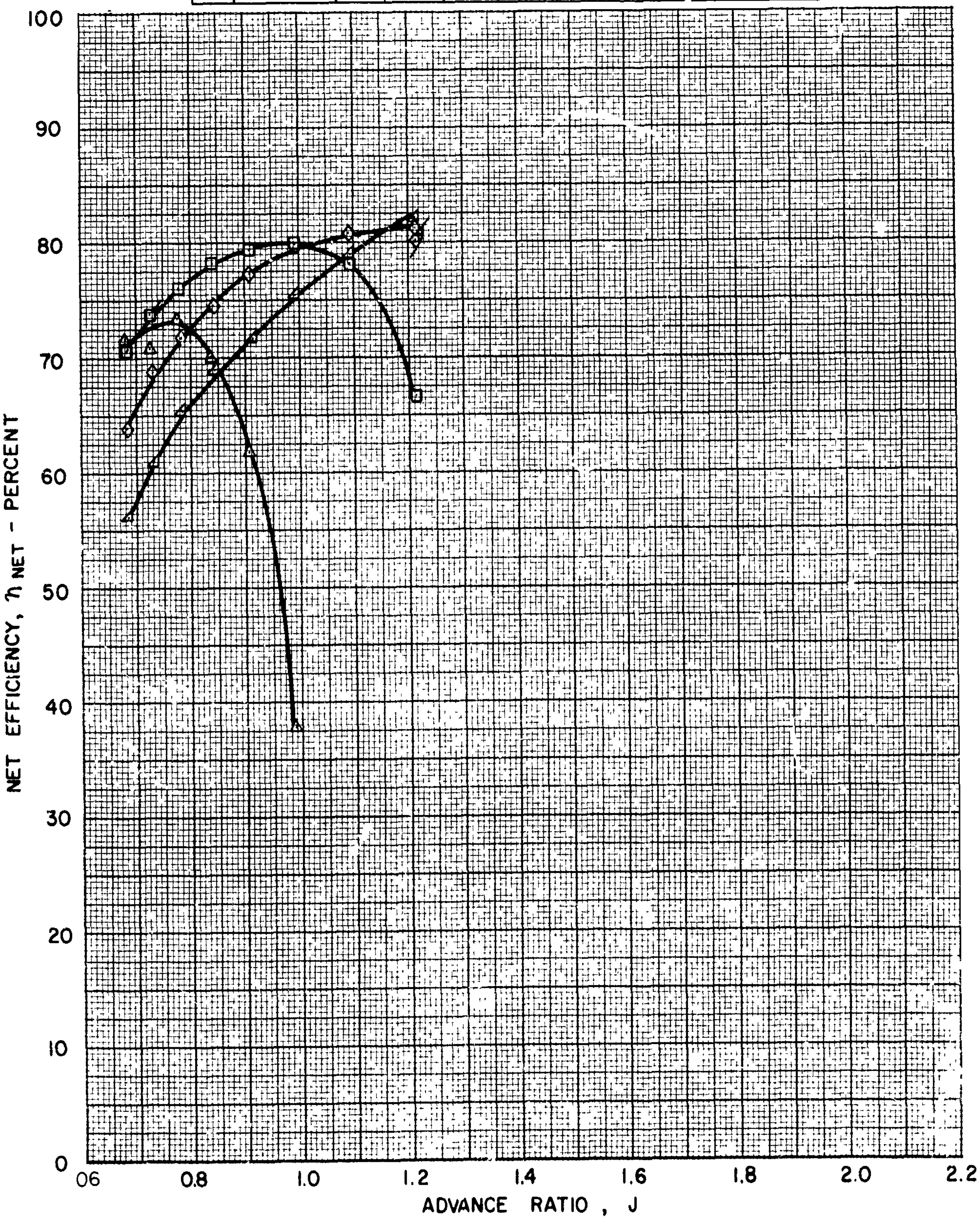

E530590-I

FIG.218

HSD SHROUDED PROPELLER TEST

EFFECT OF BLADE TIP CLEARANCE ON SHROUDED PROPELLER PERFORMANCE

SYM	RUN NO.	MACH NO.	CONFIGURATION	$\theta_{3/4}$
△	247	0.20	$L_1 C_1 E_1 B_3 P_R T_3 R_1 R_E$	20
□	252	↓	↓	25
◇	253	↓	↓	30
◿	258	↓	↓	35

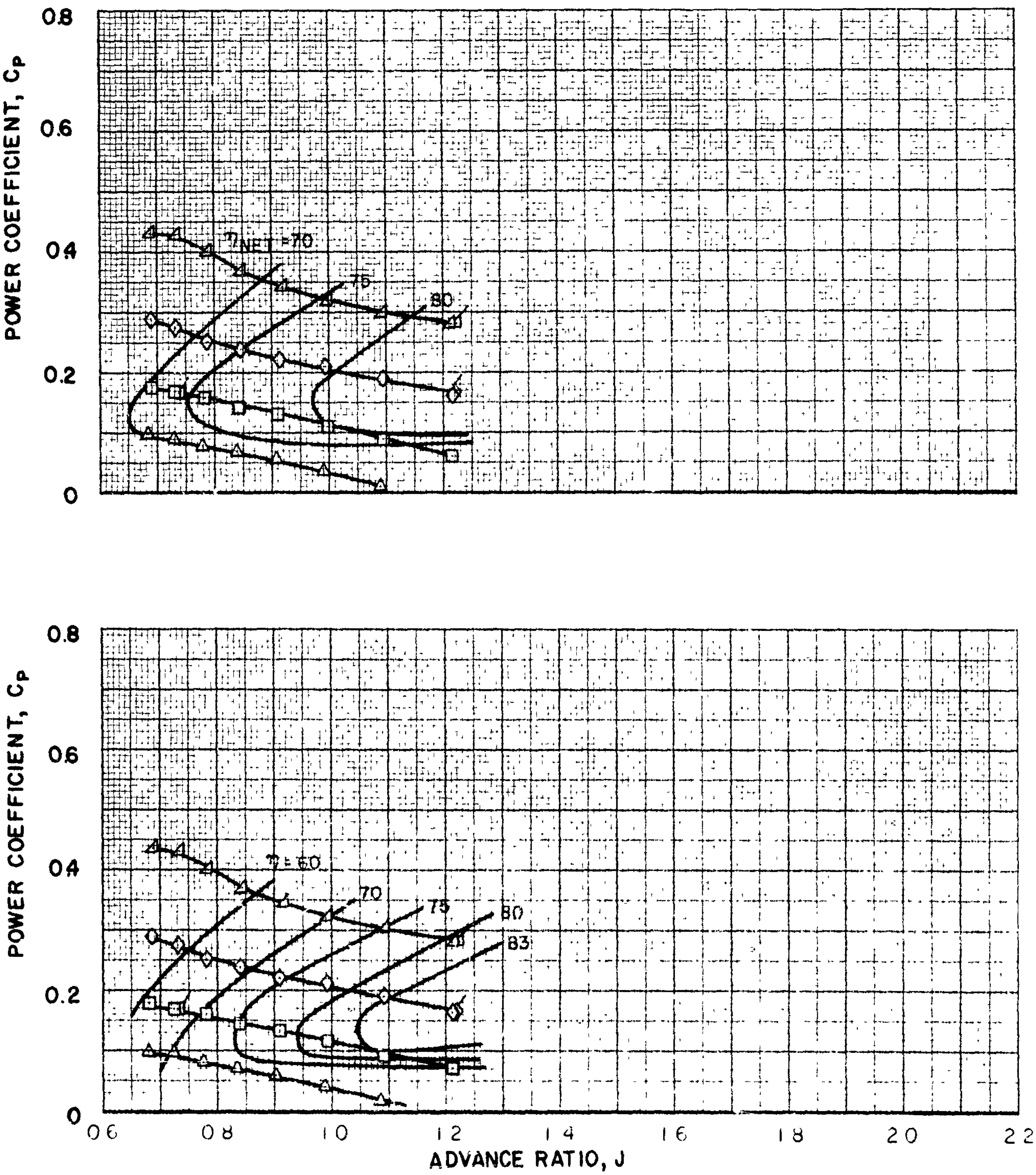

HSD SHROUDED PROPELLER TEST

EFFECT OF BLADE TIP CLEARANCE ON SHROUDED PROPELLER PERFORMANCE

SYM	RUN NO.	MACH NO.	CONFIGURATION	$\theta_{3/4}$
◇	641	0.30	L_1 C_1 E_1 B_3 P_R T_3 R_1 R_E	30
◁	642	↓	↓	34
▽	643	↓	↓	38
D	645	↓	↓	42

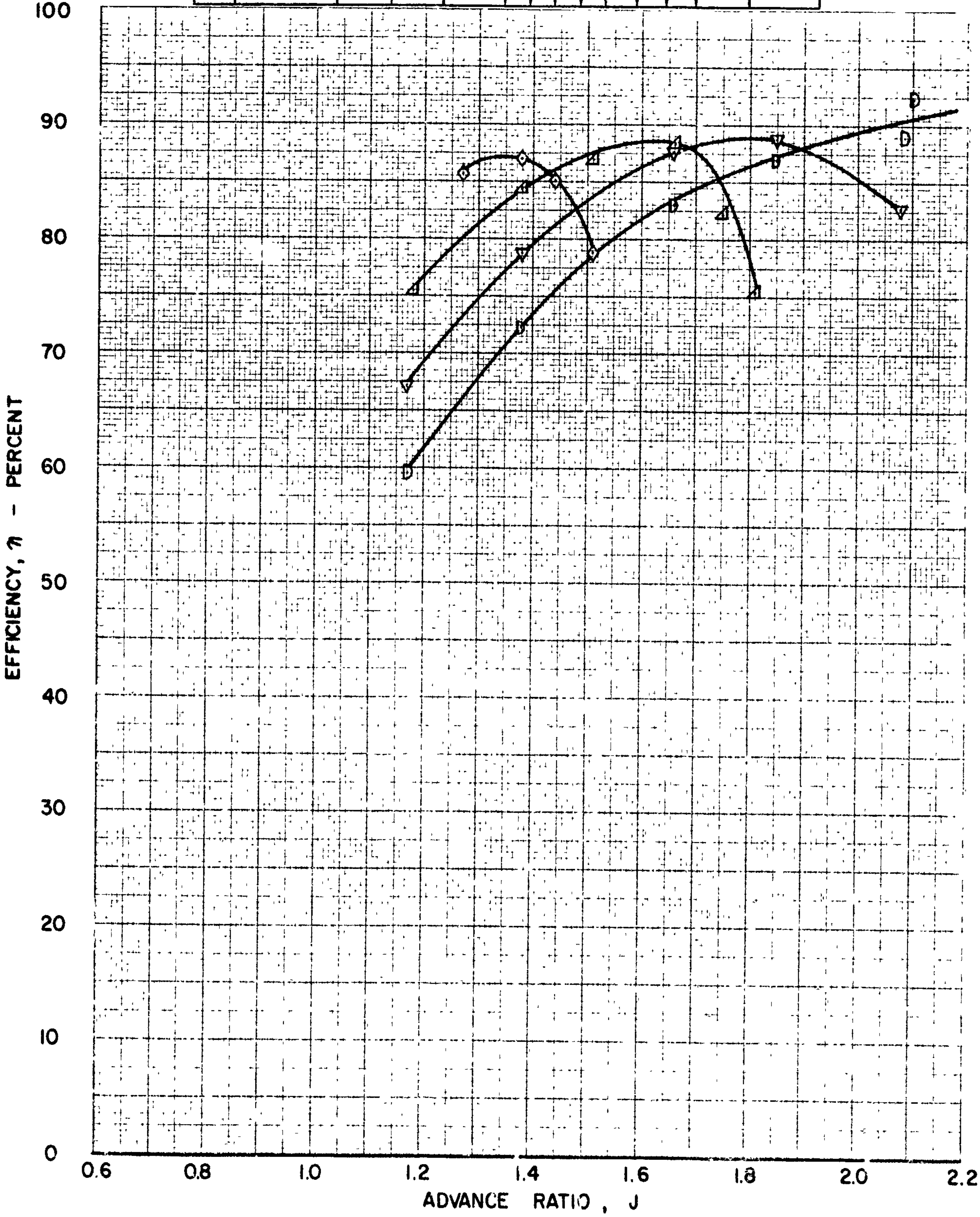

HSD SHROUDED PROPELLER TEST

EFFECT OF BLADE TIP CLEARANCE ON SHROUDED PROPELLER PERFORMANCE

SYM	RUN NO.	MACH NO.	CONFIGURATION	$\theta_{3/4}$
◇	641	0.30	L_1 C_1 E_1 B_3 P_R T_3 R_1 R_E	30
◁	642			34
▽	643			38
D	645			42

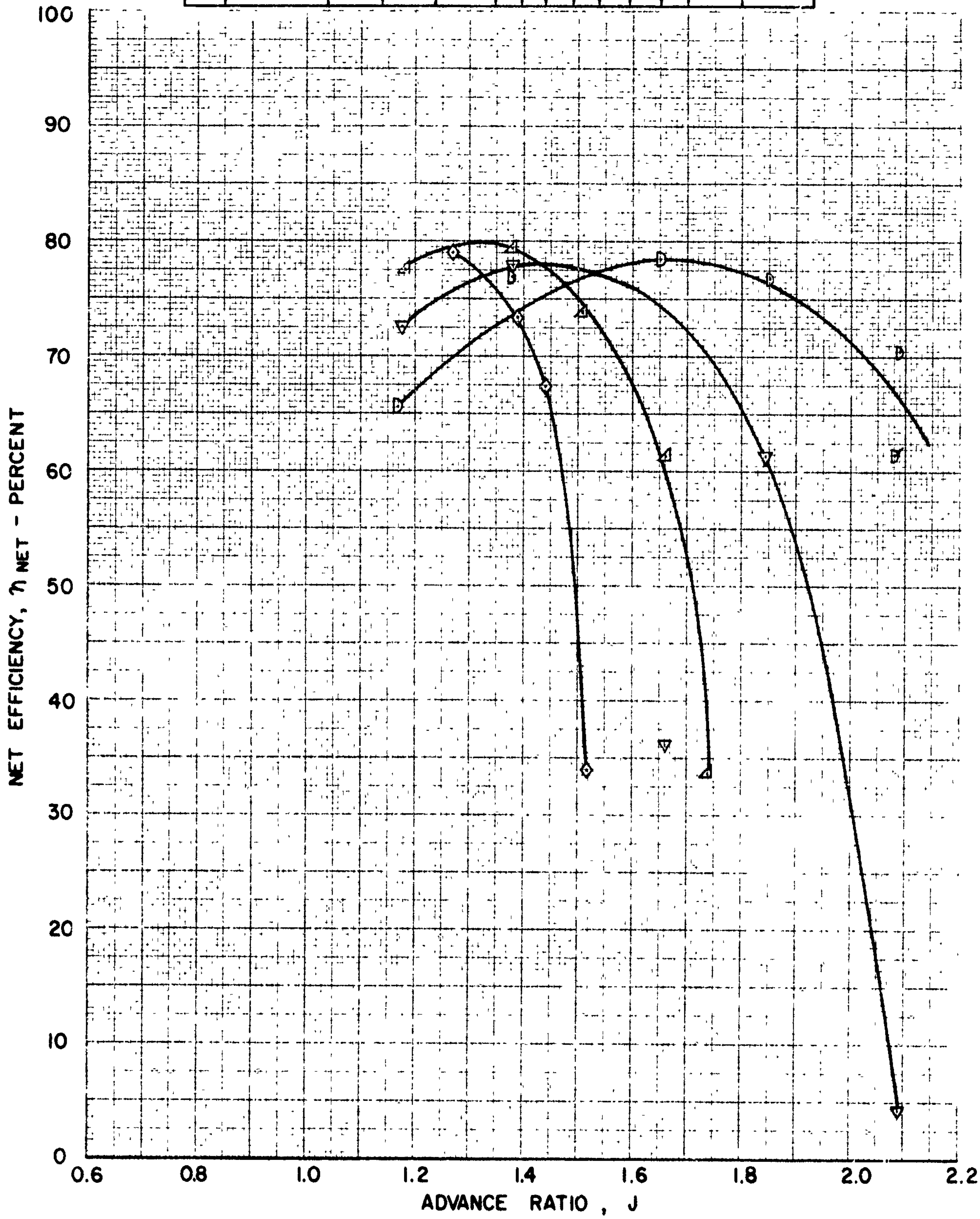

HSD SHROUDED PROPELLER TEST

EFFECT OF BLADE TIP CLEARANCE ON SHROUDED PROPELLER PERFORMANCE

SYM	RUN NO.	MACH NO.	CONFIGURATION	$\theta_{3/4}$
◇	641	0.30	$L_1\ C_1\ E_1\ B_3\ P_R\ T_3\ R_1\ R_E$	30
⊿	642	↓	↓	34
▽	643	↓	↓	38
D	645	↓	↓	42

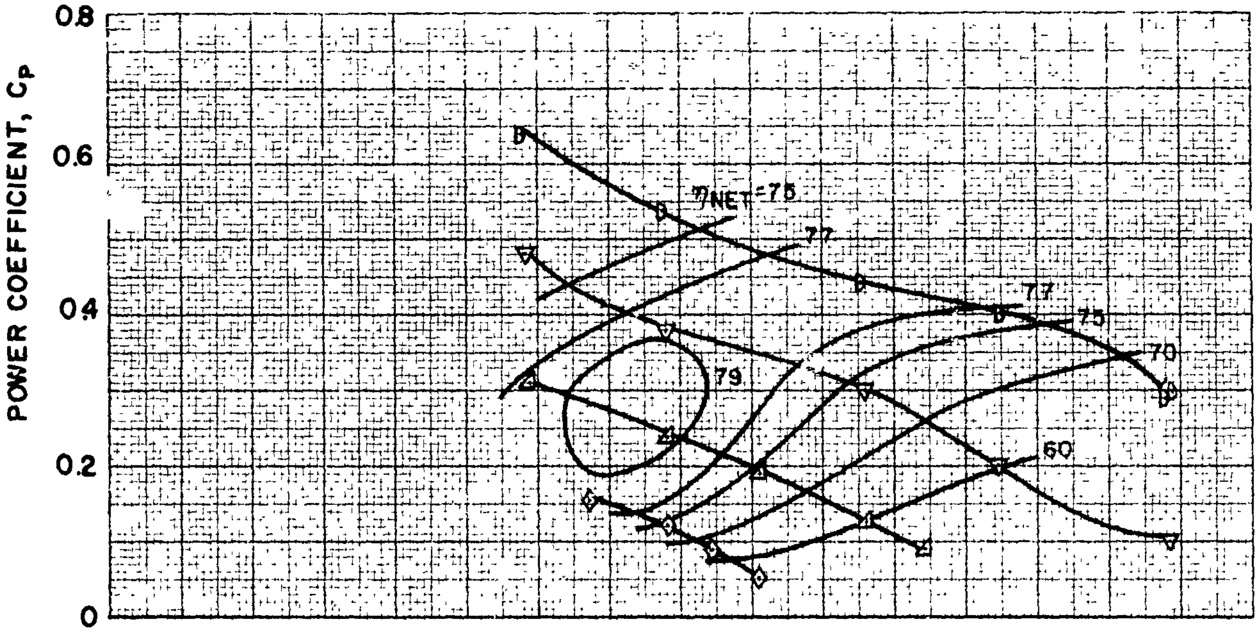

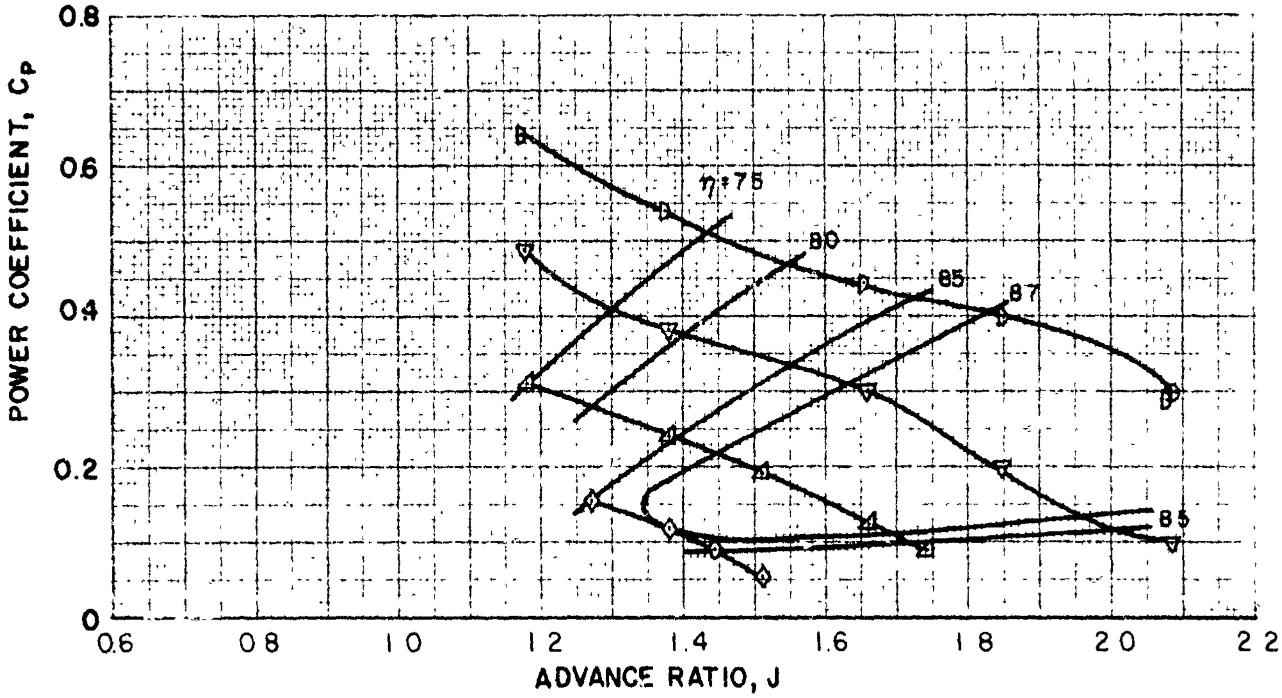

HSD SHROUDED PROPELLER TEST

EFFECT OF BLADE TIP CLEARANCE ON SHROUDED PROPELLER PERFORMANCE

SYM	RUN NO.	MACH NO.	CONFIGURATION	$\theta_{3/4}$
▽	644	0.40	$L_1\ C_1\ E_1\ B_3\ P_R\ T_3\ R_1\ R_E$	38
▷	646	↓	↓	42
◺	649	↓	↓	46
◁	651	↓	↓	50

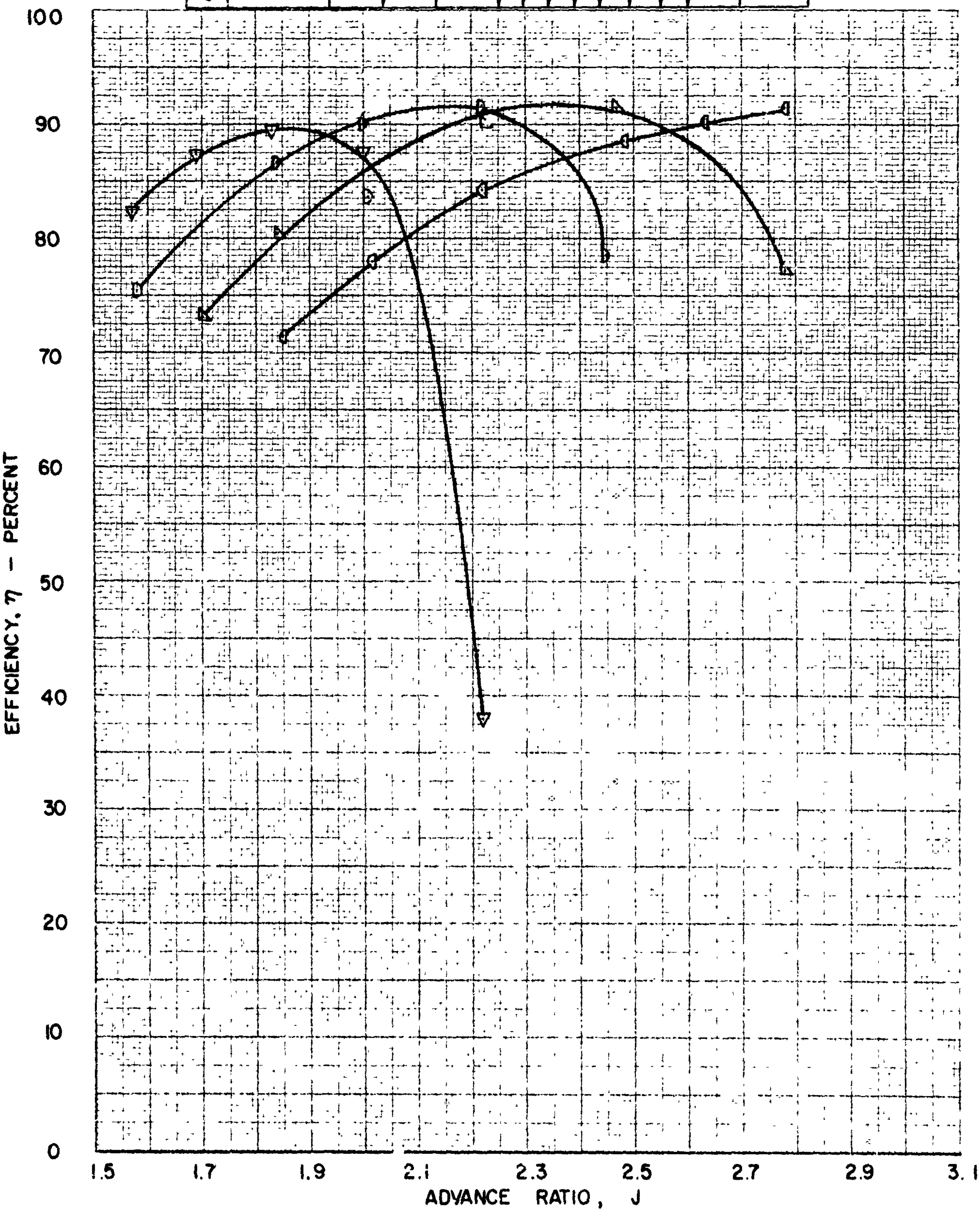

E330590-1

FIG. 223

HSD SHROUDED PROPELLER TEST

EFFECT OF BLADE TIP CLEARANCE ON SHROUDED PROPELLER PERFORMANCE

SYM	RUN NO.	MACH NO.	CONFIGURATION	$\theta_{3/4}$
▽	644	0.40	L_1 C_1 E_1 B_3 P_R T_3 R_1 R_E	38
D	646			42
◺	649			46
◖	651			50

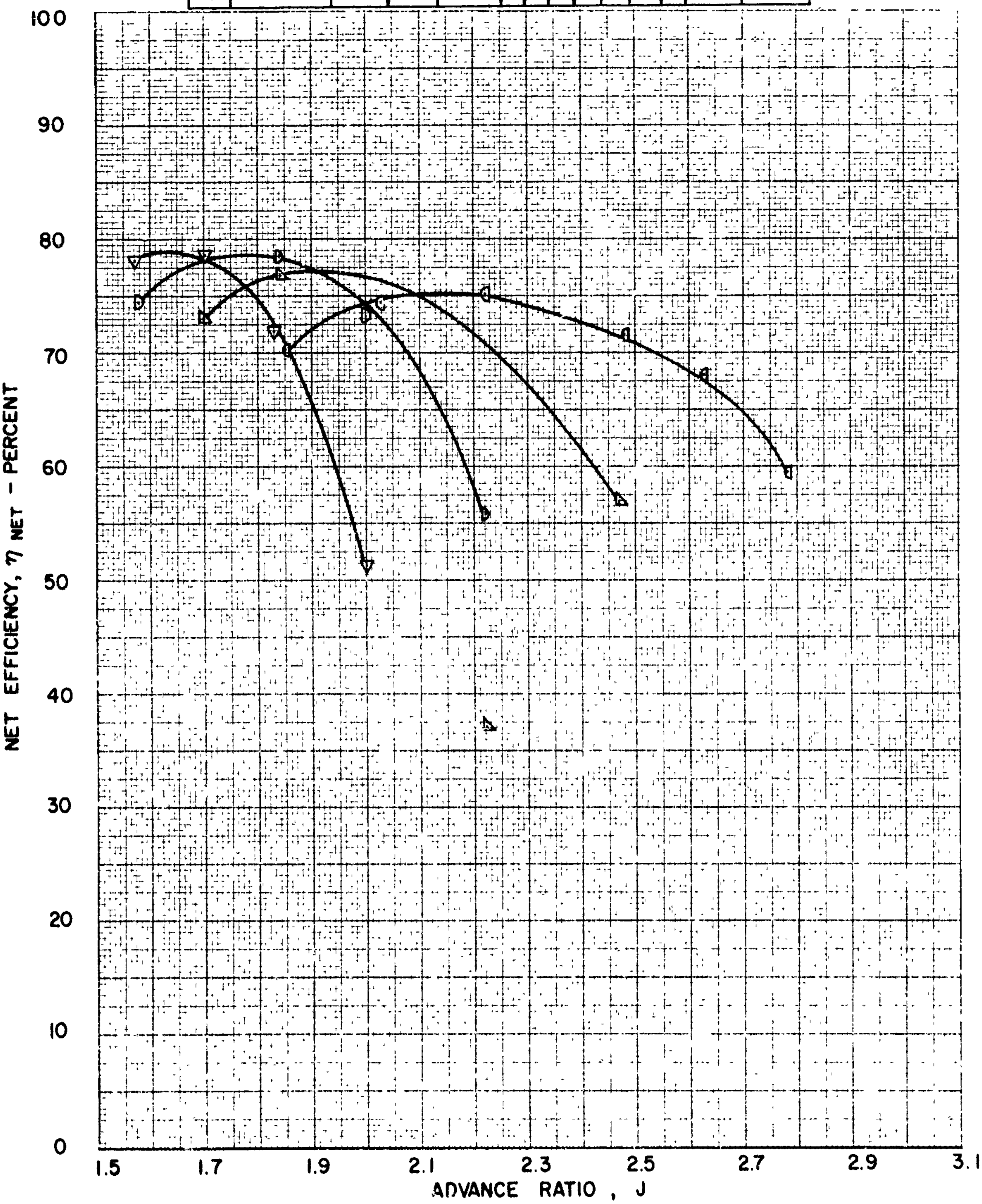

E330590-1

FIG.224

HSD SHROUDED PROPELLER TEST

EFFECT OF BLADE TIP CLEARANCE ON SHROUDED PROPELLER PERFORMANCE

SYM	RUN NO	MACH NO.	CONFIGURATION	$\theta_{3/4}$
▽	644	0.40	L_1 C_1 E_1 B_3 P_R T_3 R_1 R_E	38
D	646	↓	↓	42
◺	649	↓	↓	46
◖	651	↓	↓	50

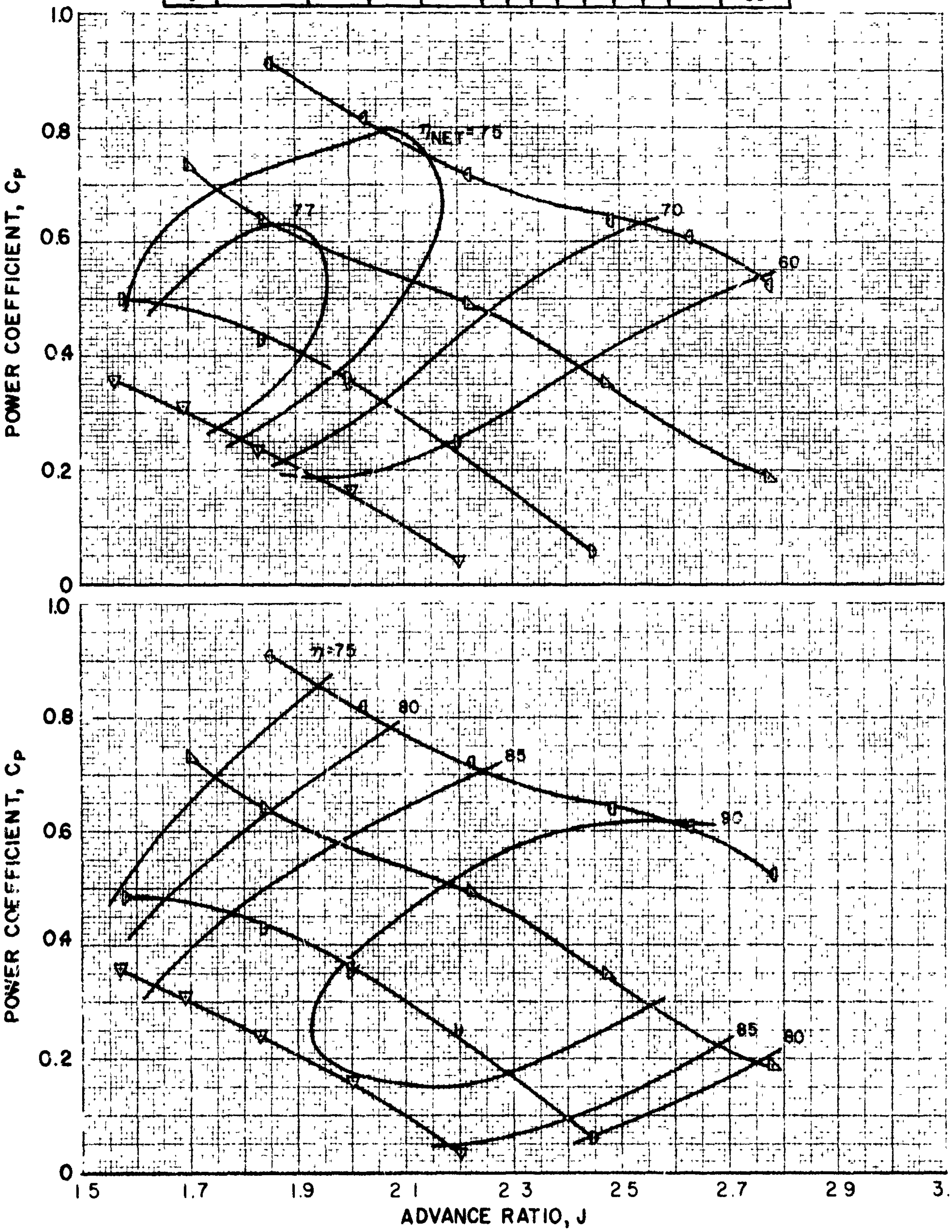

HSD SHROUDED PROPELLER TEST

EFFECT OF BLADE TIP CLEARANCE ON SHROUDED PROPELLER PERFORMANCE

SYM	RUN NO.	MACH NO.	CONFIGURATION	$\theta_{3/4}$
▷	647	0.50	L_1 C_1 E_1 B_3 P_R T_3 R_1 R_E	42
◺	650	↓	↓	46
◁	652	↓	↓	50
⊙	653	↓	↓	54

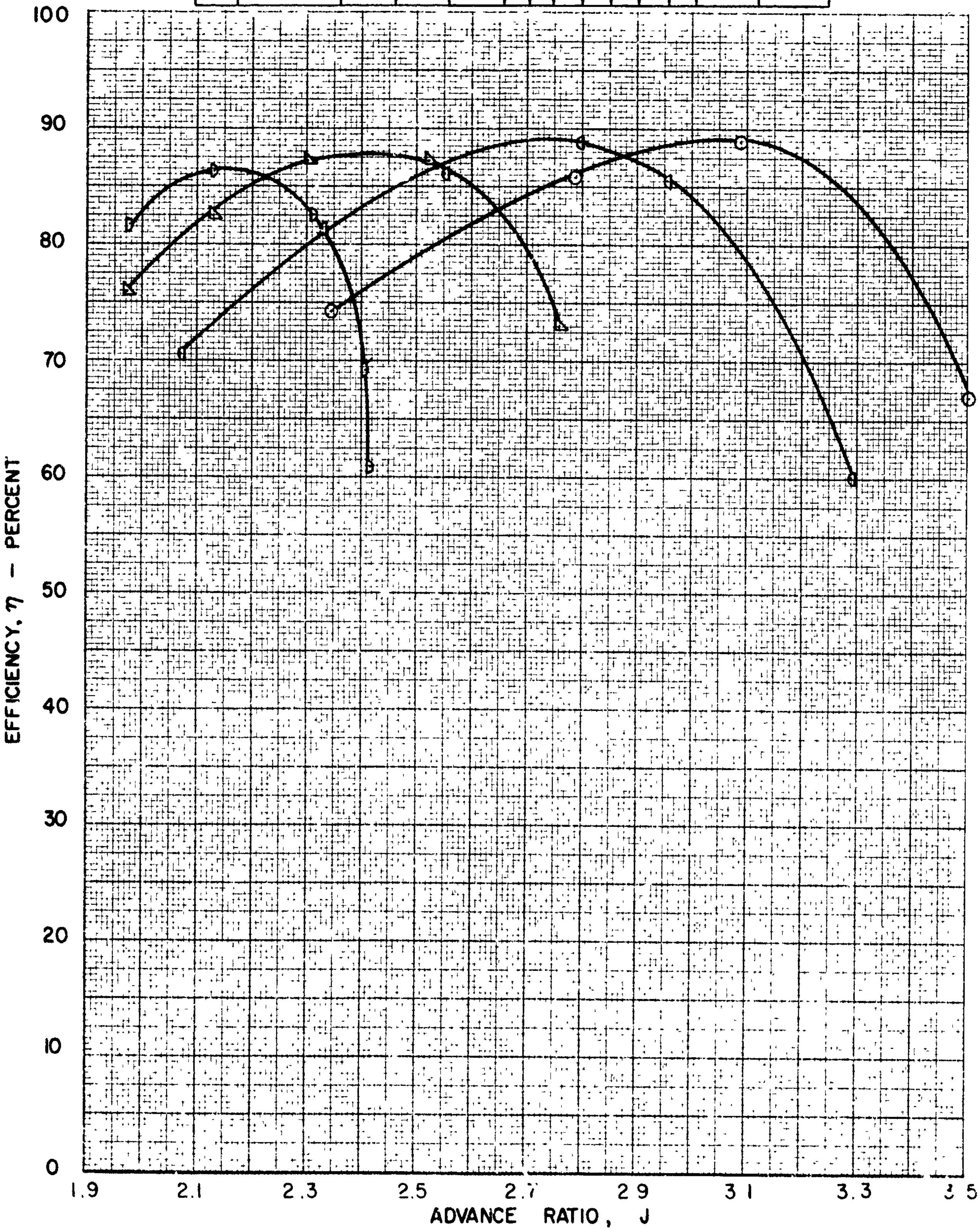

E330590-1

FIG. 226

HSD SHROUDED PROPELLER TEST

EFFECT OF BLADE TIP CLEARANCE ON SHROUDED PROPELLER PERFORMANCE

SYM	RUN NO.	MACH NO.	CONFIGURATION	$\theta_{3/4}$
D	647	0.50	L_1 C_1 E_1 B_3 P_R T_3 R_1 R_E	42
◺	650	↓	↓	46
ɑ	652	↓	↓	50
⊙	653	↓	↓	54

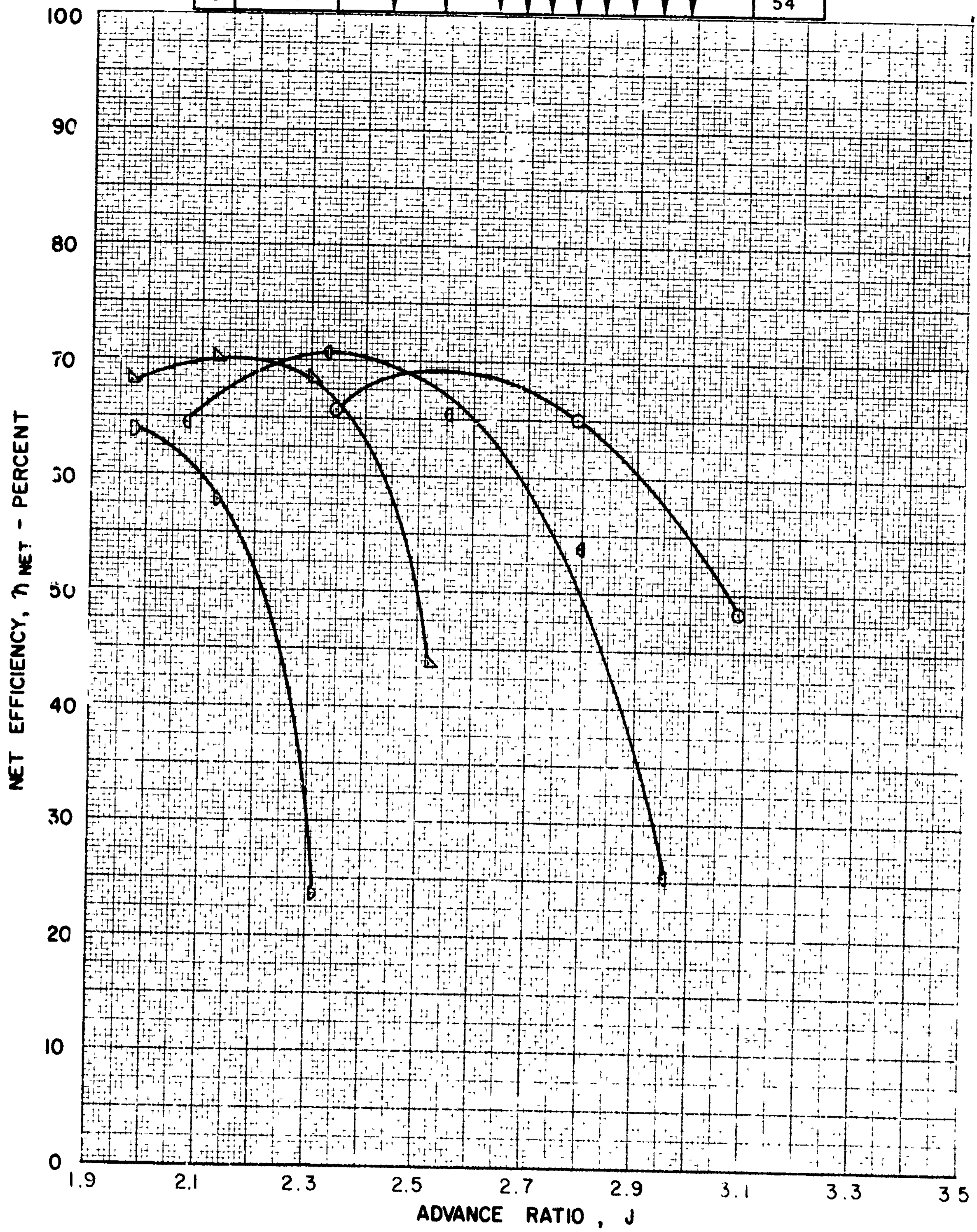

HSD SHROUDED PROPELLER TEST

EFFECT OF BLADE TIP CLEARANCE ON SHROUDED PROPELLER PERFORMANCE

SYM	RUN NO.	MACH NO.	CONFIGURATION	$\theta_{3/4}$
D	647	0.50	L_1 C_1 E_1 B_3 P_R T_3 R_1 R_E	42
▷	650	↓	↓	46
◁	652	↓	↓	50
⊙	653	↓	↓	54